

Planckian Dynamics

$$\tau_r \geq C \frac{\hbar}{k_B T} \quad (\text{SS, } \textit{Quantum Phase Transitions}, 1999)$$

School on Emergent Phenomena in
Non-Equilibrium Quantum Many-Body Systems
ICTP-SAIFR

São Paulo, Brazil
November 3,4 2025

Subir Sachdev

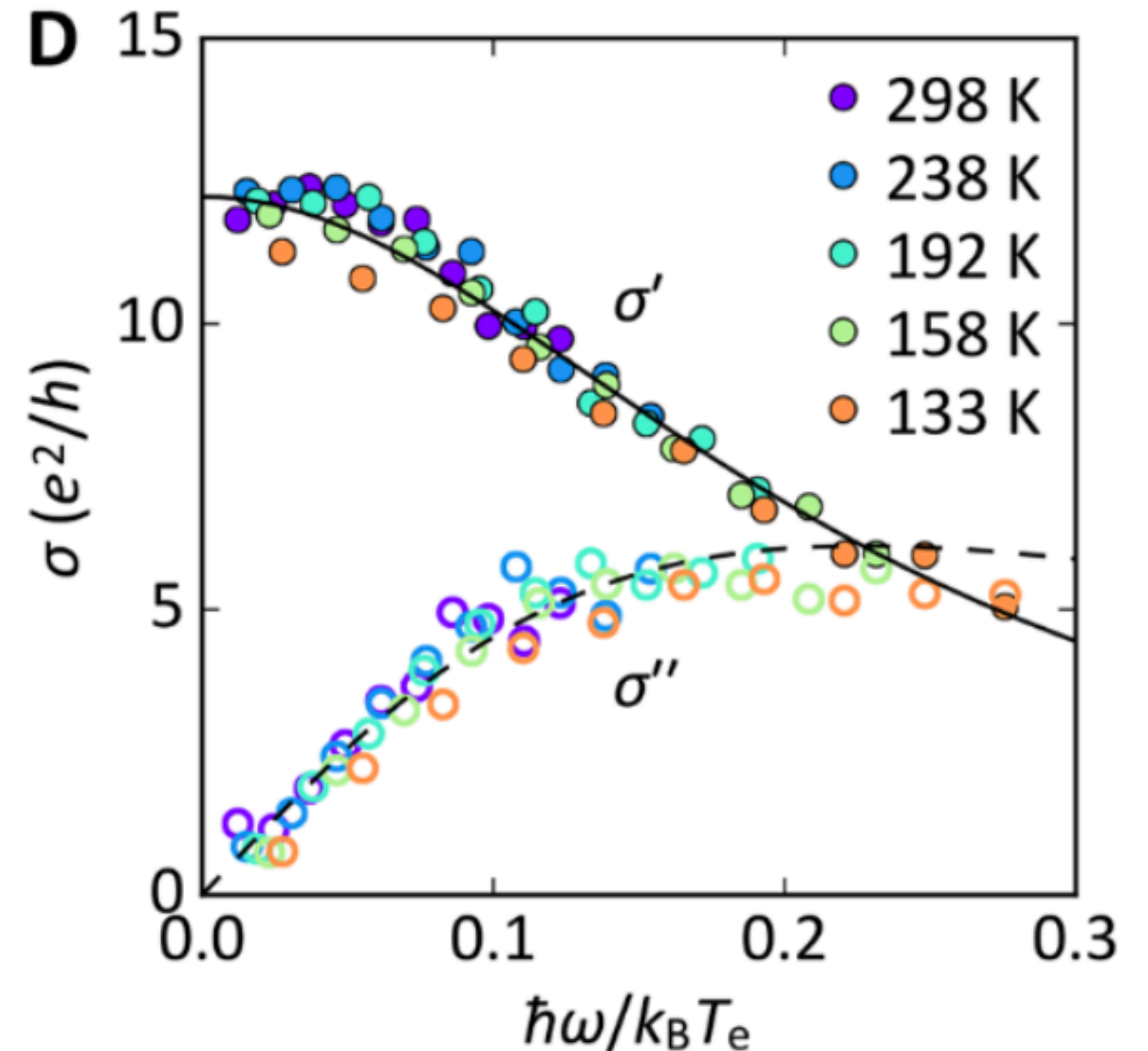
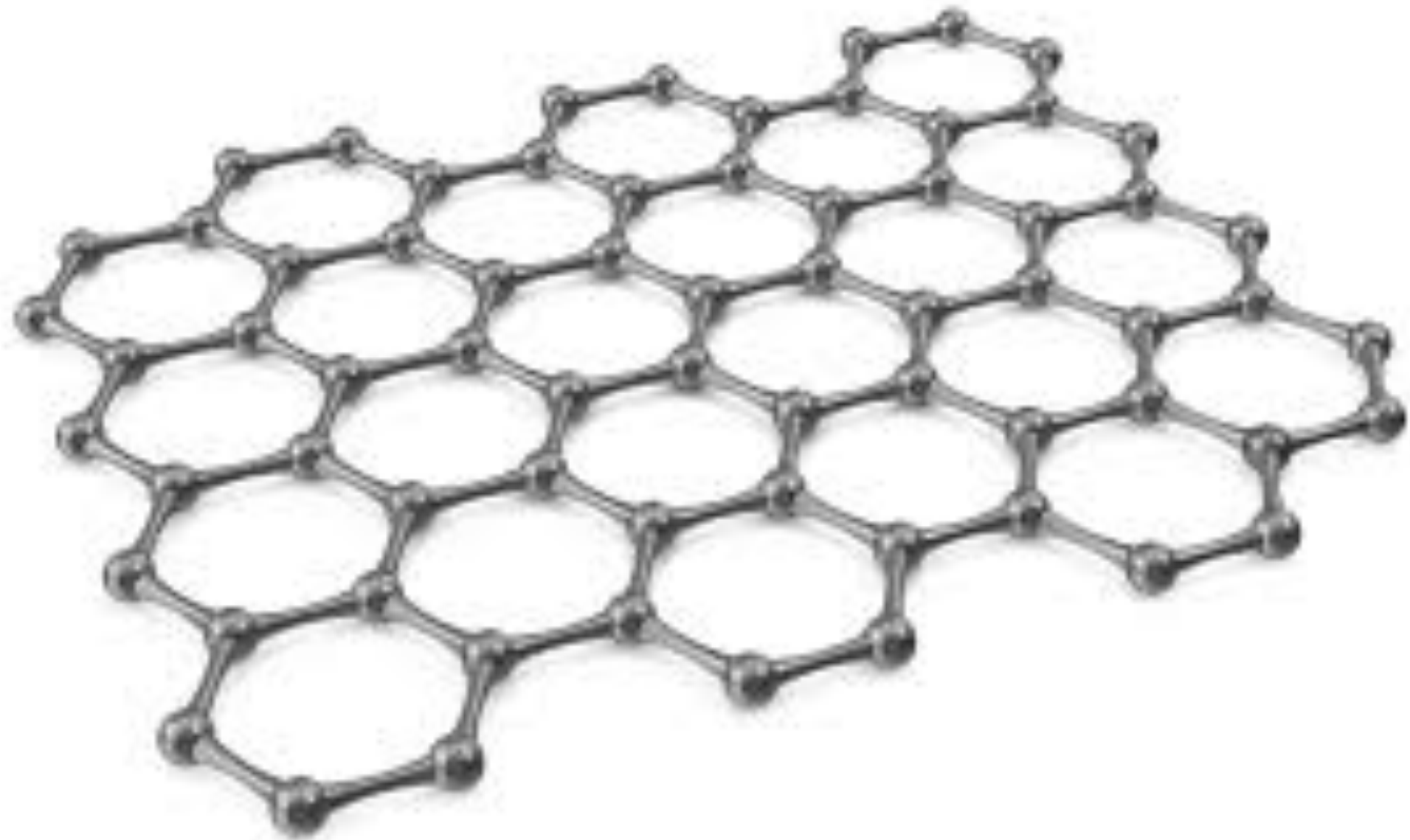


Quantum-critical conductivity of the Dirac fluid in graphene

Science **364**, 158 (2019)

Patrick Gallagher^{1,2}, Chan-Shan Yang^{1,3}, Tairu Lyu¹, Fanglin Tian^{1,4}, Rai Kou¹,
Hai Zhang^{1,5}, Kenji Watanabe⁶, Takashi Taniguchi⁶, Feng Wang^{1,2,7*}

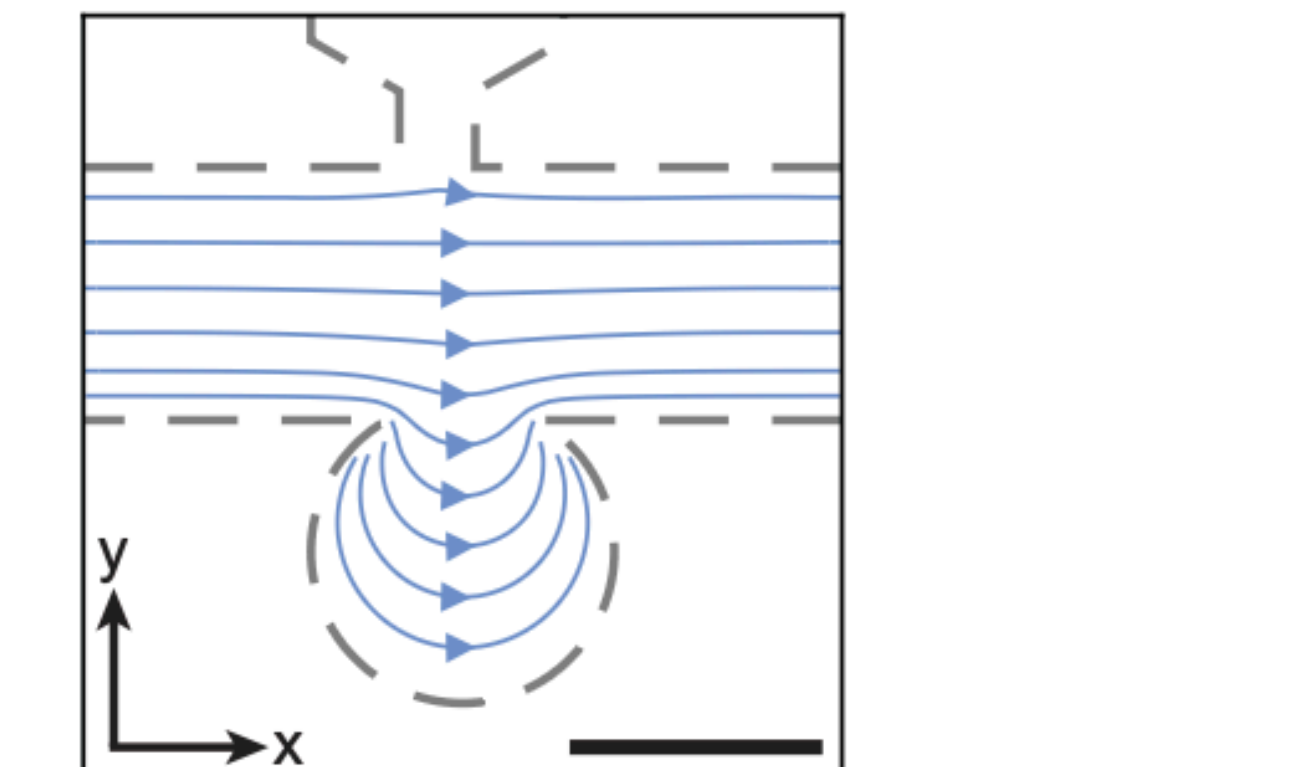
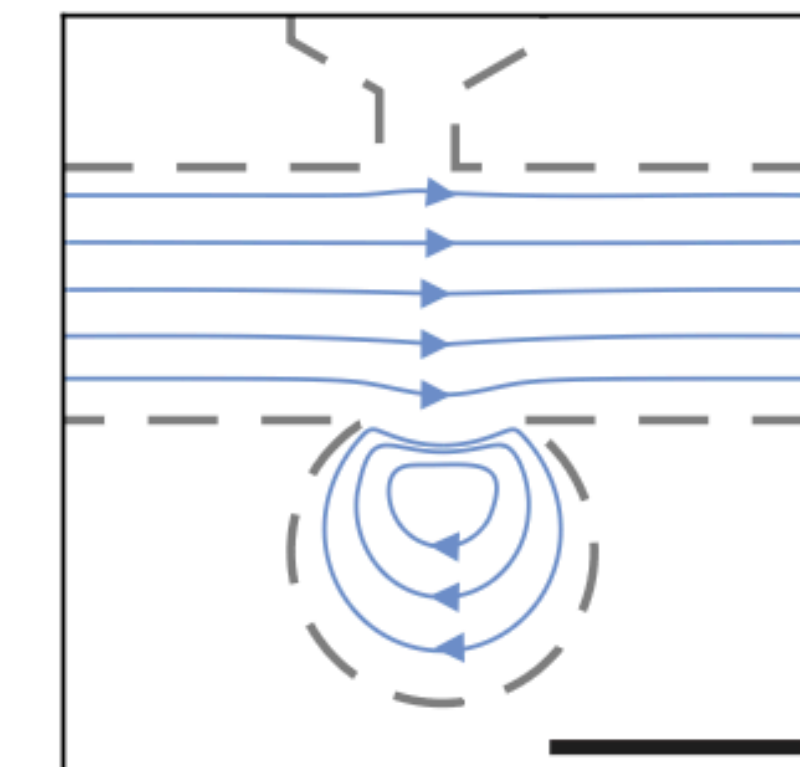
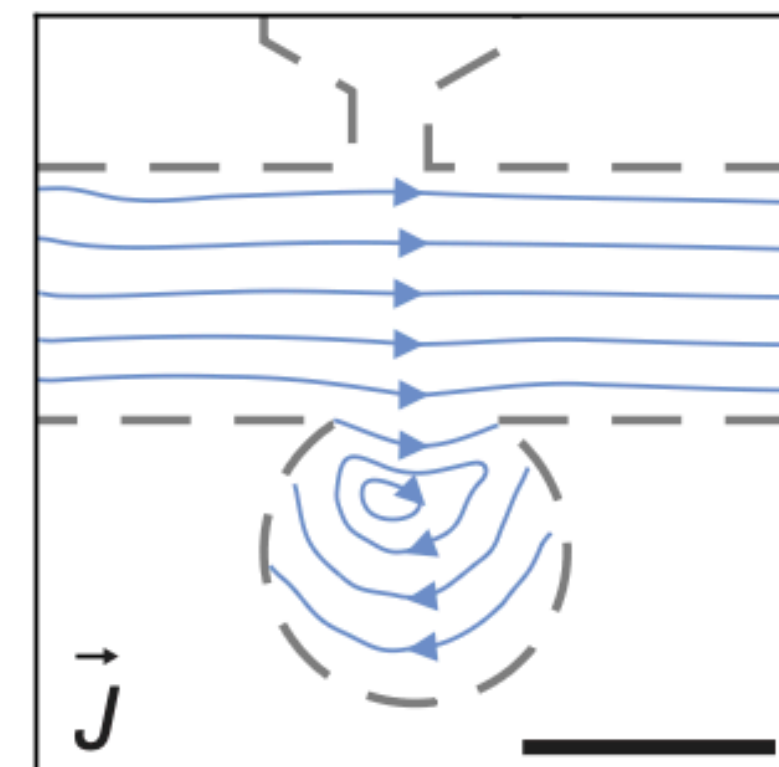
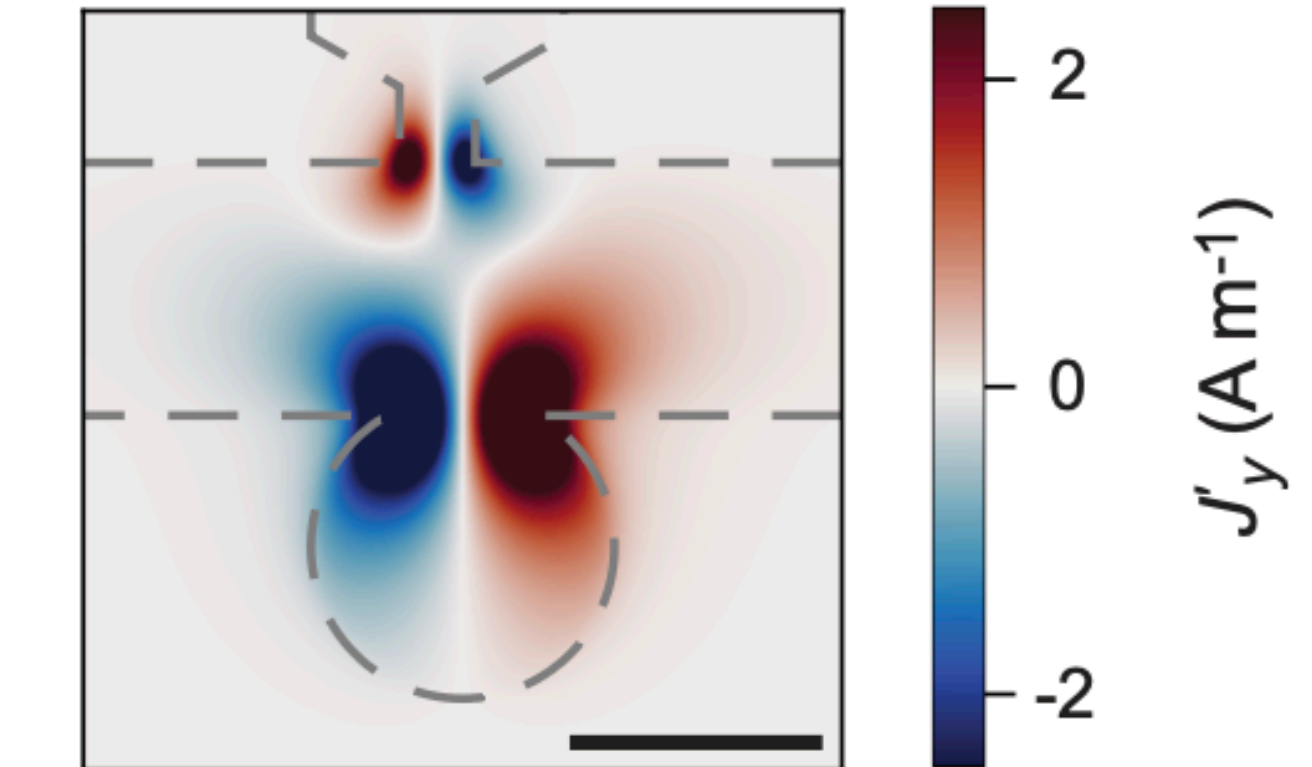
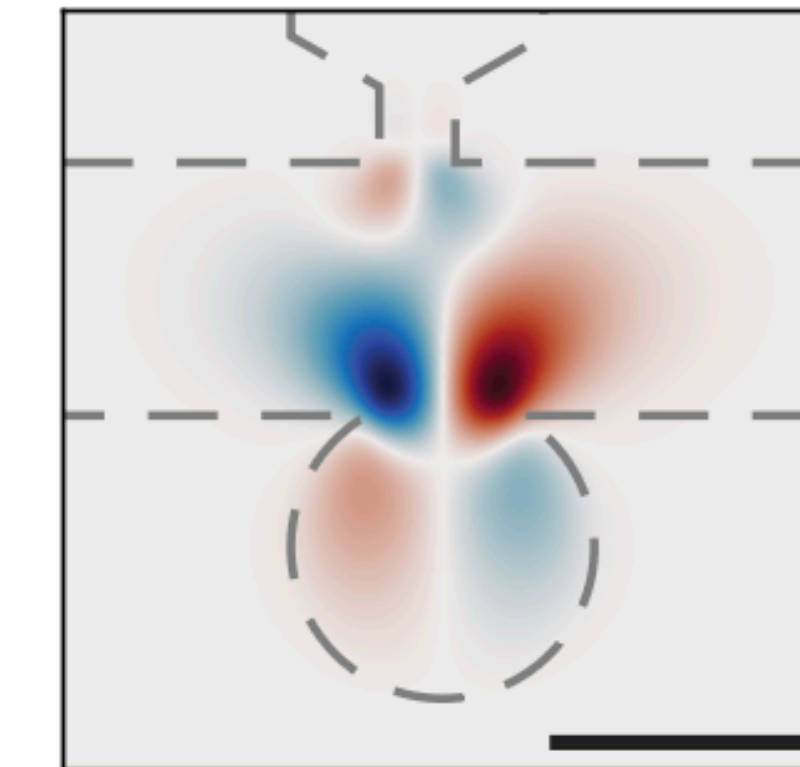
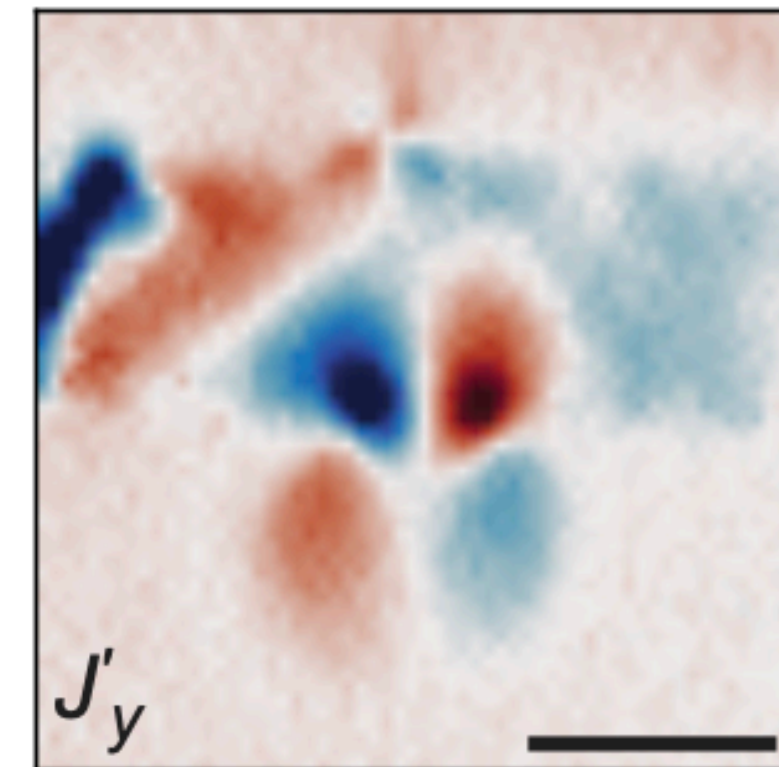
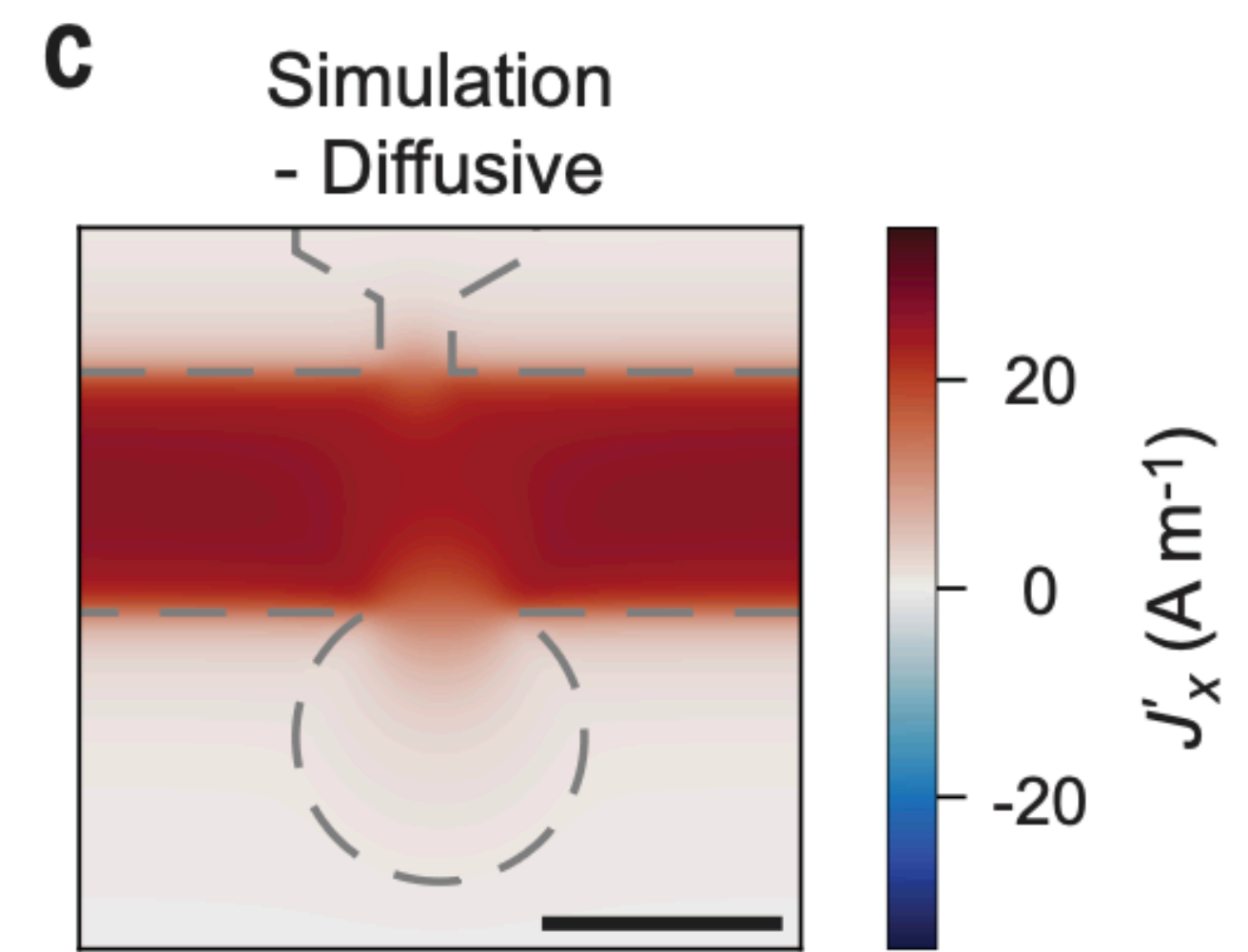
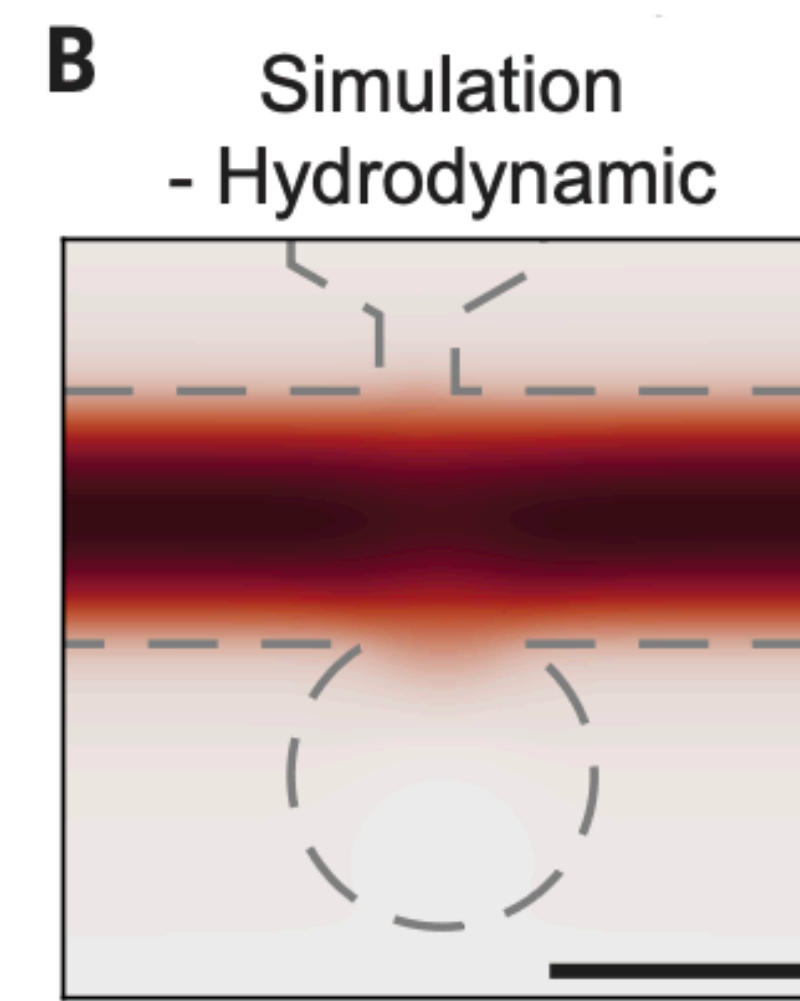
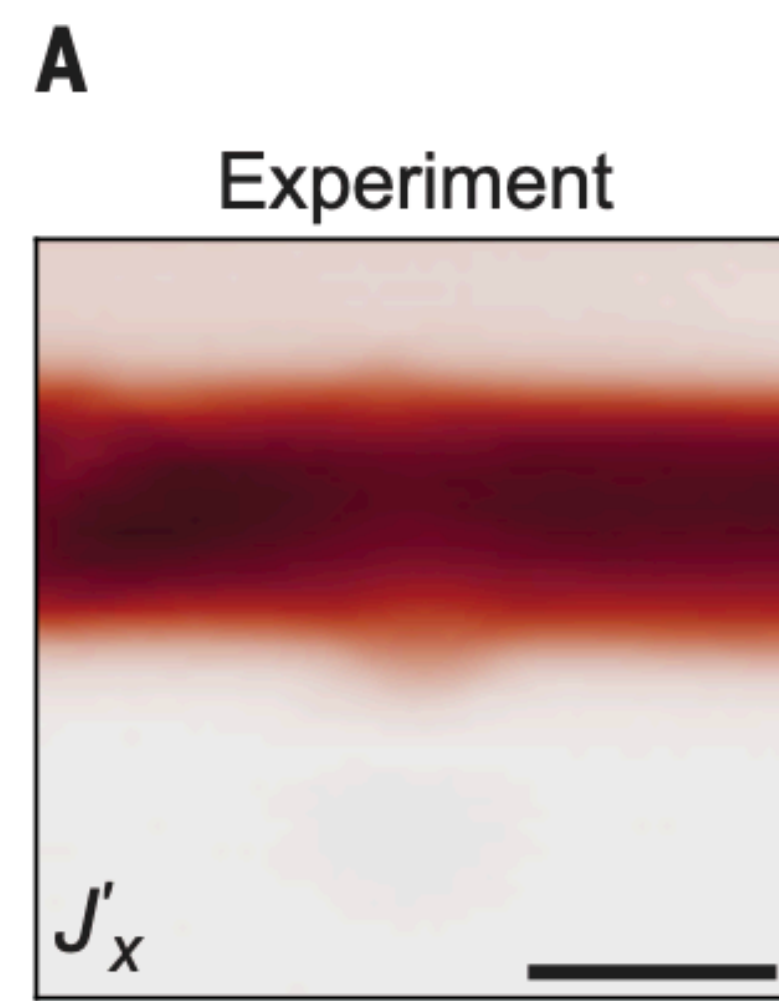
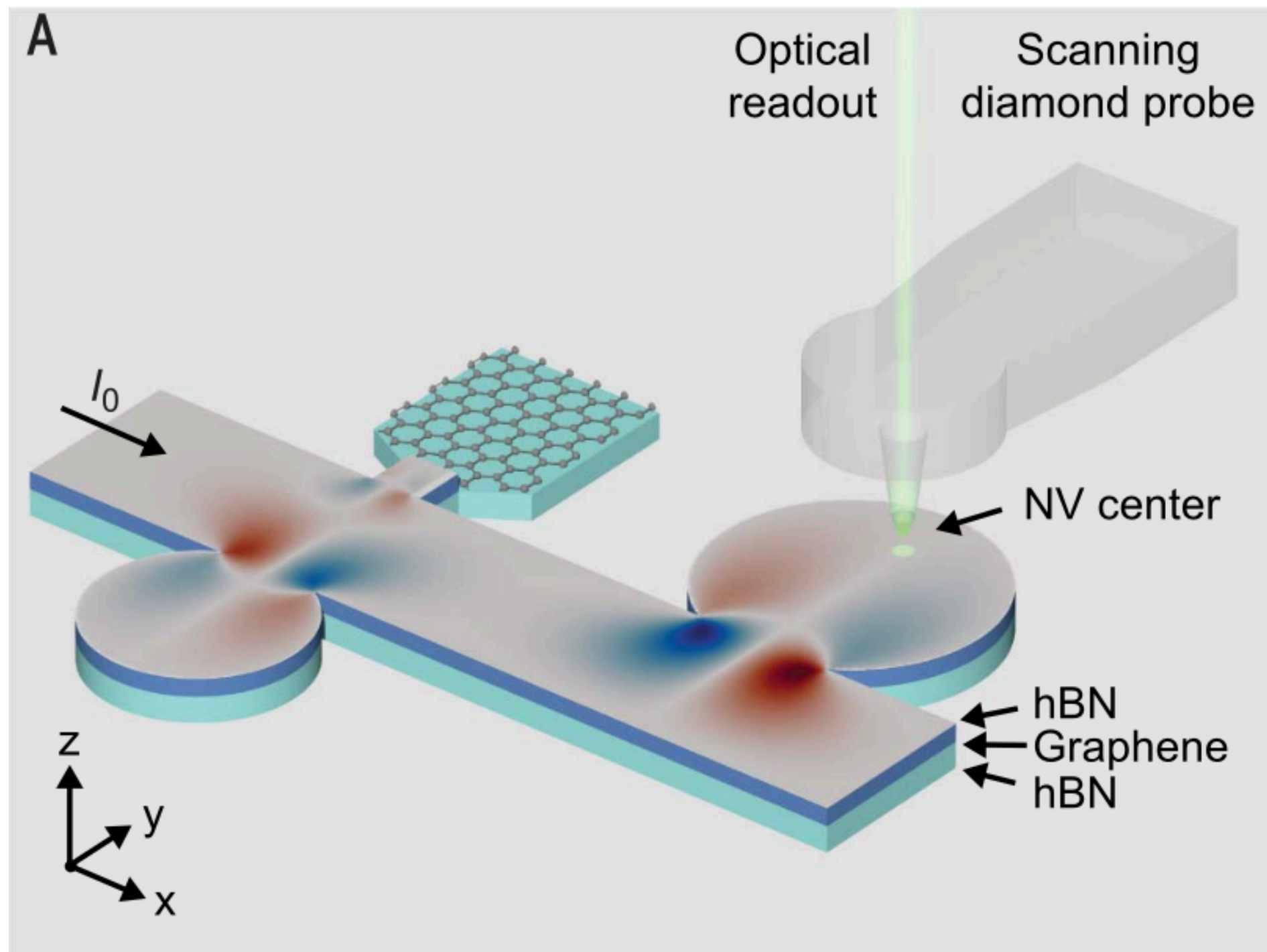
$$\sigma = \frac{e^2}{h} \mathcal{F} \left(\frac{\hbar\omega}{k_B T} \right)$$

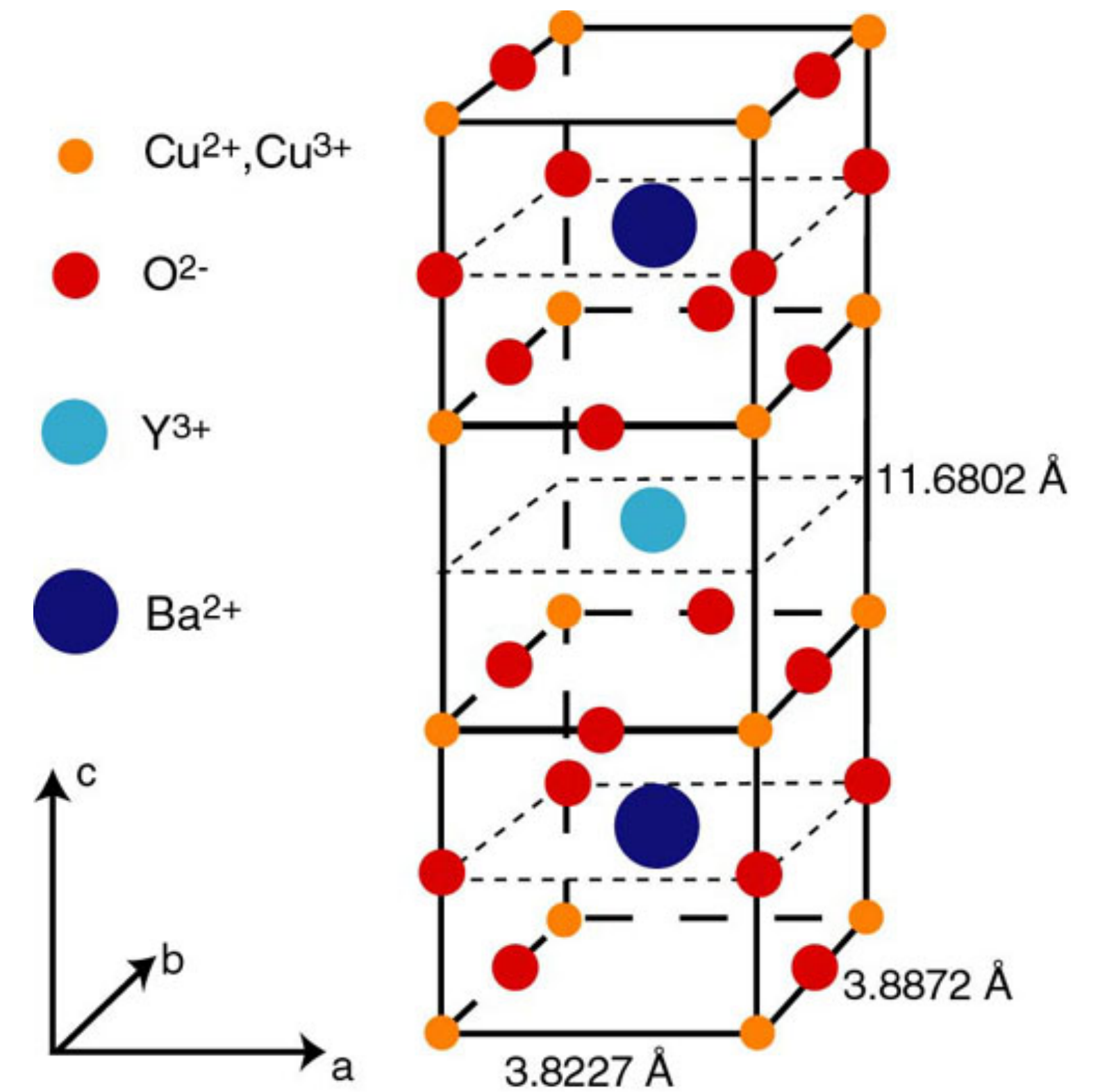
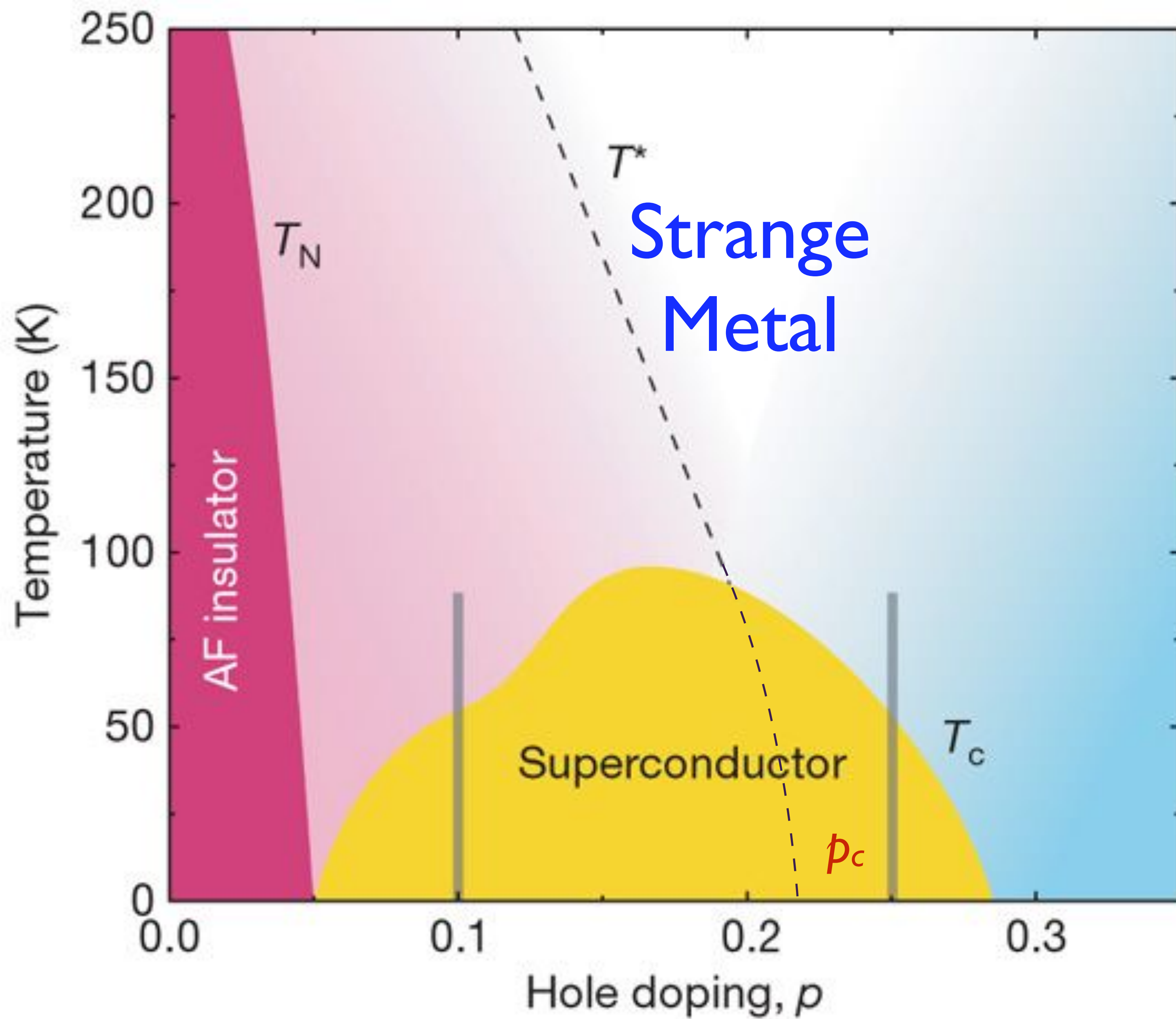


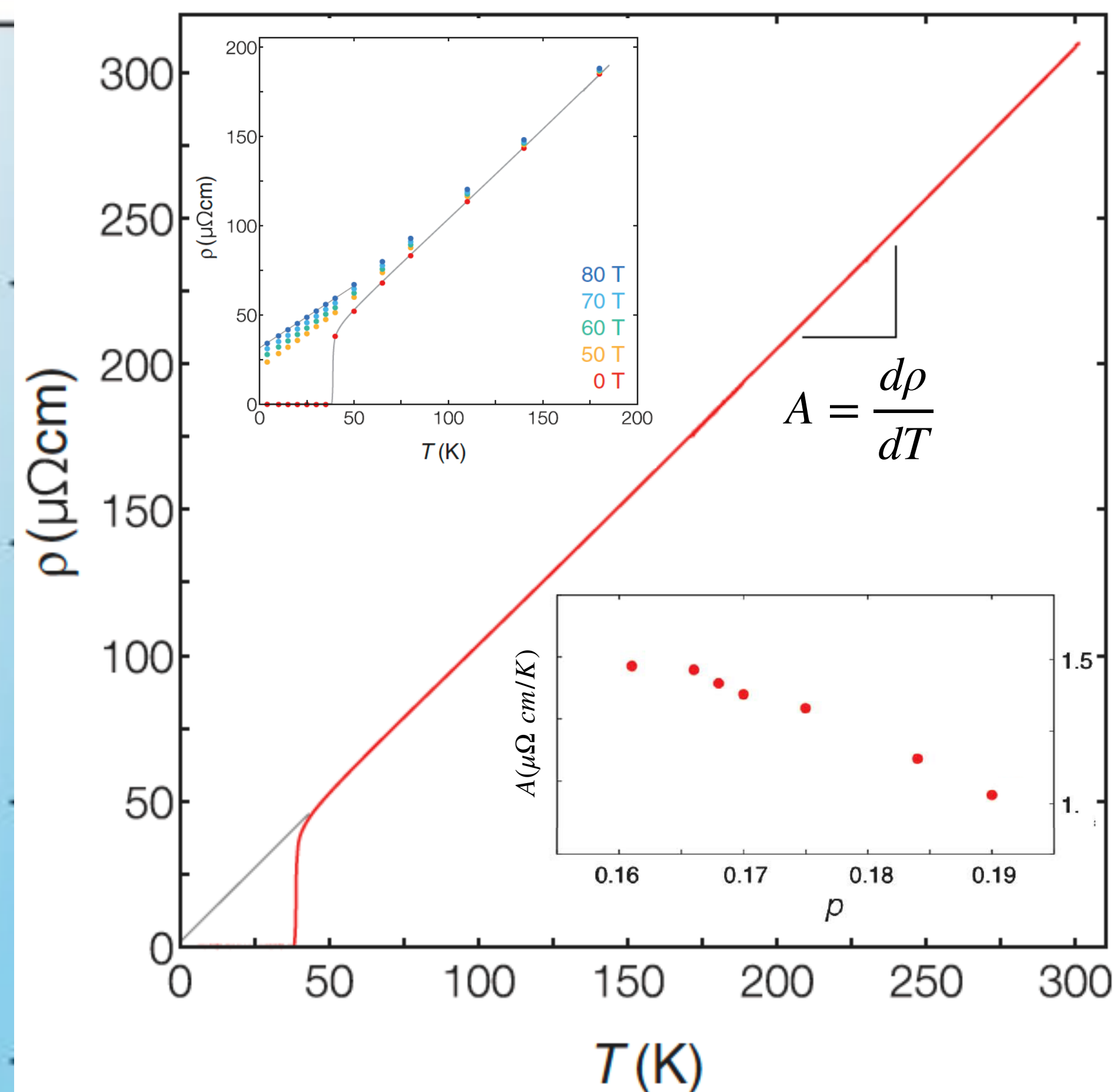
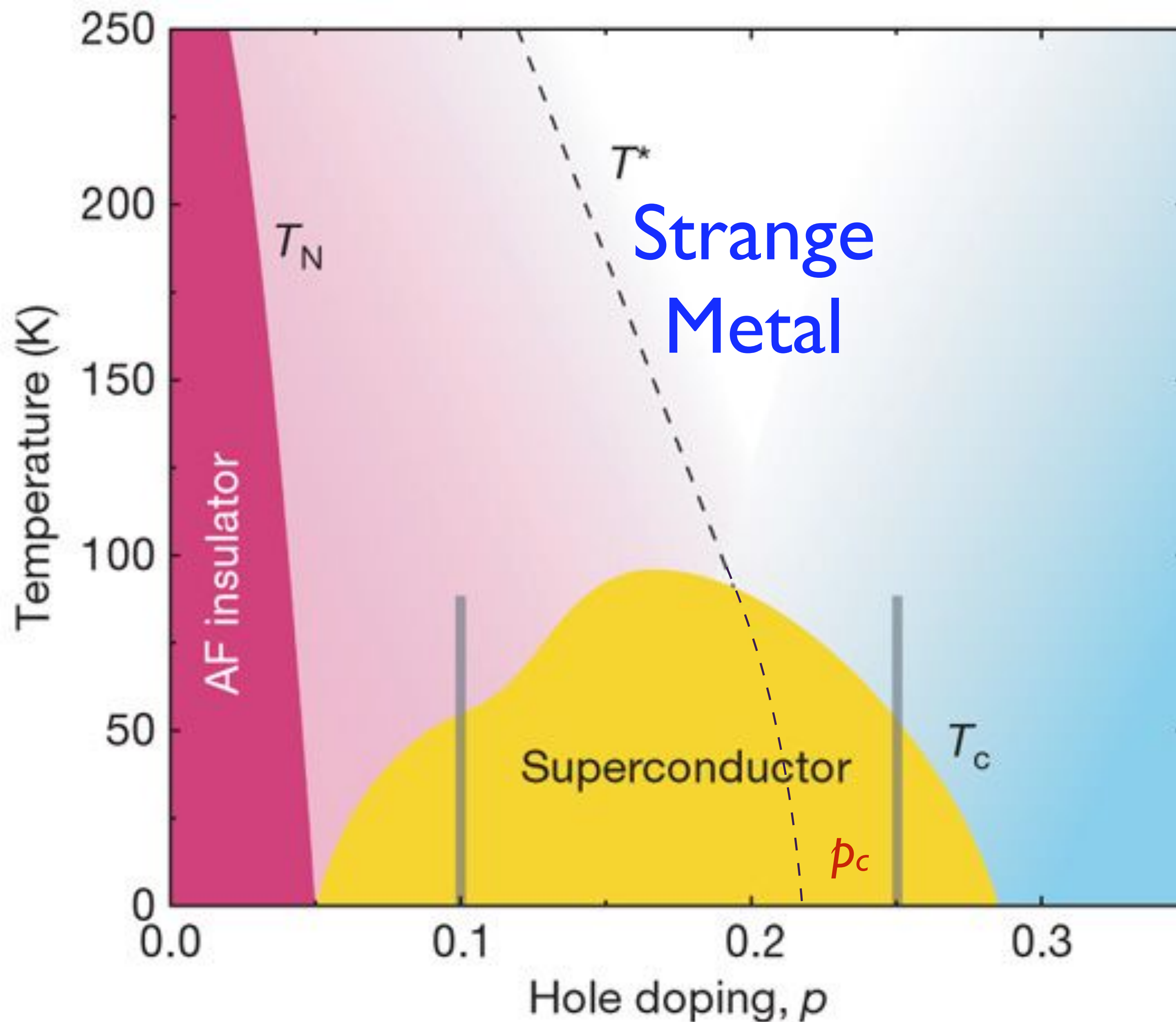
Observation of current whirlpools in graphene at room temperature

Marius L. Palm, Chaoxin Ding,
William S. Huxter, Takashi Taniguchi,
Kenji Watanabe, Christian L. Degen

Science **384**, 465 (2024)







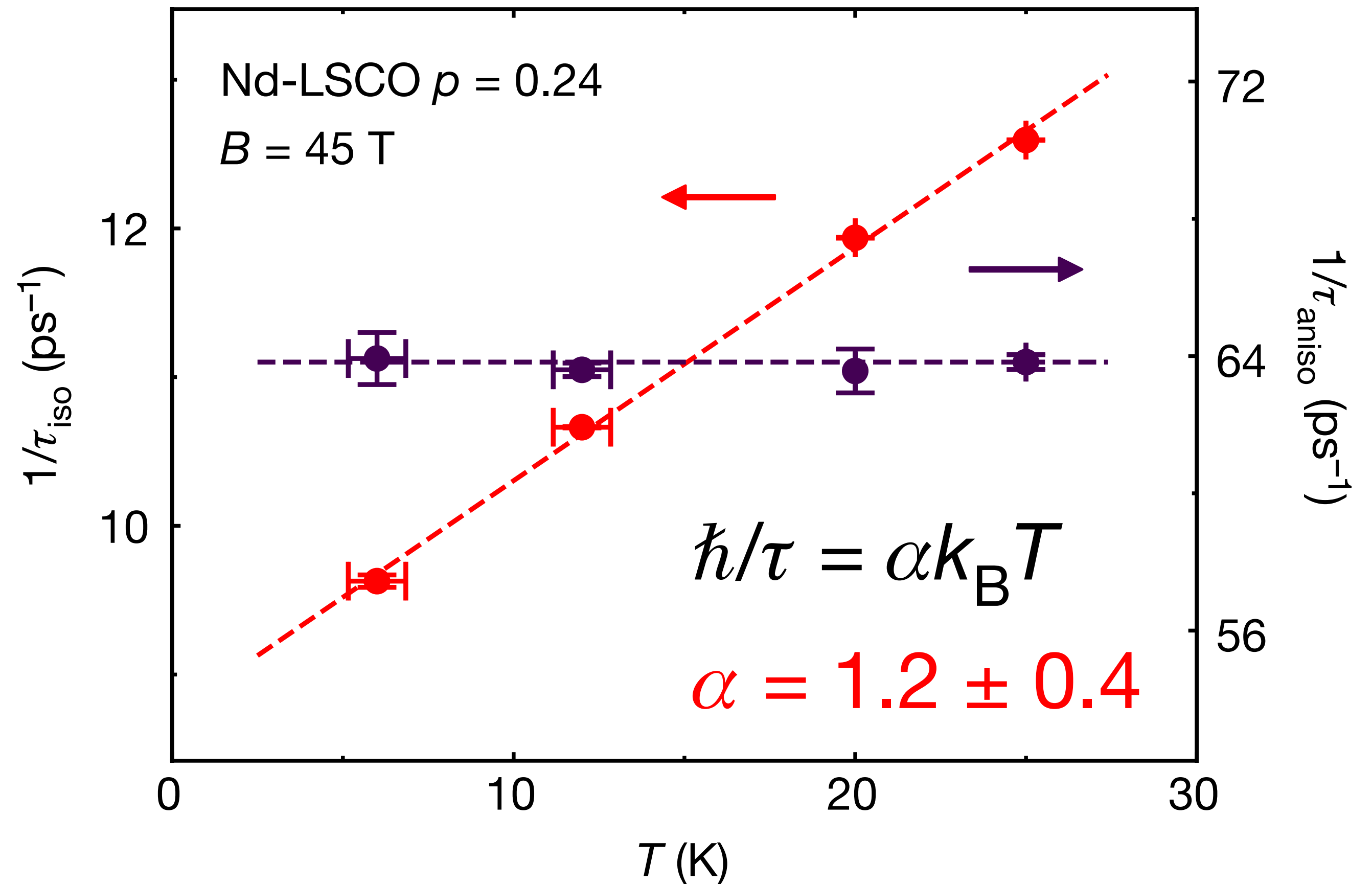
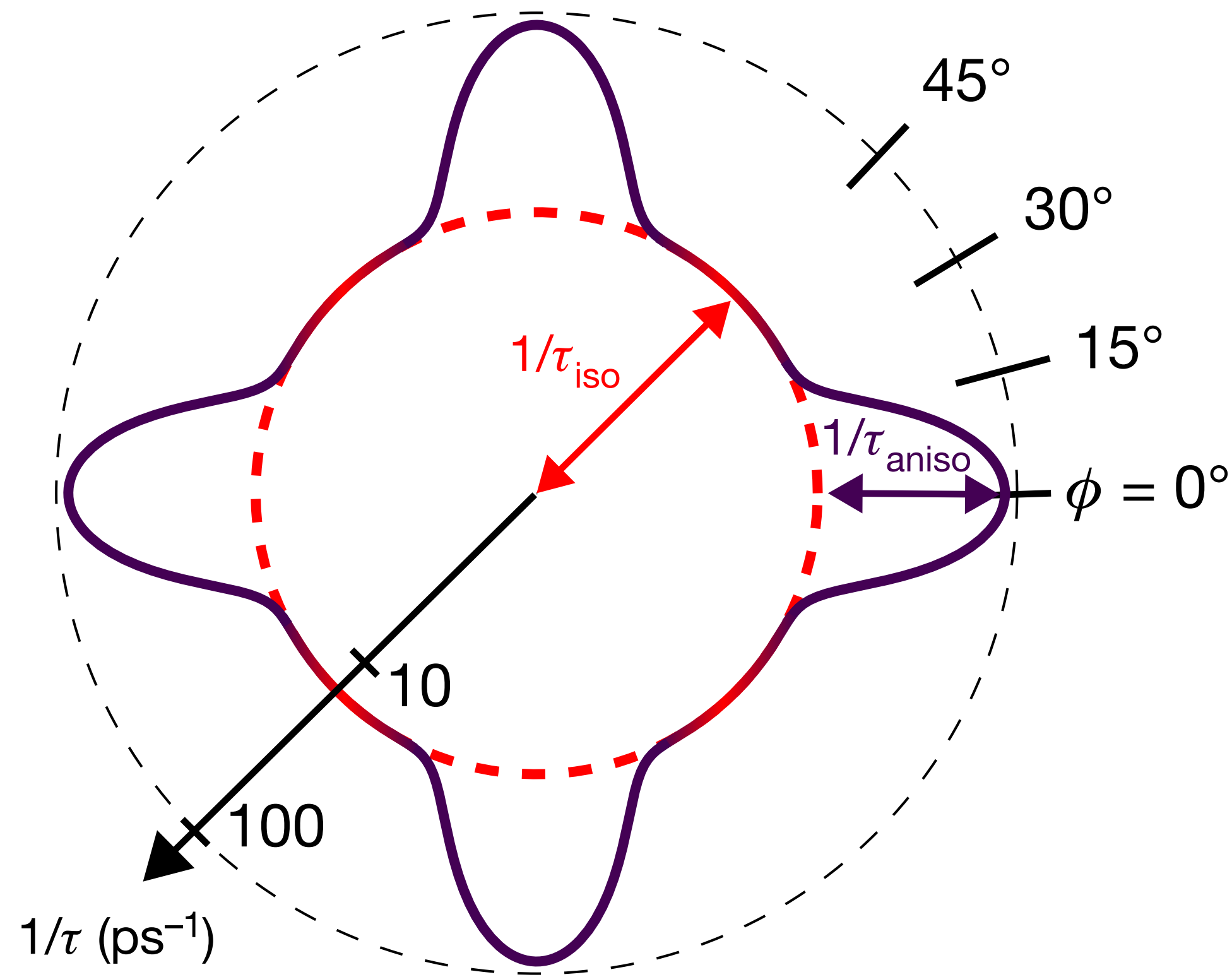
LSCO

P. Giraldo-Gallo, J.A. Galvis, Z. Stegen, K.A. Modic, F. F Balakirev, J. B. Betts, X. Lian, C. Moir, S. C. Riggs, J. Wu, A. T. Bollinger, X. He, I. Bozovic, B. J. Ramshaw, R. D. McDonald, G. S. Boebinger, A. Shekhter
 Science **361**, 479 (2018)

Linear-in temperature resistivity from an isotropic Planckian scattering rate

Nature **595**, 667-672 (2021)

G. Grissonnache, Y. Fang, A. Legros, S. Verret, F. Laliberté, C. Collignon, J. Zhou, D. Graf, P. Goddard, L. Taillefer, B. J. Ramshaw

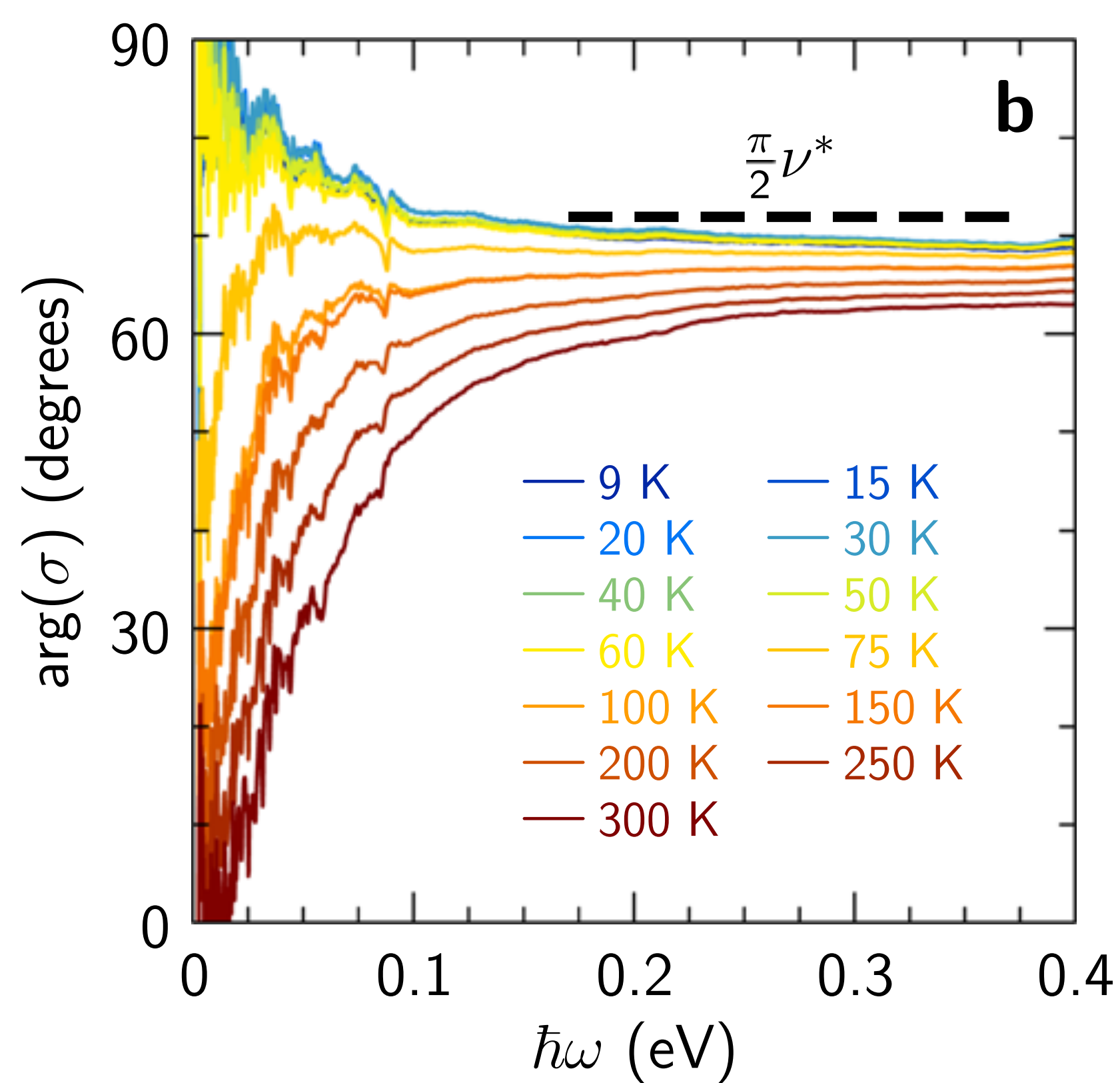
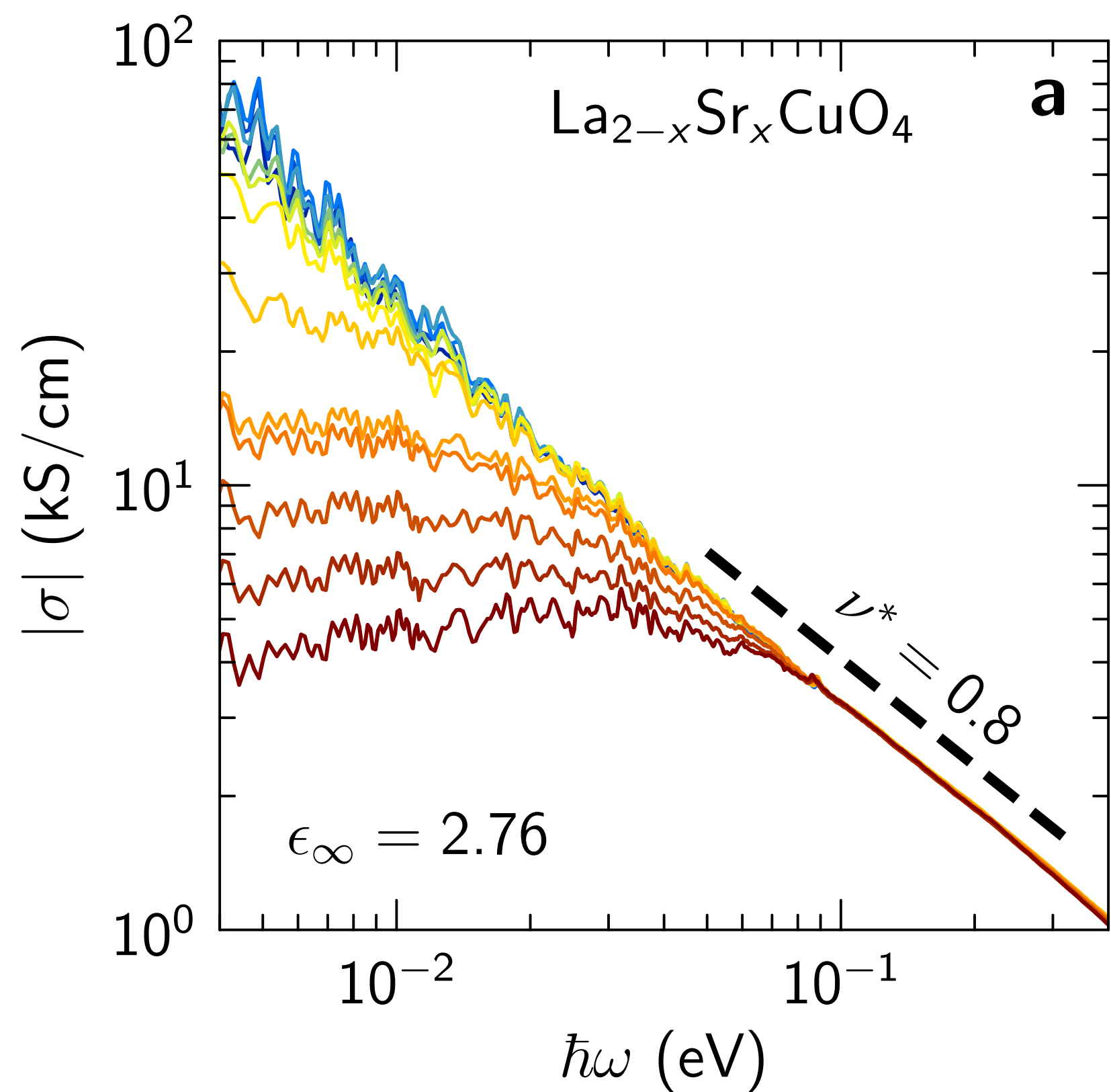


Reconciling scaling of the optical conductivity of cuprate superconductors with Planckian resistivity and specific heat

B. Michon, C. Berthod, C. W. Rischau, A. Ataei, L. Chen, S. Komiya, S. Ono, L. Taillefer, D. van der Marel, A. Georges

Nature Communications **14**, Article number: 3033 (2023)

$$\sigma(\omega) = i \frac{e^2 K / (\hbar d_c)}{\hbar \omega \frac{m^*(\omega)}{m} + i \frac{\hbar}{\tau(\omega)}}$$



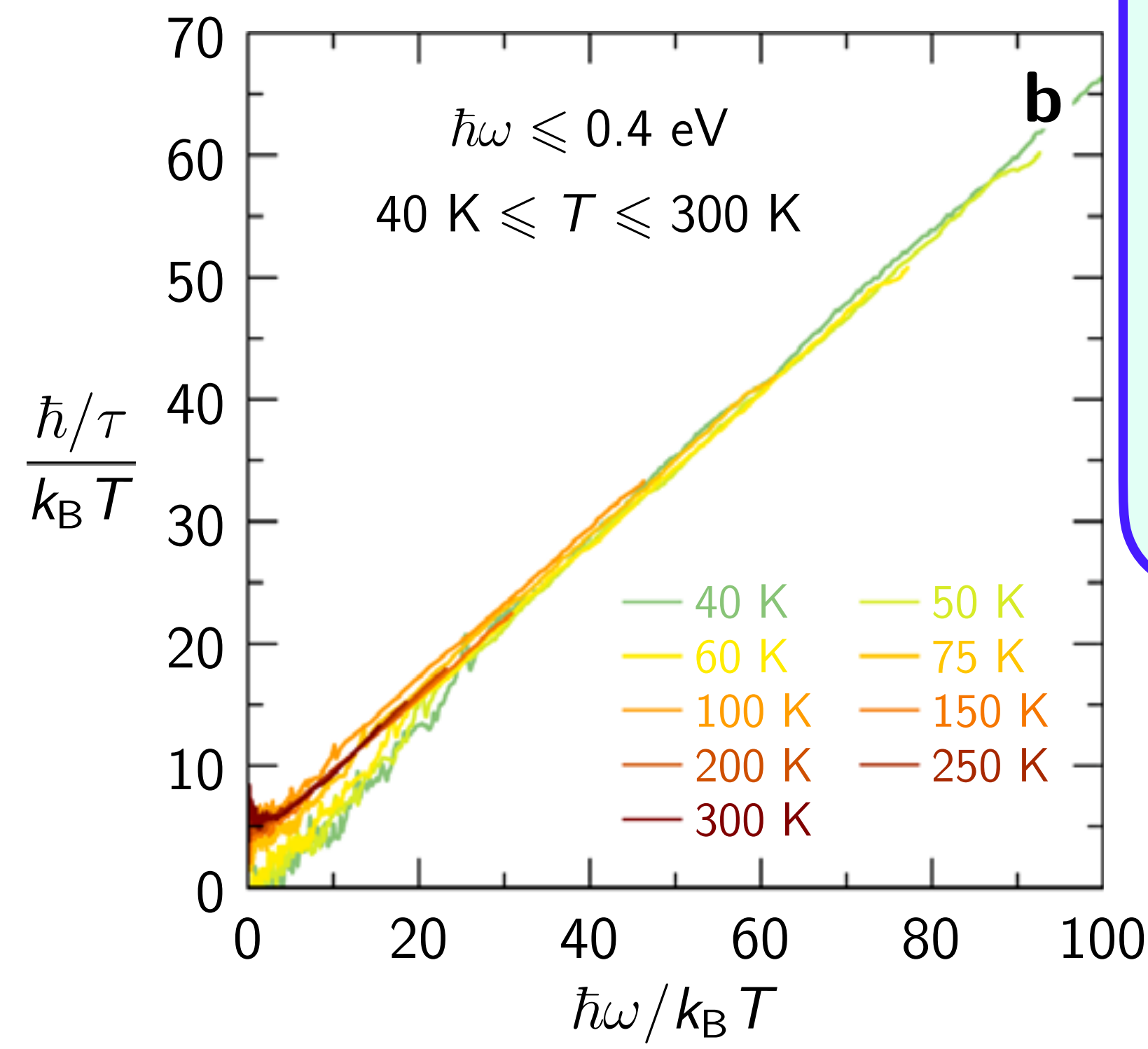
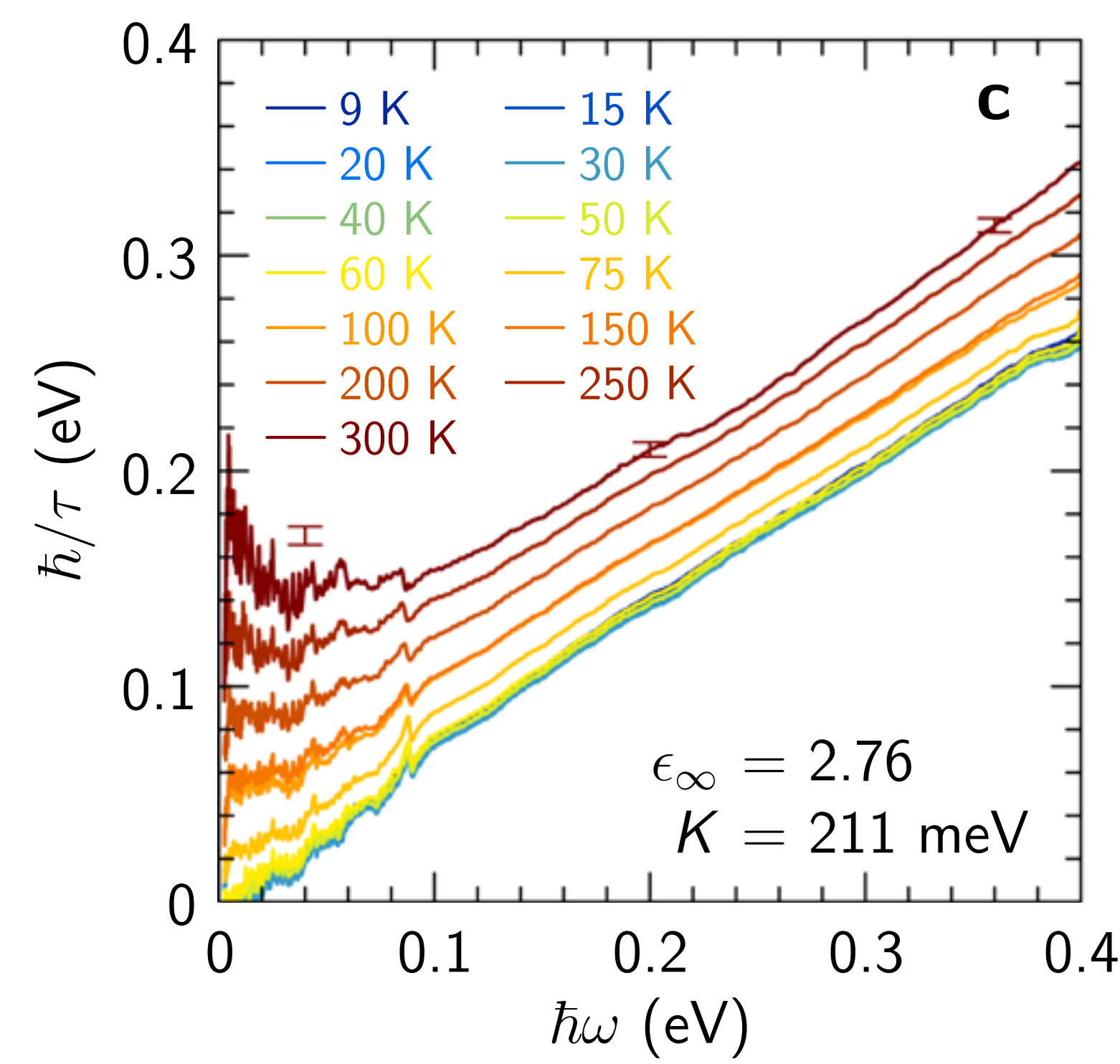
$\text{La}_{2-x}\text{Sr}_x\text{CuO}_4$
 $p = 0.24$
 $T_c = 19 \text{ K}$

Reconciling scaling of the optical conductivity of cuprate superconductors with Planckian resistivity and specific heat

B. Michon, C. Berthod, C. W. Rischau, A. Ataei, L. Chen, S. Komiya, S. Ono, L. Taillefer, D. van der Marel, A. Georges

Nature Communications **14**, Article number: 3033 (2023)

$$\sigma(\omega) = i \frac{e^2 K / (\hbar d_c)}{\hbar \omega \frac{m^*(\omega)}{m} + i \frac{\hbar}{\tau(\omega)}}$$



Planckian dynamics!

$$\tau(\omega) = \frac{\hbar}{k_B T} F\left(\frac{\hbar\omega}{k_B T}\right)$$

and entropy

$$S(T \rightarrow 0) \sim T \ln(1/T).$$

$\text{La}_{2-x}\text{Sr}_x\text{CuO}_4$
 $p = 0.24$
 $T_c = 19$ K

1. Hubbard model on the honeycomb lattice:
hydrodynamics in graphene and related materials
2. SYK as a solvable model of quantum matter
without quasiparticles
3. Hubbard model on the square lattice:
spin density wave order, and a universal theory
of strange metals from spatially random interactions.
4. Spin liquids, Fractionalized Fermi liquids (FL*)
and the cuprate phase diagram:
observation of the Yamaji effect.

Hubbard model on the honeycomb lattice: hydrodynamics in graphene and related materials

School on Emergent Phenomena in
Non-Equilibrium Quantum Many-Body Systems
ICTP-SAIFR

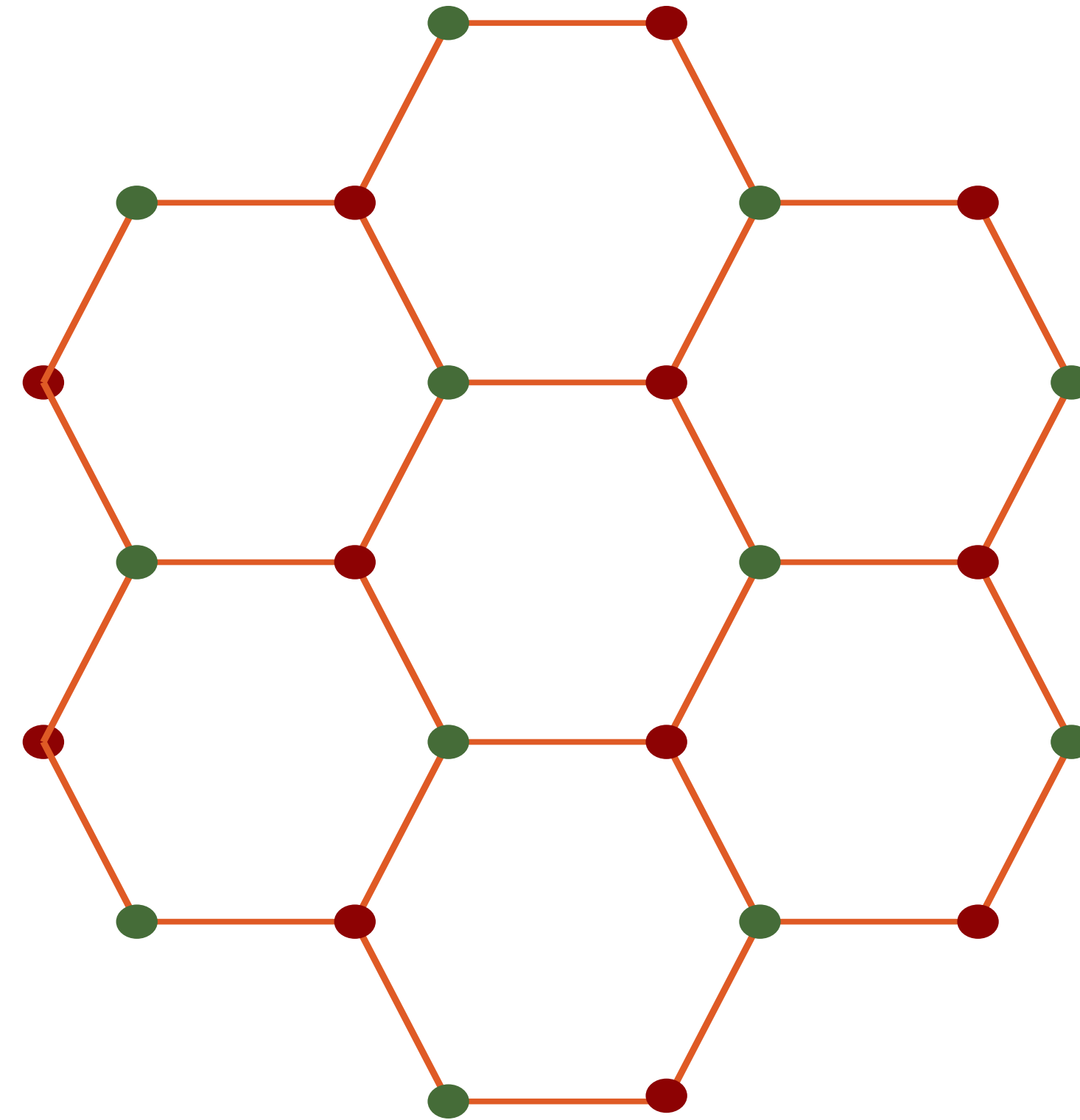
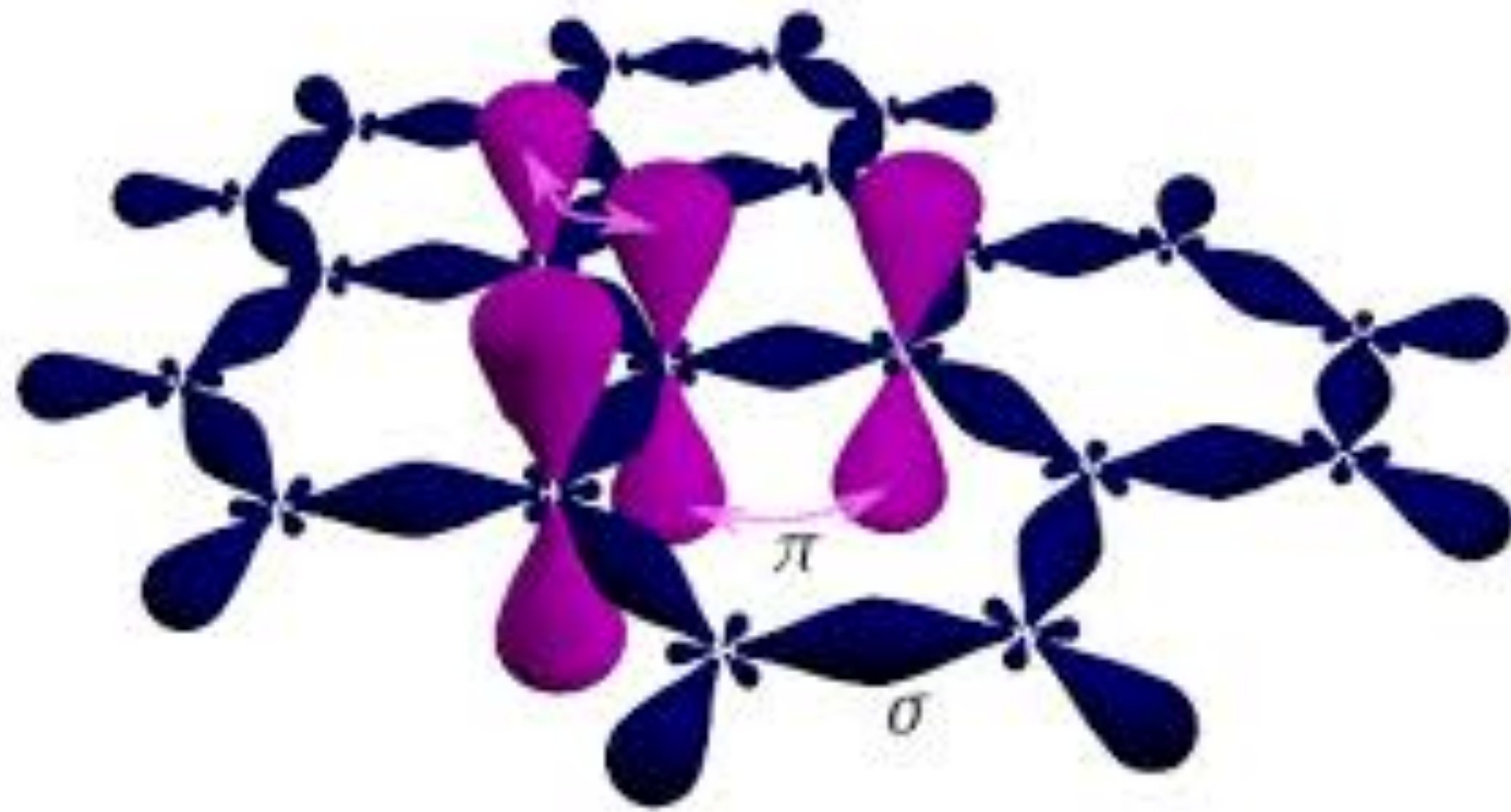
São Paulo, Brazil
November 3,4 2025

Subir Sachdev

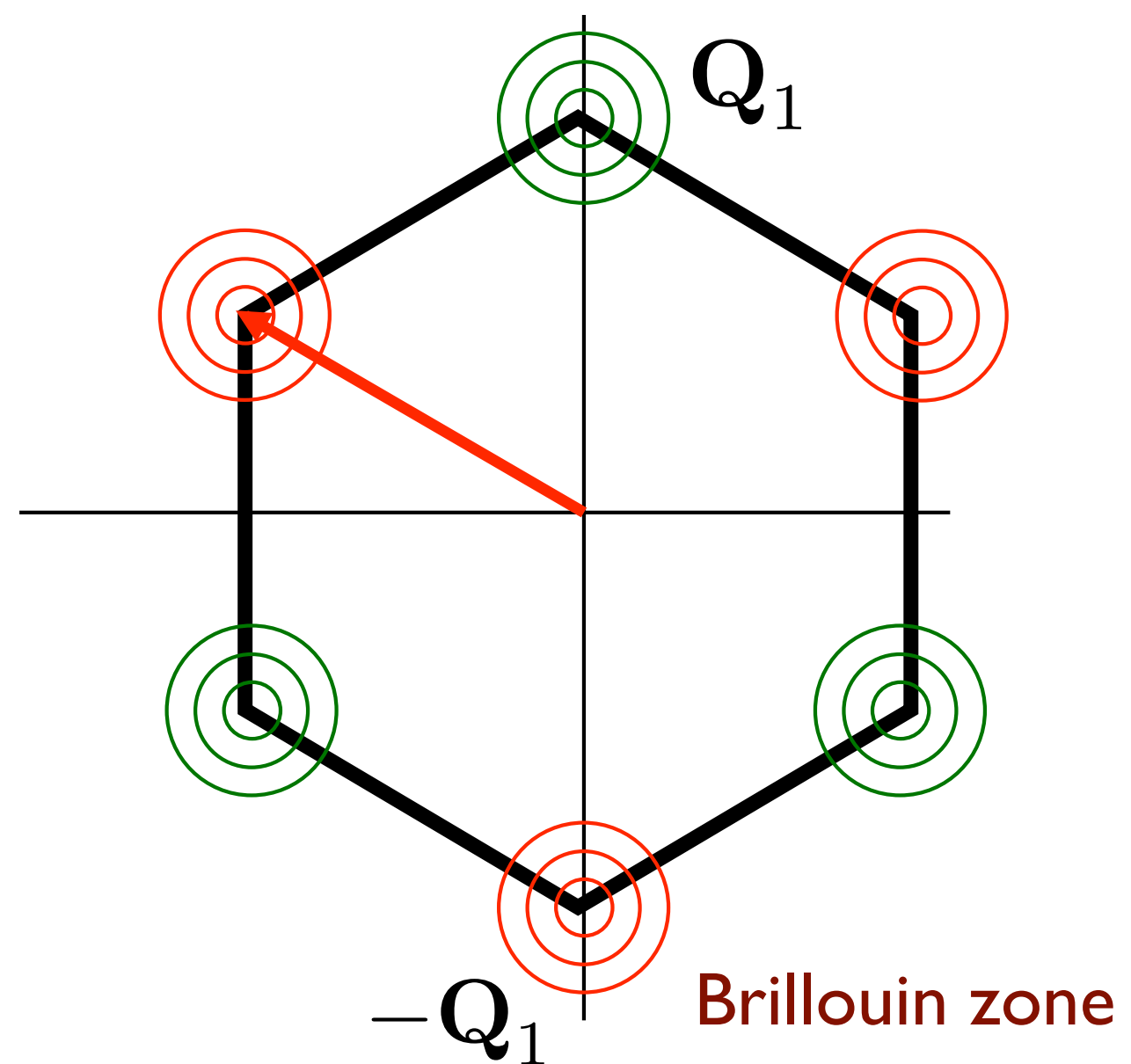
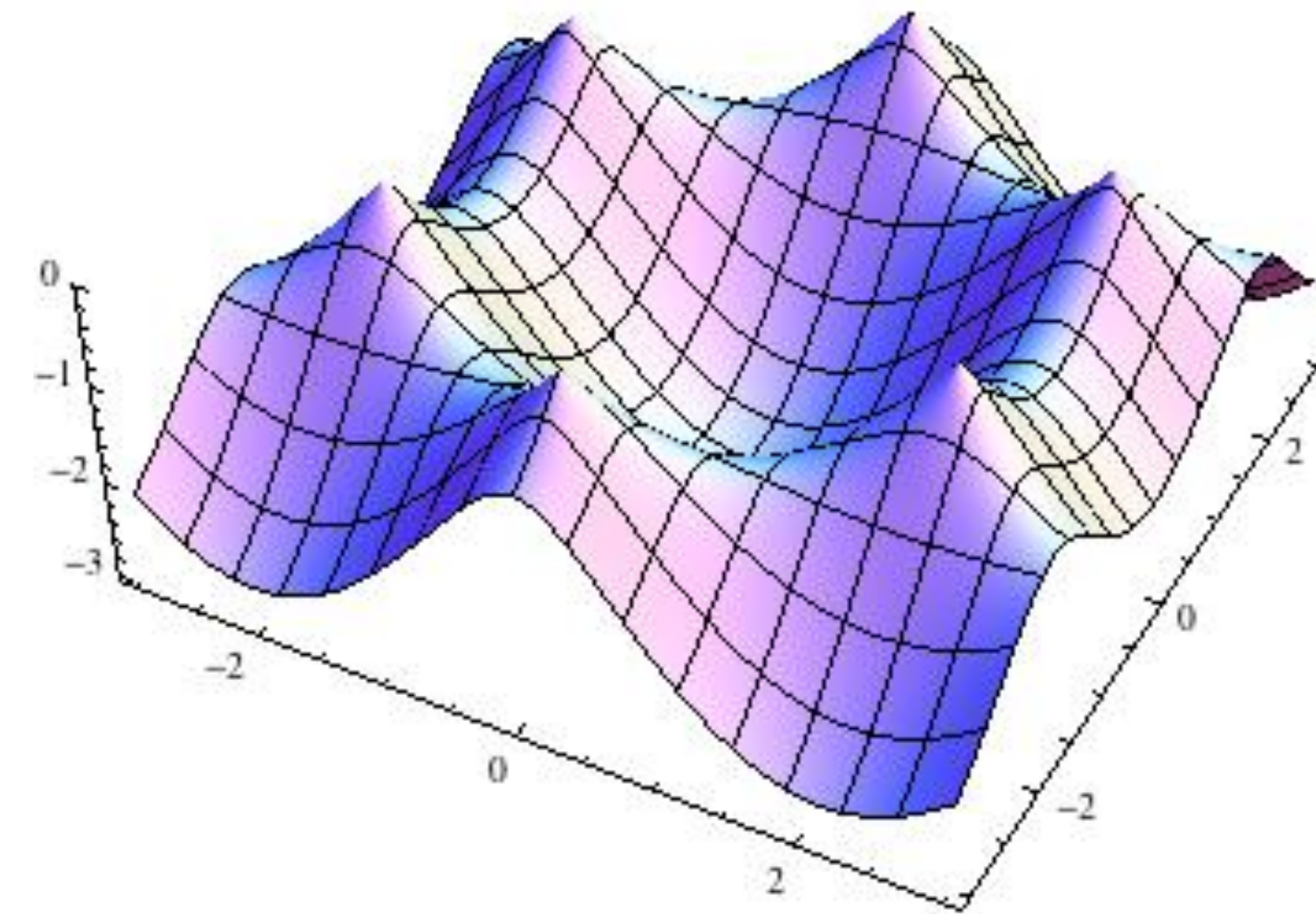
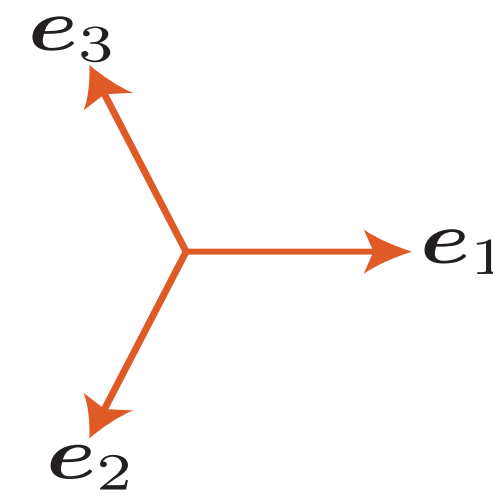
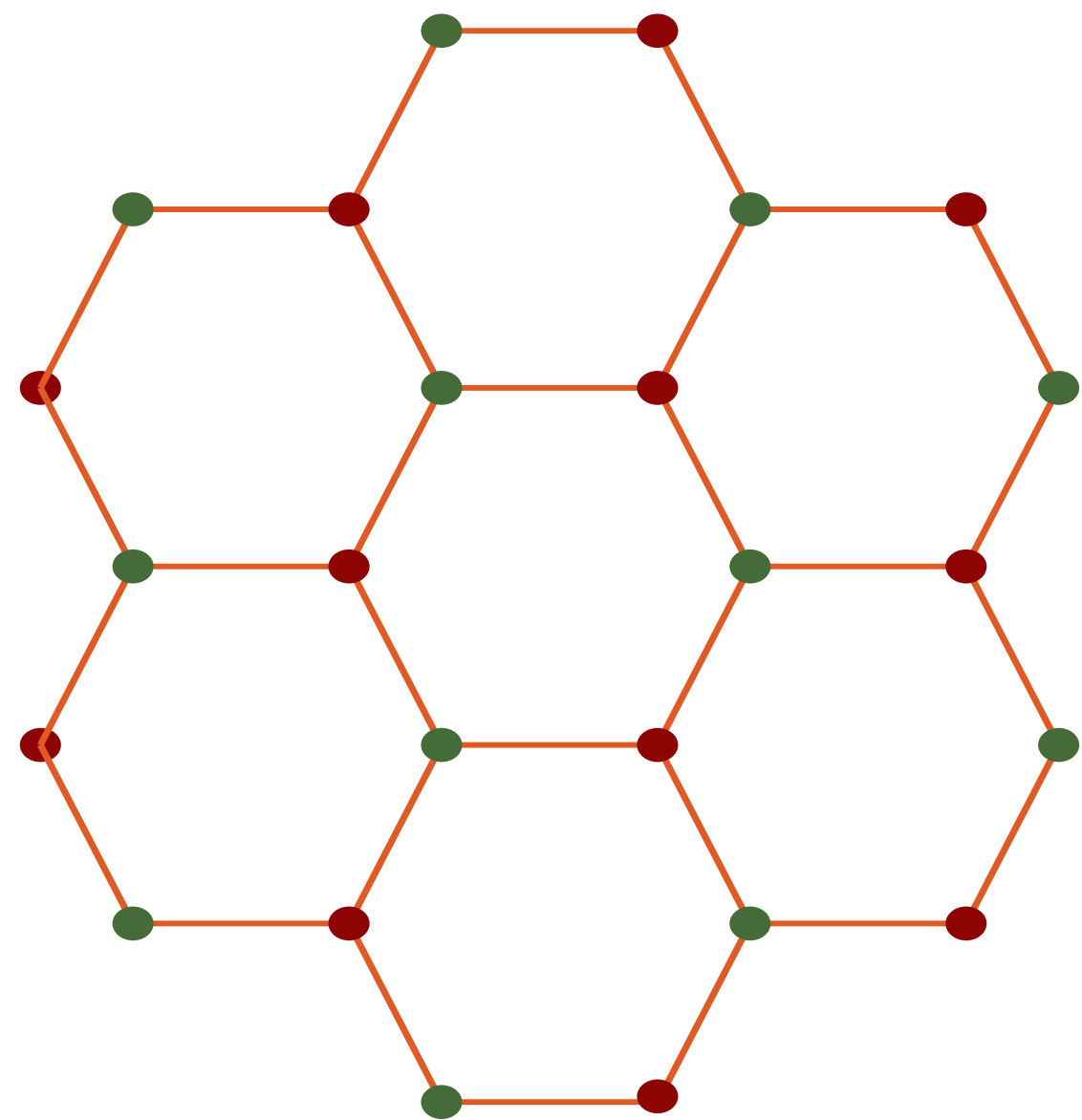


Honeycomb lattice

(describes graphene after adding long-range Coulomb interactions)



$$H = -t \sum_{\langle ij \rangle} c_{i\alpha}^\dagger c_{j\alpha} + U \sum_i \left(n_{i\uparrow} - \frac{1}{2} \right) \left(n_{i\downarrow} - \frac{1}{2} \right)$$



Semi-metal with
massless Dirac fermions
at small U/t

We define the Fourier transform of the fermions by

$$c_A(\mathbf{k}) = \sum_{\mathbf{r}} c_A(\mathbf{r}) e^{-i\mathbf{k} \cdot \mathbf{r}} \quad (4)$$

and similarly for c_B . A and B are sublattice indices. The hopping Hamiltonian is

$$H_0 = -t \sum_{\langle ij \rangle} \left(c_{Ai\alpha}^\dagger c_{Bj\alpha} + c_{Bj\alpha}^\dagger c_{Ai\alpha} \right) \quad (5)$$

where α is a spin index. If we introduce Pauli matrices τ^a in sublattice space ($a = x, y, z$), this Hamiltonian can be written as

$$H_0 = \int \frac{d^2 k}{4\pi^2} c^\dagger(\mathbf{k}) \left[-t \left(\cos(\mathbf{k} \cdot \mathbf{e}_1) + \cos(\mathbf{k} \cdot \mathbf{e}_2) + \cos(\mathbf{k} \cdot \mathbf{e}_3) \right) \tau^x + t \left(\sin(\mathbf{k} \cdot \mathbf{e}_1) + \sin(\mathbf{k} \cdot \mathbf{e}_2) + \sin(\mathbf{k} \cdot \mathbf{e}_3) \right) \tau^y \right] c(\mathbf{k}) \quad (6)$$

The low energy excitations of this Hamiltonian are near $\mathbf{k} \approx \pm \mathbf{Q}_1$.

In terms of the fields near \mathbf{Q}_1 and $-\mathbf{Q}_1$, we define

$$\begin{aligned}\psi_{A1\alpha}(\mathbf{k}) &= c_{A\alpha}(\mathbf{Q}_1 + \mathbf{k}) \\ \psi_{A2\alpha}(\mathbf{k}) &= c_{A\alpha}(-\mathbf{Q}_1 + \mathbf{k}) \\ \psi_{B1\alpha}(\mathbf{k}) &= c_{B\alpha}(\mathbf{Q}_1 + \mathbf{k}) \\ \psi_{B2\alpha}(\mathbf{k}) &= c_{B\alpha}(-\mathbf{Q}_1 + \mathbf{k})\end{aligned}\tag{7}$$

We consider Ψ to be a 8 component vector, and introduce Pauli matrices ρ^a which act in the 1, 2 valley space. Then the Hamiltonian is

$$H_0 = \int \frac{d^2k}{4\pi^2} \Psi^\dagger(\mathbf{k}) \left(v\tau^y k_x + v\tau^x \rho^z k_y \right) \Psi(\mathbf{k}),\tag{8}$$

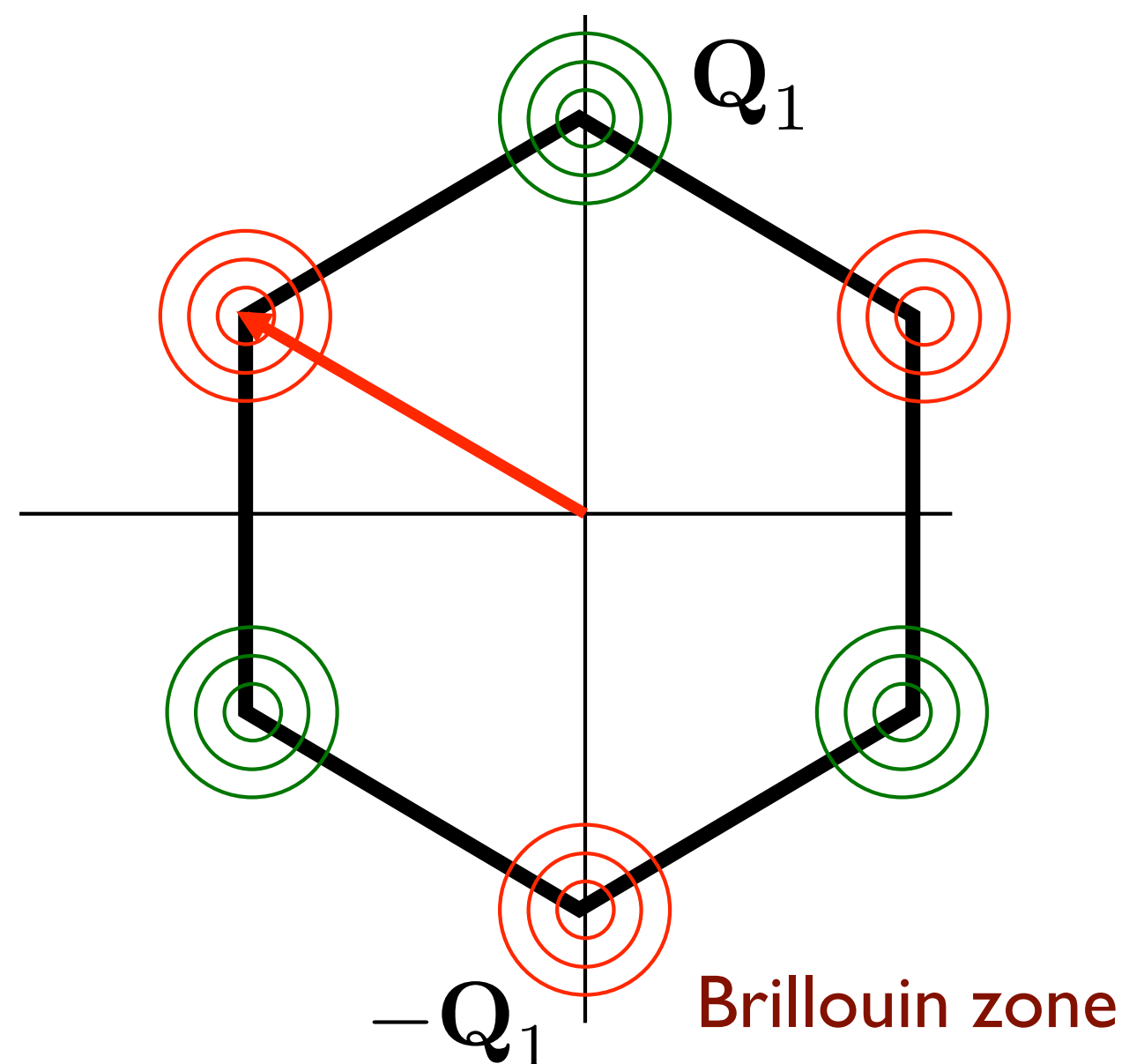
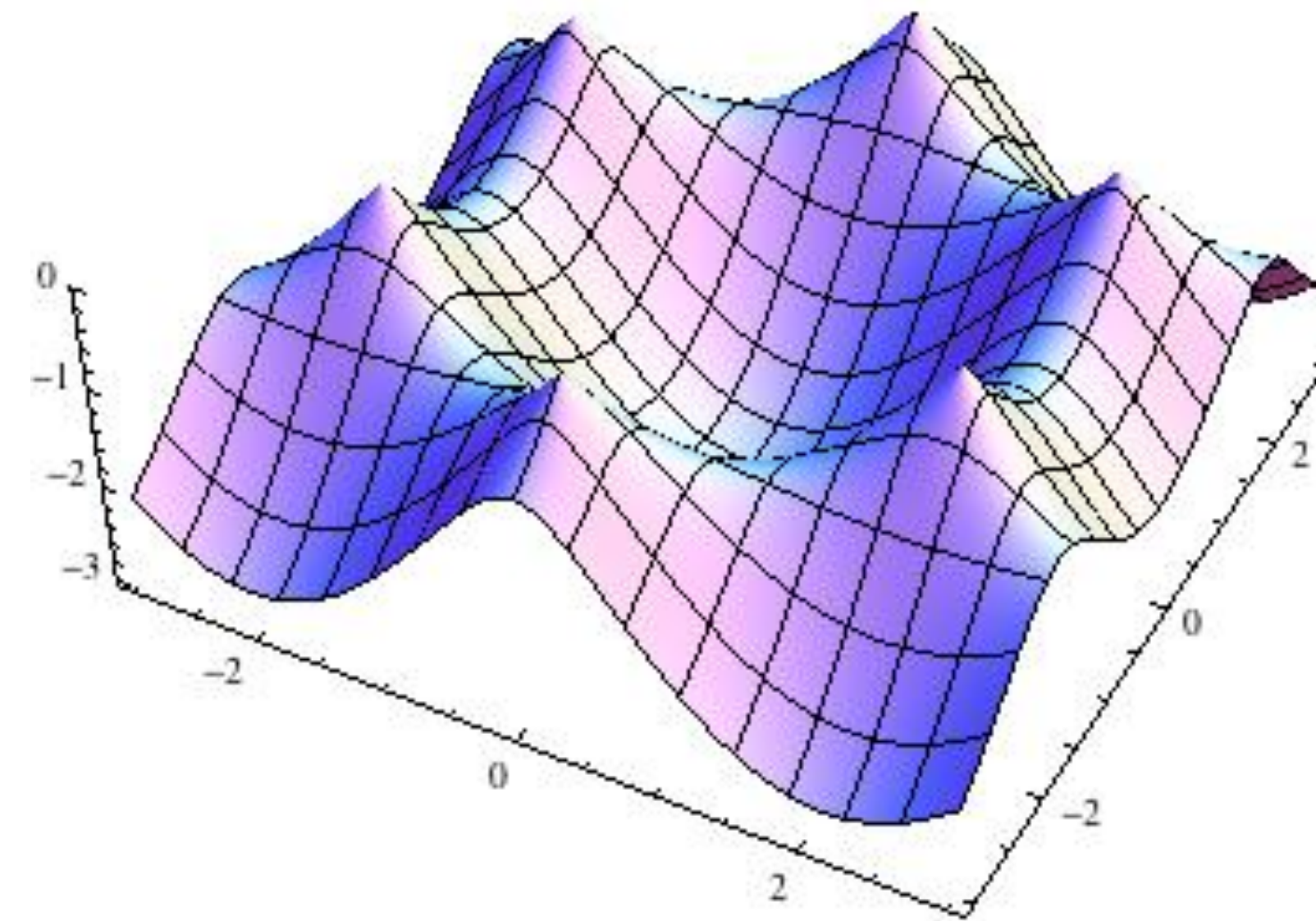
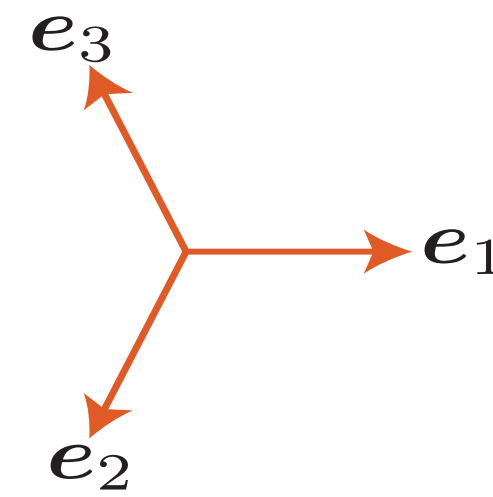
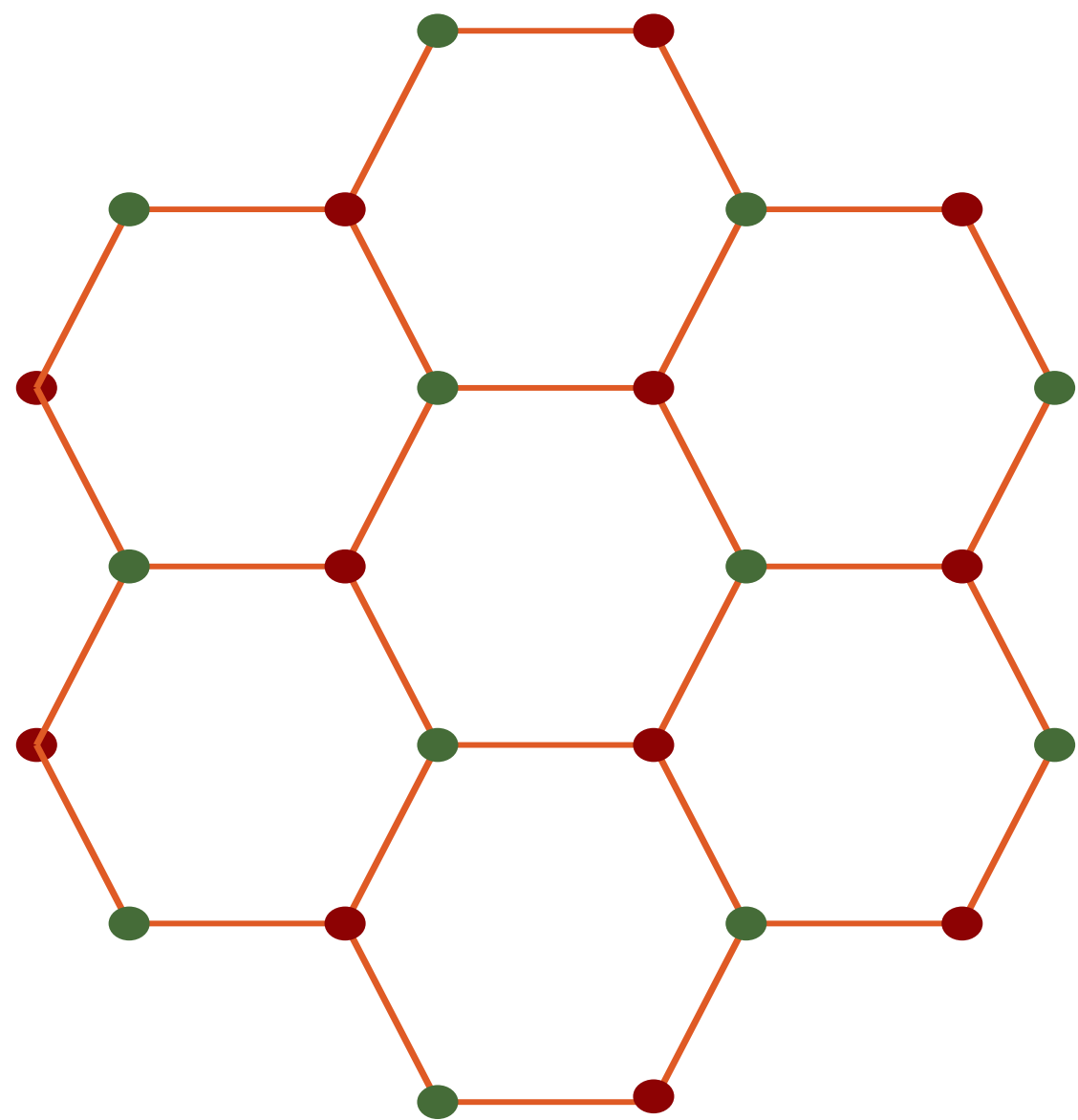
where $v = 3t/2$; below we set $v = 1$. Now define $\bar{\Psi} = \Psi^\dagger \rho^z \tau^z$. Then we can write the imaginary time Lagrangian as

$$\mathcal{L}_0 = -i\bar{\Psi} (\omega\gamma_0 + k_x\gamma_1 + k_y\gamma_2) \Psi\tag{9}$$

where

$$\gamma_0 = -\rho^z \tau^z \quad \gamma_1 = \rho^z \tau^x \quad \gamma_2 = -\tau^y\tag{10}$$

Exercise: Observe that \mathcal{L}_0 is invariant under the scaling transformation $x' = xe^{-\ell}$ and $\tau' = \tau e^{-\ell}$. Write the Hubbard interaction U in terms of the Dirac fermions, and show that it has the tree-level scaling transformation $U' = Ue^{-\ell}$. So argue that all short-range interactions are *irrelevant* in the Dirac semi-metal phase.



The theory of free Dirac fermions is invariant under conformal transformations of spacetime. This is a realization of a simple conformal field theory in 2+1 dimensions: a CFT3

The Hubbard Model at large U

$$H = - \sum_{i,j} t_{ij} c_{i\alpha}^\dagger c_{j\alpha} + U \sum_i \left(n_{i\uparrow} - \frac{1}{2} \right) \left(n_{i\downarrow} - \frac{1}{2} \right) - \mu \sum_i c_{i\alpha}^\dagger c_{i\alpha}$$

In the limit of large U , and at a density of one particle per site, this maps onto the Heisenberg antiferromagnet

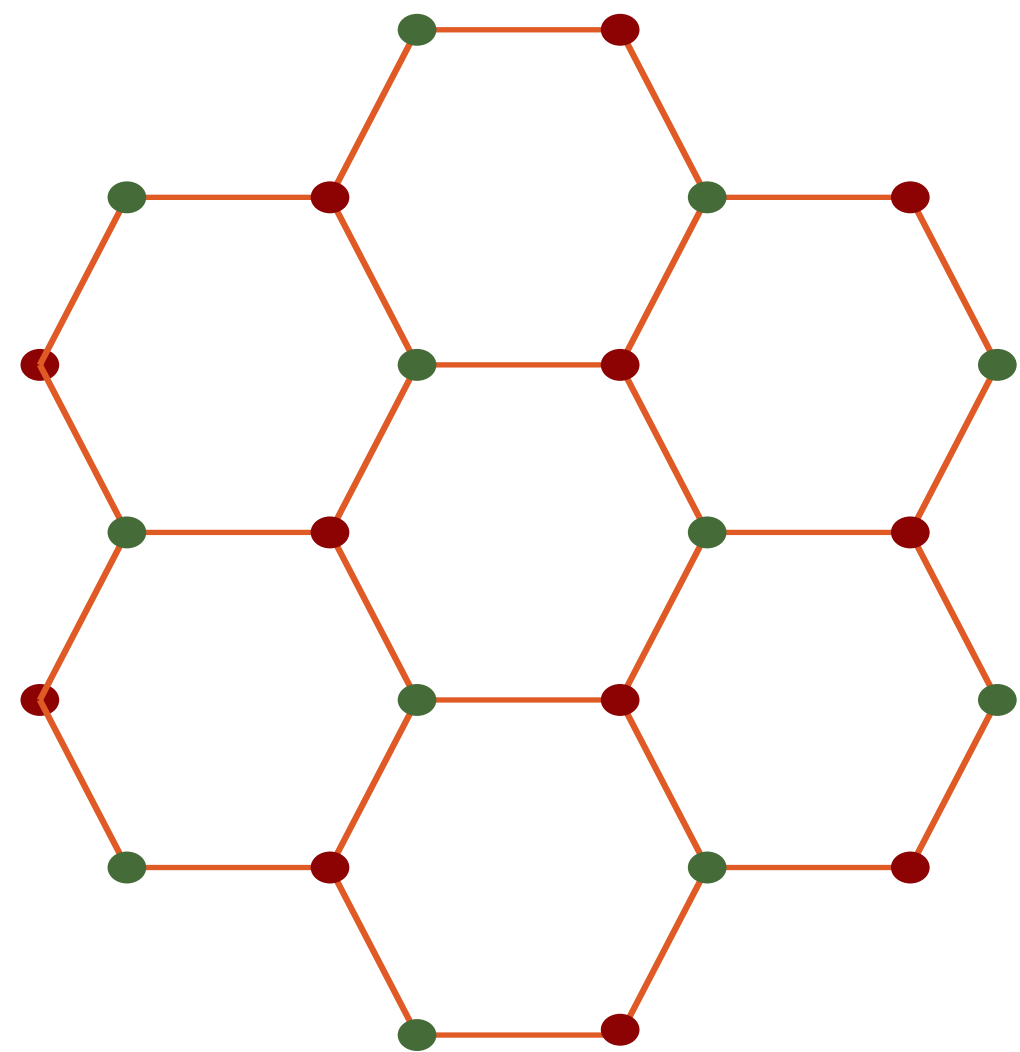
$$H_{AF} = \sum_{i < j} J_{ij} S_i^a S_j^a$$

where $a = x, y, z$,

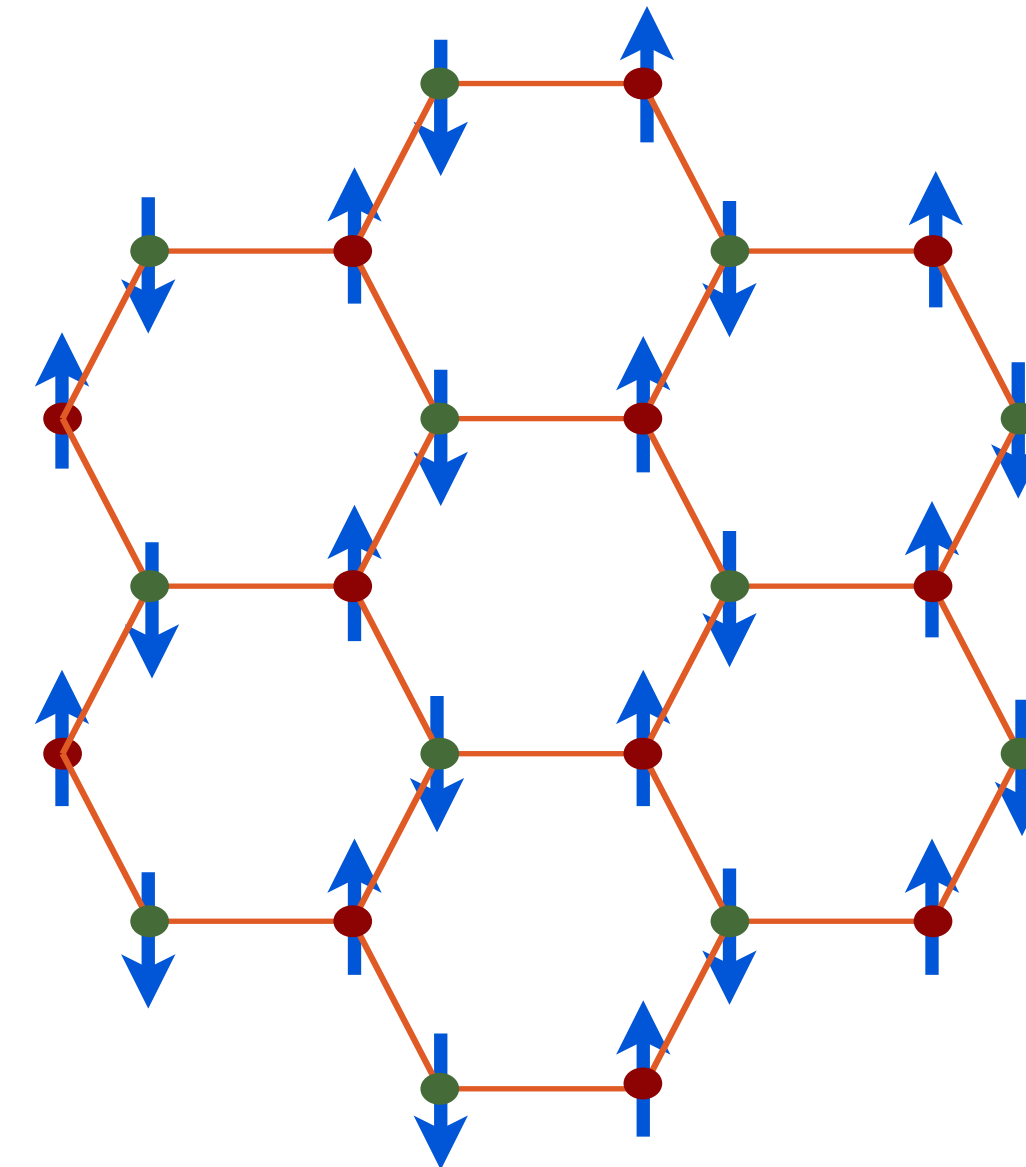
$$S_i^a = \frac{1}{2} c_{i\alpha}^{a\dagger} \sigma_{\alpha\beta}^a c_{i\beta},$$

with σ^a the Pauli matrices and

$$J_{ij} = \frac{4t_{ij}^2}{U}$$



Dirac
semi-metal



Insulating
antiferromagnet
with Neel order

U/t

Antiferromagnetism

We use the operator equation (valid on each site i):

$$U \left(n_{\uparrow} - \frac{1}{2} \right) \left(n_{\downarrow} - \frac{1}{2} \right) = -\frac{2U}{3} S^{a2} + \frac{U}{4} \quad (11)$$

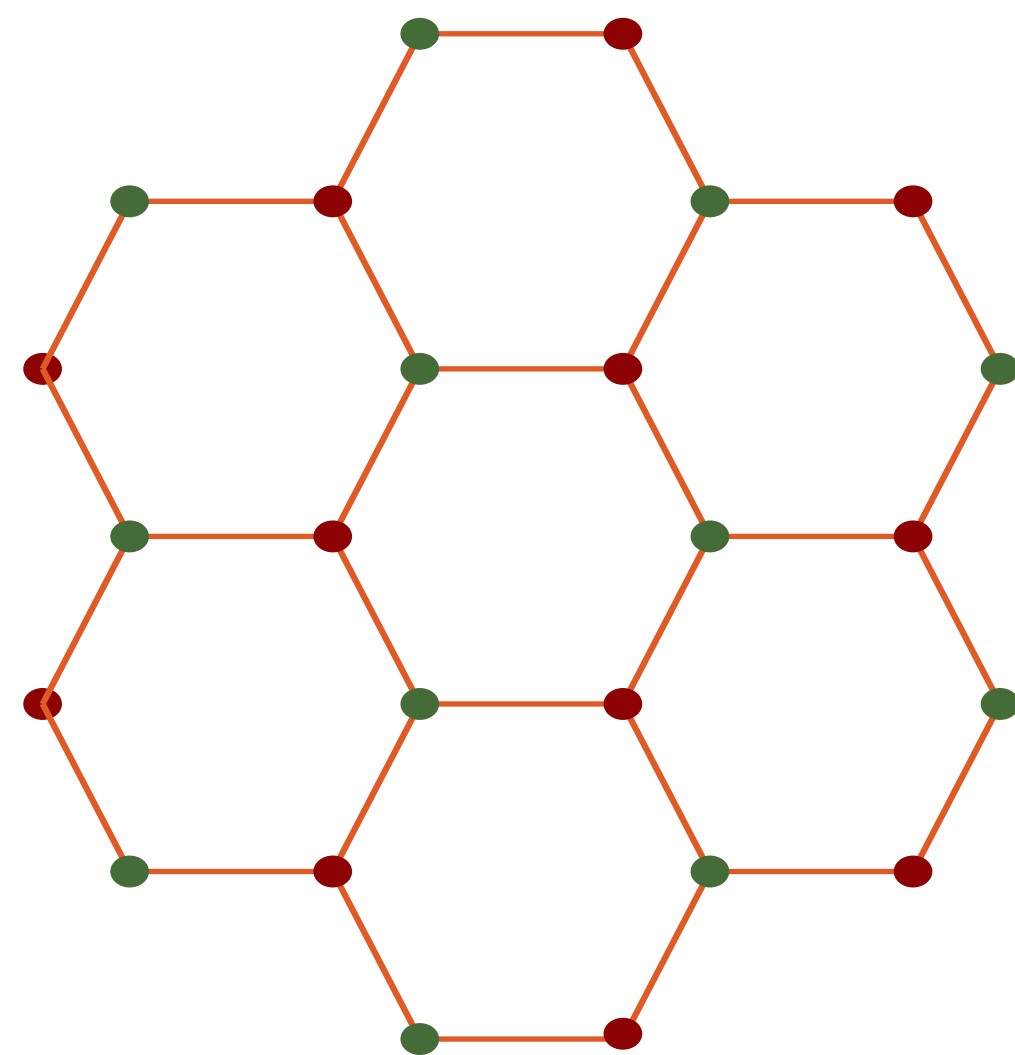
Then we decouple the interaction via

$$\exp \left(\frac{2U}{3} \sum_i \int d\tau S_i^{a2} \right) = \int \mathcal{D} J_i^a(\tau) \exp \left(- \sum_i \int d\tau \left[\frac{3}{8U} J_i^{a2} - J_i^a S_i^a \right] \right) \quad (12)$$

We now integrate out the fermions, and look for the saddle point of the resulting effective action for J_i^a .

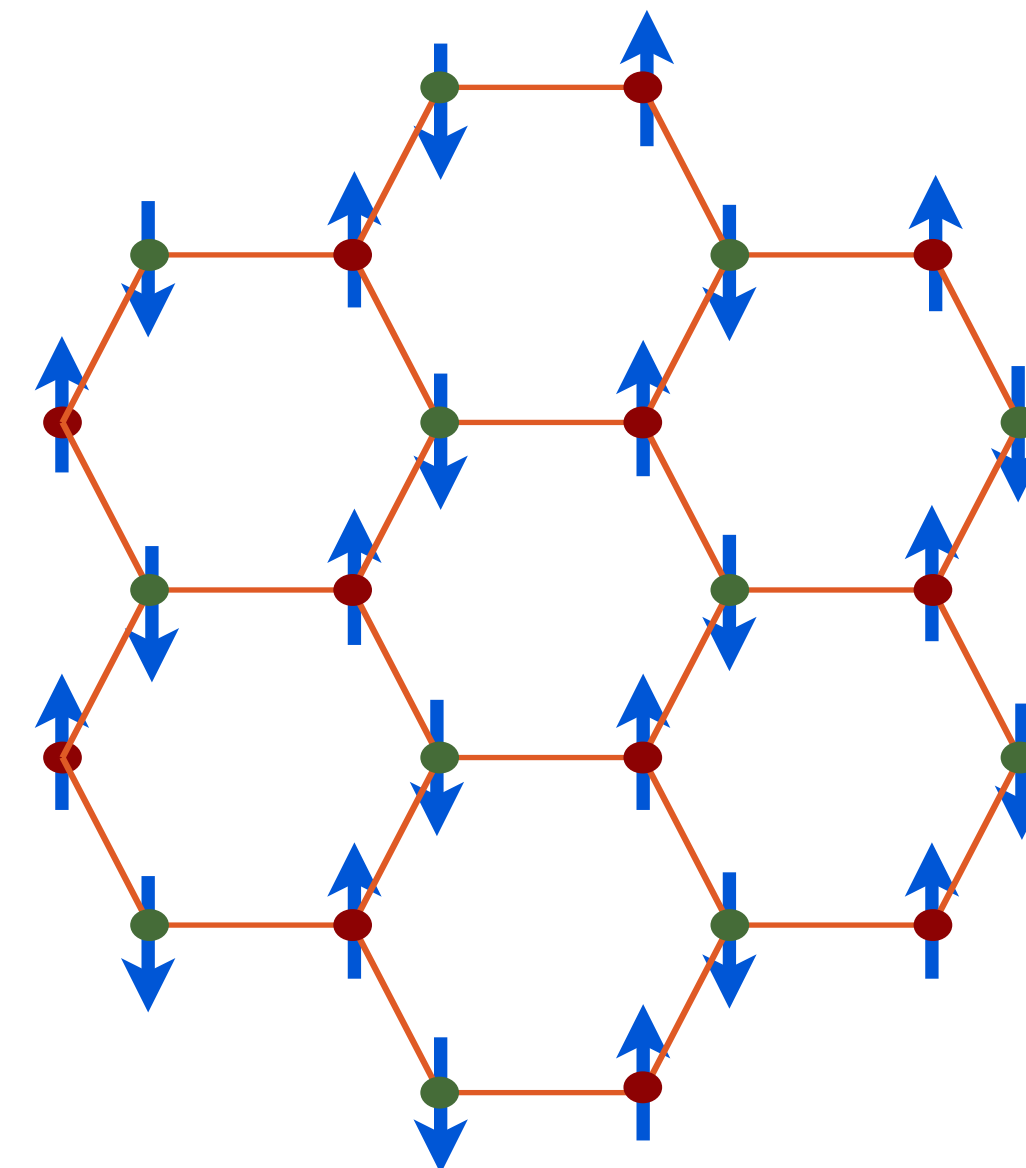
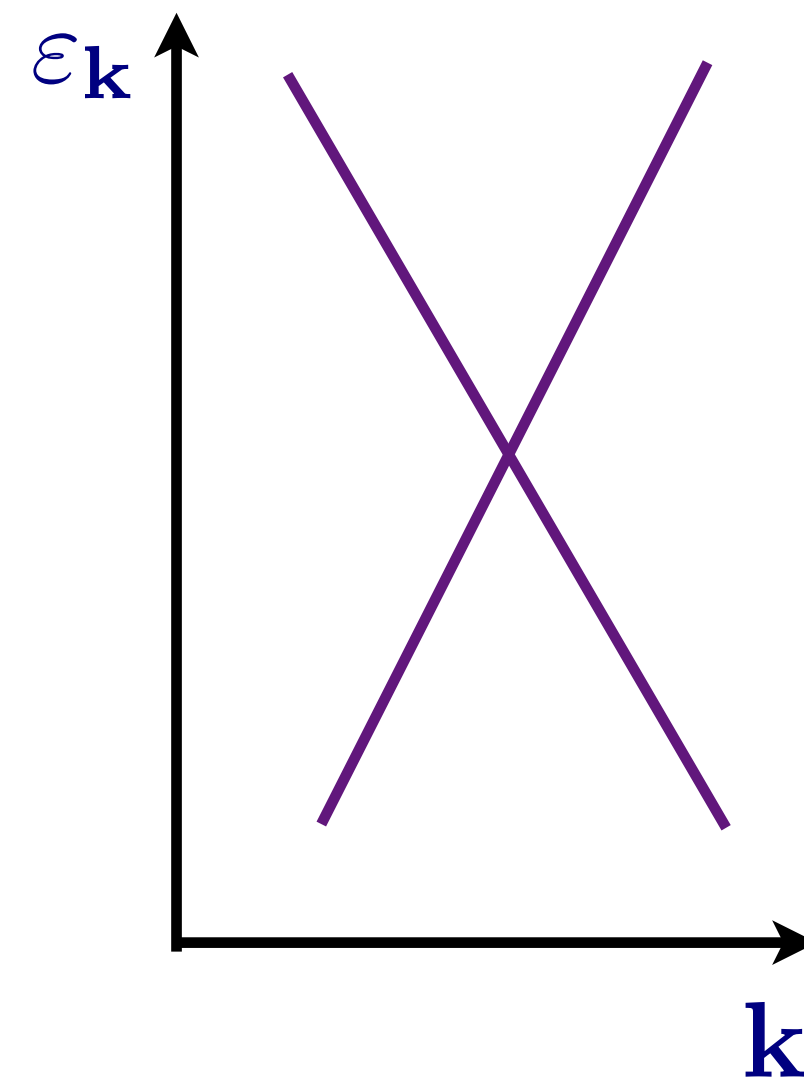
Long wavelength fluctuations about this saddle point are described by a field theory of the Néel order parameter, φ^a , coupled to the Dirac fermions in the **Gross-Neveu** model.

$$\mathcal{L} = \bar{\Psi} \gamma_{\mu} \partial_{\mu} \Psi + \frac{1}{2} \left[(\partial_{\mu} \varphi^a)^2 + s \varphi^{a2} \right] + \frac{U}{24} (\varphi^{a2})^2 - \lambda \varphi^a \bar{\Psi} \rho^z \sigma^a \Psi$$



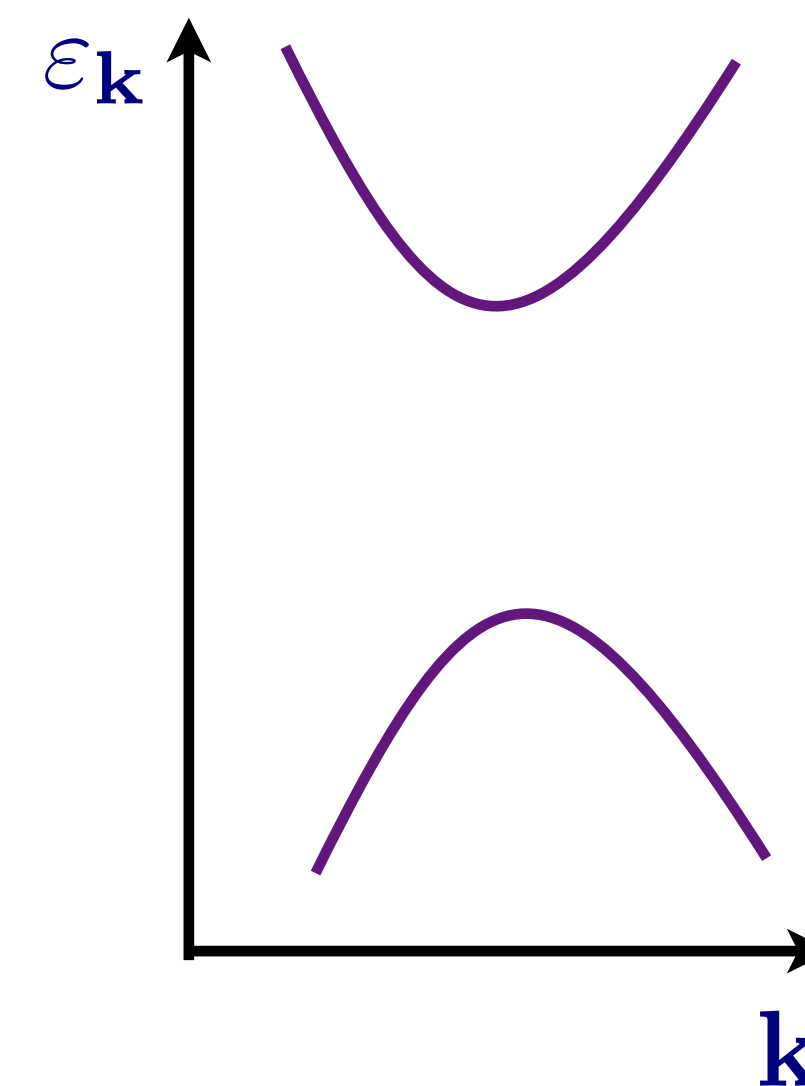
Dirac
semi-metal

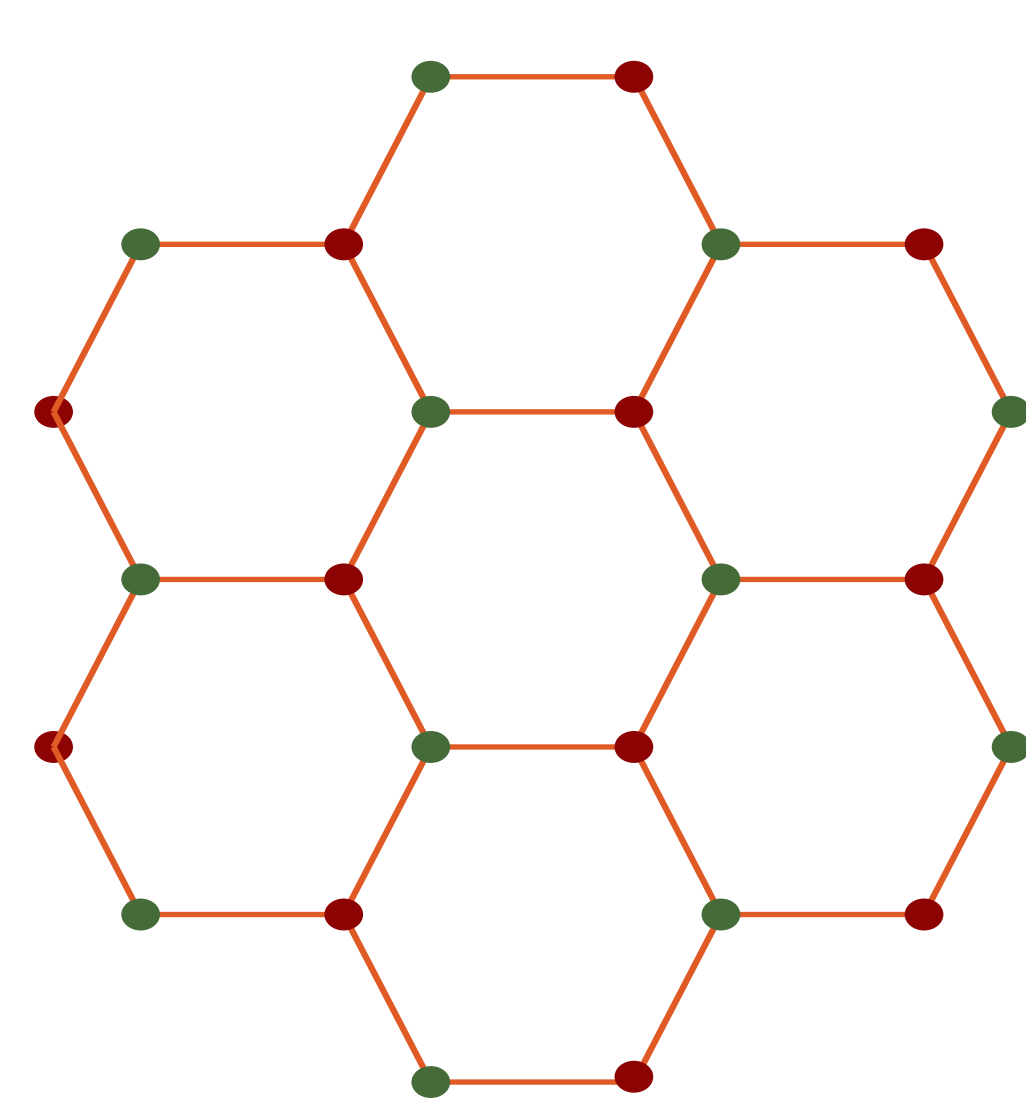
$$\langle \varphi^a \rangle = 0$$



Insulating
antiferromagnet
with Neel order

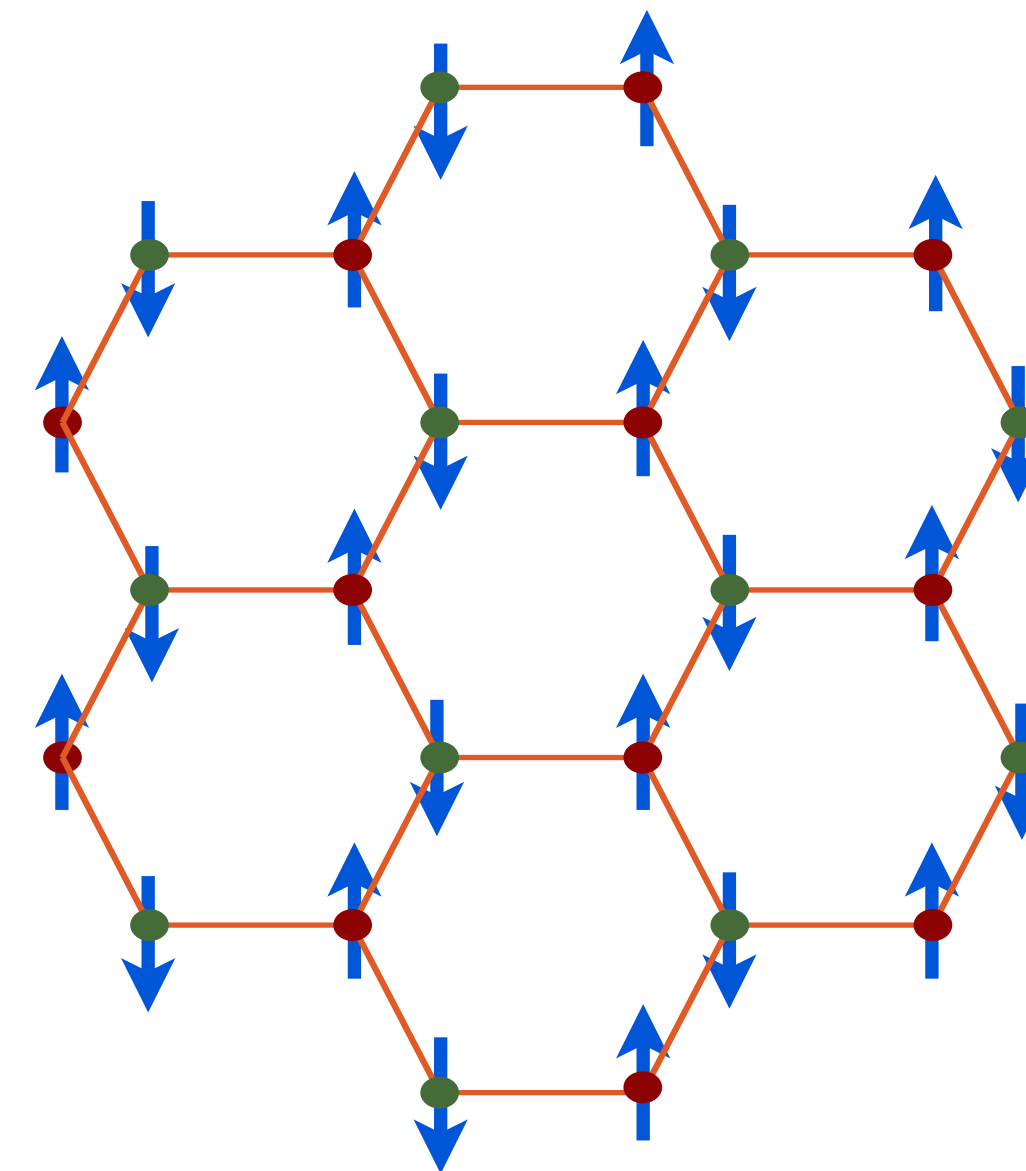
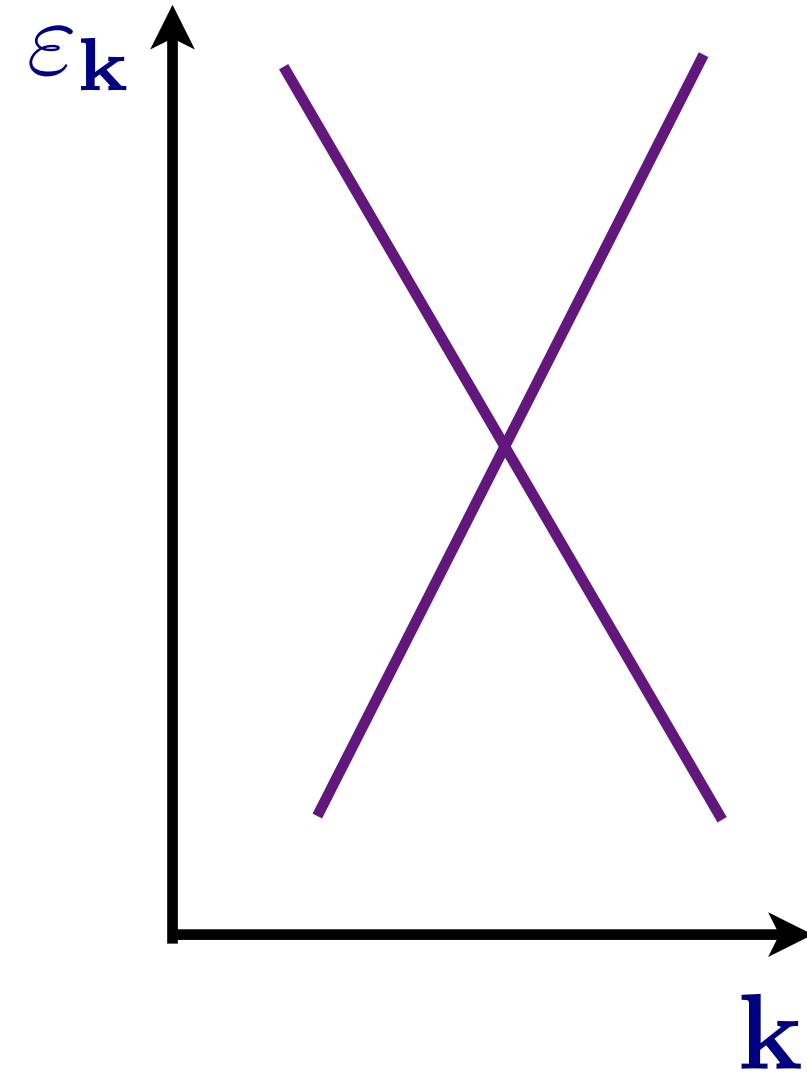
$$\langle \varphi^a \rangle \neq 0$$





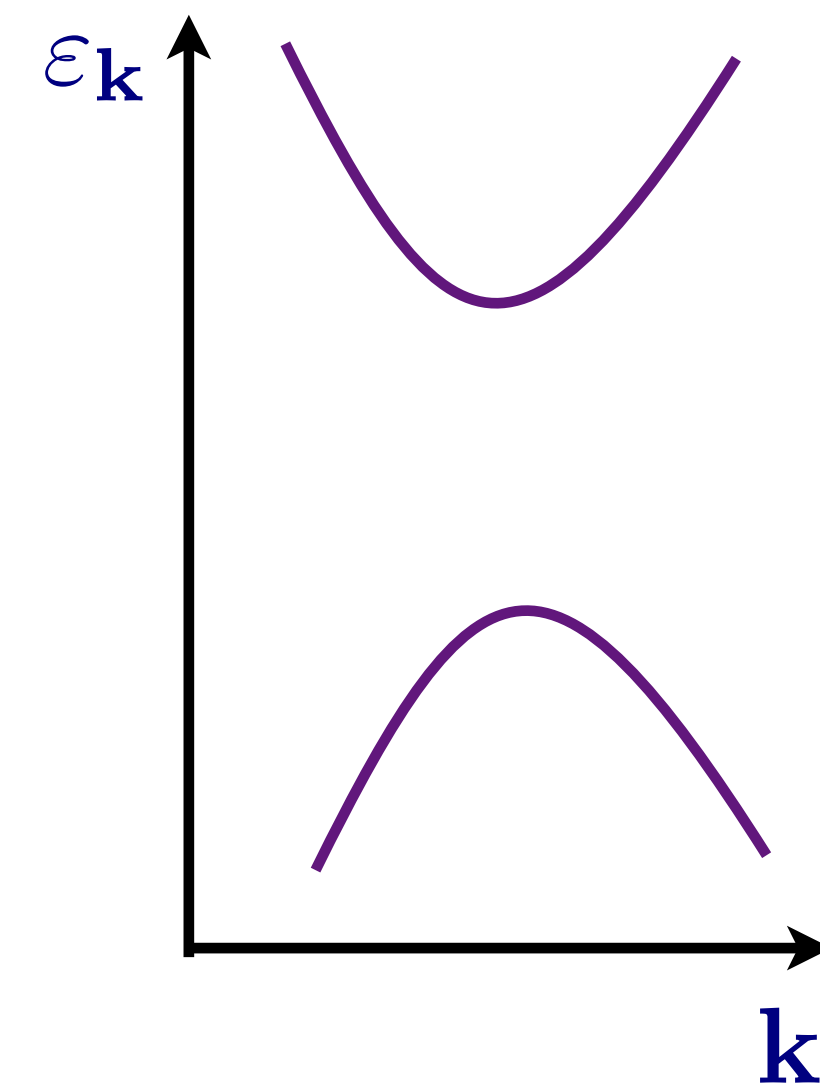
Dirac
semi-metal

$$\langle \varphi^a \rangle = 0$$



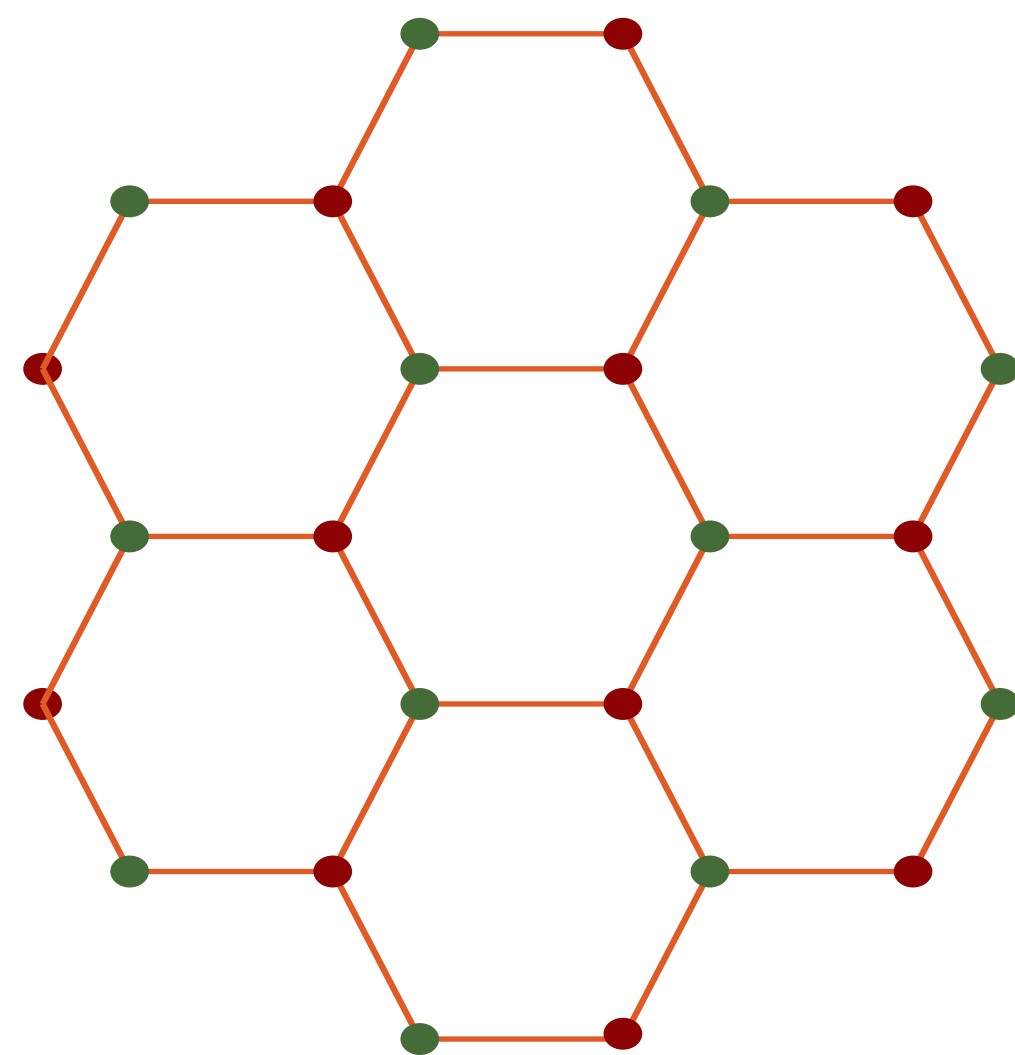
Insulating
antiferromagnet
with Neel order

$$\langle \varphi^a \rangle \neq 0$$



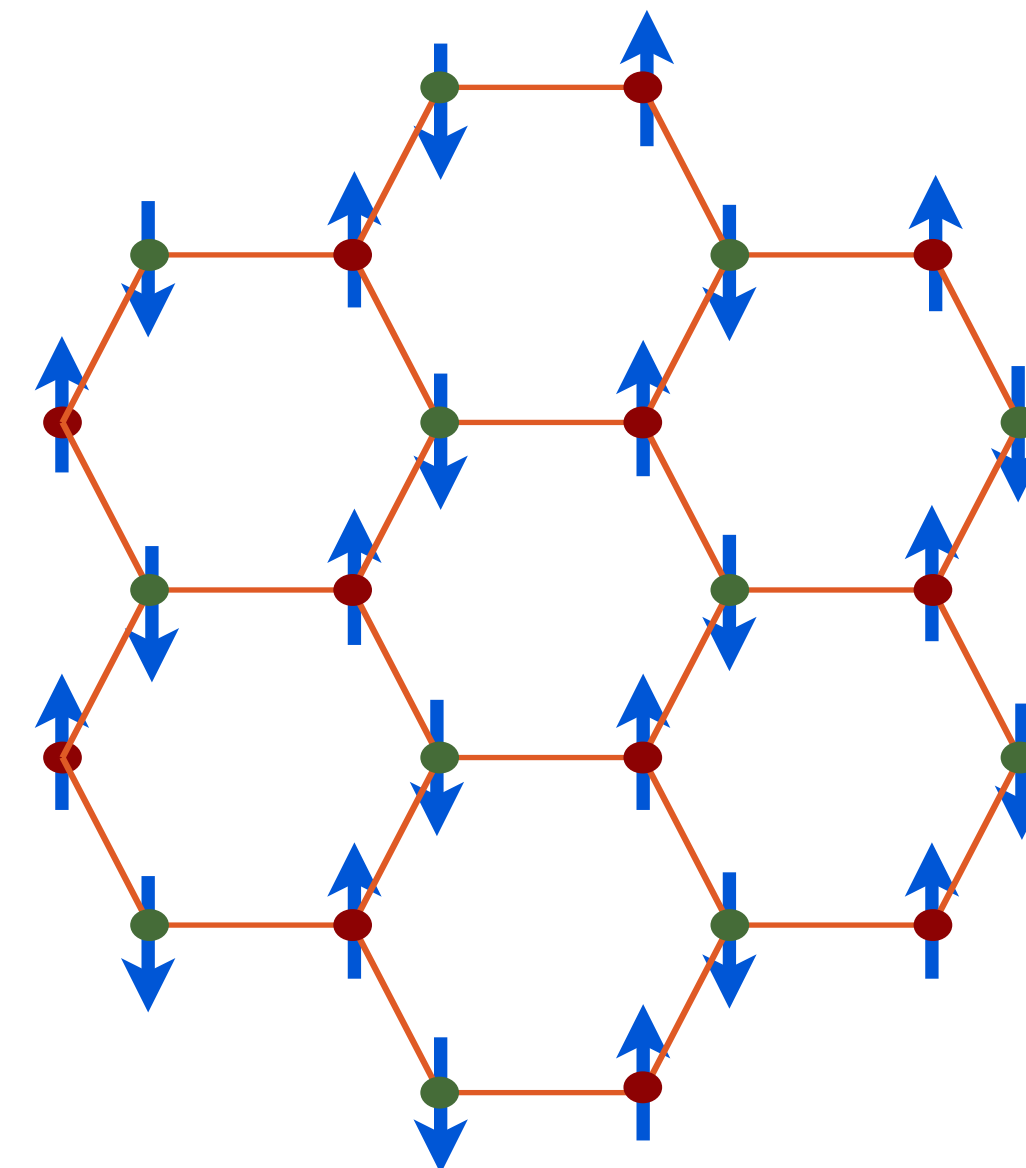
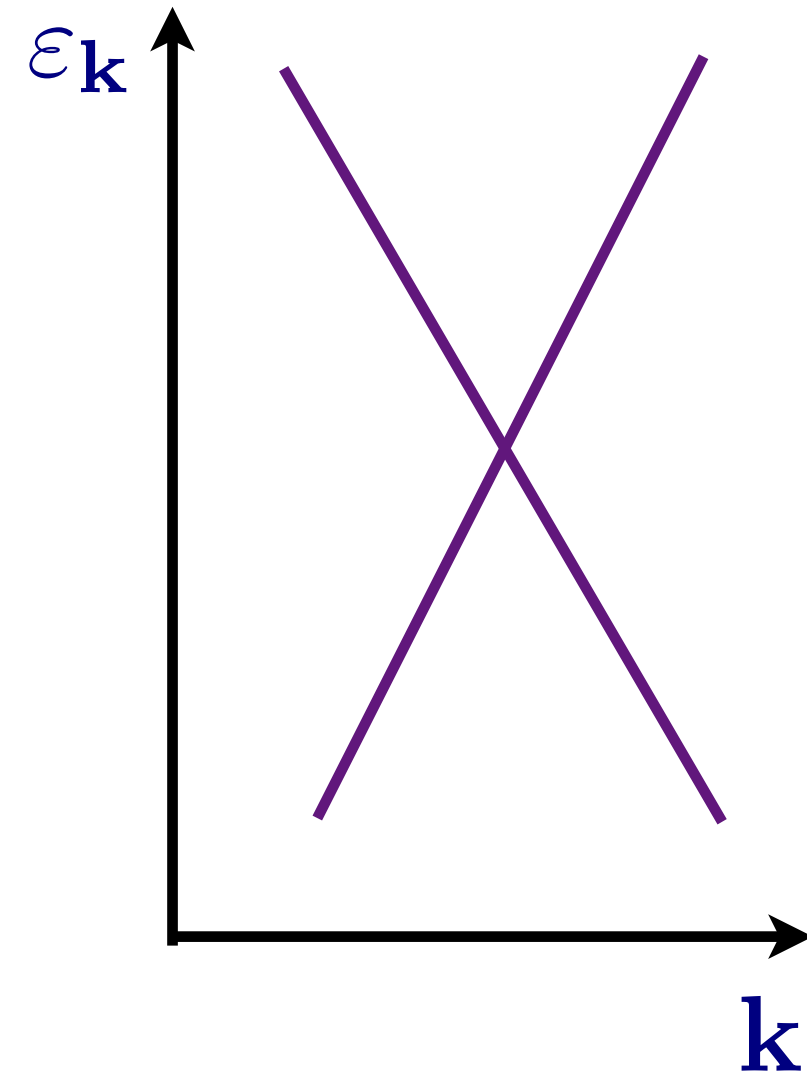
\mathcal{S}

At the quantum critical point, the non-linear couplings λ and u in the Gross-Neveu model reach non-zero fixed-point values under the renormalization group flow. The critical theory is an *interacting* CFT₃



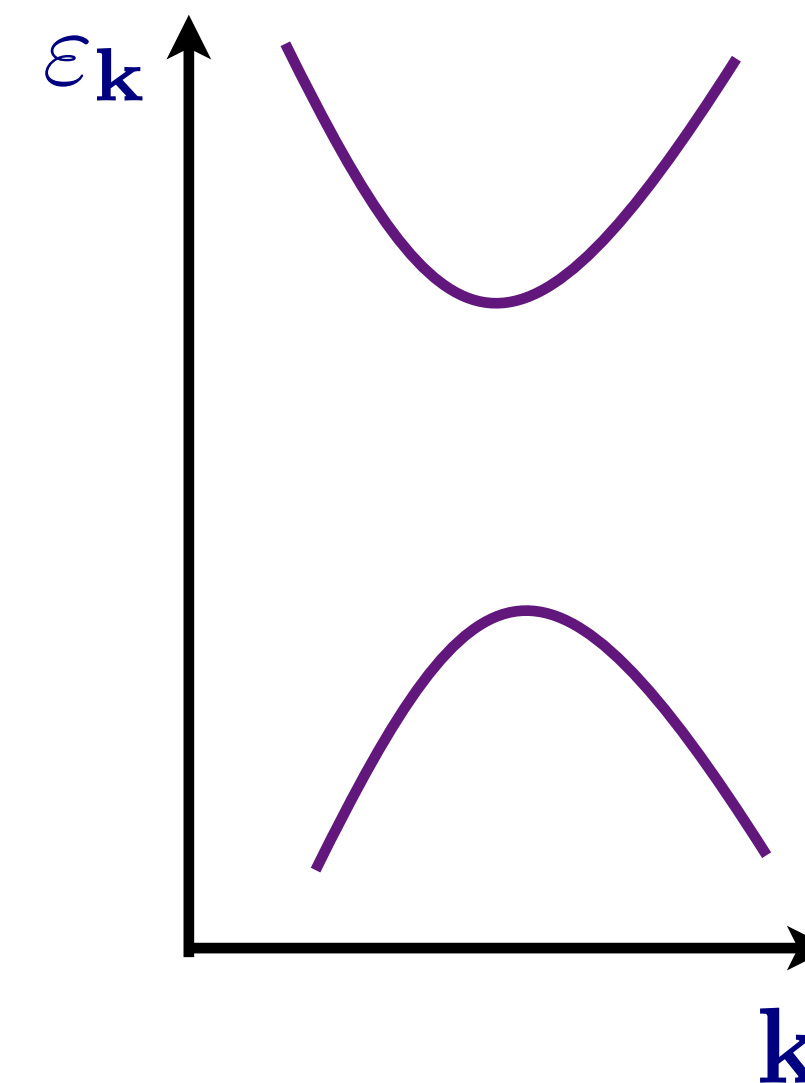
Dirac
semi-metal

$$\langle \varphi^a \rangle = 0$$



Insulating
antiferromagnet
with Neel order

$$\langle \varphi^a \rangle \neq 0$$



s

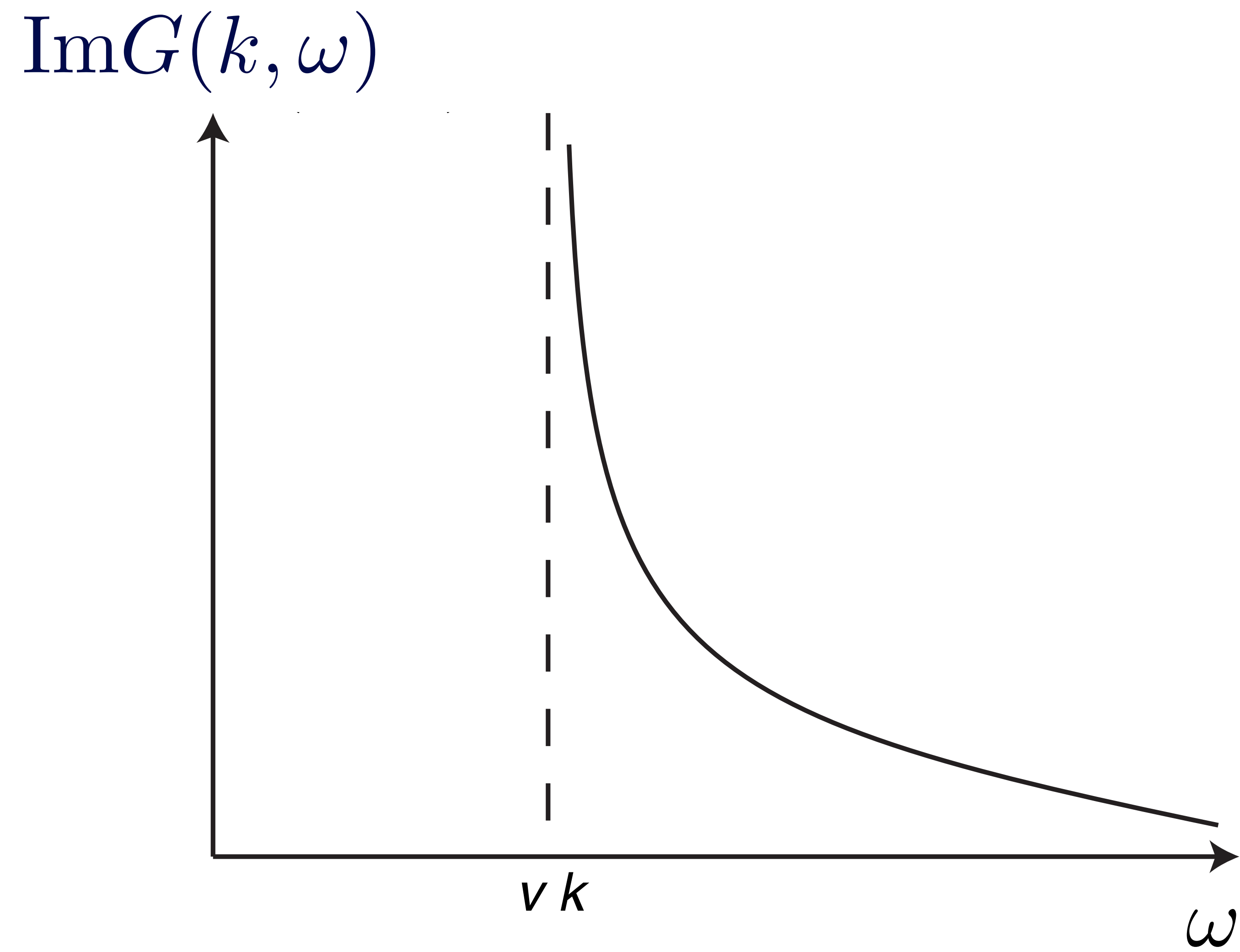
Free CFT3

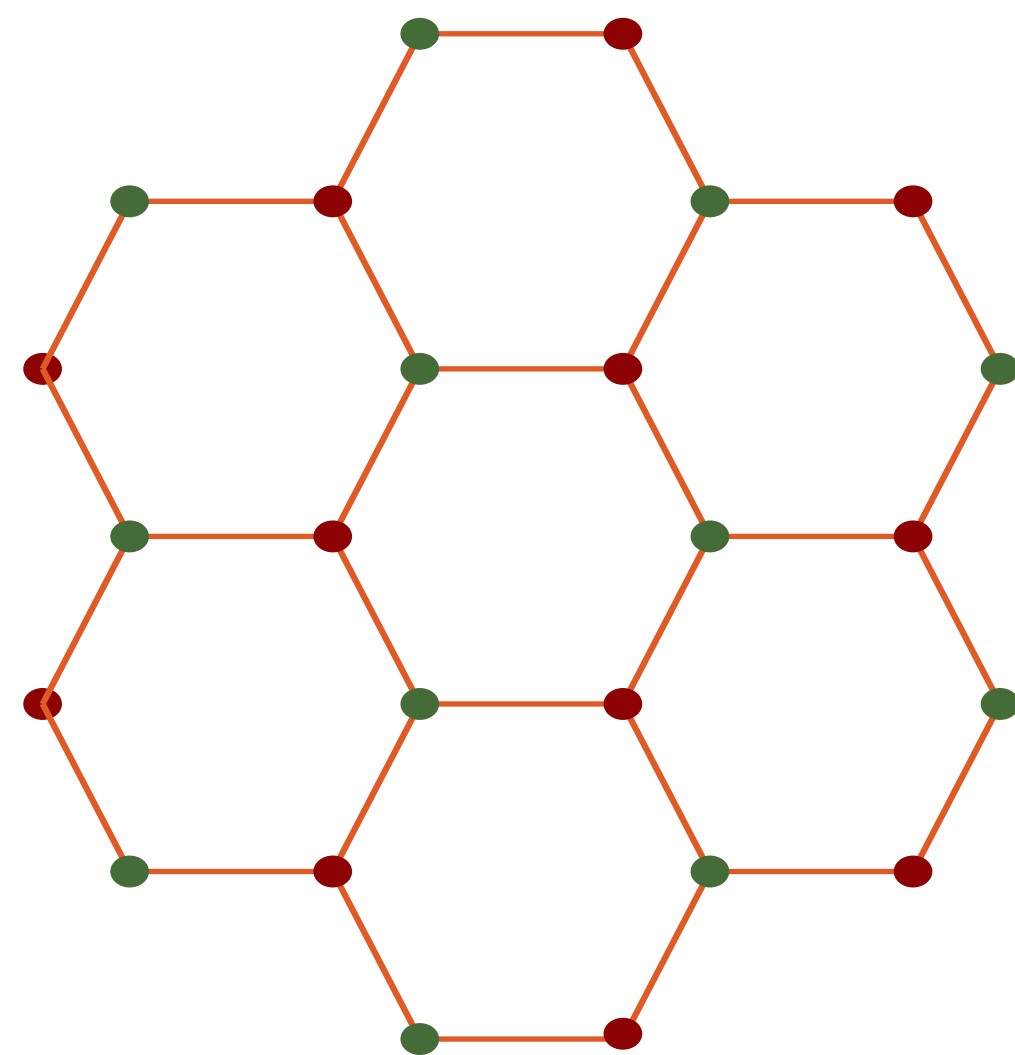
Interacting CFT3
with long-range entanglement

Electron Green's function for the interacting CFT3

$$G(k, \omega) = \langle \Psi(k, \omega); \Psi^\dagger(k, \omega) \rangle \sim \frac{i\omega + vk_x \tau^y + vk_y \tau^x \rho^z}{(\omega^2 + v^2 k_x^2 + v^2 k_y^2)^{1-\eta/2}}$$

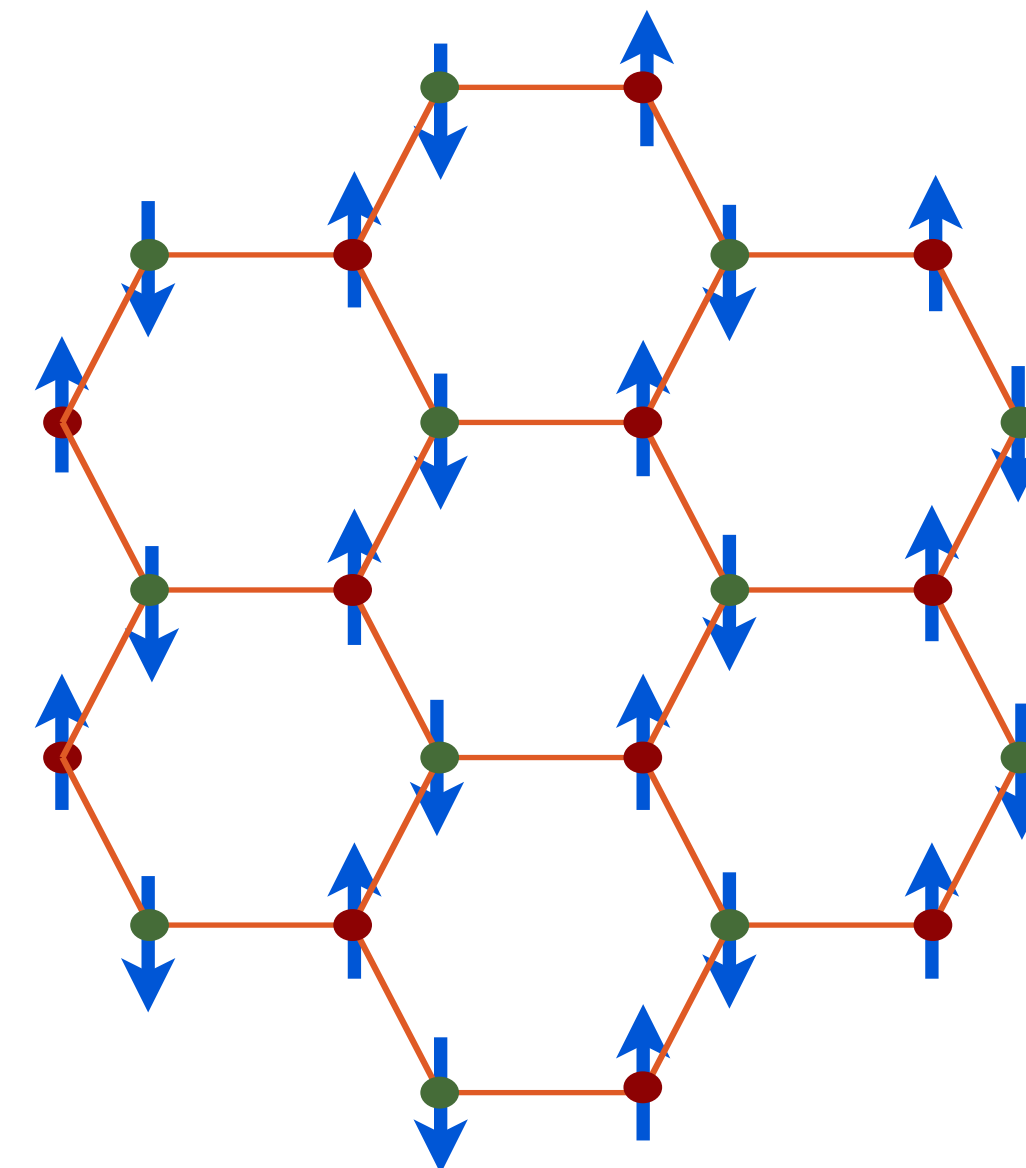
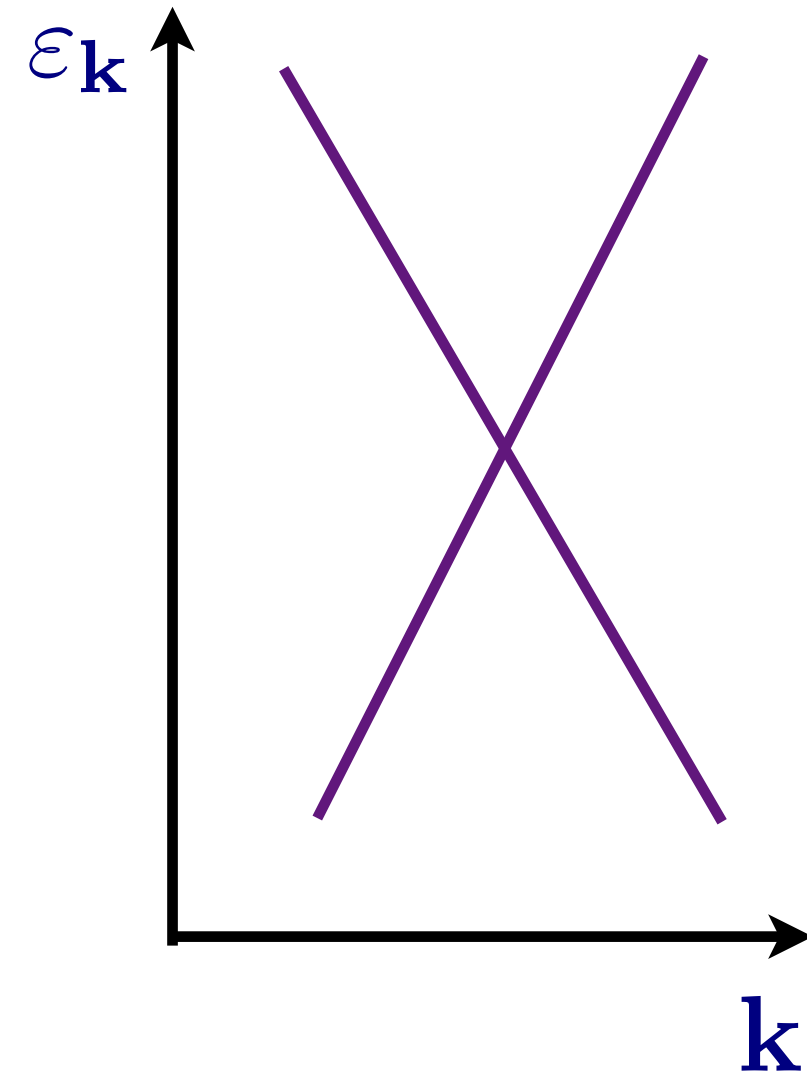
where $\eta > 0$ is the *anomalous dimension* of the fermion. Note that this leads to a fermion spectral density which has no quasiparticle pole: thus the quantum critical point has no well-defined quasiparticle excitations.





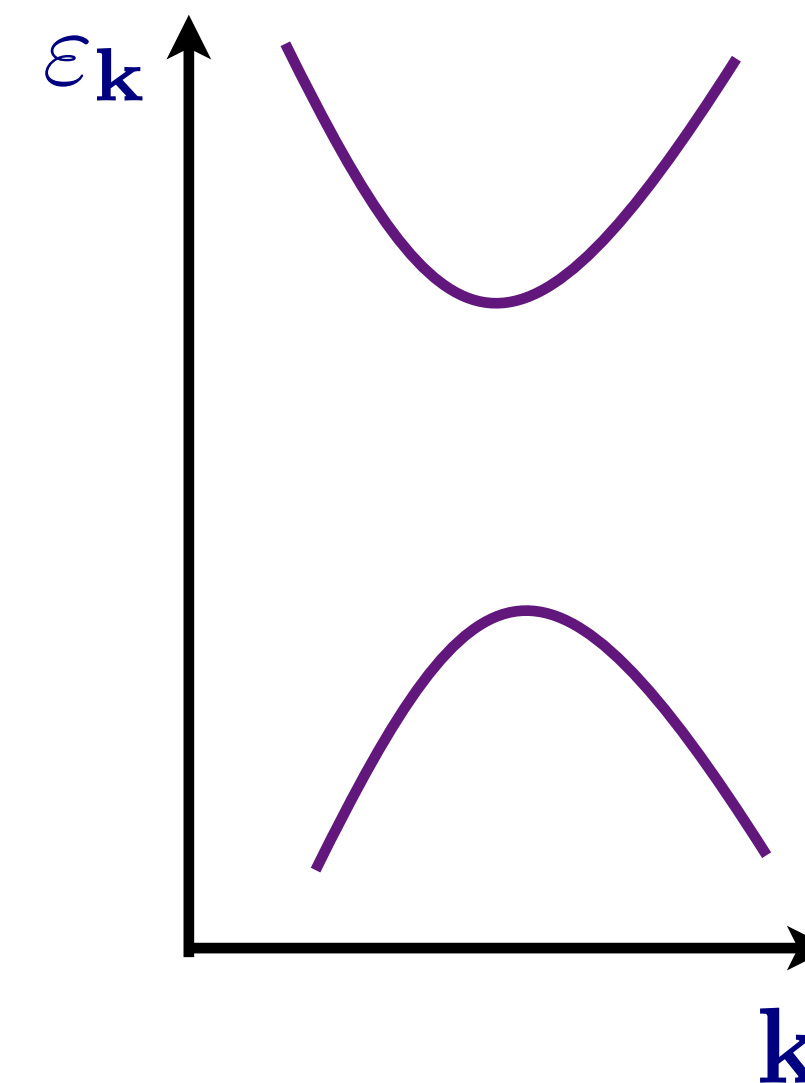
Dirac
semi-metal

$$\langle \varphi^a \rangle = 0$$



Insulating
antiferromagnet
with Neel order

$$\langle \varphi^a \rangle \neq 0$$



\mathcal{S}

Quantum phase transition described by a strongly-coupled
conformal field theory without well-defined quasiparticles

Electrical transport

The conserved electrical current is

$$J_\mu = -i\bar{\Psi}\gamma_\mu\Psi. \quad (1)$$

Let us compute its two-point correlator, $K_{\mu\nu}(k)$ at a spacetime momentum k_μ at $T = 0$. At leading order, this is given by a one fermion loop diagram which evaluates to

$$\begin{aligned} K_{\mu\nu}(k) &= \int \frac{d^3p}{8\pi^3} \frac{\text{Tr} [\gamma_\mu (i\gamma_\lambda p_\lambda + m\rho^z \sigma^z) \gamma_\nu (i\gamma_\delta (k_\delta + p_\delta) + m\rho^z \sigma^z)]}{(p^2 + m^2)((p + k)^2 + m^2)} \\ &= -\frac{2}{\pi} \left(\delta_{\mu\nu} - \frac{k_\mu k_\nu}{k^2} \right) \int_0^1 dx \frac{k^2 x(1-x)}{\sqrt{m^2 + k^2 x(1-x)}}, \end{aligned} \quad (2)$$

where the mass $m = 0$ in the semi-metal and at the quantum critical point, while $m = |\lambda N_0|$ in the insulator. Note that the current correlation is purely transverse, and this follows from the requirement of current conservation

$$k_\mu K_{\mu\nu} = 0. \quad (3)$$

Of particular interest to us is the K_{00} component, after analytic continuation to Minkowski space where the spacetime momentum k_μ is replaced by (ω, k) . The conductivity is obtained from this correlator via the Kubo formula

$$\sigma(\omega) = \lim_{k \rightarrow 0} \frac{-i\omega}{k^2} K_{00}(\omega, k). \quad (4)$$

In the insulator, where $m > 0$, analysis of the integrand in Eq. (2) shows that the spectral weight of the density correlator has a gap of $2m$ at $k = 0$, and the conductivity in Eq. (4) vanishes.

These properties are as expected in any insulator.

In the metal, and at the critical point, where $m = 0$, the fermionic spectrum is gapless, and so is that of the charge correlator. The density correlator in Eq. (2) and the conductivity in Eq. (4) evaluate to the simple universal results

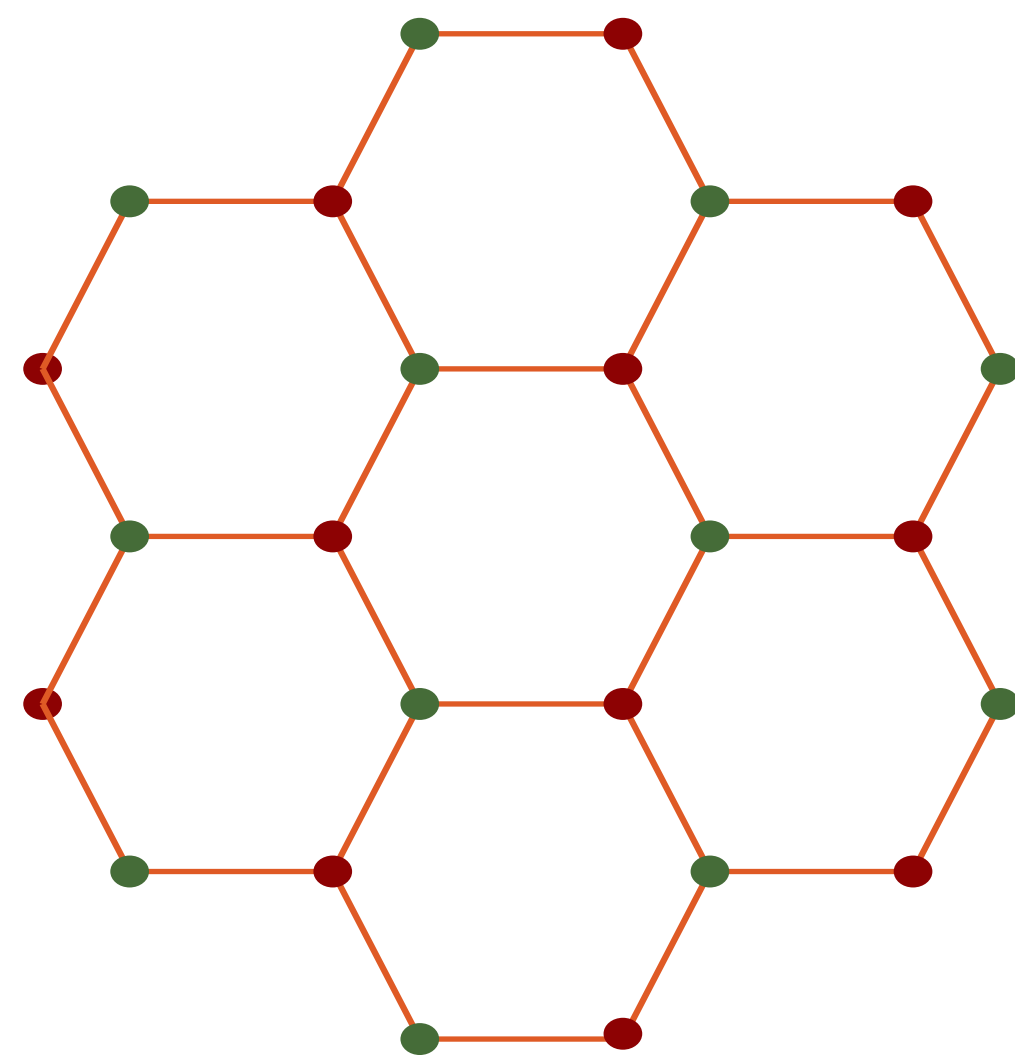
$$\begin{aligned} K_{00}(\omega, k) &= \frac{1}{4} \frac{k^2}{\sqrt{k^2 - \omega^2}} \\ \sigma(\omega) &= 1/4. \end{aligned} \quad (5)$$

Going beyond one-loop, we find *no change* in these results in the

semi-metal to all orders in perturbation theory. At the quantum critical point, there are no anomalous dimensions for the conserved current, but the amplitude does change yielding

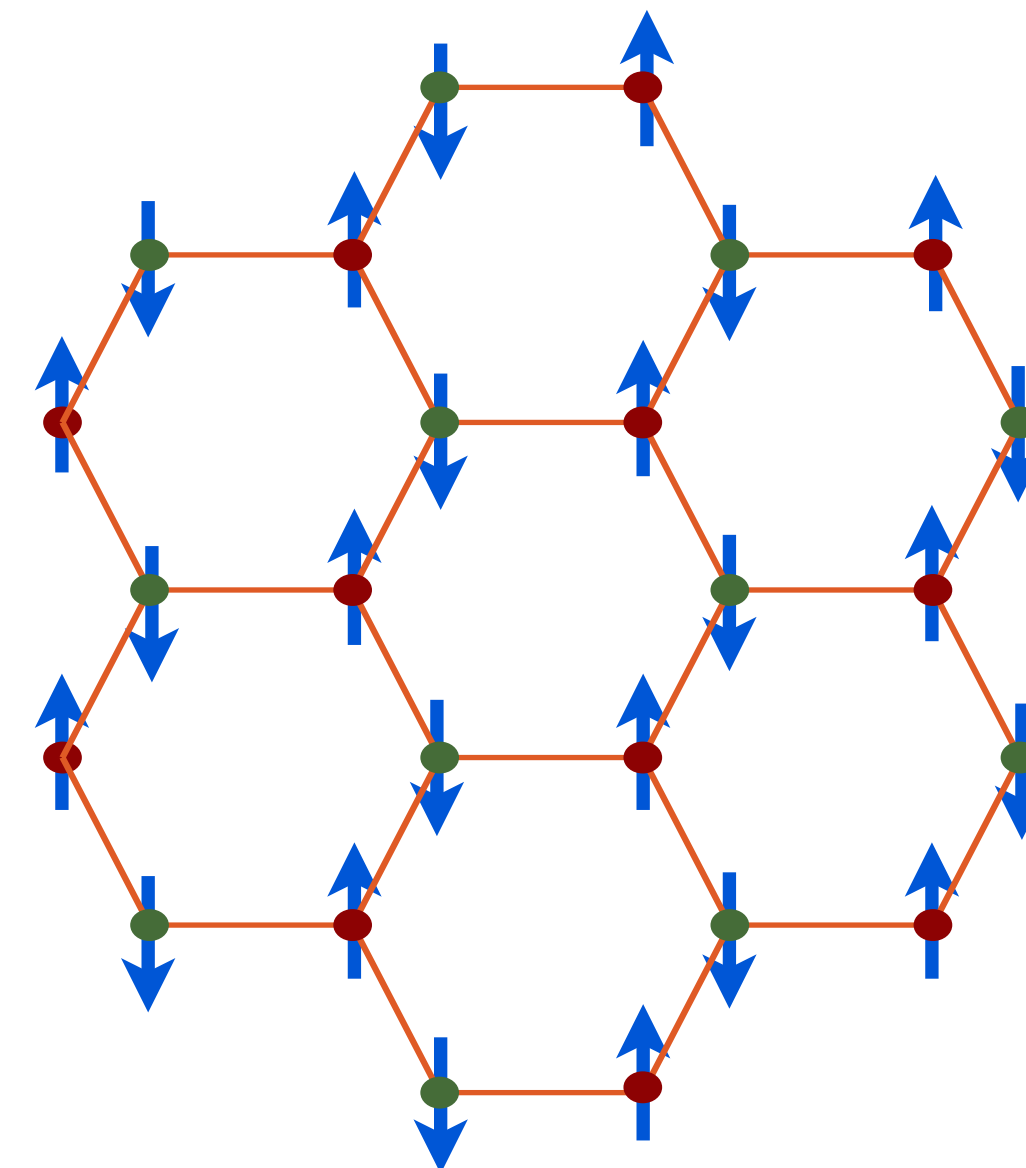
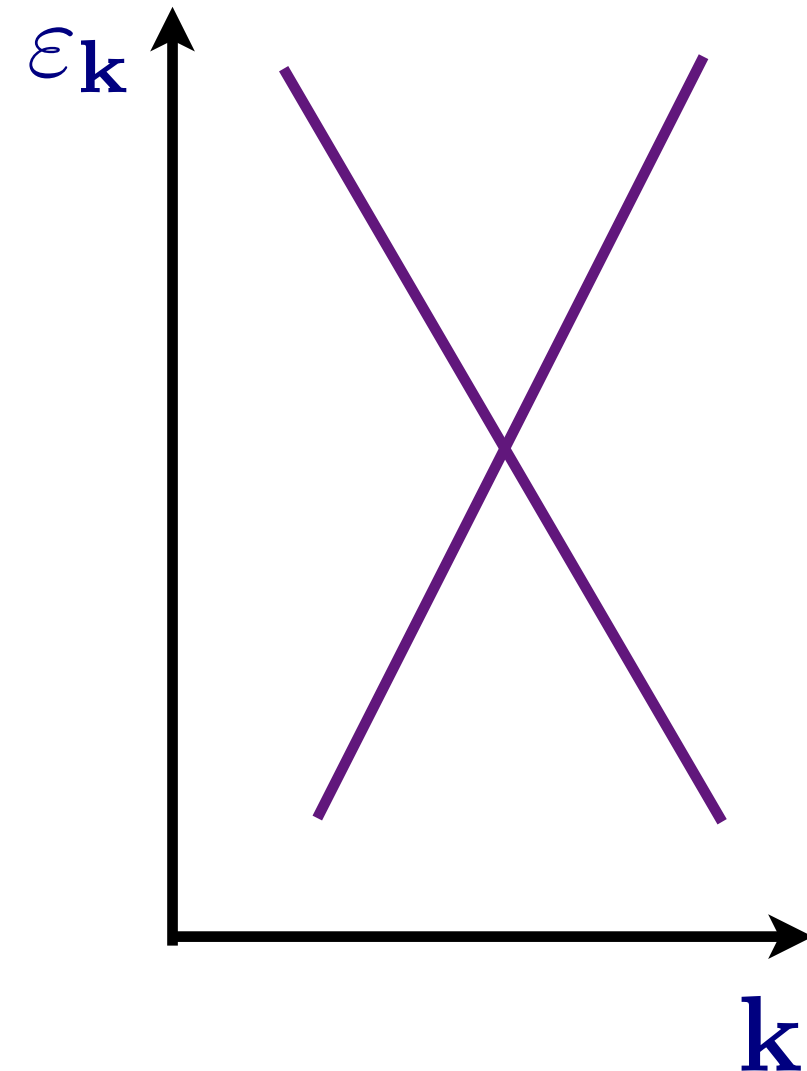
$$\begin{aligned} K_{00}(\omega, k) &= \mathcal{K} \frac{k^2}{\sqrt{k^2 - \omega^2}} \\ \sigma(\omega) &= \mathcal{K}, \end{aligned} \tag{6}$$

where \mathcal{K} is a universal number dependent only upon the universality class of the quantum critical point. The value of the \mathcal{K} for the Gross-Neveu model is not known exactly, but can be estimated by computations in the $(3 - d)$ or $1/N$ expansions.



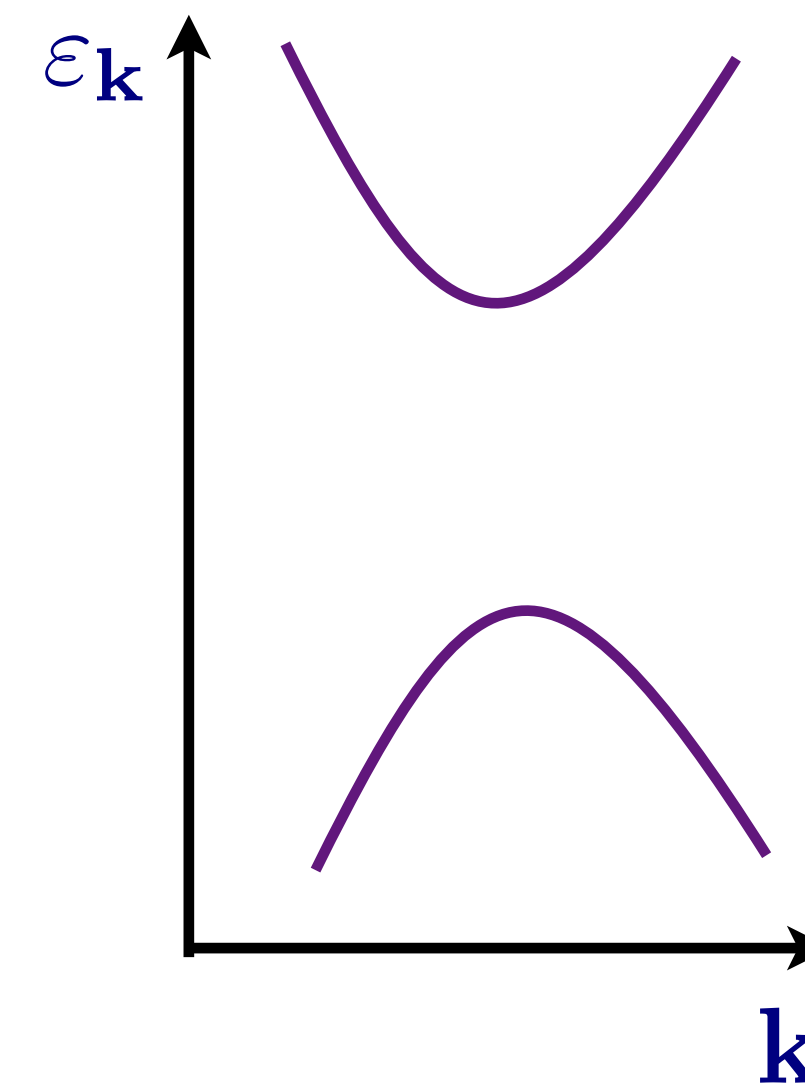
Dirac
semi-metal

$$\langle \varphi^a \rangle = 0$$



Insulating
antiferromagnet
with Neel order

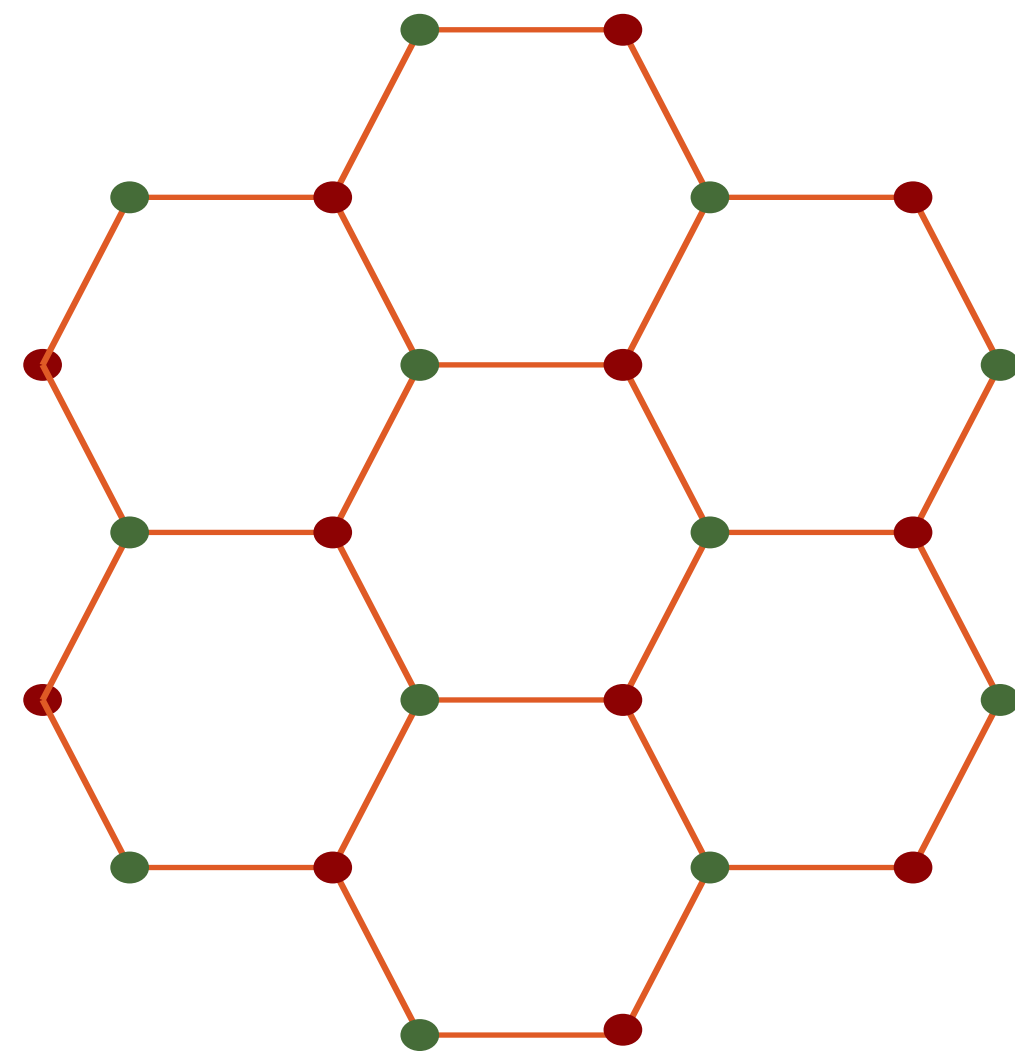
$$\langle \varphi^a \rangle \neq 0$$



s

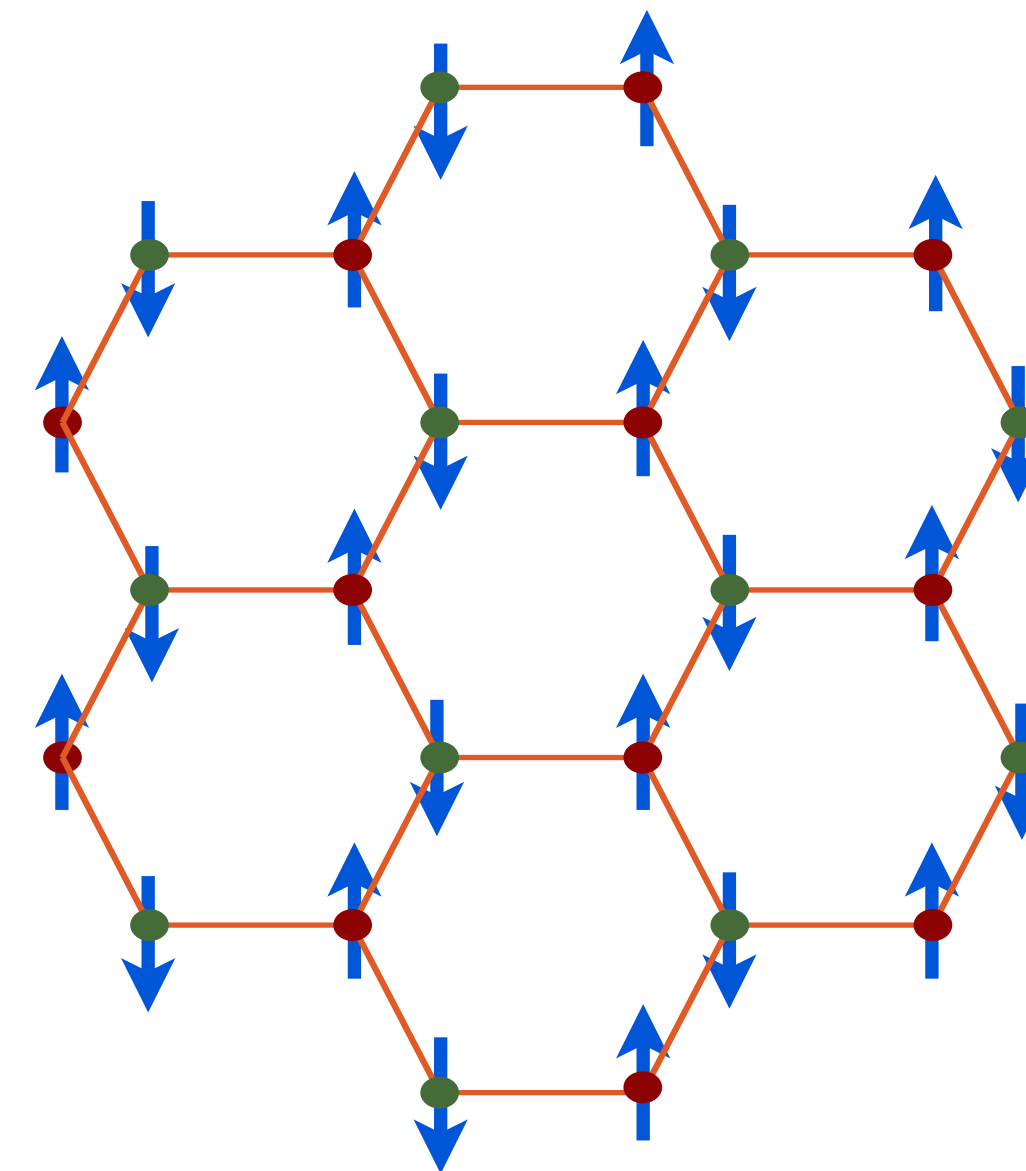
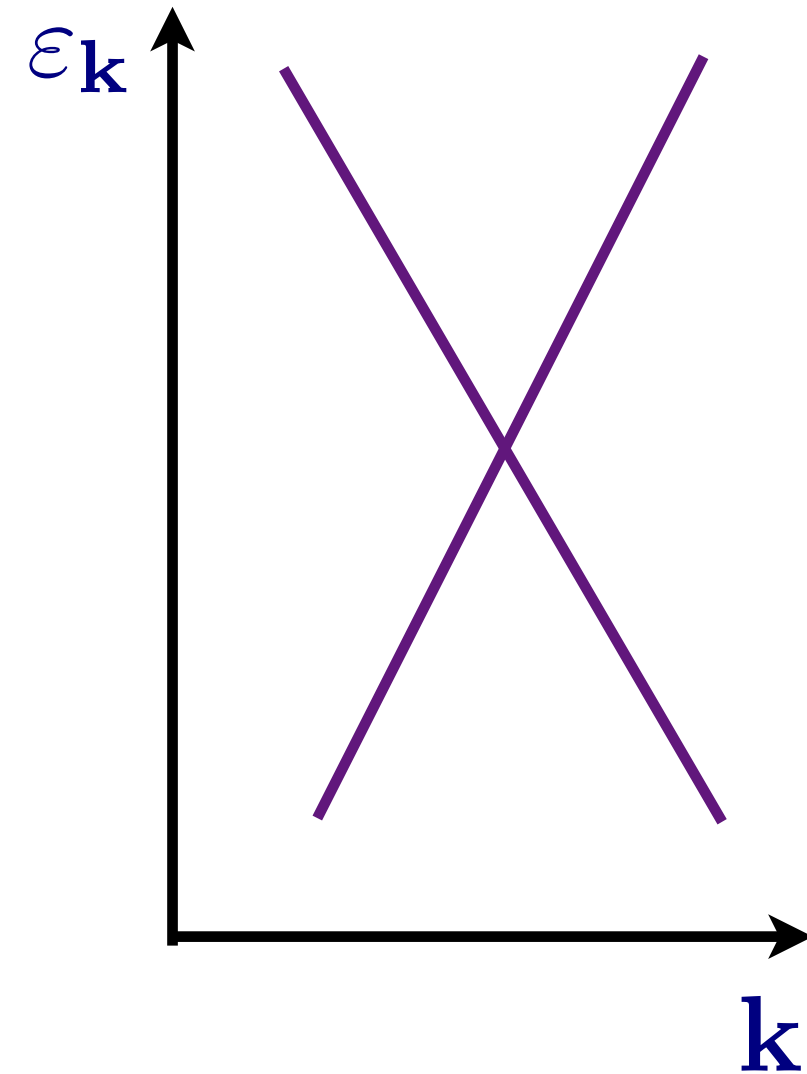
Free CFT3

Interacting CFT3
with long-range entanglement



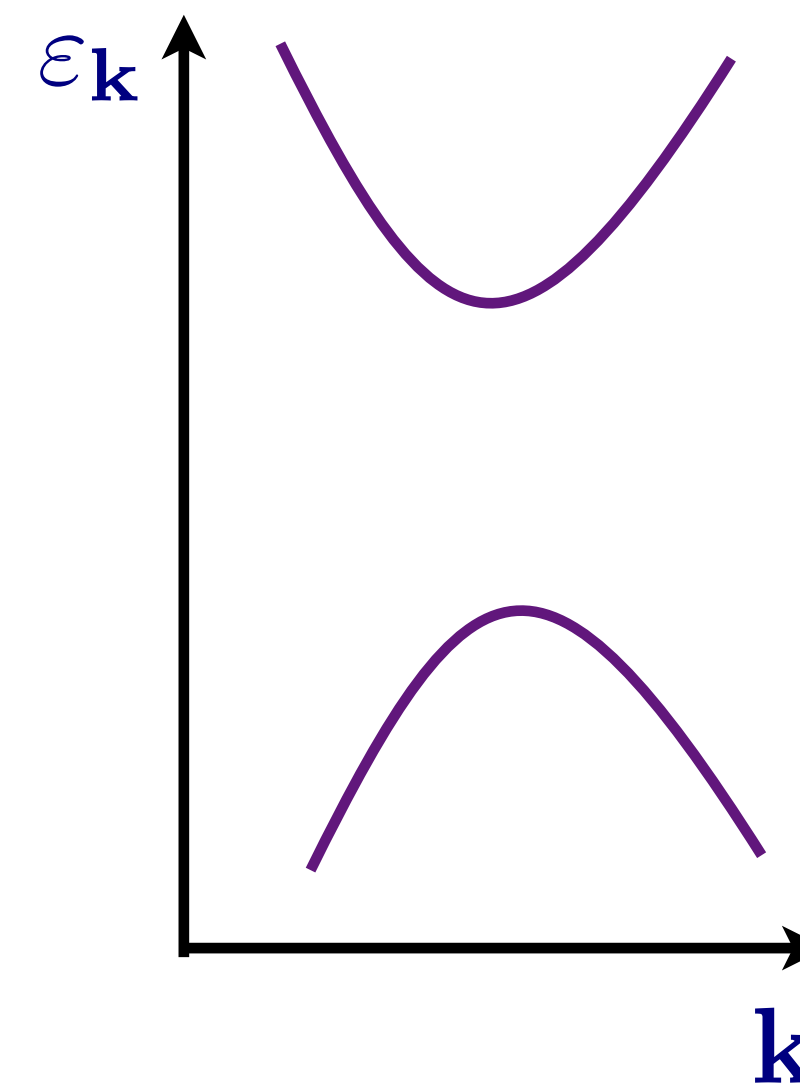
Dirac
semi-metal

$$\langle \varphi^a \rangle = 0$$



Insulating
antiferromagnet
with Neel order

$$\langle \varphi^a \rangle \neq 0$$

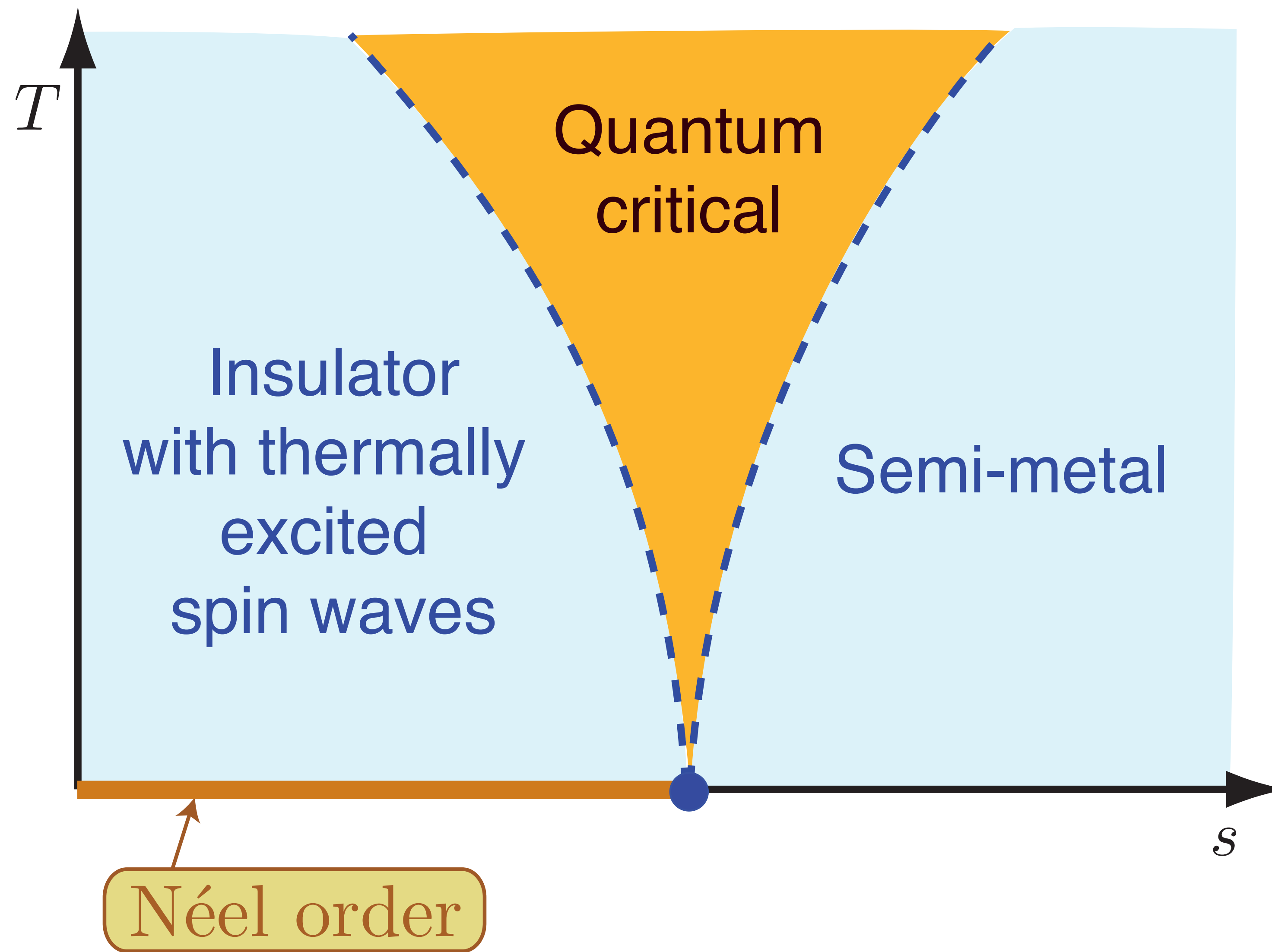


\mathcal{S}

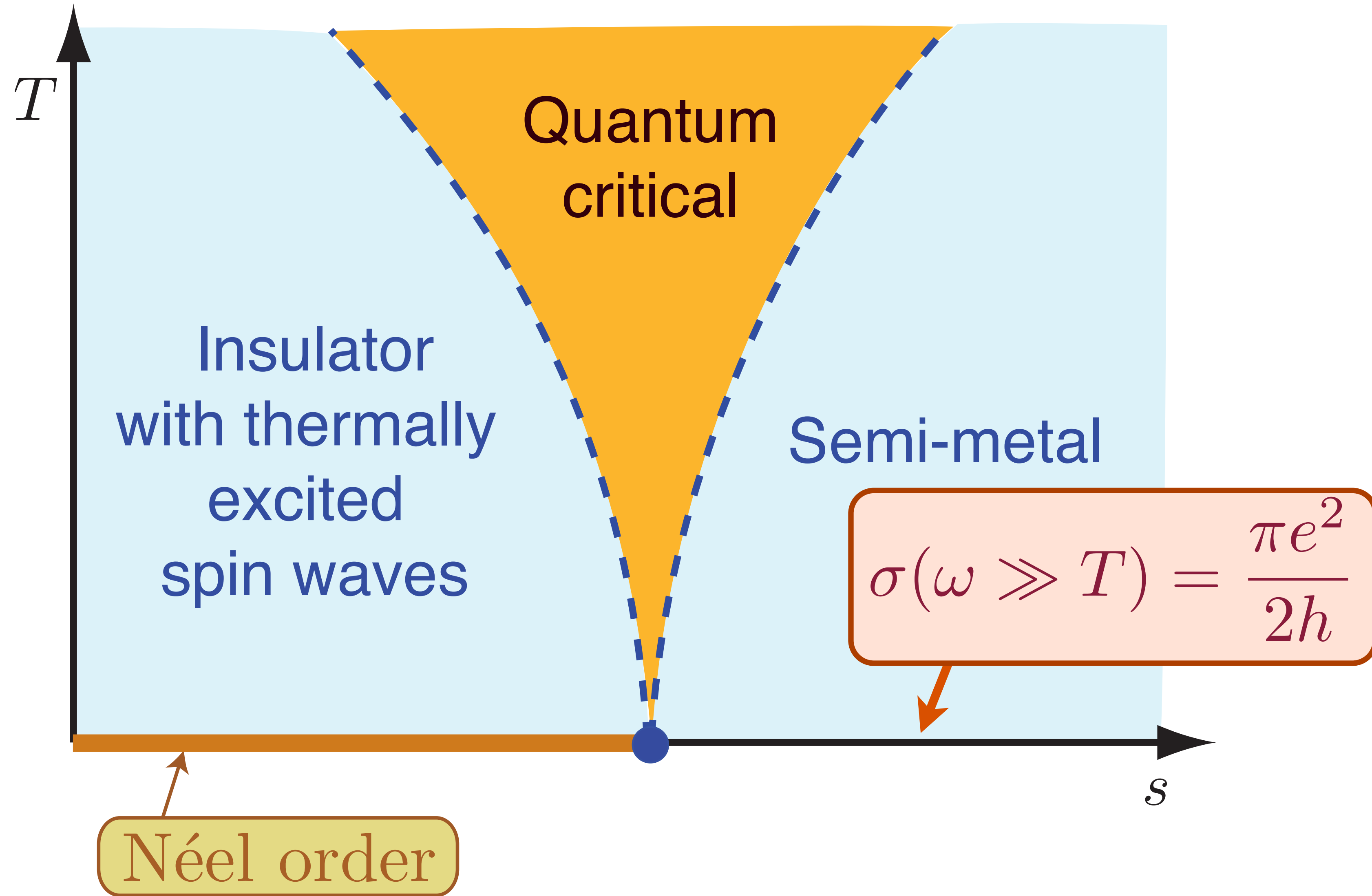
$$\sigma(\omega) = \frac{\pi e^2}{2h}$$

$$\sigma(\omega) = \frac{\mathcal{K} e^2}{\hbar}$$

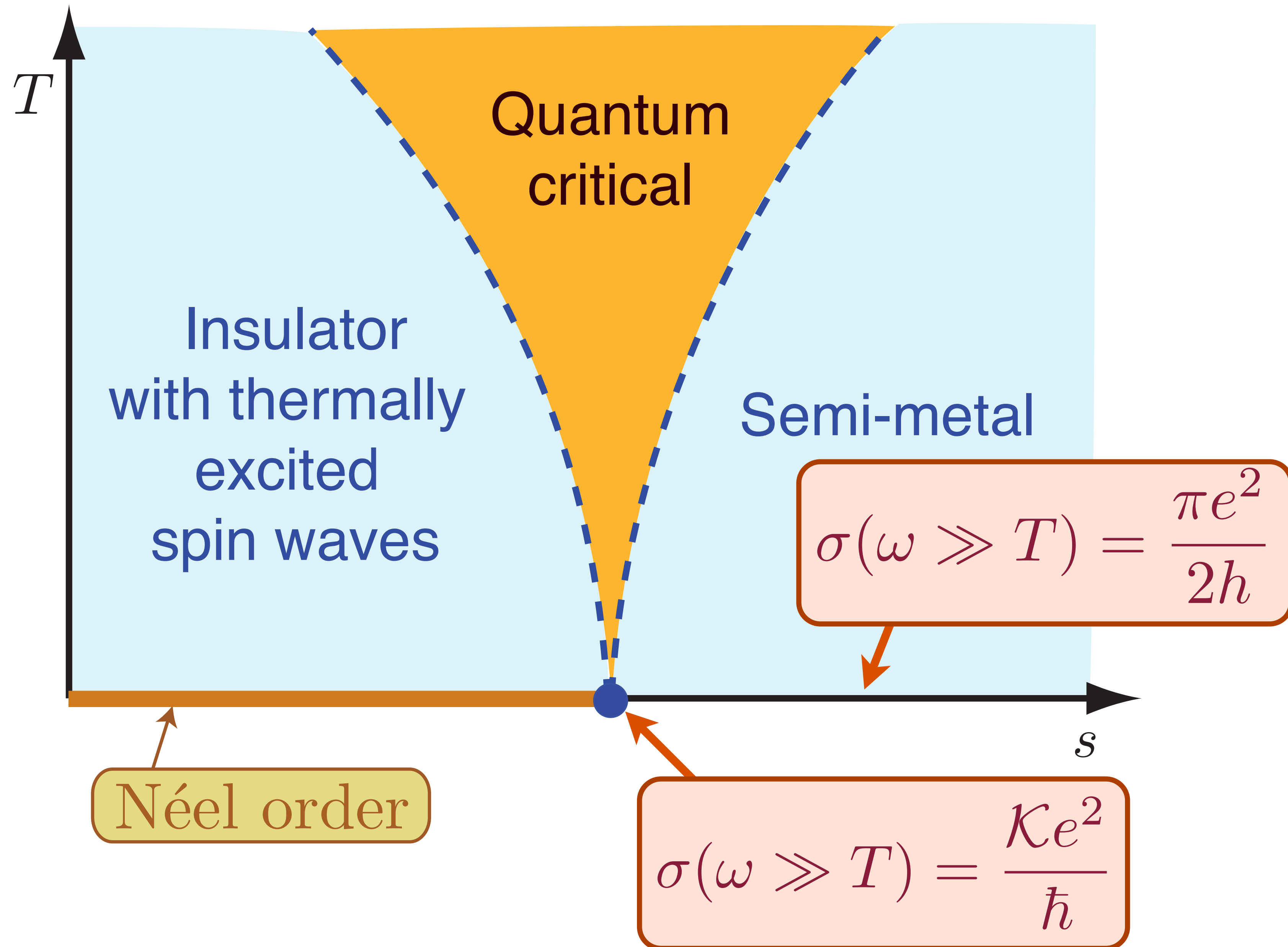
Phase diagram at non-zero temperatures



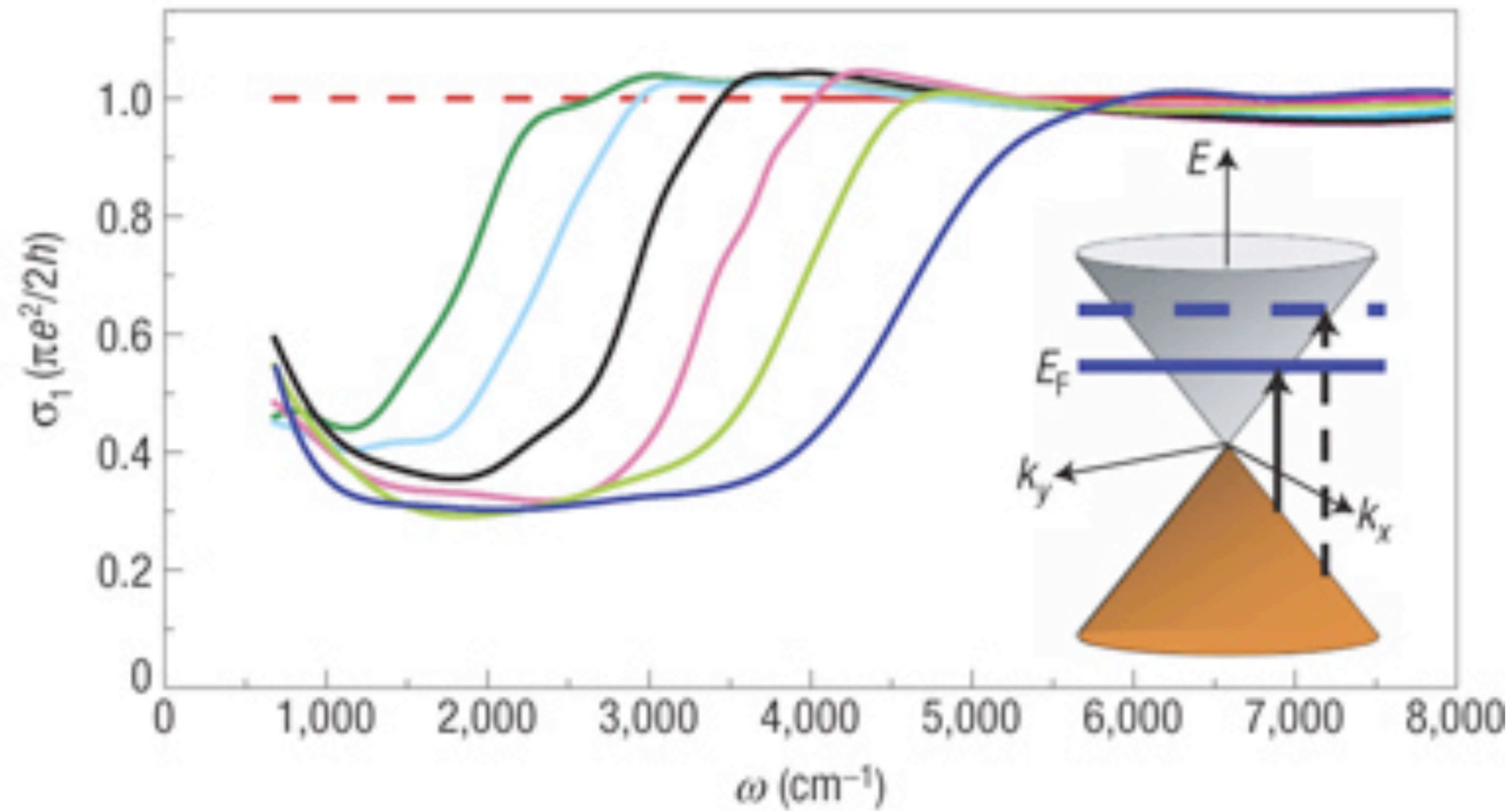
Phase diagram at non-zero temperatures



Phase diagram at non-zero temperatures



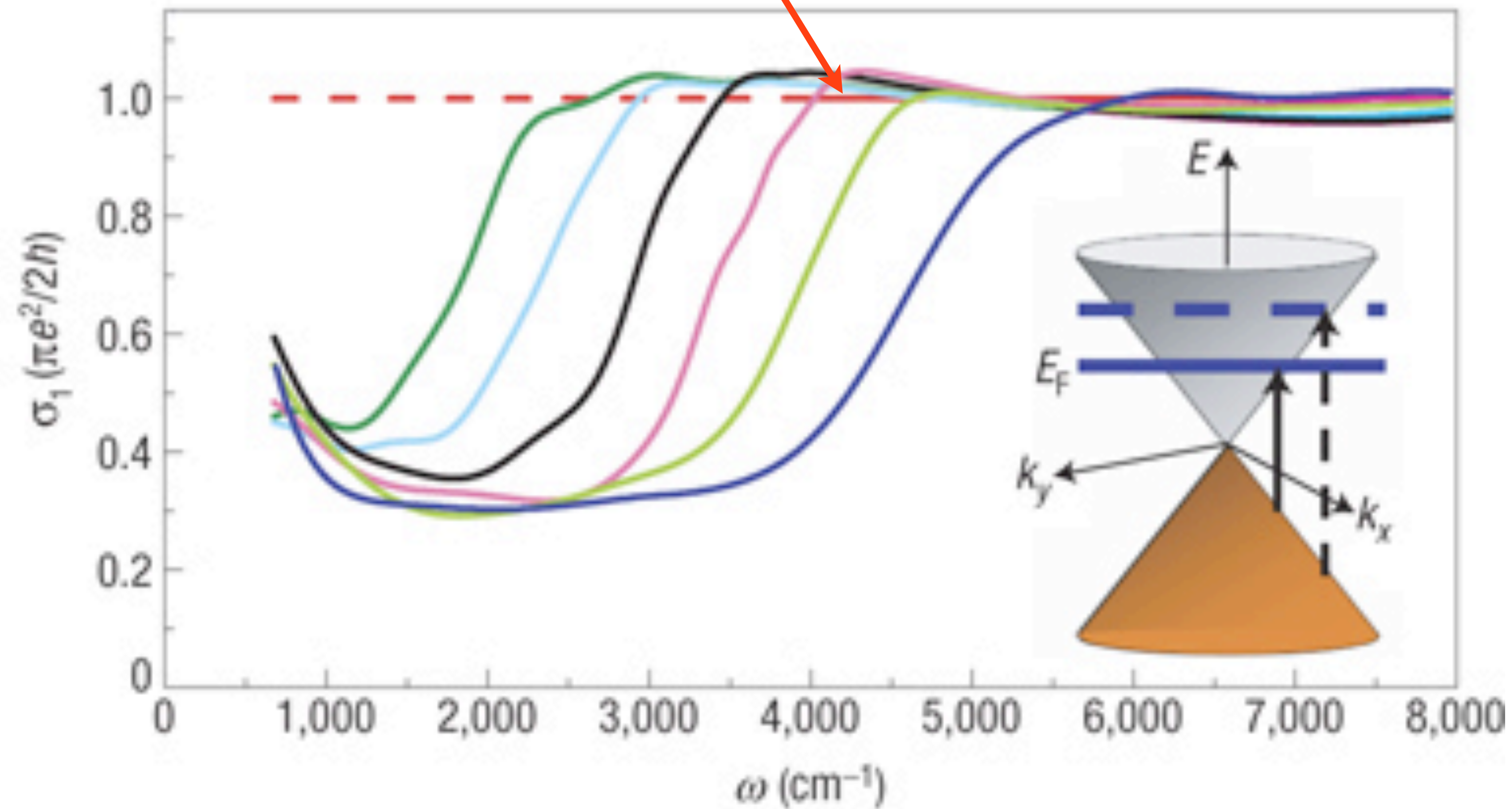
Optical conductivity of graphene



Z. Q. Li, E. A. Henriksen, Z. Jiang, Z. Hao, M. C. Martin, P. Kim, H. L. Stormer, and D. N. Basov, Nature Physics 4, 532 (2008).

Optical conductivity of graphene

Undoped graphene



Z. Q. Li, E. A. Henriksen, Z. Jiang, Z. Hao, M. C. Martin, P. Kim, H. L. Stormer, and D. N. Basov, *Nature Physics* **4**, 532 (2008).

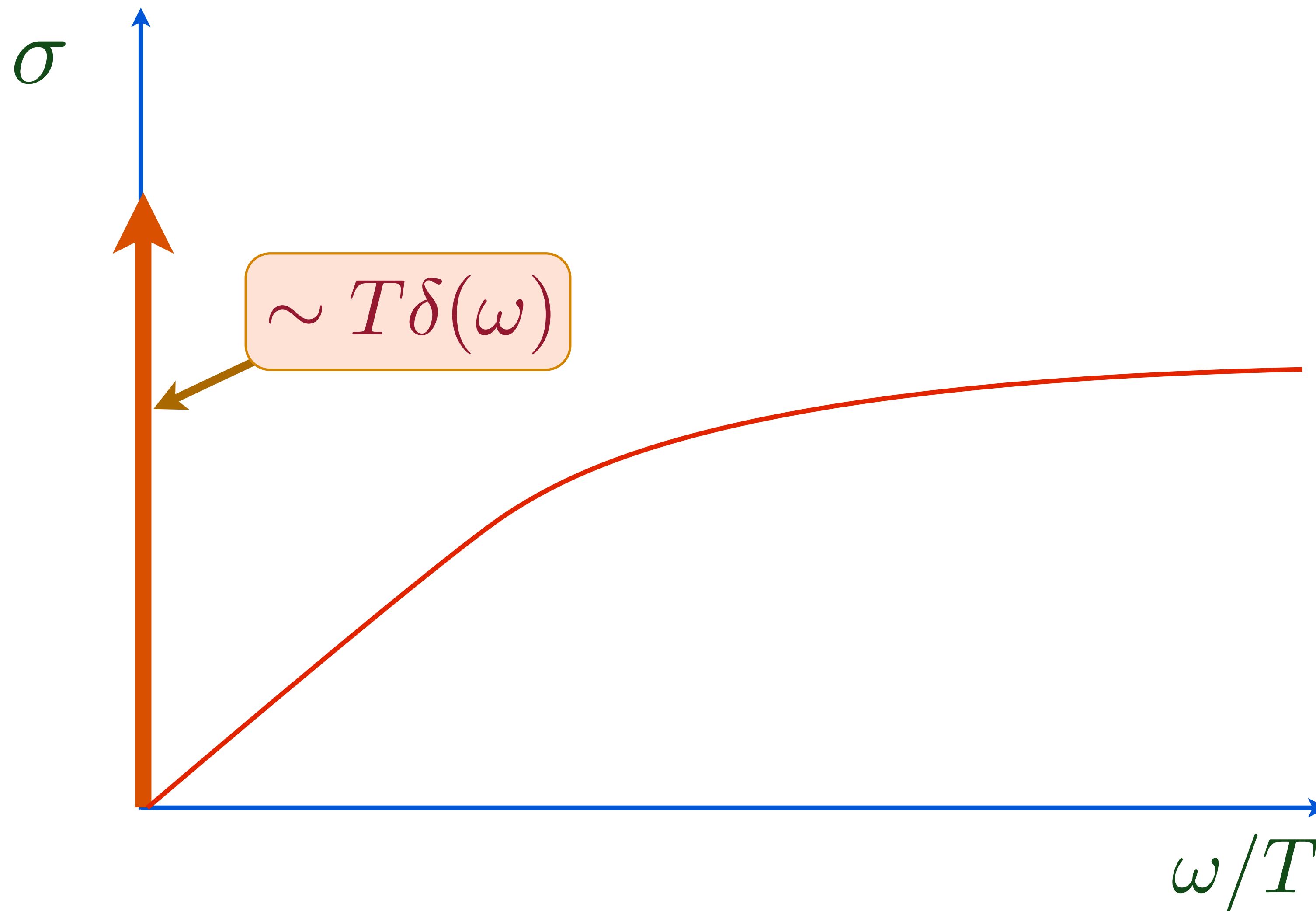
Non-zero temperatures

At the quantum-critical point at one-loop order, we can set $m = 0$, and then repeat the computation in Eq. (2) at $T > 0$. This only requires replacing the integral over the loop frequency by a summation over the Matsubara frequencies, which are quantized by odd multiples of πT . Such a computation, via Eq. (4) leads to the conductivity

$$\text{Re}[\sigma(\omega)] = (2T \ln 2) \delta(\omega) + \frac{1}{4} \tanh\left(\frac{|\omega|}{4T}\right); \quad (7)$$

the imaginary part of $\sigma(\omega)$ is the Hilbert transform of $\text{Re}[\sigma(\omega)] - 1/4$. Note that this reduces to Eq. (5) in the limit $\omega \gg T$. However, the most important new feature of Eq. (7) arises for $\omega \ll T$, where we find a delta function at zero frequency in the real part. Thus the d.c. conductivity is infinite at this order, arising from the collisionless transport of thermally excited carriers.

Electrical transport in a free CFT3 for $T > 0$



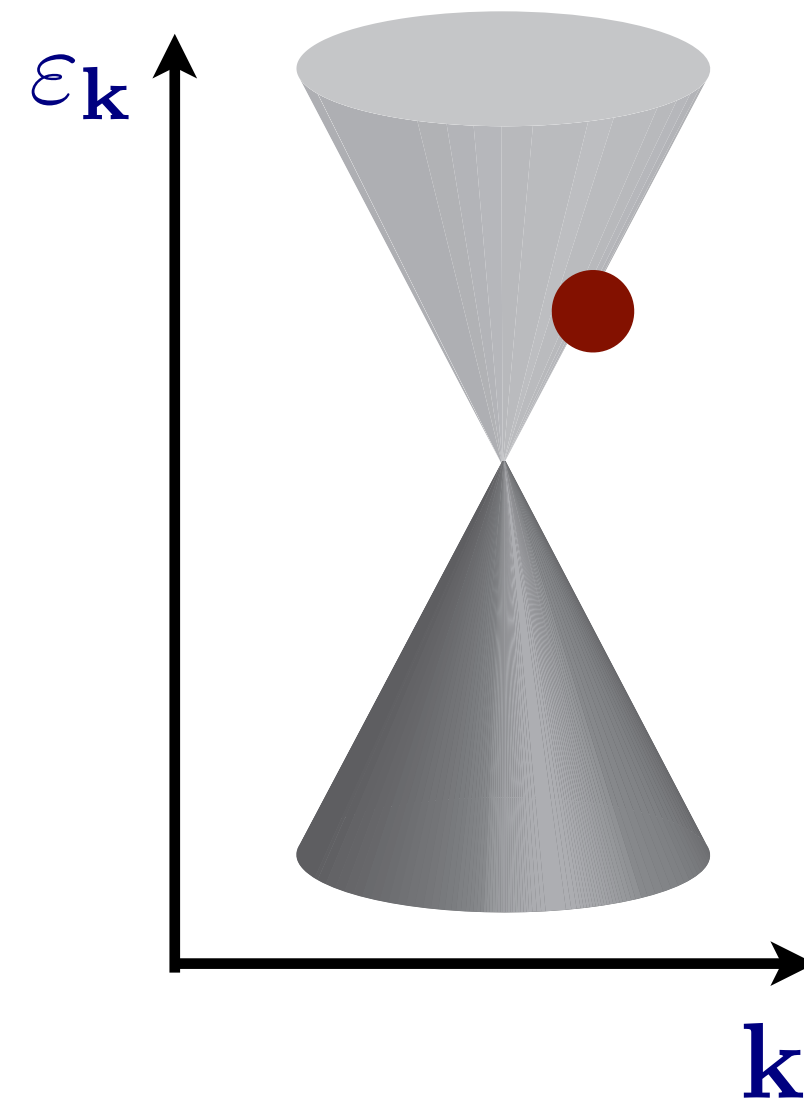
Particles



Momentum



Current



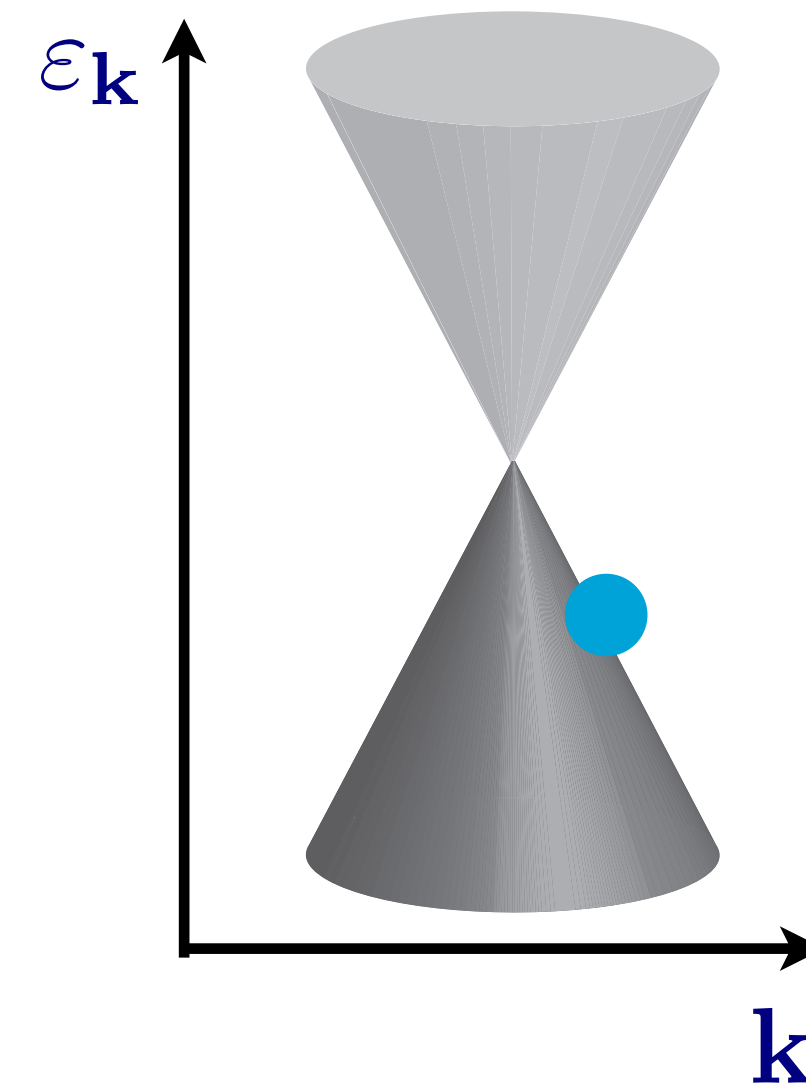
Holes



Momentum



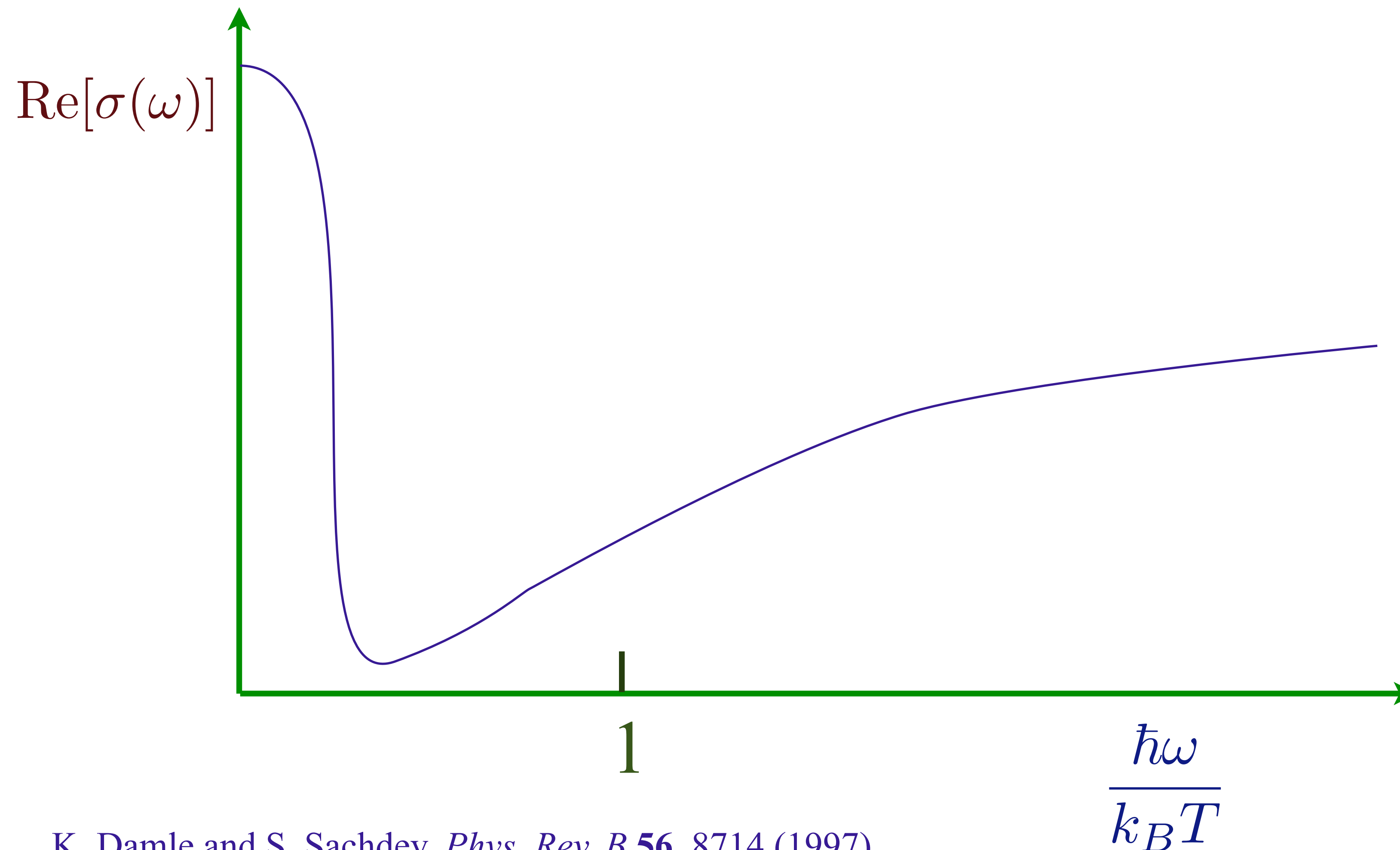
Current



Particle hole symmetry: current carrying state has zero momentum,
and collisions can relax current to zero

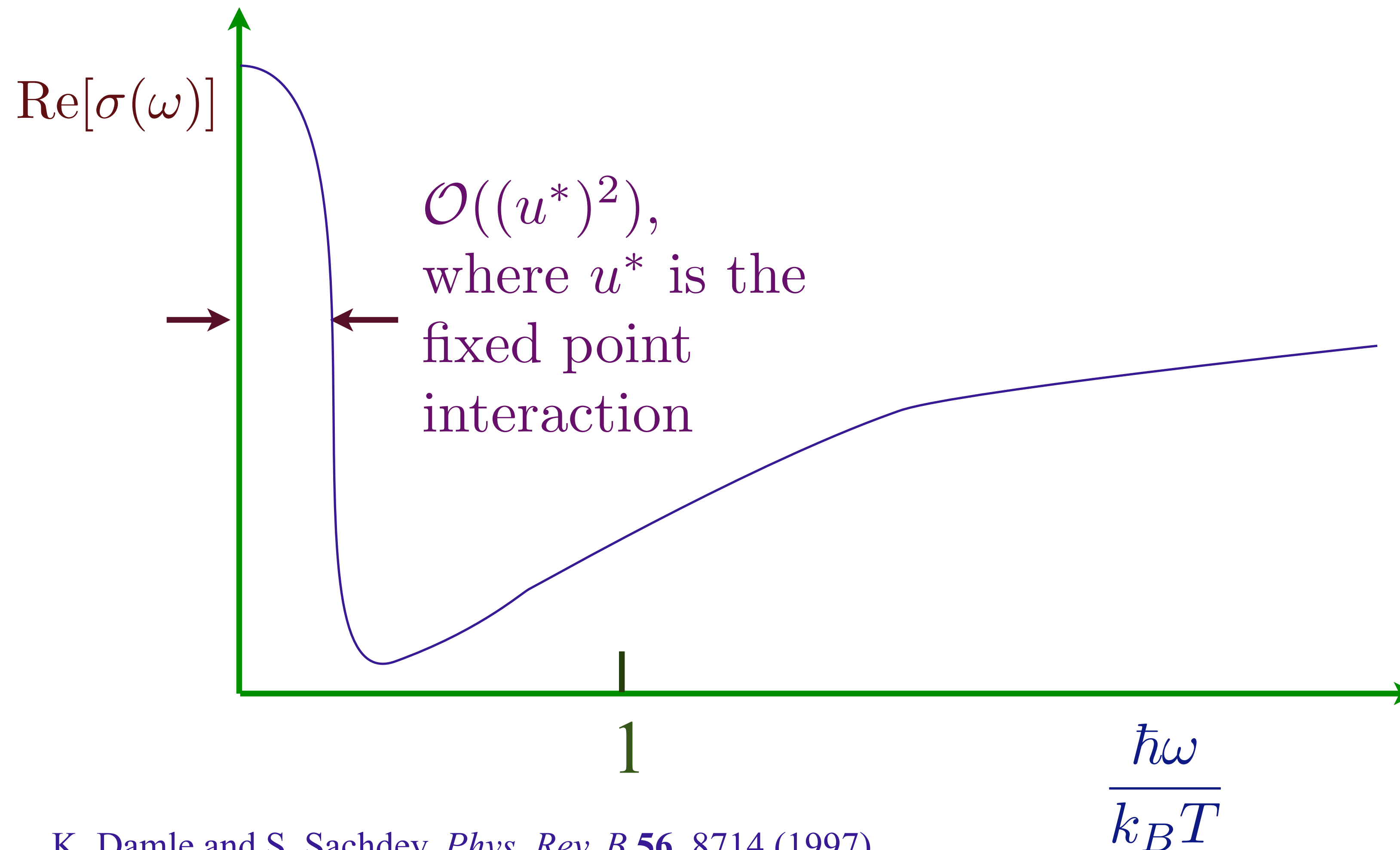
Electrical transport for a (weakly) interacting CFT3

$$\sigma(\omega, T) = \frac{e^2}{h} \Sigma \left(\frac{\hbar\omega}{k_B T} \right) ; \quad \Sigma \rightarrow \text{a universal function}$$



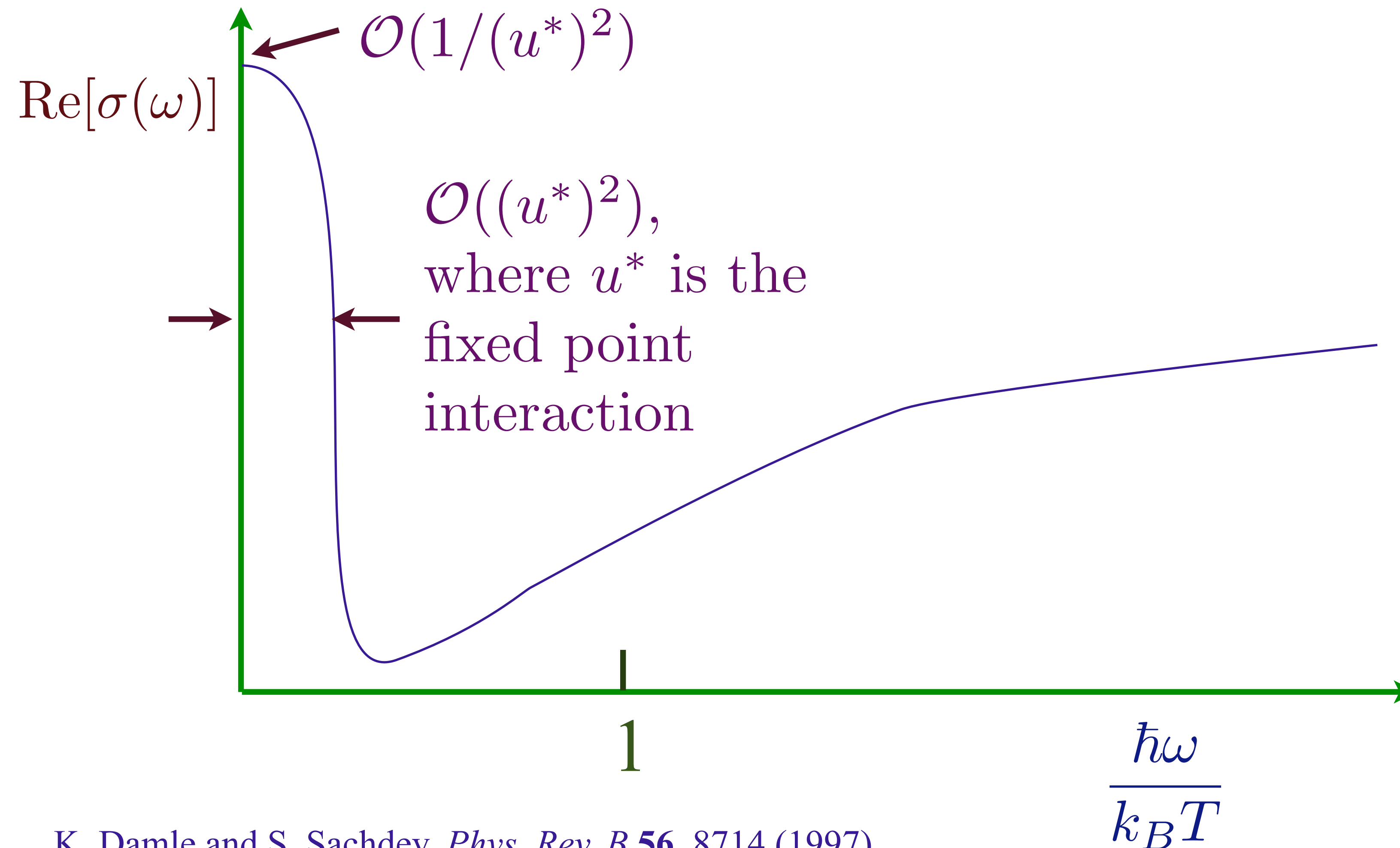
Electrical transport for a (weakly) interacting CFT3

$$\sigma(\omega, T) = \frac{e^2}{h} \Sigma \left(\frac{\hbar\omega}{k_B T} \right) ; \quad \Sigma \rightarrow \text{a universal function}$$



Electrical transport for a (weakly) interacting CFT3

$$\sigma(\omega, T) = \frac{e^2}{h} \Sigma \left(\frac{\hbar\omega}{k_B T} \right) ; \quad \Sigma \rightarrow \text{a universal function}$$



Graphene has long-range Coulomb interactions

Lars Fritz, Joerg Schmalian,
Markus Mueller, S.S.,
PRB **78**, 085416 (2008)

$$\begin{aligned} H &= H_0 + H_1 \\ H_0 &= \int d\mathbf{x} \left[v_F \Psi_a^\dagger (-i\sigma^i \partial_i) \Psi_a \right] \\ H_1 &= \frac{1}{2} \int \frac{d^2 k_1}{(2\pi)^2} \frac{d^2 k_2}{(2\pi)^2} \frac{d^2 q}{(2\pi)^2} \Psi_a^\dagger(\mathbf{k}_2 - \mathbf{q}) \Psi_a(\mathbf{k}_2) \frac{2\pi e^2}{\varepsilon |\mathbf{q}|} \Psi_b^\dagger(\mathbf{k}_1 + \mathbf{q}) \Psi_b(\mathbf{k}_1), \end{aligned}$$

with $a = 1, \dots, N$ labeling the "flavors" of fermions ($N = 4$ in graphene, accounting for 2 valleys and 2 spin projections). We define the "fine-structure constant"

$$\alpha \equiv \frac{e^2}{\varepsilon v_F},$$

and the RG equation for the dimensionless α is

$$\frac{d\alpha}{d\ell} = -\frac{\alpha^2}{4} + \mathcal{O}(\alpha^3).$$

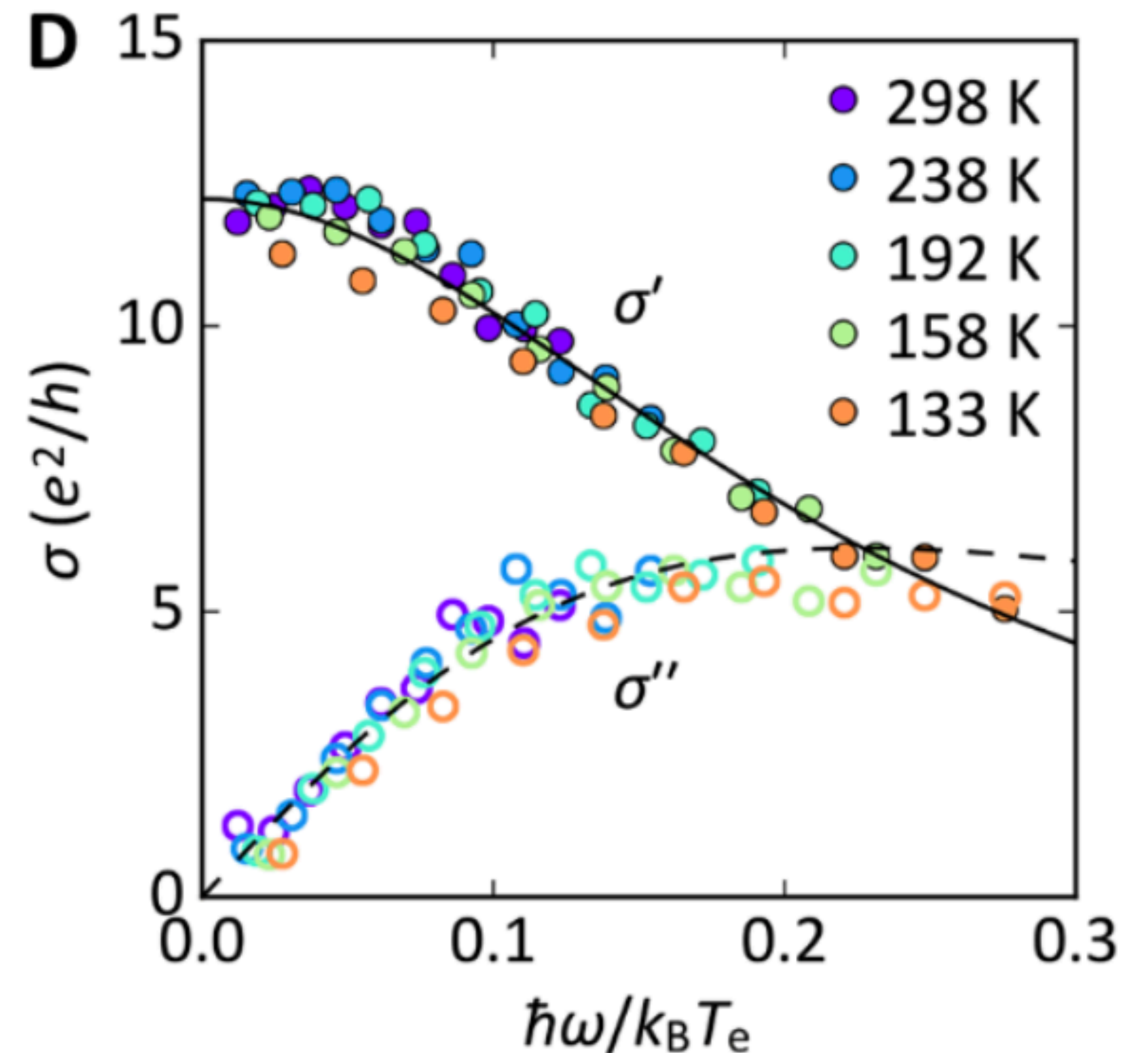
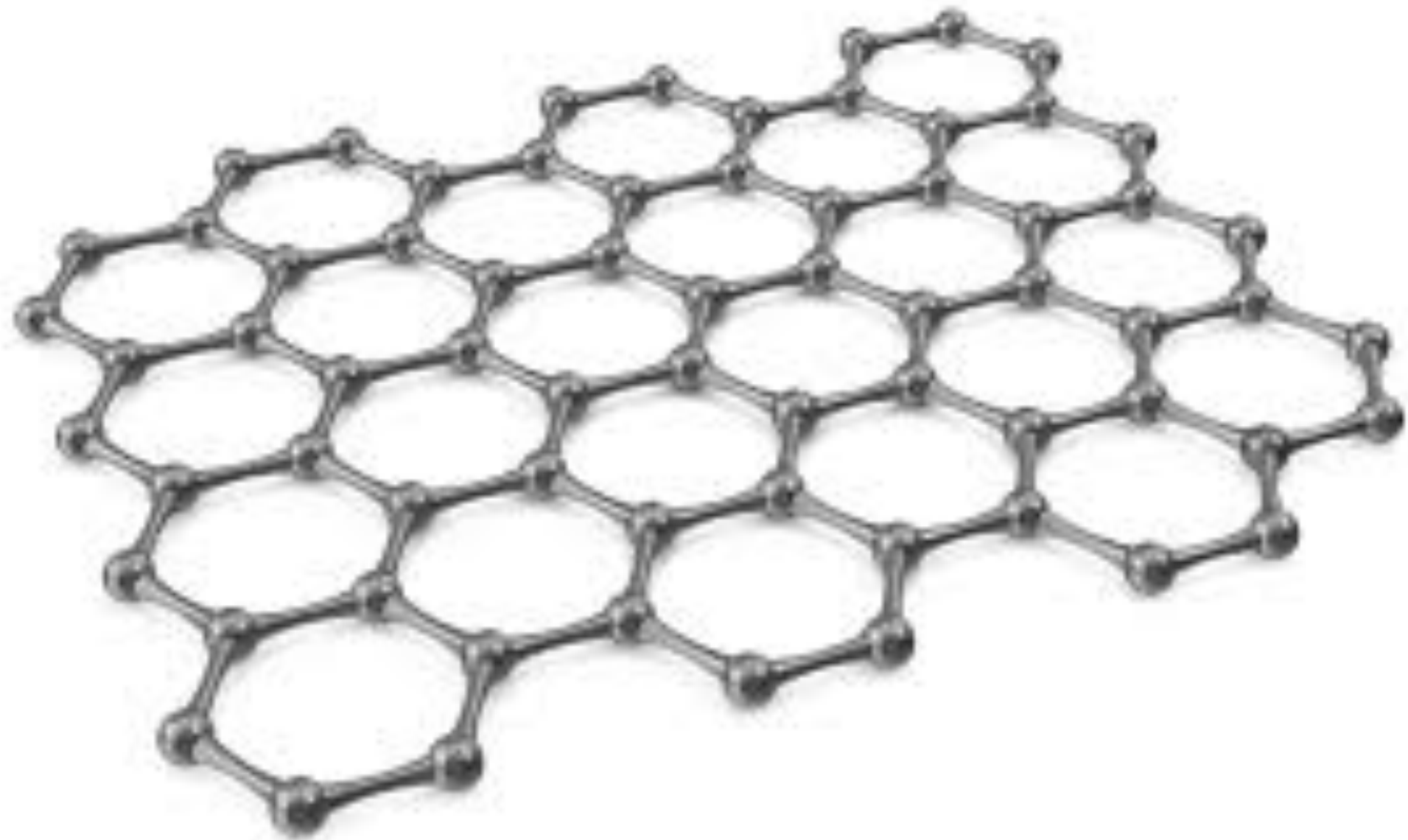
So α flows logarithmically slowly to zero, as the temperature is lowered. At intermediate temperatures, we can view $\alpha \approx \text{constant}$, and then graphene behaves like a CFT3.

Quantum-critical conductivity of the Dirac fluid in graphene

Science **364**, 158 (2019)

Patrick Gallagher^{1,2}, Chan-Shan Yang^{1,3}, Tairu Lyu¹, Fanglin Tian^{1,4}, Rai Kou¹,
Hai Zhang^{1,5}, Kenji Watanabe⁶, Takashi Taniguchi⁶, Feng Wang^{1,2,7*}

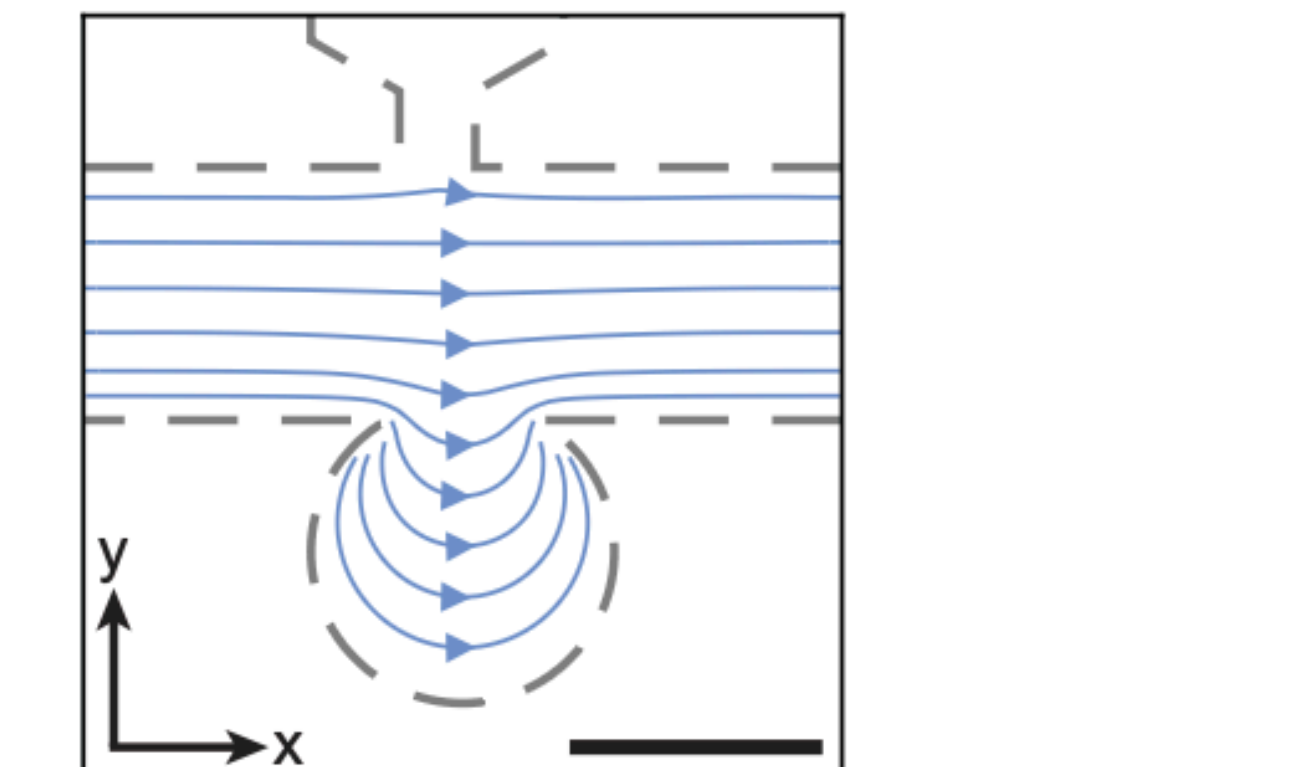
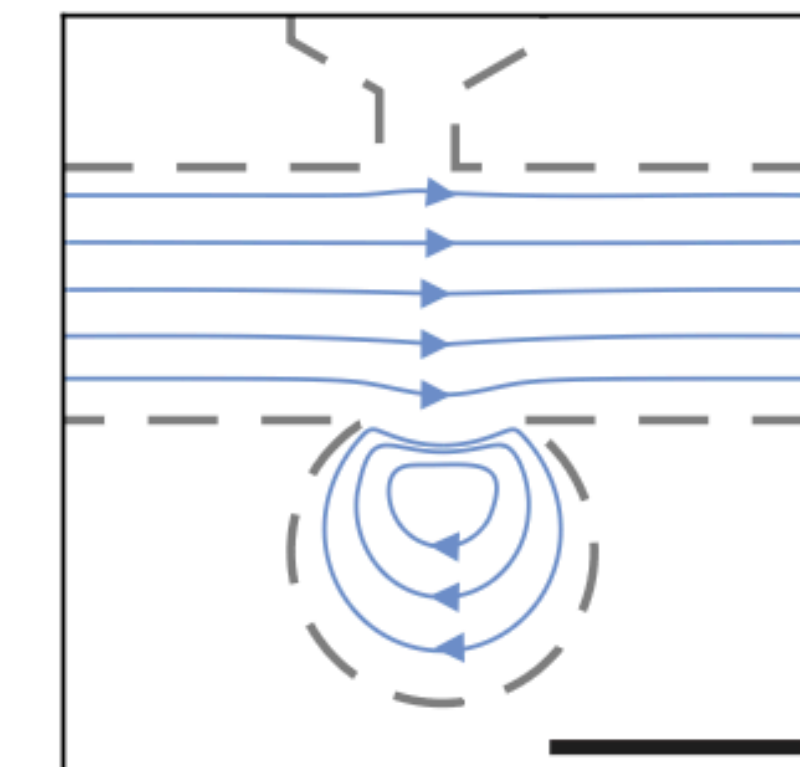
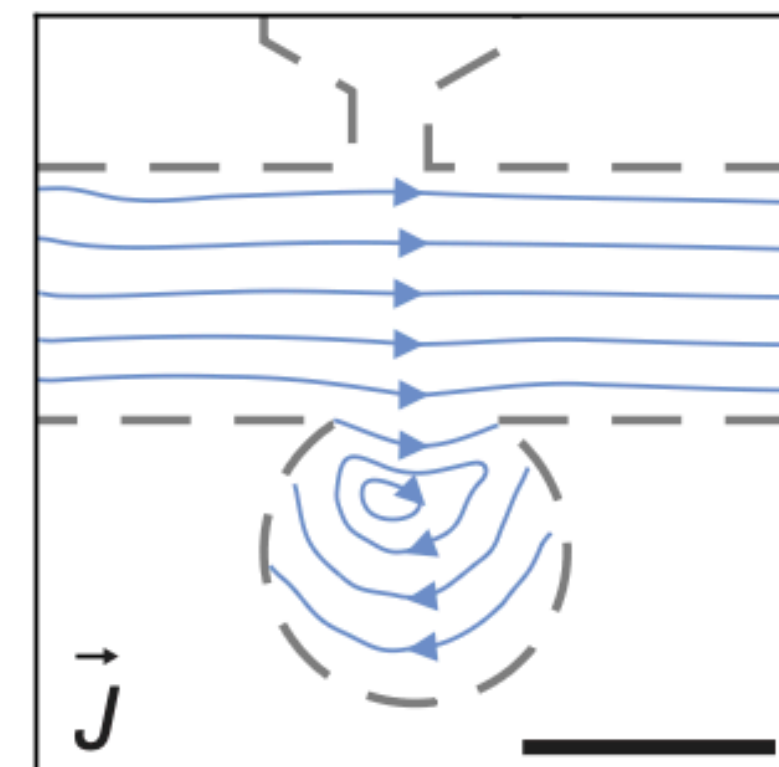
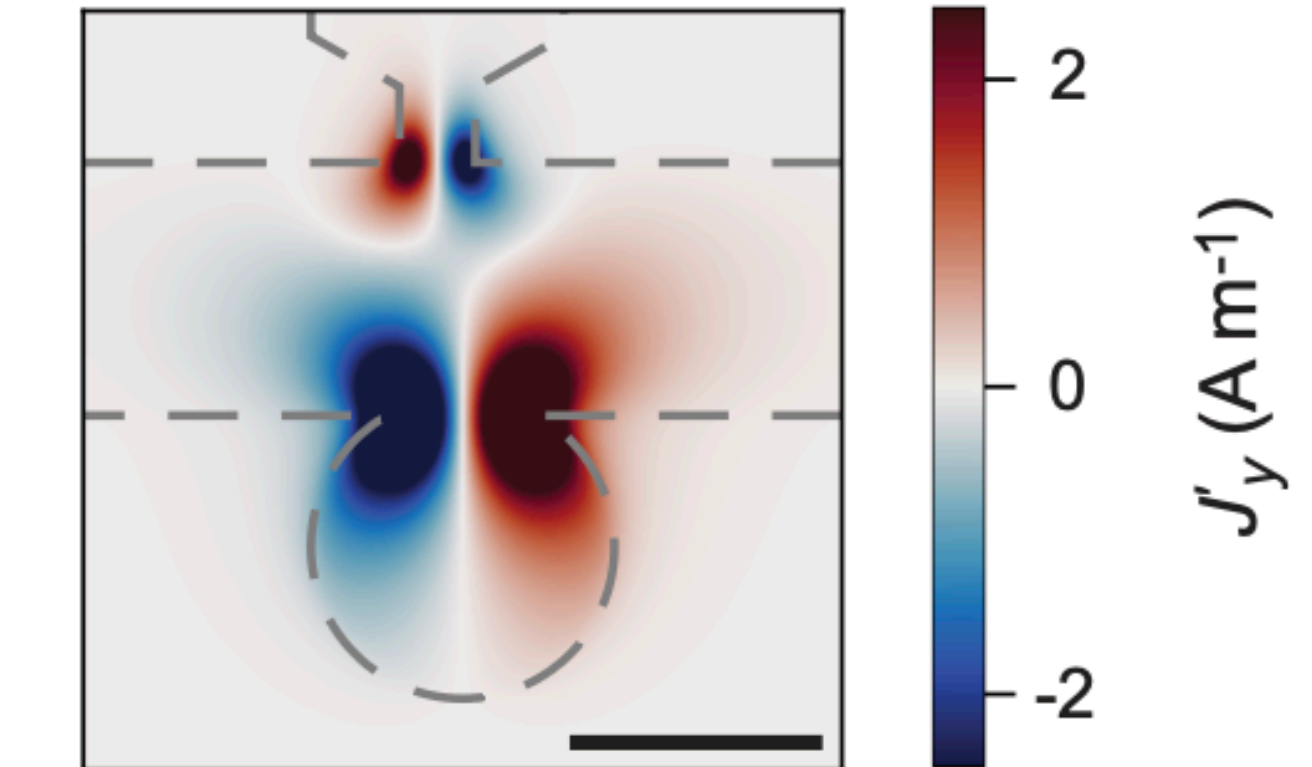
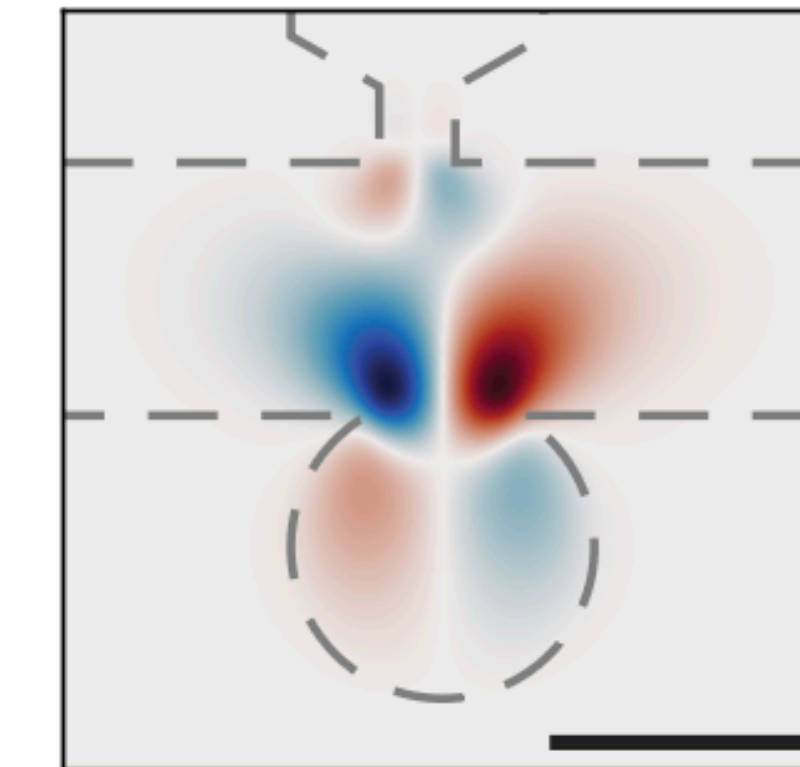
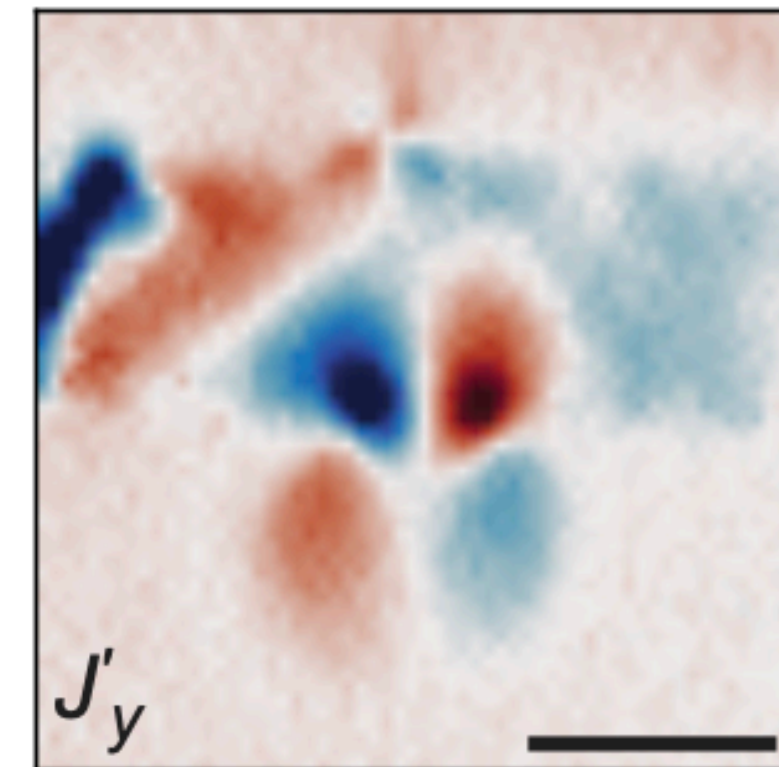
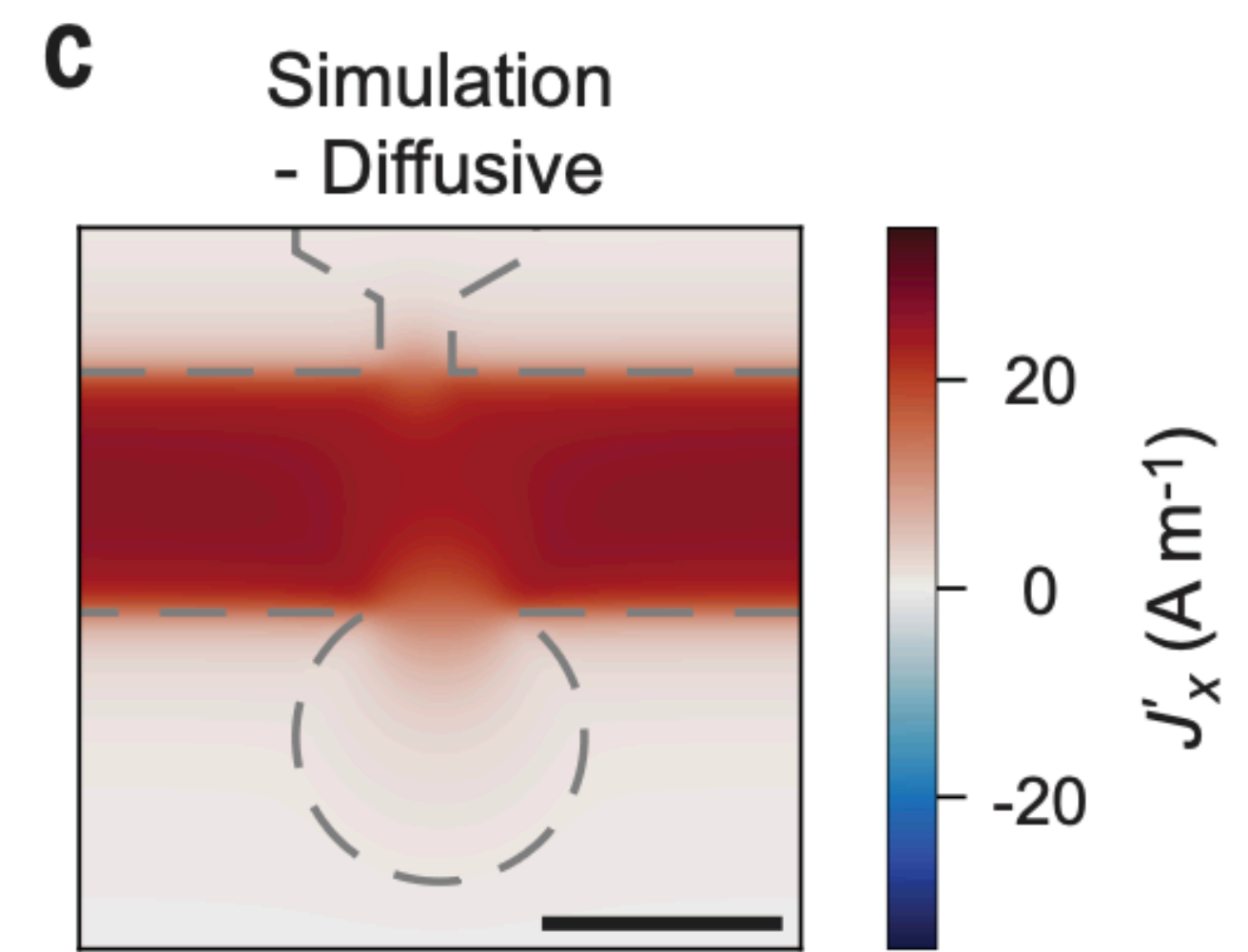
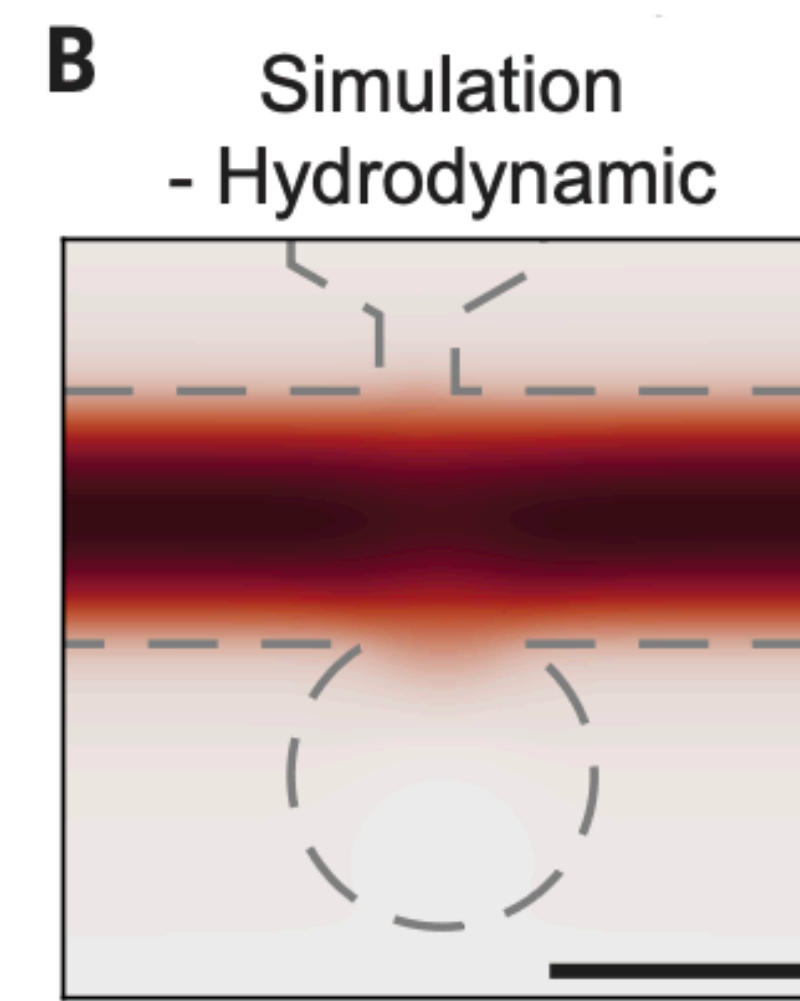
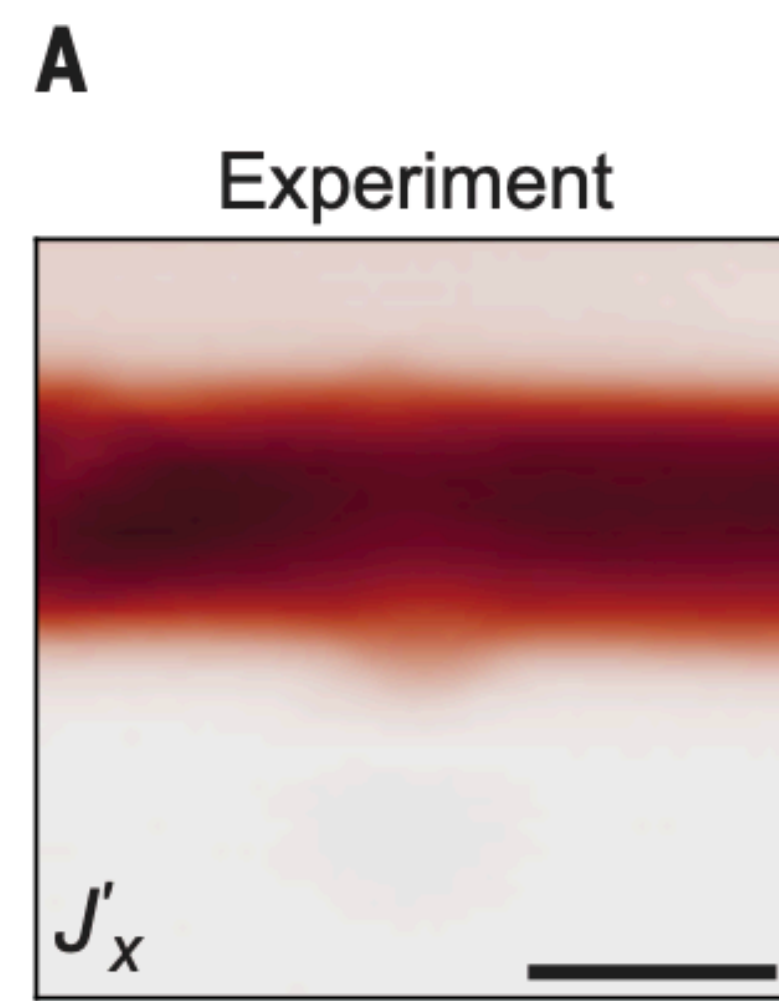
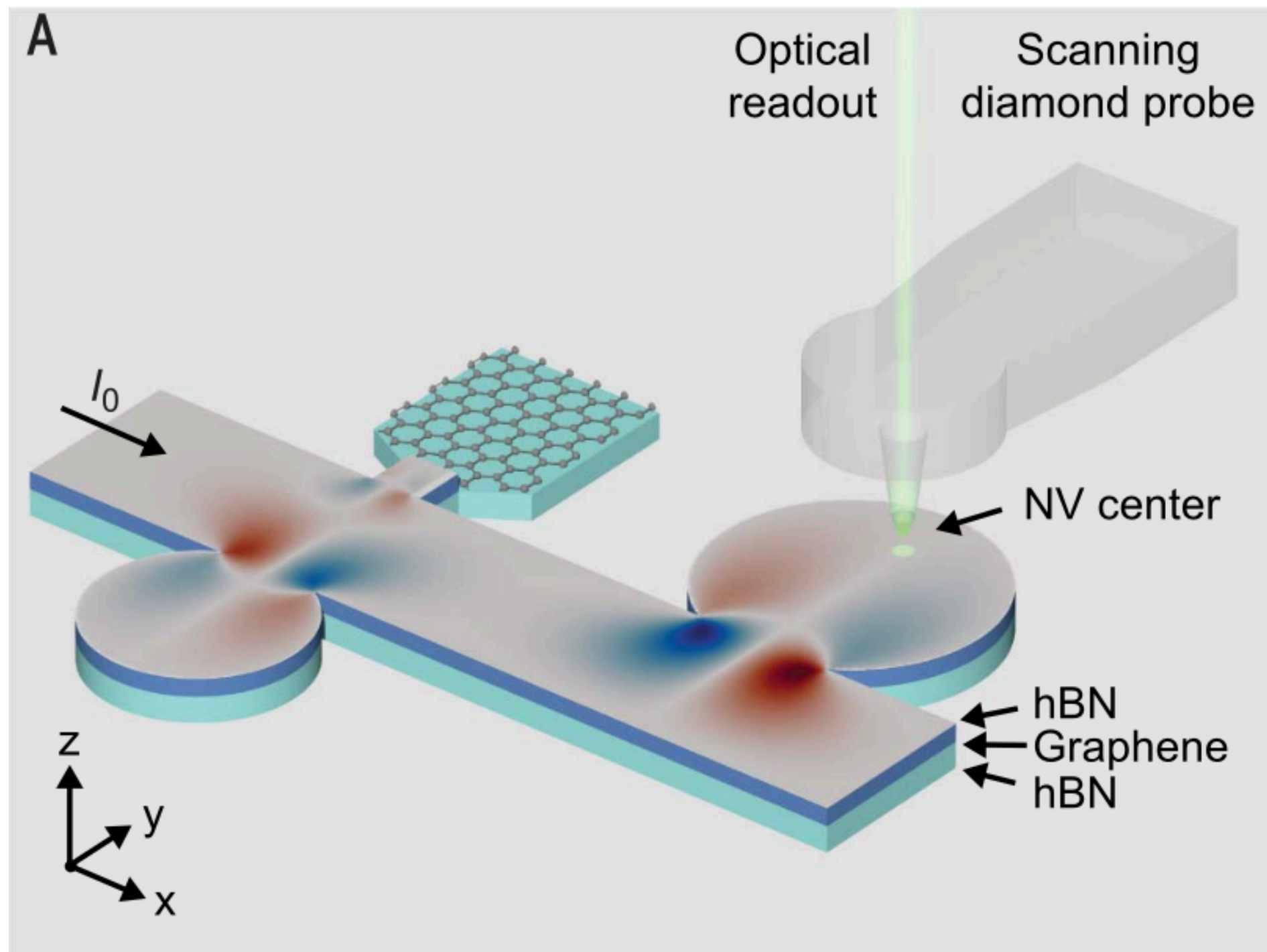
$$\sigma = \frac{e^2}{h} \mathcal{F} \left(\frac{\hbar\omega}{k_B T} \right)$$



Observation of current whirlpools in graphene at room temperature

Marius L. Palm, Chaoxin Ding,
William S. Huxter, Takashi Taniguchi,
Kenji Watanabe, Christian L. Degen

Science **384**, 465 (2024)



1. Hubbard model on the honeycomb lattice:
hydrodynamics in graphene and related materials
2. SYK as a solvable model of quantum matter
without quasiparticles
3. Hubbard model on the square lattice:
spin density wave order, and a universal theory
of strange metals from spatially random interactions.
4. Spin liquids, Fractionalized Fermi liquids (FL*)
and the cuprate phase diagram:
observation of the Yamaji effect.

SYK as a solvable model of quantum matter without quasiparticles

School on Emergent Phenomena in
Non-Equilibrium Quantum Many-Body Systems
ICTP-SAIFR

São Paulo, Brazil
November 3,4 2025

Subir Sachdev



A simple model of a metal with quasiparticles

$$H = \frac{1}{(N)^{1/2}} \sum_{i,j=1}^N t_{ij} c_i^\dagger c_j - \mu \sum_i c_i^\dagger c_i$$

$$c_i c_j + c_j c_i = 0 \quad , \quad c_i c_j^\dagger + c_j^\dagger c_i = \delta_{ij}$$

$$\frac{1}{N} \sum_i c_i^\dagger c_i = \mathcal{Q}$$

t_{ij} are independent random variables with $\overline{t_{ij}} = 0$ and $\overline{|t_{ij}|^2} = t^2$

A simple model of a metal with quasiparticles

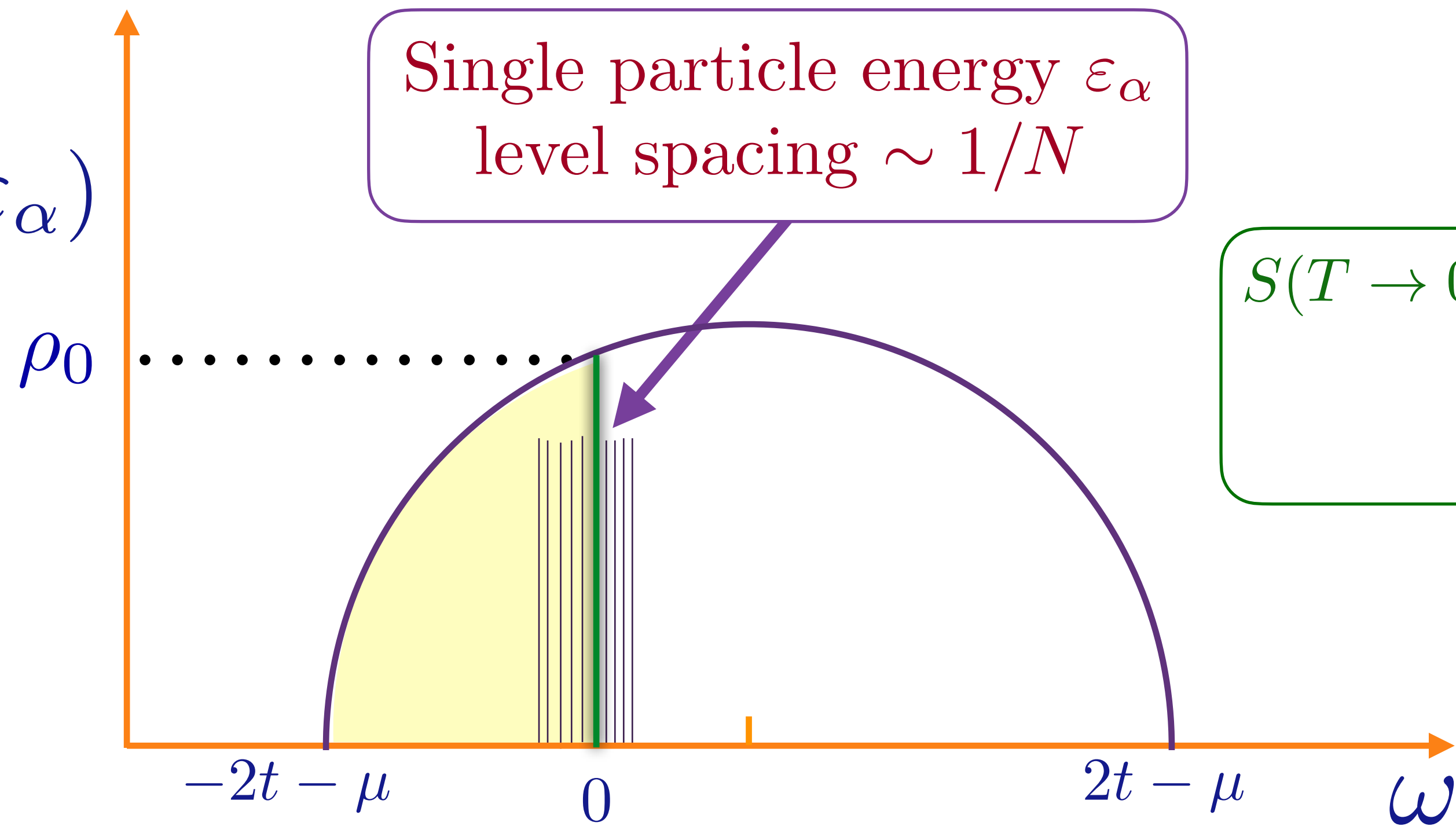
Feynman graph expansion in $t_{ij..}$, and graph-by-graph average, yields exact equations in the large N limit:

$$G(\tau) \equiv -T_\tau \left\langle c_i(\tau) c_i^\dagger(0) \right\rangle$$
$$G(i\omega) = \frac{1}{i\omega + \mu - \Sigma(i\omega)} \quad , \quad \Sigma(\tau) = t^2 G(\tau)$$
$$G(\tau = 0^-) = Q.$$

$G(\omega)$ can be determined by solving a quadratic equation.

A simple model of a metal with quasiparticles

$$\rho(\omega) = \frac{1}{N} \sum_{\alpha} \delta(\omega - \varepsilon_{\alpha})$$

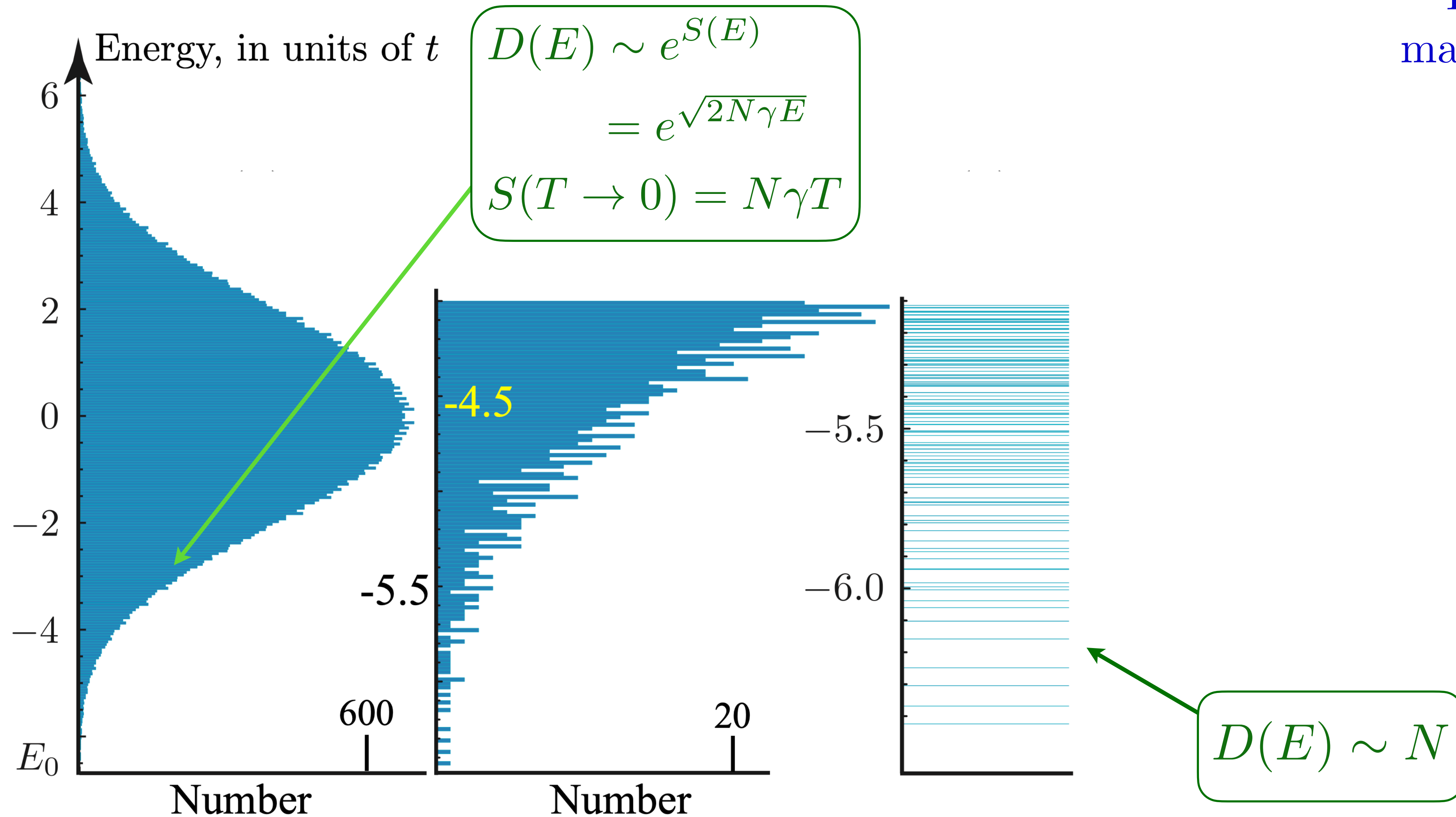


$$S(T \rightarrow 0) = N\gamma T$$
$$\gamma = \frac{\pi^2}{3} \rho_0$$

Many-body density of states

$$D(E) = \sum_i \delta(E - E_i); \quad E_0 + E_i \Rightarrow \text{Many body eigenvalue}$$

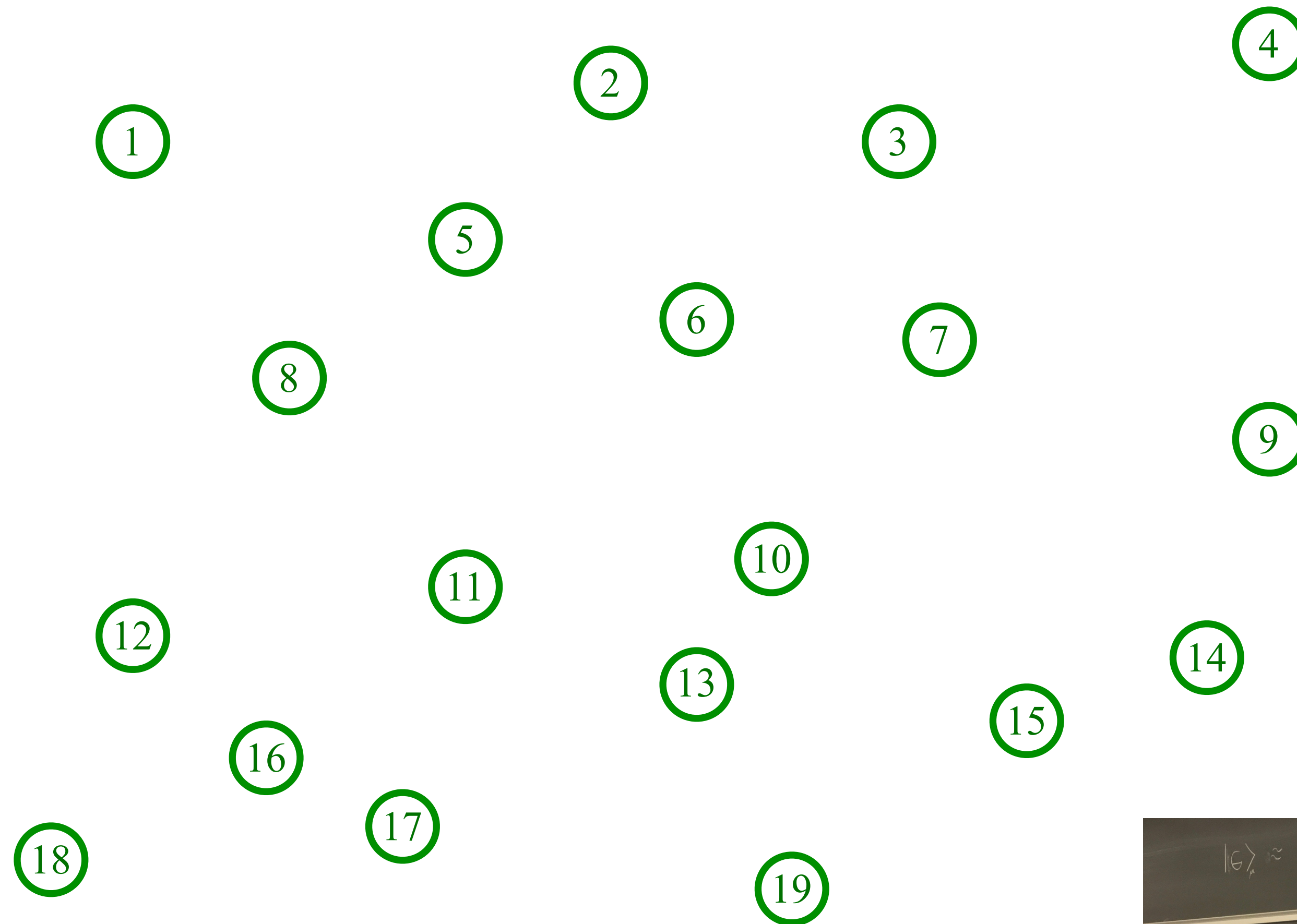
For random
matrix model:
 $E_0 + E_i =$
 $\sum_{\alpha} n_{\alpha} \varepsilon_{\alpha}$
 $n_{\alpha} = 0, 1,$
occupation
number



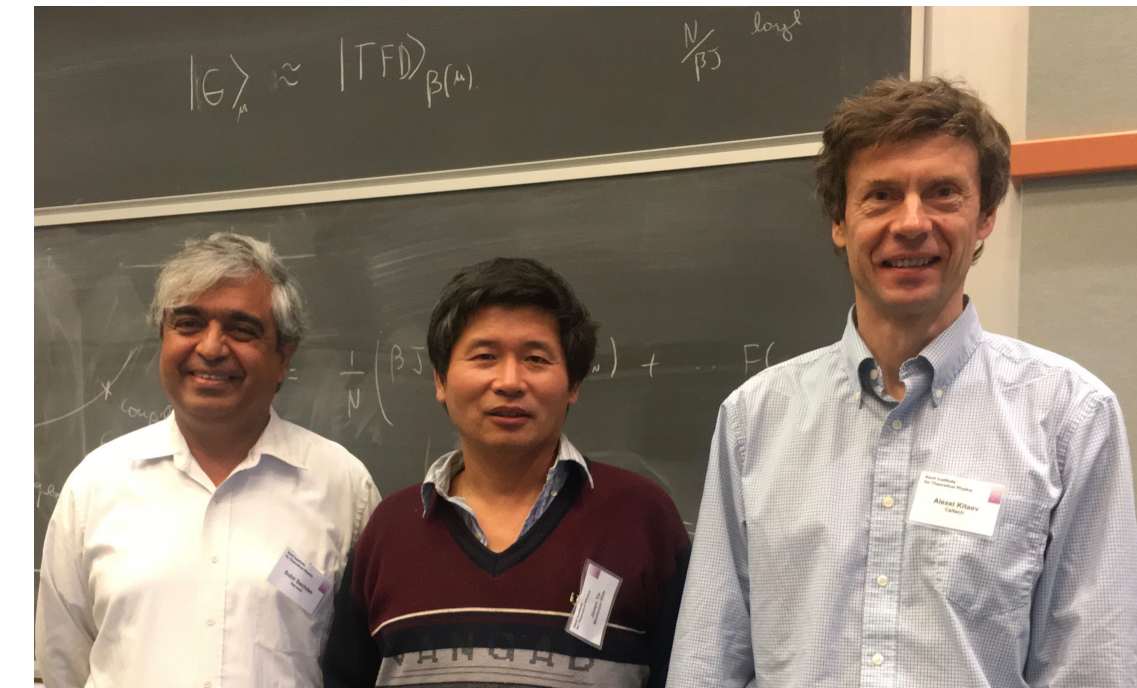
Random matrix model

The SYK model

Sachdev, Ye (1993); Kitaev (2015)

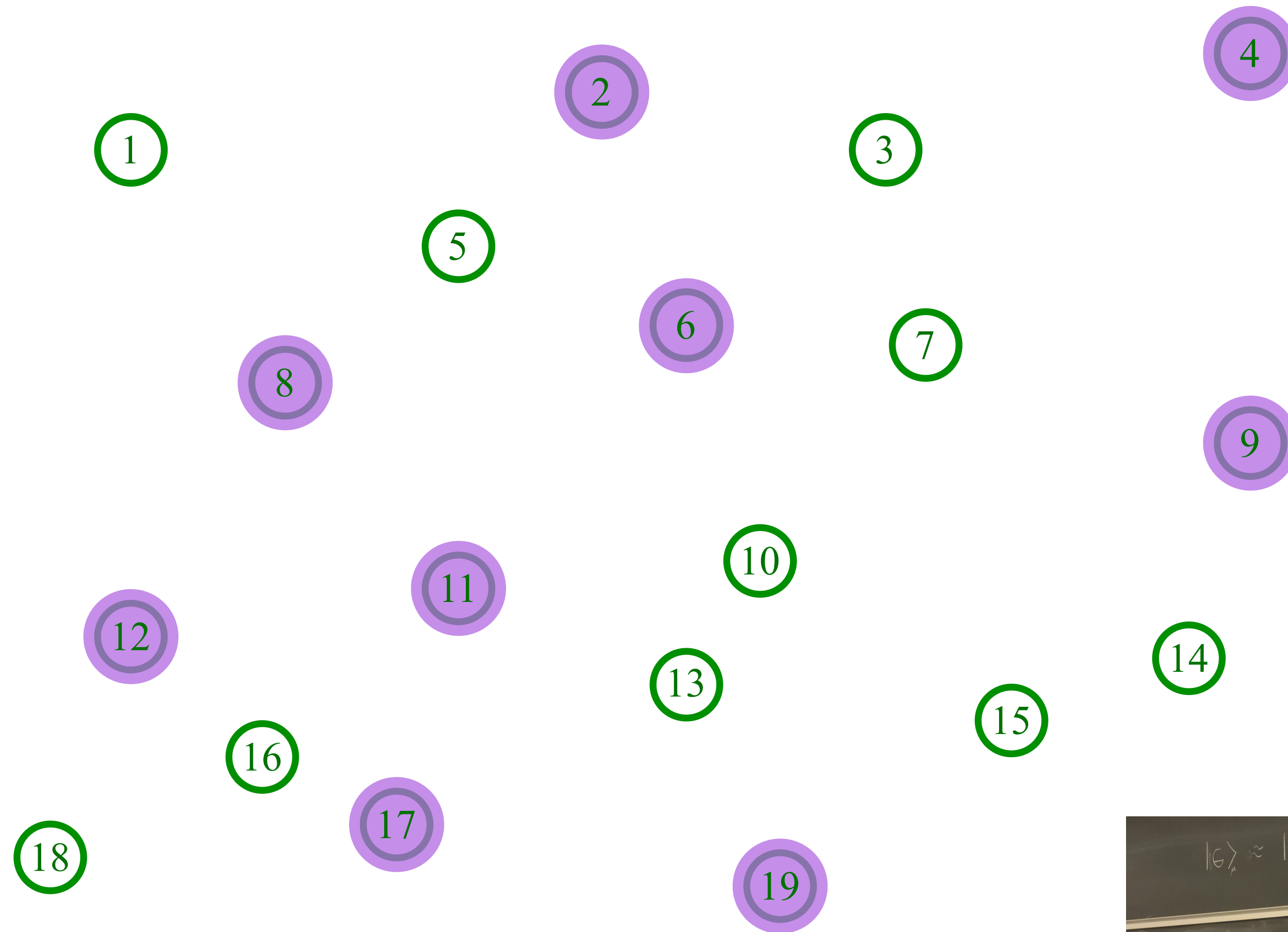


Pick a set of random positions

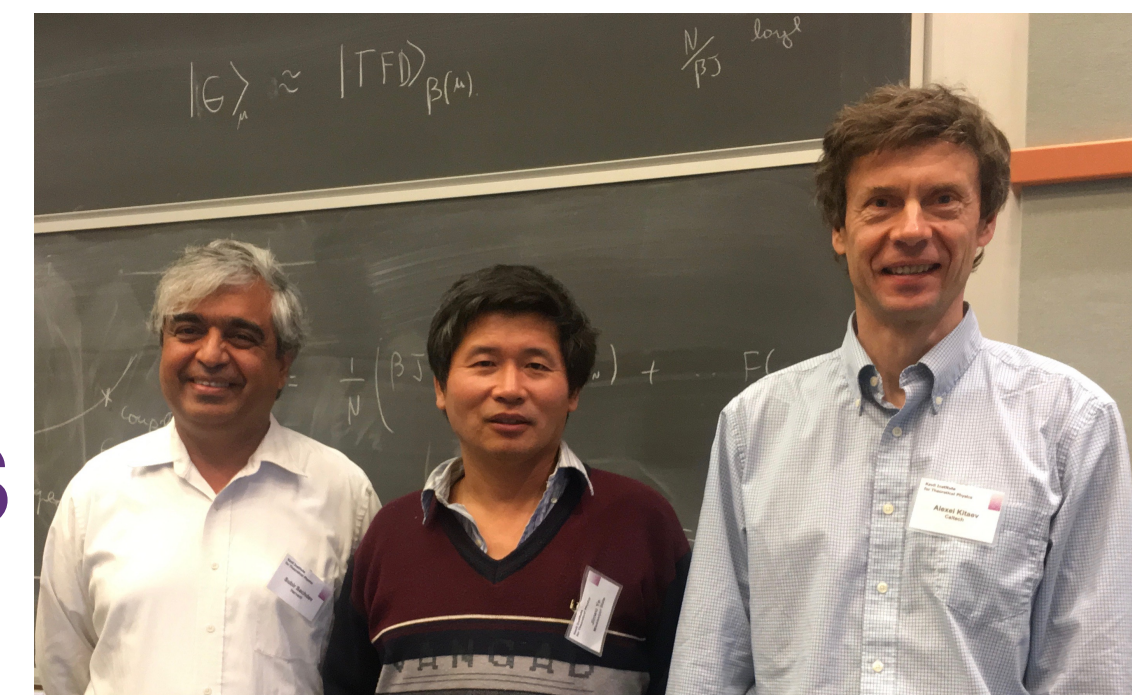


The SYK model

Sachdev, Ye (1993); Kitaev (2015)

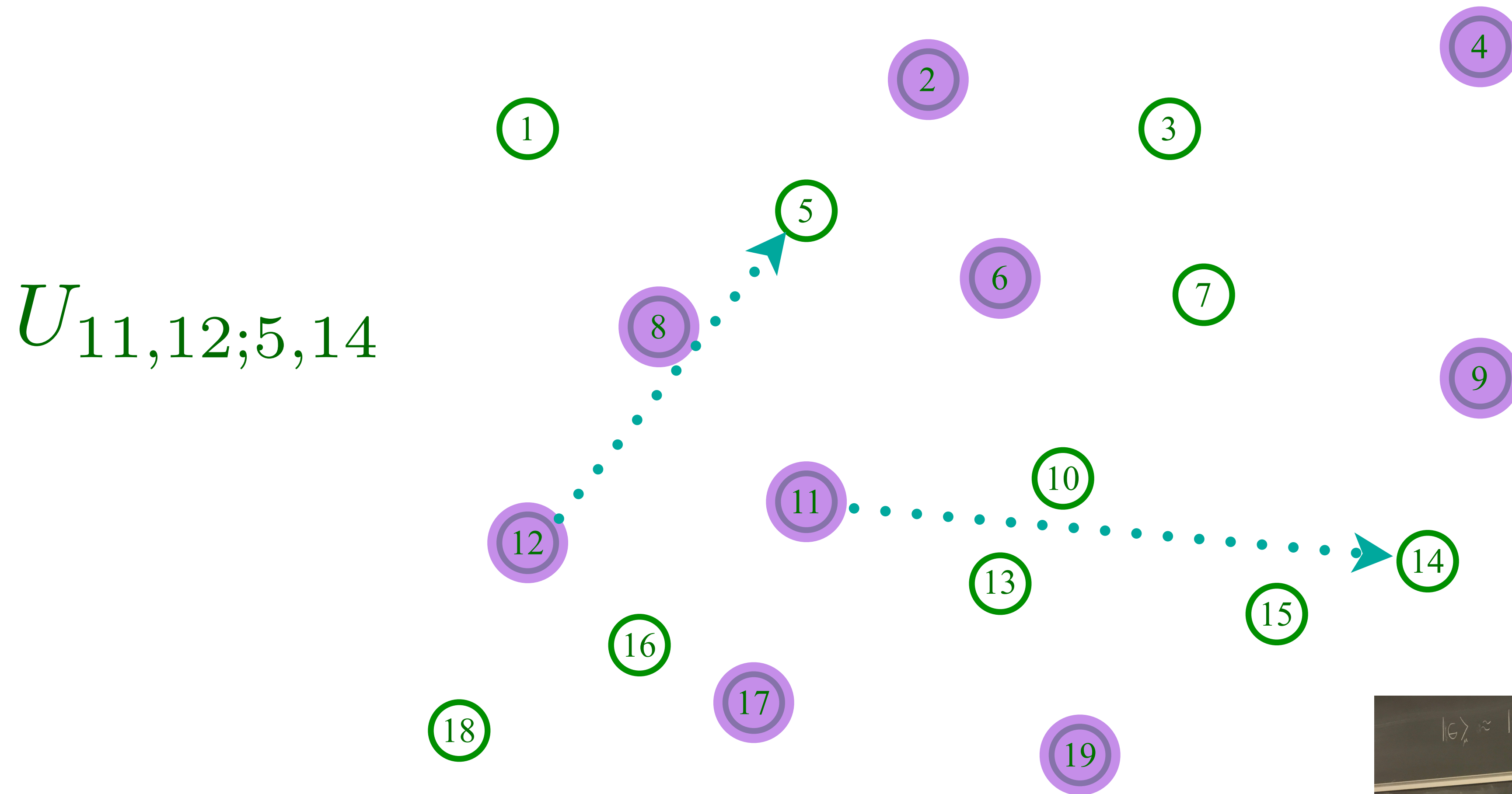


Place electrons randomly on some sites

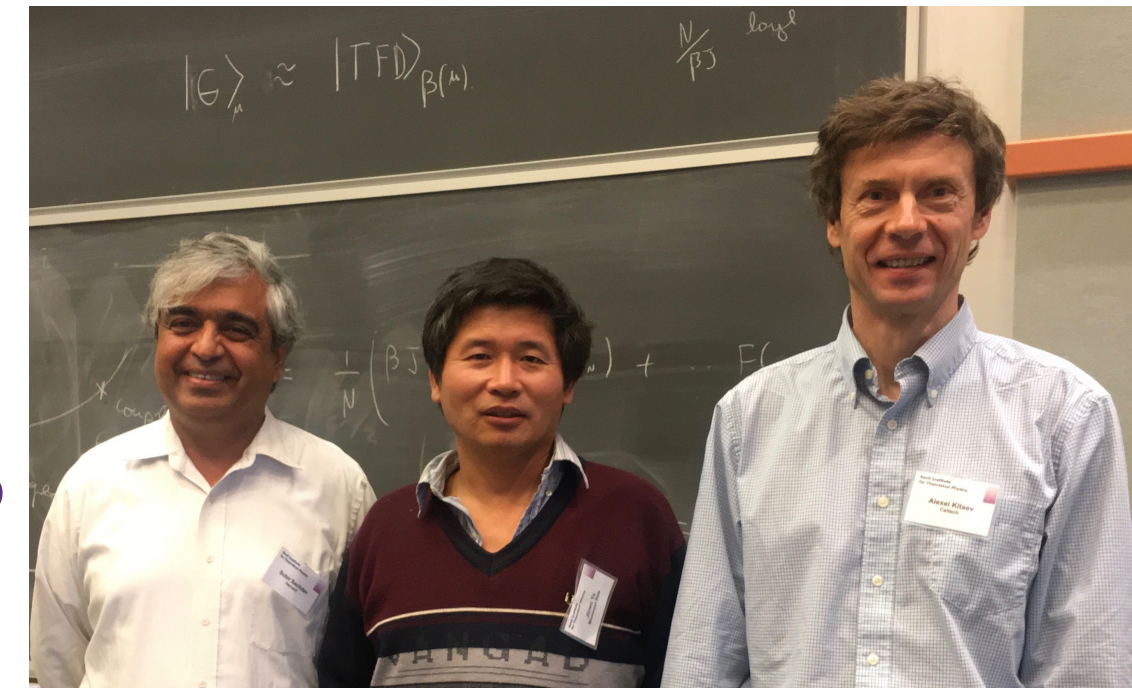


The SYK model

Sachdev, Ye (1993); Kitaev (2015)



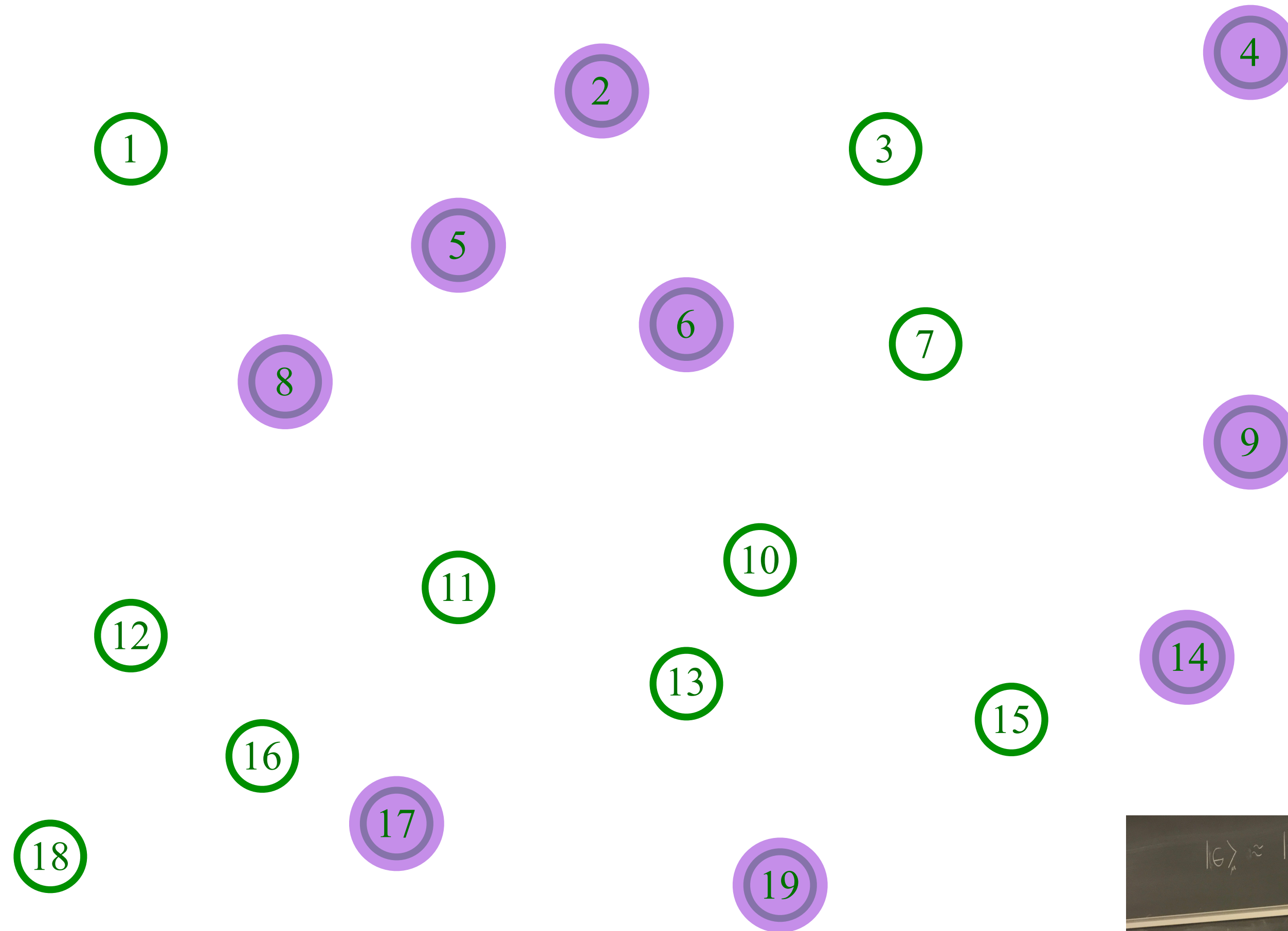
Place electrons randomly on some sites



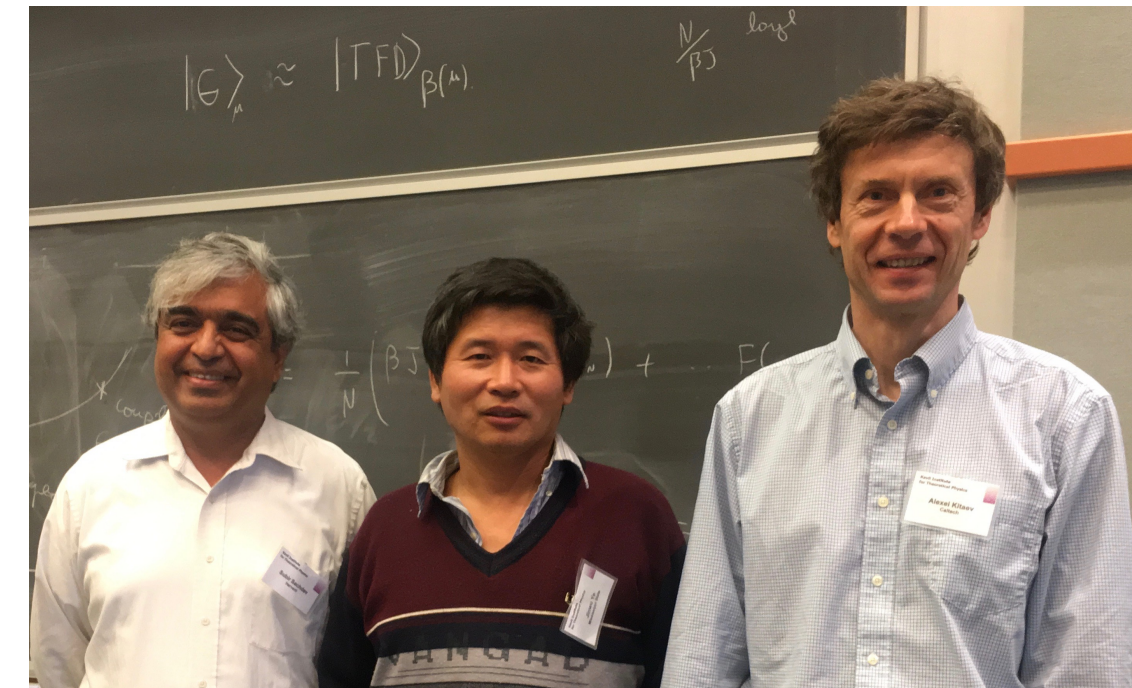
The SYK model

Sachdev, Ye (1993); Kitaev (2015)

$$U_{11,12;5,14}$$

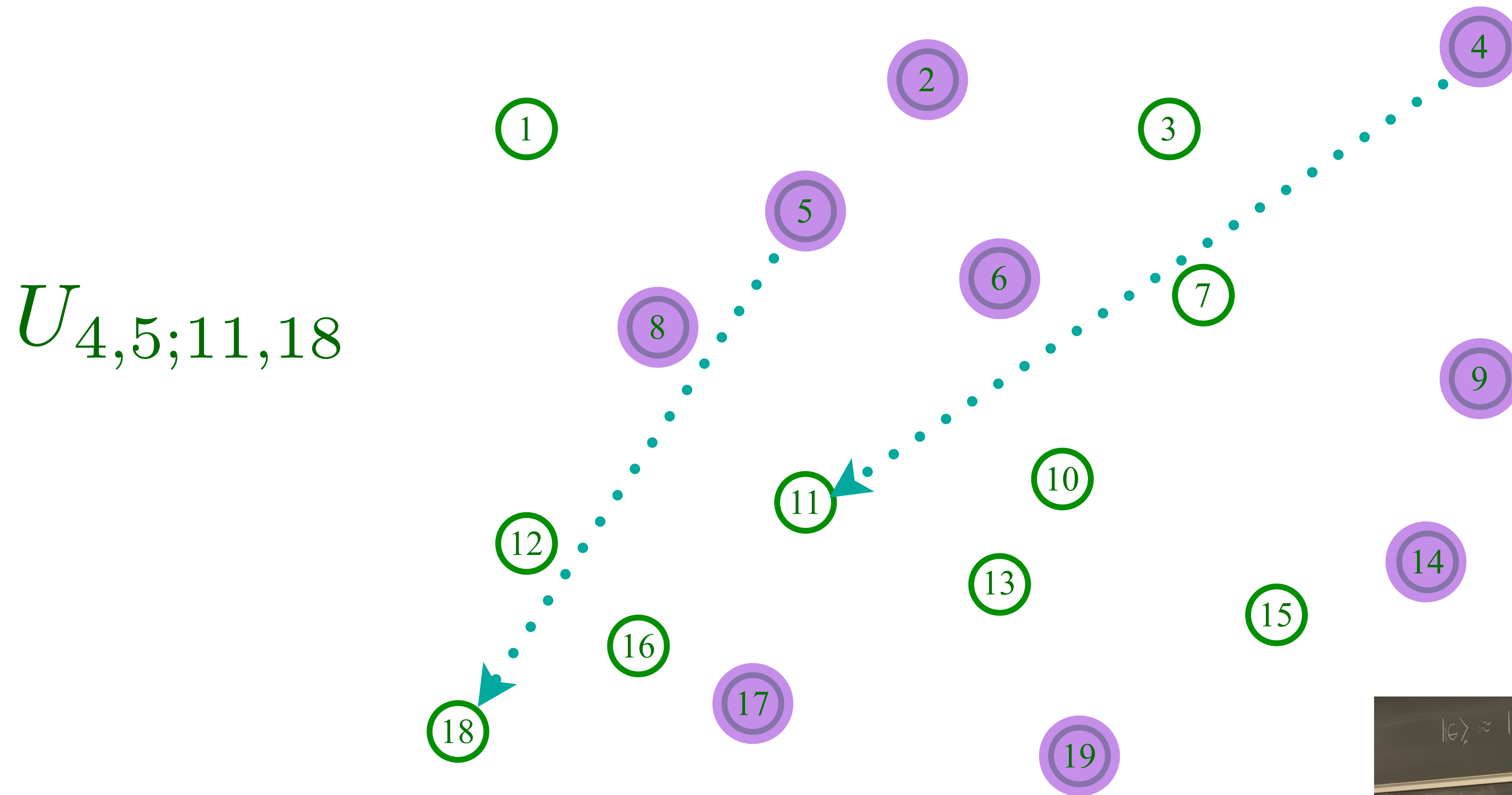


Entangle electrons pairwise randomly

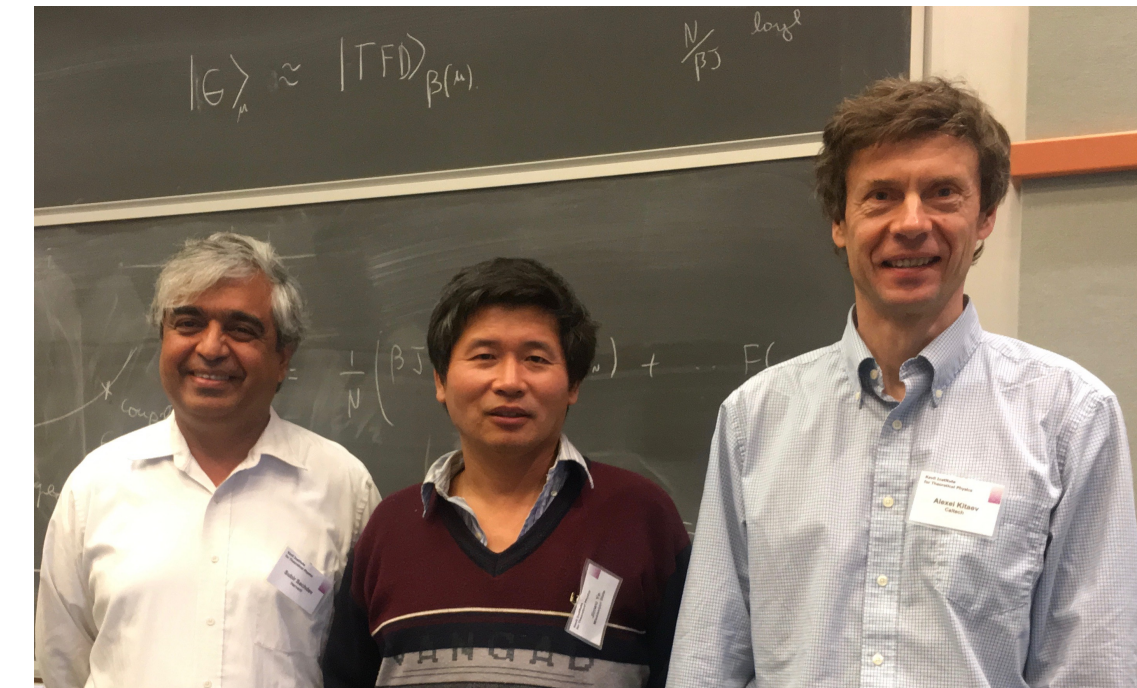


The SYK model

Sachdev, Ye (1993); Kitaev (2015)



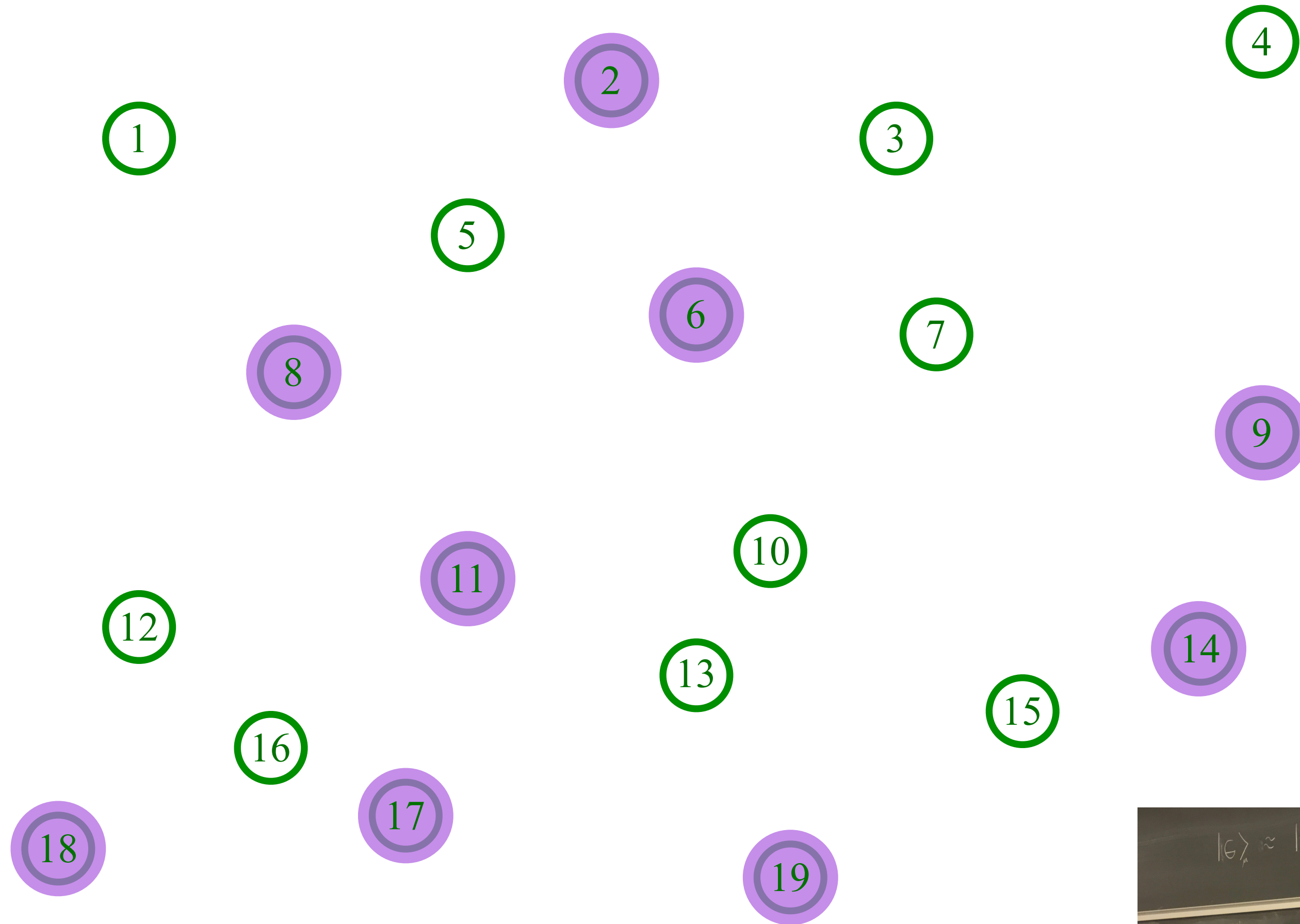
Entangle electrons pairwise randomly



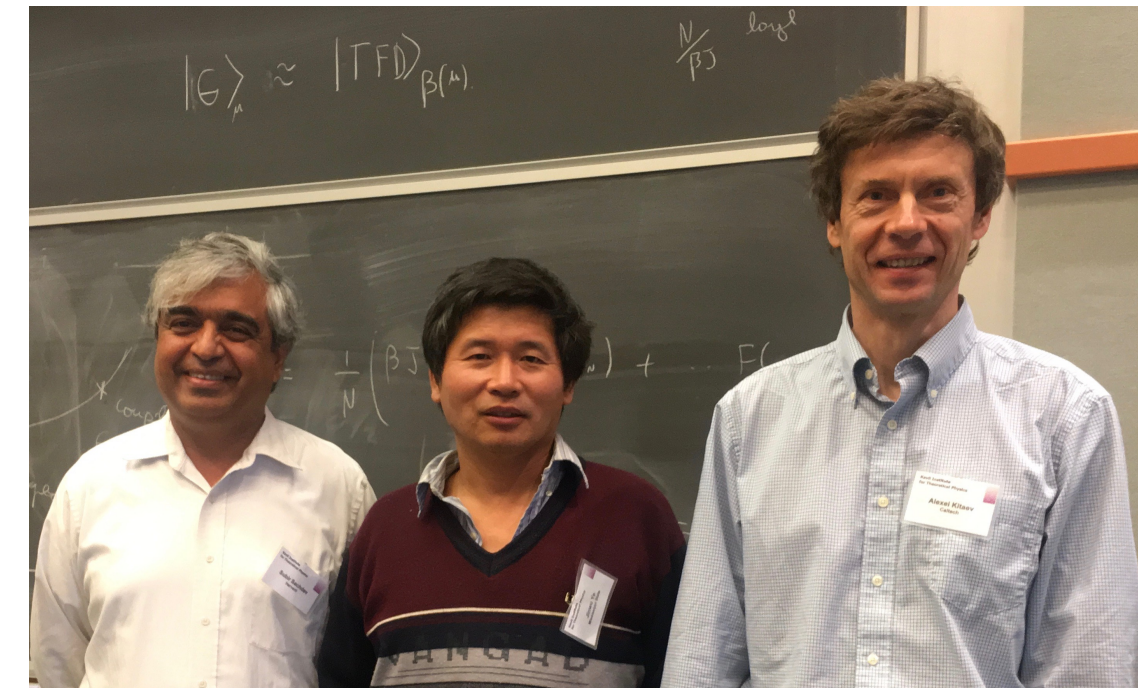
The SYK model

Sachdev, Ye (1993); Kitaev (2015)

$$U_{4,5;11,18}$$

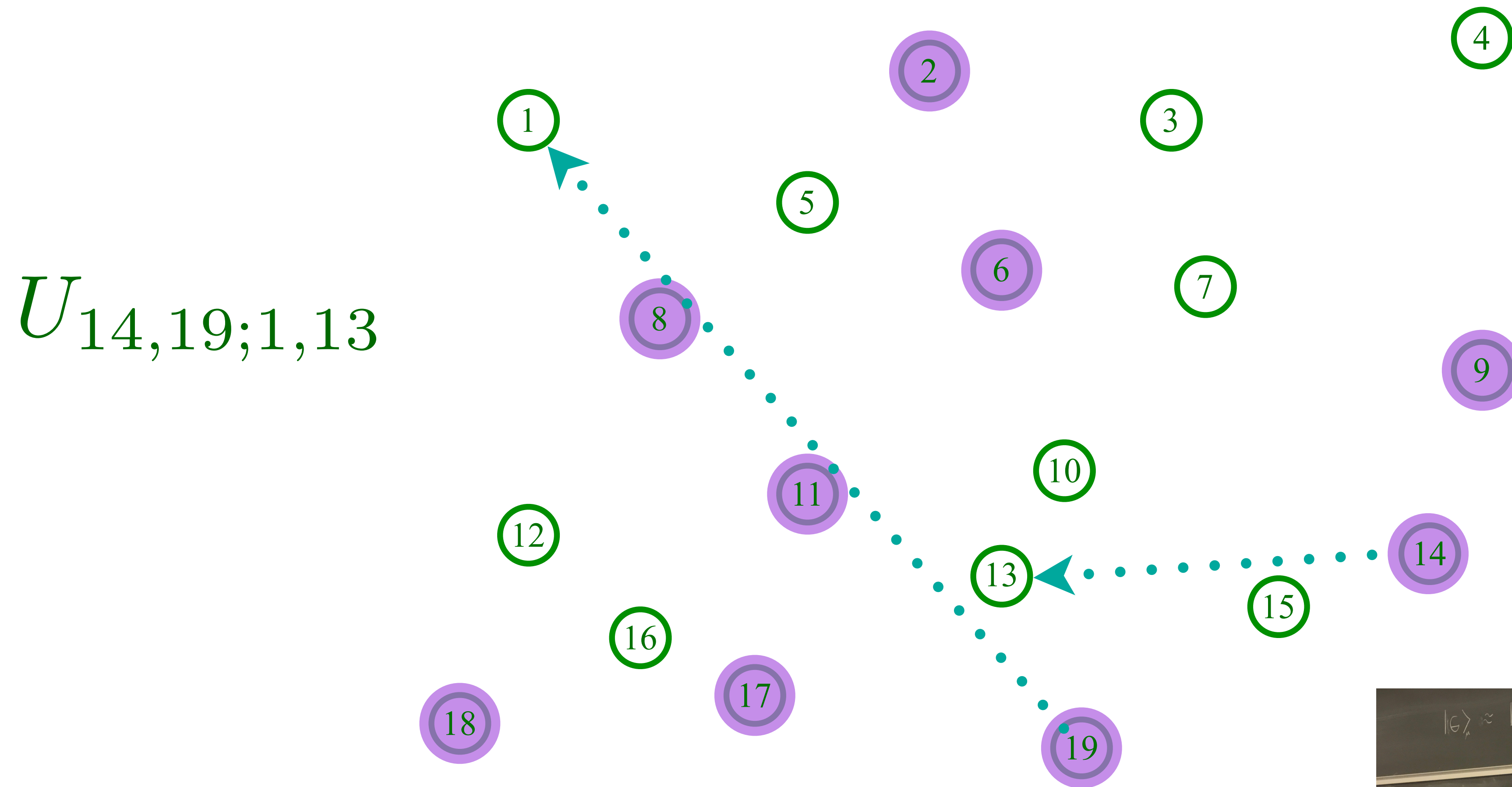


Entangle electrons pairwise randomly

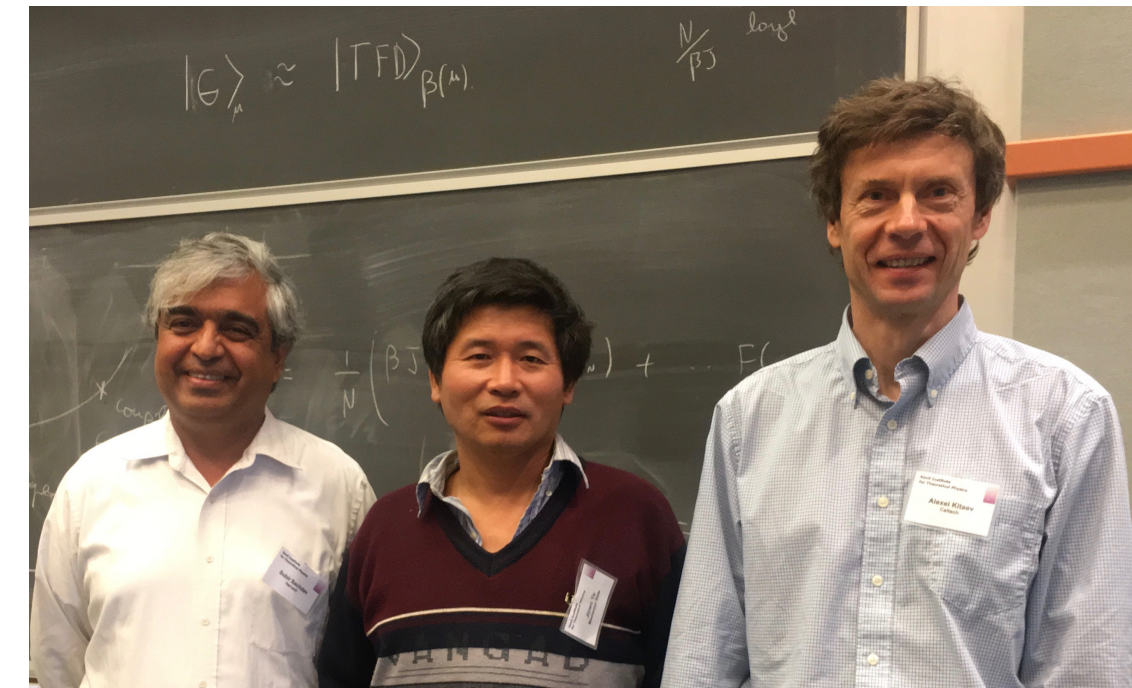


The SYK model

Sachdev, Ye (1993); Kitaev (2015)



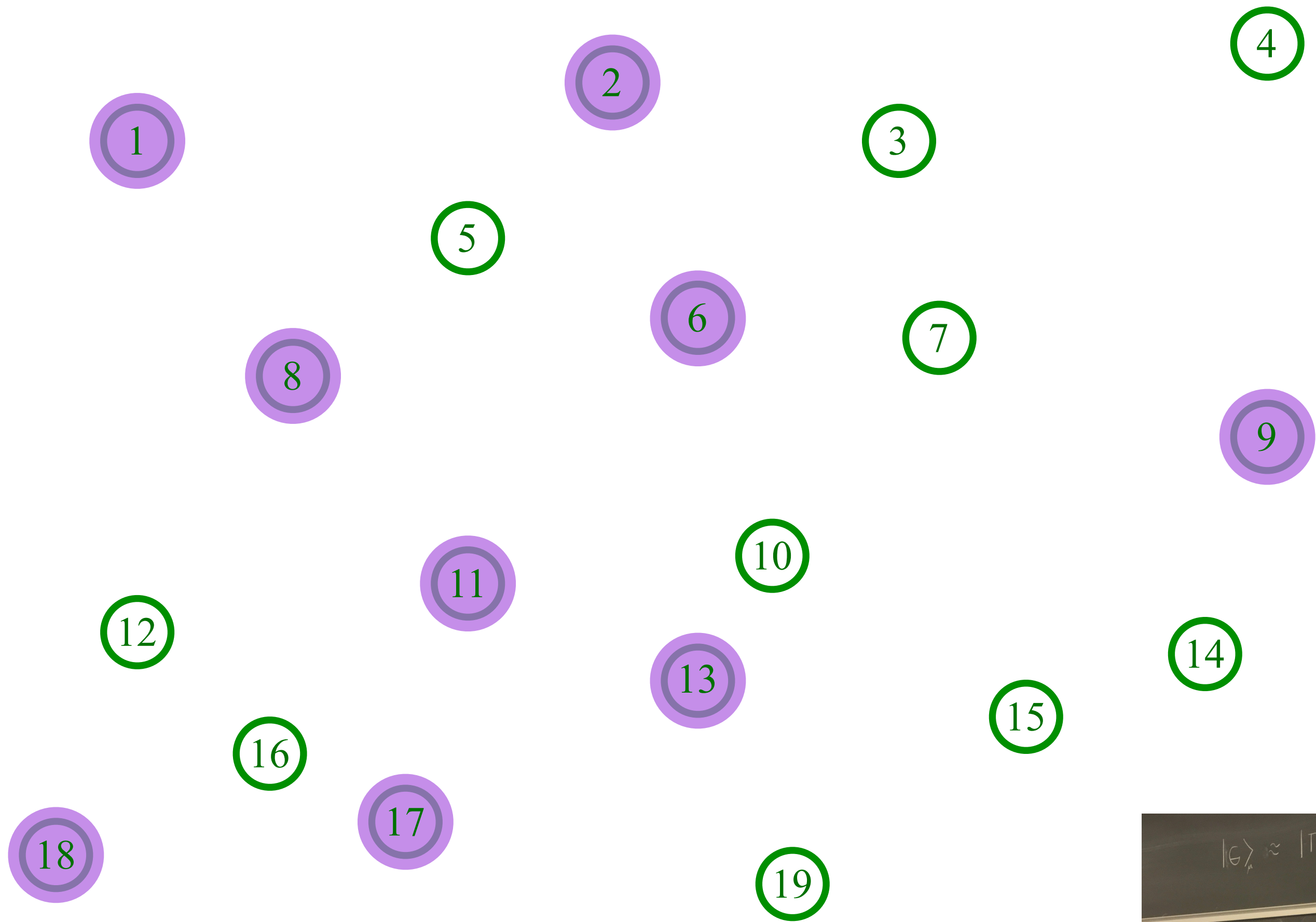
Entangle electrons pairwise randomly



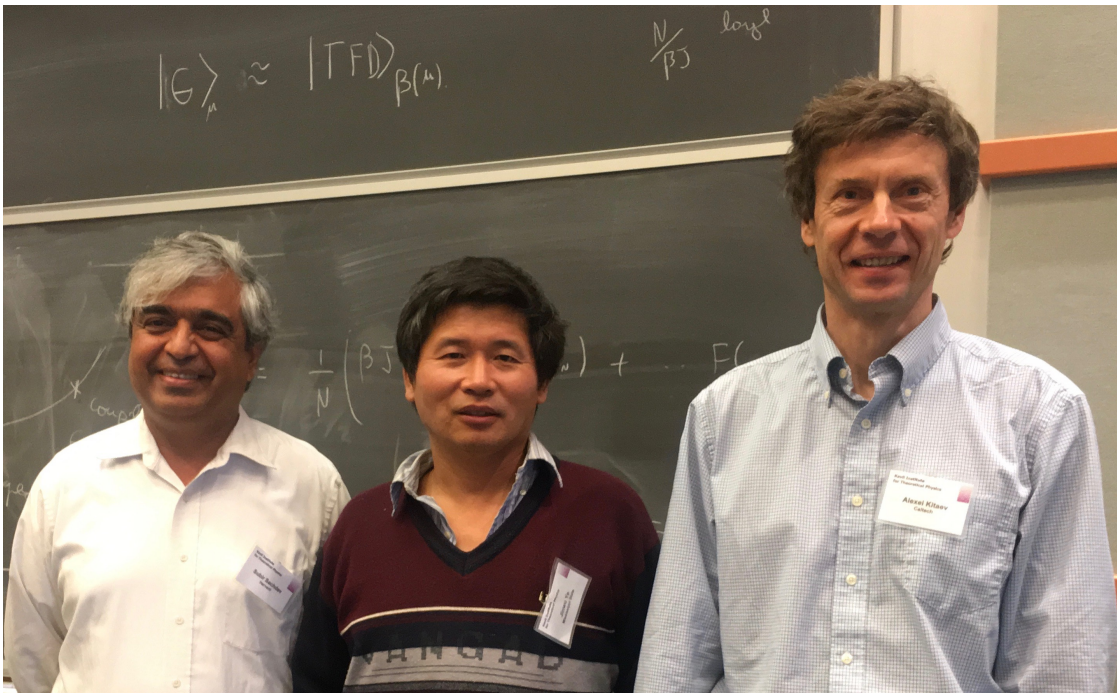
The SYK model

Sachdev, Ye (1993); Kitaev (2015)

$$U_{14,19;1,13}$$



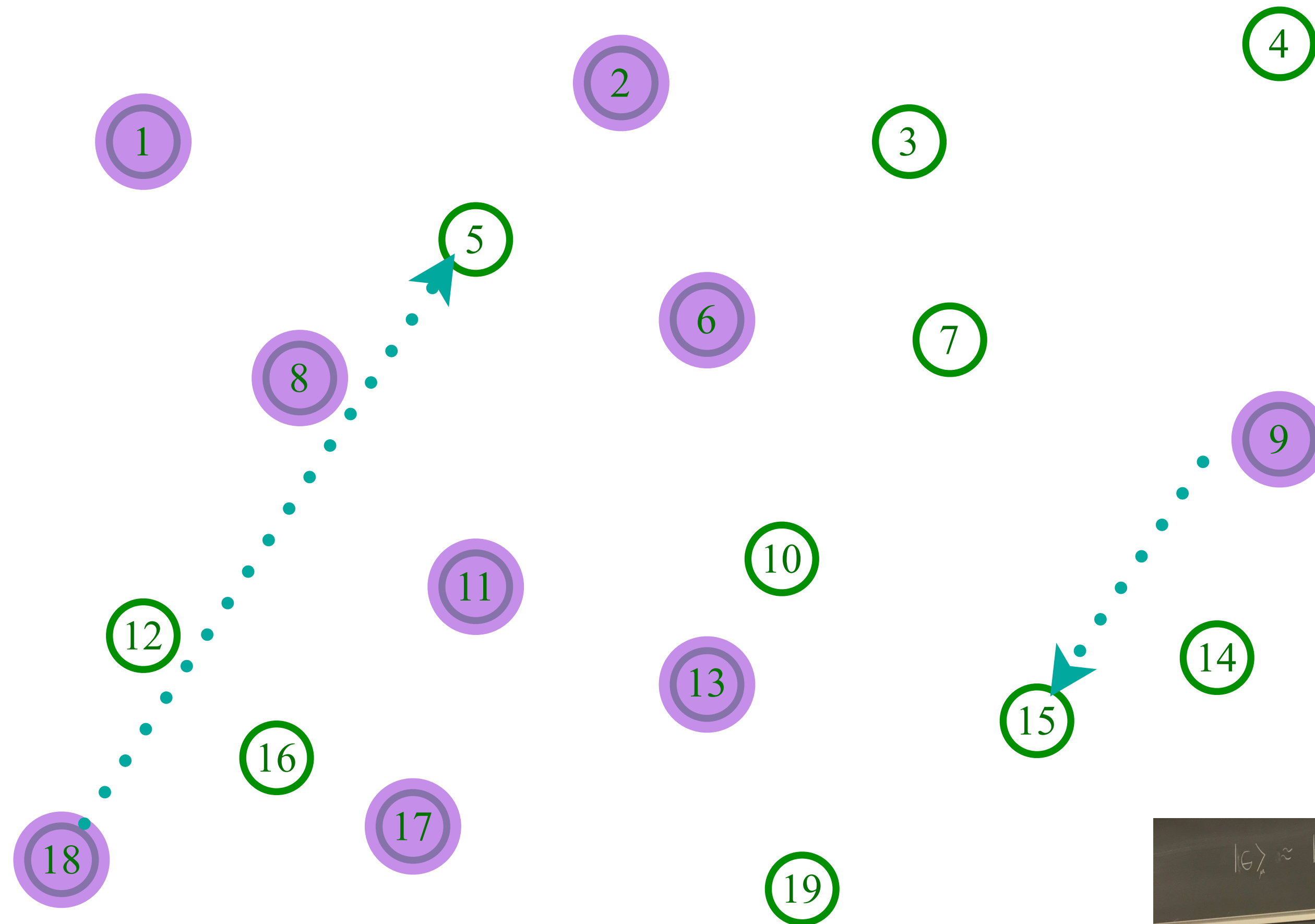
Entangle electrons pairwise randomly



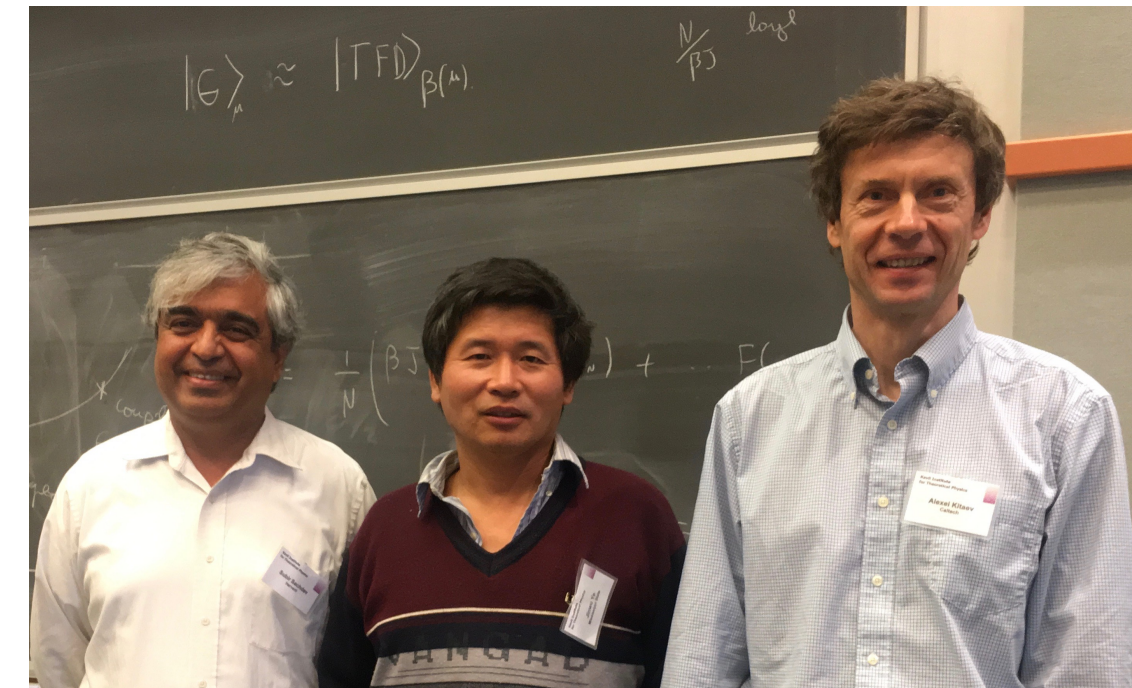
The SYK model

Sachdev, Ye (1993); Kitaev (2015)

$$U_{9,18;5,15}$$



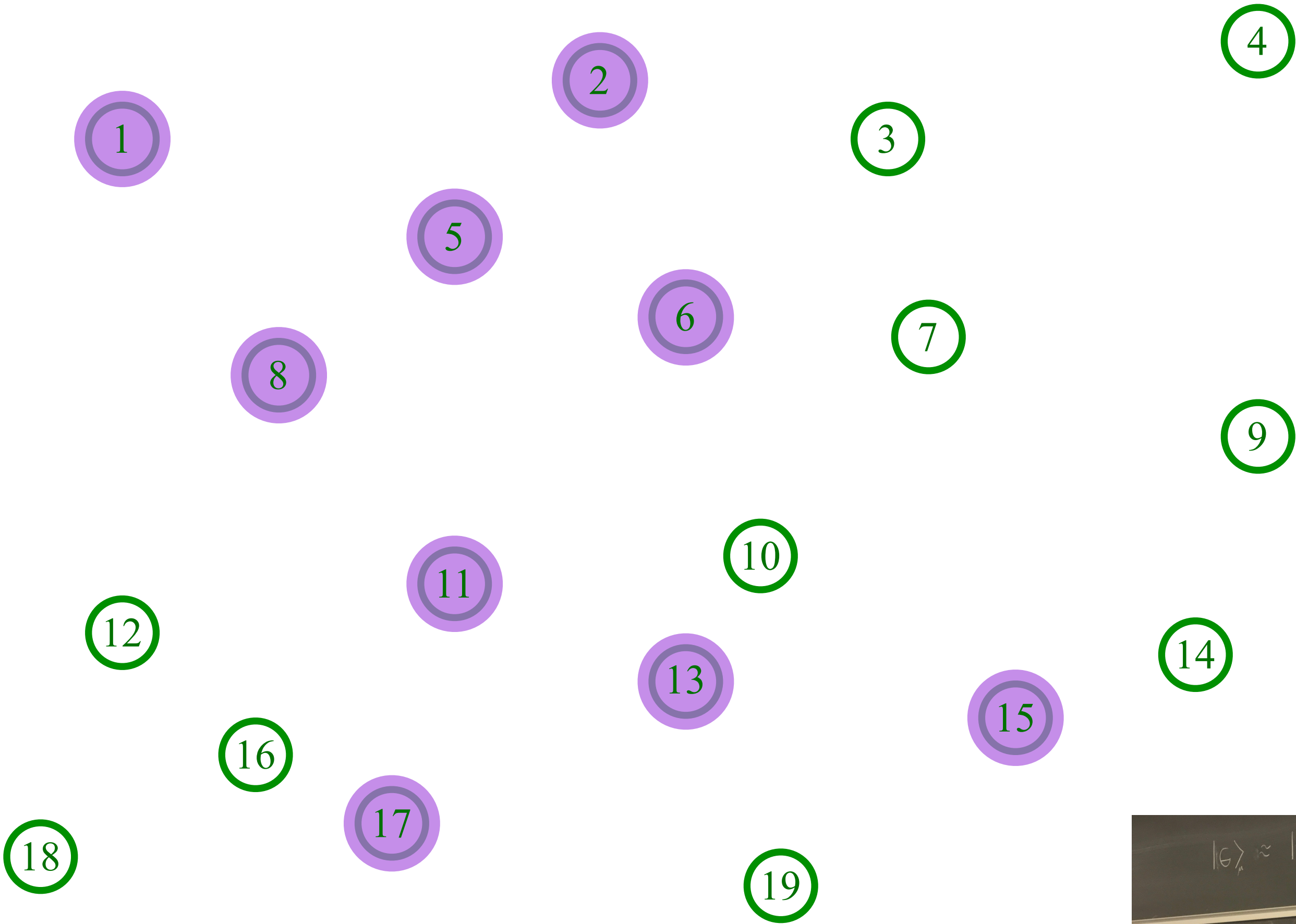
Entangle electrons pairwise randomly



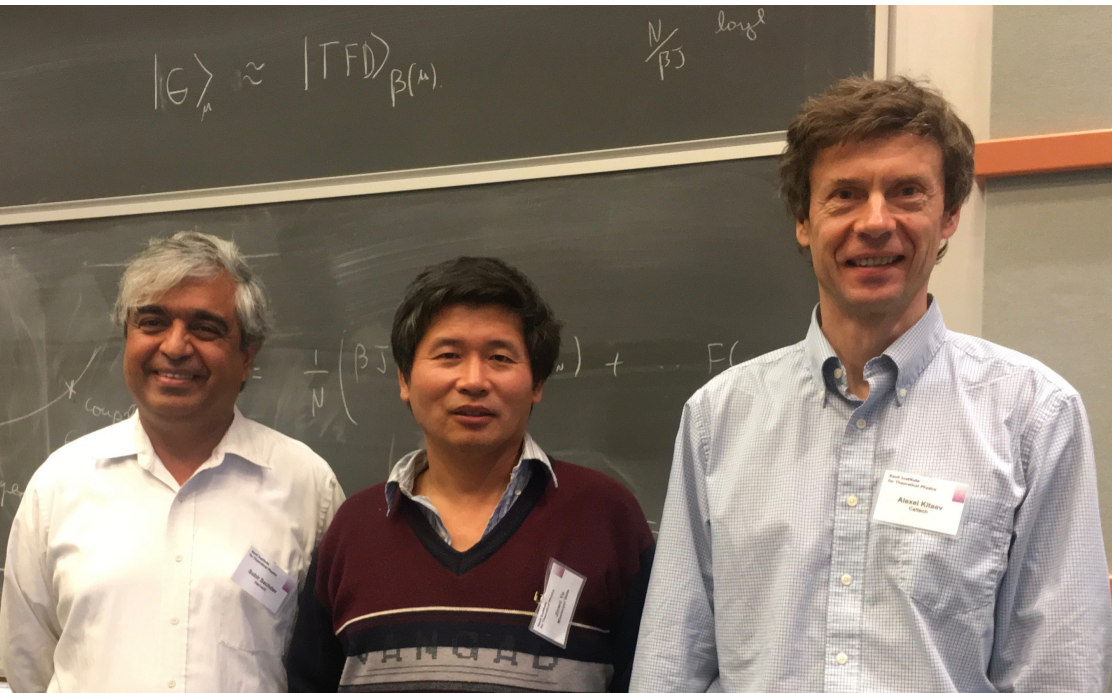
The SYK model

Sachdev, Ye (1993); Kitaev (2015)

$$U_{9,18;5,15}$$



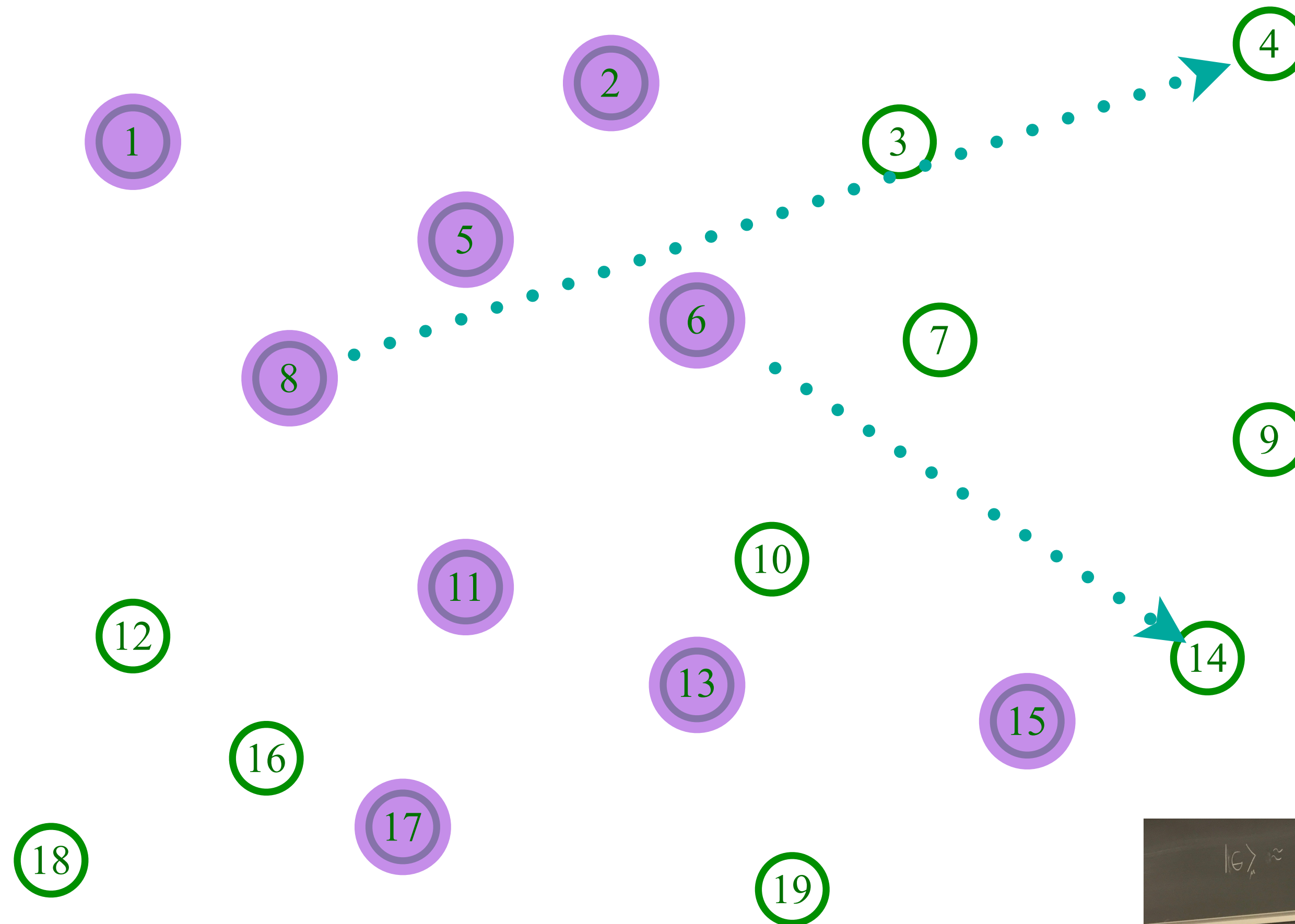
Entangle electrons pairwise randomly



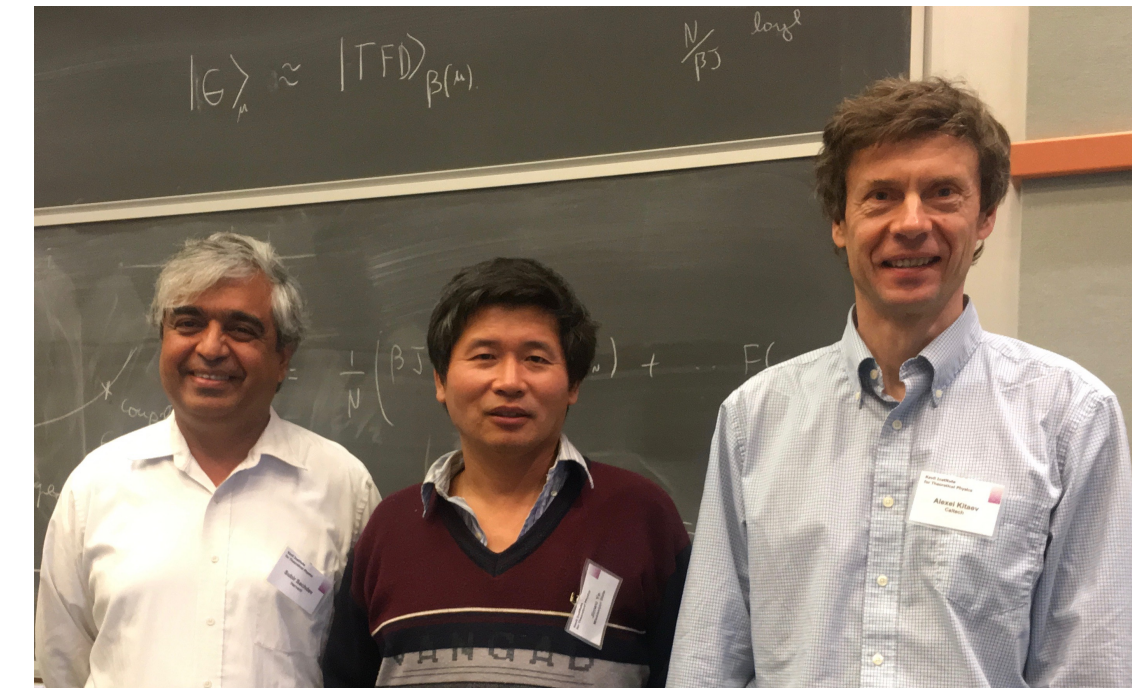
The SYK model

Sachdev, Ye (1993); Kitaev (2015)

$$U_{6,8;4,14}$$



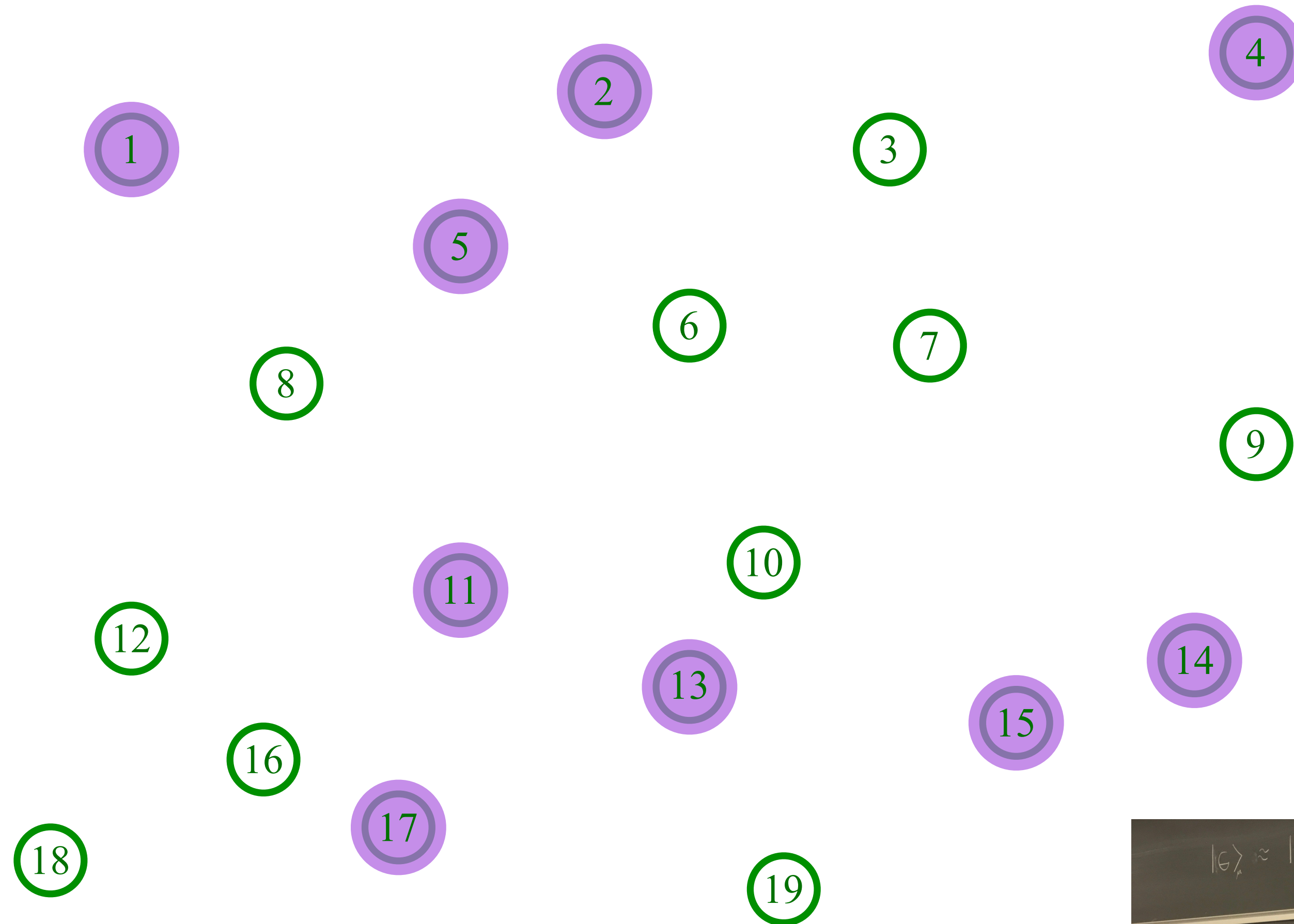
Entangle electrons pairwise randomly



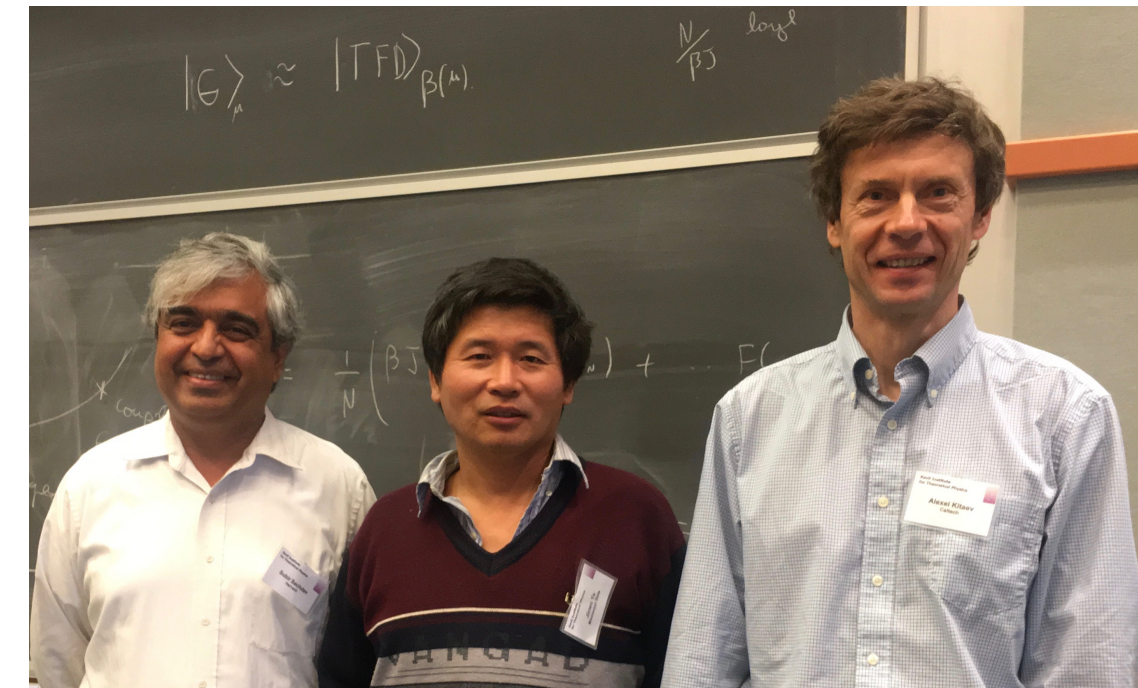
The SYK model

Sachdev, Ye (1993); Kitaev (2015)

$$U_{6,8;4,14}$$



Entangle electrons pairwise randomly



The Sachdev-Ye-Kitaev (SYK) model

(See also: the “2-Body Random Ensemble” in nuclear physics; did not obtain the large N limit;
T.A. Brody, J. Flores, J.B. French, P.A. Mello, A. Pandey, and S.S.M. Wong, Rev. Mod. Phys. **53**, 385 (1981))

$$\mathcal{H} = \frac{1}{(2N)^{3/2}} \sum_{\alpha, \beta, \gamma, \delta=1}^N U_{\alpha\beta;\gamma\delta} c_{\alpha}^{\dagger} c_{\beta}^{\dagger} c_{\gamma} c_{\delta} - \mu \sum_{\alpha} c_{\alpha}^{\dagger} c_{\alpha}$$

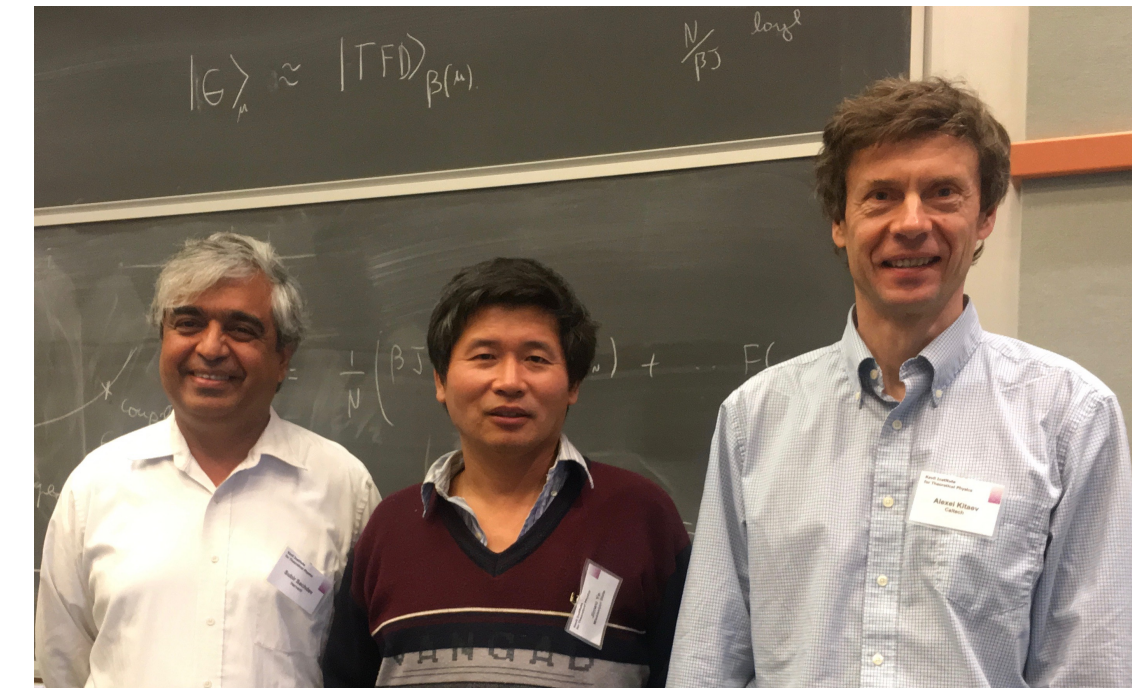
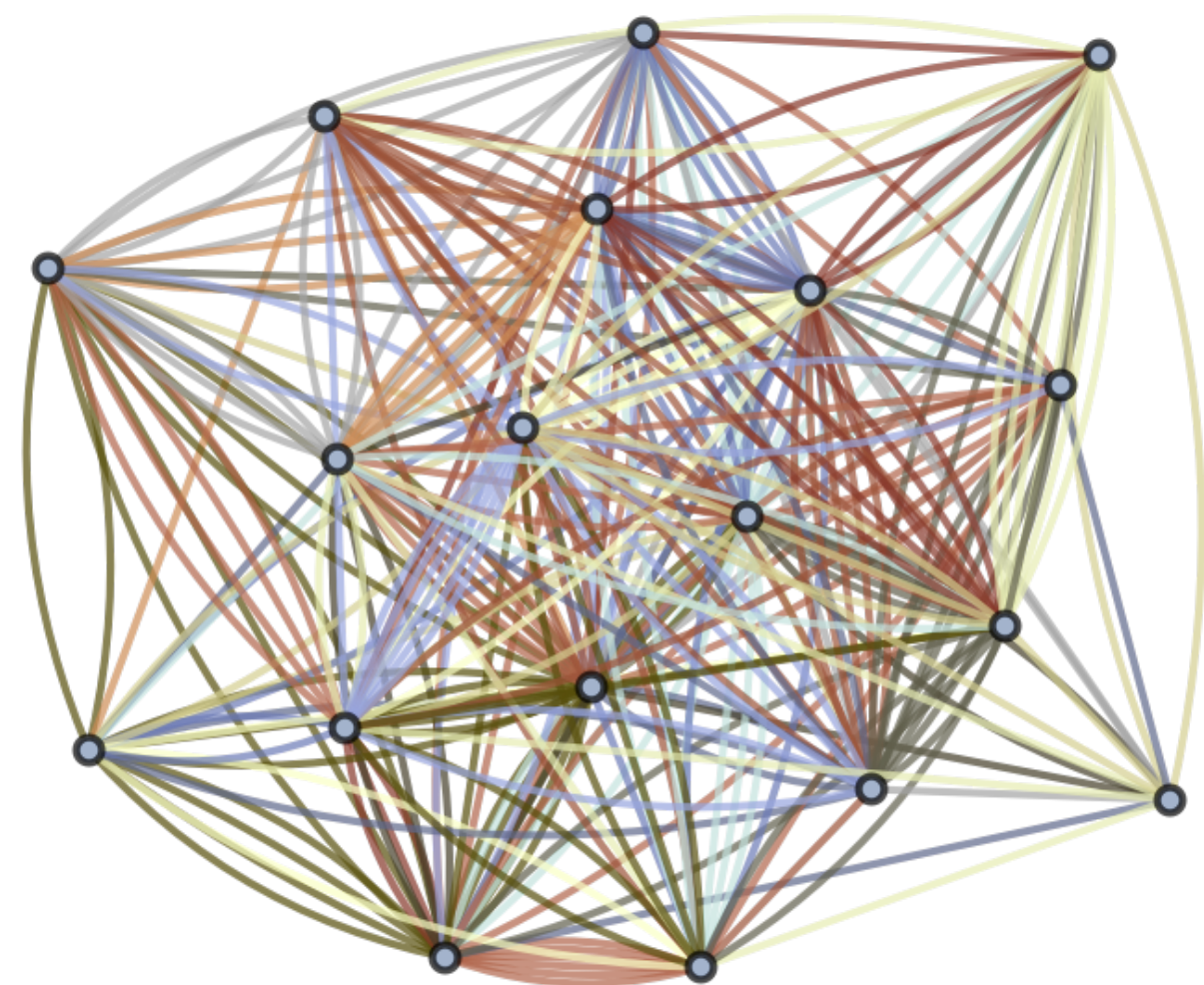
$$c_{\alpha} c_{\beta} + c_{\beta} c_{\alpha} = 0 \quad , \quad c_{\alpha} c_{\beta}^{\dagger} + c_{\beta}^{\dagger} c_{\alpha} = \delta_{\alpha\beta}$$

$$\mathcal{Q} = \frac{1}{N} \sum_{\alpha} c_{\alpha}^{\dagger} c_{\alpha} ; \quad [\mathcal{H}, \mathcal{Q}] = 0 ; \quad 0 \leq \mathcal{Q} \leq 1$$

$U_{\alpha\beta;\gamma\delta}$ are independent random variables with $\overline{U_{\alpha\beta;\gamma\delta}} = 0$ and $\overline{|U_{\alpha\beta;\gamma\delta}|^2} = U^2$
 $N \rightarrow \infty$ yields critical strange metal.

S. Sachdev and J. Ye, PRL **70**, 3339 (1993)

A. Kitaev, unpublished; S. Sachdev, PRX **5**, 041025 (2015)

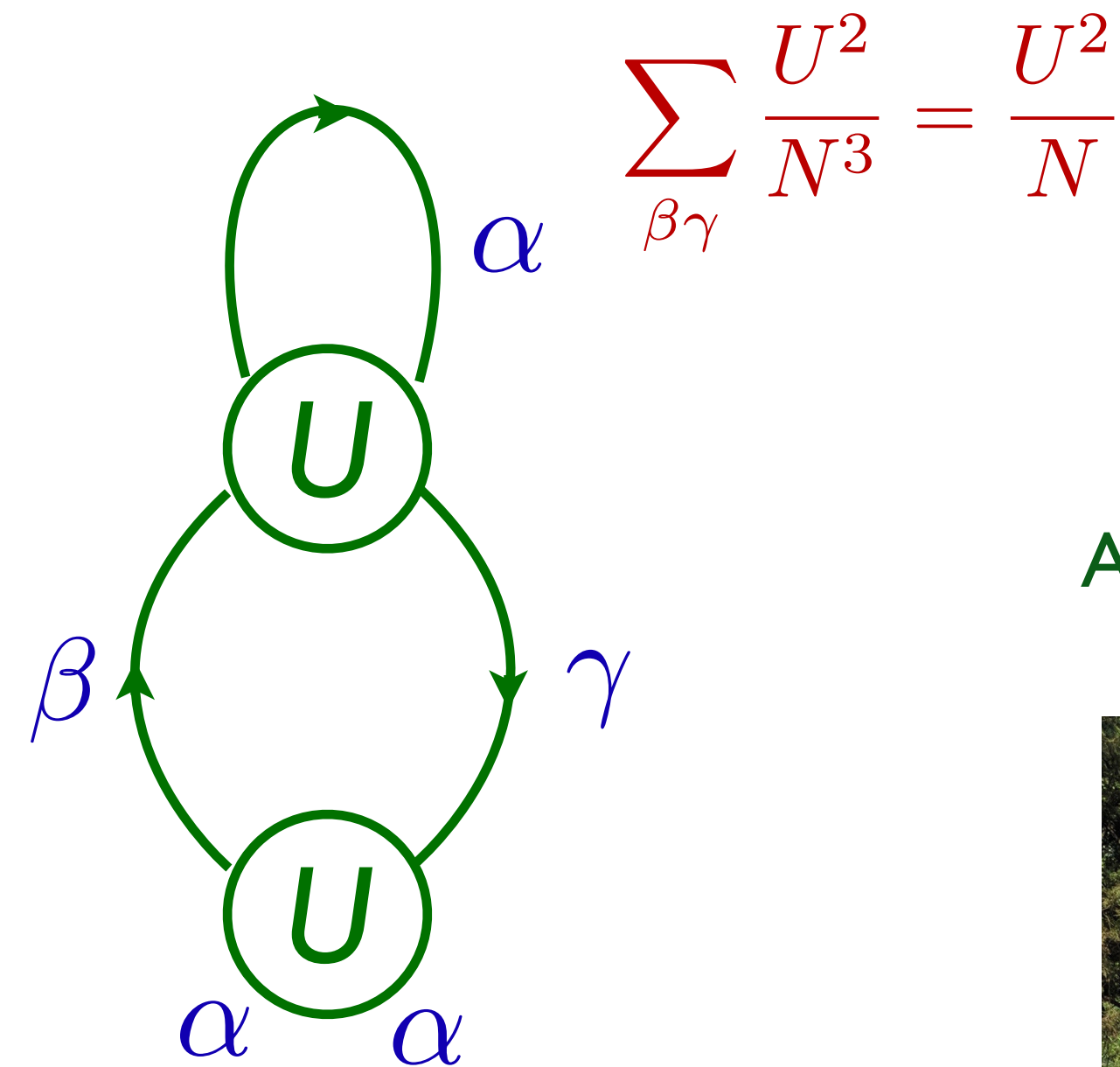
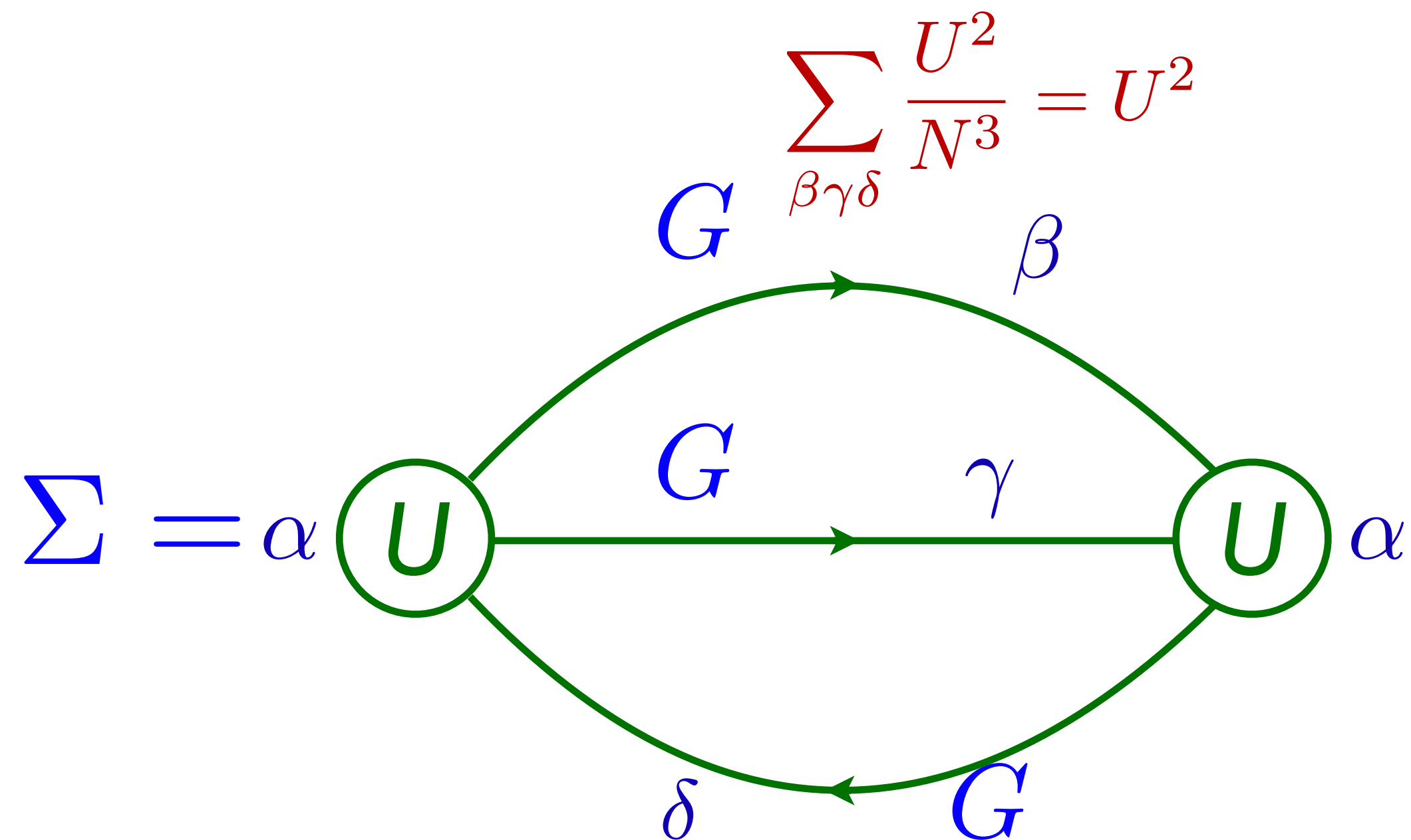


The Sachdev-Ye-Kitaev (SYK) model

Feynman graph expansion in $U_{\alpha\beta;\gamma\delta}$, and graph-by-graph average, yields exact equations in the large N limit:

$$G(i\omega) = \frac{1}{i\omega + \mu - \Sigma(i\omega)} \quad , \quad \Sigma(\tau) = -U^2 G^2(\tau) G(-\tau)$$

$$G(\tau = 0^-) = \mathcal{Q}.$$



S. Sachdev and J. Ye,
PRL **70**, 3339 (1993)

A. Georges and O. Parcollet
PRB **59**, 5341 (1999)



G - Σ path integral

After introducing replicas $a = 1 \dots n$, and integrating out the disorder, the partition function can be written as

$$Z = \int \mathcal{D}c_{\alpha a}(\tau) \exp \left[- \sum_{ia} \int_0^\beta d\tau c_{\alpha a}^\dagger \left(\frac{\partial}{\partial \tau} - \mu \right) c_{\alpha a} \right. \\ \left. - \frac{U^2}{4N^3} \sum_{ab} \int_0^\beta d\tau d\tau' \left| \sum_i c_{\alpha a}^\dagger(\tau) c_{\alpha b}(\tau') \right|^4 \right].$$

For simplicity, we neglect the replica indices, and introduce the identity

$$1 = \int \mathcal{D}G(\tau_1, \tau_2) \mathcal{D}\Sigma(\tau_1, \tau_2) \exp \left[-N \int_0^\beta d\tau_1 d\tau_2 \Sigma(\tau_1, \tau_2) \left(G(\tau_2, \tau_1) \right. \right. \\ \left. \left. + \frac{1}{N} \sum_\alpha c_\alpha(\tau_2) c_\alpha^\dagger(\tau_1) \right) \right].$$

Then the partition function can be written as a path integral with an action S analogous to a Luttinger-Ward functional

G - Σ
path
integral

Then the partition function can be written as a path integral with an action S analogous to a Luttinger-Ward functional

$$Z = \int \mathcal{D}G(\tau_1, \tau_2) \mathcal{D}\Sigma(\tau_1, \tau_2) \exp(-NS)$$
$$S = \ln \det [\delta(\tau_1 - \tau_2)(\partial_{\tau_1} + \mu) - \Sigma(\tau_1, \tau_2)]$$
$$+ \int d\tau_1 d\tau_2 [\Sigma(\tau_1, \tau_2)G(\tau_2, \tau_1) + (U^2/2)G^2(\tau_2, \tau_1)G^2(\tau_1, \tau_2)]$$

G - Σ path integral

Then the partition function can be written as a path integral with an action S analogous to a Luttinger-Ward functional

$$Z = \int \mathcal{D}G(\tau_1, \tau_2) \mathcal{D}\Sigma(\tau_1, \tau_2) \exp(-NS)$$
$$S = \ln \det [\delta(\tau_1 - \tau_2)(\partial_{\tau_1} + \mu) - \Sigma(\tau_1, \tau_2)]$$
$$+ \int d\tau_1 d\tau_2 [\Sigma(\tau_1, \tau_2)G(\tau_2, \tau_1) + (U^2/2)G^2(\tau_2, \tau_1)G^2(\tau_1, \tau_2)]$$

Saddle-point equations:

$$G(i\omega) = \frac{1}{i\omega + \mu - \Sigma(i\omega)} \quad , \quad \Sigma(\tau) = -U^2 G^2(\tau)G(-\tau)$$
$$G(\tau = 0^-) = Q.$$

G - Σ path integral

Then the partition function can be written as a path integral with an action S analogous to a Luttinger-Ward functional

$$Z = \int \mathcal{D}G(\tau_1, \tau_2) \mathcal{D}\Sigma(\tau_1, \tau_2) \exp(-NS)$$
$$S = \ln \det [\delta(\tau_1 - \tau_2)(\partial_{\tau_1} + \mu) - \Sigma(\tau_1, \tau_2)]$$
$$+ \int d\tau_1 d\tau_2 [\Sigma(\tau_1, \tau_2)G(\tau_2, \tau_1) + (U^2/2)G^2(\tau_2, \tau_1)G^2(\tau_1, \tau_2)]$$

Saddle-point equations:

$$G(i\omega) = \frac{1}{i\omega + \mu - \Sigma(i\omega)} \quad , \quad \Sigma(\tau) = -U^2 G^2(\tau)G(-\tau)$$
$$G(\tau = 0^-) = Q.$$

Solution at long times, and at $T = 0$: $G(\tau) \sim |\tau|^{-1/2}$
 \Rightarrow indication there are no quasiparticles

The SYK model

$$G(i\omega) = \frac{1}{i\omega + \mu - \Sigma(i\omega)} \quad , \quad \Sigma(\tau) = -U^2 G^2(\tau) G(-\tau)$$
$$\Sigma(z) = \mu - \frac{1}{A} \sqrt{z} + \dots \quad , \quad G(z) = \frac{A}{\sqrt{z}}$$

At frequencies $\ll U$, the $i\omega + \mu$ can be dropped, and without it equations are invariant under the reparametrization and gauge transformations.

The singular part of the self-energy and the Green's function obey

$$\int_0^\beta d\tau_2 \Sigma_{\text{sing}}(\tau_1, \tau_2) G(\tau_2, \tau_3) = -\delta(\tau_1 - \tau_3)$$

$$\Sigma_{\text{sing}}(\tau_1, \tau_2) = -U^2 G^2(\tau_1, \tau_2) G(\tau_2, \tau_1)$$

The SYK model

$$\int_0^\beta d\tau_2 \Sigma(\tau_1, \tau_2) G(\tau_2, \tau_3) = -\delta(\tau_1 - \tau_3)$$

$$\Sigma(\tau_1, \tau_2) = -U^2 G^2(\tau_1, \tau_2) G(\tau_2, \tau_1)$$

These equations are invariant under

$$\tau = f(\sigma)$$

$$G(\tau_1, \tau_2) = [f'(\sigma_1) f'(\sigma_2)]^{-1/4} \frac{g(\sigma_1)}{g(\sigma_2)} \tilde{G}(\sigma_1, \sigma_2)$$

$$\Sigma(\tau_1, \tau_2) = [f'(\sigma_1) f'(\sigma_2)]^{-3/4} \frac{g(\sigma_1)}{g(\sigma_2)} \tilde{\Sigma}(\sigma_1, \sigma_2)$$

where $f(\sigma)$ and $g(\sigma)$ are arbitrary functions.

The SYK model

$$\int_0^\beta d\tau_2 \Sigma(\tau_1, \tau_2) G(\tau_2, \tau_3) = -\delta(\tau_1 - \tau_3)$$

$$\Sigma(\tau_1, \tau_2) = -U^2 G^2(\tau_1, \tau_2) G(\tau_2, \tau_1)$$

These equations are invariant under

$$\tau = f(\sigma)$$

$$G(\tau_1, \tau_2) = [f'(\sigma_1) f'(\sigma_2)]^{-1/4} \frac{g(\sigma_1)}{g(\sigma_2)} \tilde{G}(\sigma_1, \sigma_2)$$

$$\Sigma(\tau_1, \tau_2) = [f'(\sigma_1) f'(\sigma_2)]^{-3/4} \frac{g(\sigma_1)}{g(\sigma_2)} \tilde{\Sigma}(\sigma_1, \sigma_2)$$

where $f(\sigma)$ and $g(\sigma)$ are arbitrary functions.

We can map the $T = 0$ solution to the $T > 0$ solution by

$$\tau = \frac{1}{\pi T} \tan(\pi T \sigma)$$

$$g(\sigma) = e^{-2\pi \mathcal{E} T \sigma}$$

A. Kitaev, 2015

S. Sachdev, PRX **5**, 041025 (2015)

The complex SYK model

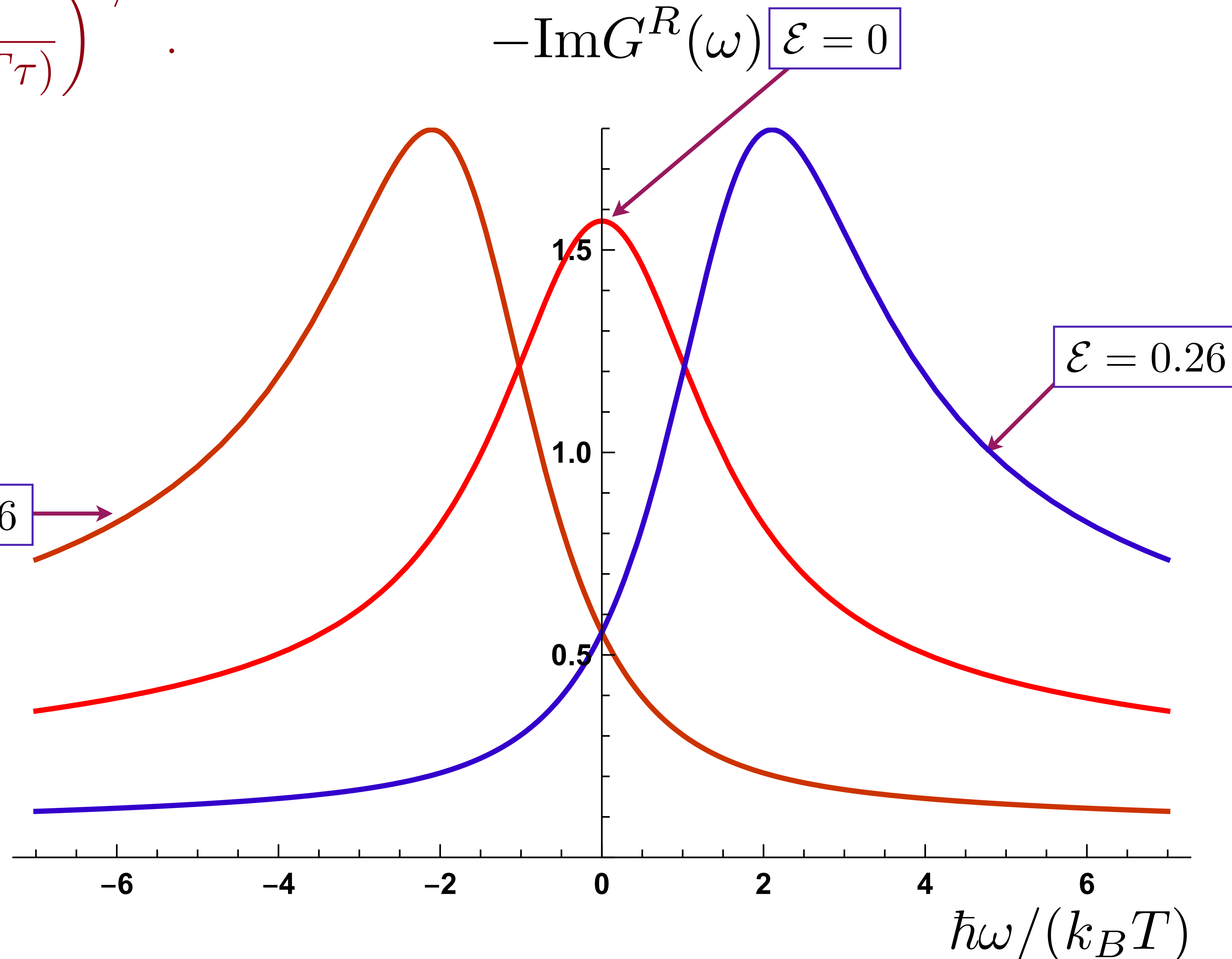
$$G_*(\tau) = -C \frac{e^{-2\pi\mathcal{E}T\tau}}{\sqrt{1 + e^{-4\pi\mathcal{E}}}} \left(\frac{T}{\sin(\pi T\tau)} \right)^{1/2}.$$

$$G_*^R(\omega) = \frac{-iC e^{-i\theta}}{(2\pi T)^{1/2}} \frac{\Gamma\left(\frac{1}{4} - \frac{i\omega}{2\pi T} + i\mathcal{E}\right)}{\Gamma\left(\frac{3}{4} - \frac{i\omega}{2\pi T} + i\mathcal{E}\right)}.$$

$$e^{2\pi\mathcal{E}} = \frac{\sin(\pi/4 + \theta)}{\sin(\pi/4 - \theta)}$$

$$C = \left(\frac{\pi}{U^2 \cos(2\theta)} \right)^{1/4}$$

\mathcal{E} is a known function of \mathcal{Q}
(Luttinger relation)



S. Sachdev and J. Ye, PRL **70**, 3339 (1993)

A. Georges and O. Parcollet PRB **59**, 5341 (1999)

S. Sachdev, PRX **5**, 041025 (2015)

The complex SYK model

$$G_*(\tau) = -C \frac{e^{-2\pi\mathcal{E}T\tau}}{\sqrt{1 + e^{-4\pi\mathcal{E}}}} \left(\frac{T}{\sin(\pi T\tau)} \right)^{1/2}.$$

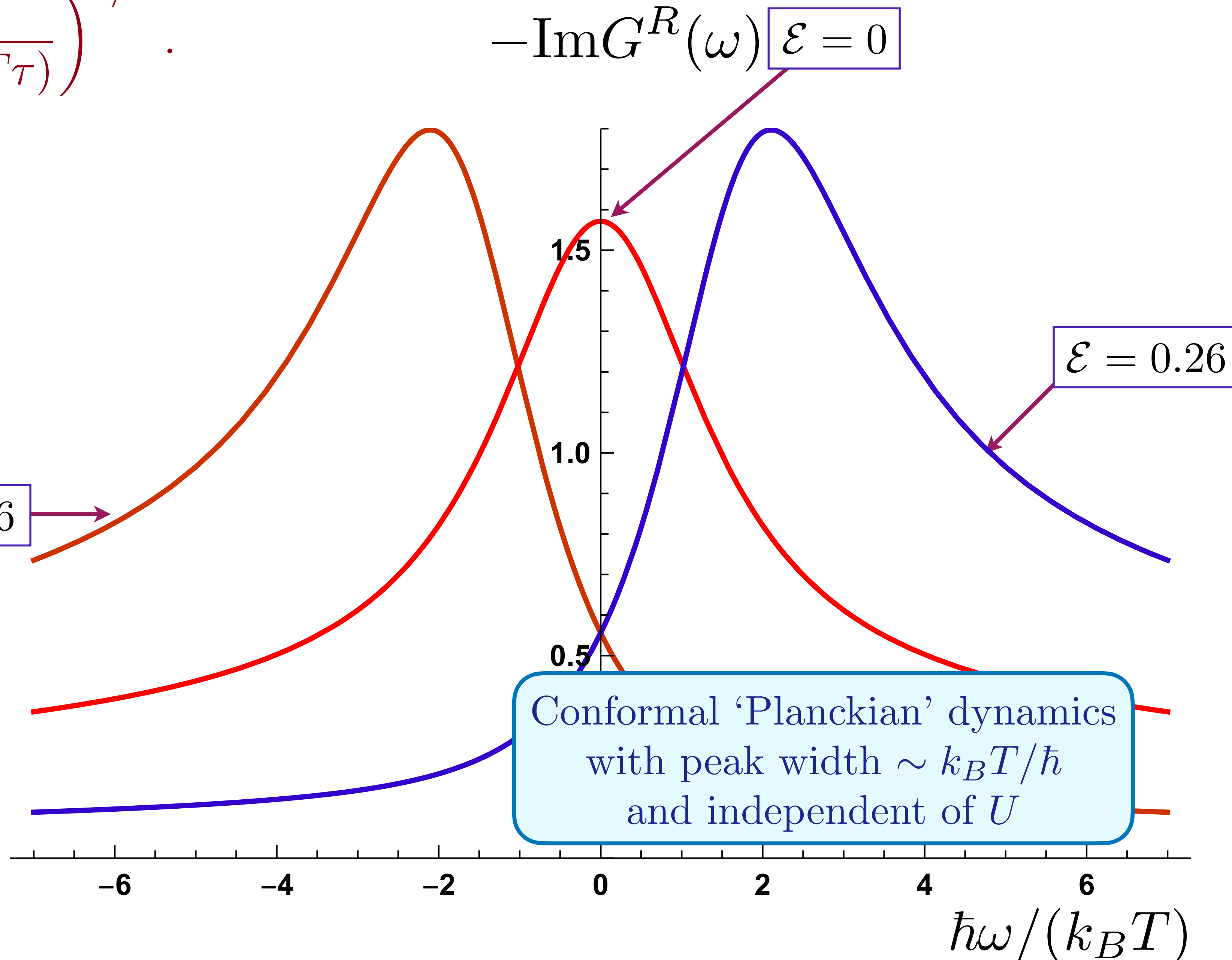
$$G_*^R(\omega) = \frac{-iC e^{-i\theta}}{(2\pi T)^{1/2}} \frac{\Gamma\left(\frac{1}{4} - \frac{i\omega}{2\pi T} + i\mathcal{E}\right)}{\Gamma\left(\frac{3}{4} - \frac{i\omega}{2\pi T} + i\mathcal{E}\right)}.$$

$$e^{2\pi\mathcal{E}} = \frac{\sin(\pi/4 + \theta)}{\sin(\pi/4 - \theta)}$$

$$C = \left(\frac{\pi}{U^2 \cos(2\theta)} \right)^{1/4}$$

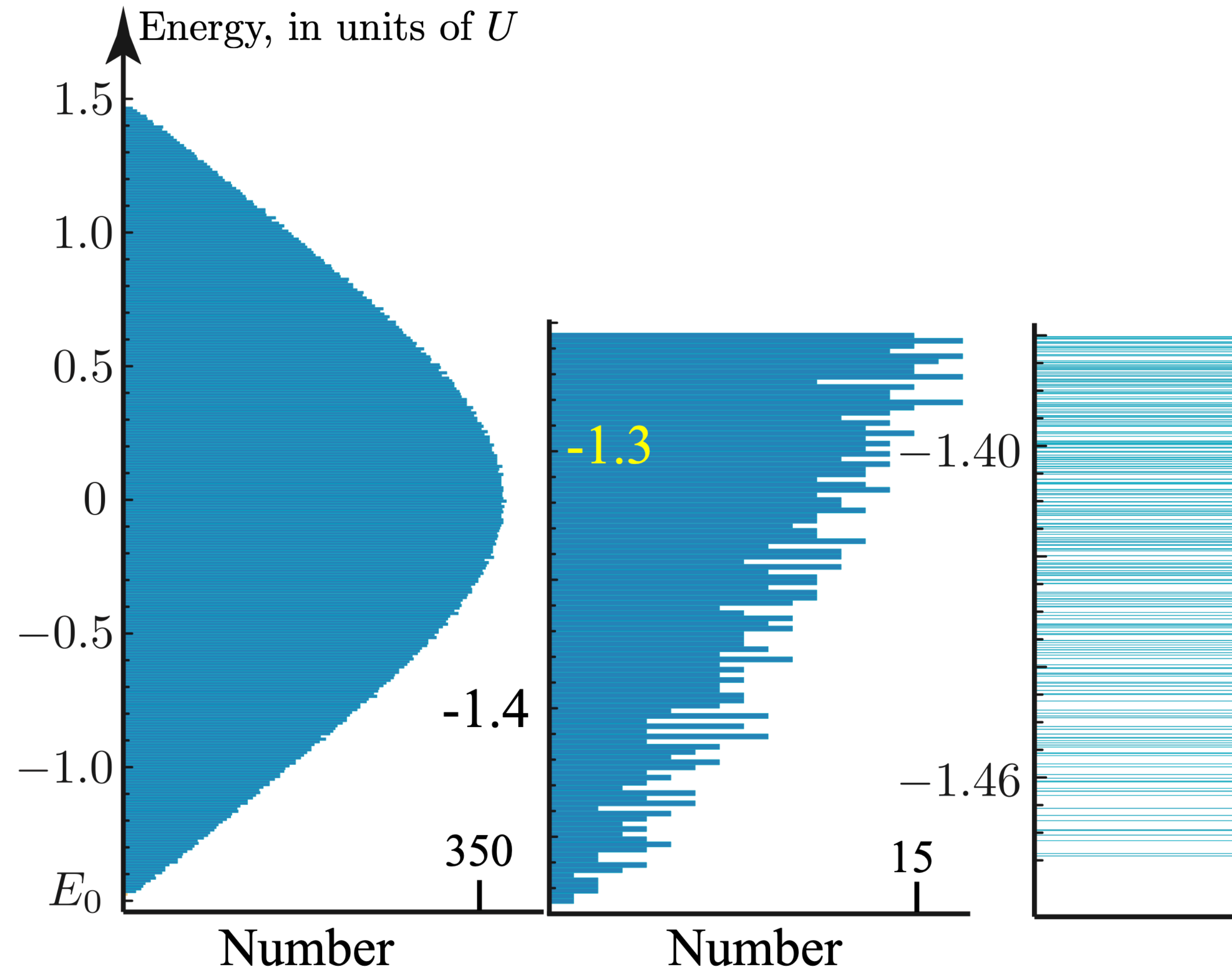
\mathcal{E} is a known function of \mathcal{Q}
(Luttinger relation)

S. Sachdev and J. Ye, PRL **70**, 3339 (1993)
A. Georges and O. Parcollet PRB **59**, 5341 (1999)
S. Sachdev, PRX **5**, 041025 (2015)



Many-body density of states

$$D(E) = \sum_i \delta(E - E_i); \quad E_0 + E_i \Rightarrow \text{Many body eigenvalue}$$



Complex SYK model

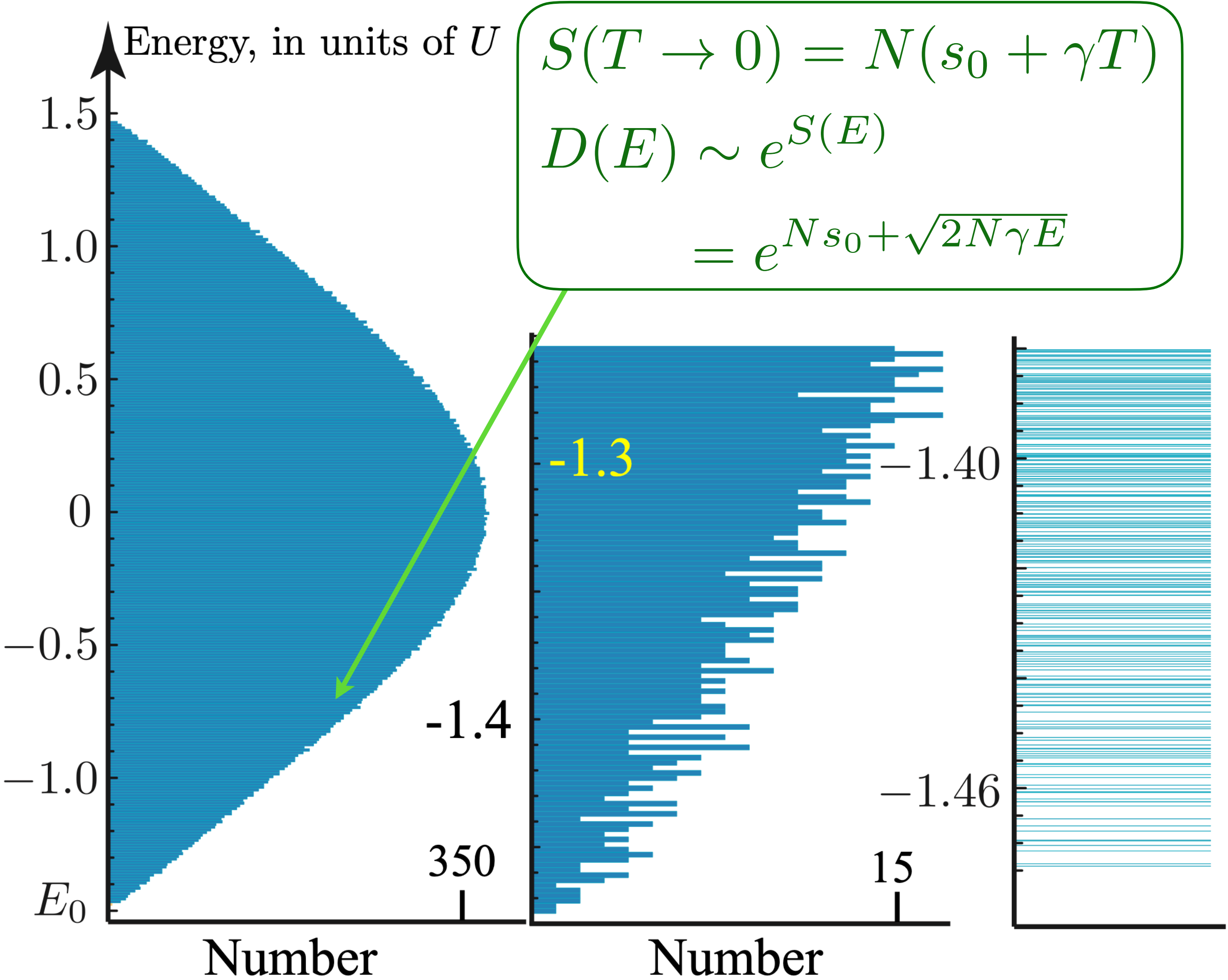
Many-body density of states

$$D(E) = \sum_i \delta(E - E_i); \quad E_0 + E_i \Rightarrow \text{Many body eigenvalue}$$

At $Q = 1/2$

$$s_0 = \frac{\text{Catalan}}{\pi} + \frac{\ln 2}{4} = 0.46484769917 \dots$$

A. Georges, O. Parcollet, and S. Sachdev,
PRB **63**, 134406 (2001)



$$S(T \rightarrow 0) = N(s_0 + \gamma T)$$
$$D(E) \sim e^{S(E)}$$
$$= e^{N s_0 + \sqrt{2N\gamma E}}$$

Complex SYK model

Many-body density of states

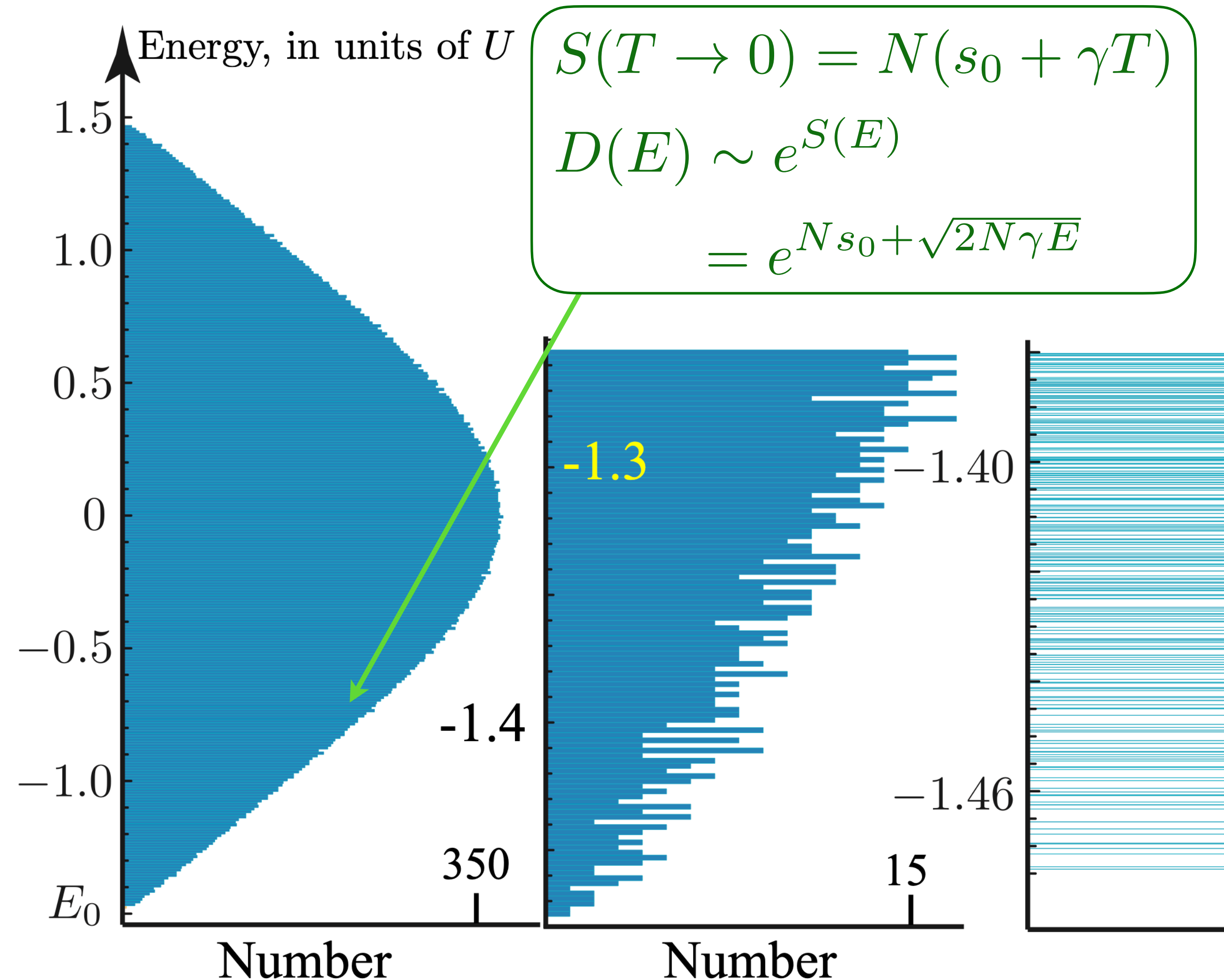
Boltzmann

$$D(E) = \sum_i \delta(E - E_i); \quad E_0 + E_i \Rightarrow \text{Many body eigenvalue}$$

At $Q = 1/2$

$$s_0 = \frac{\text{Catalan}}{\pi} + \frac{\ln 2}{4} \\ = 0.46484769917 \dots$$

A. Georges, O. Parcollet, and S. Sachdev,
PRB **63**, 134406 (2001)



Energy level
spacing $\sim e^{-N s_0} !$

No quasiparticle decomposition:
wavefunctions change chaotically
from one state to the next.

Complex SYK model

(Numerics: G. Tarnopolsky)

Many-body density of states

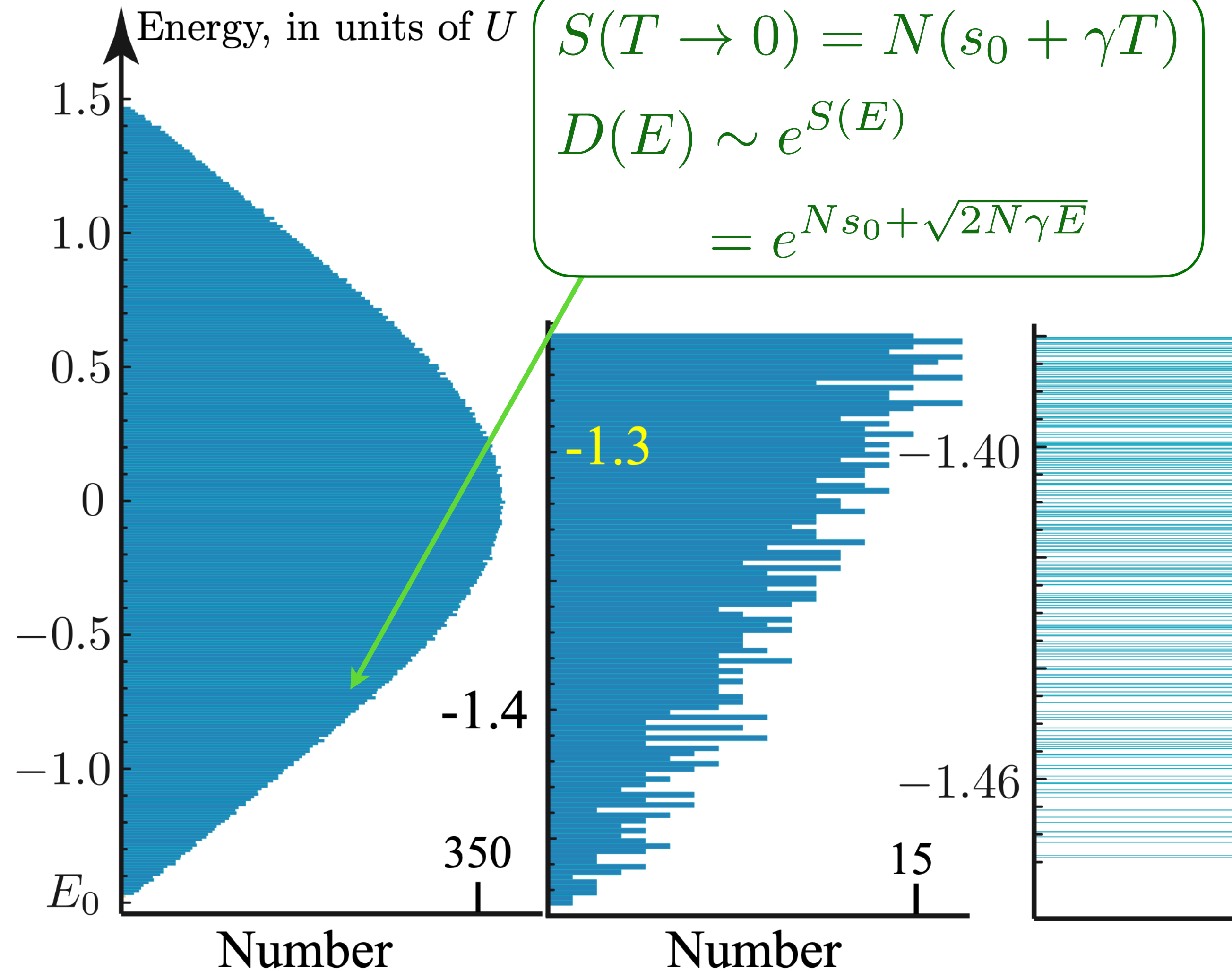
Beyond Boltzmann

$$D(E) = \sum_i \delta(E - E_i); \quad E_0 + E_i \Rightarrow \text{Many body eigenvalue}$$

At $Q = 1/2$

$$s_0 = \frac{\text{Catalan}}{\pi} + \frac{\ln 2}{4} = 0.46484769917 \dots$$

A. Georges, O. Parcollet, and S. Sachdev,
PRB **63**, 134406 (2001)



$$S(T \rightarrow 0) = N(s_0 + \gamma T)$$
$$D(E) \sim e^{S(E)}$$
$$= e^{N s_0 + \sqrt{2N\gamma E}}$$

$$D(E) \sim N^{-1} \exp(N s_0) \sinh(\sqrt{2N\gamma E})$$

Complex SYK model

Many-body density of states

Beyond Boltzmann

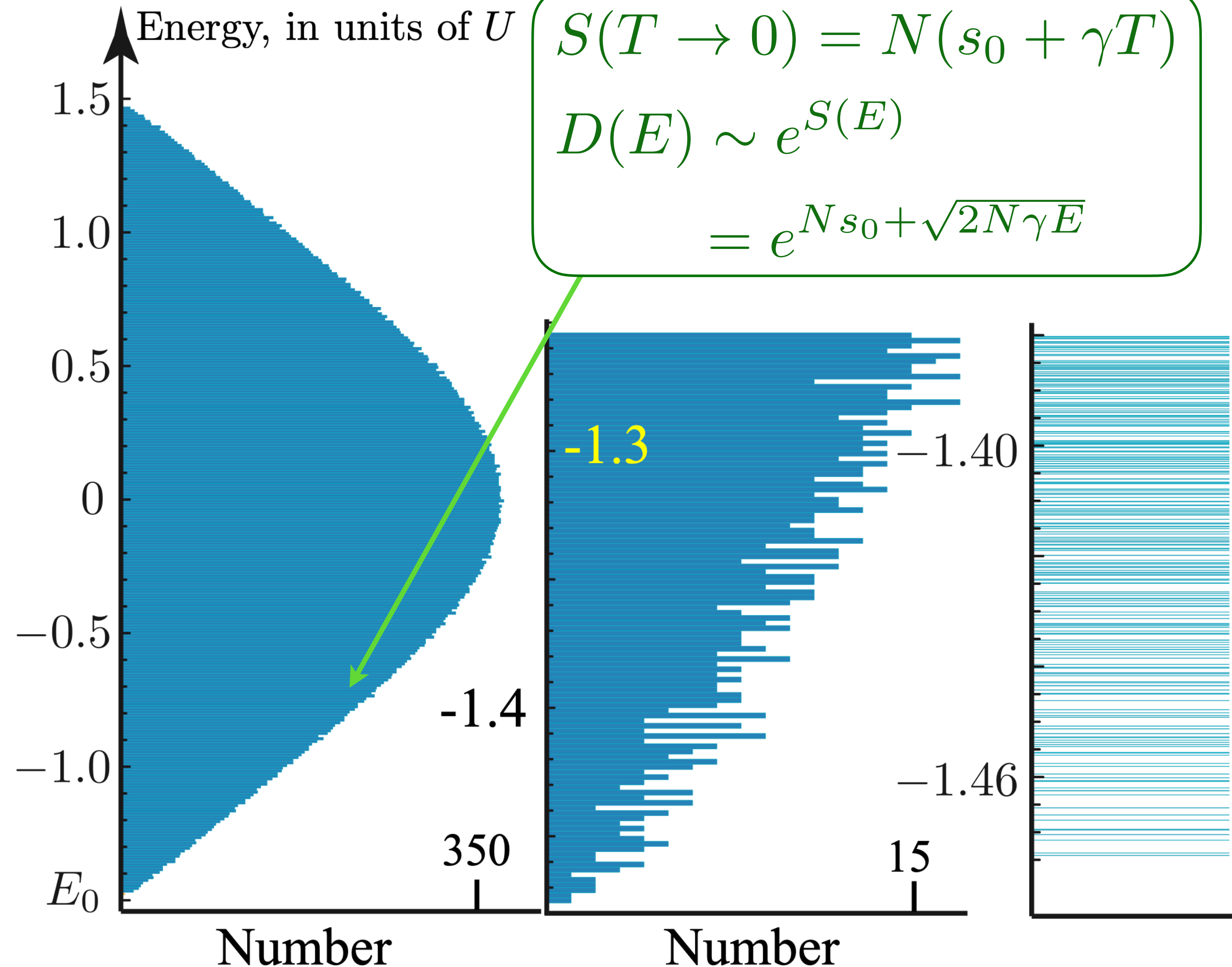
$$D(E) = \sum_i \delta(E - E_i); \quad E_0 + E_i \Rightarrow \text{Many body eigenvalue}$$

At $Q = 1/2$

$$s_0 = \frac{\text{Catalan}}{\pi} + \frac{\ln 2}{4} \\ = 0.46484769917 \dots$$

A. Georges, O. Parcollet, and S. Sachdev,
PRB **63**, 134406 (2001)

$$D(E) \sim N^{-1} \exp(N s_0) \sinh(\sqrt{2N\gamma E})$$



$$S(T \rightarrow 0) = N(s_0 + \gamma T) \\ D(E) \sim e^{S(E)} \\ = e^{N s_0 + \sqrt{2N\gamma E}}$$

Complex SYK model

Many-body density of states

Beyond Boltzmann

$$D(E) = \sum_i \delta(E - E_i); \quad E_0 + E_i \Rightarrow \text{Many body eigenvalue}$$

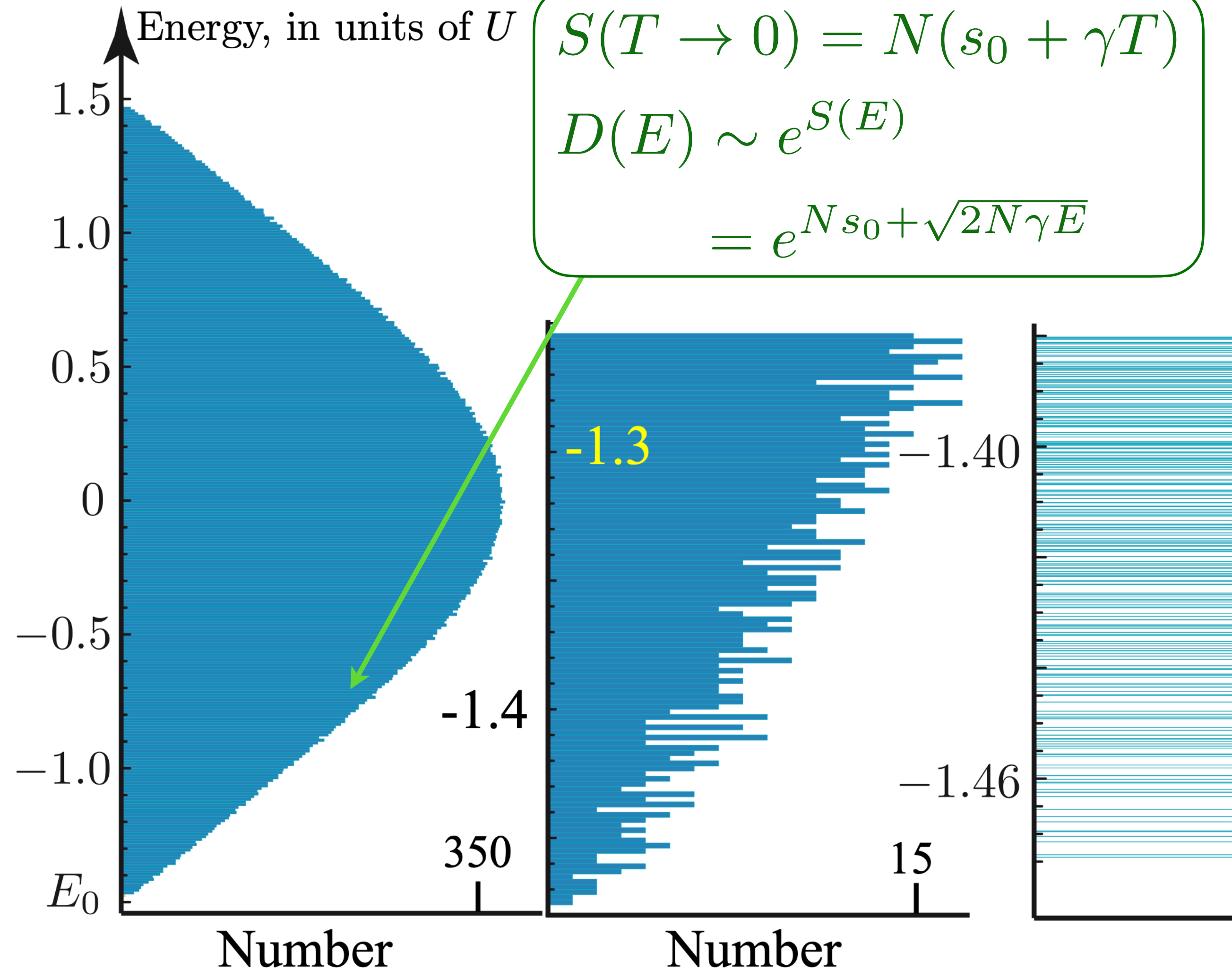
At $Q = 1/2$

$$s_0 = \frac{\text{Catalan}}{\pi} + \frac{\ln 2}{4} \\ = 0.46484769917 \dots$$

A. Georges, O. Parcollet, and S. Sachdev,
PRB **63**, 134406 (2001)

$$D(E) \sim N^{-1} \exp(N s_0) \sinh(\sqrt{2N\gamma E})$$

J. S. Cotler et al.,
JHEP 05 (2017) 118



Complex SYK model

(Numerics: G. Tarnopolsky)

Many-body density of states

Beyond Boltzmann

$$D(E) = \sum_i \delta(E - E_i); \quad E_0 + E_i \Rightarrow \text{Many body eigenvalue}$$

At $Q = 1/2$

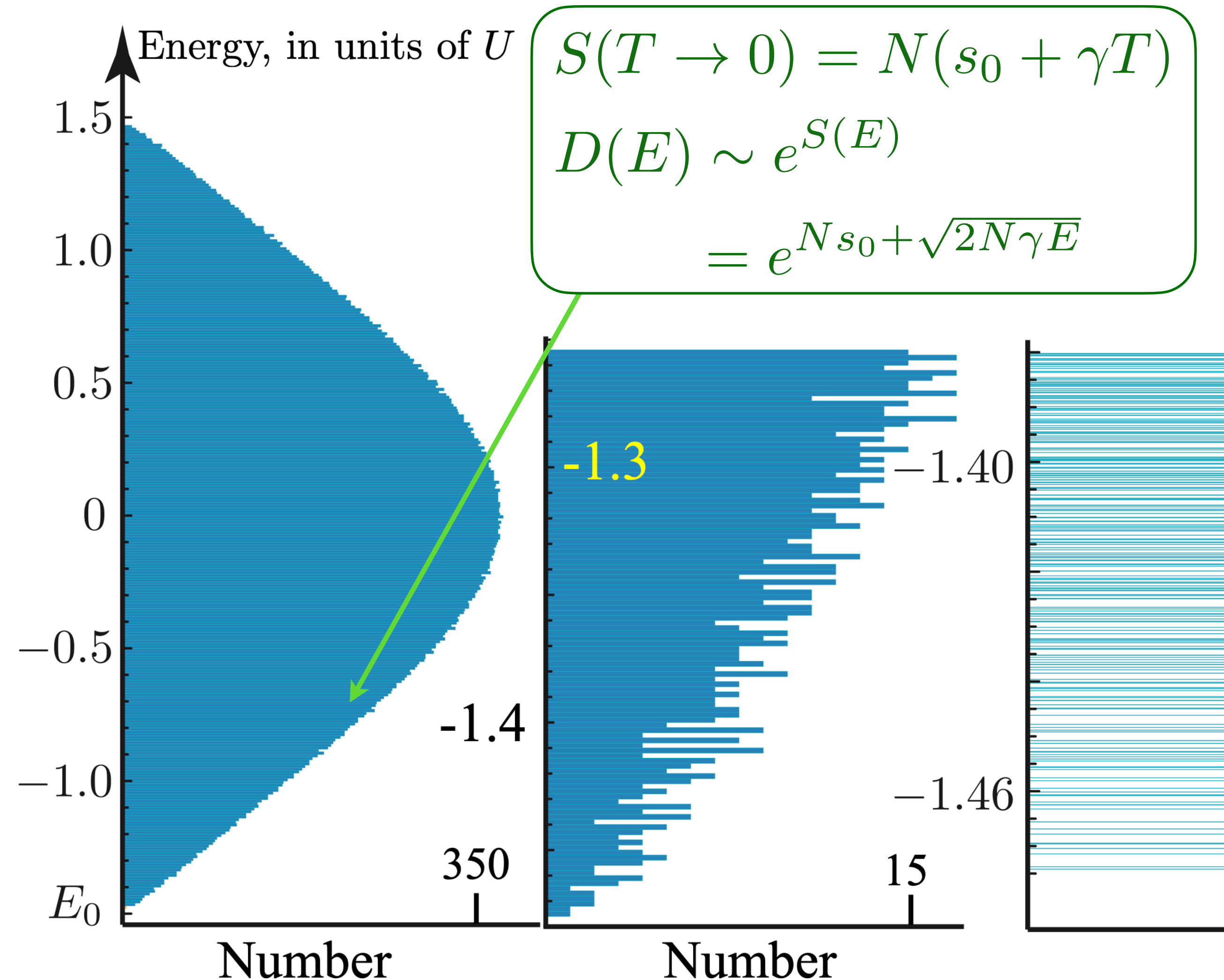
$$s_0 = \frac{\text{Catalan}}{\pi} + \frac{\ln 2}{4} \\ = 0.46484769917 \dots$$

A. Georges, O. Parcollet, and S. Sachdev,
PRB **63**, 134406 (2001)

$$D(E) \sim N^{-1} \exp(N s_0) \sinh(\sqrt{2N\gamma E})$$

J. S. Cotler et al.,
JHEP 05 (2017) 118

Yingfei Gu, A. Kitaev, S. Sachdev, and
G. Tarnopolsky, JHEP 02 (2020) 157



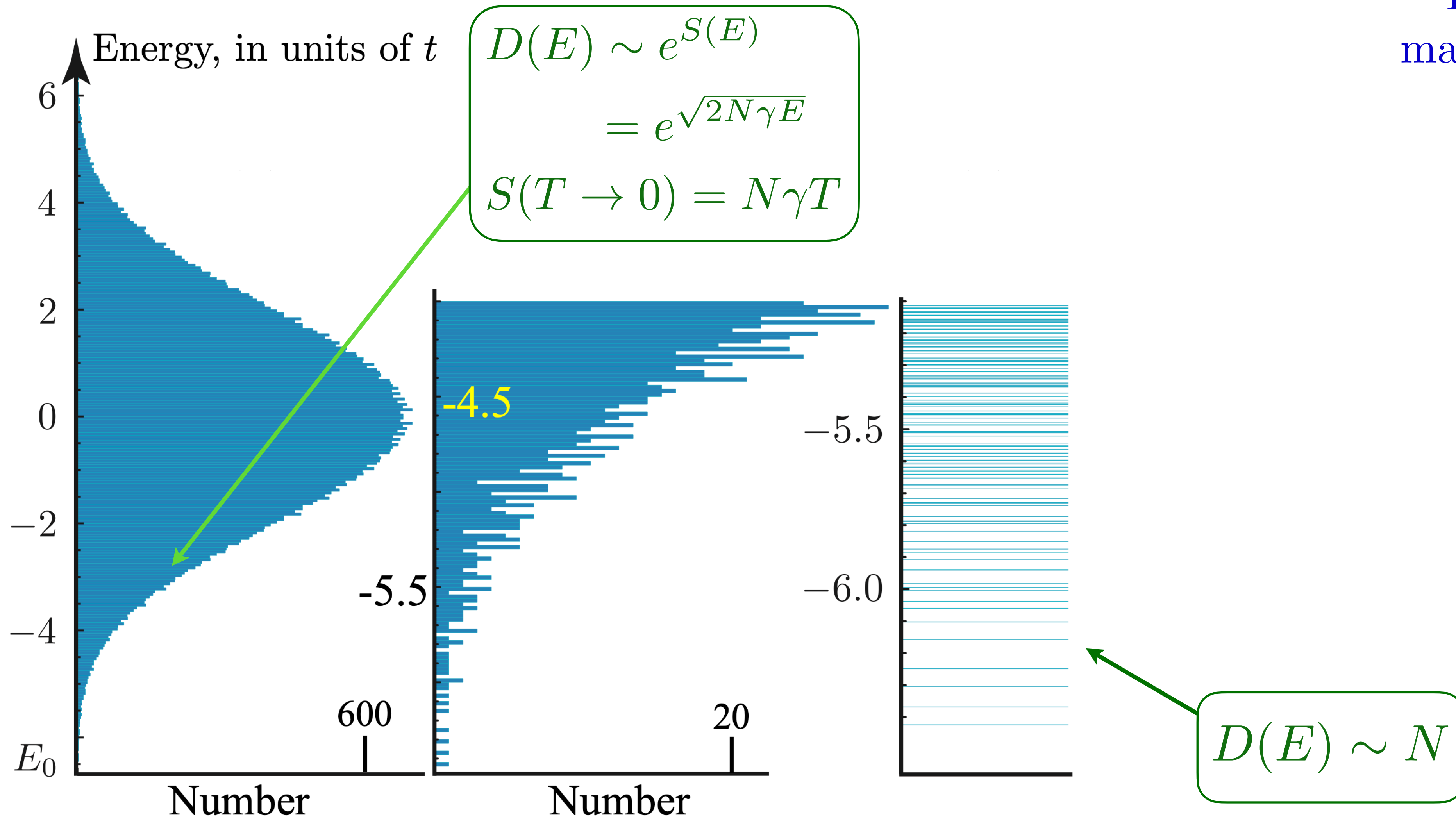
Complex SYK model

(Numerics: G. Tarnopolsky)

Many-body density of states

$$D(E) = \sum_i \delta(E - E_i); \quad E_0 + E_i \Rightarrow \text{Many body eigenvalue}$$

For random
matrix model:
 $E_0 + E_i =$
 $\sum_{\alpha} n_{\alpha} \varepsilon_{\alpha}$
 $n_{\alpha} = 0, 1,$
occupation
number



Random matrix model

Yukawa-SYK model

$$\mathcal{H} = -\mu \sum_i \psi_i^\dagger \psi_i + \sum_\ell \frac{1}{2} (\pi_\ell^2 + \omega_0^2 \phi_\ell^2) + \frac{1}{N} \sum_{ij\ell} g_{ij\ell} \psi_i^\dagger \psi_j \phi_\ell$$

with $g_{ij\ell}$ independent random numbers with zero mean.

W. Fu, D. Gaiotto, J. Maldacena, and S. Sachdev, PRD **95**, 026009 (2017)

J. Murugan, D. Stanford, and E. Witten, JHEP 08, 146 (2017)

A. A. Patel and S. Sachdev, PRB **98**, 125134 (2018)

E. Marcus and S. Vandoren, JHEP 01, 166 (2018)

Yuxuan Wang, PRL **124**, 017002 (2020)

I. Esterlis and J. Schmalian, PRB **100**, 115132 (2019)

Yuxuan Wang and A. V. Chubukov, PRR **2**, 033084 (2020)

E. E. Aldape, T. Cookmeyer, A. A. Patel, and E. Altman, PRB **105**, 235111 (2022)

Jaewon Kim, E. Altman, and Xiangyu Cao, PRB **103**, 081113 (2021)

W. Wang, A. Davis, G. Pan, Yuxuan Wang, and Zi Yang Meng, PRB **103**, 195108 (2021)

I. Esterlis, H. Guo, A. A. Patel, and S. Sachdev, PRB **103**, 235129 (2021).

Yukawa-SYK model

These results can also be obtained from the saddle-point of a G - Σ - D - Π action, obtained using replica methods as for the SYK model.

$$\begin{aligned} \mathcal{Z} &= \int \mathcal{D}G \mathcal{D}\Sigma \mathcal{D}D \mathcal{D}\Pi \exp(-N S_{\text{all}}) \\ S_{\text{all}} &= -\ln \det(\partial_\tau + -\mu + \Sigma) + \frac{1}{2} \ln \det(-\partial_\tau^2 + \omega_0^2 - \Pi) \\ &\quad + \int d\tau \int d\tau' \left[-\Sigma(\tau'; \tau) G(\tau; \tau') + \frac{1}{2} \Pi(\tau'; \tau) D(\tau; \tau') \right. \\ &\quad \left. + \frac{g^2}{2} G(\tau; \tau') G(\tau'; \tau) D(\tau; \tau') \right]. \end{aligned}$$

Yukawa-SYK model

These results can also be obtained from the saddle-point of a G - Σ - D - Π action, obtained using replica methods as for the SYK model.

$$\mathcal{Z} = \int \mathcal{D}G \mathcal{D}\Sigma \mathcal{D}D \mathcal{D}\Pi \exp(-N S_{\text{all}})$$

Saddle-point equations:

$$\Sigma(\tau) = g^2 D(\tau) G(\tau),$$

$$\Pi(\tau) = -g^2 G(-\tau) G(\tau),$$

$$G(i\omega) = \frac{1}{i\omega + \mu - \Sigma(i\omega)},$$

$$D(i\Omega) = \frac{1}{\Omega^2 + \omega_0^2 - \Pi(i\Omega)}.$$

Yukawa-SYK model

$$\mathcal{H} = -\mu \sum_i \psi_i^\dagger \psi_i + \sum_\ell \frac{1}{2} (\pi_\ell^2 + \omega_0^2 \phi_\ell^2) + \frac{1}{N} \sum_{ij\ell} g_{ij\ell} \psi_i^\dagger \psi_j \phi_\ell$$

with $g_{ij\ell}$ independent random numbers with zero mean. The large N equations for the Green's functions and self energies of the fermions (G, Σ) and bosons (D, Π) are

$$G(i\omega_n) = \frac{1}{i\omega_n + \mu - \Sigma(i\omega_n)} \quad , \quad D(i\omega_n) = \frac{1}{\omega_n^2 + \omega_0^2 - \Pi(i\omega_n)}$$
$$\Sigma(\tau) = g^2 G(\tau) D(\tau) \quad , \quad \Pi(\tau) = -g^2 G(\tau) G(-\tau)$$

Make the low frequency ansatz

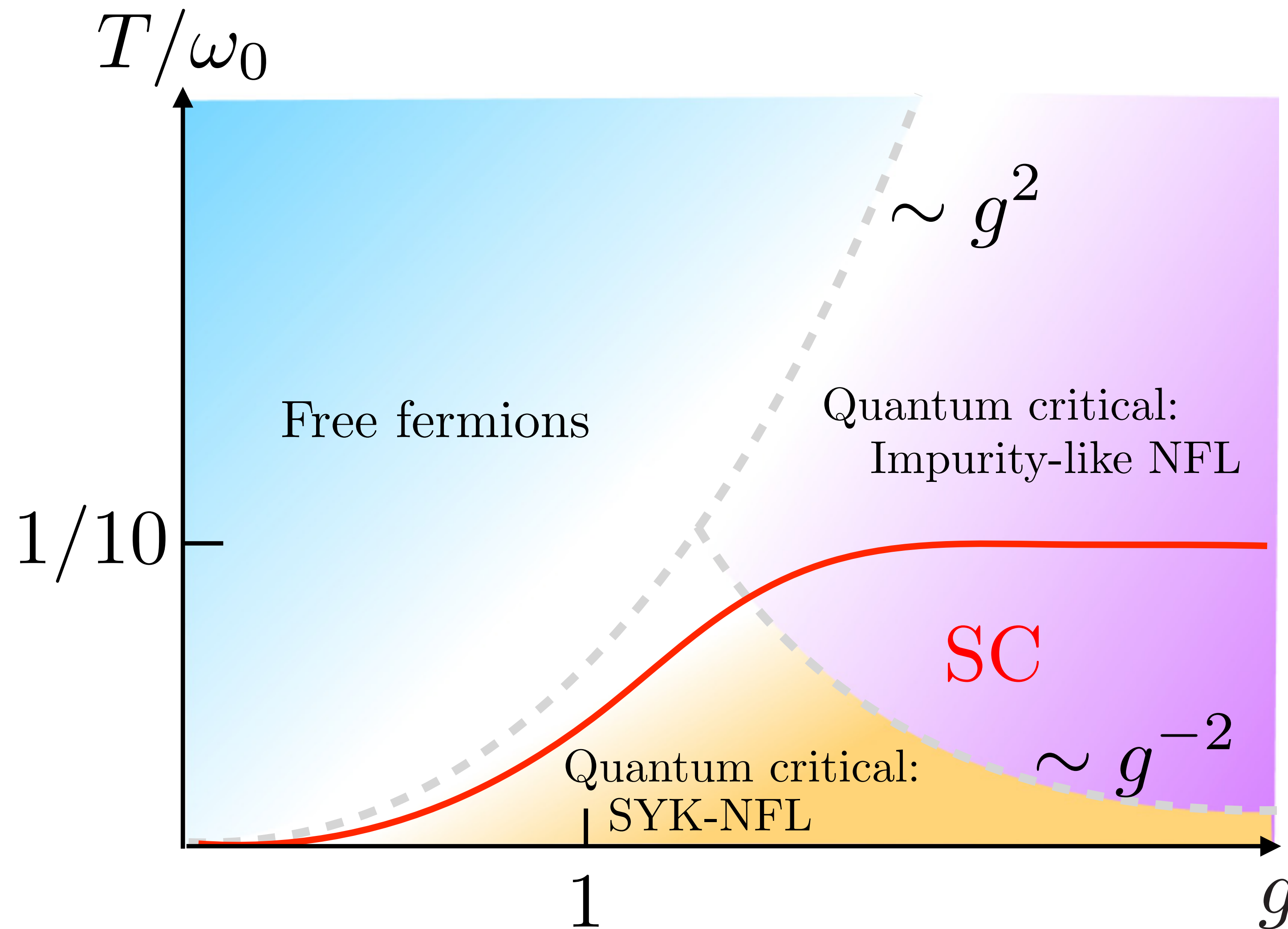
$$G(i\omega) \sim -i \text{sgn}(\omega) |\omega|^{-(1-2\Delta)} \quad , \quad D(i\omega) \sim |\omega|^{1-4\Delta} \quad , \quad \frac{1}{4} < \Delta < \frac{1}{2}$$

A consistent solution exists for

$$\frac{4\Delta - 1}{2(2\Delta - 1)[\sec(2\pi\Delta) - 1]} = 1 \quad , \quad \Delta = 0.42037 \dots$$

I. Esterlis and J. Schmalian,
PRB **100**, 115132 (2019)
See also Yuxuan Wang,
PRL **124**, 017002 (2020)

Yukawa-SYK model



I. Esterlis and J. Schmalian,
PRB **100**, 115132 (2019)
See also Yuxuan Wang,
PRL **124**, 017002 (2020)

Yukawa-SYK model

arXiv > cond-mat > arXiv:2511.01030

Search...

Help | Adva

Condensed Matter > Strongly Correlated Electrons

[Submitted on 2 Nov 2025]

Superlinear Hall angle and carrier mobility from non-Boltzmann magnetotransport in the spatially disordered Yukawa-SYK model on a square lattice

[Davide Valentinis](#), [Jörg Schmalian](#), [Subir Sachdev](#), [Aavishkar A. Patel](#)

Exact numerical results for the DC magnetoconductivity tensor of the two-dimensional spatially disordered Yukawa-Sachdev-Ye-Kitaev (2D-YSYK) model on a square lattice, at first order in applied perpendicular magnetic field, are obtained from the self-consistent disorder-averaged solution of the 2D-YSYK saddle-point equations. This system describes fermions endowed with a Fermi surface and coupled to a bosonic scalar field through spatially random Yukawa interactions. The resulting local and energy-dependent fermionic self-energies are employed in the Kubo formalism to calculate the longitudinal and Hall conductivities, the Hall coefficient, the carrier mobility, and the cotangent of the Hall angle, at fixed fermion density. From the interplay between YSYK interactions and square-lattice embedding, and the non-Boltzmann frequency-dependent self energies, we find nontrivial evolution of the magnetotransport coefficients as a function of temperature and YSYK interaction strength, notably a superlinear evolution of the Hall-angle cotangent and the inverse carrier mobility with temperature, concomitant with linear-in-temperature resistivity, in an extended crossover regime above the low-temperature Marginal Fermi Liquid (MFL) ground state. Our model and results provide a controlled theoretical framework to interpret linear magnetotransport experiments in strange-metal phases found in strongly correlated solid-state electron systems.

1. Hubbard model on the honeycomb lattice:
hydrodynamics in graphene and related materials
2. SYK as a solvable model of quantum matter
without quasiparticles
3. Hubbard model on the square lattice:
spin density wave order, and a universal theory
of strange metals from spatially random interactions.
4. Spin liquids, Fractionalized Fermi liquids (FL*)
and the cuprate phase diagram:
observation of the Yamaji effect.

Hubbard model on the square lattice: spin density wave order, and a universal theory of strange metals from spatially random interactions

School on Emergent Phenomena in
Non-Equilibrium Quantum Many-Body Systems
ICTP-SAIFR

São Paulo, Brazil
November 3,4 2025

Subir Sachdev



The Hubbard Model

$$H = - \sum_{i < j} t_{ij} c_{i\alpha}^\dagger c_{j\alpha} + U \sum_i \left(n_{i\uparrow} - \frac{1}{2} \right) \left(n_{i\downarrow} - \frac{1}{2} \right) - \mu \sum_i c_{i\alpha}^\dagger c_{i\alpha}$$

$t_{ij} \rightarrow$ “hopping”. $U \rightarrow$ local repulsion, $\mu \rightarrow$ chemical potential

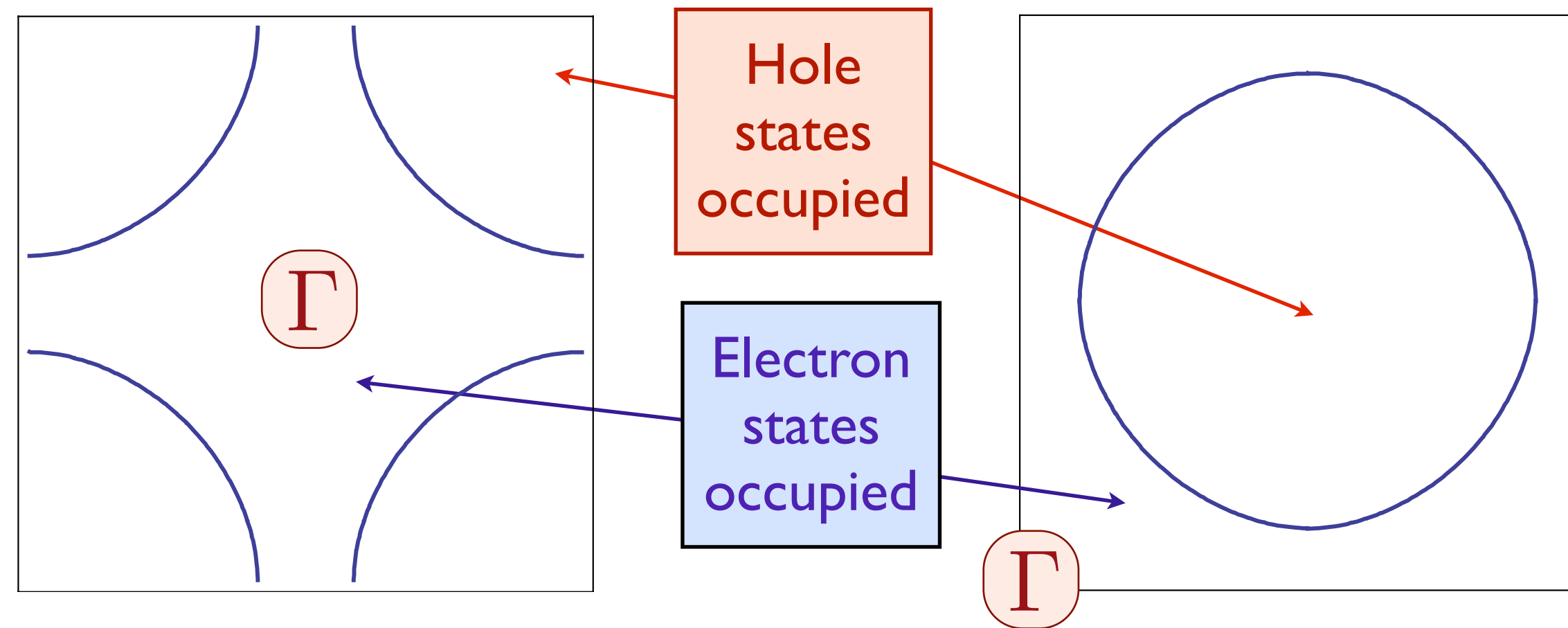
Spin index $\alpha = \uparrow, \downarrow$

$$n_{i\alpha} = c_{i\alpha}^\dagger c_{i\alpha}$$

$$\begin{aligned} c_{i\alpha}^\dagger c_{j\beta} + c_{j\beta} c_{i\alpha}^\dagger &= \delta_{ij} \delta_{\alpha\beta} \\ c_{i\alpha} c_{j\beta} + c_{j\beta} c_{i\alpha} &= 0 \end{aligned}$$

Will study on the square lattice

Fermi surfaces in electron- and hole-doped cuprates



Effective Hamiltonian for quasiparticles:

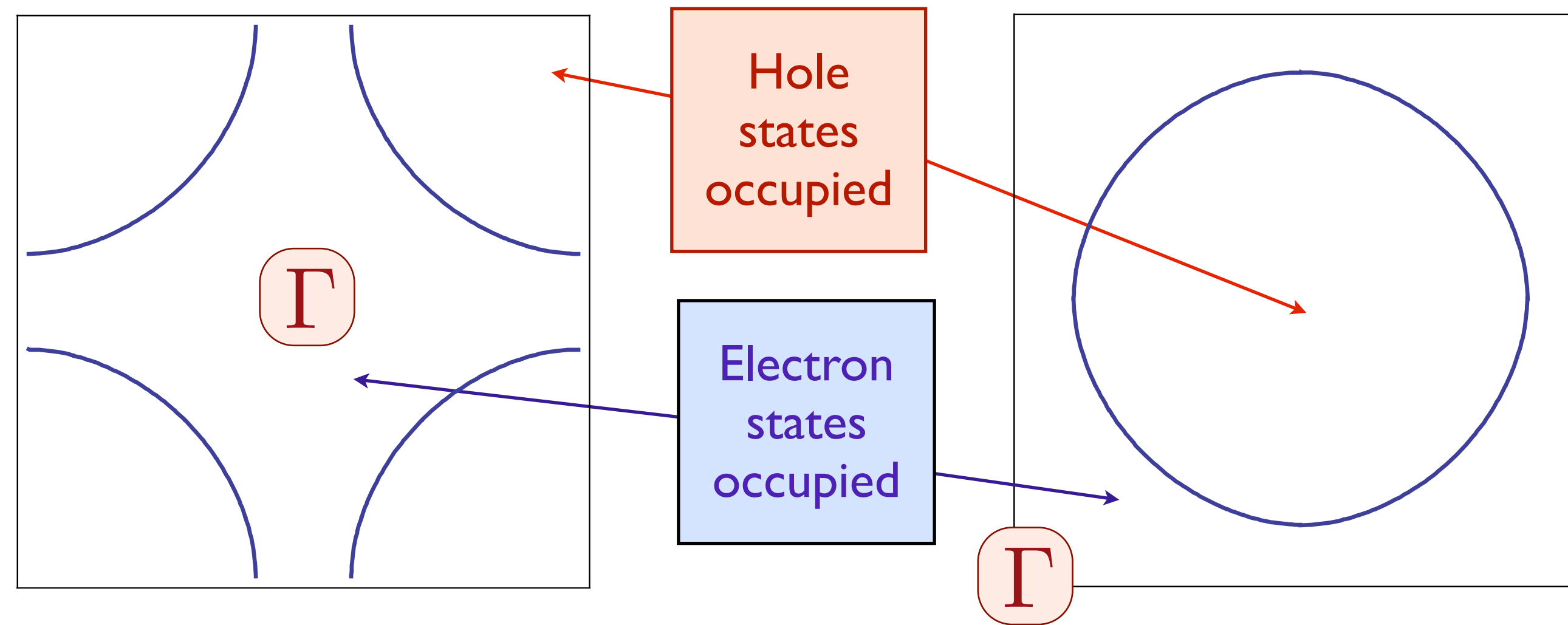
$$H_0 = - \sum_{i < j} t_{ij} c_{i\alpha}^\dagger c_{j\alpha} \equiv \sum_{\mathbf{k}} \epsilon_{\mathbf{k}} c_{\mathbf{k}\alpha}^\dagger c_{\mathbf{k}\alpha}$$

with t_{ij} non-zero for first, second and third neighbor, leads to satisfactory agreement with experiments. The area of the occupied electron states, \mathcal{A}_e , from Luttinger's theory is

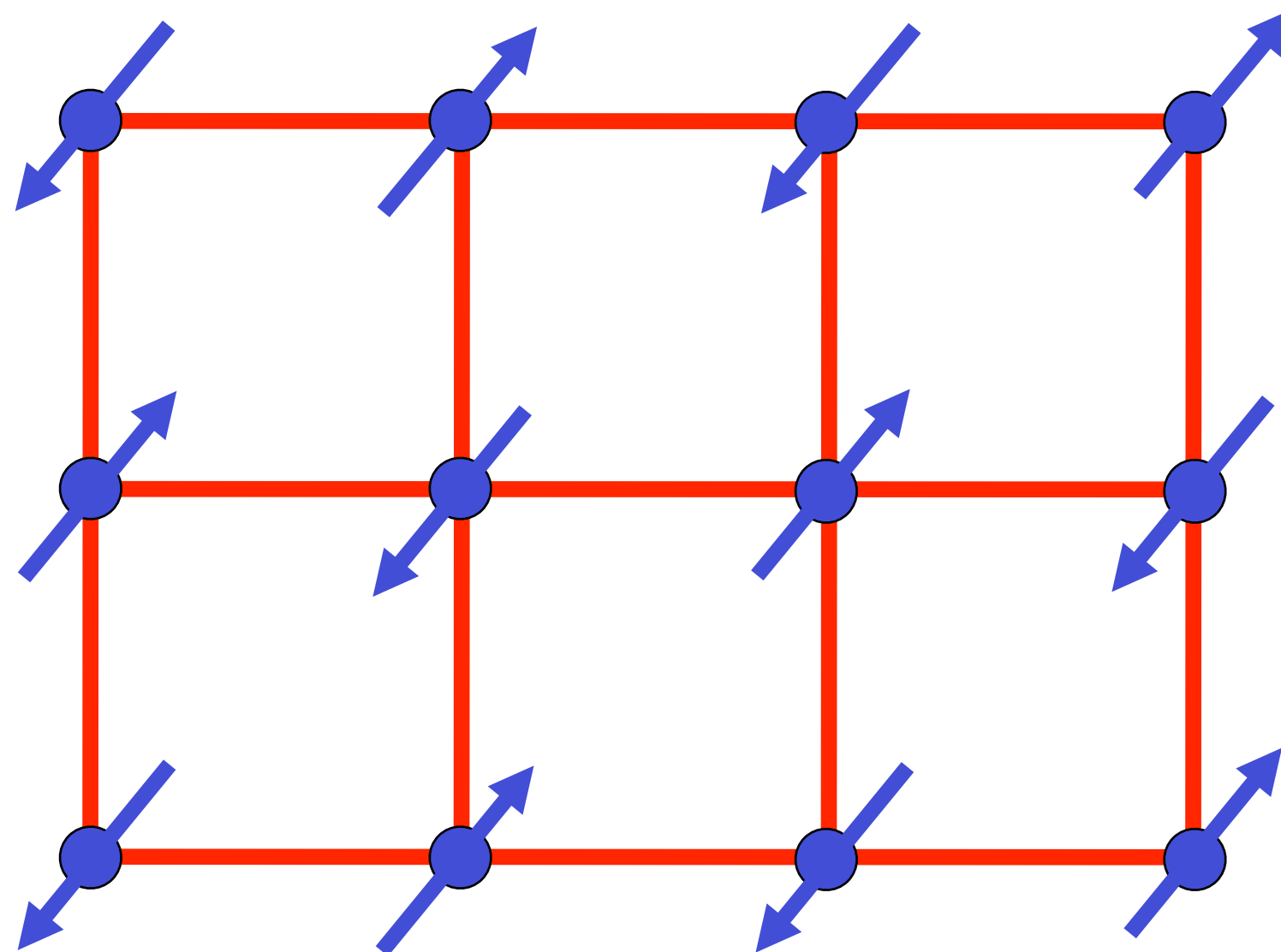
$$\frac{2\mathcal{A}_e}{4\pi^2} = \begin{cases} (1 - x) & \text{for hole-doping } x \\ (1 + p) & \text{for electron-doping } p \end{cases}$$

The area of the occupied hole states, \mathcal{A}_h , which form a closed Fermi surface and so appear in quantum oscillation experiments is $\mathcal{A}_h = 4\pi^2 - \mathcal{A}_e$.

Fermi surface+antiferromagnetism



+



The electron spin polarization obeys

$$\langle \vec{S}(\mathbf{r}, \tau) \rangle = \vec{\varphi}(\mathbf{r}, \tau) e^{i\mathbf{K} \cdot \mathbf{r}}$$

where $\mathbf{K} = (\pi, \pi)$ is the ordering wavevector.

Fermi surface+antiferromagnetism

We use the operator equation (valid on each site i):

$$U \left(n_{\uparrow} - \frac{1}{2} \right) \left(n_{\downarrow} - \frac{1}{2} \right) = -\frac{2U}{3} \vec{S}^2 + \frac{U}{4} \quad (1)$$

Then we decouple the interaction via

$$\exp \left(\frac{2U}{3} \sum_i \int d\tau \vec{S}_i^2 \right) = \int \mathcal{D} \vec{J}_i(\tau) \exp \left(- \sum_i \int d\tau \left[\frac{3}{8U} \vec{J}_i^2 - \vec{J}_i \vec{S}_i \right] \right) \quad (2)$$

We now integrate out the fermions, and look for the saddle point of the resulting effective action for \vec{J}_i . At the saddle-point we find that the lowest energy is achieved when the vector has opposite orientations on the A and B sublattices. Anticipating this, we look for a continuum limit in terms of a field $\vec{\varphi}_i$ where

$$\vec{J}_i = \vec{\varphi}_i e^{i\mathbf{K} \cdot \mathbf{r}_i} \quad (3)$$

Fermi surface+antiferromagnetism

In this manner, we obtain the “spin-fermion” model

$$\begin{aligned}\mathcal{Z} &= \int \mathcal{D}c_\alpha \mathcal{D}\vec{\varphi} \exp(-\mathcal{S}) \\ \mathcal{S} &= \int d\tau \sum_{\mathbf{k}} c_{\mathbf{k}\alpha}^\dagger \left(\frac{\partial}{\partial \tau} - \varepsilon_{\mathbf{k}} \right) c_{\mathbf{k}\alpha} \\ &\quad - \lambda \int d\tau \sum_i c_{i\alpha}^\dagger \vec{\varphi}_i \cdot \vec{\sigma}_{\alpha\beta} c_{i\beta} e^{i\mathbf{K} \cdot \mathbf{r}_i} \\ &\quad + \int d\tau d^2r \left[\frac{1}{2} (\nabla_r \vec{\varphi})^2 + \frac{1}{2} (\partial_\tau \vec{\varphi})^2 + \frac{s}{2} \vec{\varphi}^2 + \frac{u}{4} \vec{\varphi}^4 \right]\end{aligned}$$

Fermi surface+antiferromagnetism

In the Hamiltonian form (ignoring, for now, the time dependence of $\vec{\varphi}$), the coupling between $\vec{\varphi}$ and the electrons takes the form

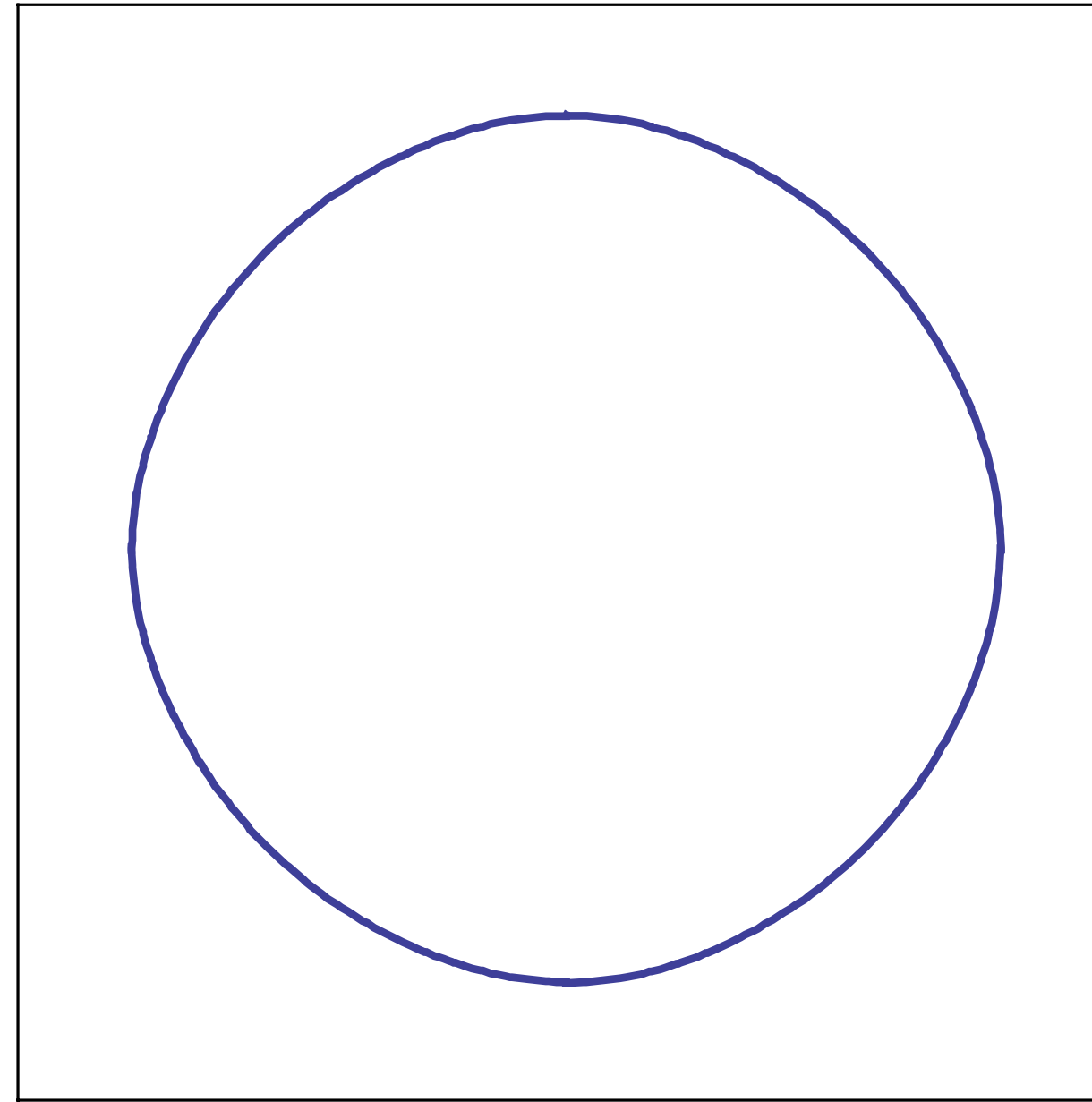
$$H_{\text{sdw}} = \lambda \sum_{\mathbf{k}, \mathbf{q}, \alpha, \beta} \vec{\varphi}_{\mathbf{q}} \cdot c_{\mathbf{k}+\mathbf{q}, \alpha}^{\dagger} \vec{\sigma}_{\alpha\beta} c_{\mathbf{k}+\mathbf{K}, \beta}$$

where $\vec{\sigma}$ are the Pauli matrices, the boson momentum \mathbf{q} is small, while the fermion momentum \mathbf{k} extends over the entire Brillouin zone. In the antiferromagnetically ordered state, we may take $\vec{\varphi} \propto (0, 0, 1)$, and the electron dispersions obtained by diagonalizing $H_0 + H_{\text{sdw}}$ are

$$E_{\mathbf{k}\pm} = \frac{\varepsilon_{\mathbf{k}} + \varepsilon_{\mathbf{k}+\mathbf{K}}}{2} \pm \sqrt{\left(\frac{\varepsilon_{\mathbf{k}} - \varepsilon_{\mathbf{k}+\mathbf{K}}}{2}\right)^2 + \lambda^2 |\vec{\varphi}|^2}$$

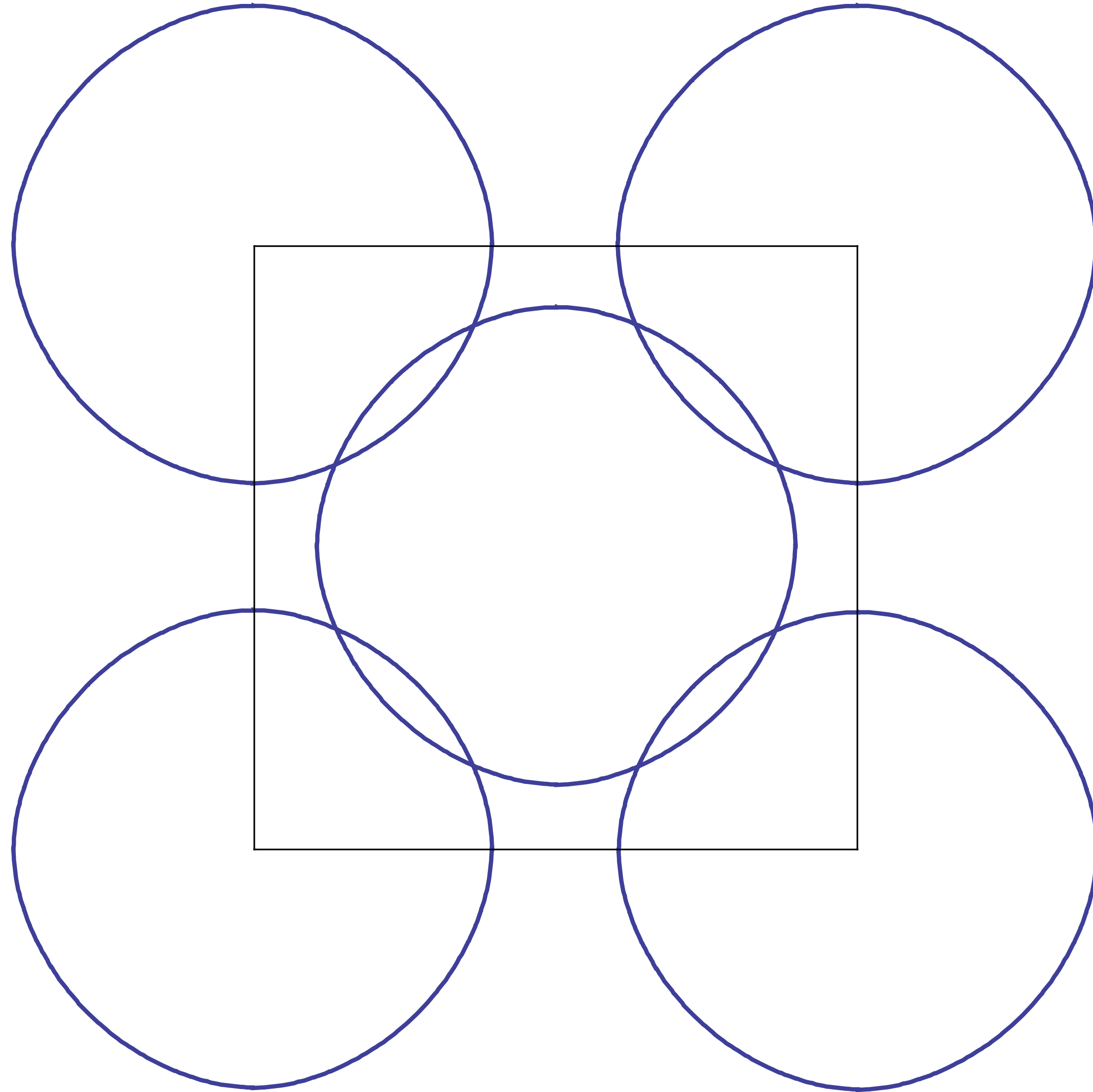
This leads to the Fermi surfaces shown in the following slides as a function of increasing $|\vec{\varphi}|$.

Fermi surface+antiferromagnetism



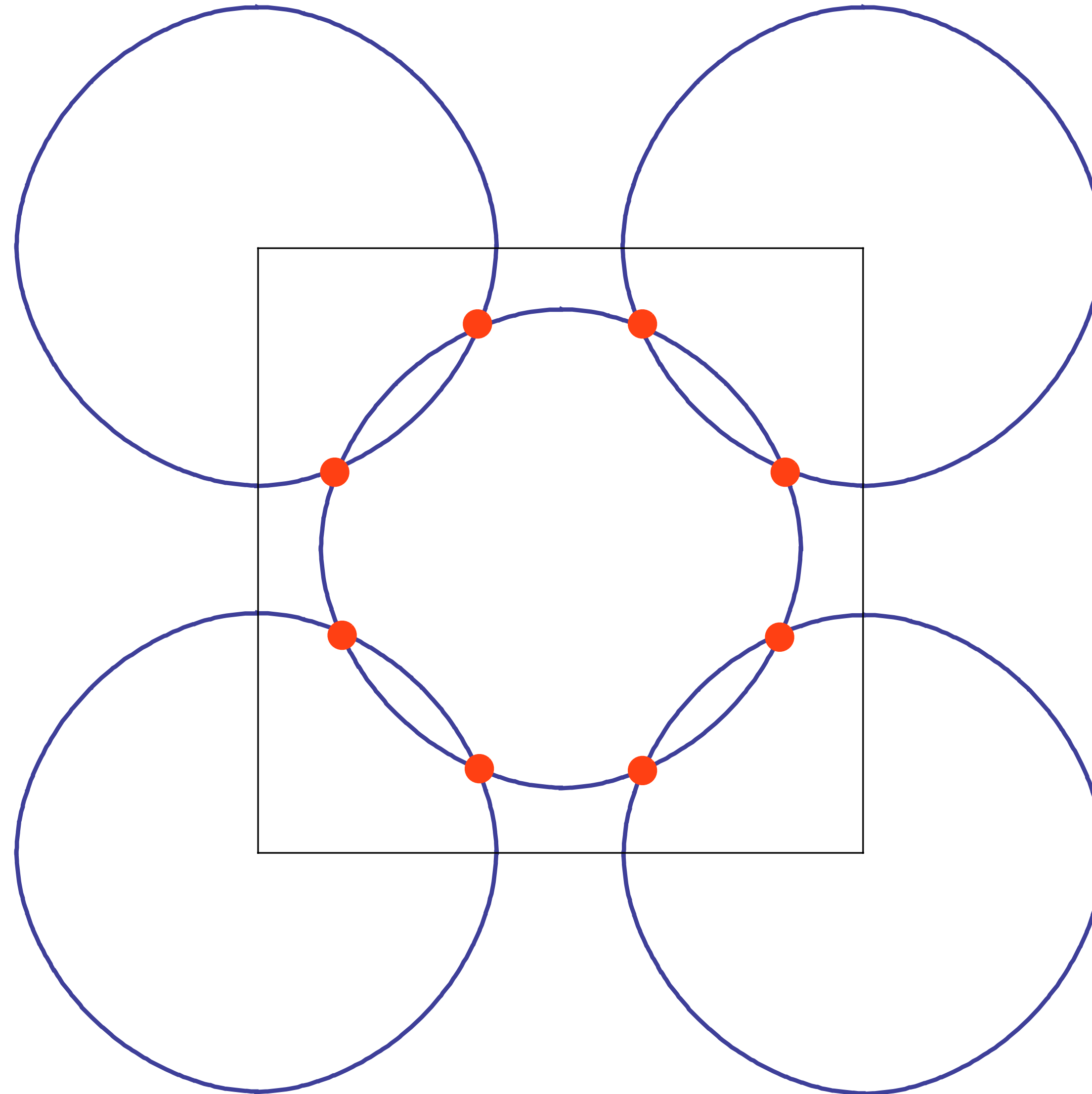
Metal with “large” Fermi surface

Fermi surface+antiferromagnetism



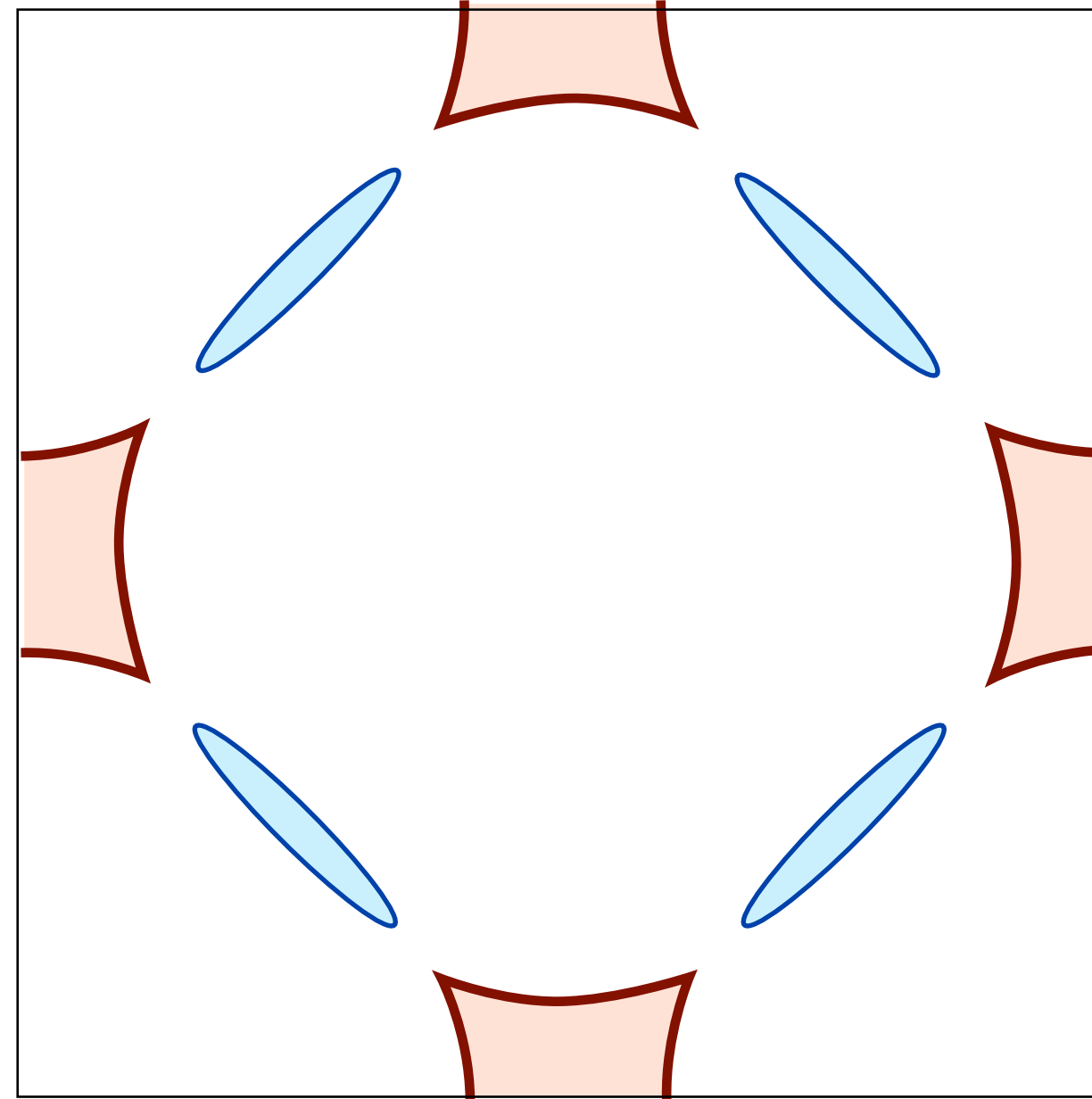
Fermi surfaces translated by $\mathbf{K} = (\pi, \pi)$.

Fermi surface+antiferromagnetism



“Hot” spots

Fermi surface+antiferromagnetism

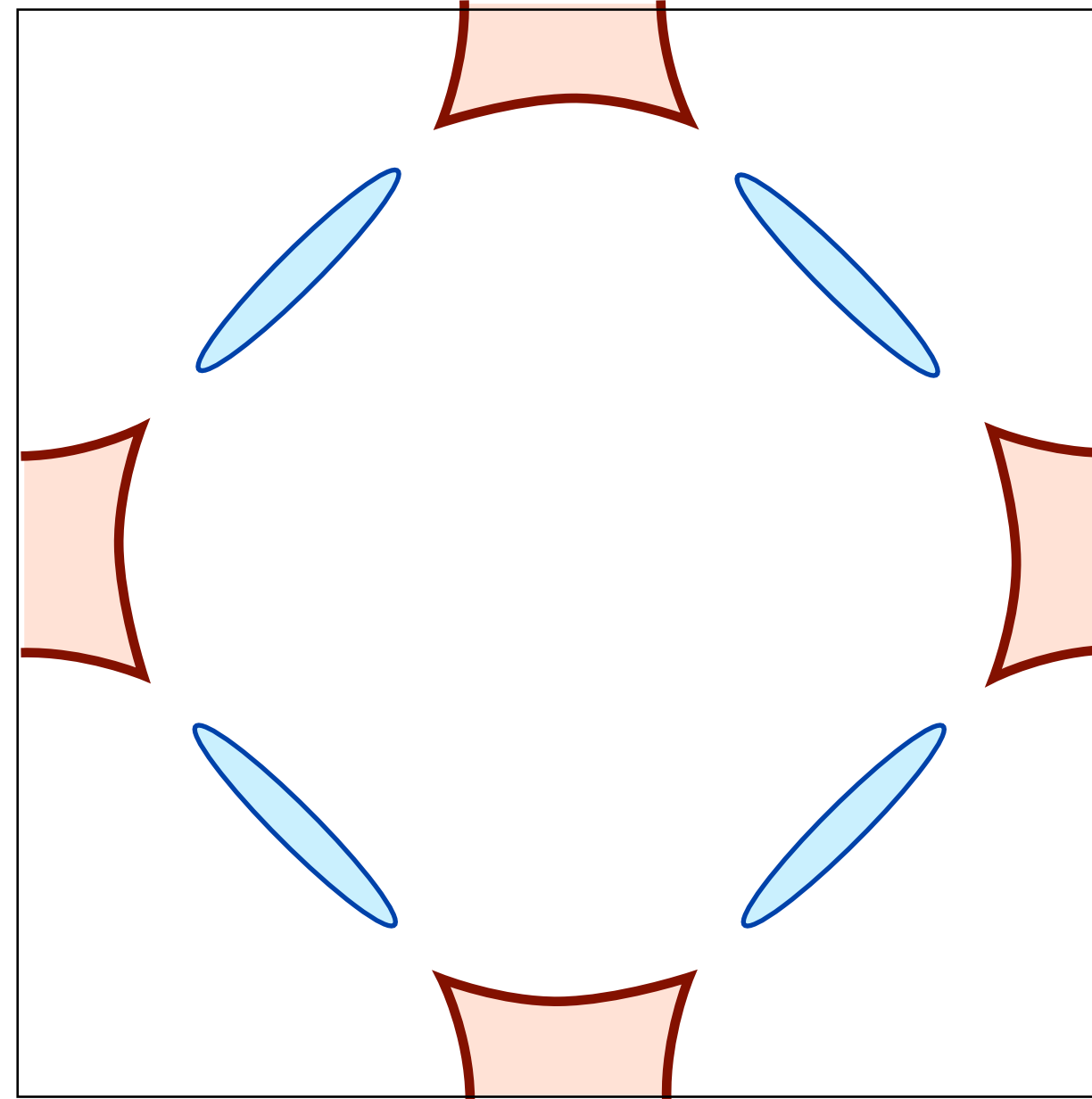


Electron and hole pockets in
antiferromagnetic phase with $\langle \vec{\varphi} \rangle \neq 0$

Fermi surface+antiferromagnetism

Obeys Luttinger volume
in reduced Brillouin zone:

$$2 \times \frac{1}{(2\pi)^2/2} \times (-2\mathcal{A}_h + \mathcal{A}_e) = -2p.$$

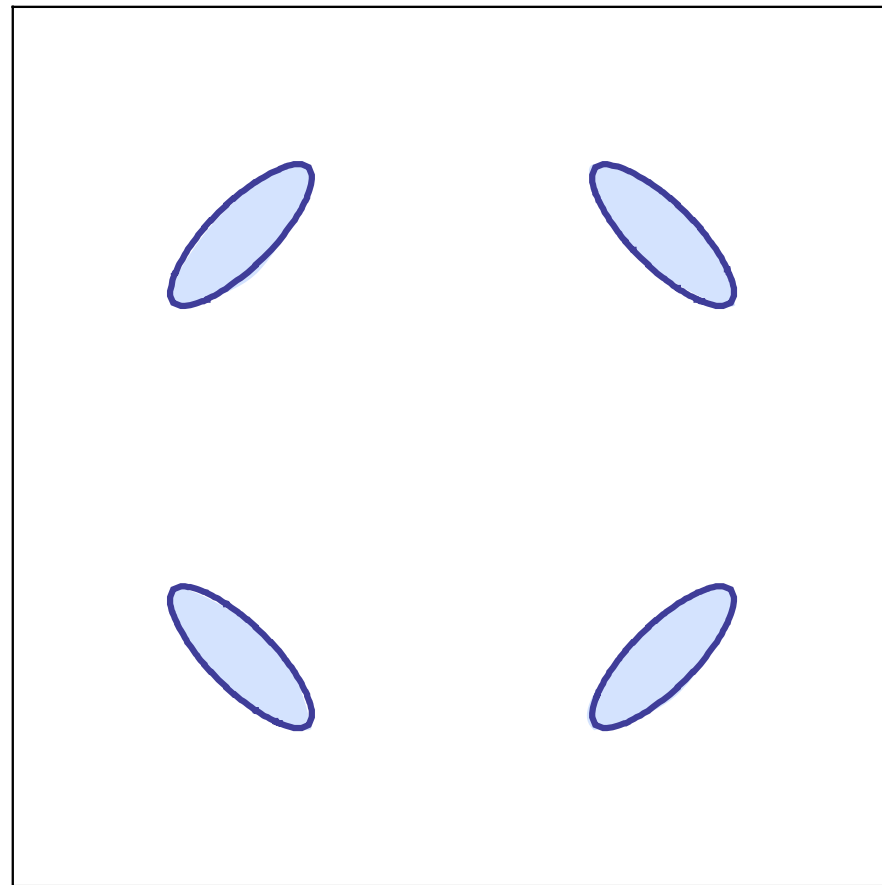


Electron and hole pockets in
antiferromagnetic phase with $\langle \vec{\varphi} \rangle \neq 0$

Square lattice Hubbard model with hole doping

$$\langle \vec{\varphi} \rangle \neq 0$$

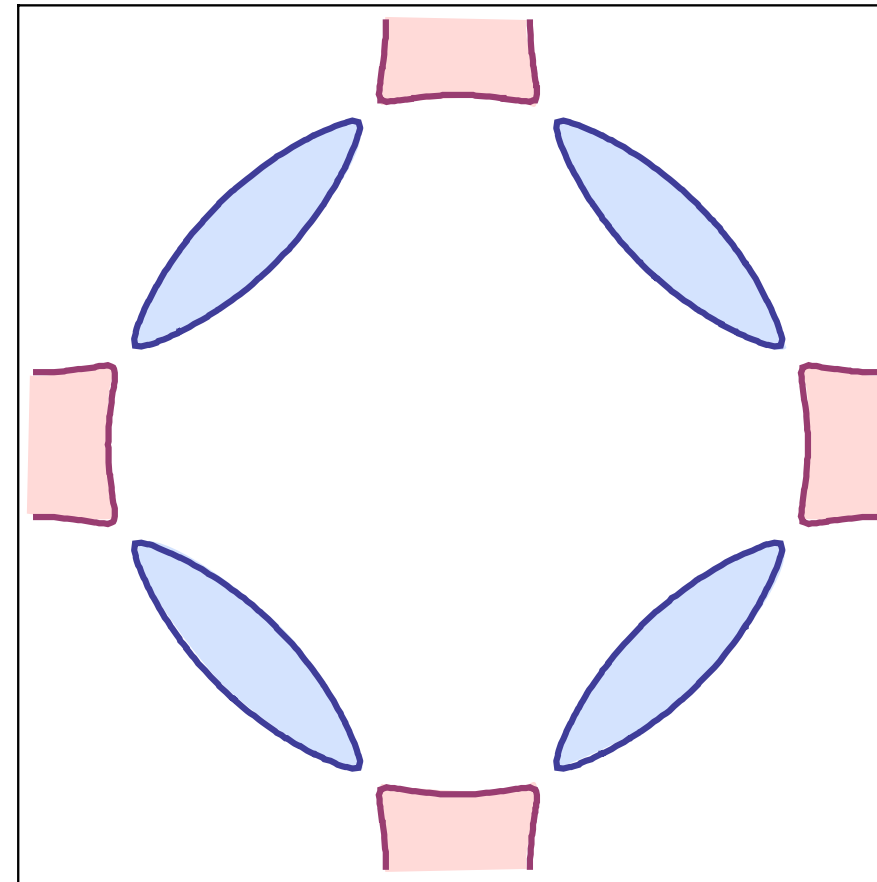
and large



Metal with
hole pockets

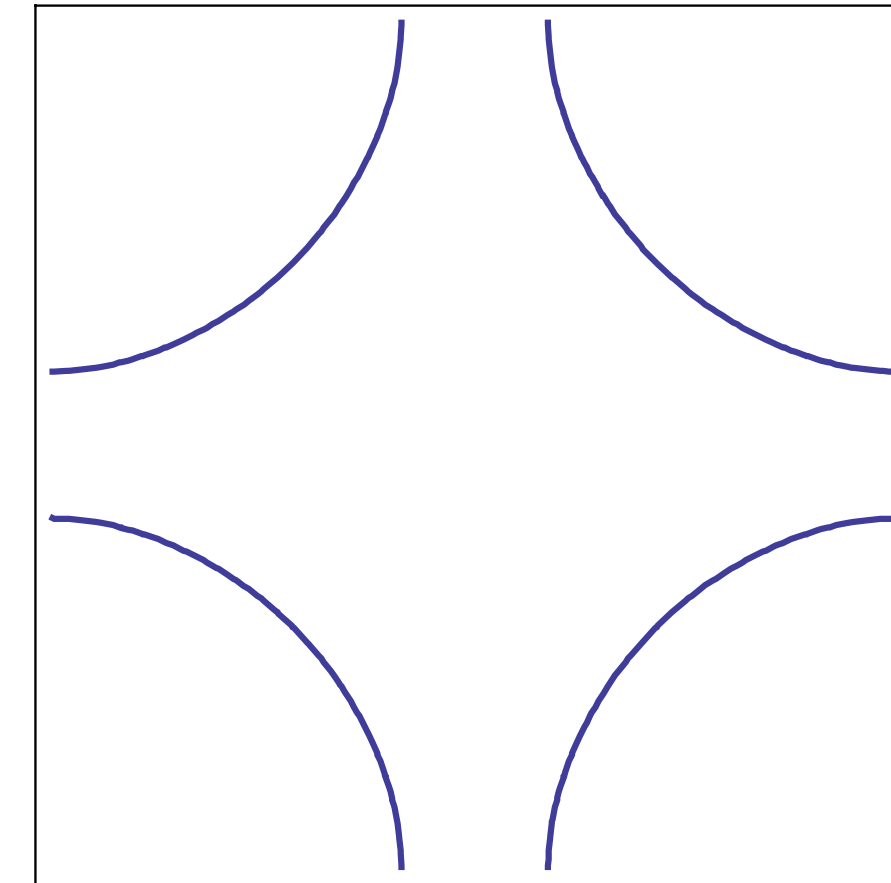
$$\langle \vec{\varphi} \rangle \neq 0$$

and small



Metal with
electron and
hole pockets

$$\langle \vec{\varphi} \rangle = 0$$



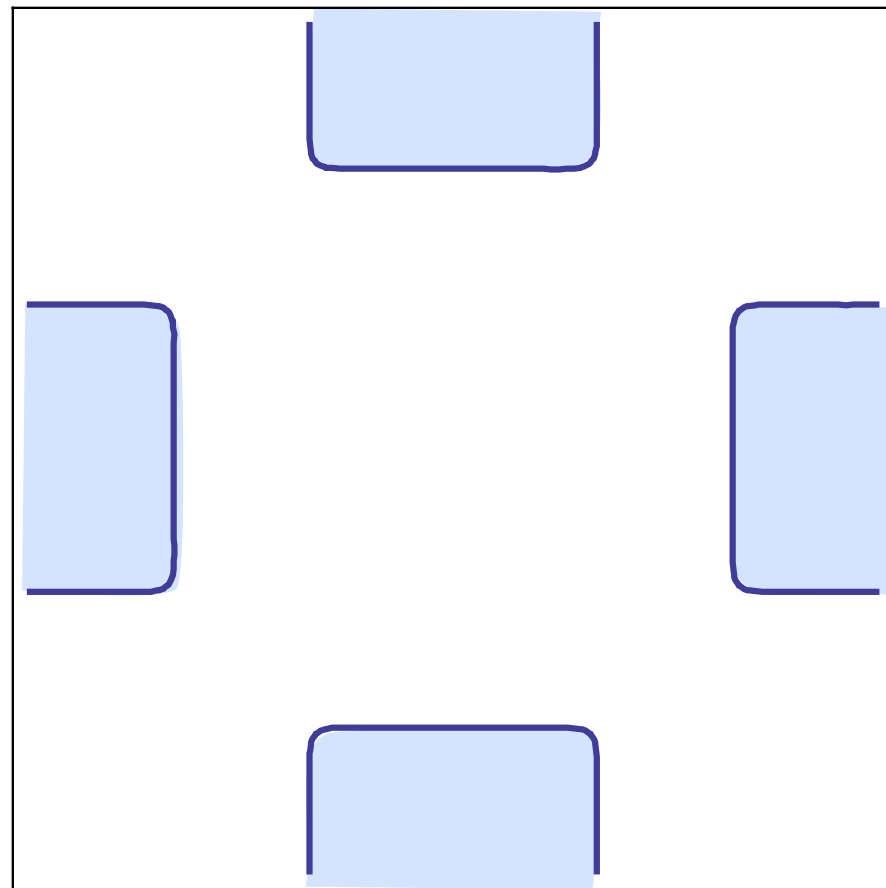
Metal with
"large" Fermi
surface

S

Square lattice Hubbard model with electron doping

$$\langle \vec{\varphi} \rangle \neq 0$$

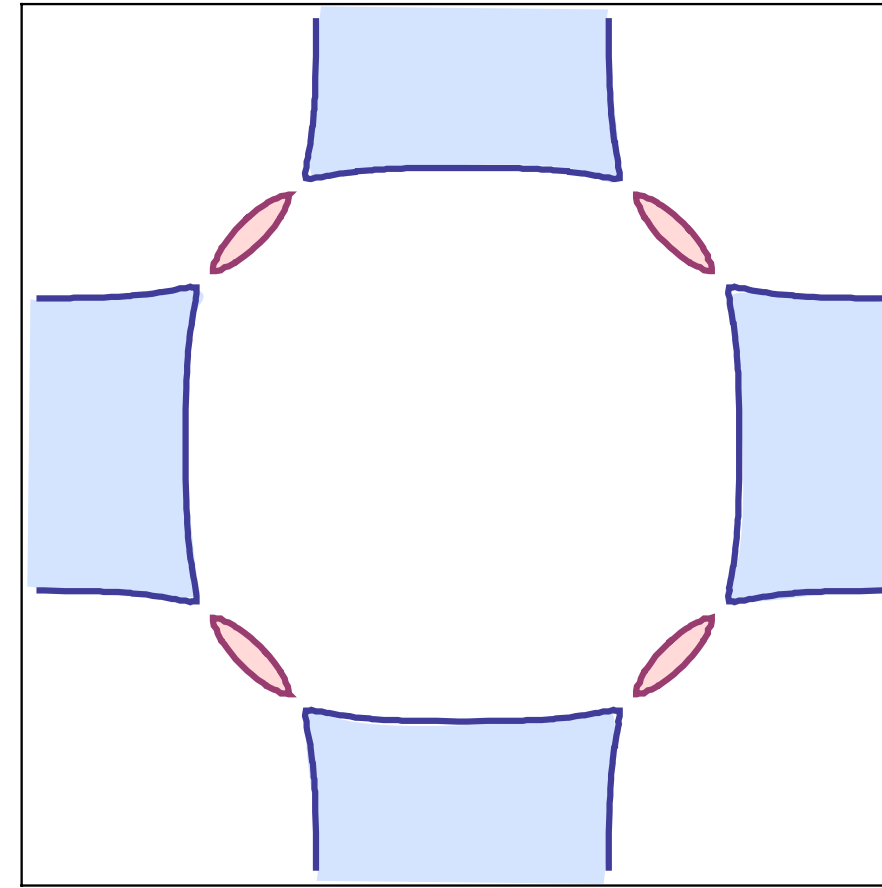
and large



Metal with
electron pockets

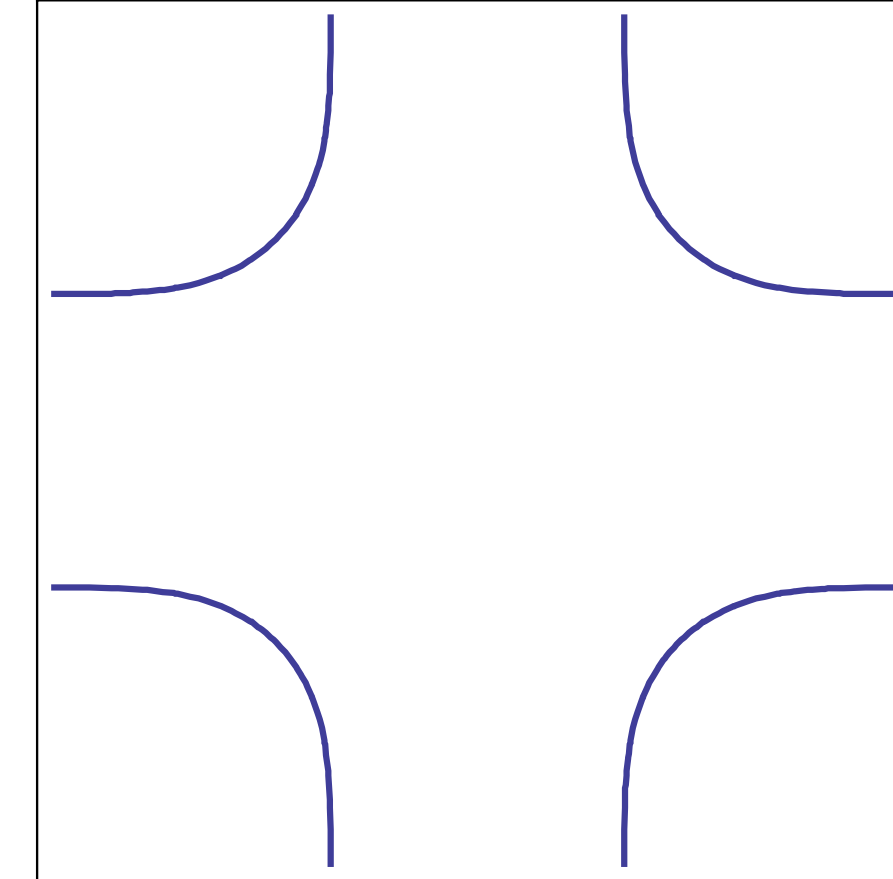
$$\langle \vec{\varphi} \rangle \neq 0$$

and small



Metal with
electron and
hole pockets

$$\langle \vec{\varphi} \rangle = 0$$



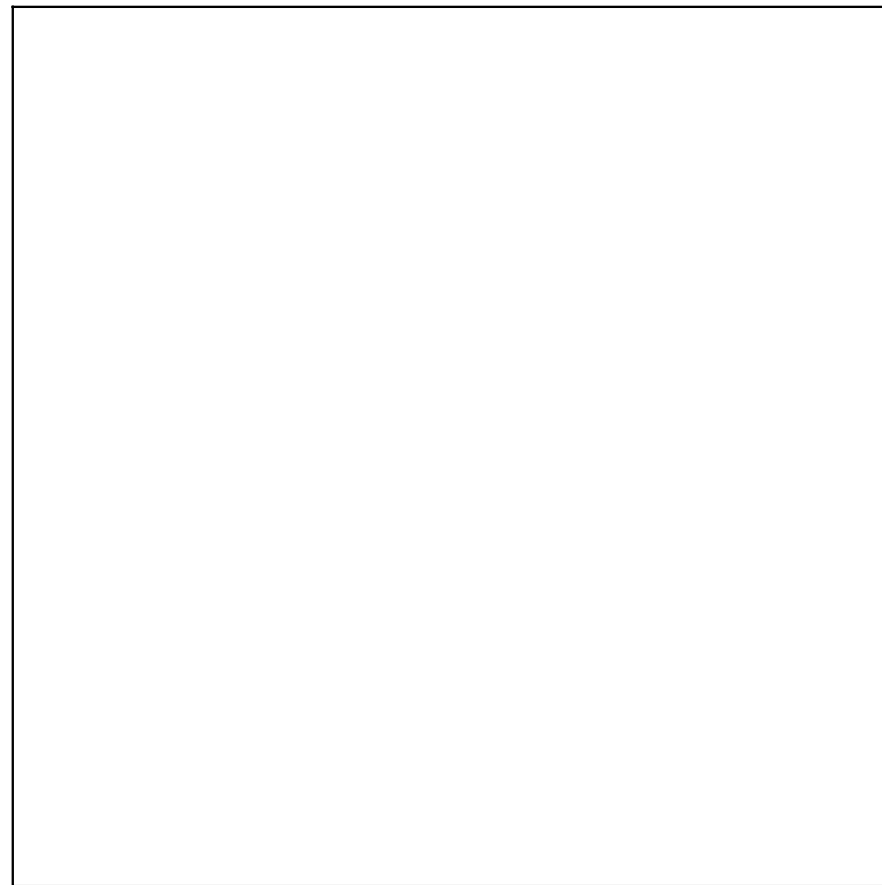
Metal with
“large” Fermi
surface

S

Square lattice Hubbard model with no doping

$$\langle \vec{\varphi} \rangle \neq 0$$

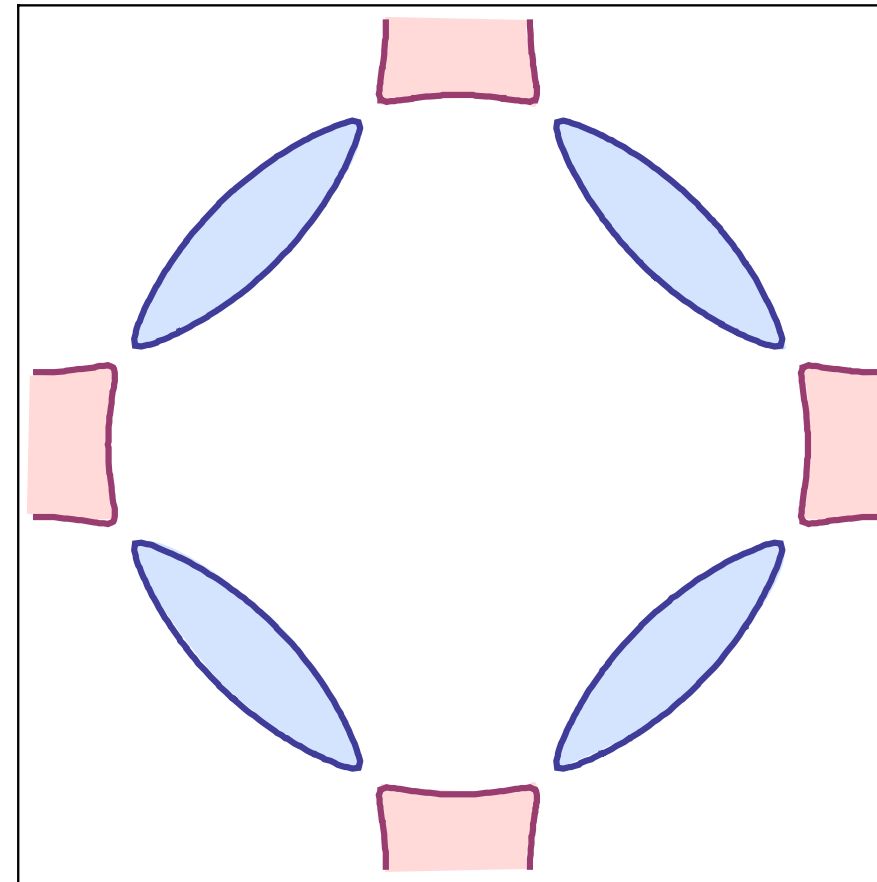
and large



Insulator

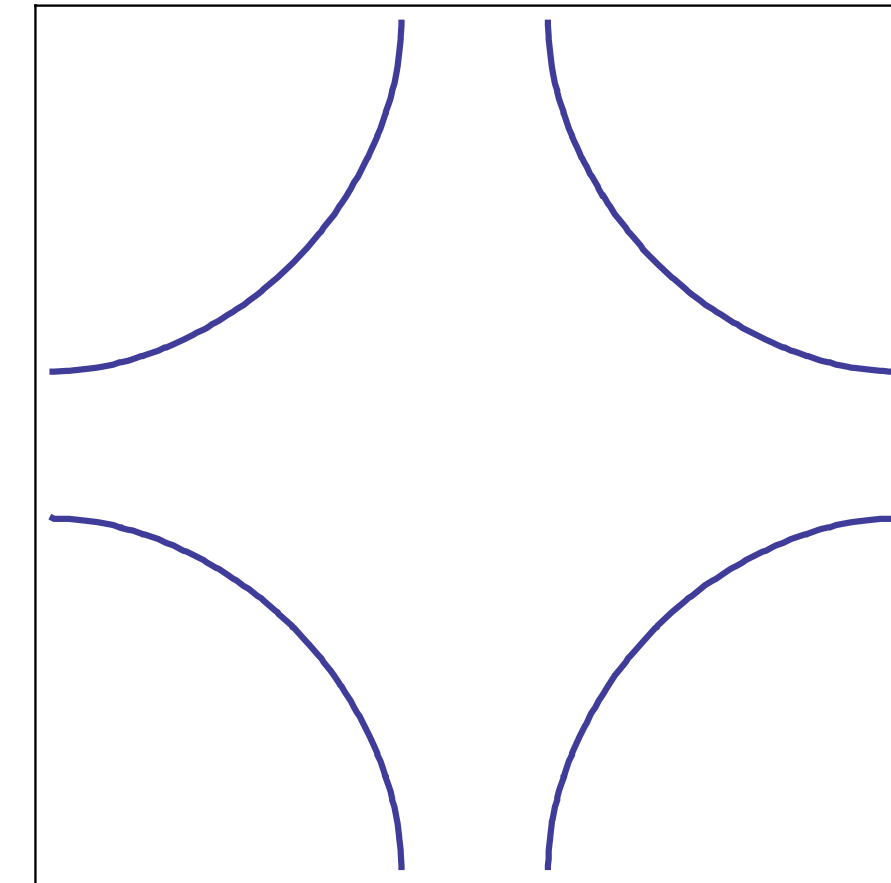
$$\langle \vec{\varphi} \rangle \neq 0$$

and small



Metal with
electron and
hole pockets

$$\langle \vec{\varphi} \rangle = 0$$



Metal with
“large” Fermi
surface

S

Fermi surface+antiferromagnetism

We use the operator equation (valid on each site i):

$$U \left(n_{\uparrow} - \frac{1}{2} \right) \left(n_{\downarrow} - \frac{1}{2} \right) = -\frac{2U}{3} \vec{S}^2 + \frac{U}{4} \quad (1)$$

Then we decouple the interaction via

$$\exp \left(\frac{2U}{3} \sum_i \int d\tau \vec{S}_i^2 \right) = \int \mathcal{D} \vec{J}_i(\tau) \exp \left(- \sum_i \int d\tau \left[\frac{3}{8U} \vec{J}_i^2 - \vec{J}_i \vec{S}_i \right] \right) \quad (2)$$

We now integrate out the fermions, and look for the saddle point of the resulting effective action for \vec{J}_i . At the saddle-point we find that the lowest energy is achieved when the vector has opposite orientations on the A and B sublattices. Anticipating this, we look for a continuum limit in terms of a field $\vec{\varphi}_i$ where

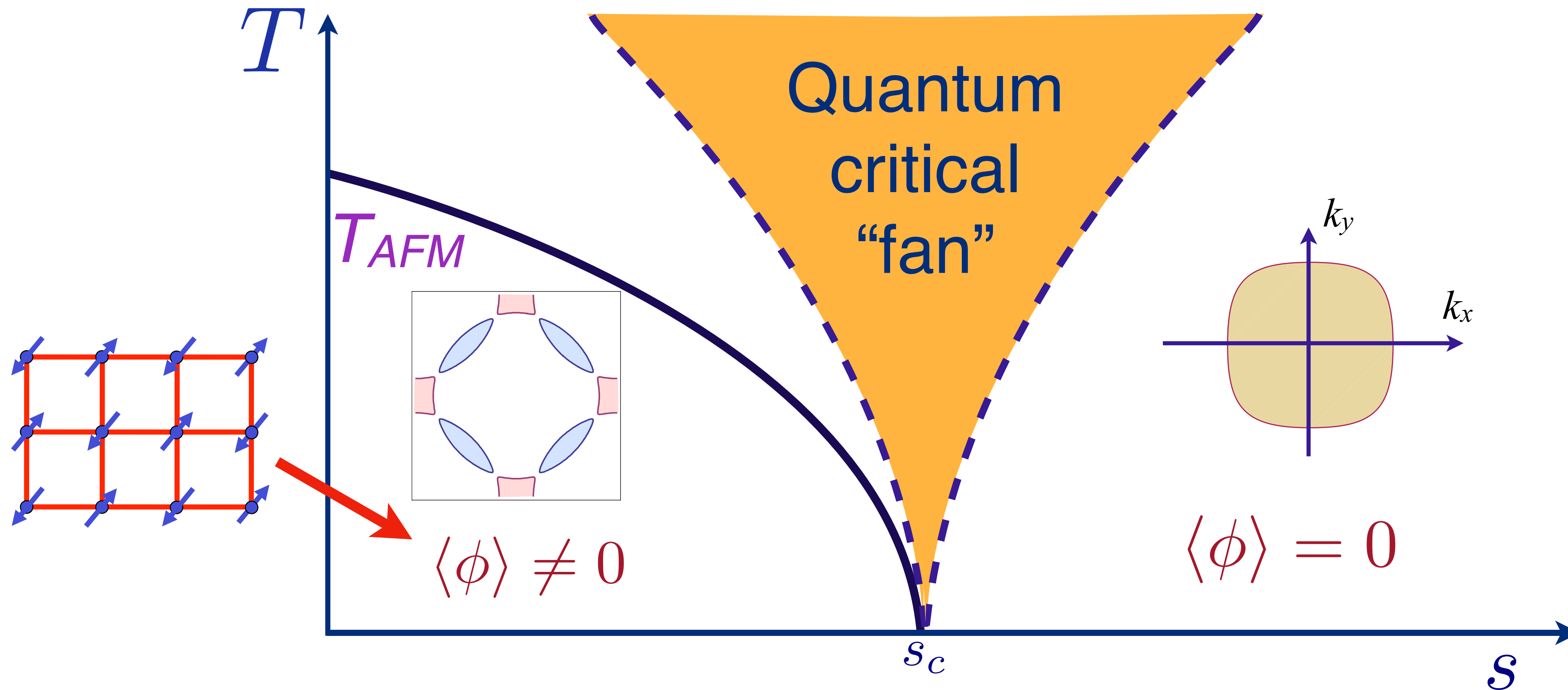
$$\vec{J}_i = \vec{\varphi}_i e^{i\mathbf{K} \cdot \mathbf{r}_i} \quad (3)$$

Hertz effective action

Integrate out the fermions to obtain the Hertz effective action

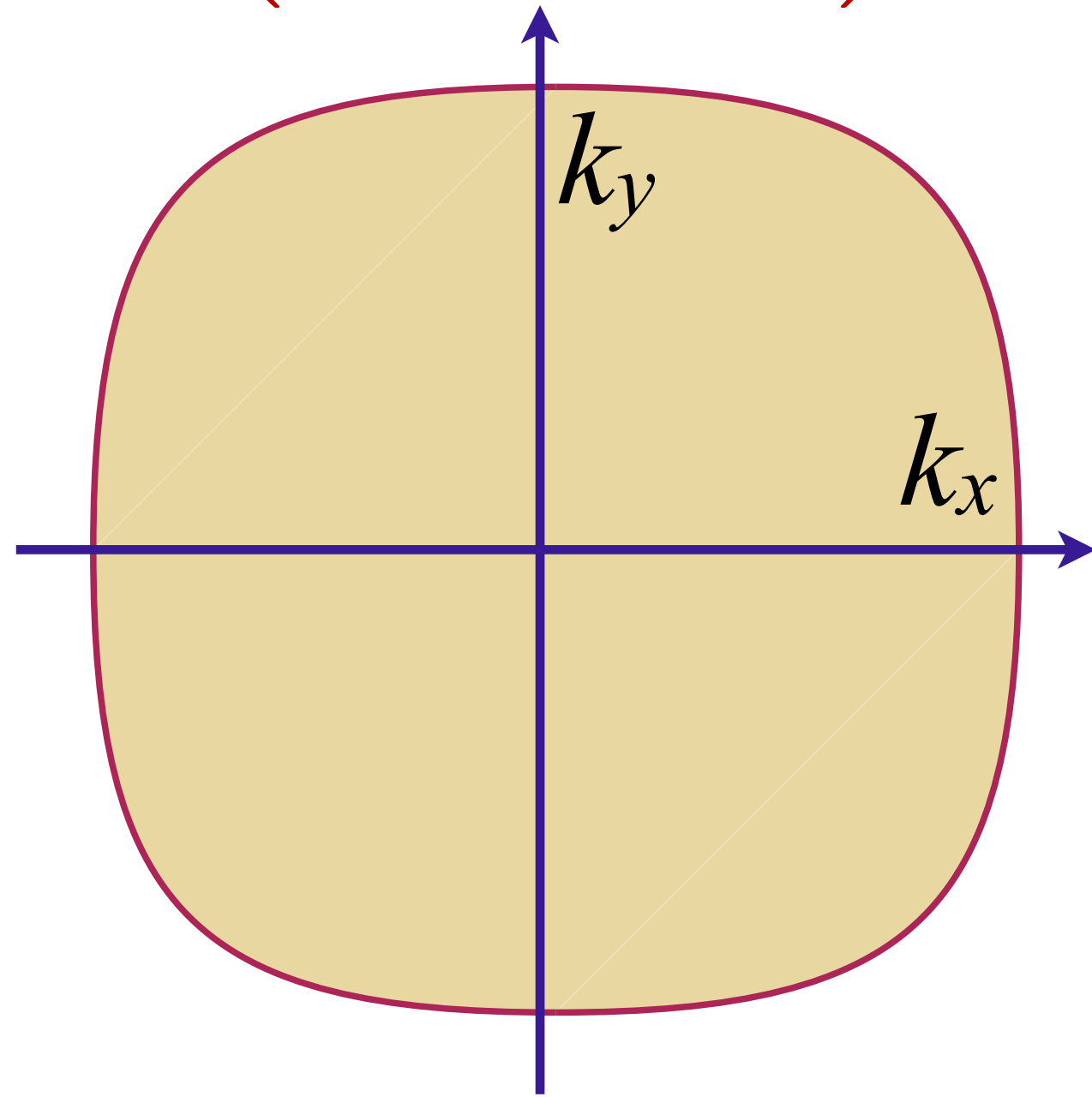
$$\begin{aligned}\mathcal{S}_H[\vec{\varphi}] &= \sum_{\mathbf{k}, \omega} |\vec{\varphi}(\mathbf{k}, i\omega)|^2 \left[\frac{3}{8U} - \chi(\mathbf{K} + \mathbf{k}, i\omega) \right] + \dots \\ &= \sum_{\mathbf{k}, \omega} |\vec{\varphi}(\mathbf{k}, i\omega)|^2 \left[k^2 + |\omega| + s \right] + \dots\end{aligned}$$

Fermi surface reconstruction from spin density wave (SDW) order



Fermi surface + critical boson with no spatial disorder

$$c_{\mathbf{k}\sigma}^\dagger \left(\frac{\partial}{\partial \tau} + \varepsilon(\mathbf{k}) \right) c_{\mathbf{k}\sigma}$$



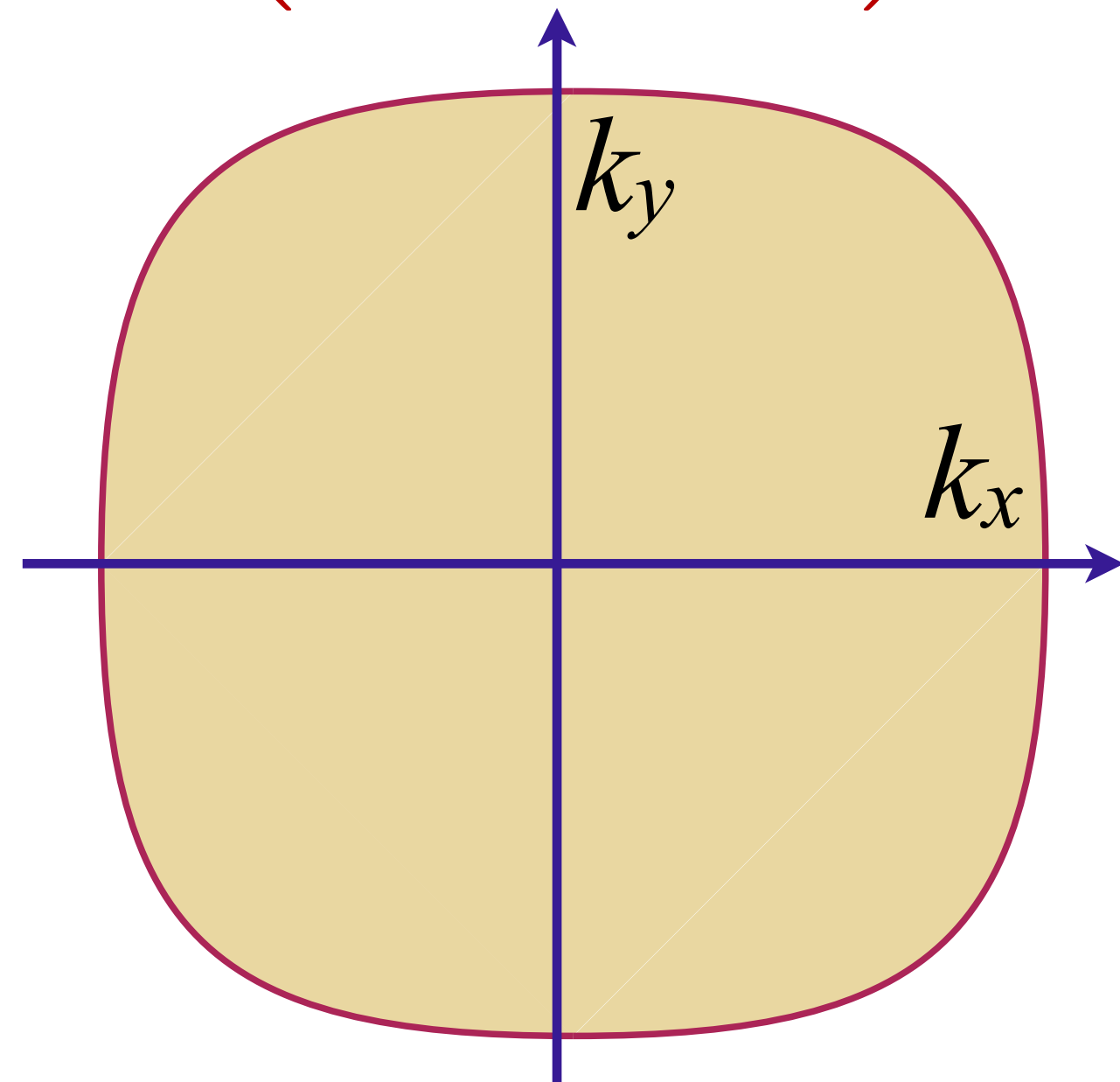
$$+s [\phi(\mathbf{r})]^2$$

$$+g c_\sigma^\dagger(\mathbf{r}) \tau_{\sigma\sigma'}^a c_{\sigma'}(\mathbf{r}) \phi_a(\mathbf{r}) e^{i\mathbf{K}\cdot\mathbf{r}}$$

$$+K [\nabla_{\mathbf{r}} \phi(\mathbf{r})]^2 + u [\phi(\mathbf{r})]^4$$

Fermi surface + critical boson with no spatial disorder

$$c_{\mathbf{k}\sigma}^\dagger \left(\frac{\partial}{\partial \tau} + \varepsilon(\mathbf{k}) \right) c_{\mathbf{k}\sigma}$$



$$+s [\phi(\mathbf{r})]^2$$

$$+g c_\sigma^\dagger(\mathbf{r}) \tau_{\sigma\sigma'}^a c_{\sigma'}(\mathbf{r}) \phi_a(\mathbf{r}) e^{i\mathbf{K}\cdot\mathbf{r}}$$

$$+K [\nabla_{\mathbf{r}} \phi(\mathbf{r})]^2 + u [\phi(\mathbf{r})]^4$$

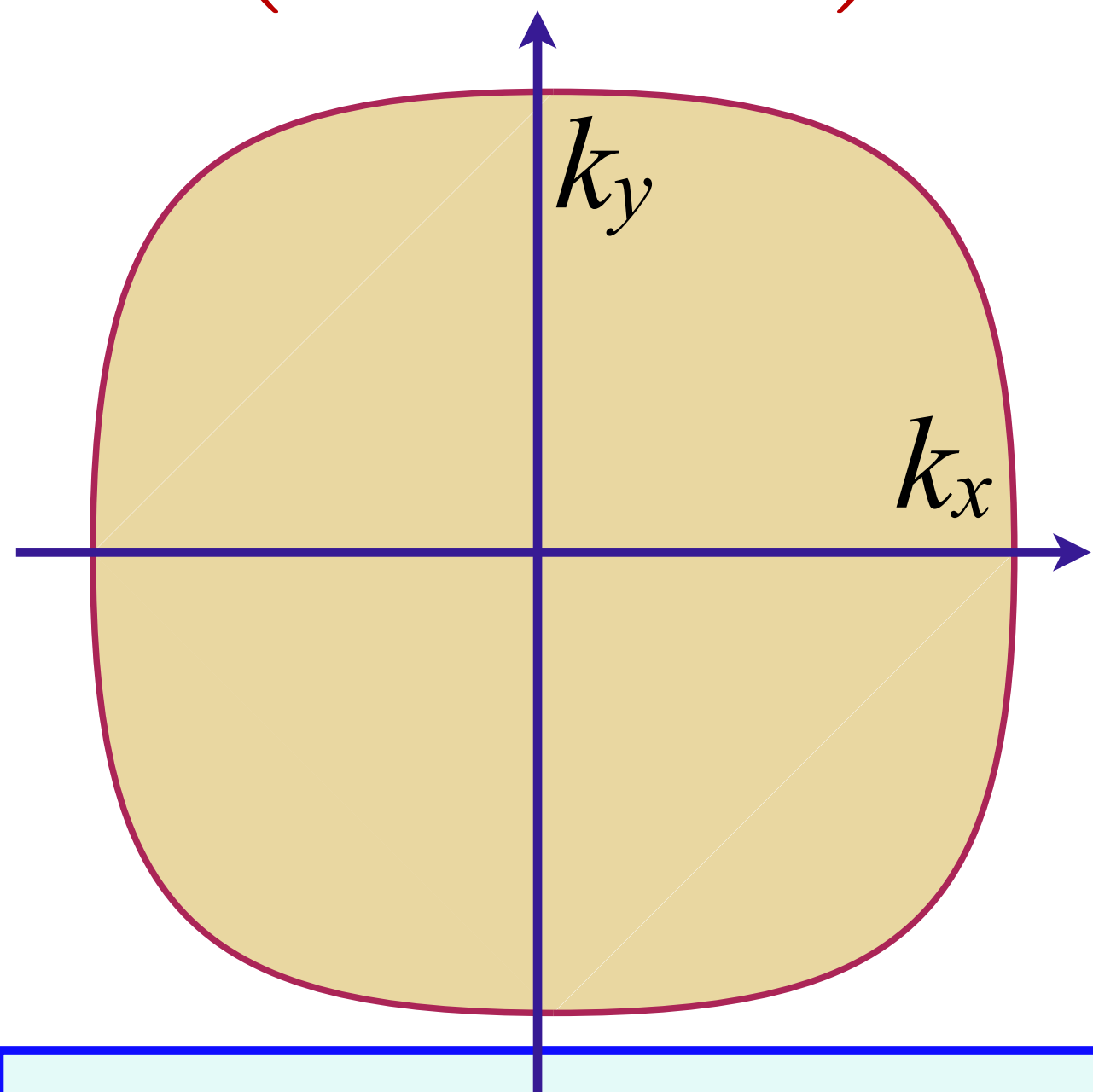
A. A. Patel and S. S.,
PRB **90**, 165146 (2014)

Not a strange metal, despite strongly coupled quantum criticality.

Extreme drag: the fermions c “drag” the bosons ϕ as they move, and so electrical current does not relax, even though strong c - ϕ scattering leads to absence of c quasiparticles.

Fermi surface + critical boson with potential disorder

$$c_{\mathbf{k}\sigma}^\dagger \left(\frac{\partial}{\partial \tau} + \varepsilon(\mathbf{k}) \right) c_{\mathbf{k}\sigma}$$



$$+s [\phi(\mathbf{r})]^2$$

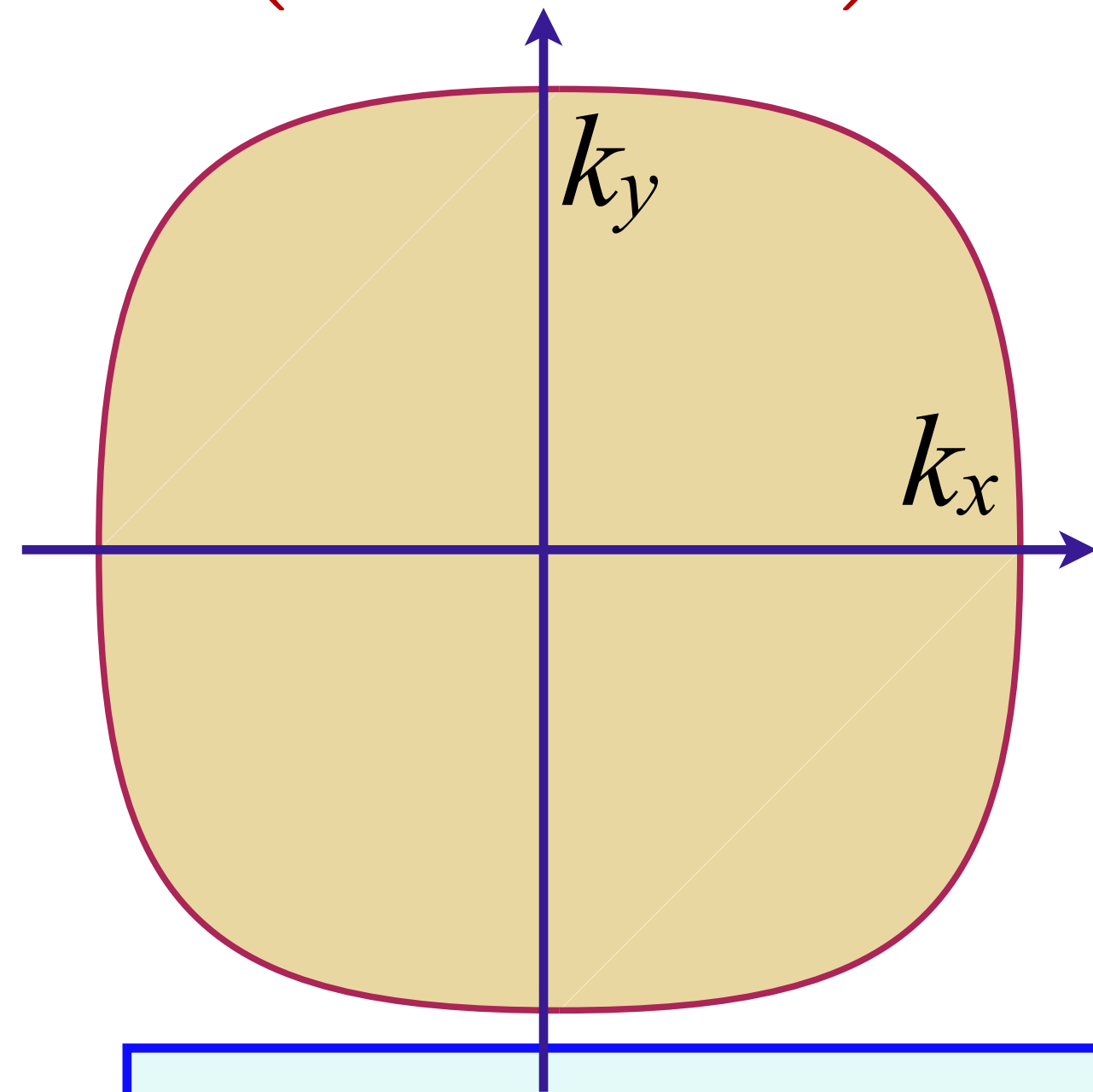
$$+g c_\sigma^\dagger(\mathbf{r}) \tau_{\sigma\sigma'}^a c_{\sigma'}(\mathbf{r}) \phi_a(\mathbf{r}) e^{i\mathbf{K}\cdot\mathbf{r}}$$

$$+K [\nabla_{\mathbf{r}} \phi(\mathbf{r})]^2 + u [\phi(\mathbf{r})]^4 + v(\mathbf{r}) c_\sigma^\dagger(\mathbf{r}) c_\sigma(\mathbf{r})$$

Spatially random potential $v(\mathbf{r})$ with $\overline{v(\mathbf{r})} = 0$, $\overline{v(\mathbf{r})v(\mathbf{r}')} = v^2 \delta(\mathbf{r} - \mathbf{r}')$

Fermi surface + critical boson with potential and coupling disorder

$$c_{\mathbf{k}\sigma}^\dagger \left(\frac{\partial}{\partial \tau} + \varepsilon(\mathbf{k}) \right) c_{\mathbf{k}\sigma}$$



$$+s [\phi(\mathbf{r})]^2 + [g + g'(\mathbf{r})] c_\sigma^\dagger(\mathbf{r}) \tau_{\sigma\sigma'}^a c_{\sigma'}(\mathbf{r}) \phi_a(\mathbf{r}) e^{i\mathbf{K}\cdot\mathbf{r}} \\ + K [\nabla_{\mathbf{r}} \phi(\mathbf{r})]^2 + u [\phi(\mathbf{r})]^4 + v(\mathbf{r}) c_\sigma^\dagger(\mathbf{r}) c_\sigma(\mathbf{r})$$

Aavishkar A. Patel, Haoyu Guo, Ilya Esterlis, S. S., *Science* **381**, 790 (2023)

Spatially random potential $v(\mathbf{r})$ with $\overline{v(\mathbf{r})} = 0$, $\overline{v(\mathbf{r})v(\mathbf{r}')} = v^2 \delta(\mathbf{r} - \mathbf{r}')$
 Spatially random coupling $g'(\mathbf{r})$ with $\overline{g'(\mathbf{r})} = 0$, $\overline{g'(\mathbf{r})g'(\mathbf{r}')} = g'^2 \delta(\mathbf{r} - \mathbf{r}')$

Can rescale $\phi(\mathbf{r})$ to transfer disorder to random mass $s + s'(\mathbf{r})$ (and vice versa),
 but $g'(\mathbf{r})$ yields a better perturbative SYK-type analysis.

2d-YSYK model: Fermi surface + critical boson with interaction disorder

Note: we are considering the simpler case of ordering at $\mathbf{K} = 0$ (e.g. ferromagnetism).
But $\mathbf{K} \neq 0$ results are very similar in the presence of disorder

All results are obtained from the large N saddle-point and response functions of this G - Σ - D - Π theory:

$$\mathcal{Z} = \int \mathcal{D}G \mathcal{D}\Sigma \mathcal{D}D \mathcal{D}\Pi \exp(-N S_{\text{all}})$$

$$\begin{aligned} S_{\text{all}} = & -\ln \det(\partial_\tau + \varepsilon(\mathbf{k}) - \mu + \Sigma) + \frac{1}{2} \ln \det(-\partial_\tau^2 + \mathbf{q}^2 + m_b^2 - \Pi) \\ & + \int d\tau d^2r \int d\tau' d^2r' \left[-\Sigma(\tau', \mathbf{r}'; \tau, \mathbf{r}) G(\tau, \mathbf{r}; \tau', \mathbf{r}') + \frac{1}{2} \Pi(\tau', \mathbf{r}'; \tau, \mathbf{r}) D(\tau, \mathbf{r}; \tau', \mathbf{r}') \right. \\ & + \frac{g^2}{2} G(\tau, \mathbf{r}; \tau', \mathbf{r}') G(\tau', \mathbf{r}'; \tau, \mathbf{r}) D(\tau, \mathbf{r}; \tau', \mathbf{r}') + \frac{v^2}{2} G(\tau, \mathbf{r}; \tau', \mathbf{r}') G(\tau', \mathbf{r}'; \tau, \mathbf{r}) \delta(\mathbf{r} - \mathbf{r}') \\ & \left. + \frac{g'^2}{2} G(\tau, \mathbf{r}; \tau', \mathbf{r}') G(\tau', \mathbf{r}'; \tau, \mathbf{r}) D(\tau, \mathbf{r}; \tau', \mathbf{r}') \delta(\mathbf{r} - \mathbf{r}') \right]. \end{aligned}$$

2d-YSYK model: Fermi surface + critical boson with interaction disorder

All results are obtained from the large N saddle-point and response functions of this G - Σ - D - Π theory:

$$\mathcal{Z} = \int \mathcal{D}G \mathcal{D}\Sigma \mathcal{D}D \mathcal{D}\Pi \exp(-N S_{\text{all}})$$

Saddle-point equations

$$\Sigma = \text{Diagram: A horizontal solid line labeled } G \text{ connects two white circles. A wavy line labeled } D \text{ connects the same two circles above the } G \text{ line.}$$

$$\Sigma(\tau, \mathbf{r}) = g^2 D(\tau, \mathbf{r}) G(\tau, \mathbf{r}) + v^2 G(\tau, \mathbf{r}) \delta^2(\mathbf{r}) + g'^2 G(\tau, \mathbf{r}) D(\tau, \mathbf{r}) \delta^2(\mathbf{r}),$$

$$\Pi(\tau, \mathbf{r}) = -g^2 G(-\tau, -\mathbf{r}) G(\tau, \mathbf{r}) - g'^2 G(-\tau, \mathbf{r}) G(\tau, \mathbf{r}) \delta^2(\mathbf{r}),$$

$$G(i\omega, \mathbf{k}) = \frac{1}{i\omega - \varepsilon(\mathbf{k}) + \mu - \Sigma(i\omega, \mathbf{k})},$$

$$D(i\Omega, \mathbf{q}) = \frac{1}{\Omega^2 + \mathbf{q}^2 + m_b^2 - \Pi(i\Omega, \mathbf{q})}.$$

$$\Pi = \text{Diagram: A thick circular loop labeled } G \text{ connects two white circles. A wavy line labeled } G \text{ connects the same two circles below the } G \text{ loop.}$$

Fermi surface + critical boson with no spatial disorder

Solution of Migdal-Eliashberg equations for electron (G)
and boson (D) Green's functions at small ω :

P.A. Lee (1989)

$$\Sigma(\hat{\mathbf{k}}, i\omega) \sim -i \text{sgn}(\omega) |\omega|^{2/3}, \quad G(\mathbf{k}, i\omega) = \frac{1}{i\omega - \varepsilon(\mathbf{k}) - \Sigma(\hat{\mathbf{k}}, i\omega)}, \quad D(\mathbf{q}, i\Omega) = \frac{1}{\Omega^2 + q^2 + \gamma |\Omega|/q}$$

Fermi surface + critical boson with no spatial disorder

Solution of Migdal-Eliashberg equations for electron (G) and boson (D) Green's functions at small ω :

P.A. Lee (1989)

$$\Sigma(\hat{\mathbf{k}}, i\omega) \sim -i \operatorname{sgn}(\omega) |\omega|^{2/3}, \quad G(\mathbf{k}, i\omega) = \frac{1}{i\omega - \varepsilon(\mathbf{k}) - \Sigma(\hat{\mathbf{k}}, i\omega)}, \quad D(\mathbf{q}, i\Omega) = \frac{1}{\Omega^2 + q^2 + \gamma |\Omega|/q}$$

Fermi surface + critical boson with potential and interaction disorder

Boson Green's function: $D(q, i\Omega) \sim 1/(q^2 + \gamma |\Omega|)$

Fermion self energy:

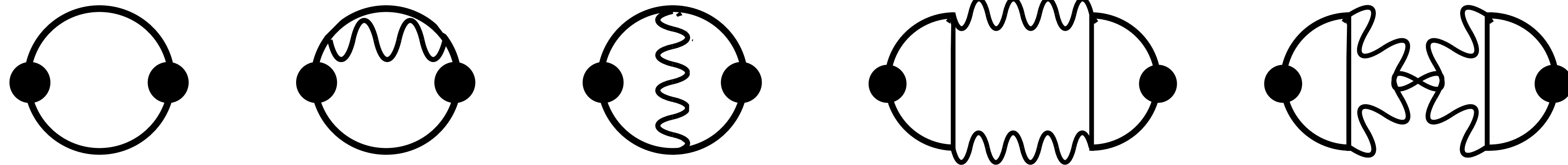
$$\Sigma(i\omega) \sim -iv^2 \operatorname{sgn}(\omega) - i \left(\frac{g^2}{v^2} + g'^2 \right) \omega \ln(1/|\omega|); \quad \frac{1}{\tau_{\text{in}}(\omega)} \sim \left(\frac{g^2}{v^2} + g'^2 \right) |\omega|$$

Marginal Fermi liquid self energy and $T \ln(1/T)$ specific heat

Aavishkar A. Patel, Haoyu Guo, Ilya Esterlis, S. S., *Science* **381**, 790 (2023)

2d-YSYK model: Fermi surface + critical boson with interaction disorder

Optical conductivity—Diagrams



Fermi surface + critical boson with no spatial disorder

$$\text{Re} [\sigma(\omega)] = C |\omega|^{-2/3}$$

Yong Baek Kim, A. Furusaki, Xiao-Gang Wen,
and P. A. Lee, PRB **50**, 17917 (1994).

Fermi surface + critical boson with no spatial disorder

$$\text{Re} [\sigma(\omega)] = C |\omega|^{-2/3}$$

Yong Baek Kim, A. Furusaki, Xiao-Gang Wen,
and P. A. Lee, PRB **50**, 17917 (1994).

$$C = 0; \quad \sigma(\omega) \sim i/(\omega) + \omega^0 + \dots$$

Haoyu Guo, Aavishkar Patel, Ilya Esterlis, S.S. PRB **106**, 115151 (2022)

Z. Darius Shi, D.V. Else, H. Goldman and T. Senthil, SciPost Phys. **14**, 113 (2023)



Fermi surface + critical boson with no spatial disorder

$$\text{Re} [\sigma(\omega)] = C |\omega|^{-2/3}$$

Yong Baek Kim, A. Furusaki, Xiao-Gang Wen,
and P. A. Lee, PRB **50**, 17917 (1994).

$$C = 0; \quad \sigma(\omega) \sim i/(\omega) + \omega^0 + \dots$$

Haoyu Guo, Aavishkar Patel, Ilya Esterlis, S.S. PRB **106**, 115151 (2022)
Z. Darius Shi, D.V. Else, H. Goldman and T. Senthil, SciPost Phys. **14**, 113 (2023)



Fermi surface + critical boson with potential and interaction disorder

$$\text{Conductivity: } \sigma(\omega) \sim \frac{1}{\frac{1}{\tau_{\text{trans}}(\omega)} - i\omega \frac{m_{\text{trans}}^*(\omega)}{m}}$$

$$\frac{1}{\tau_{\text{trans}}(\omega)} \sim v^2 + g'^2 |\omega| \quad ; \quad \frac{m_{\text{trans}}^*(\omega)}{m} \sim \frac{2g'^2}{\pi} \ln(\Lambda/\omega)$$

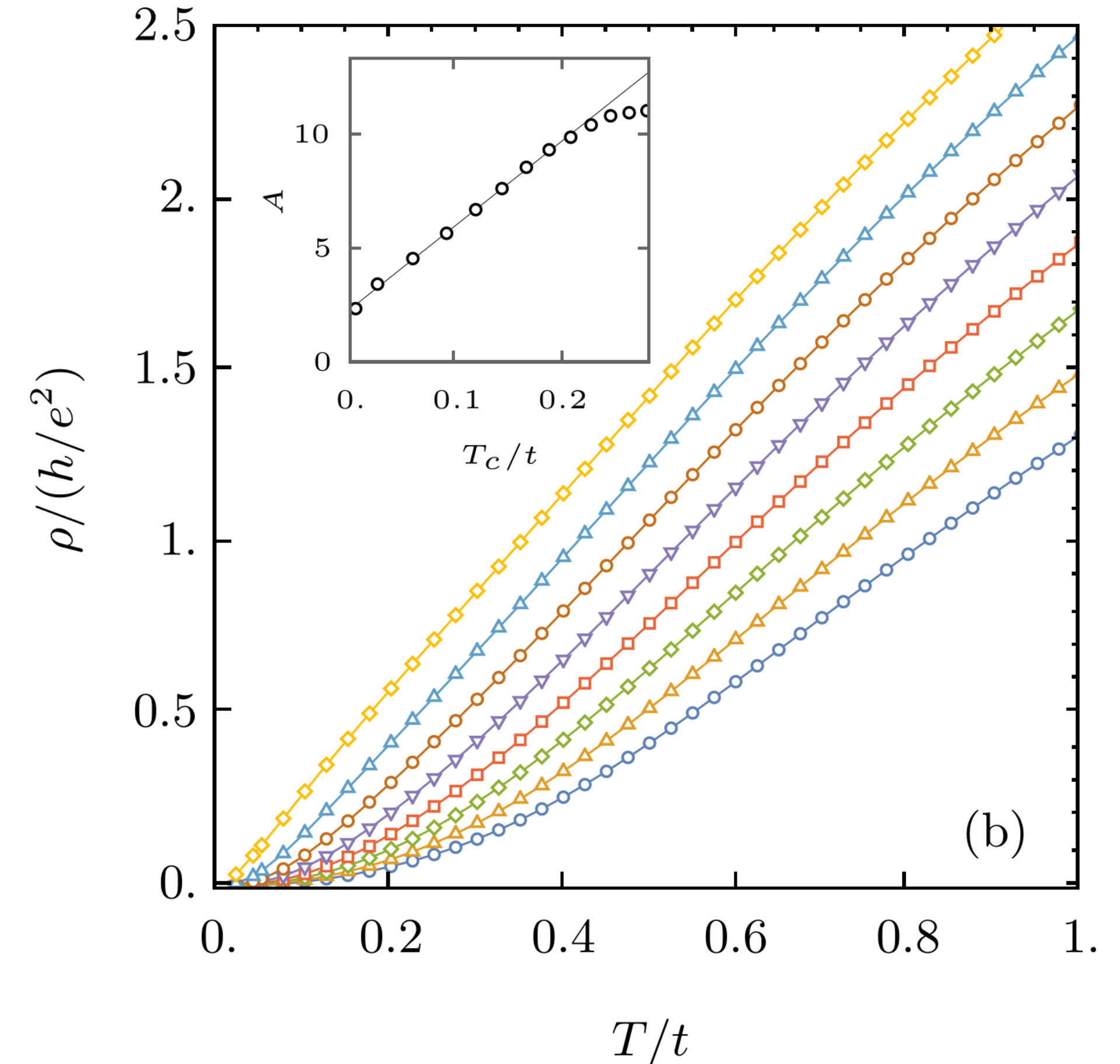
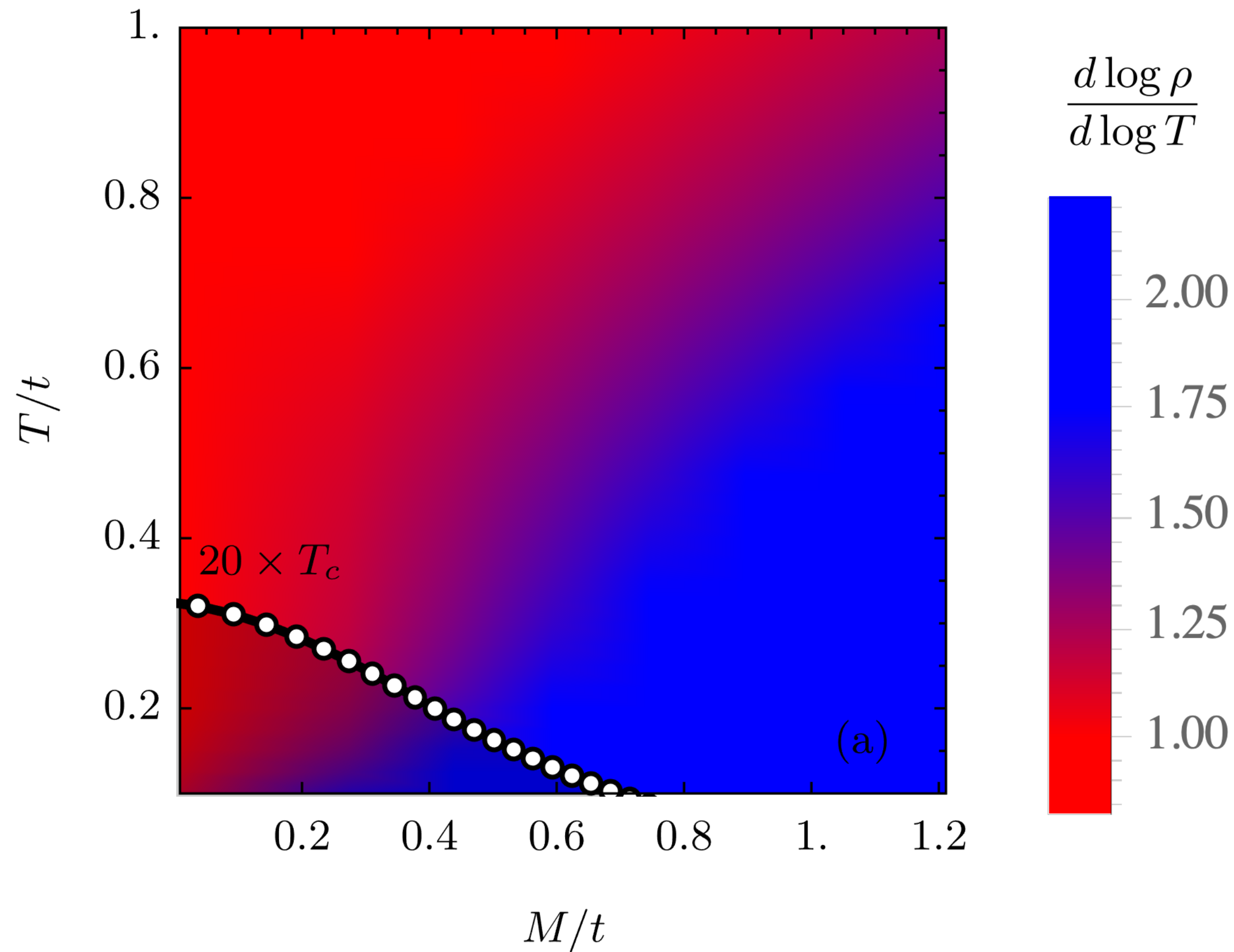
Aavishkar A. Patel, Haoyu
Guo, Ilya Esterlis, S. S.,
Science **381**, 790 (2023)

Residual resistivity is determined by v^2 ; Linear-in- T resistivity determined by g'^2 ;
Transport insensitive to g ; Marginal Fermi liquid self energy and $T \ln(1/T)$ specific heat.

Strange metal and superconductor in the two-dimensional Yukawa-Sachdev-Ye-Kitaev model

$g = 0$

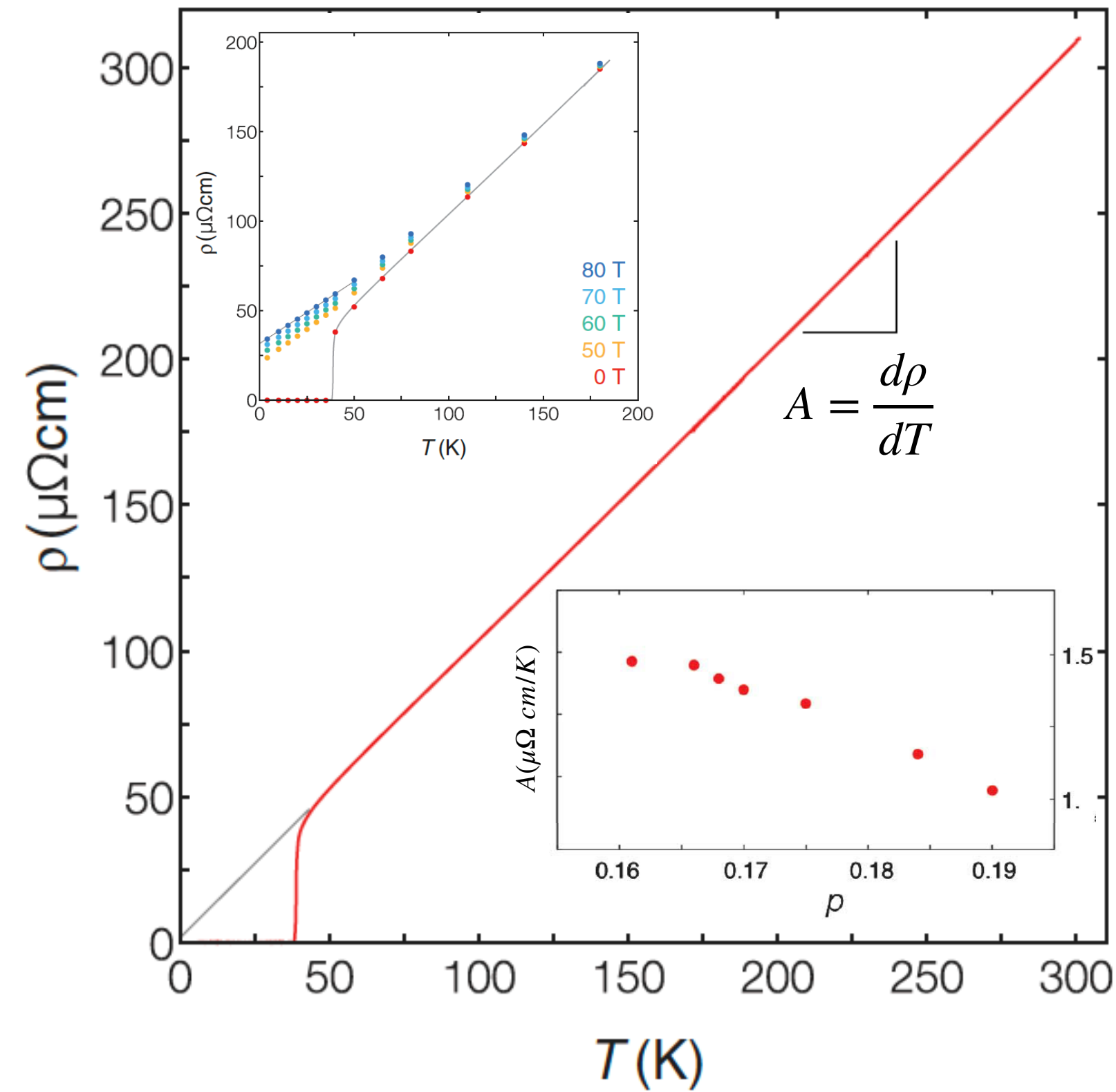
Chenyuan Li, Aavishkar A. Patel, Haoyu Guo, Davide Valentini, Jorg Schmalian, S.S., Ilya Esterlis, PRL **133**, 186502 (2024)



Strange metal and superconductor in the two-dimensional Yukawa-Sachdev-Ye-Kitaev model

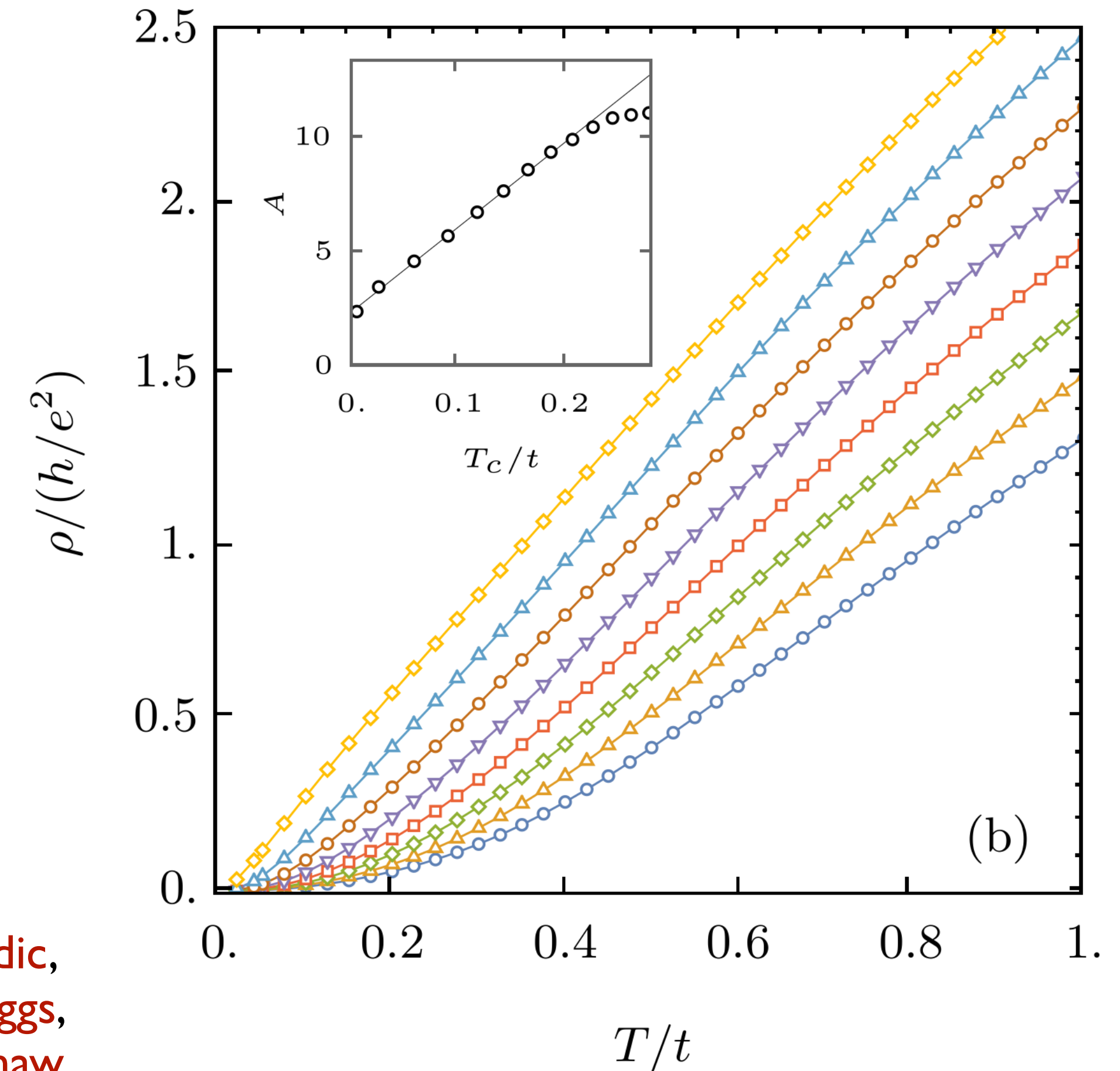
$$g = 0$$

Chenyuan Li, Aavishkar A. Patel, Haoyu Guo, Davide Valentini, Jorg Schmalian, S.S., Ilya Esterlis, PRL **133**, 186502 (2024)



LSCO

P. Giraldo-Gallo, J.A. Galvis, Z. Stegen, K.A. Modic,
F. F. Balakirev, J. B. Betts, X. Lian, C. Moir, S. C. Riggs,
J. Wu, A. T. Bollinger, X. He, I. Bozovic, B. J. Ramshaw,
R. D. McDonald, G. S. Boebinger, A. Shekhter
Science **361**, 479 (2018)

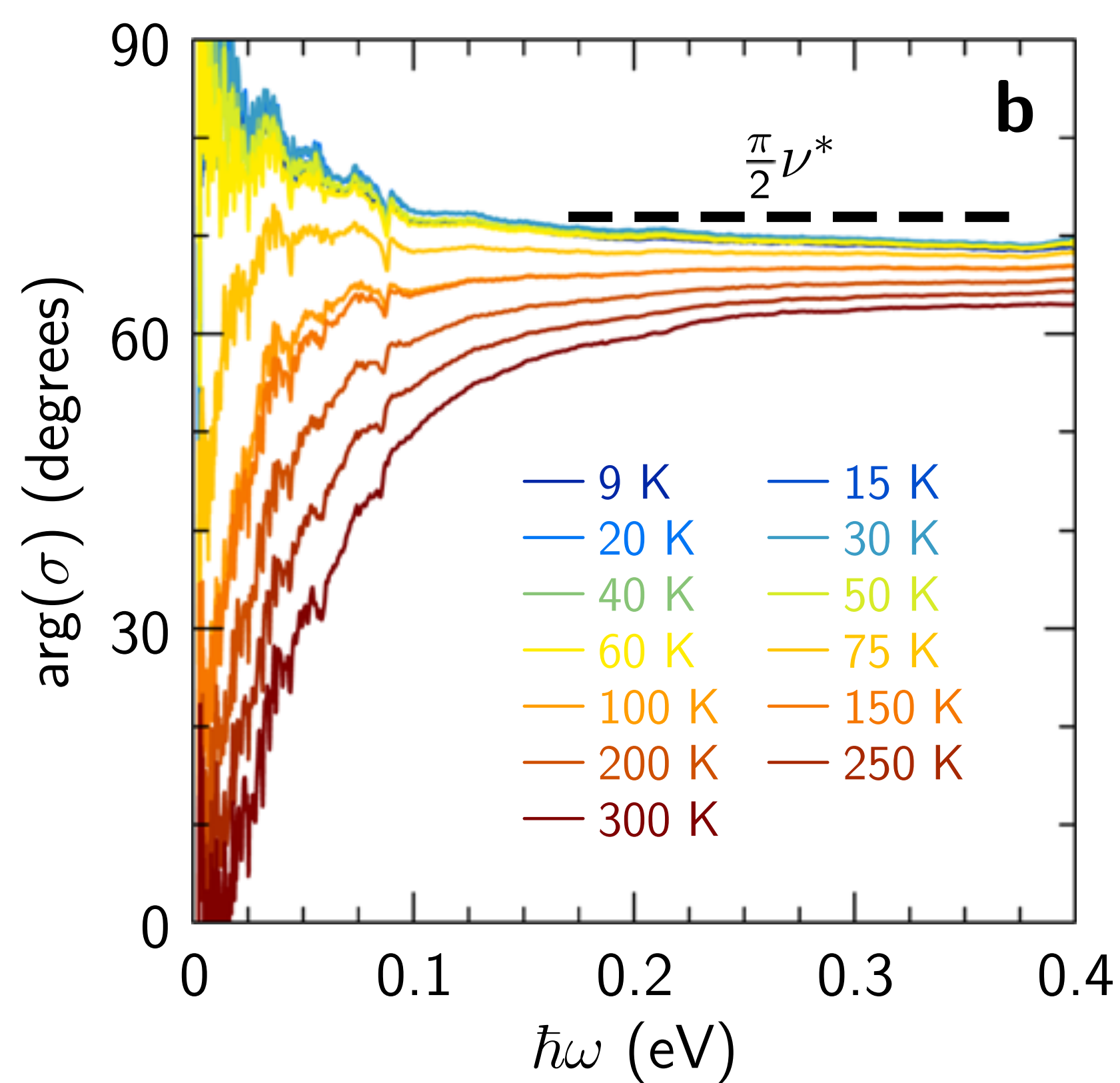
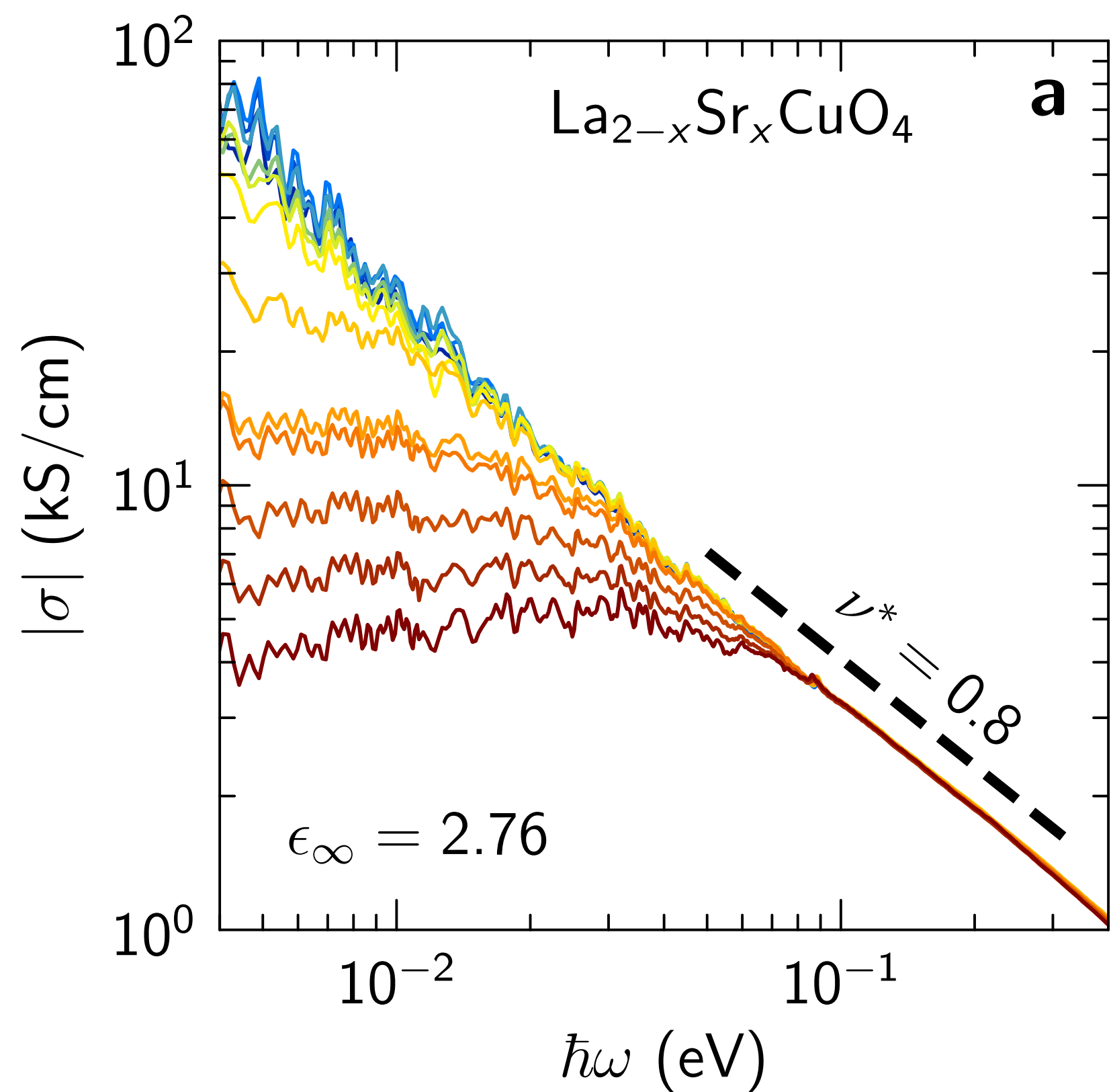


Reconciling scaling of the optical conductivity of cuprate superconductors with Planckian resistivity and specific heat

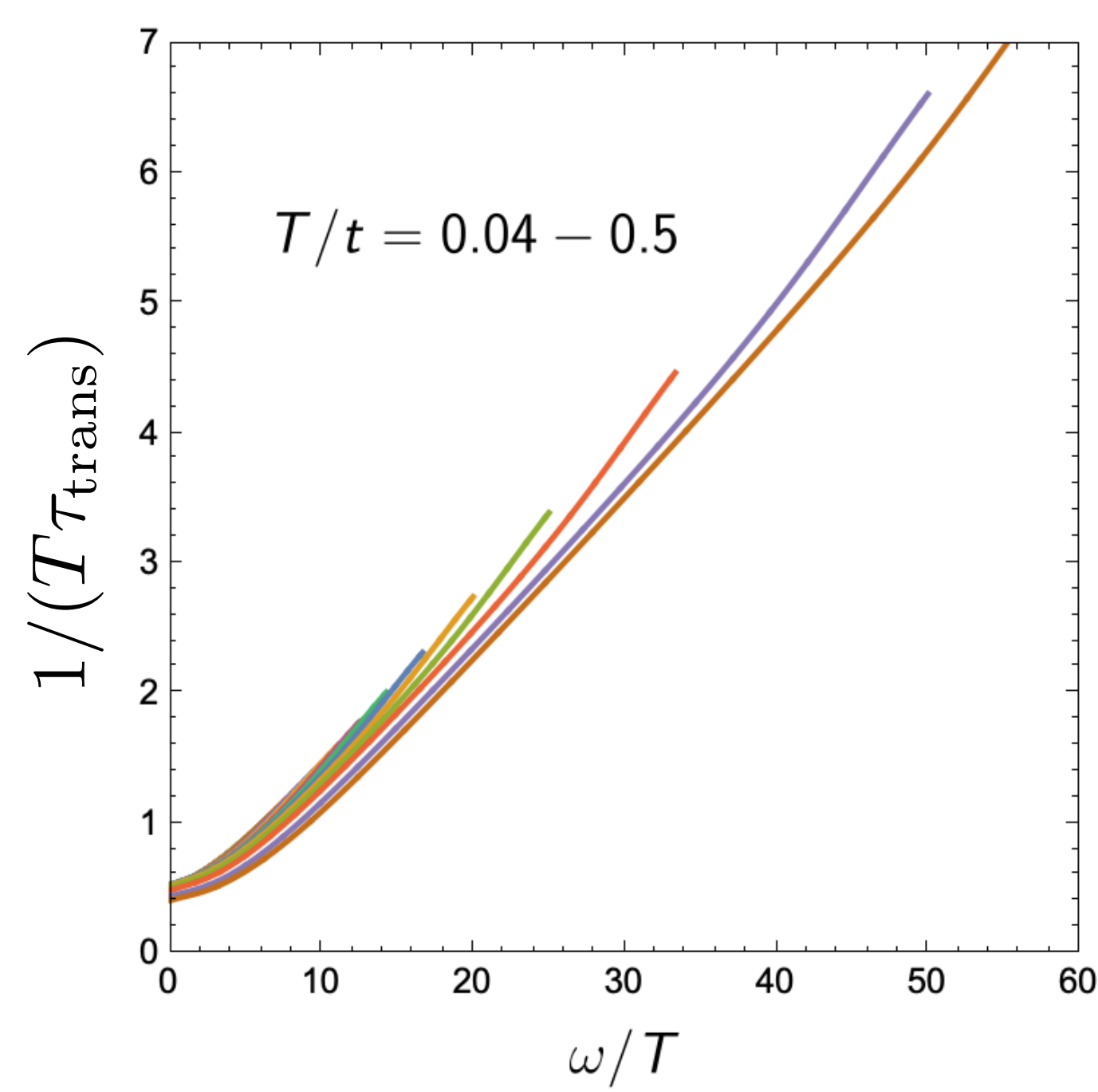
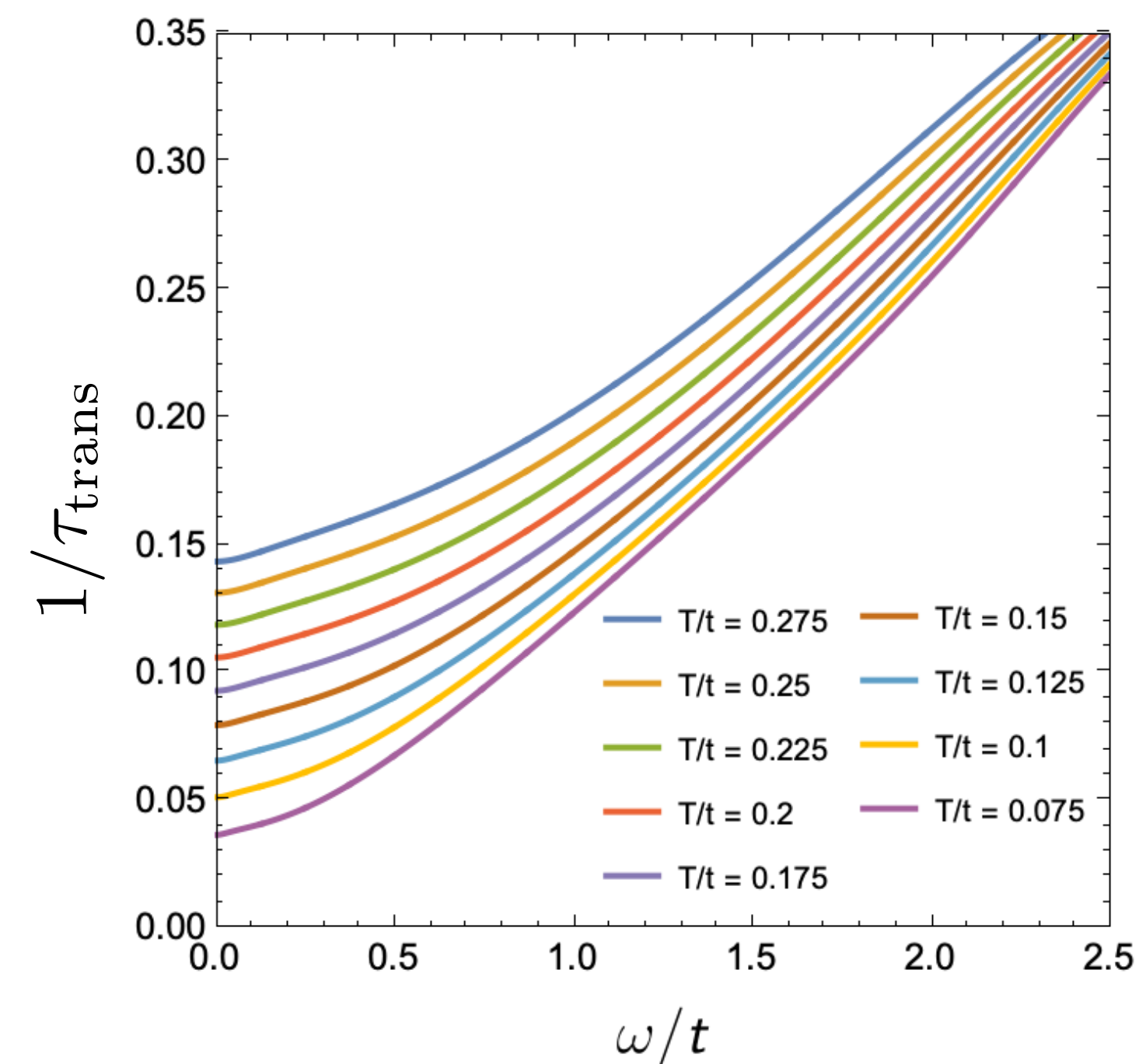
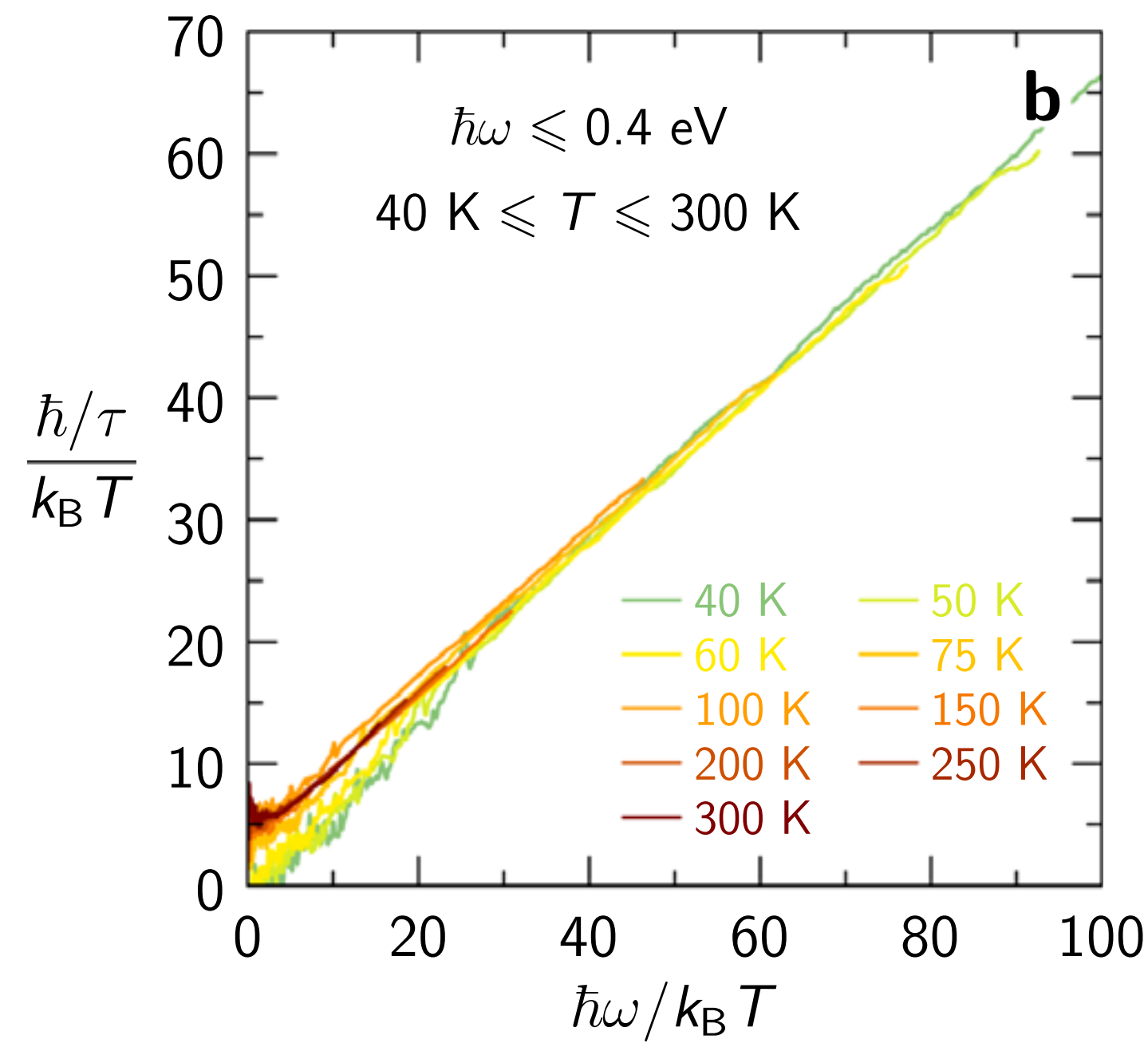
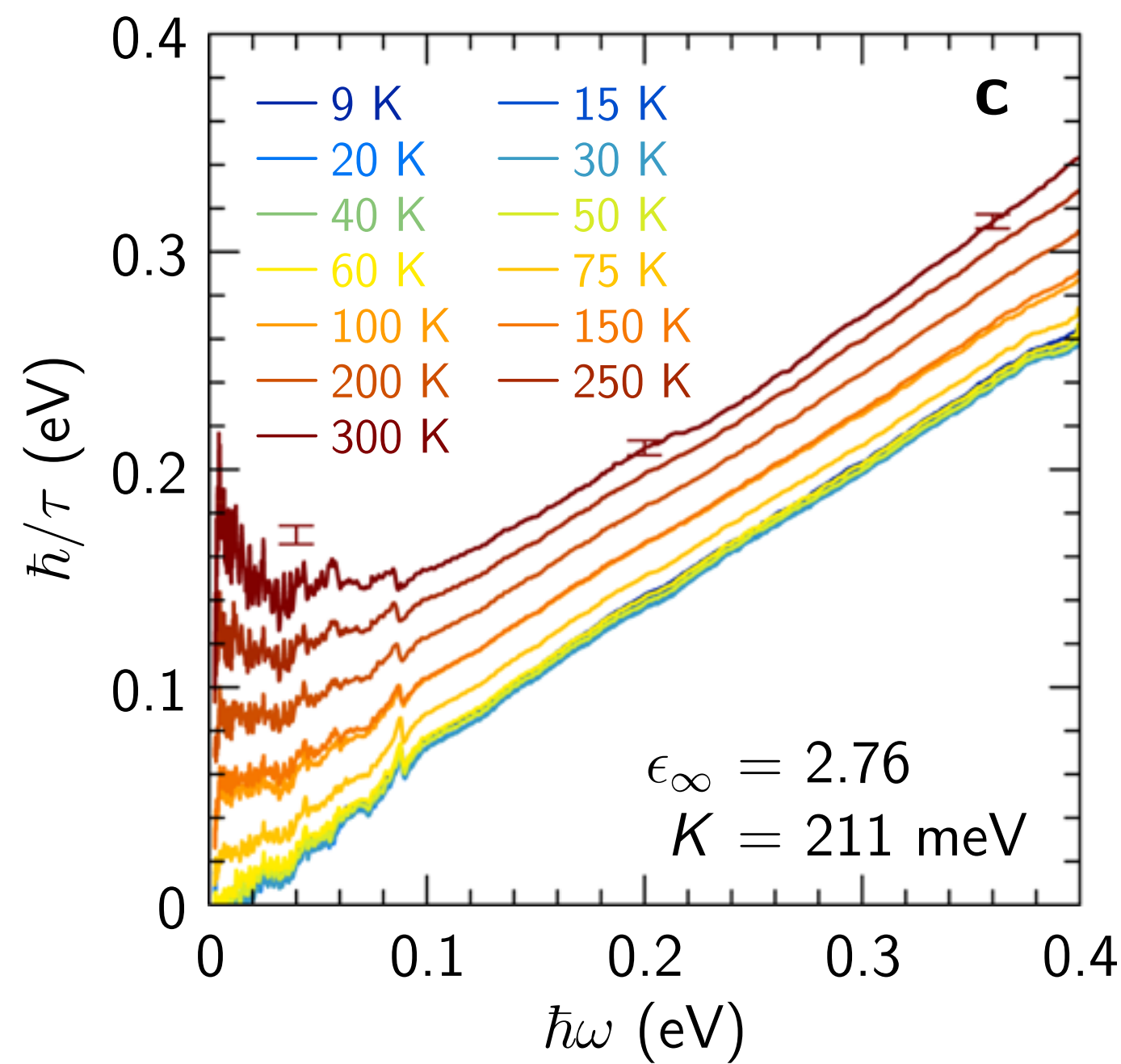
B. Michon, C. Berthod, C. W. Rischau, A. Ataei, L. Chen, S. Komiya, S. Ono, L. Taillefer, D. van der Marel, A. Georges

Nature Communications **14**, Article number: 3033 (2023)

$$\sigma(\omega) = i \frac{e^2 K / (\hbar d_c)}{\hbar \omega \frac{m^*(\omega)}{m} + i \frac{\hbar}{\tau(\omega)}}$$



$\text{La}_{2-x}\text{Sr}_x\text{CuO}_4$
 $p = 0.24$
 $T_c = 19 \text{ K}$



From
optical conductivity
data of
Michon et al. (2023)

$$\frac{\hbar}{\tau} = k_B T \Phi_\tau \left(\frac{\hbar\omega}{k_B T} \right)$$

2d-YSYK theory

Chenyuan Li, Aavishkar A. Patel, Haoyu Guo, Davide Valentini, Jorg Schmalian, S.S., Ilya Esterlis, PRL **133**, 186502 (2024)

1. Hubbard model on the honeycomb lattice:
hydrodynamics in graphene and related materials
2. SYK as a solvable model of quantum matter
without quasiparticles
3. Hubbard model on the square lattice:
spin density wave order, and a universal theory
of strange metals from spatially random interactions.

4. Spin liquids, Fractionalized Fermi liquids (FL*)
and the cuprate phase diagram:
observation of the Yamaji effect.

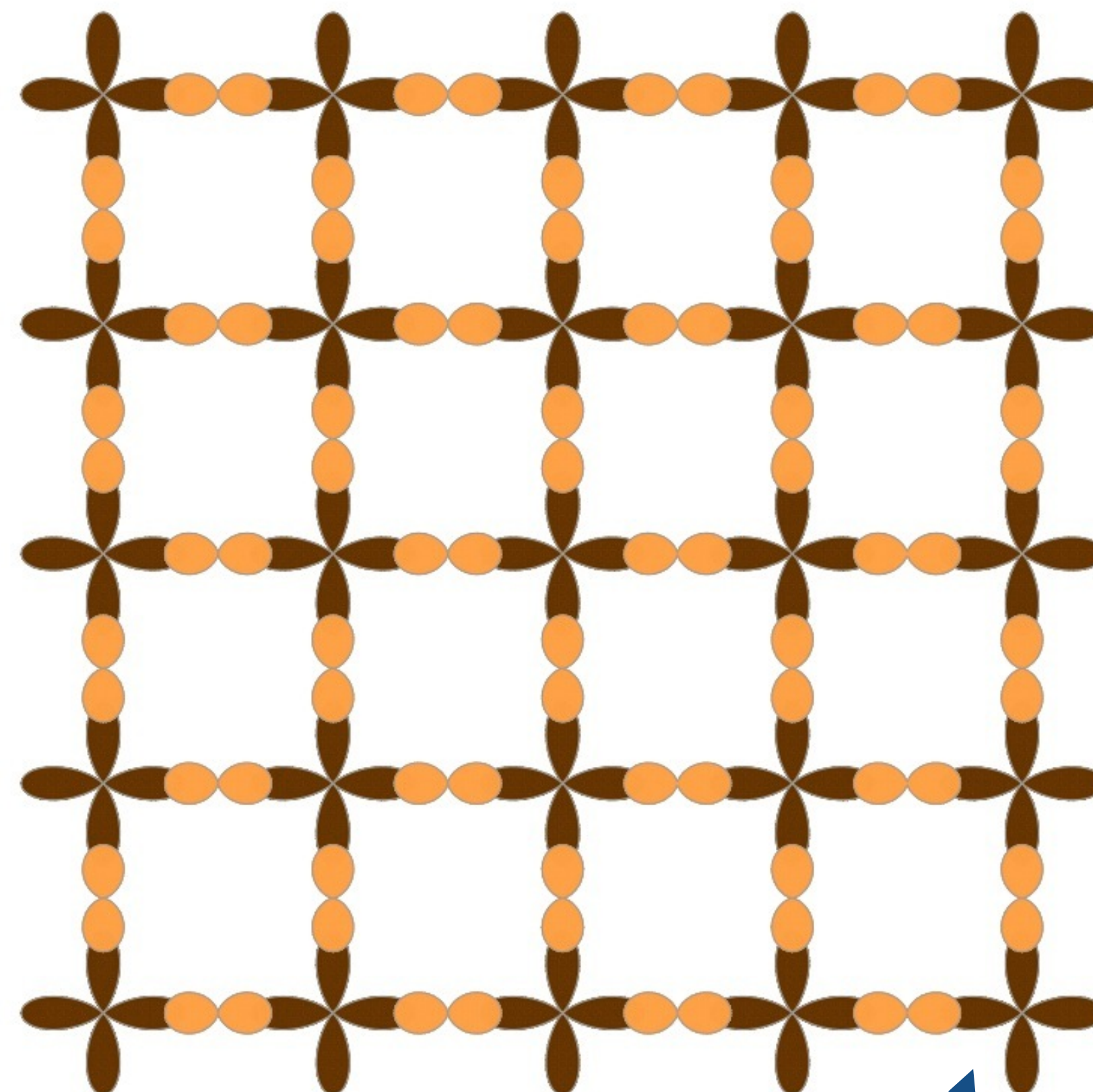
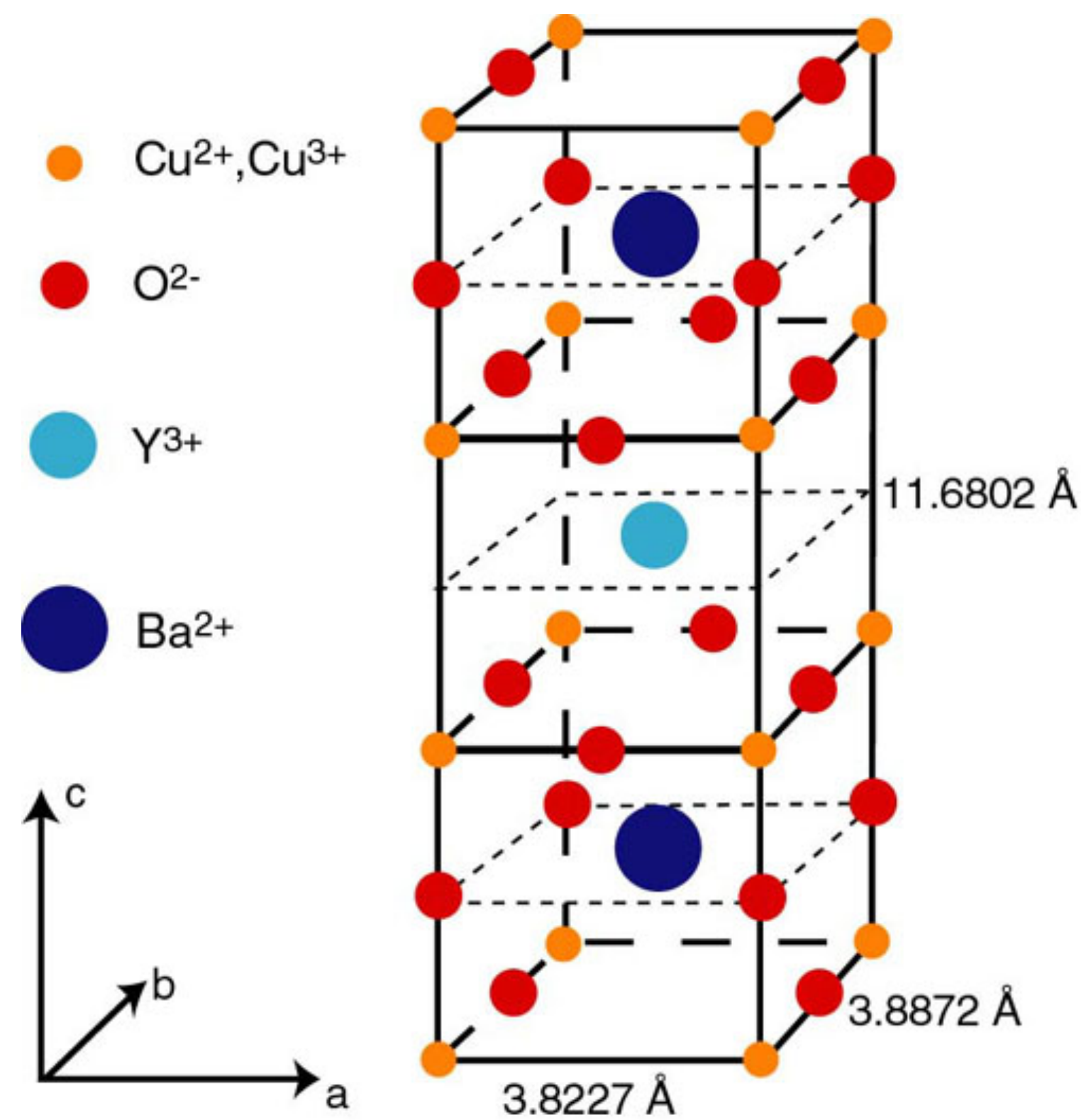
Spin liquids, Fractionalized Fermi liquids (FL*) and the cuprate phase diagram: observation of the Yamaji effect

School on Emergent Phenomena in
Non-Equilibrium Quantum Many-Body Systems
ICTP-SAIFR

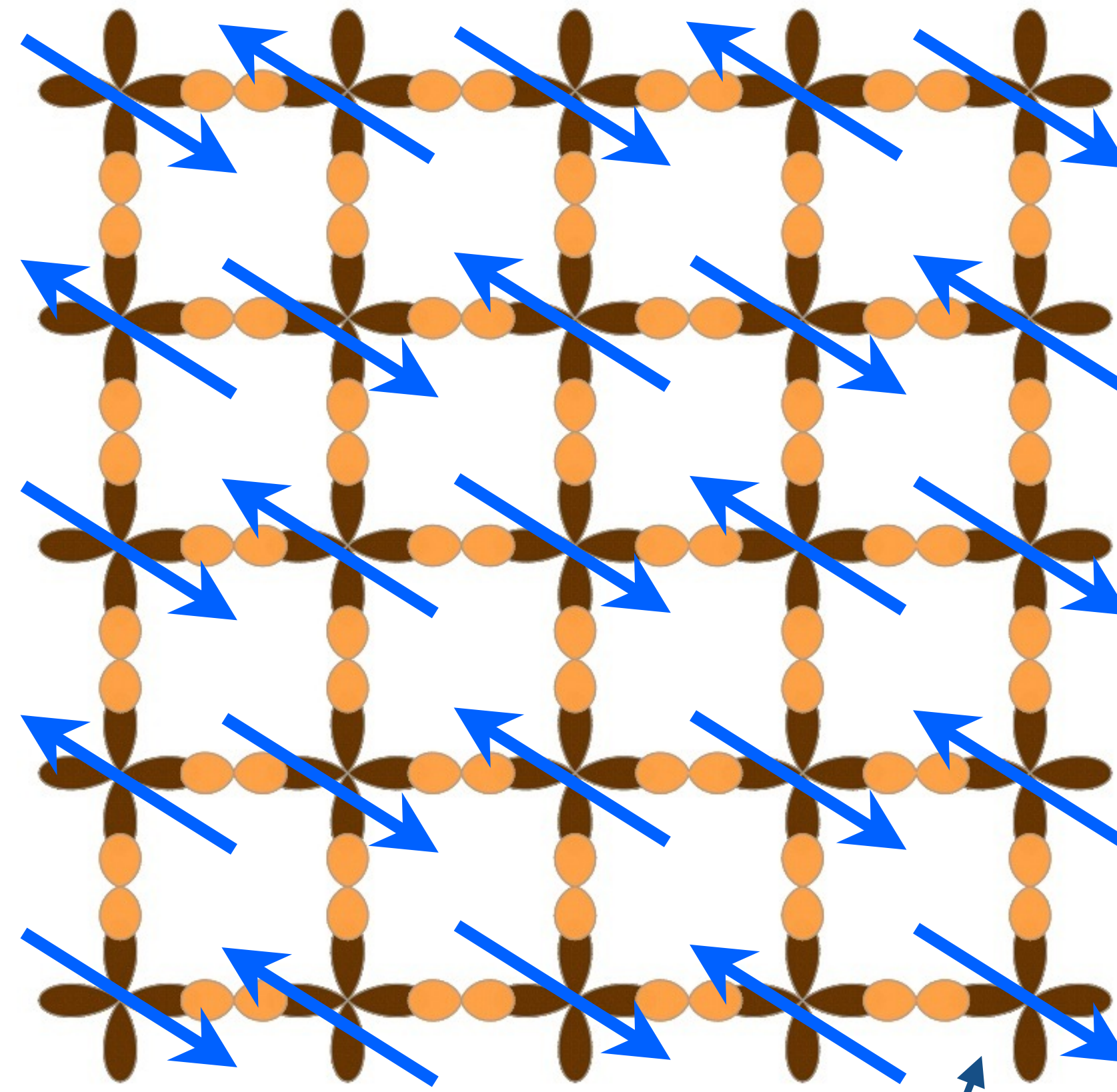
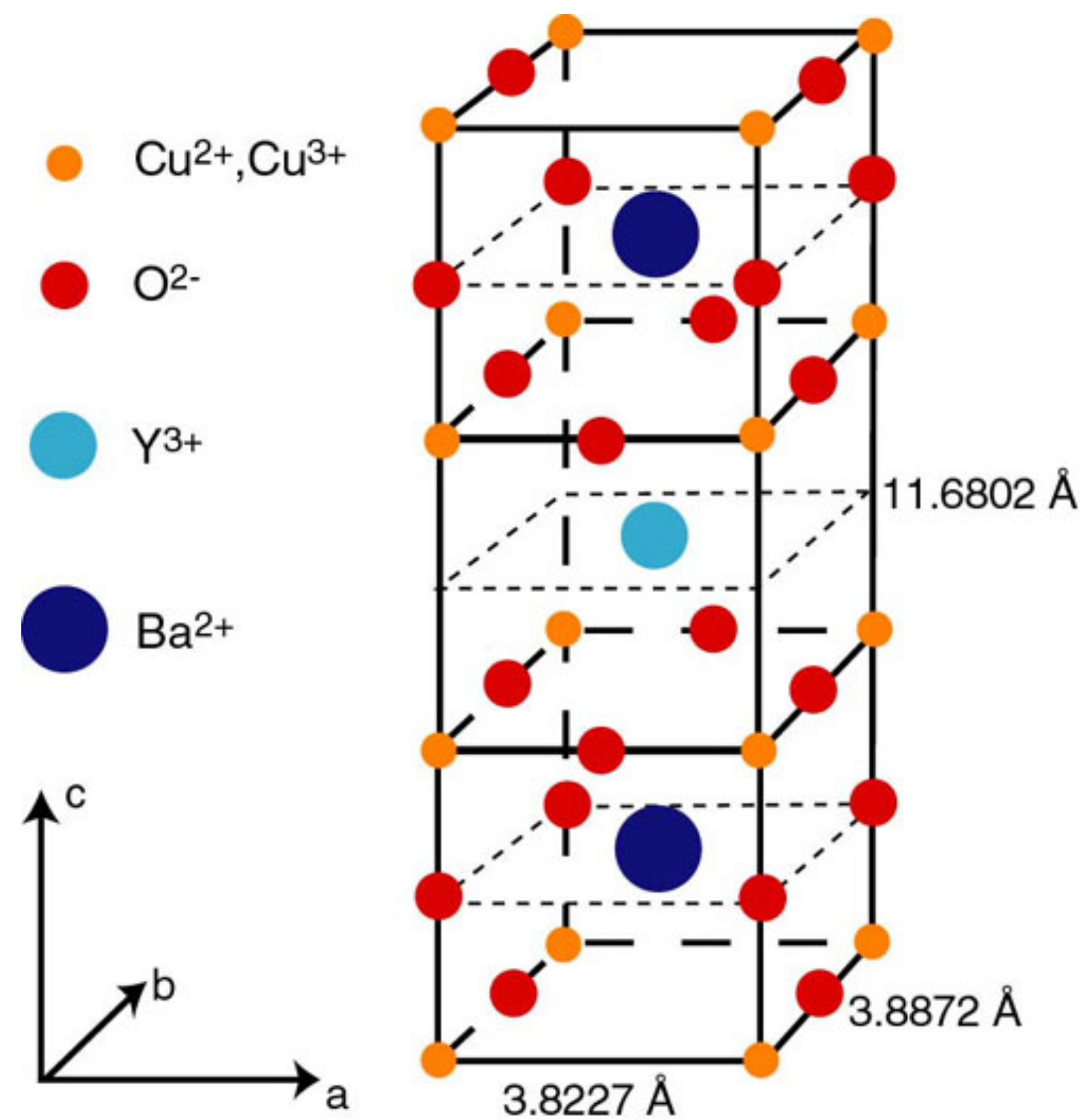
São Paulo, Brazil
November 3,4 2025

Subir Sachdev





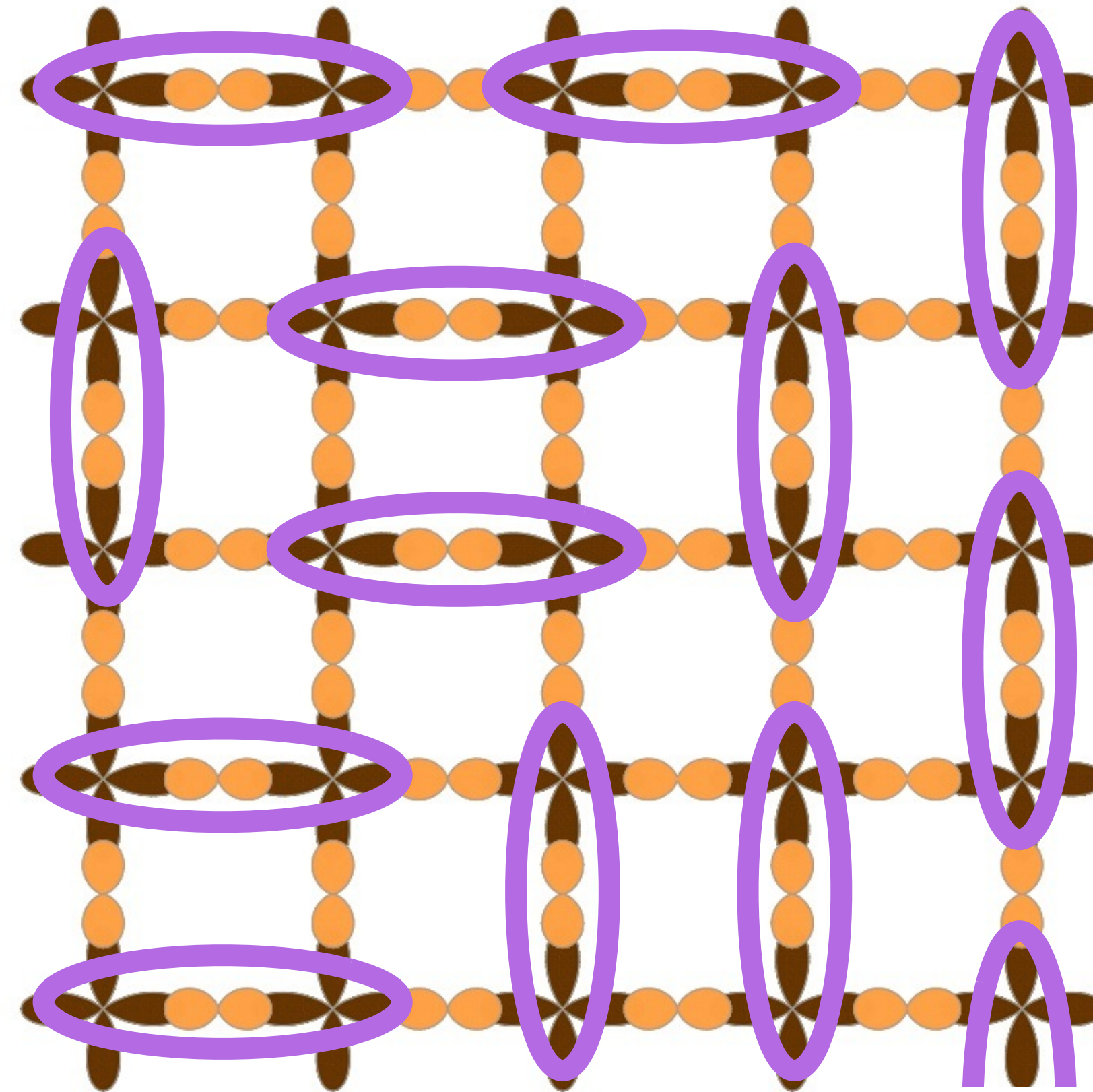
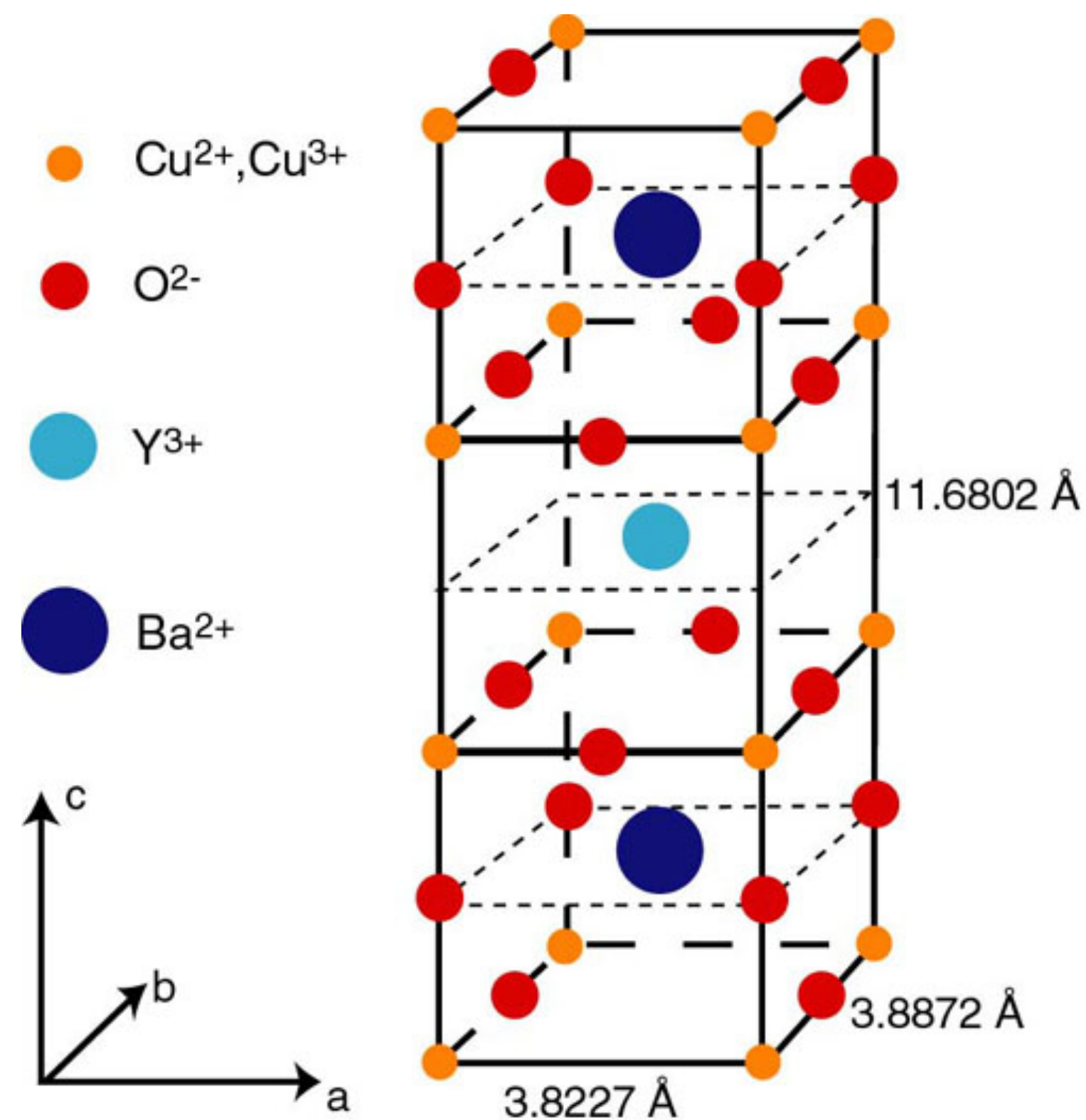
Cu



Cu



Antiferromagnetic insulator at a density of one electron per Cu



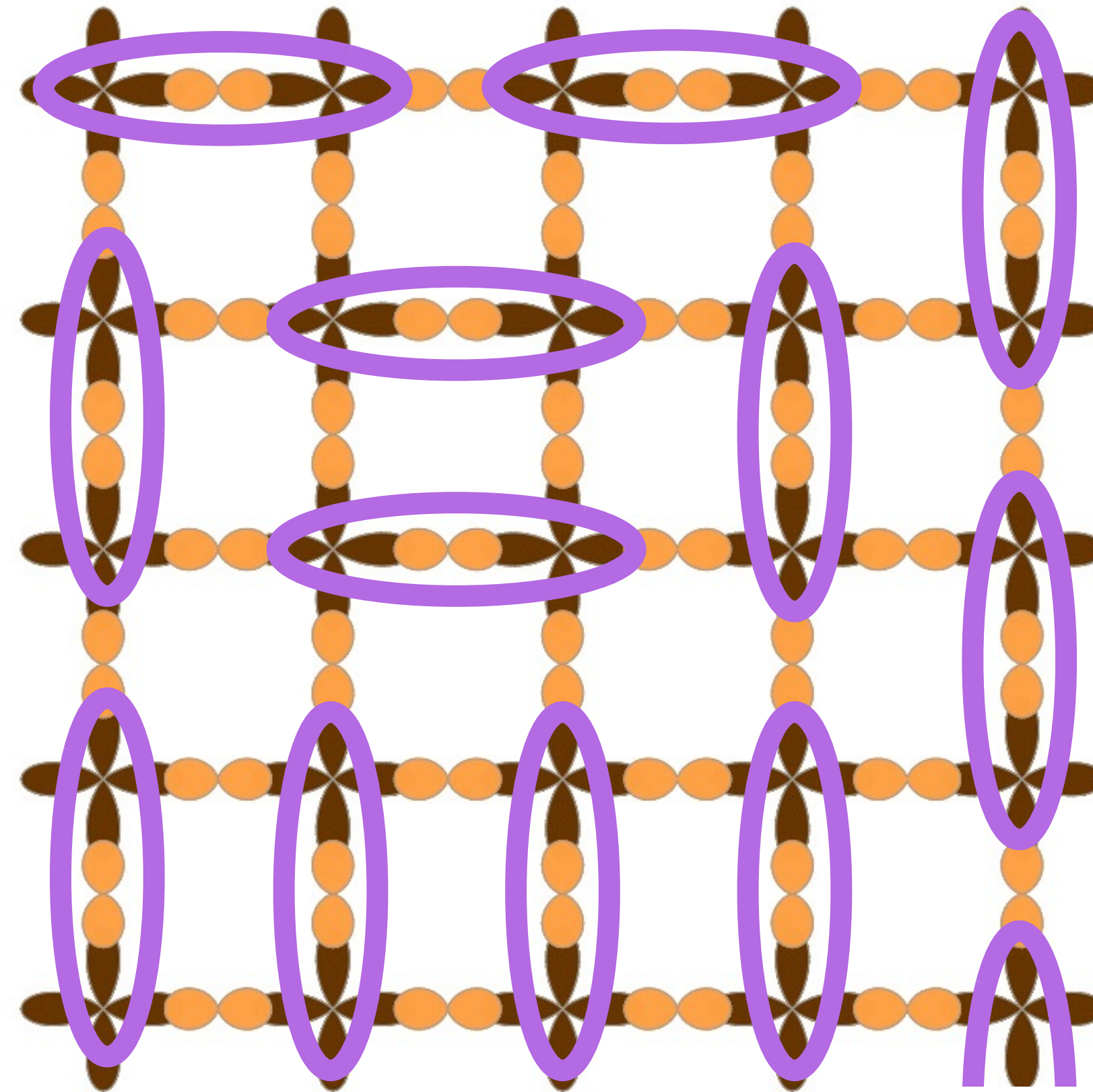
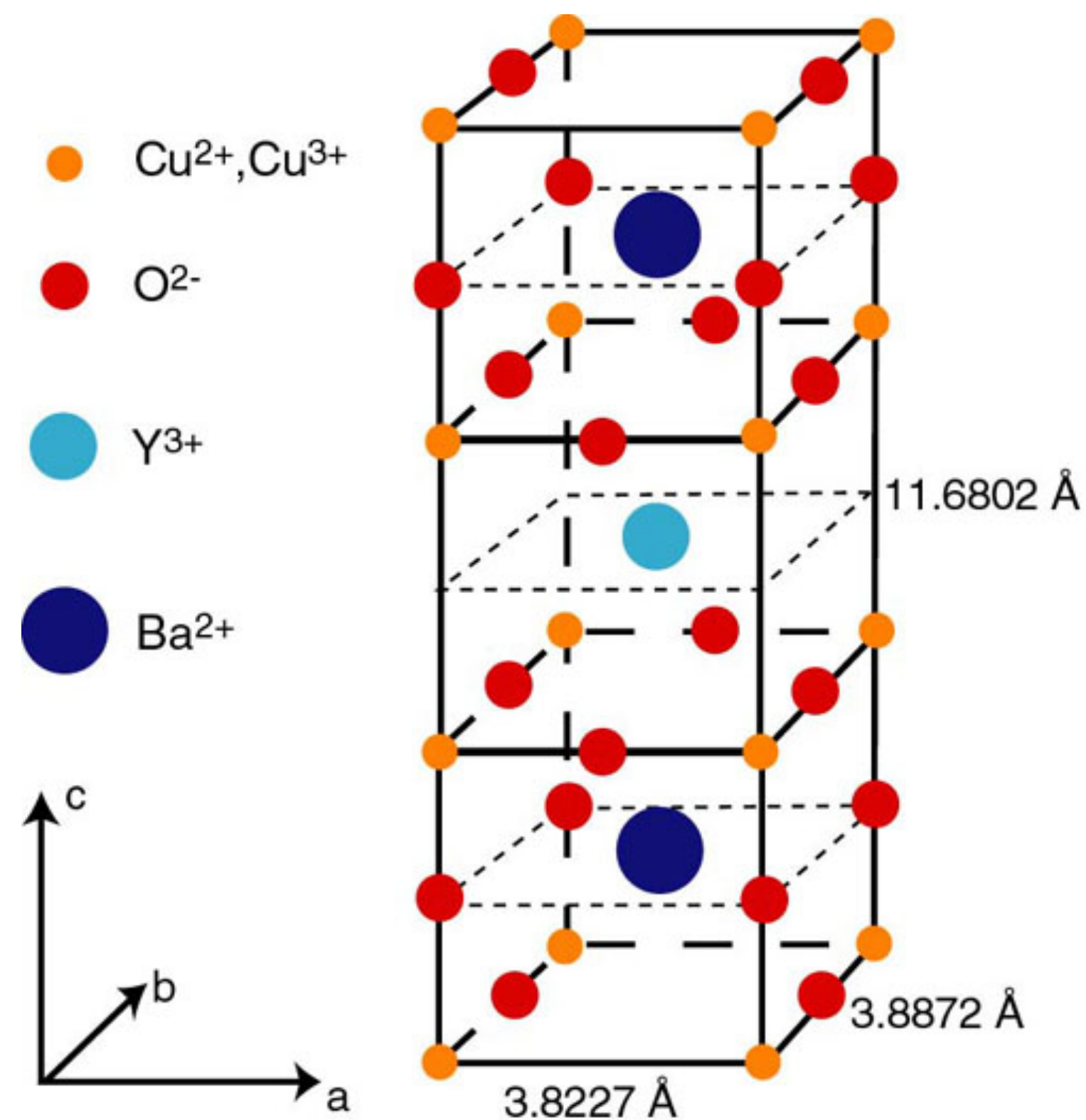
$$|G\rangle = \sum_{\mathcal{D}} c_{\mathcal{D}} |\mathcal{D}\rangle$$

$\mathcal{D} \rightarrow$ dimer covering
 of lattice

$$\text{YBa}_2\text{Cu}_3\text{O}_{6+x}$$

$$\text{Oval} = \frac{1}{\sqrt{2}} (|\uparrow\downarrow\rangle - |\downarrow\uparrow\rangle)$$

P.W.Anderson and G. Baskaran (1988): The key to high temperature superconductivity
 is the formation of a “resonating valence bond state”
 (a type of **quantum spin liquid**) which entangles the electrons on Cu



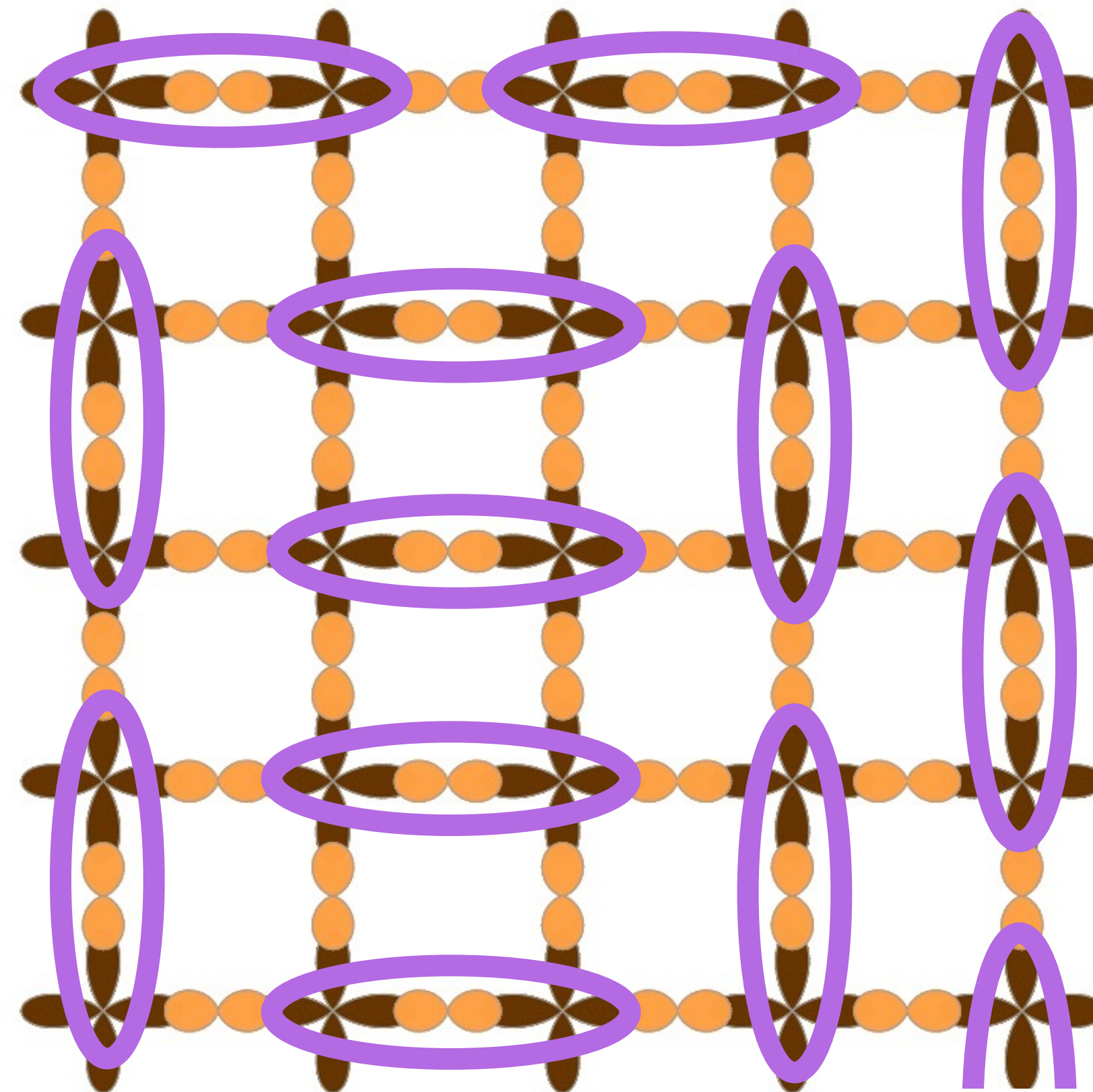
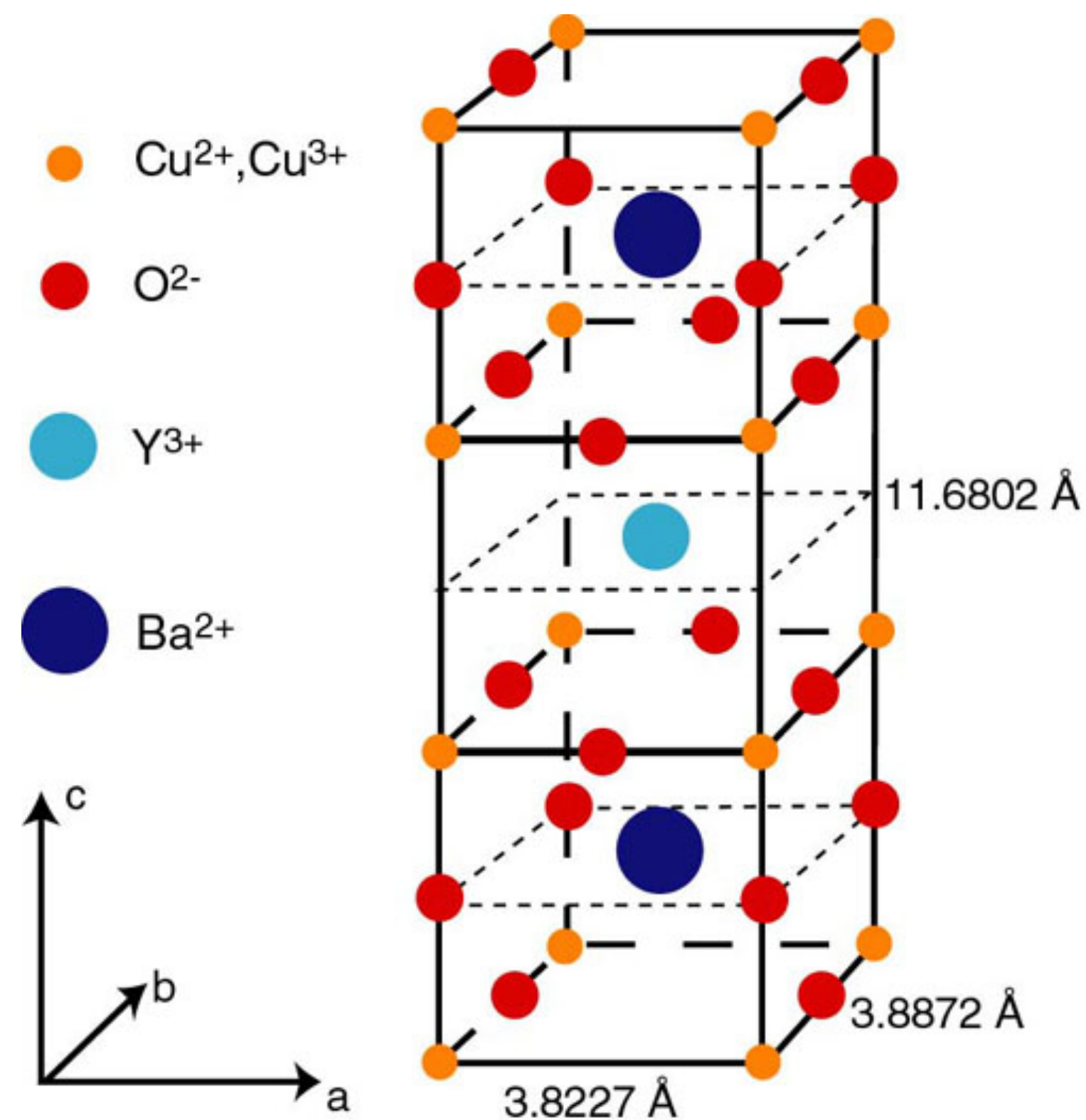
$$|G\rangle = \sum_{\mathcal{D}} c_{\mathcal{D}} |\mathcal{D}\rangle$$

$\mathcal{D} \rightarrow$ dimer covering
 of lattice



$$\text{Oval} = \frac{1}{\sqrt{2}} (|\uparrow\downarrow\rangle - |\downarrow\uparrow\rangle)$$

P.W.Anderson and G. Baskaran (1988): The key to high temperature superconductivity
 is the formation of a “resonating valence bond state”
 (a type of **quantum spin liquid**) which entangles the electrons on Cu



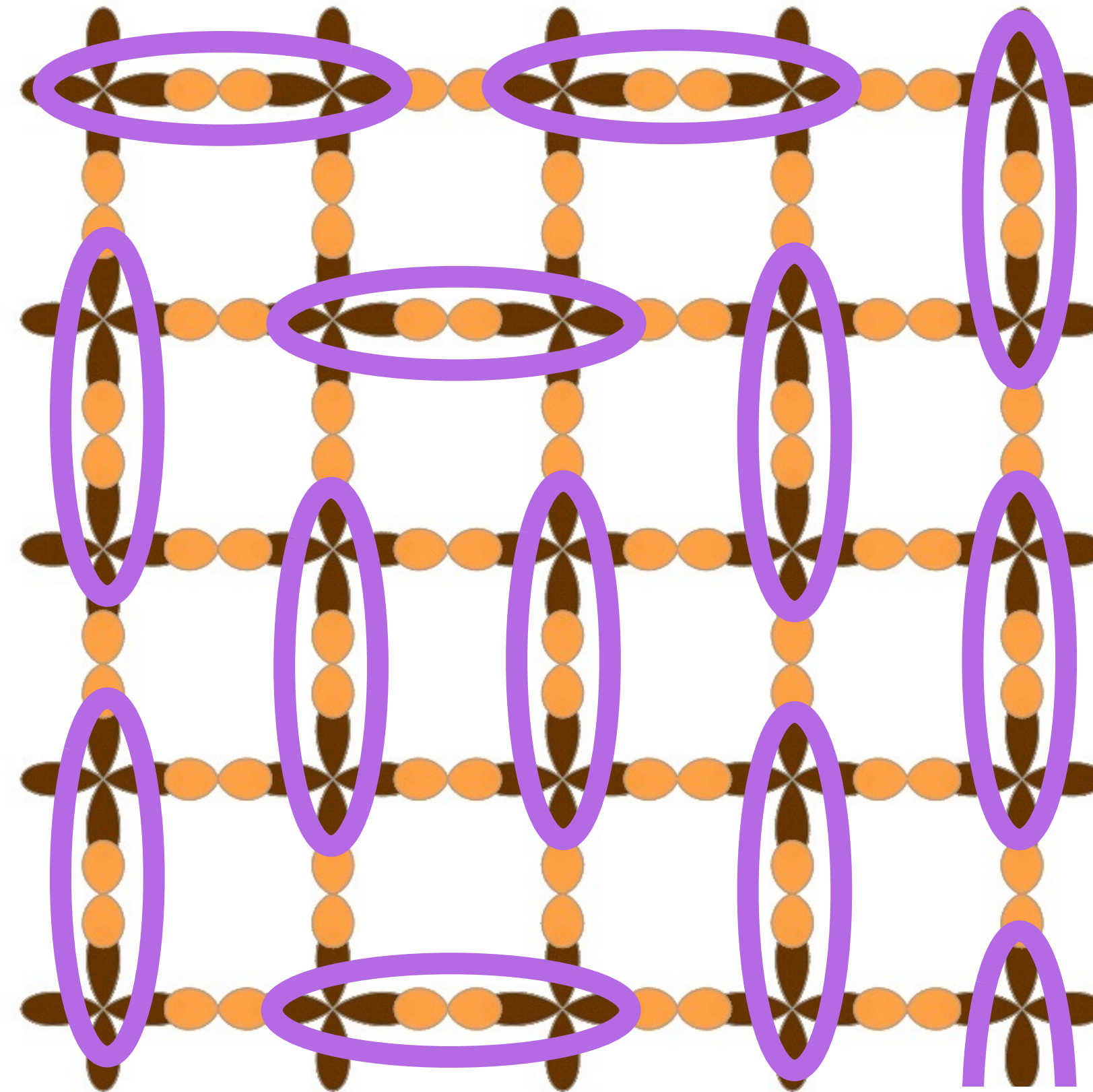
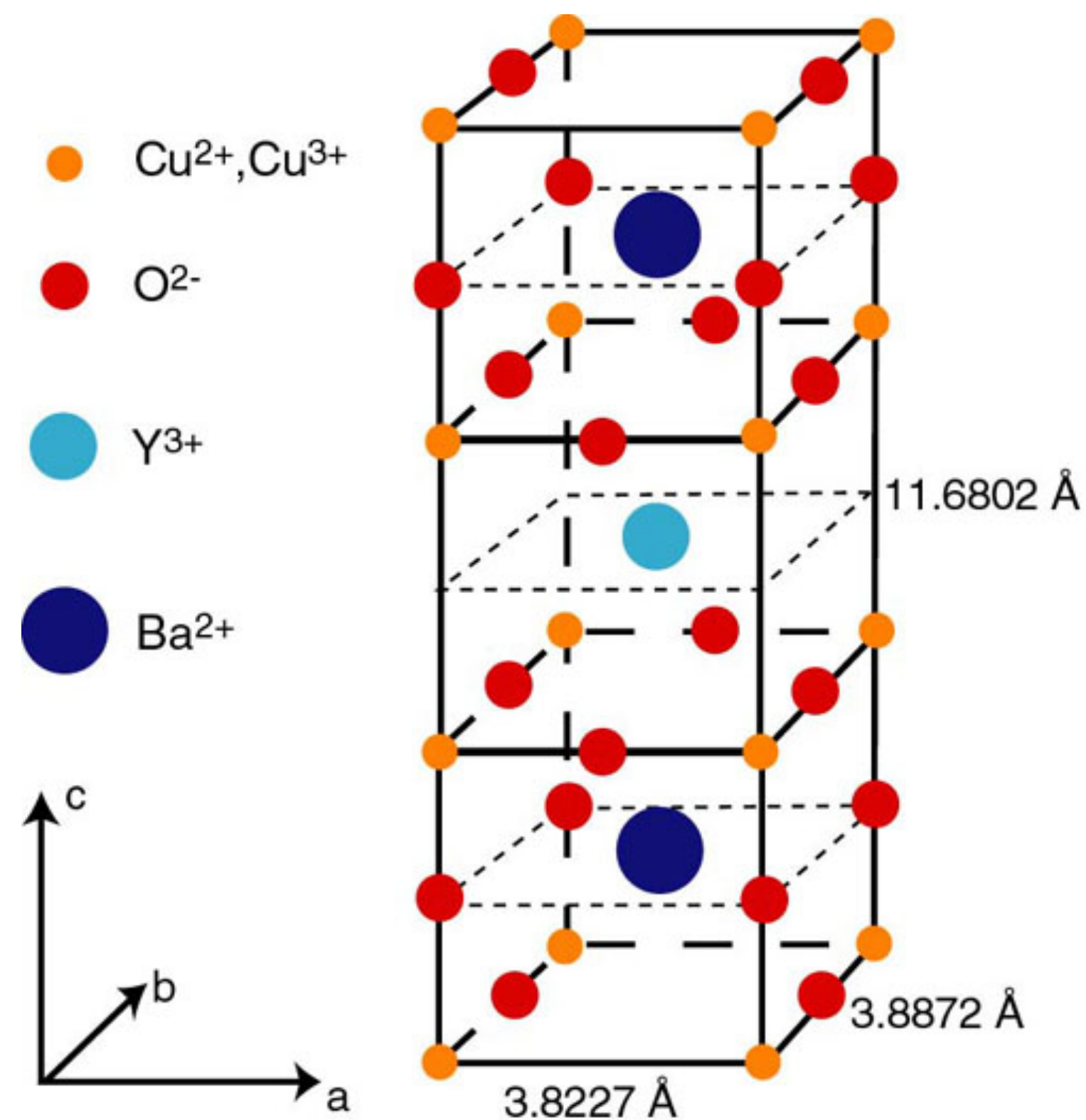
$$|G\rangle = \sum_{\mathcal{D}} c_{\mathcal{D}} |\mathcal{D}\rangle$$

$\mathcal{D} \rightarrow$ dimer covering
 of lattice



$$\text{Oval} = \frac{1}{\sqrt{2}} (|\uparrow\downarrow\rangle - |\downarrow\uparrow\rangle)$$

P.W.Anderson and G. Baskaran (1988): The key to high temperature superconductivity
 is the formation of a “resonating valence bond state”
 (a type of **quantum spin liquid**) which entangles the electrons on Cu



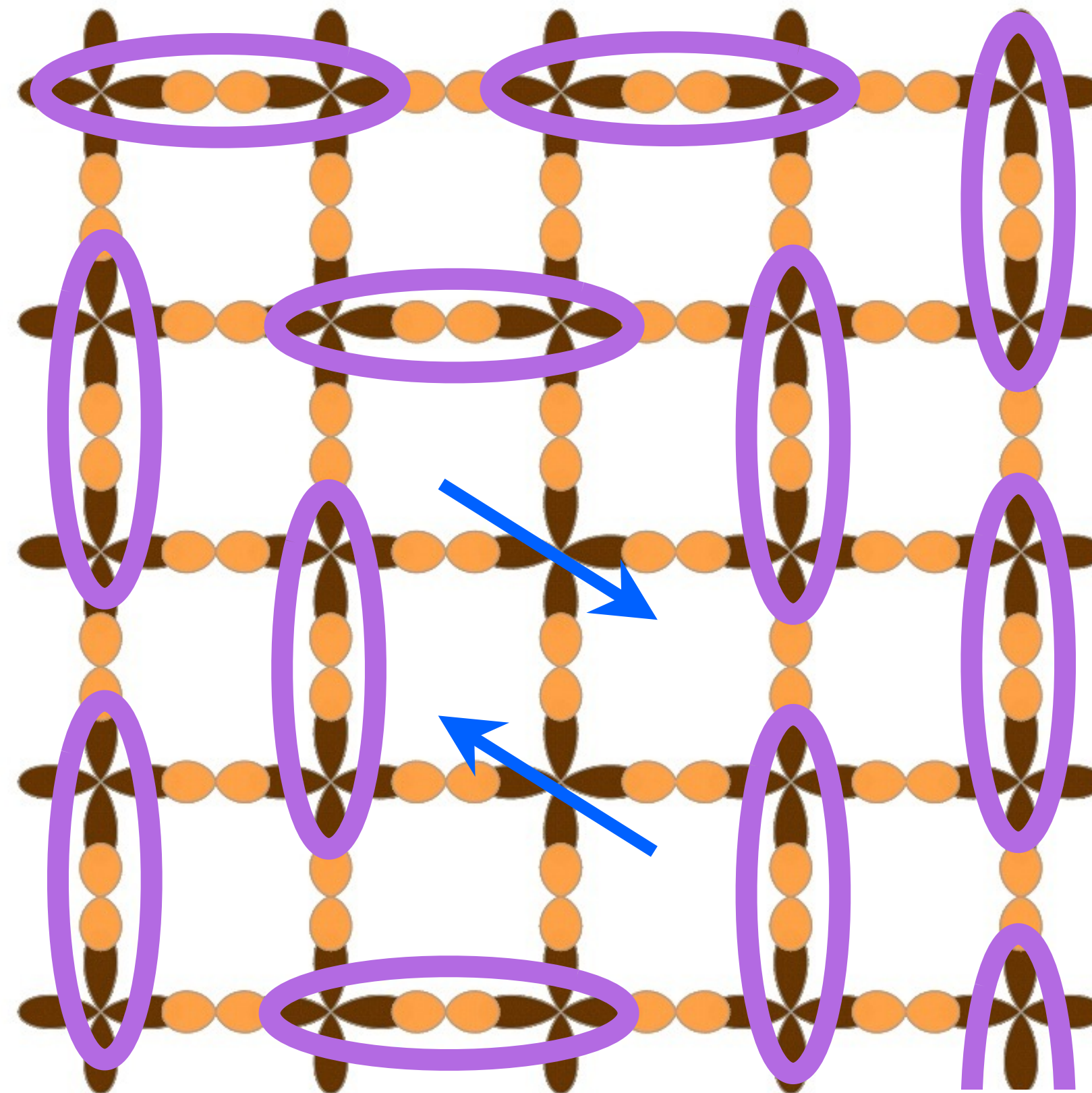
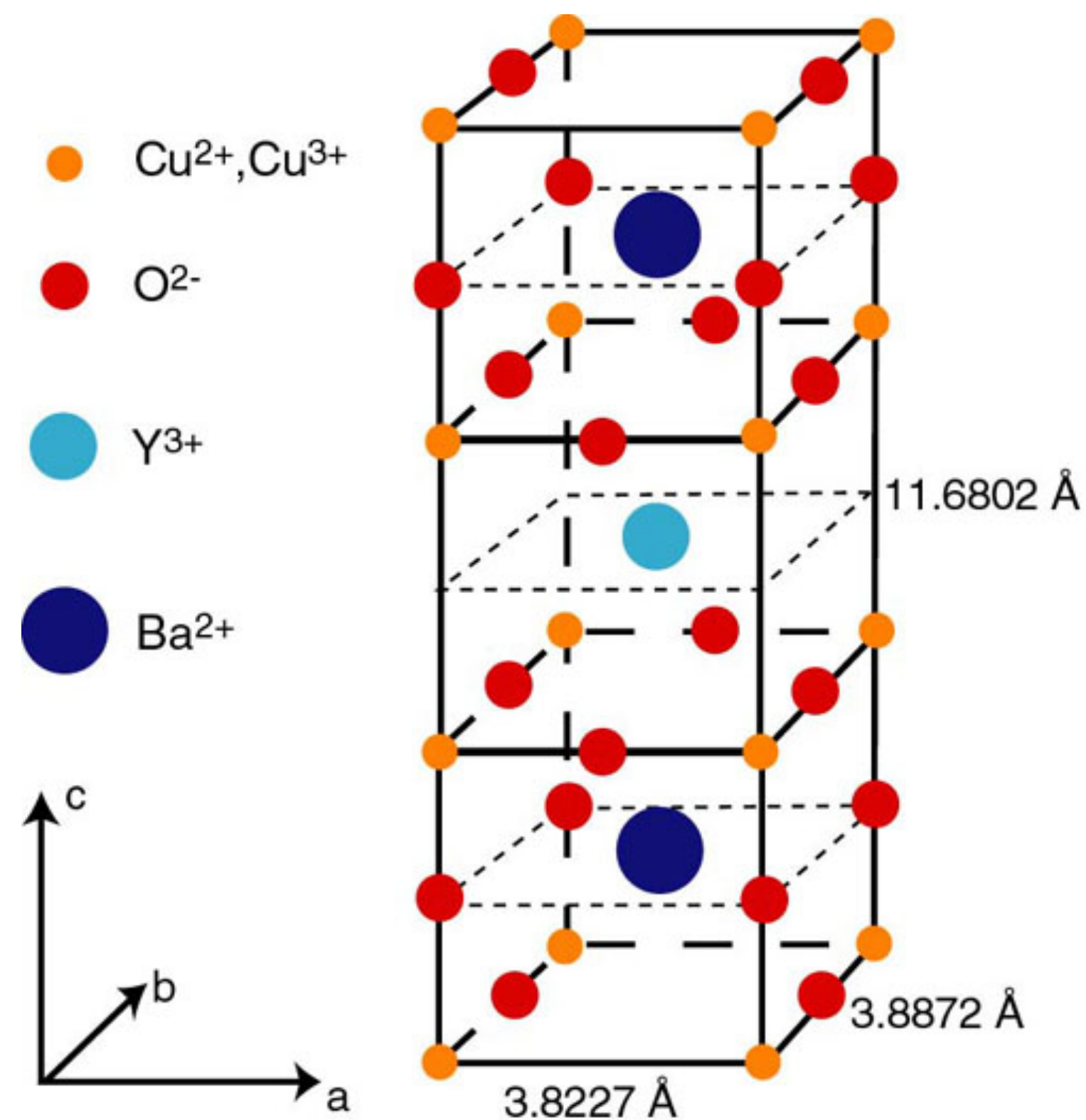
$$|G\rangle = \sum_{\mathcal{D}} c_{\mathcal{D}} |\mathcal{D}\rangle$$

$\mathcal{D} \rightarrow$ dimer covering
 of lattice



$$\text{Oval} = \frac{1}{\sqrt{2}} (|\uparrow\downarrow\rangle - |\downarrow\uparrow\rangle)$$

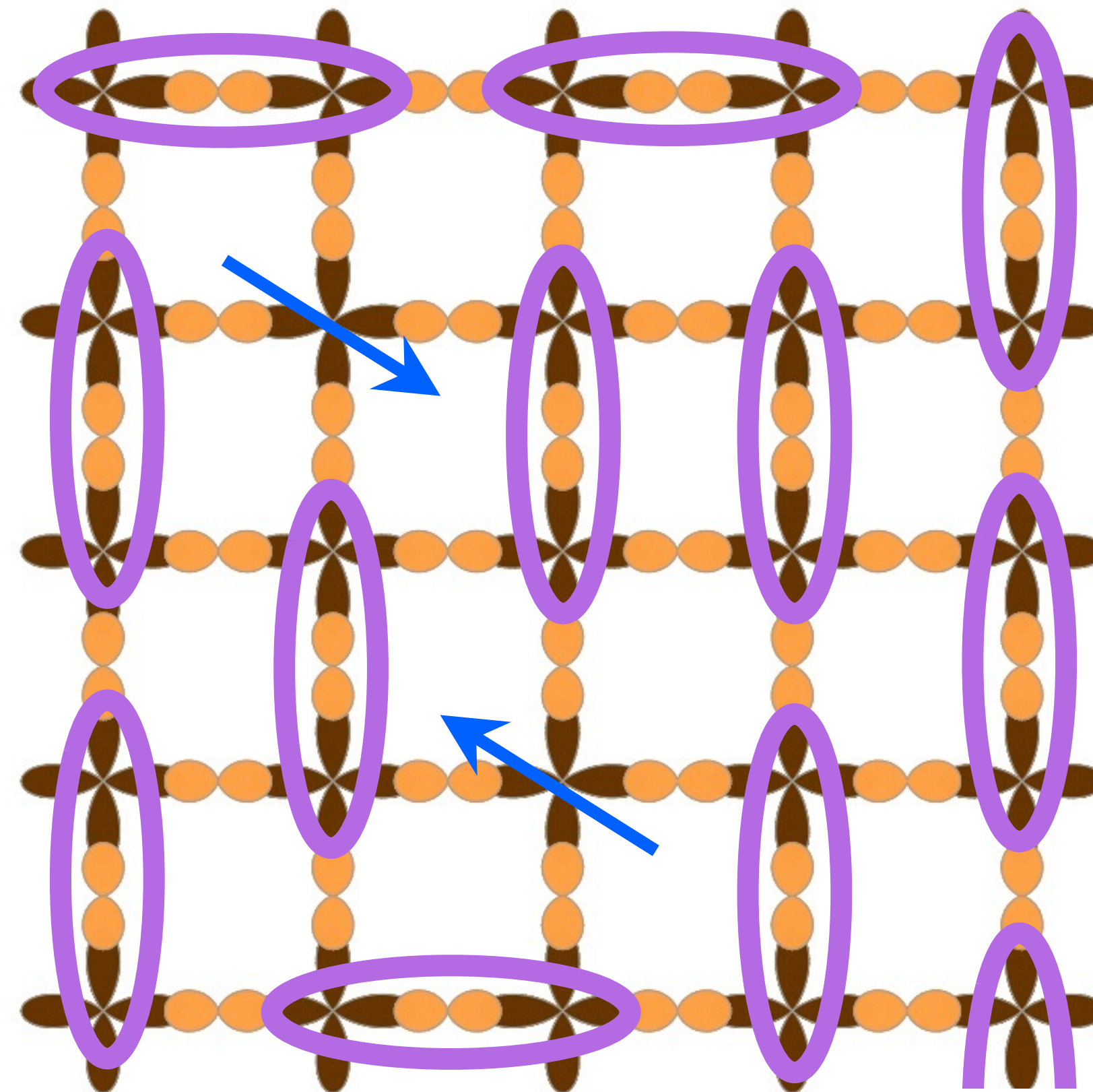
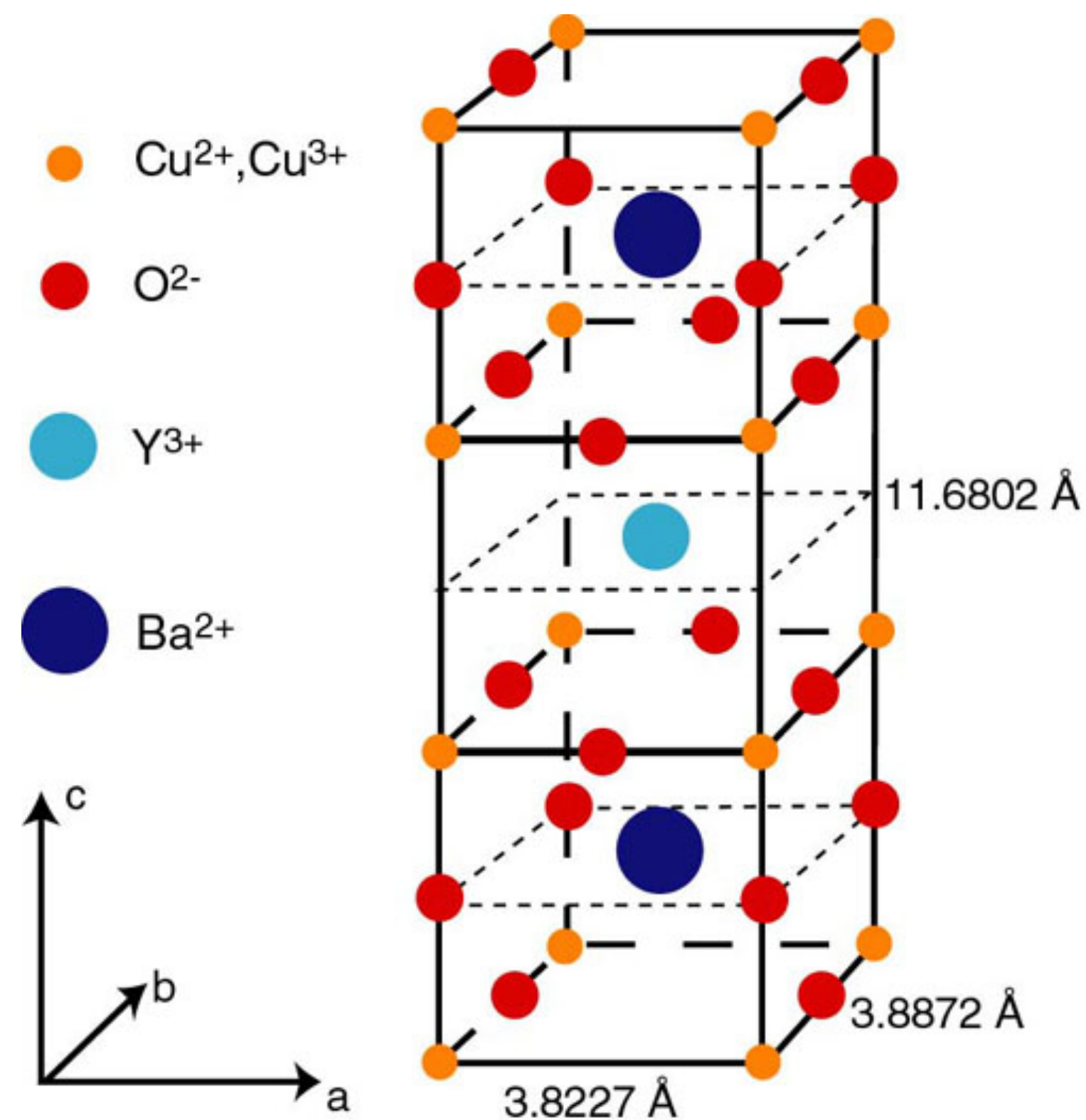
P.W.Anderson and G. Baskaran (1988): The key to high temperature superconductivity
 is the formation of a “resonating valence bond state”
 (a type of **quantum spin liquid**) which entangles the electrons on Cu



$$\text{YBa}_2\text{Cu}_3\text{O}_{6+x}$$

$$\text{Oval} = \frac{1}{\sqrt{2}} (|\uparrow\downarrow\rangle - |\downarrow\uparrow\rangle)$$

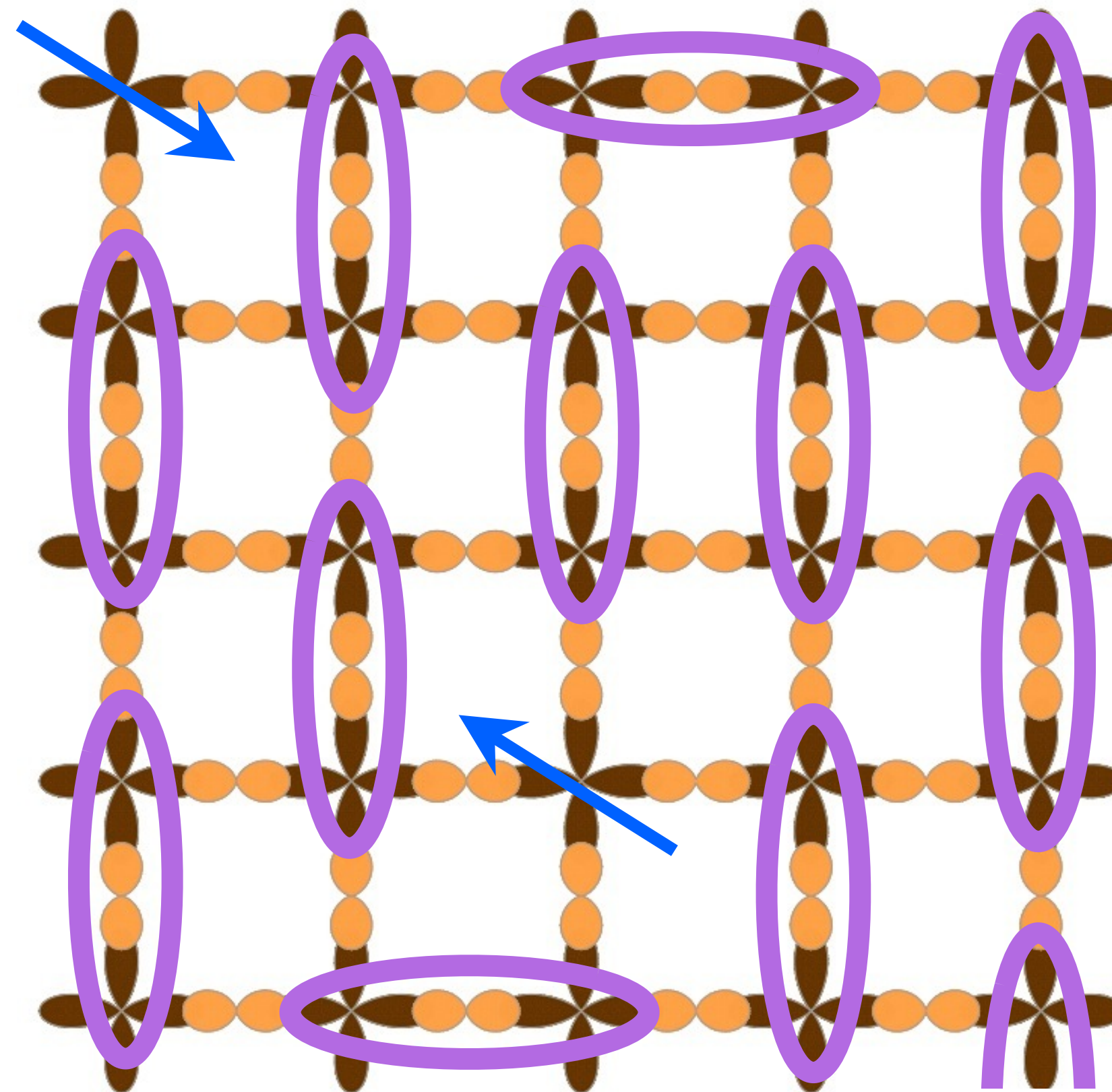
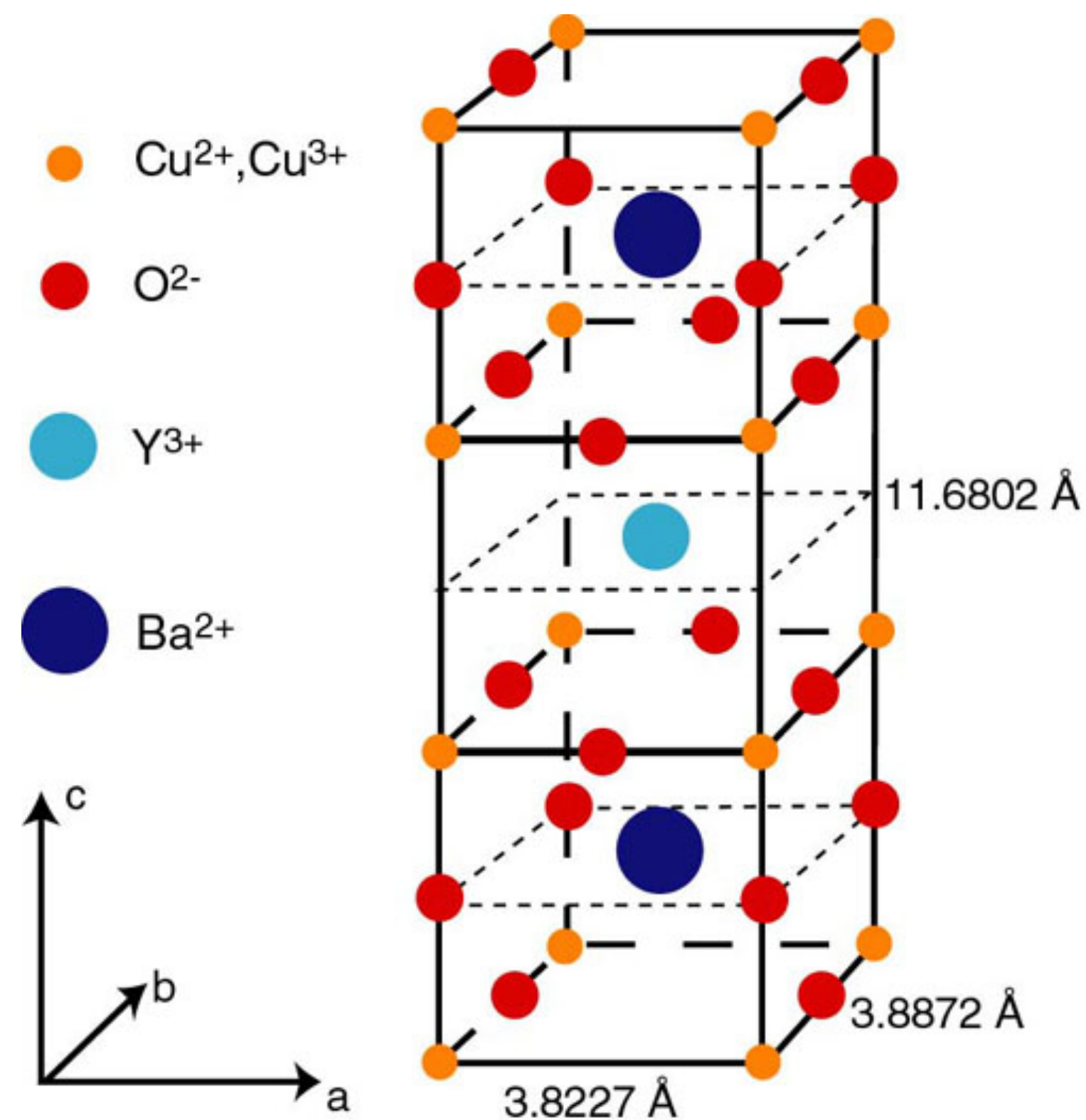
Key feature: fractionalization. Excitations are particle-like, but cannot be created by local operators: they are classified under distinct superselection/anyon sectors.



$$\text{YBa}_2\text{Cu}_3\text{O}_{6+x}$$

$$\text{Oval} = \frac{1}{\sqrt{2}} (|\uparrow\downarrow\rangle - |\downarrow\uparrow\rangle)$$

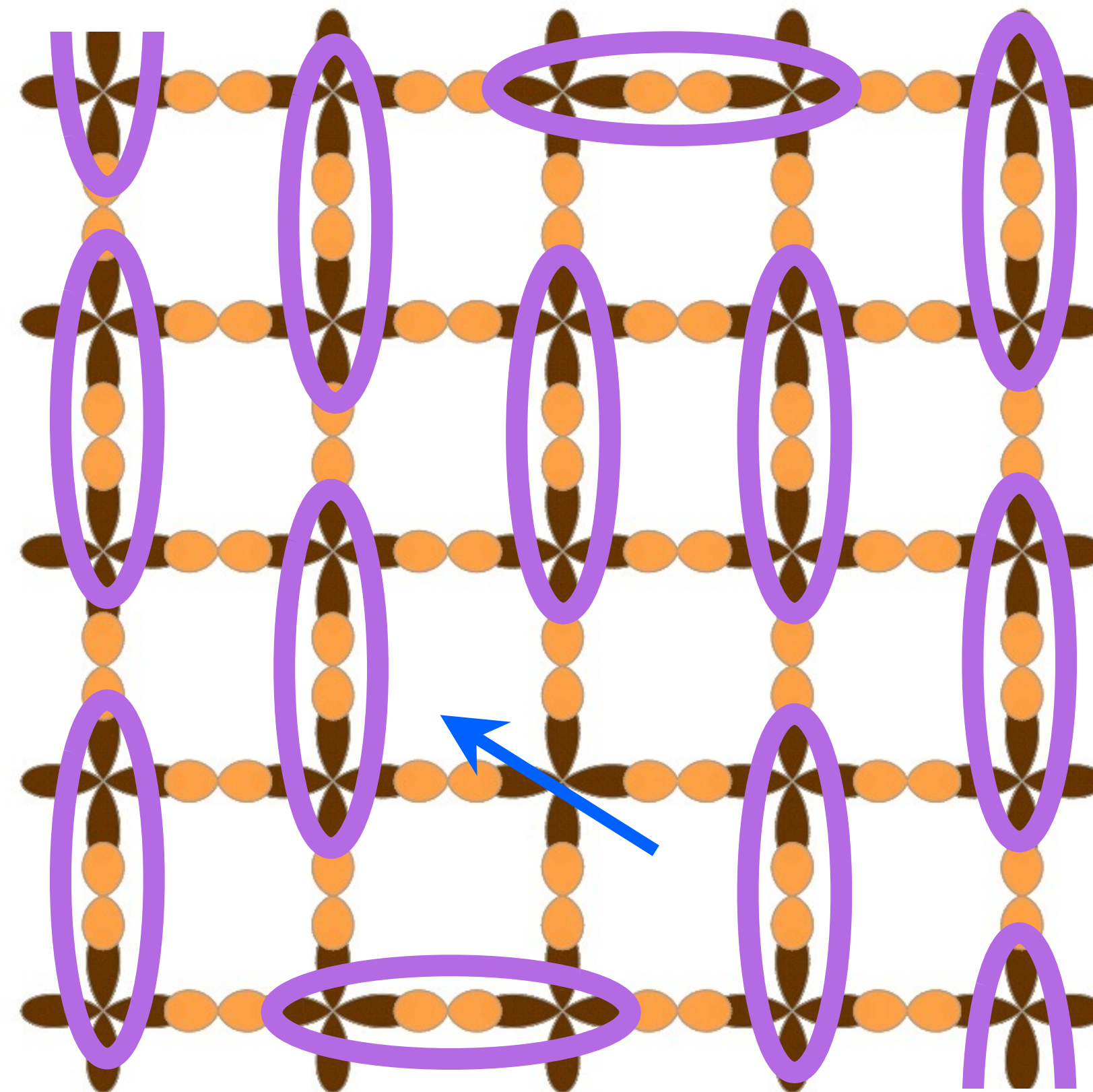
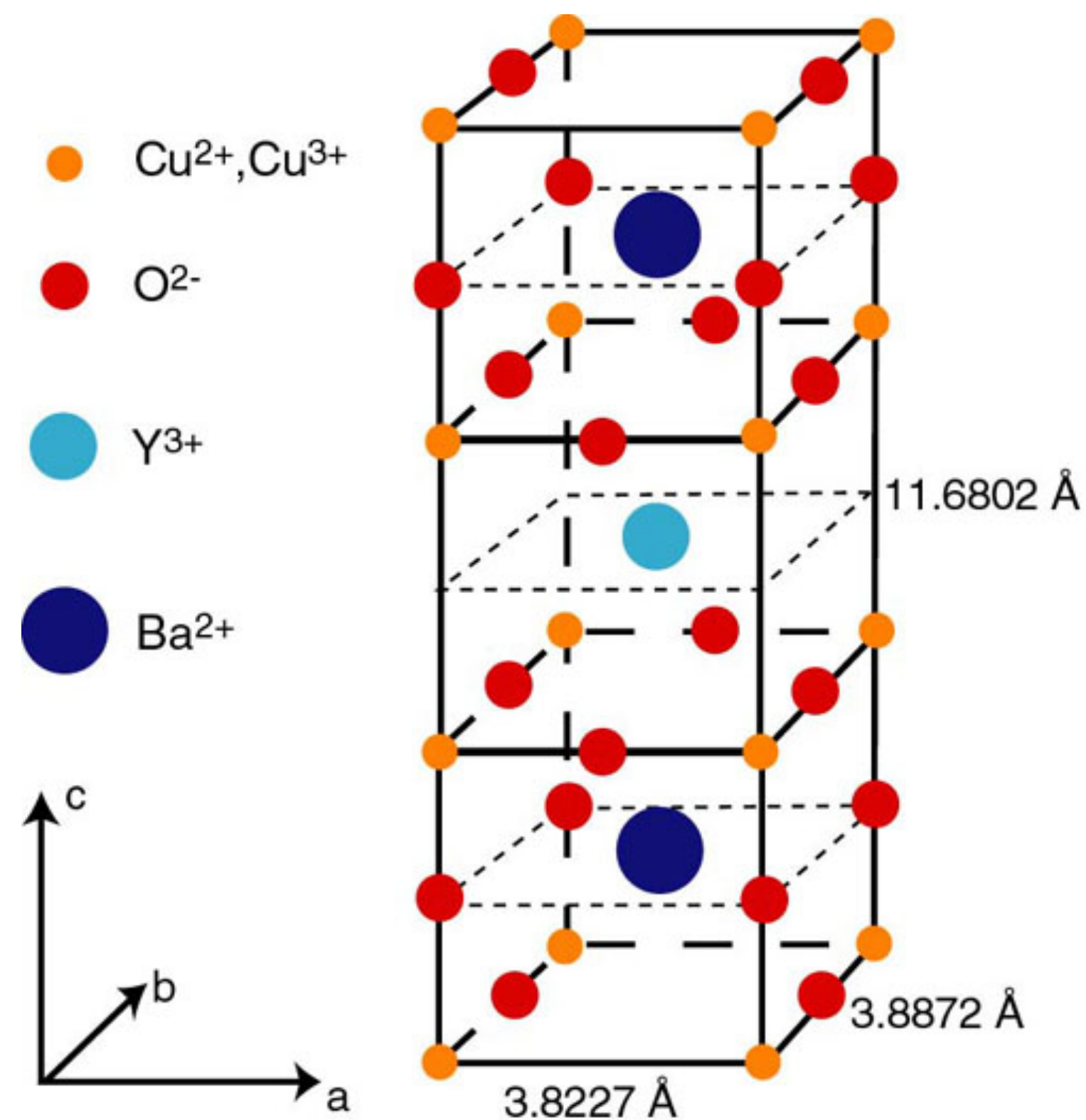
Key feature: fractionalization. Excitations are particle-like, but cannot be created by local operators: they are classified under distinct superselection/anyon sectors.



$$\text{YBa}_2\text{Cu}_3\text{O}_{6+x}$$

$$\bigcirc = \frac{1}{\sqrt{2}} (|\uparrow\downarrow\rangle - |\downarrow\uparrow\rangle)$$

Key feature: fractionalization. Excitations are particle-like, but cannot be created by local operators: they are classified under distinct superselection/anyon sectors.

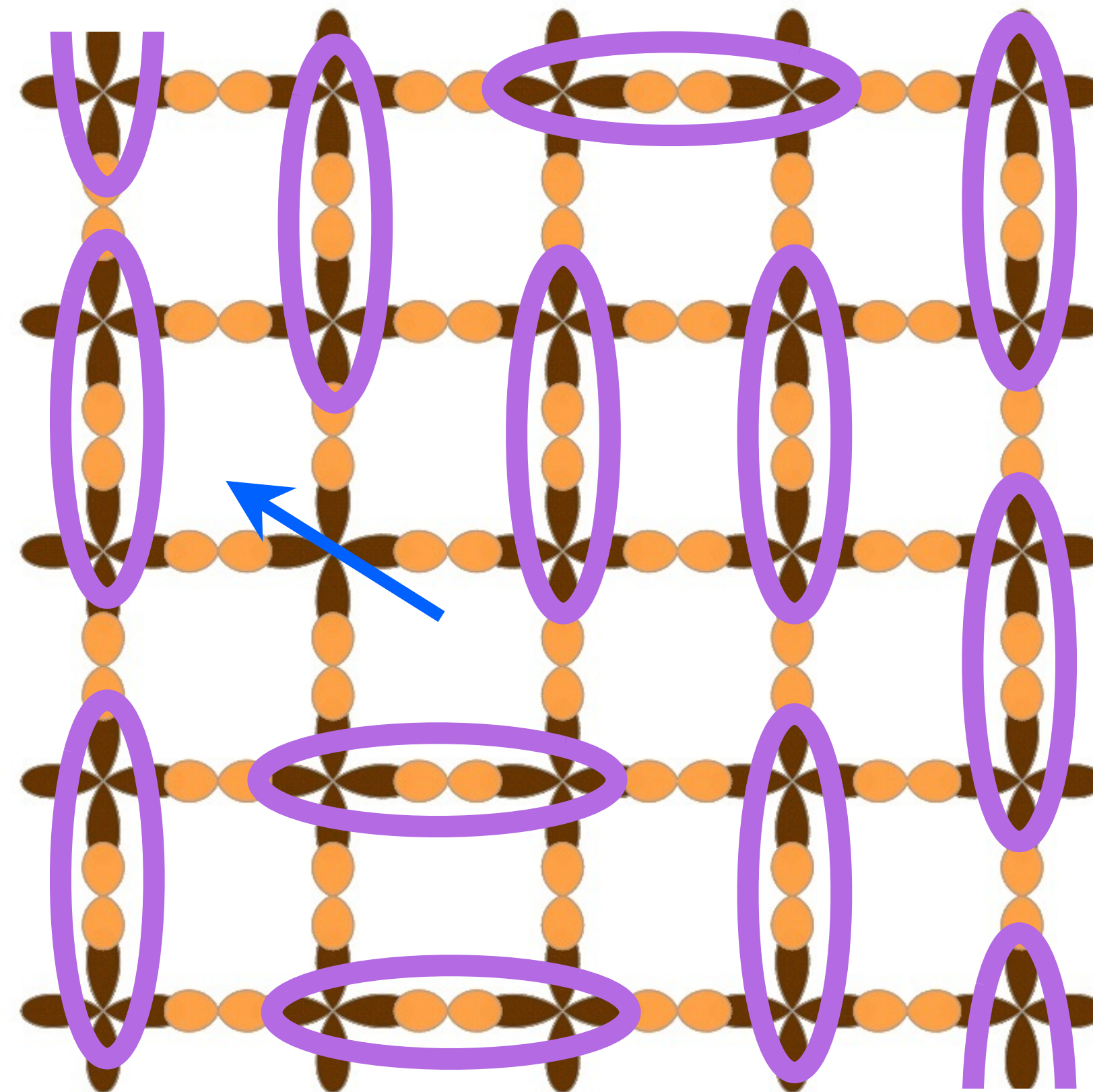
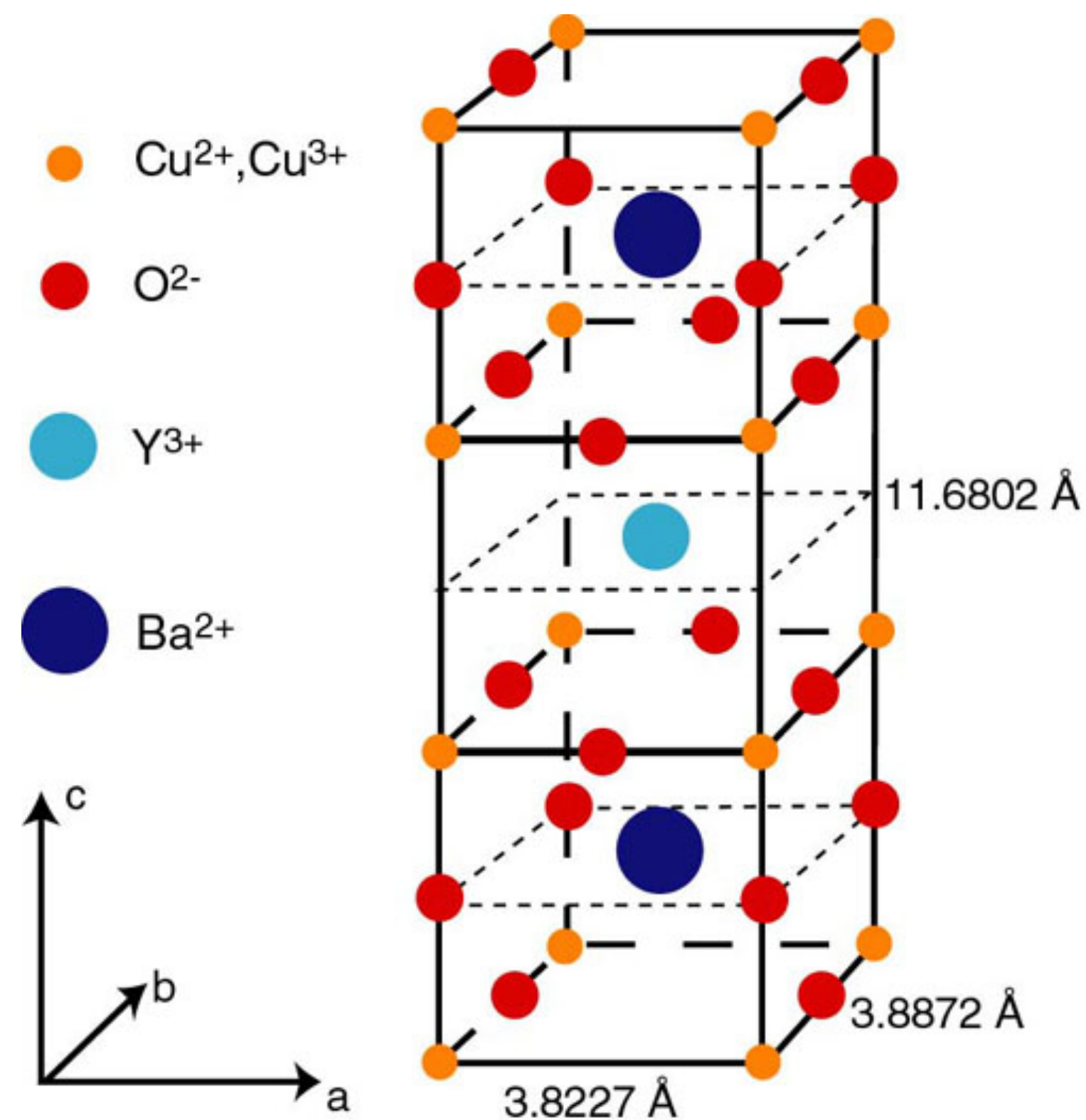


Spin $S=1/2$,
 charge
 neutral
 spinon

$$\text{YBa}_2\text{Cu}_3\text{O}_{6+x}$$

$$\bigcirc = \frac{1}{\sqrt{2}} (|\uparrow\downarrow\rangle - |\downarrow\uparrow\rangle)$$

Key feature: fractionalization. Excitations are particle-like, but cannot be created by local operators: they are classified under distinct superselection/anyon sectors.

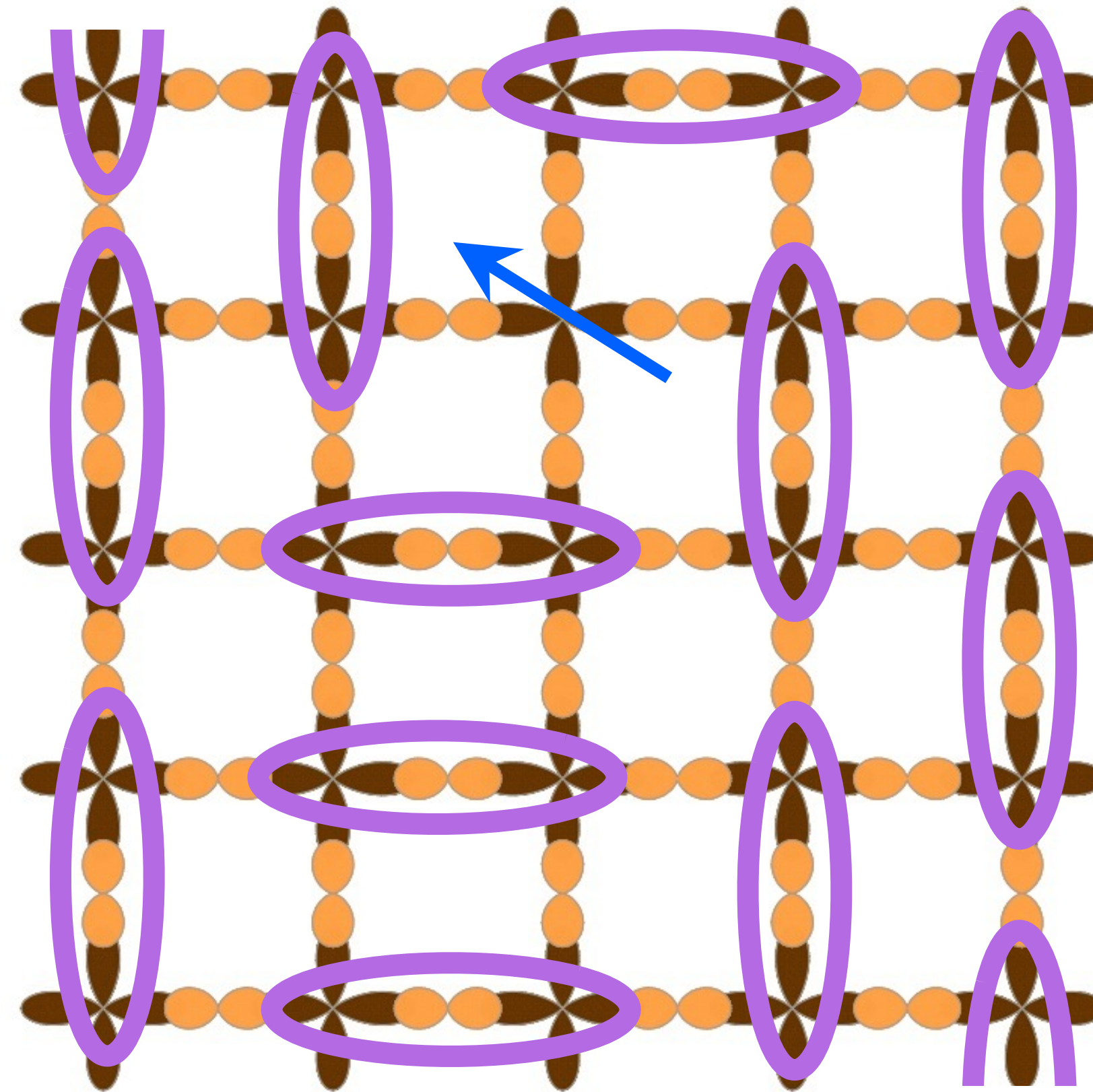
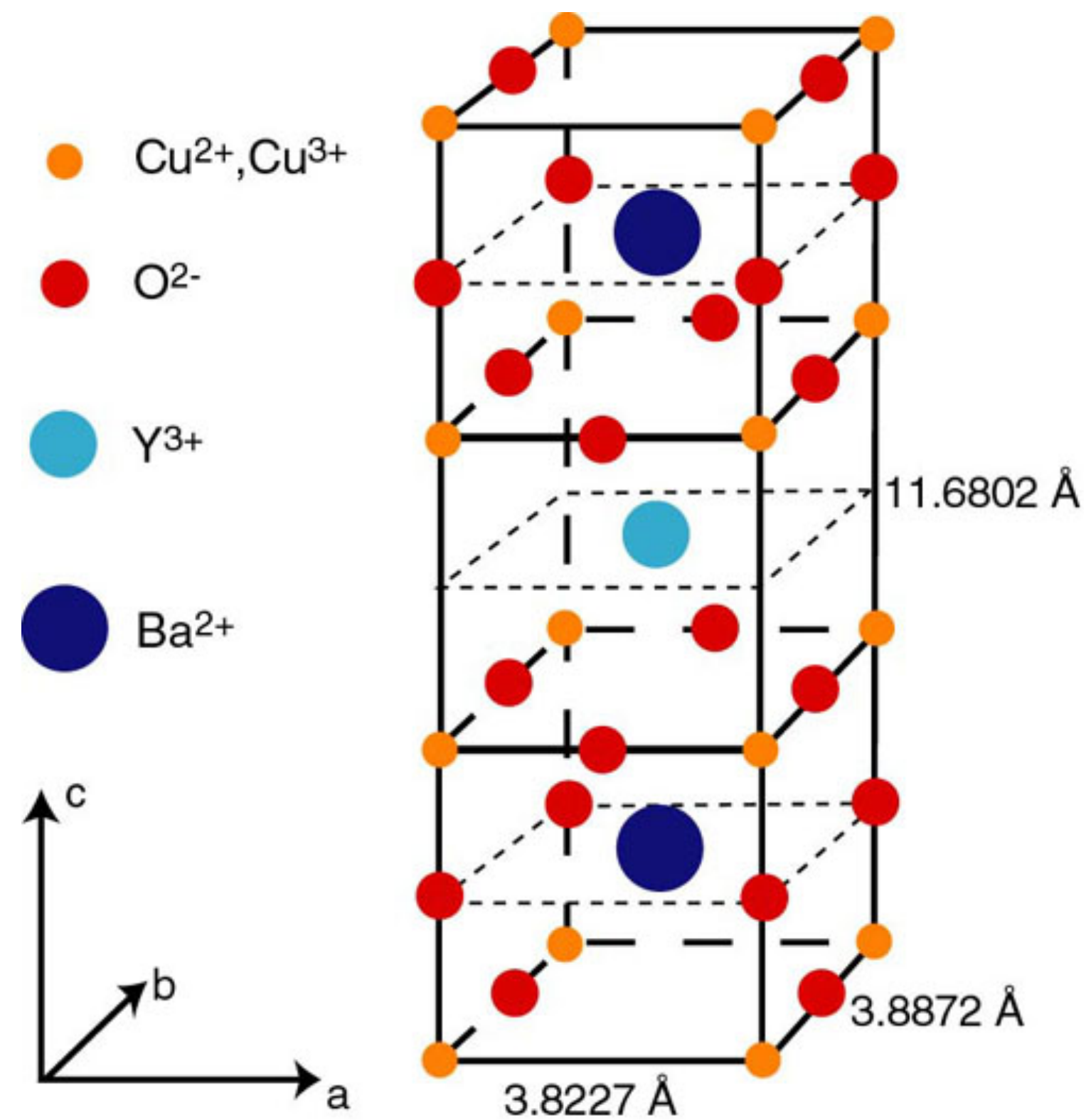


Spin $S=1/2$,
 charge
 neutral
 spinon

$$\text{YBa}_2\text{Cu}_3\text{O}_{6+x}$$

$$\text{Oval} = \frac{1}{\sqrt{2}} (|\uparrow\downarrow\rangle - |\downarrow\uparrow\rangle)$$

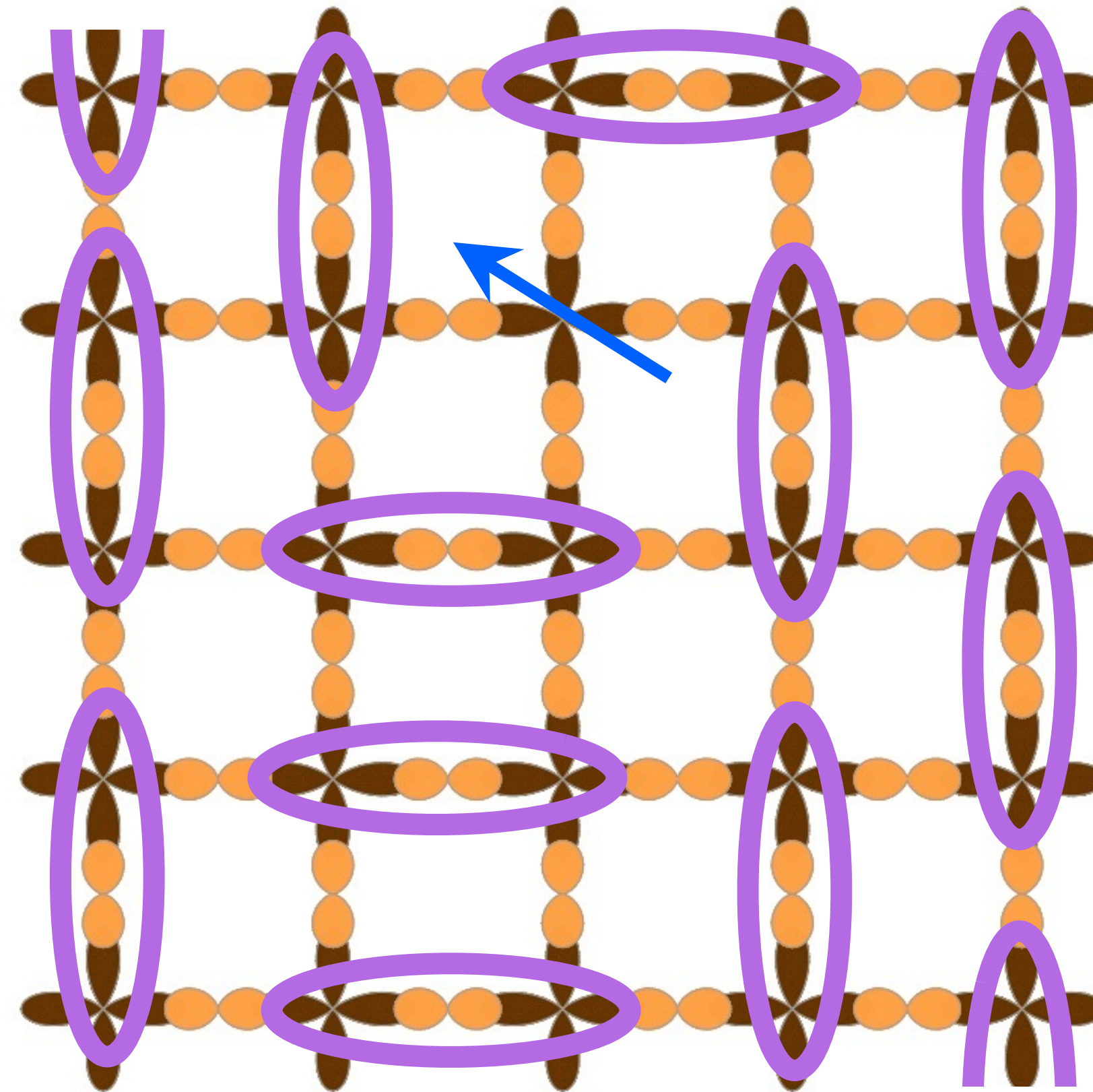
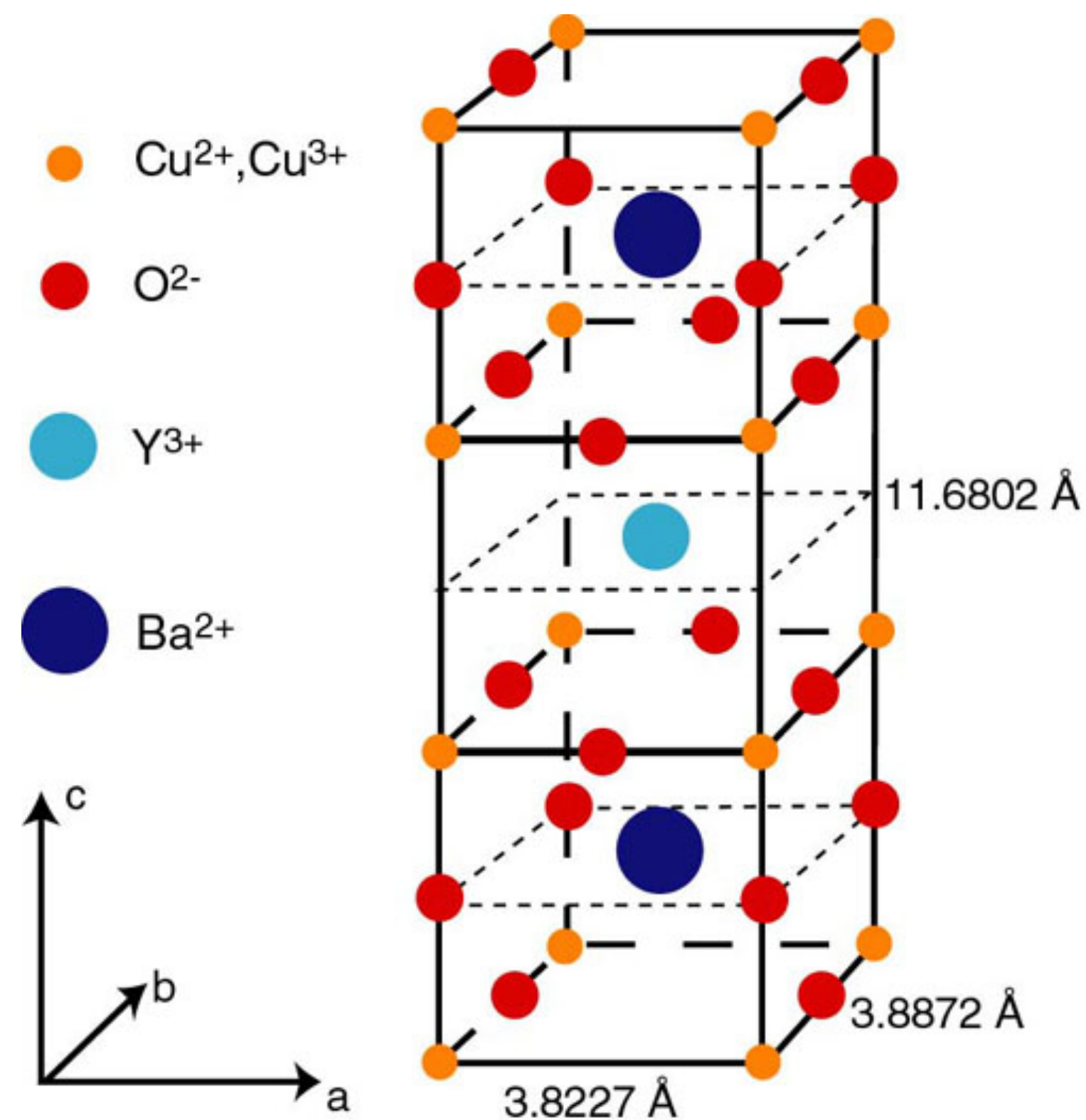
Key feature: fractionalization. Excitations are particle-like, but cannot be created by local operators: they are classified under distinct superselection/anyon sectors.



Spin $S=1/2$,
 charge
 neutral
 spinon

$$\text{YBa}_2\text{Cu}_3\text{O}_{6+x} \quad \text{Oval} = \frac{1}{\sqrt{2}} (|\uparrow\downarrow\rangle - |\downarrow\uparrow\rangle)$$

Key feature: fractionalization. Excitations are particle-like, but cannot be created by local operators: they are classified under distinct superselection/anyon sectors.

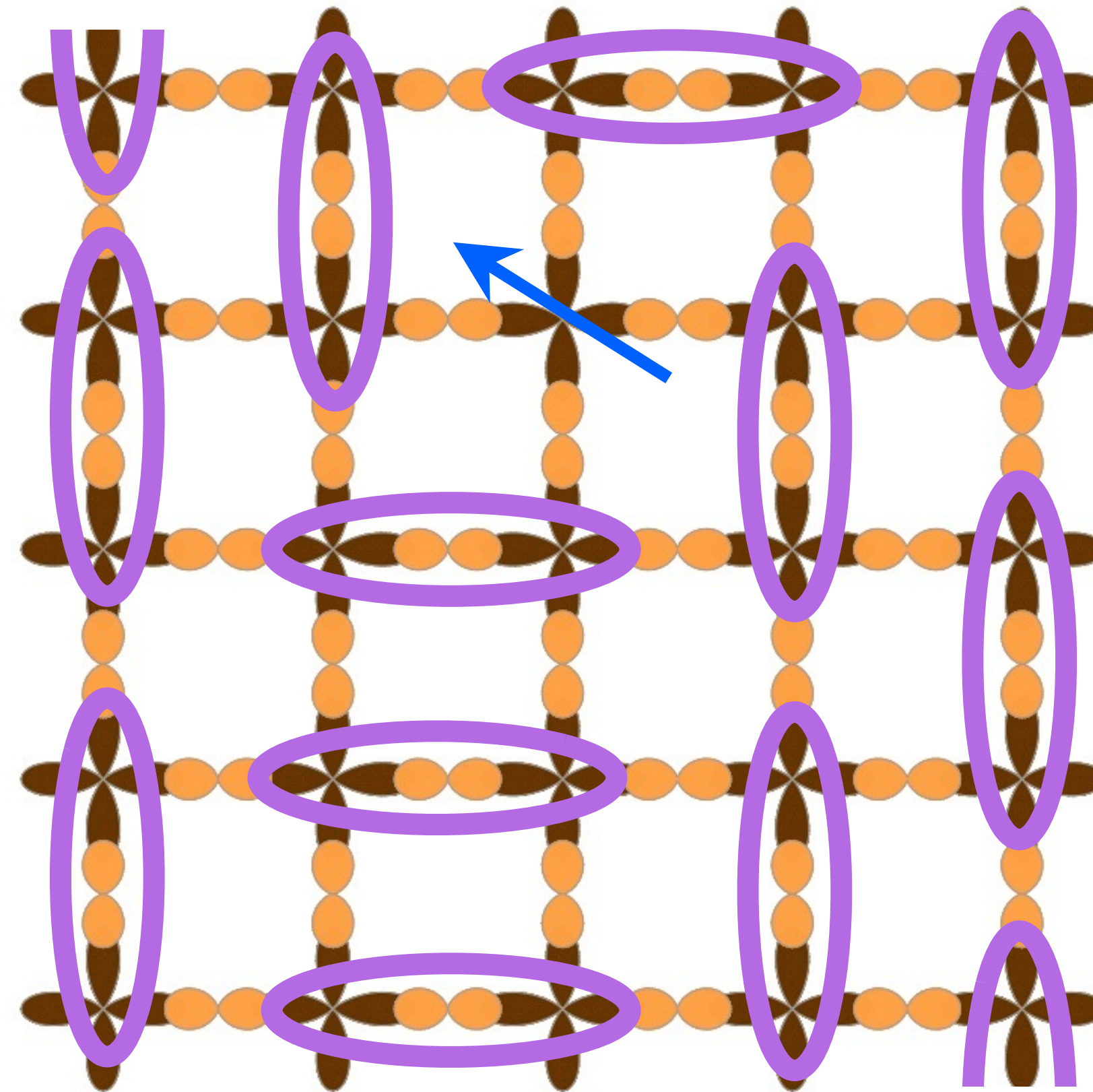
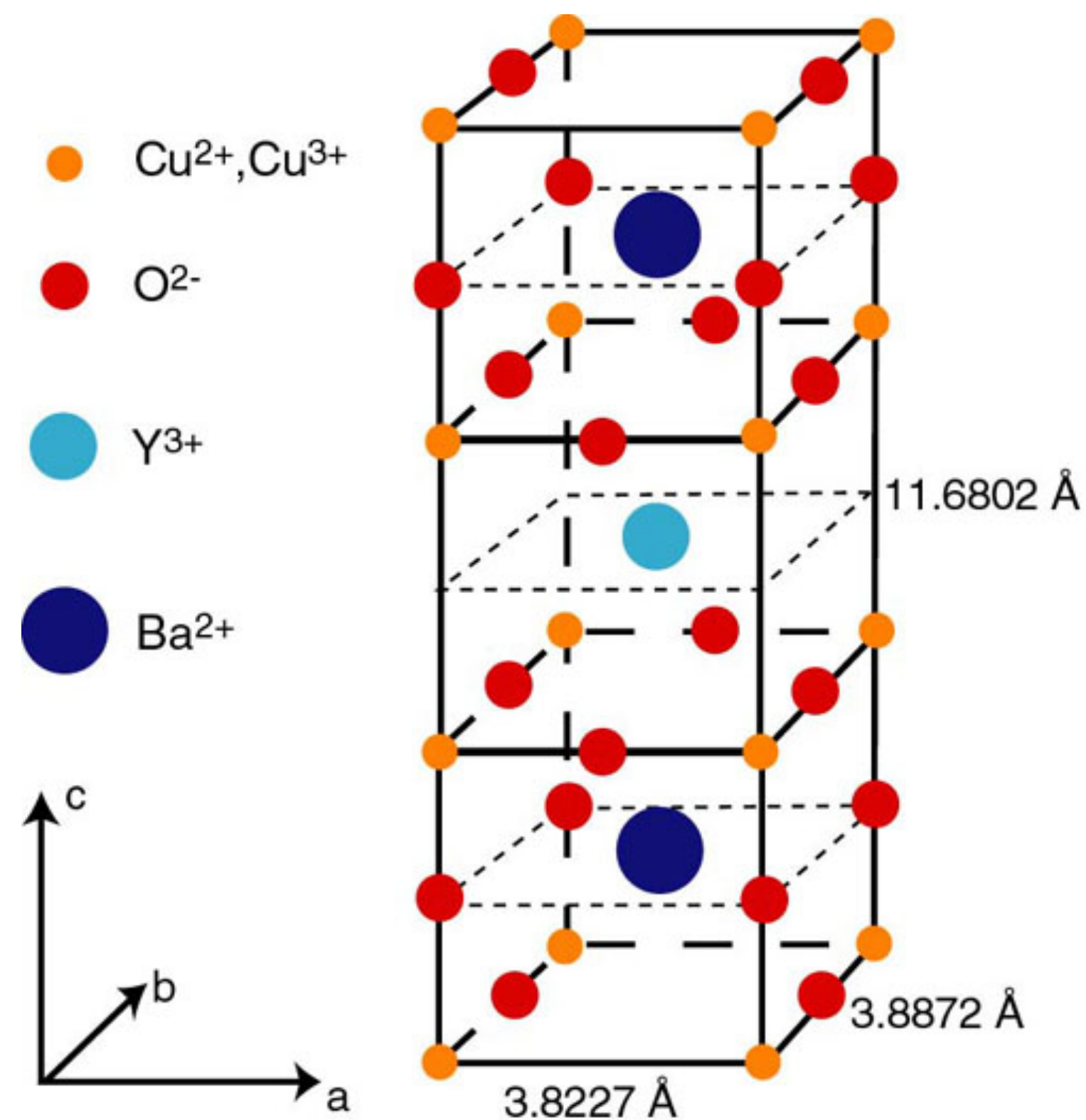


Spin $S=1/2$,
 charge
 neutral
 spinon

$$\text{YBa}_2\text{Cu}_3\text{O}_{6+x}$$

$$\text{Oval} = \frac{1}{\sqrt{2}} (|\uparrow\downarrow\rangle - |\downarrow\uparrow\rangle)$$

Key feature: fractionalization. Excitations are particle-like, but cannot be created by local operators: they are classified under distinct superselection/anyon sectors.
 Kitaev: this is useful for quantum error correction.

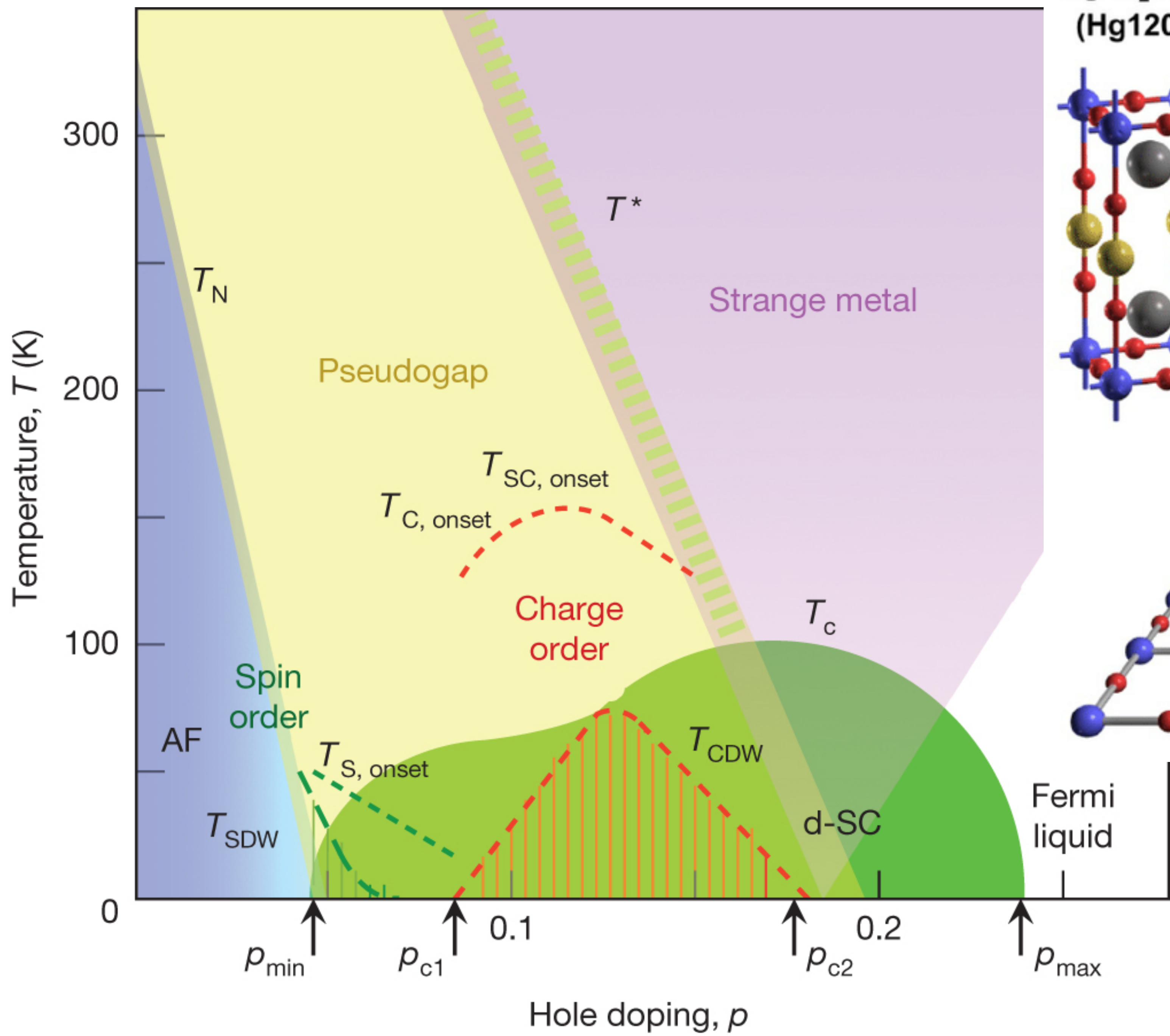


Spin $S=1/2$,
 charge
 neutral
 spinon

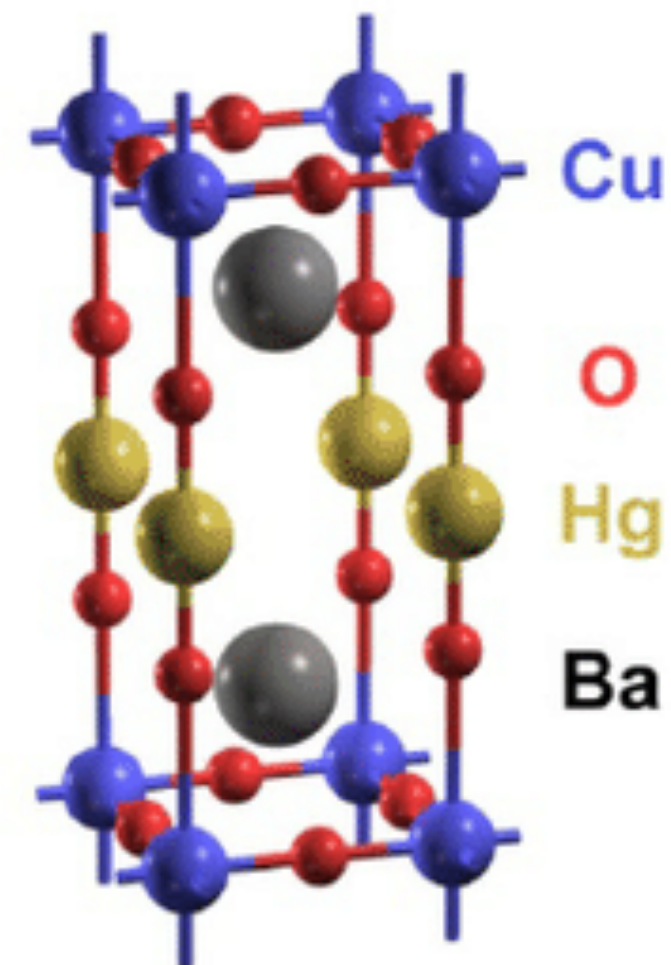


$$\text{Oval} = \frac{1}{\sqrt{2}} (|\uparrow\downarrow\rangle - |\downarrow\uparrow\rangle)$$

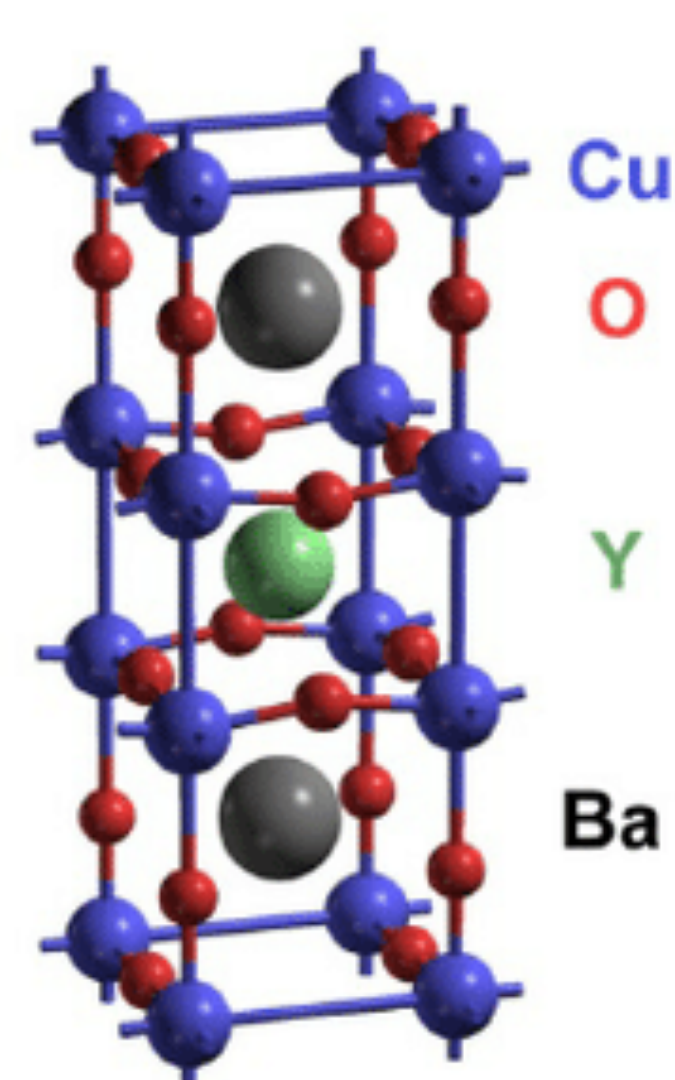
- Theory of gapped spin liquids of insulators in two dimensions. ✓
 The simplest, and closest to Anderson's RVB state, is the \mathbb{Z}_2 spin liquid (Read and S.S. 1991), with the same anyons as the toric code (Kitaev 1996). Implemented in Google's fault tolerant qubit.



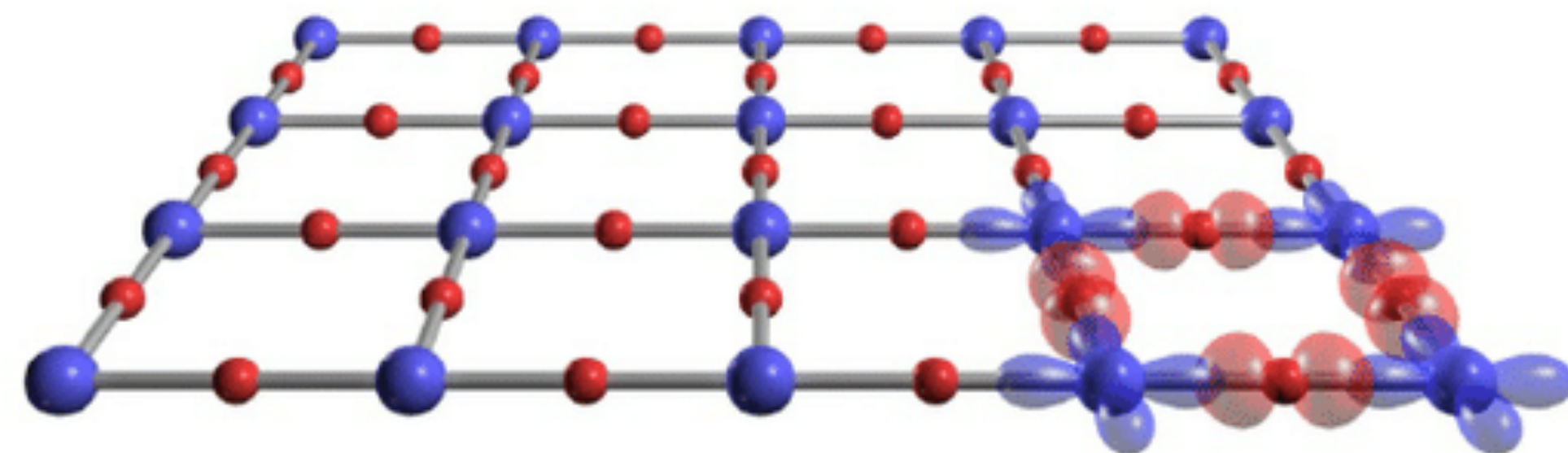
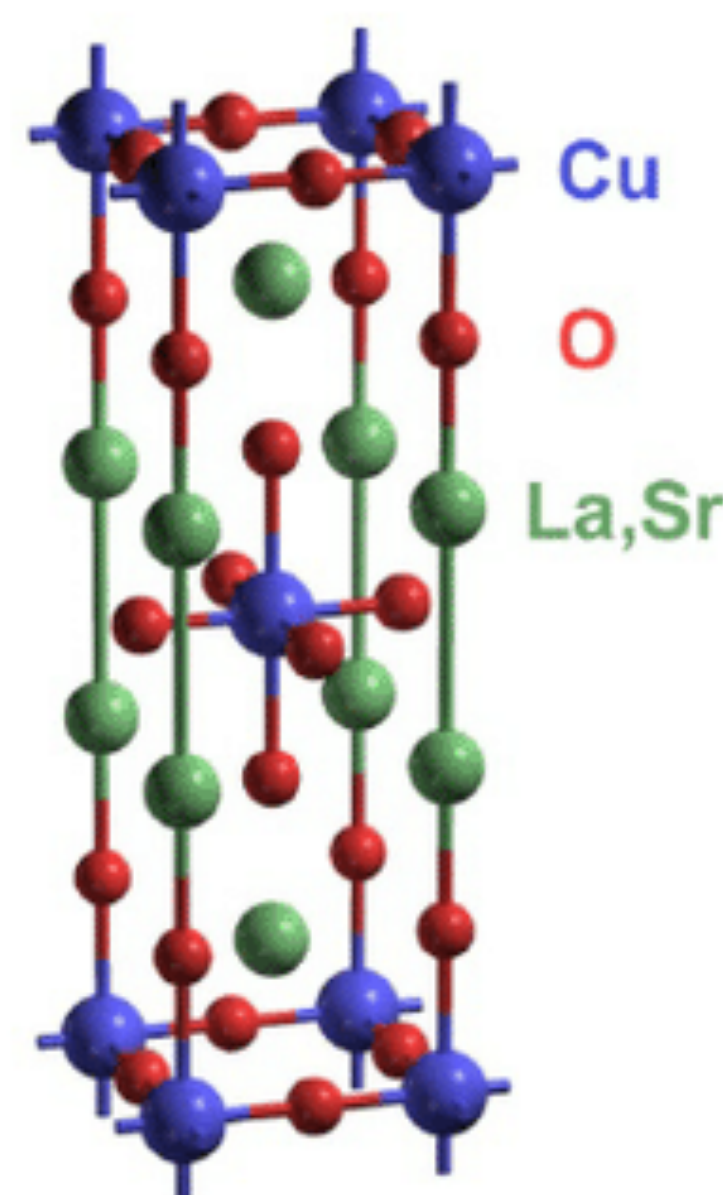
$\text{HgBa}_2\text{CuO}_{4+\delta}$
(Hg1201)

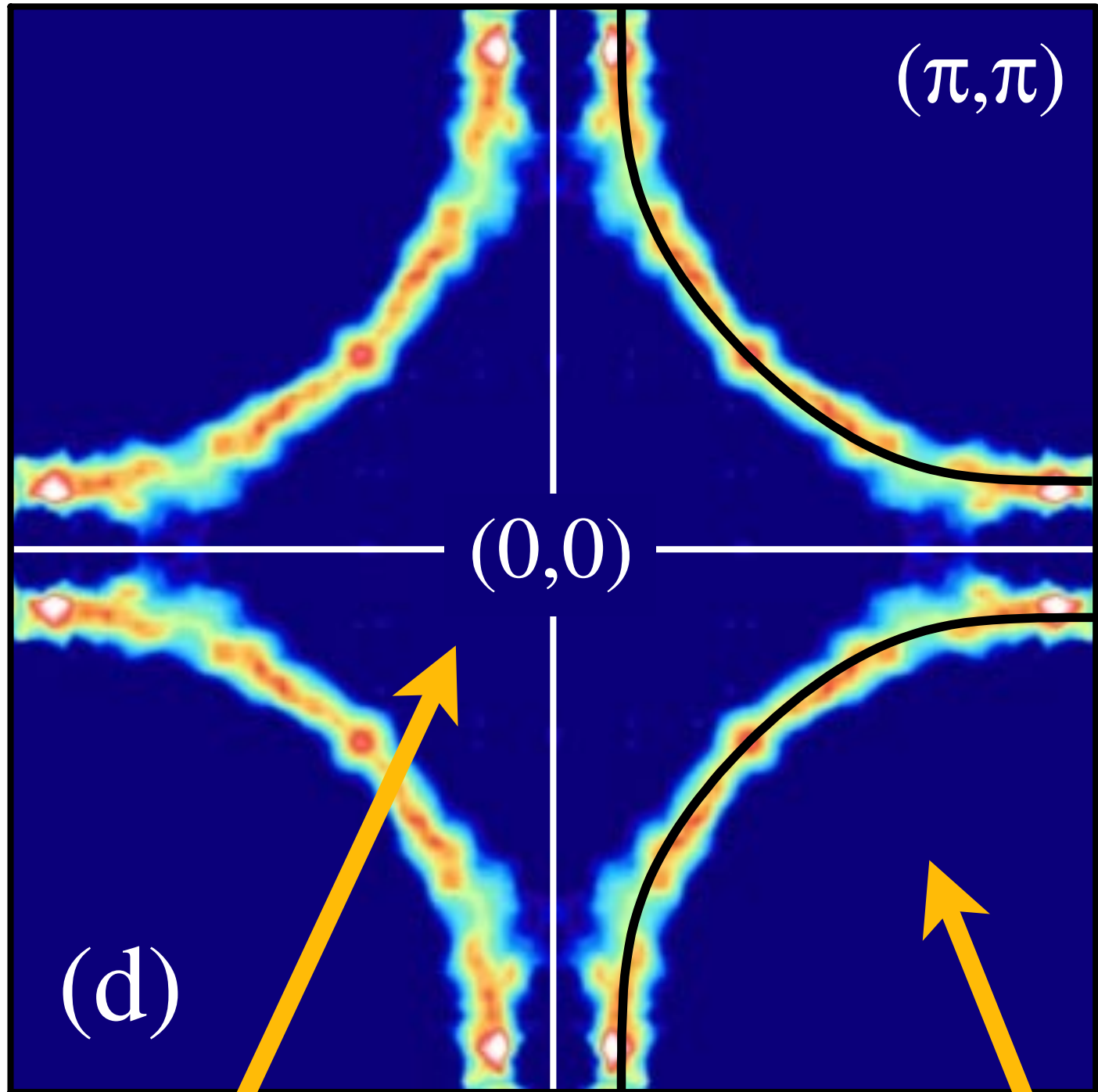
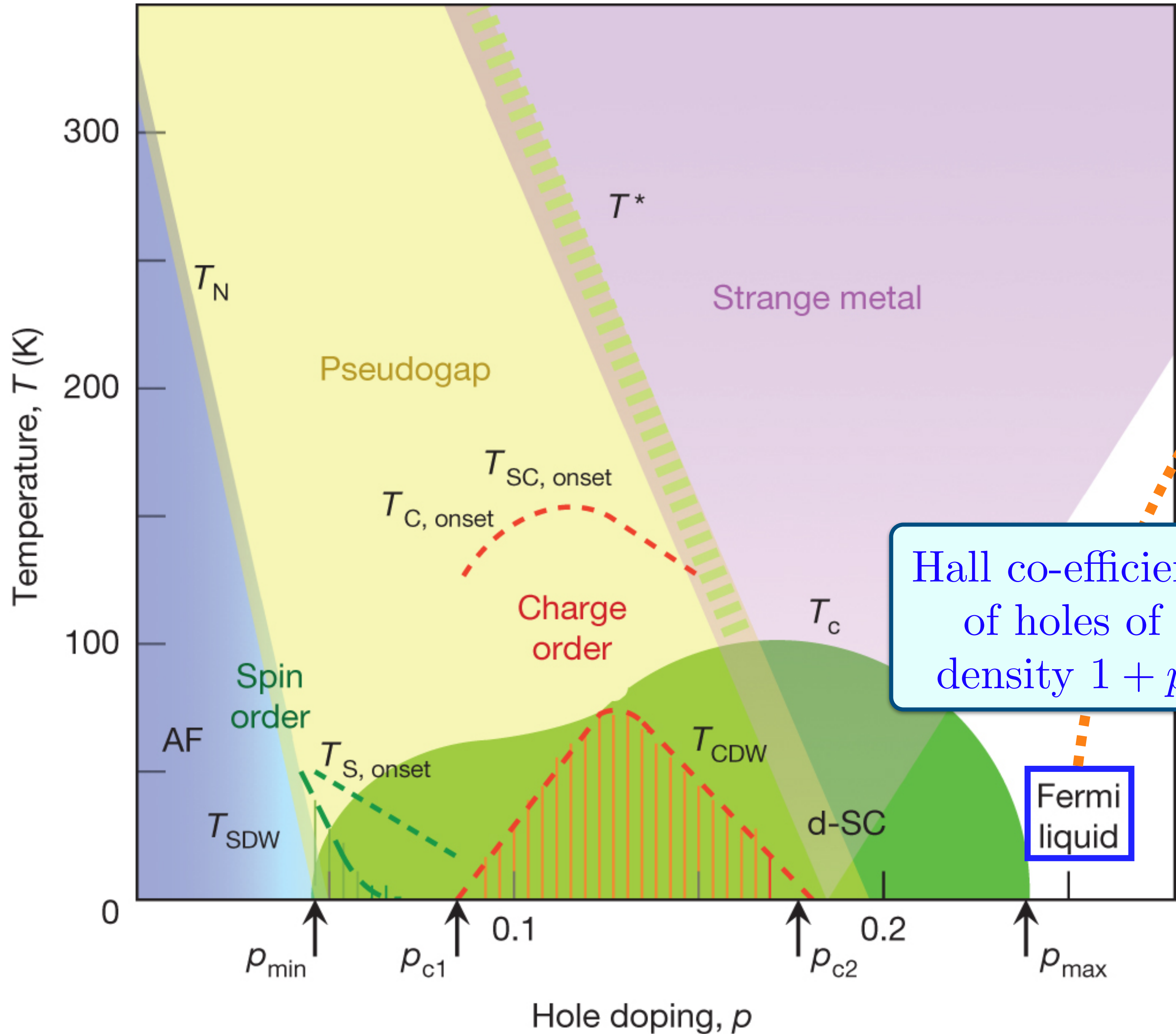


$\text{YBa}_2\text{Cu}_3\text{O}_{7-\delta}$
(YBCO)



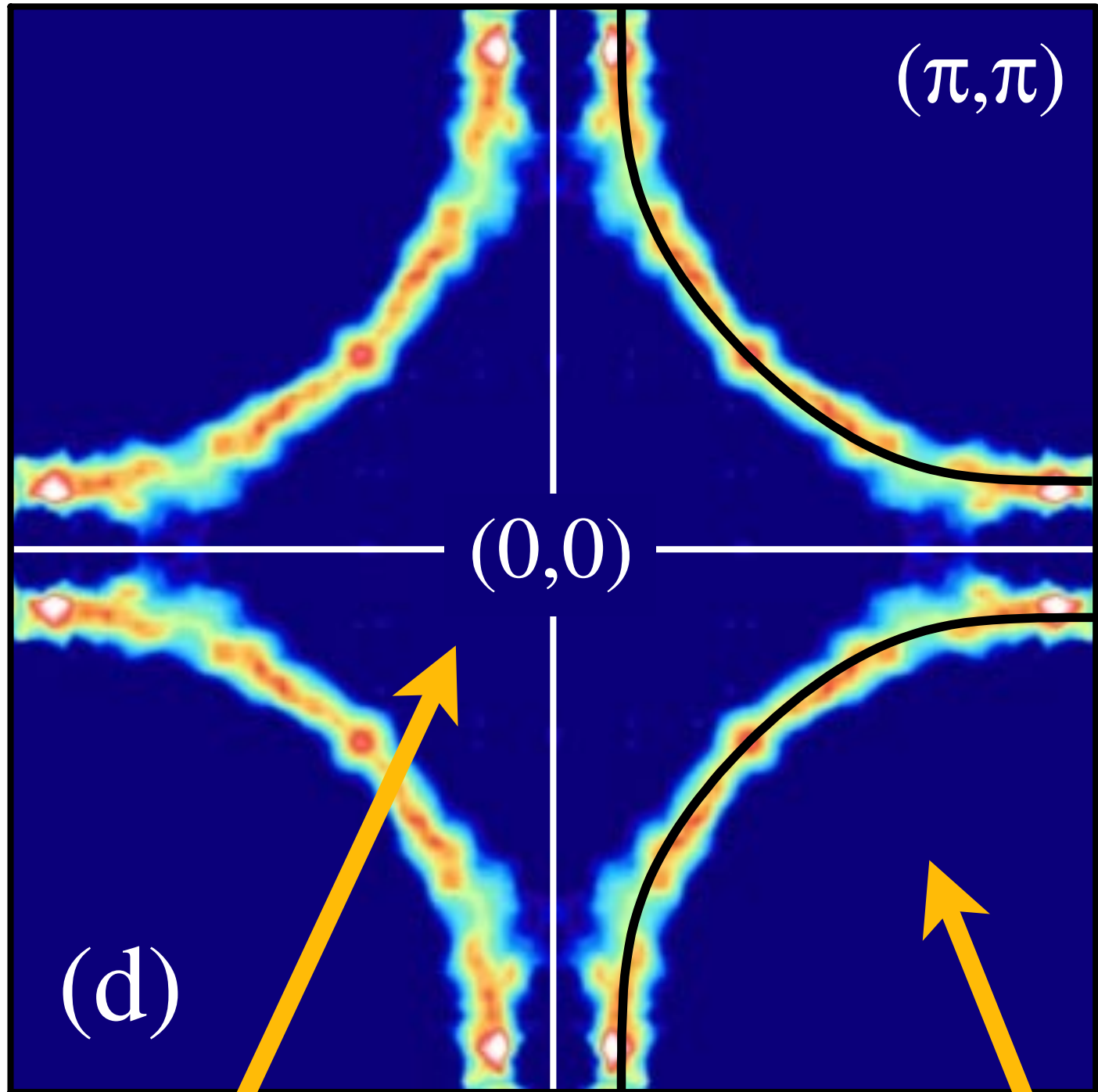
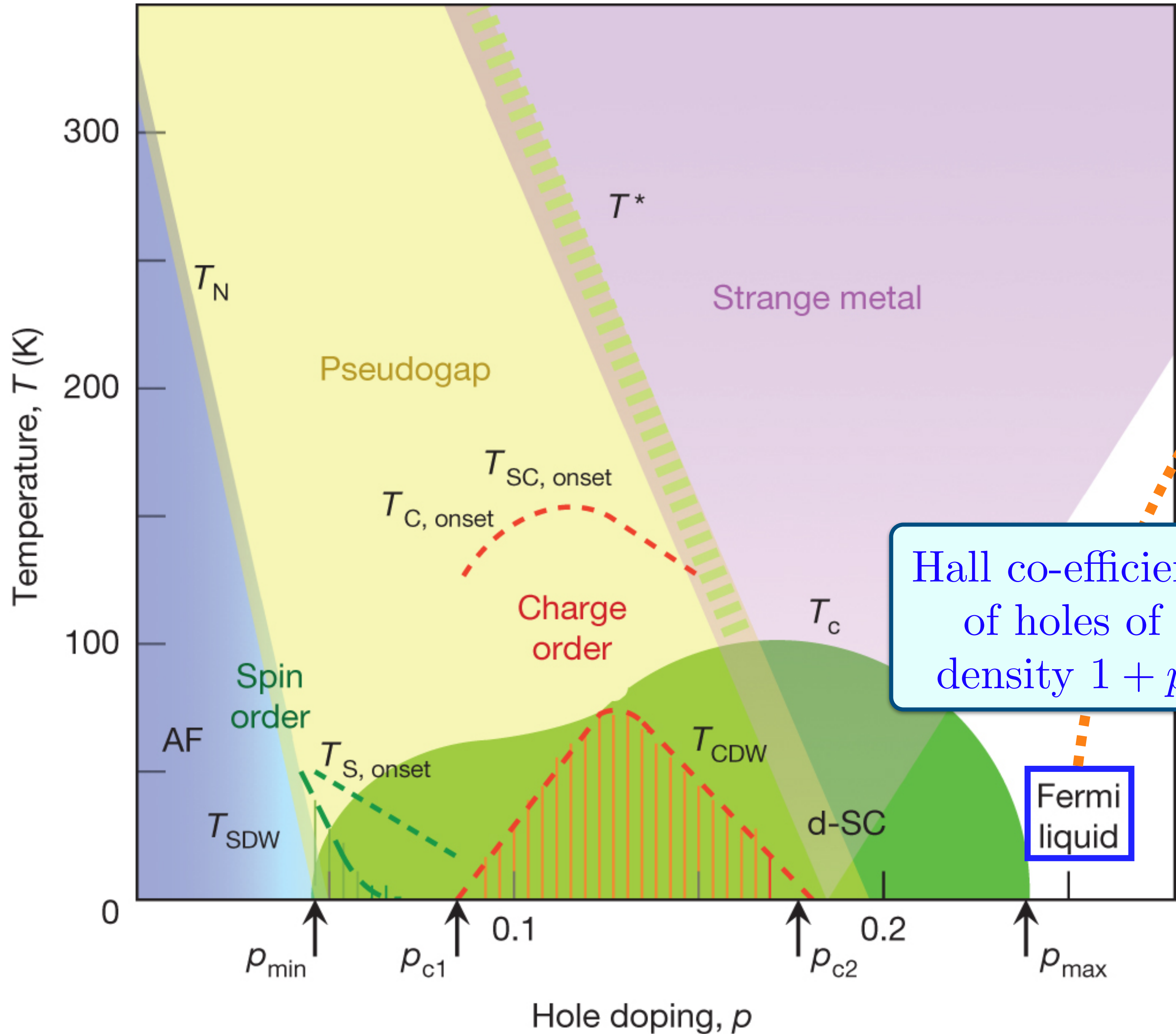
$\text{La}_{2-x}\text{Sr}_x\text{CuO}_4$
(LSCO)





$1-p$ electrons $1+p$ holes

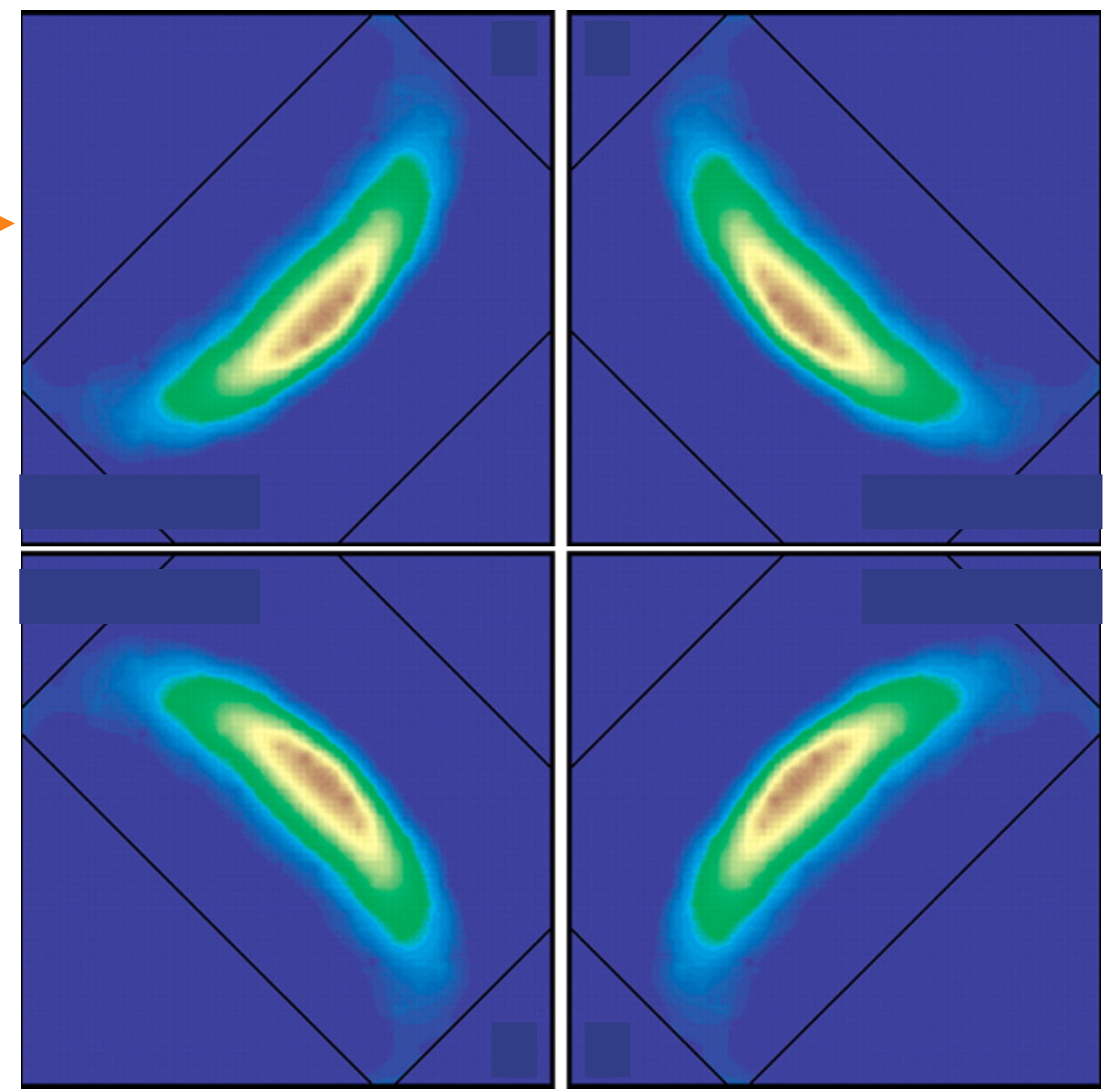
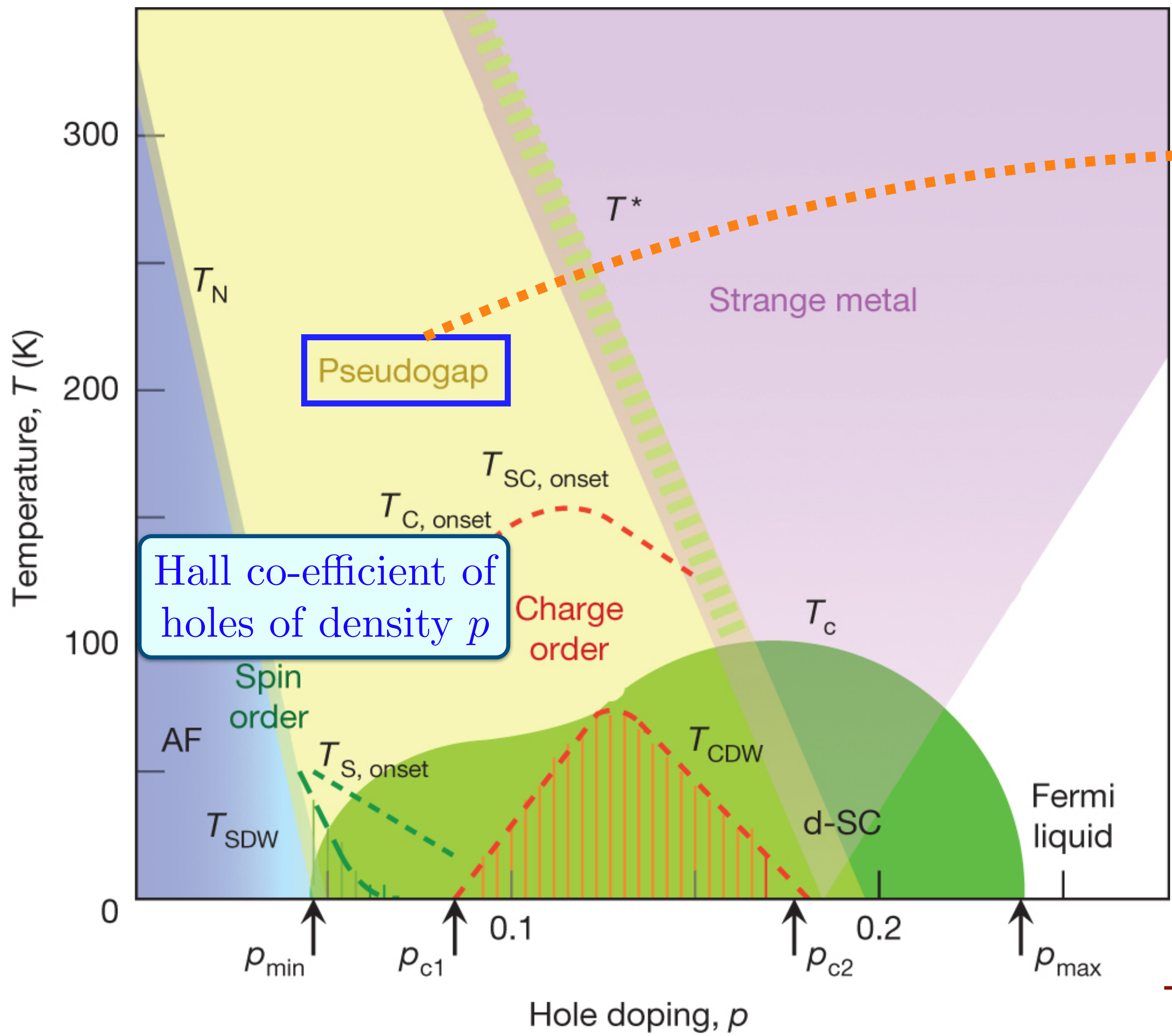
Luttinger, 1960: Area enclosed by the Fermi surface is the same as that for free fermions *with the same symmetry*.



Luttinger, 1960: Area enclosed by the Fermi surface is the same as that for free fermions *with the same symmetry*.
Oshikawa, 2000: Area constrained by a 't Hooft anomaly of global U(1) and translations

Keimer, Kivelson, Norman, Uchida, and Zaanen, *Nature* **518**, 179 (2015)

Kyle M. Shen *et al.*, *Science* **307**, 901 (2005)



‘Fermi arcs’ ?

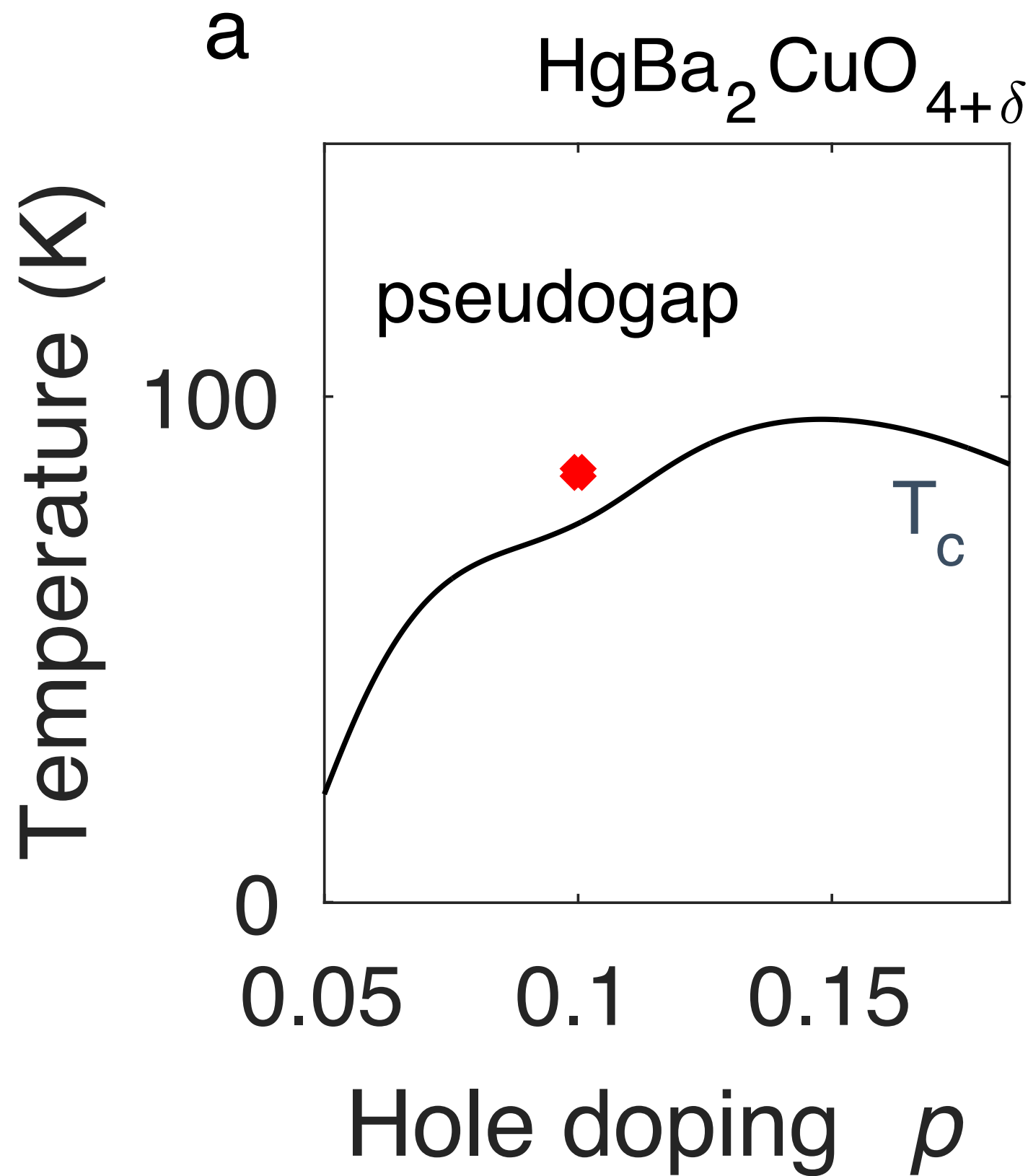
T. Senthil, S. S., M.Vojta, *PRL* **90**, 216403 (2003)

Observation of the Yamaji effect in a cuprate superconductor

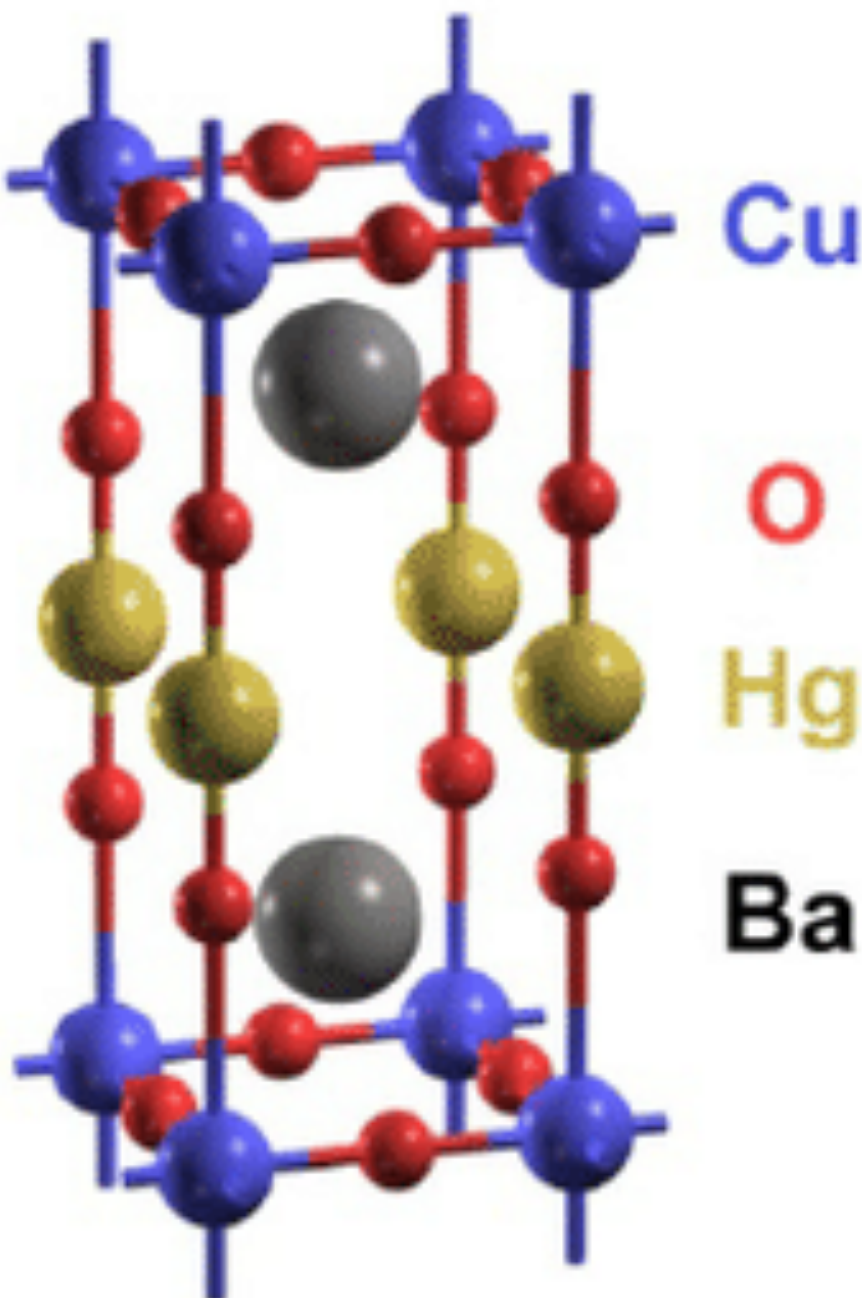
Mun K. Chan¹, Katherine A. Schreiber¹, Oscar E. Ayala-Valenzuela¹,
Eric D. Bauer², Arkady Shekhter¹ & Neil Harrison¹

nature physics
arXiv:2411.10631

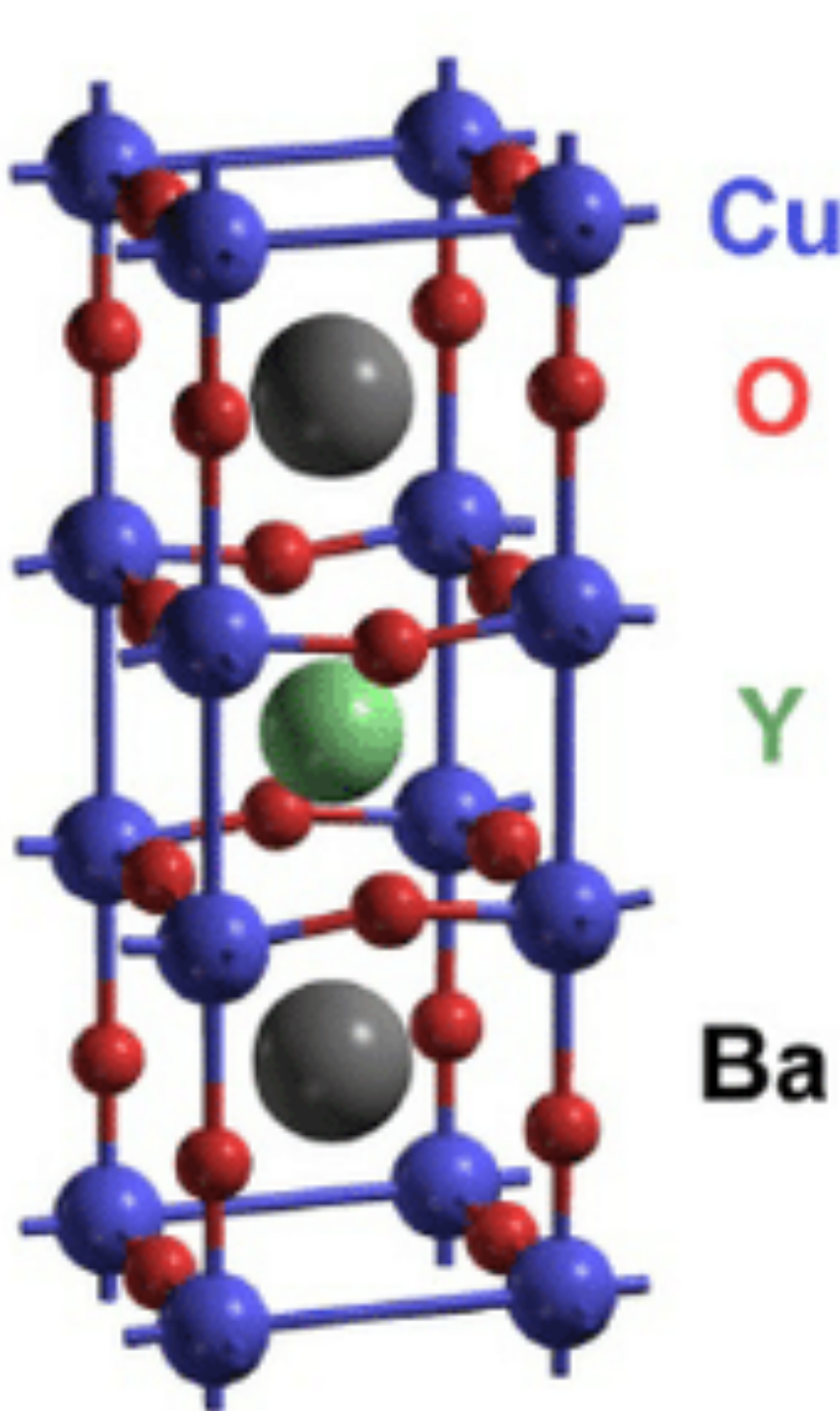
Published online: 16 September 2025



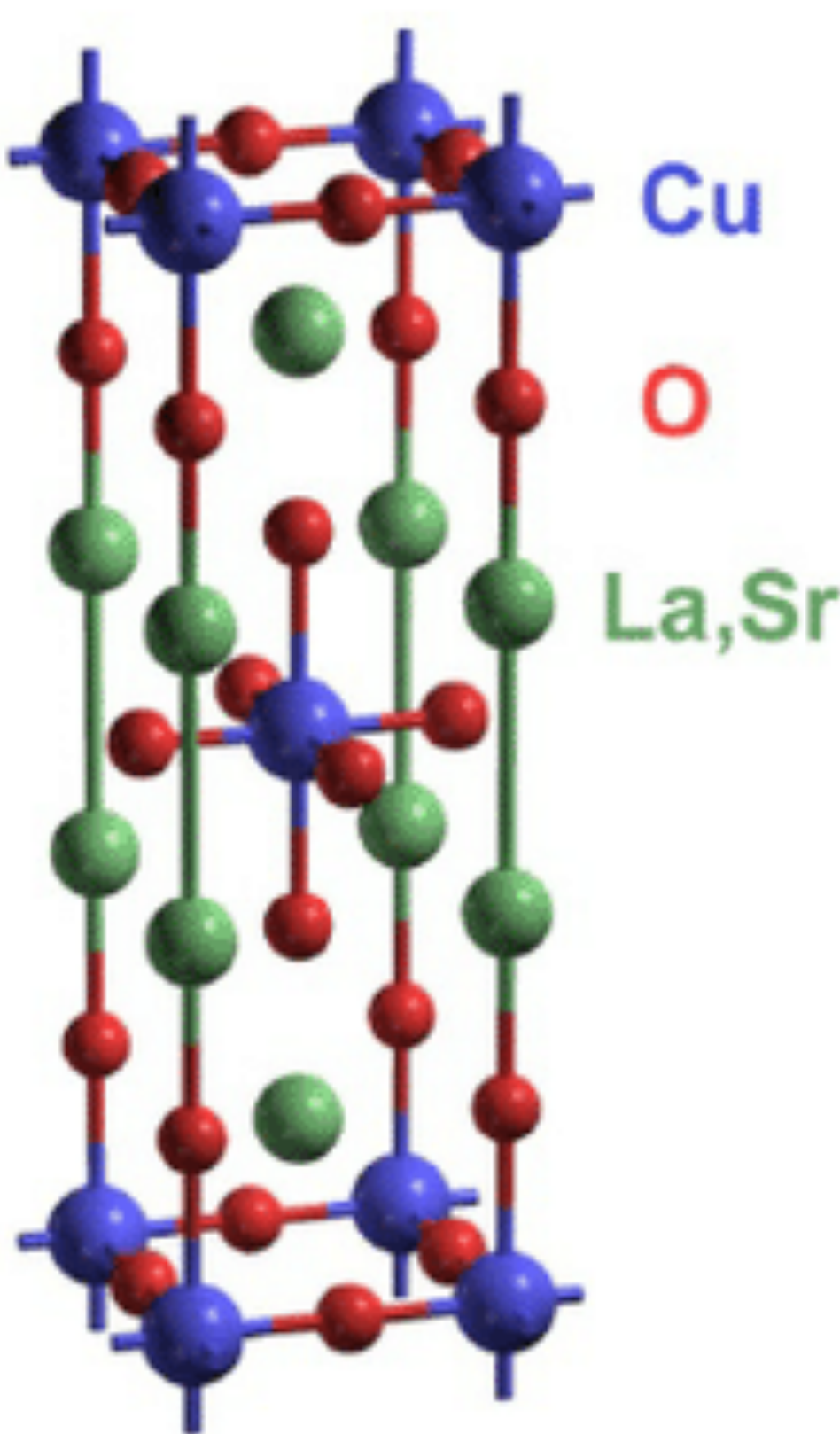
$\text{HgBa}_2\text{CuO}_{4+\delta}$
(Hg1201)



$\text{YBa}_2\text{Cu}_3\text{O}_{7-\delta}$
(YBCO)



$\text{La}_{2-x}\text{Sr}_x\text{CuO}_4$
(LSCO)



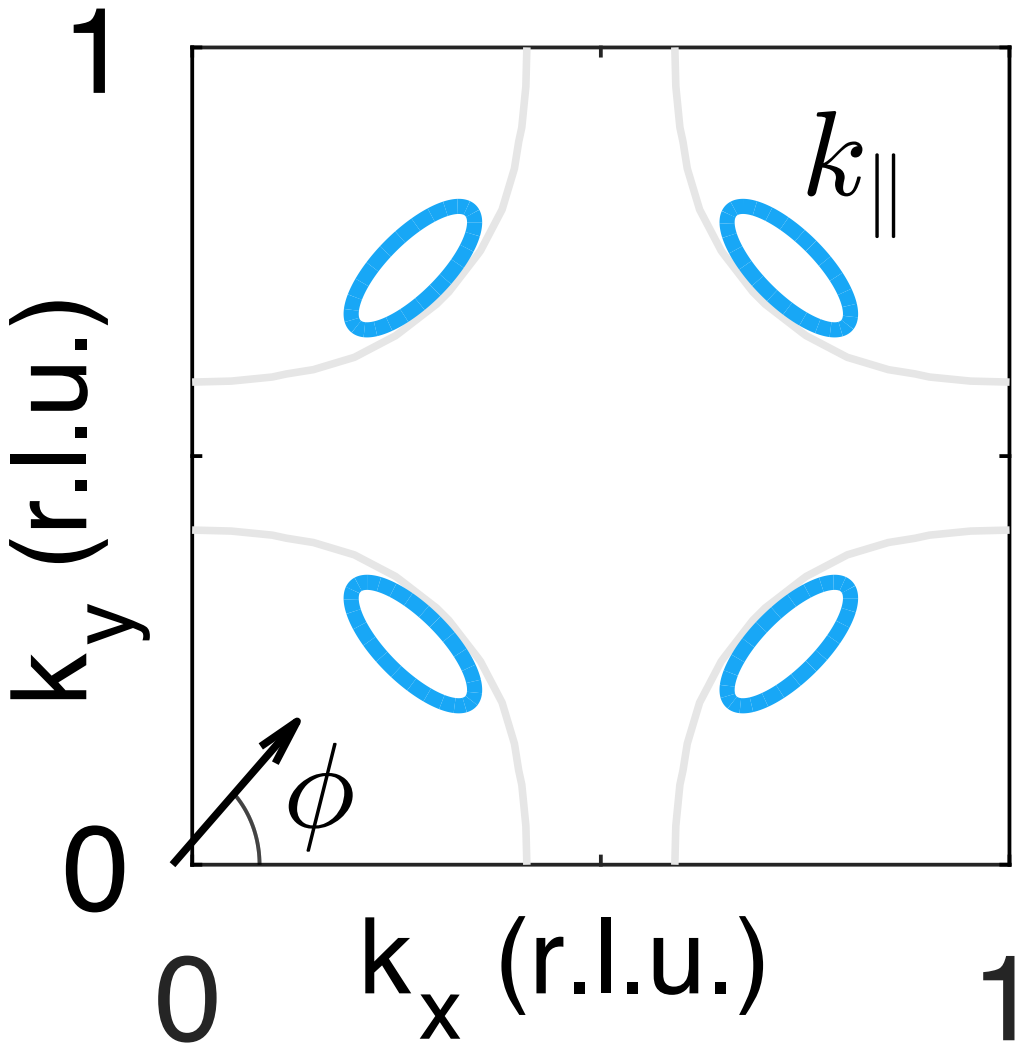
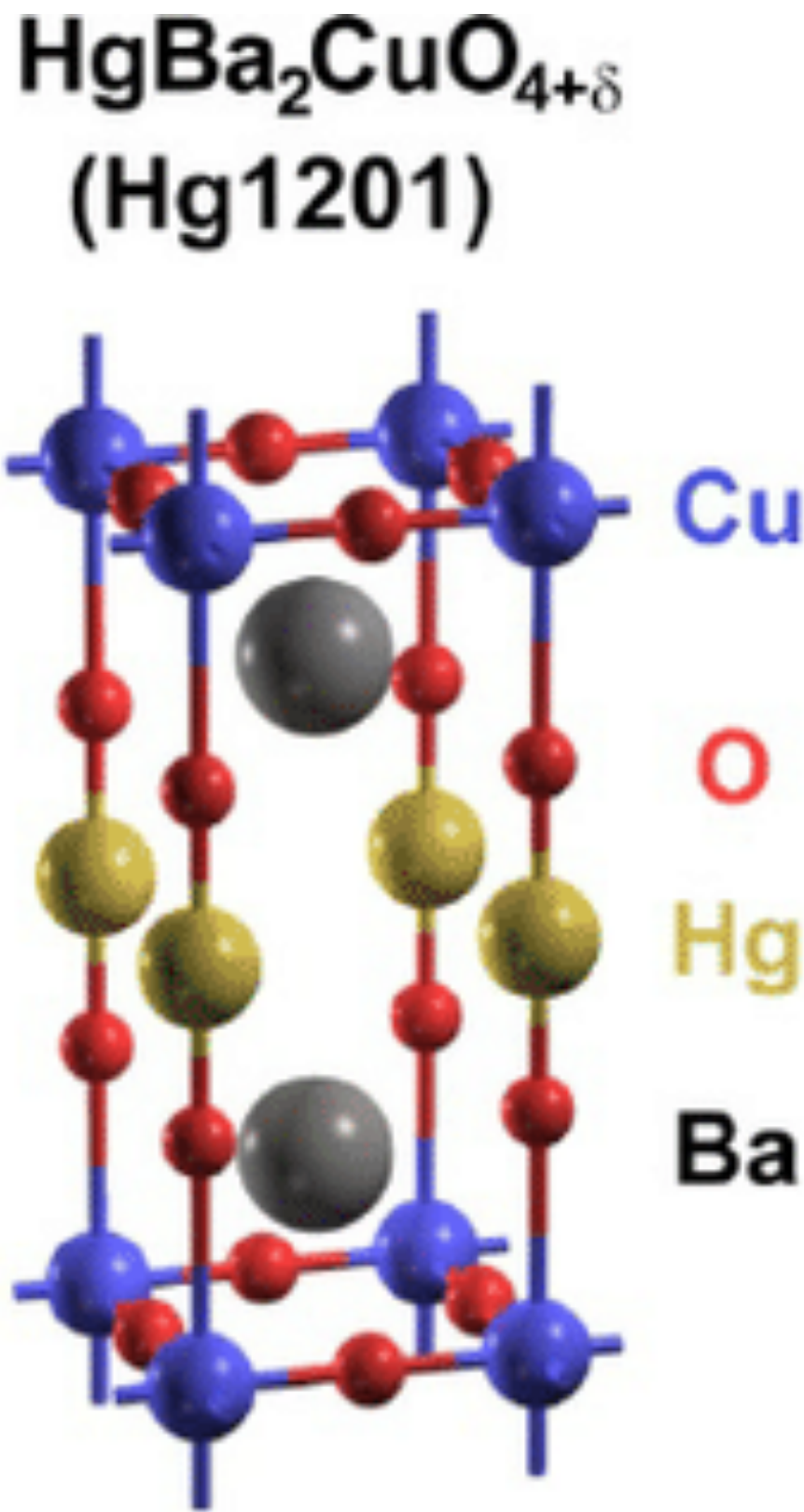
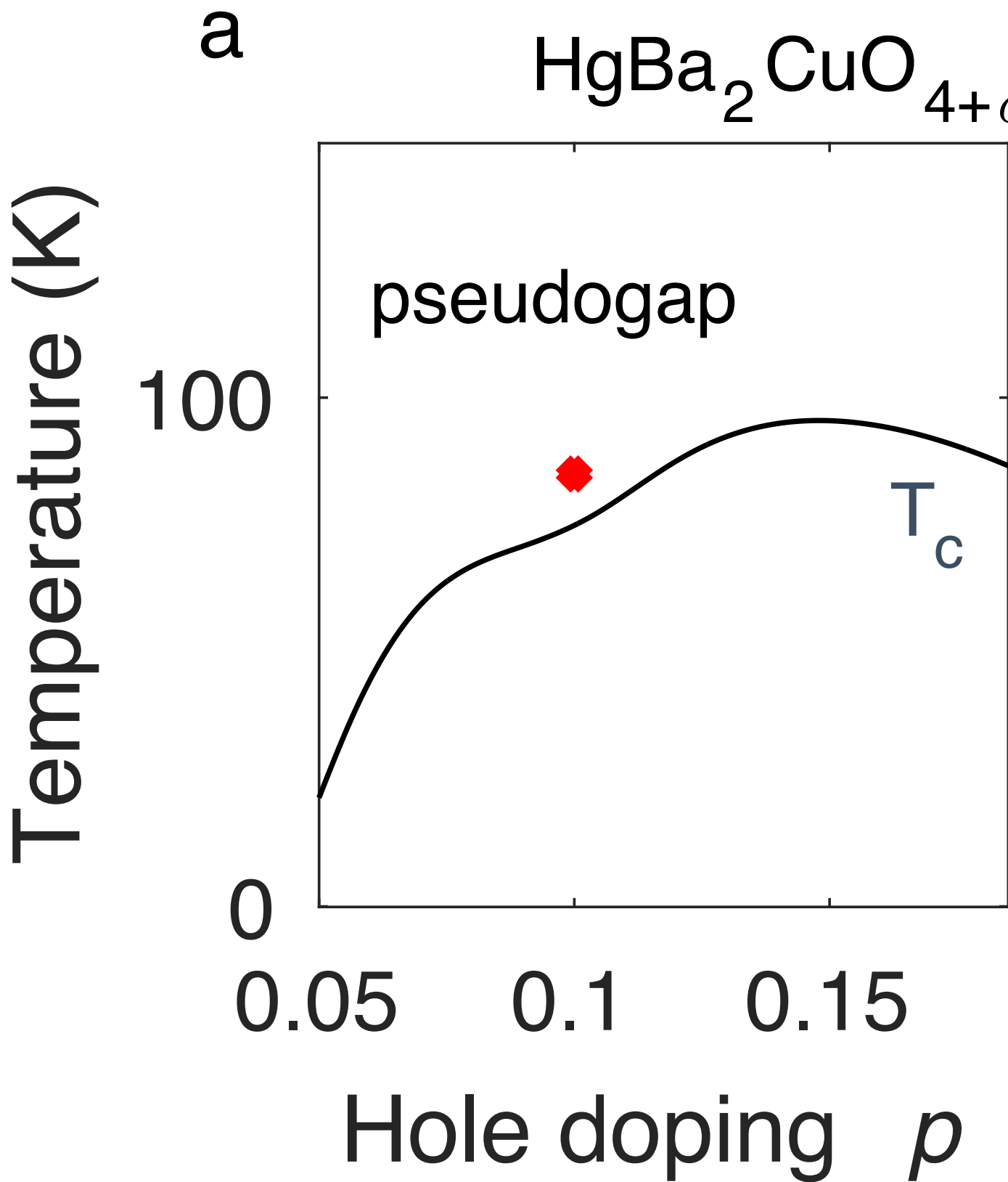
Observation of the Yamaji effect in a cuprate superconductor

nature physics

arXiv:2411.10631

Mun K. Chan¹, Katherine A. Schreiber¹, Oscar E. Ayala-Valenzuela¹,
Eric D. Bauer², Arkady Shekhter¹ & Neil Harrison¹

Published online: 16 September 2025



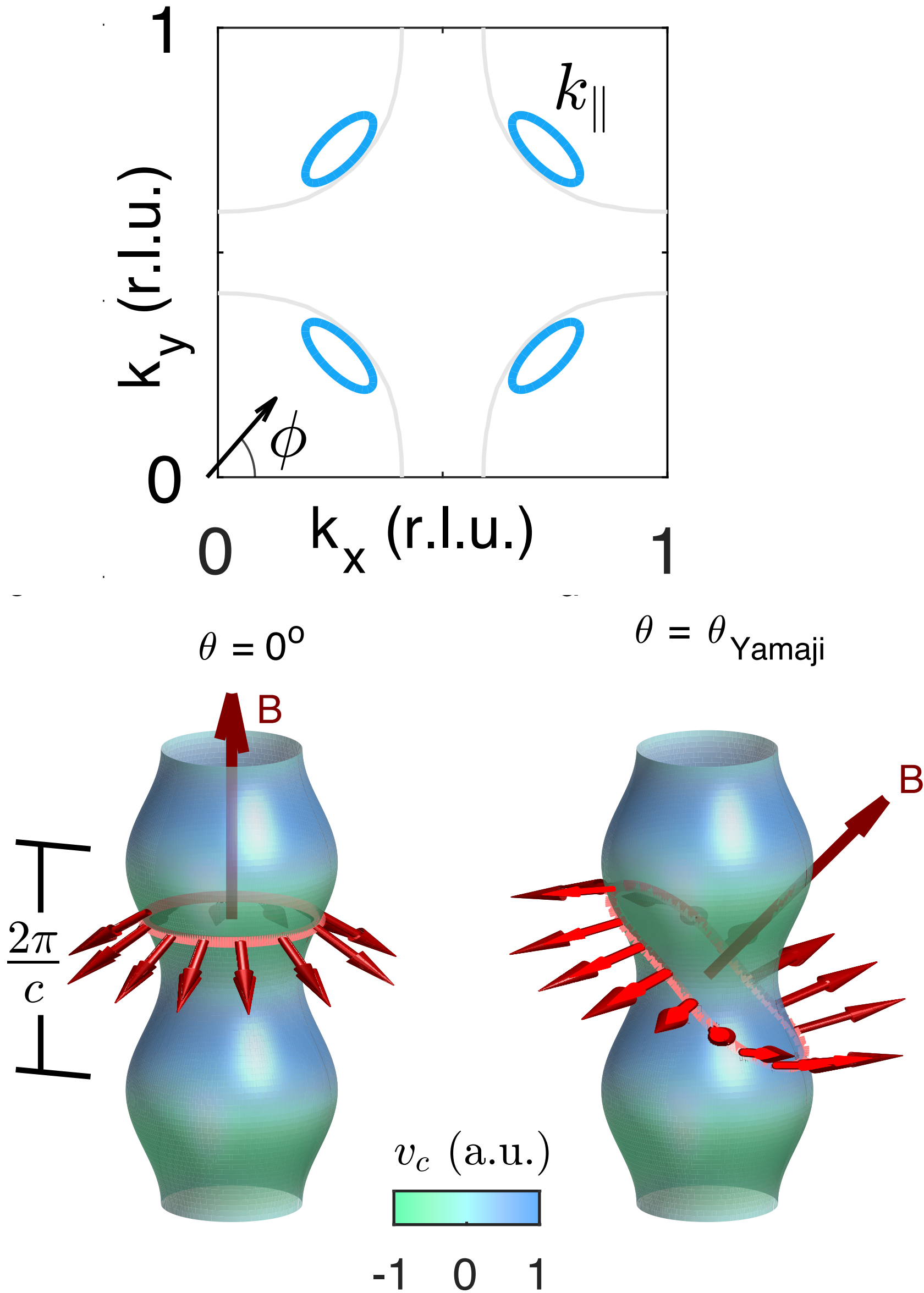
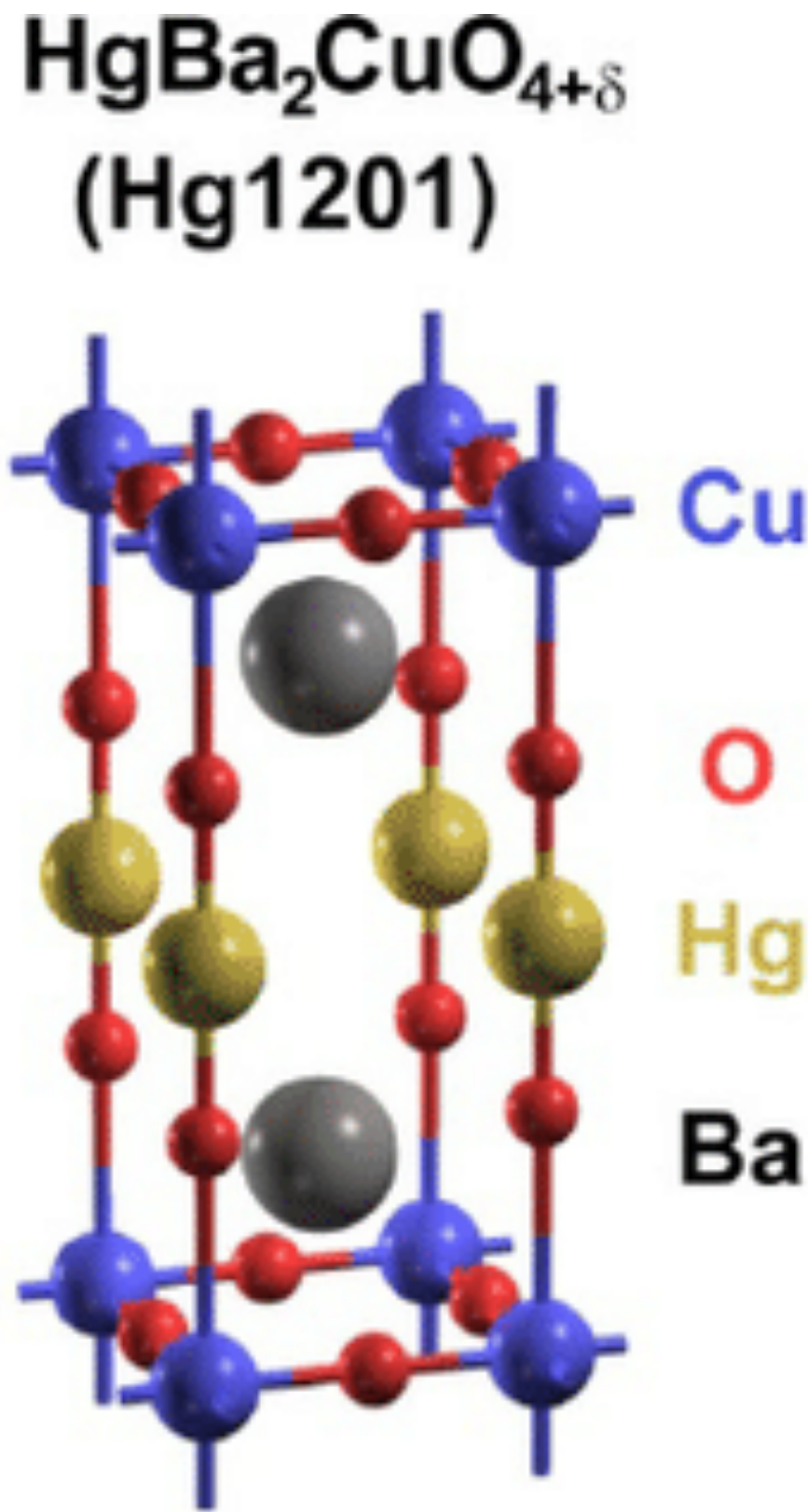
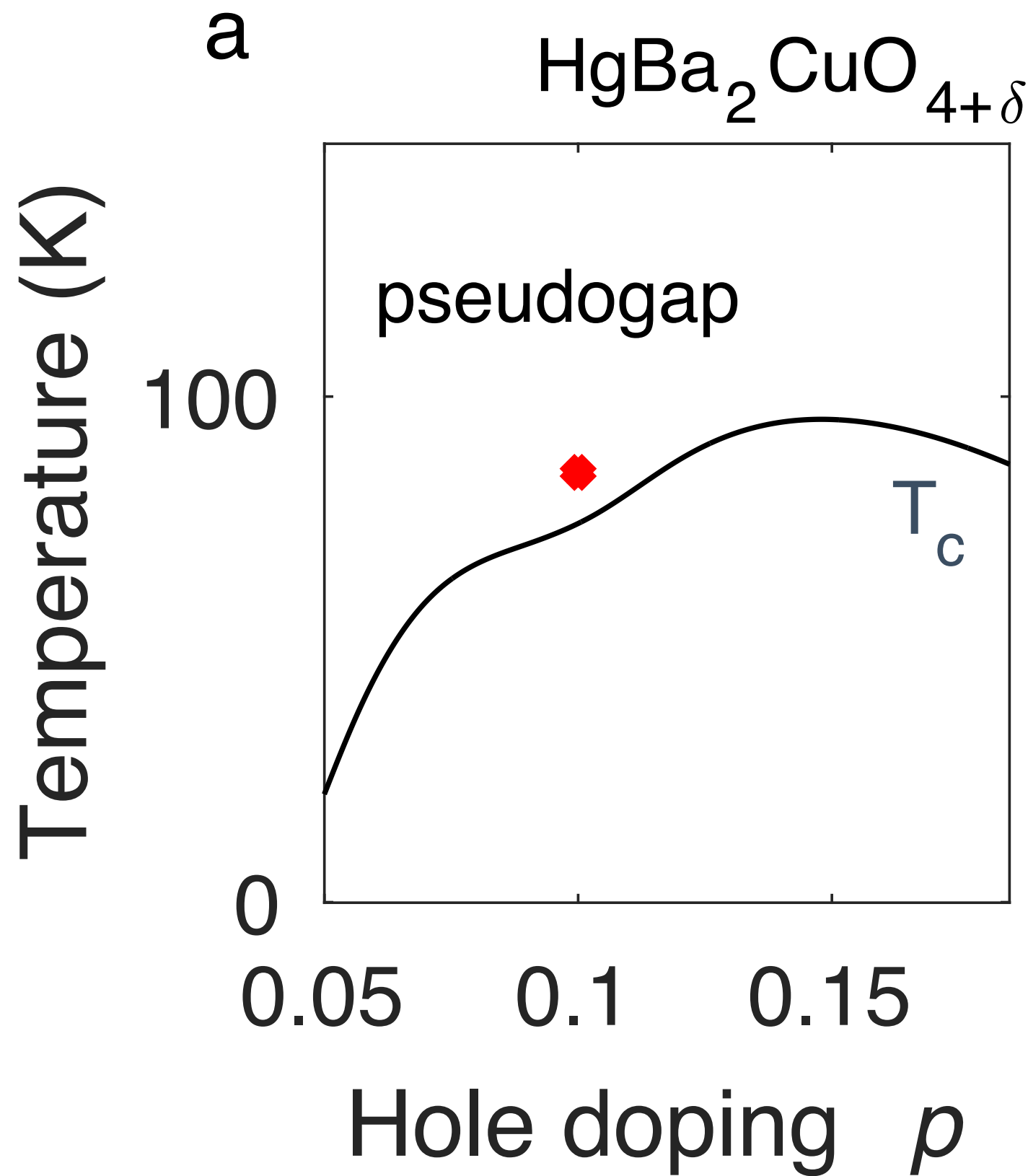
Observation of the Yamaji effect in a cuprate superconductor

nature physics

arXiv:2411.10631

Mun K. Chan¹✉, Katherine A. Schreiber¹, Oscar E. Ayala-Valenzuela¹,
Eric D. Bauer², Arkady Shekhter¹ & Neil Harrison¹

Published online: 16 September 2025



At the Yamaji angle, the orbits in the plane orthogonal to \mathbf{B} have an area which is independent of momentum in the c direction, to first order in the hopping along the c direction.

K.Yamaji JPSJ **58**, 1520 (1989)

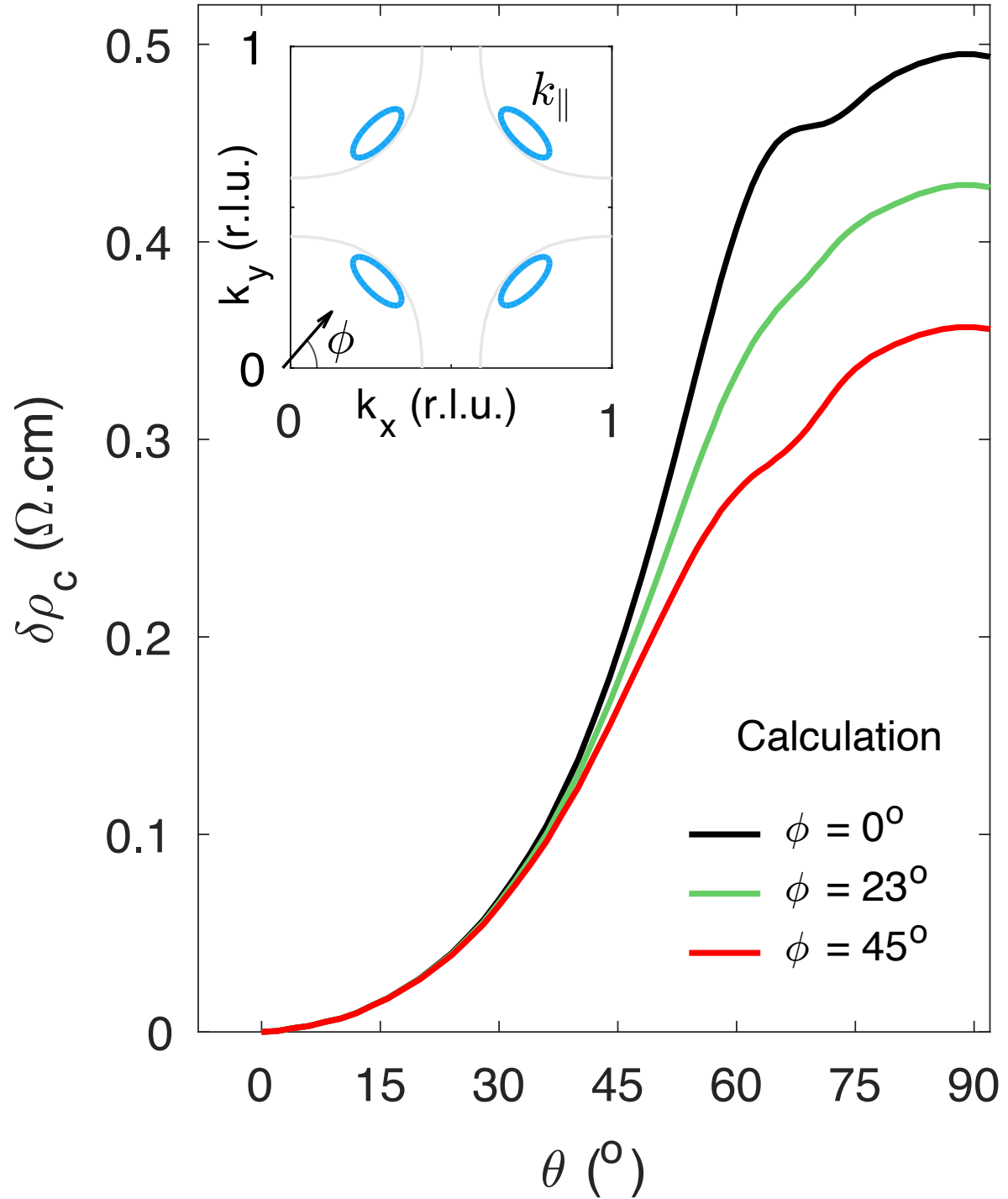
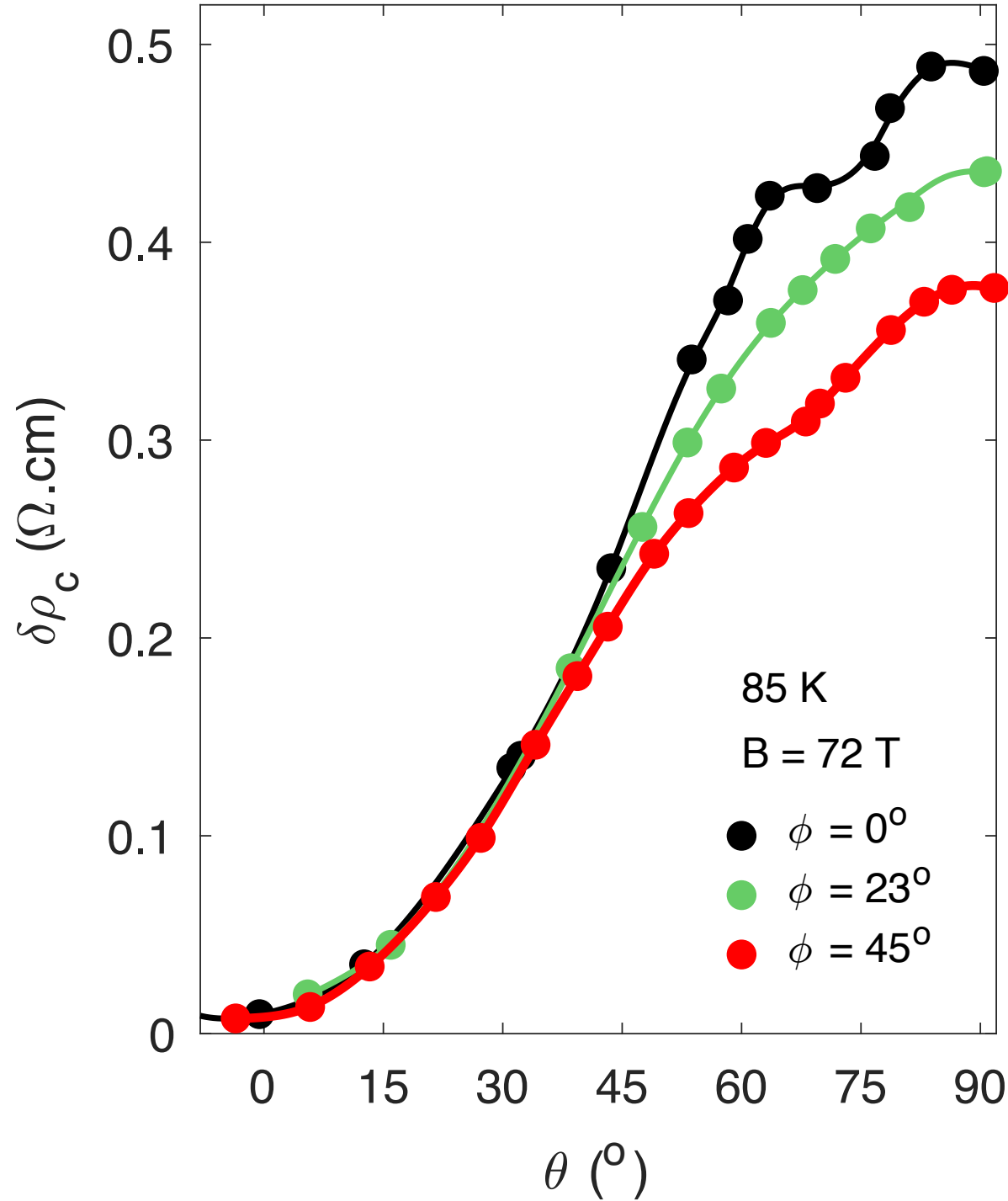
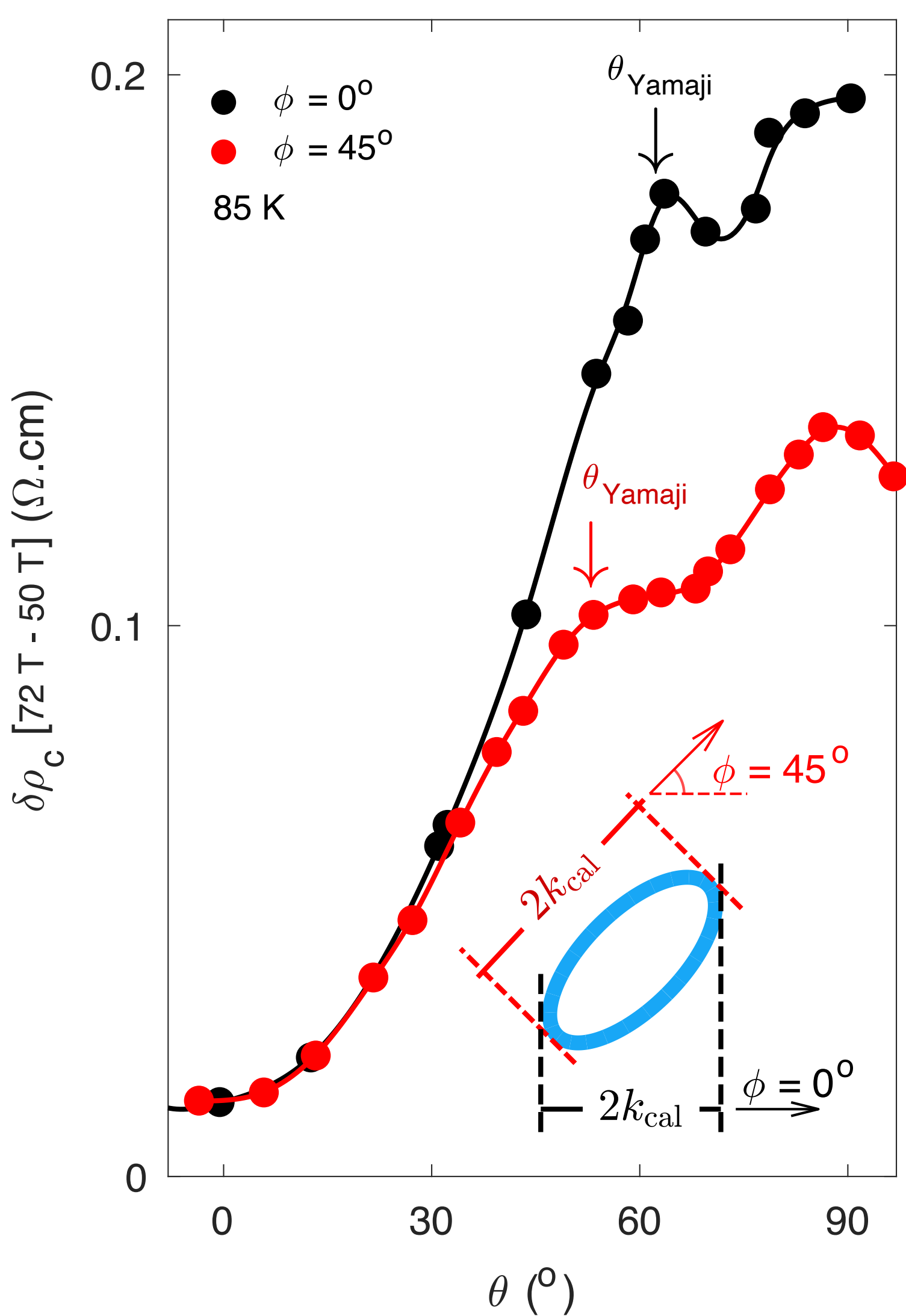
Observation of the Yamaji effect in a cuprate superconductor

nature physics

arXiv:2411.10631

Mun K. Chan¹, Katherine A. Schreiber¹, Oscar E. Ayala-Valenzuela¹,
Eric D. Bauer², Arkady Shekhter¹ & Neil Harrison¹

Published online: 16 September 2025

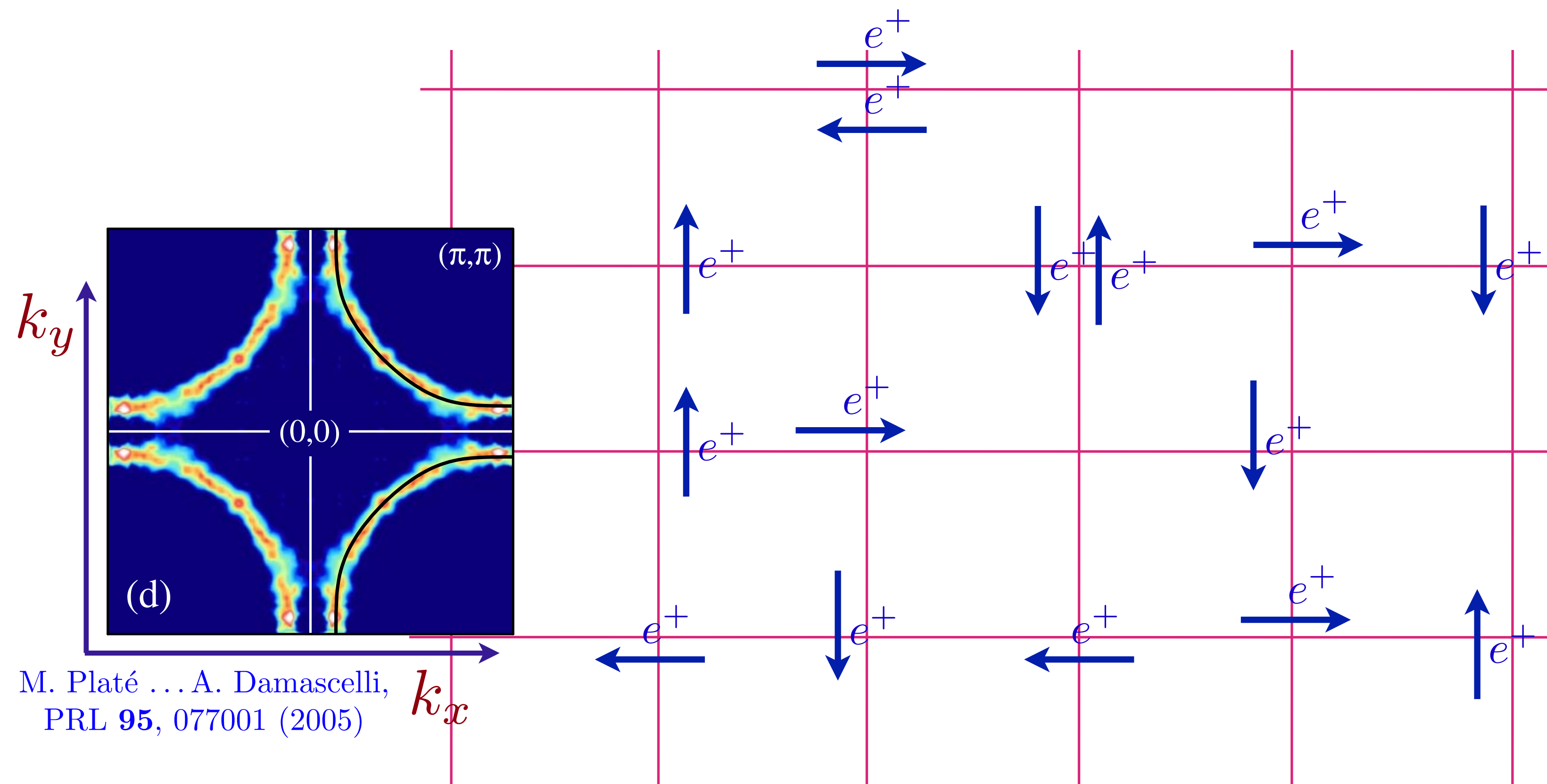


Doping
 $p = 0.1$

“The small size of the pockets determined from the Yamaji effect is ... approximately 1.3% of the Brillouin zone area”

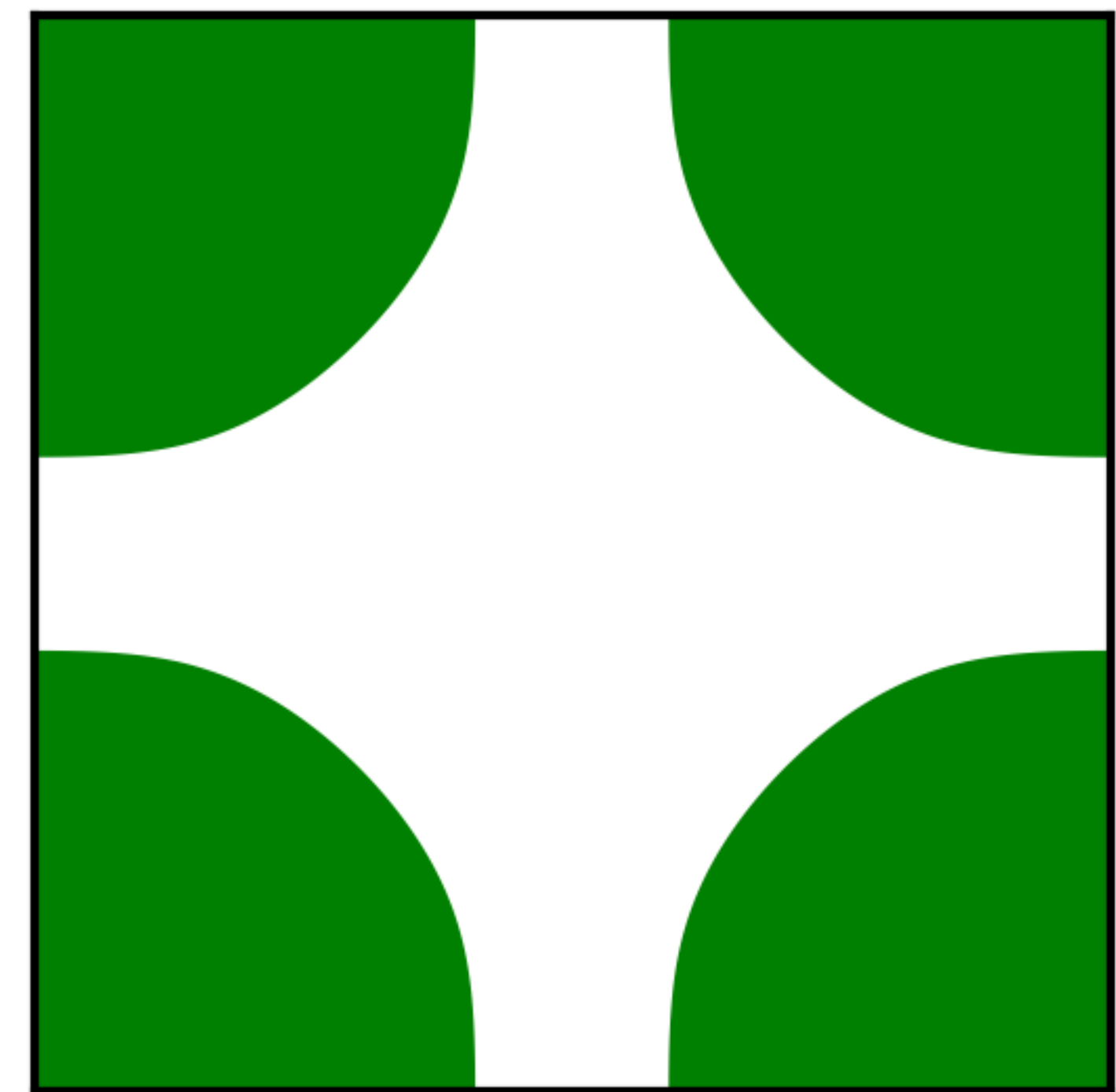
**Metals obtained by
doping Mott insulators**

Ordinary metal



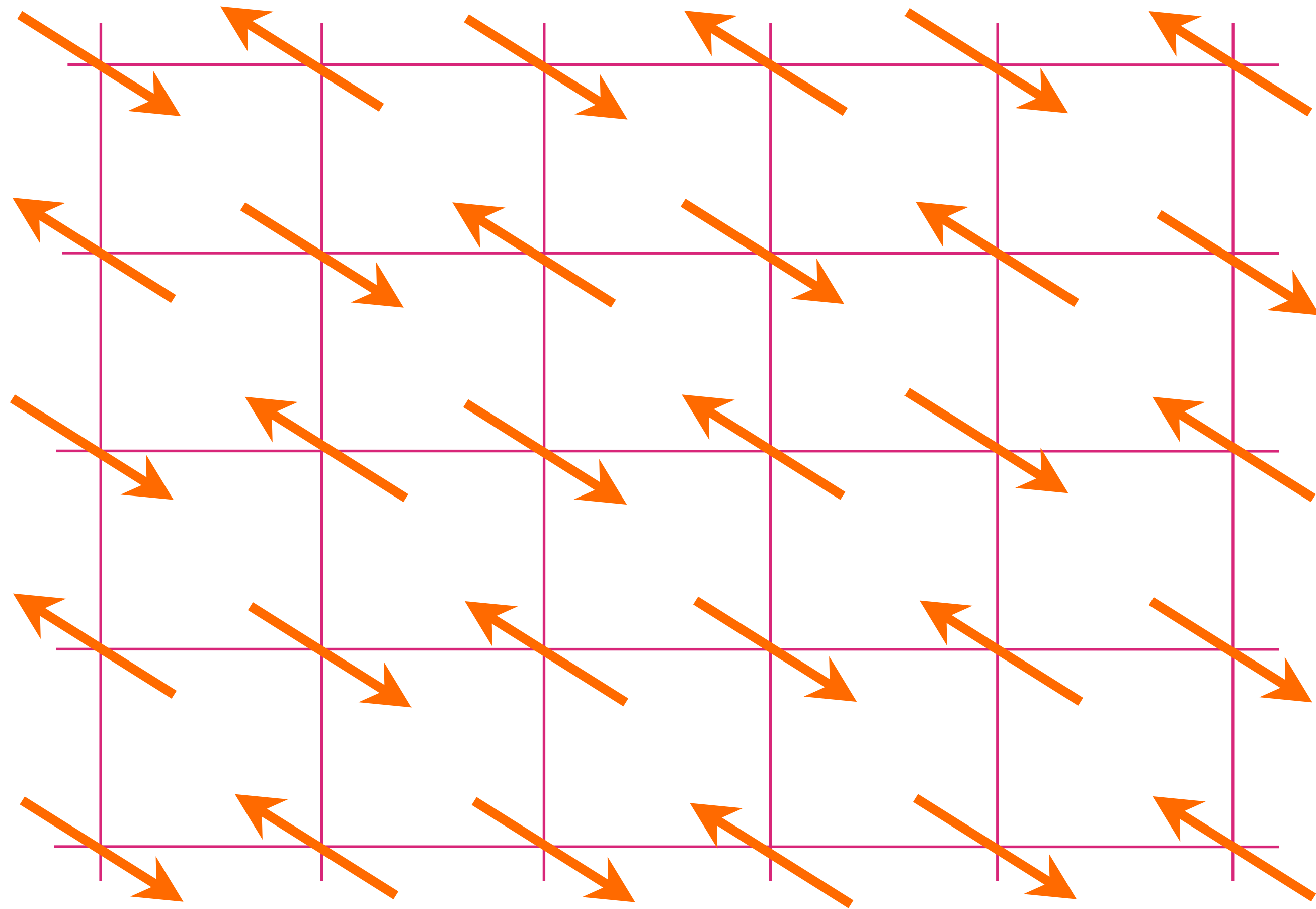
At large p , we obtain a gas of nearly free fermionic holes of density $1+p$ (relative to the filled band with 2 electrons per site)

Luttinger area.
No broken symmetry



Area $(1 + p)/2$

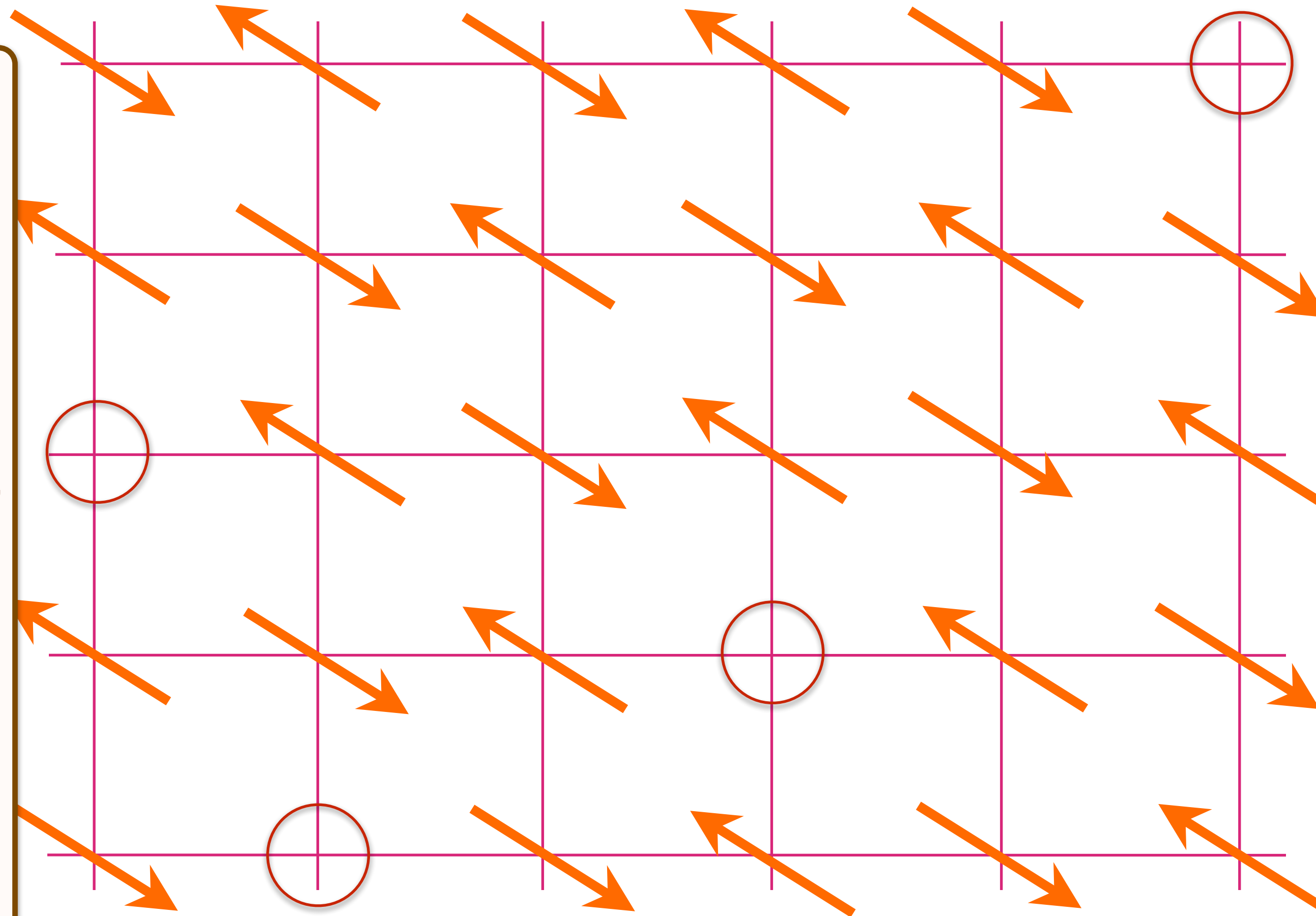
Insulating antiferromagnet



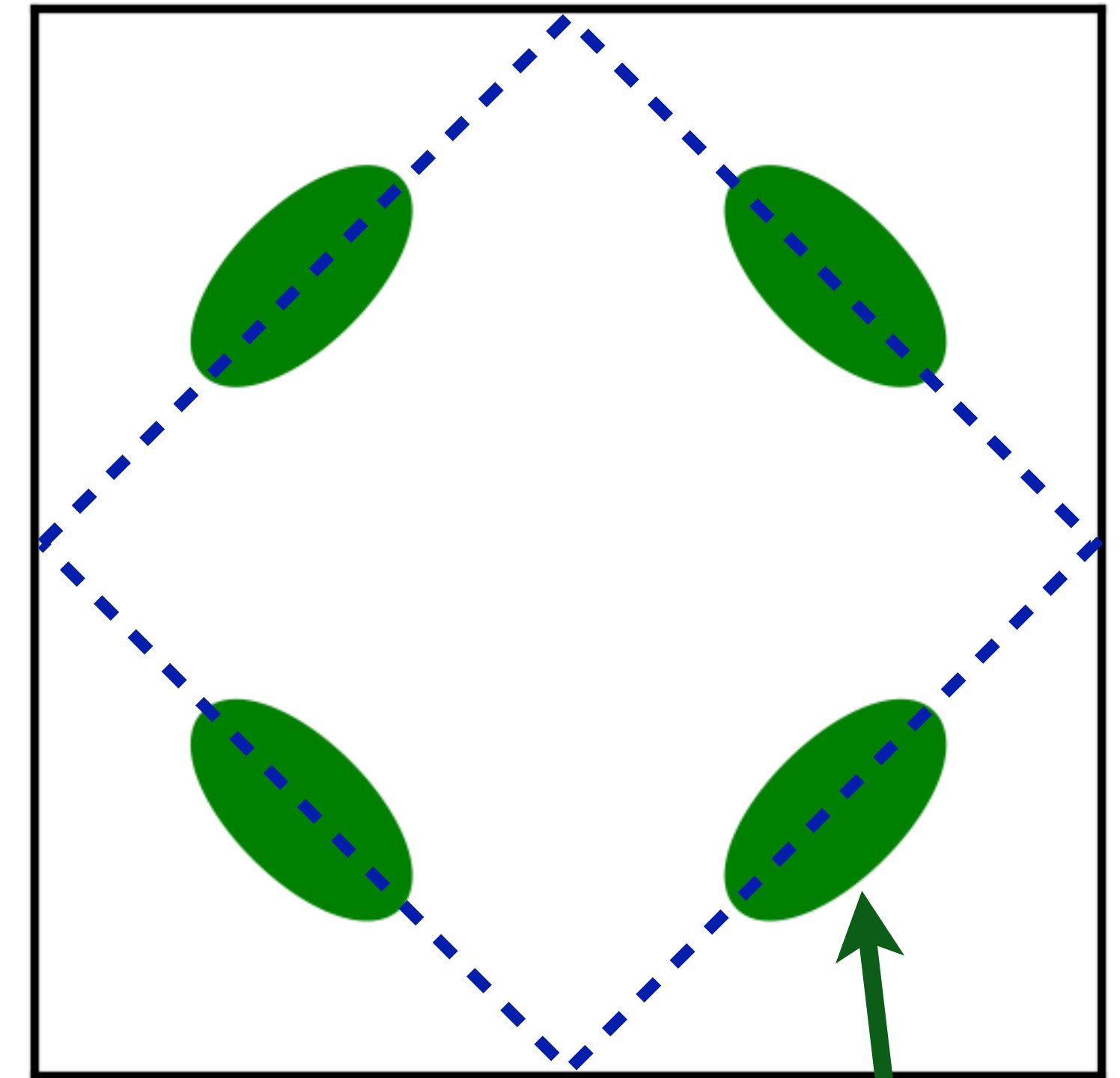
Doping an insulating antiferromagnet with holes of density p

AF metal

Fermi liquid
with density
 p of spin
 $1/2$, charge
 $+e$ holes.
Yamaji effect
requires
inter-layer
spin
correlations
(not present
in Hg-1201).



Luttinger area.
Broken symmetry



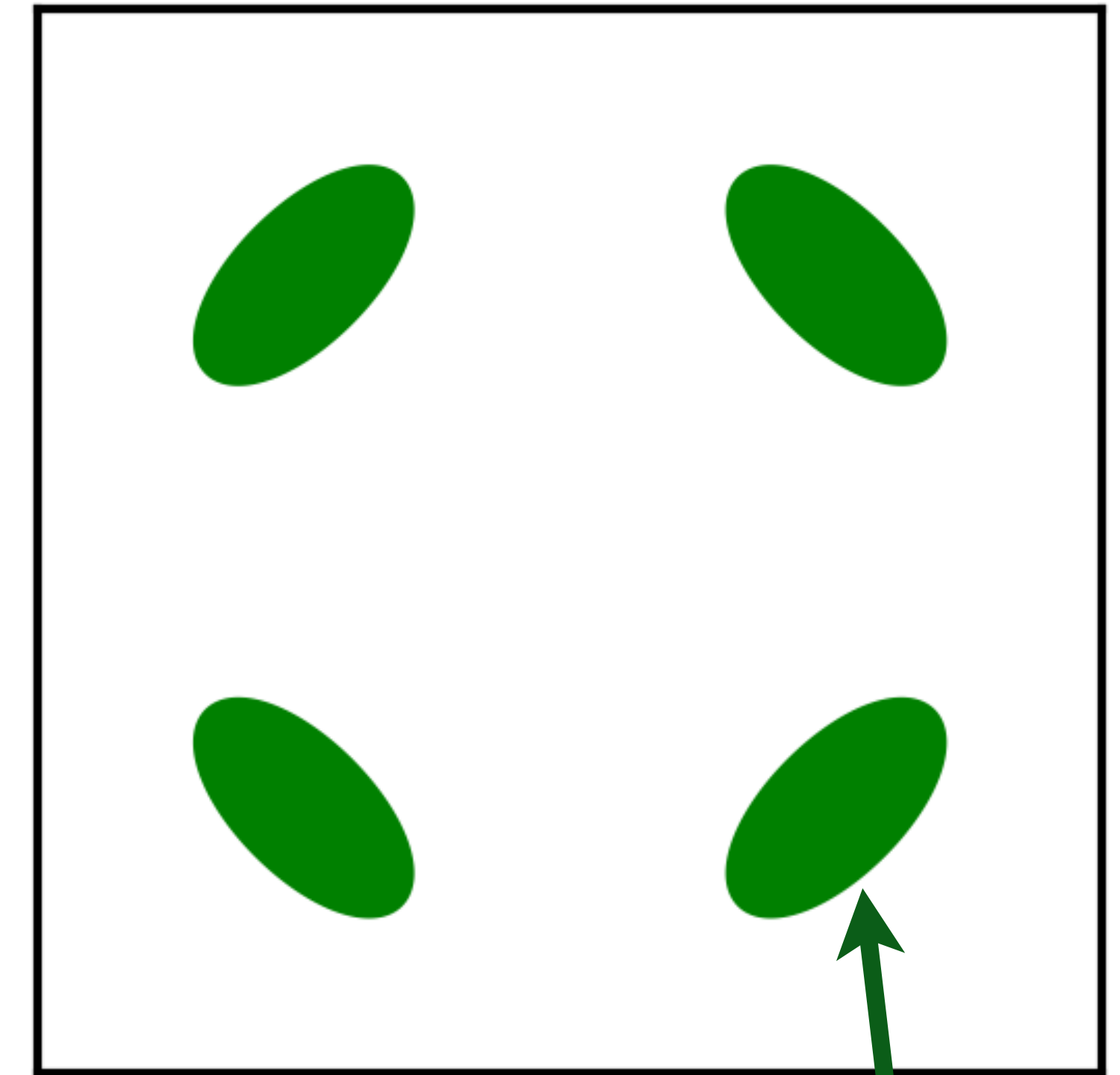
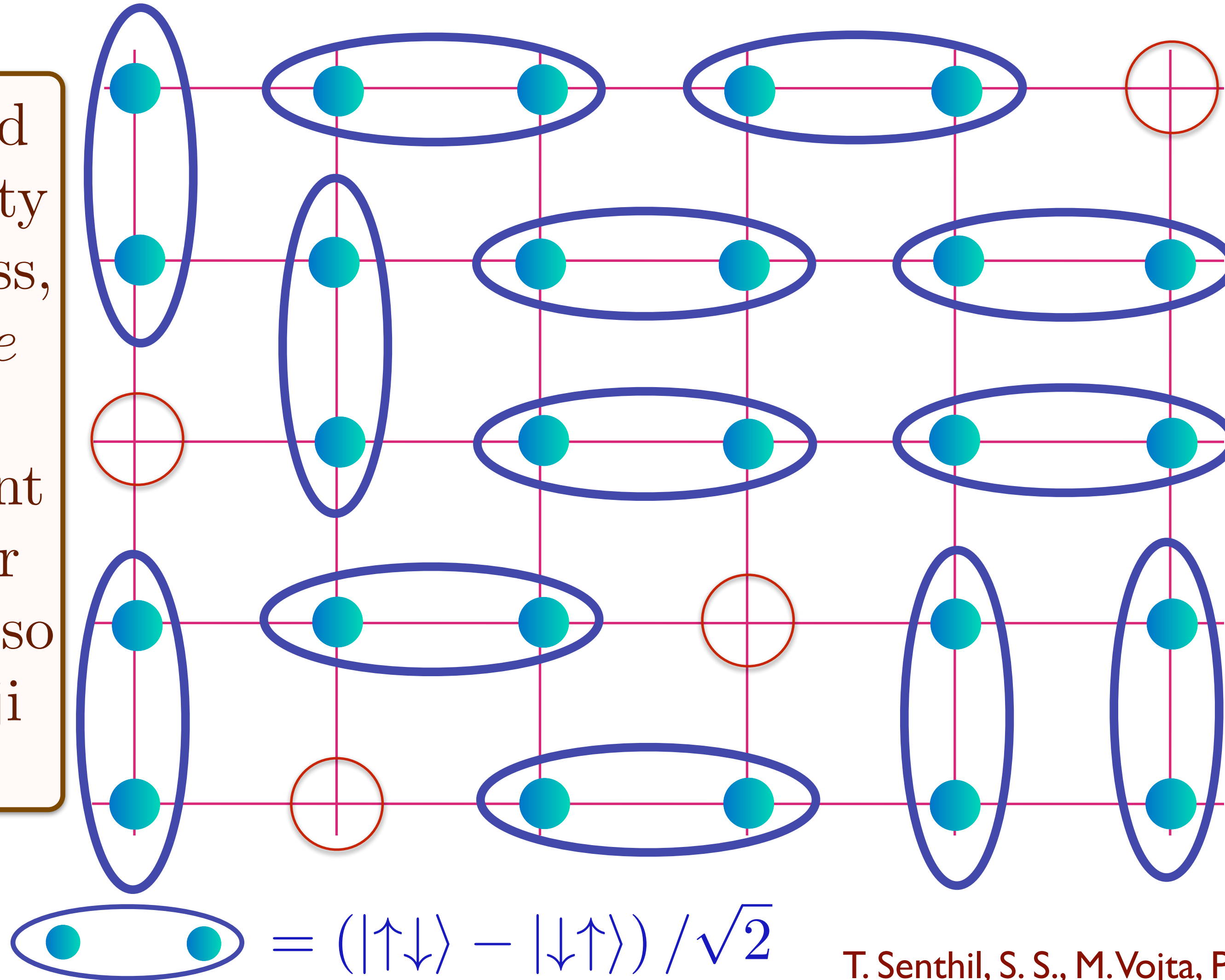
Area $p/4$

Doping an insulating antiferromagnet with holes of density p

Holon metal

Oshikawa anomaly is satisfied by sum of spin liquid (1) and Fermi surface anomalies (p)

Spin liquid with density p of spinless, charge $+e$ 'holons'. No coherent inter-layer transport, so no Yamaji effect.



Area $p/4$

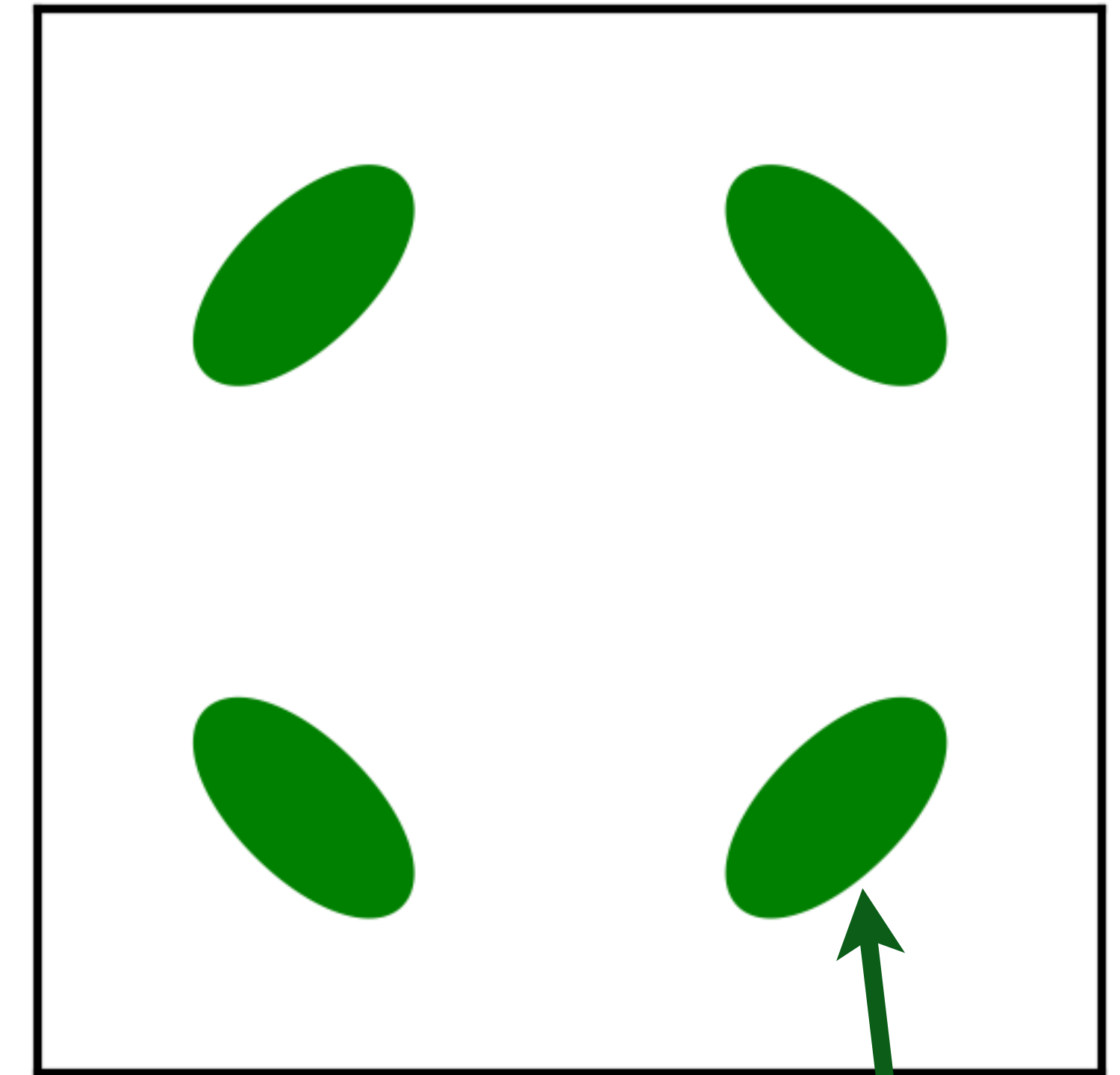
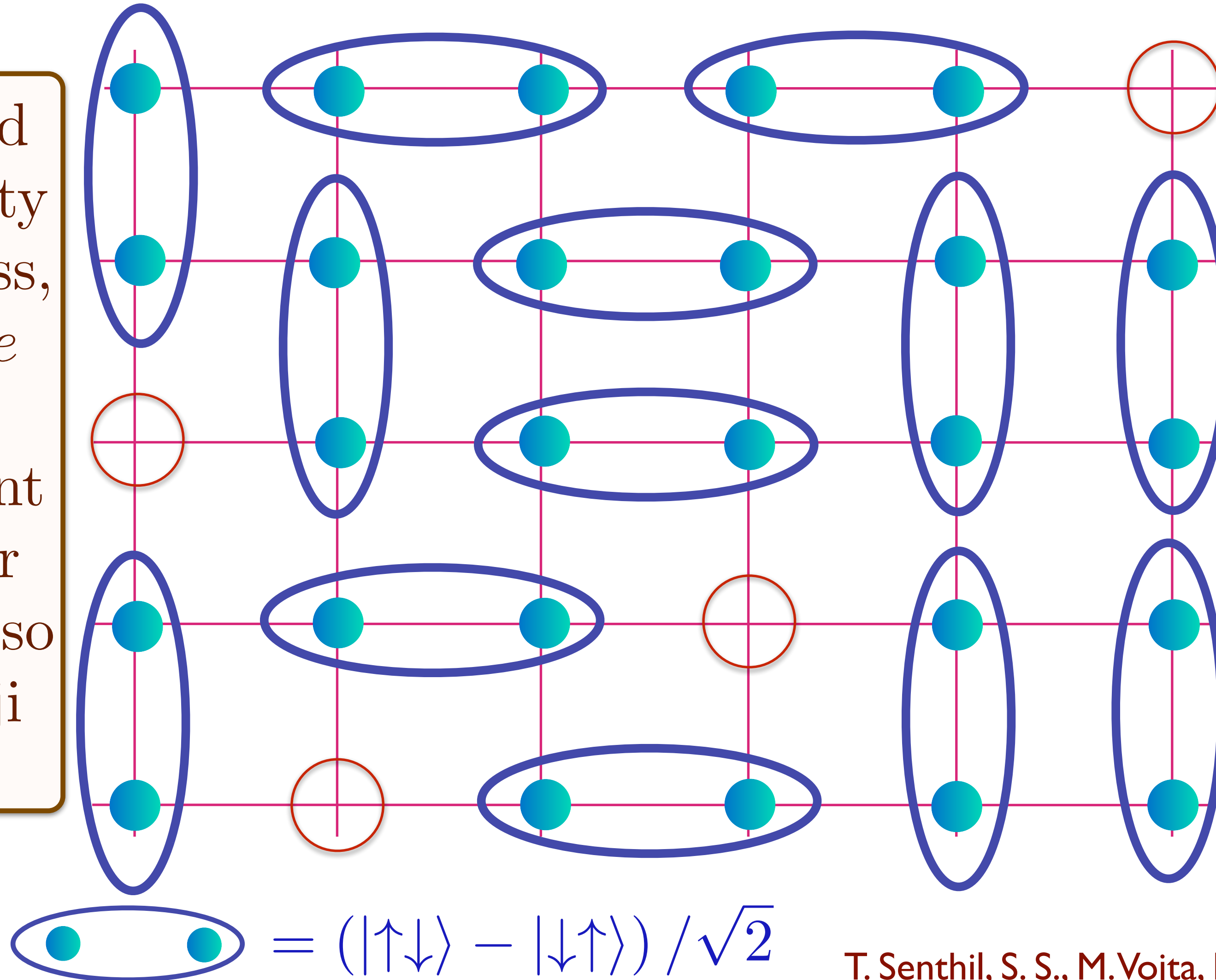
T. Senthil, S. S., M. Vojta, PRL **90**, 216403 (2003);
R. K. Kaul, A. Kolezhuk, M. Levin, S. S., T. Senthil, PRB **75**, 235122 (2007);
R. K. Kaul, Y. B. Kim, S. S., T. Senthil, Nature Physics **4**, 28 (2008)

Doping an insulating antiferromagnet with holes of density p

Holon metal

Oshikawa anomaly is satisfied by sum of spin liquid (1) and Fermi surface anomalies (p)

Spin liquid with density p of spinless, charge $+e$ 'holons'. No coherent inter-layer transport, so no Yamaji effect.



Area $p/4$

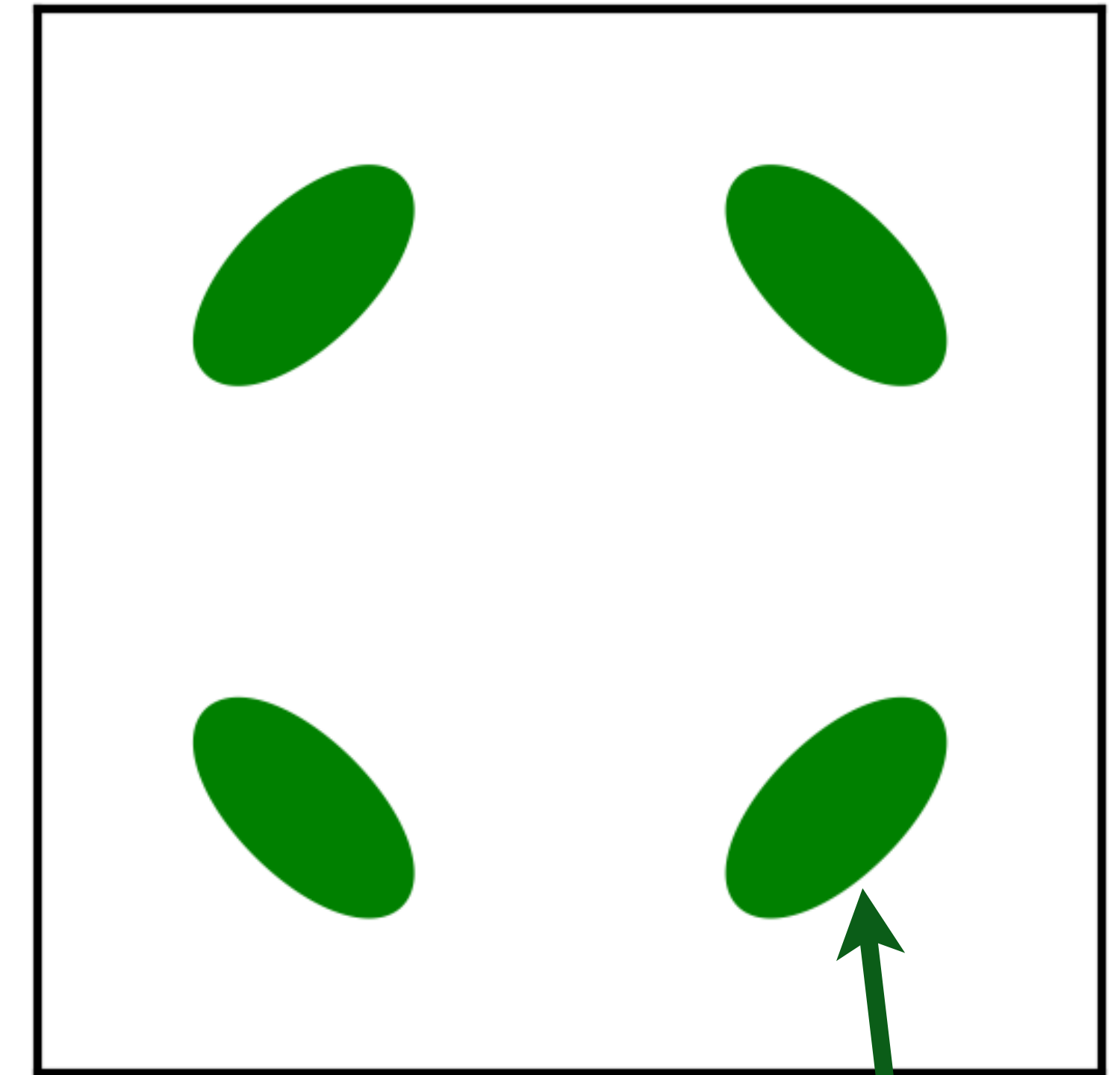
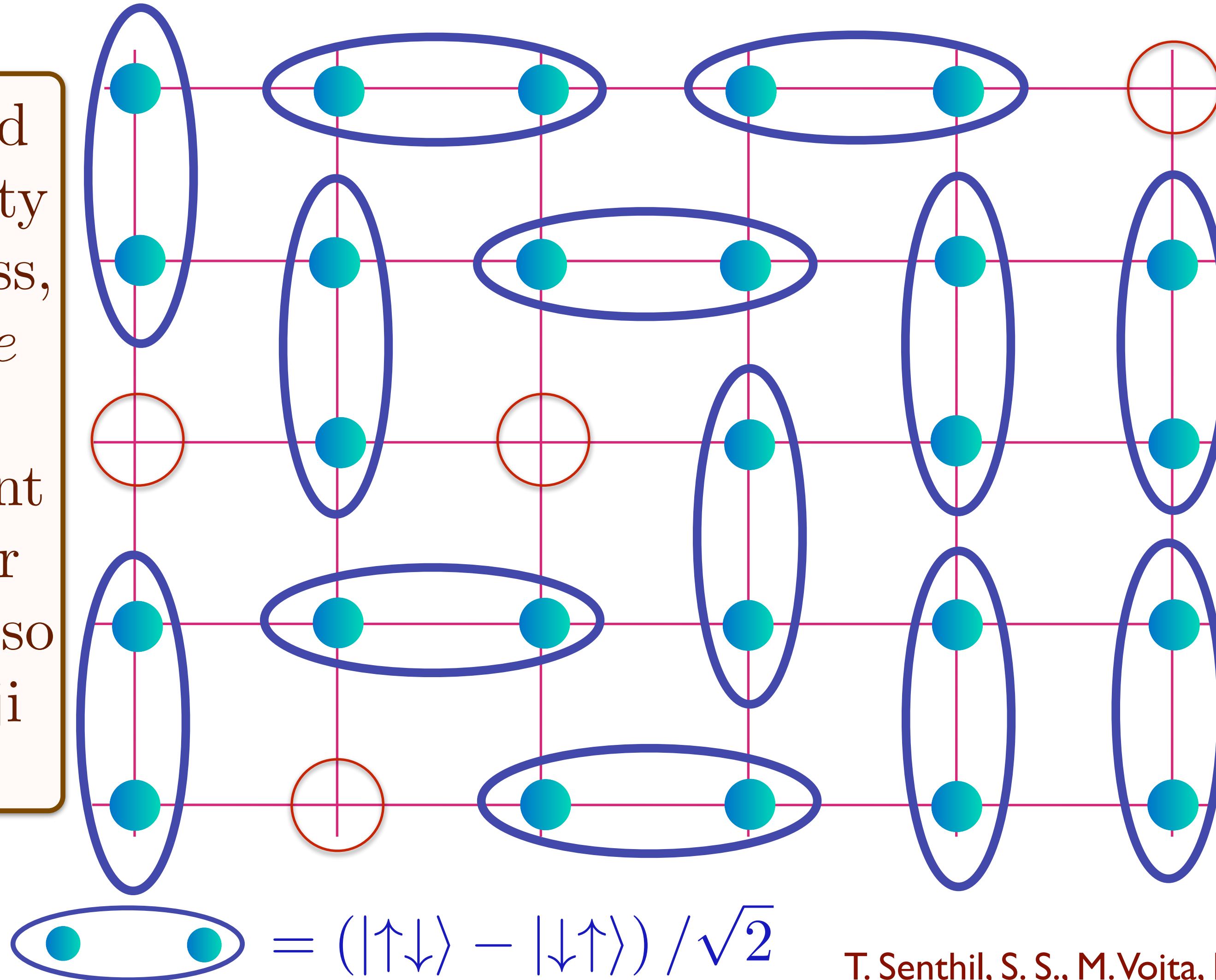
T. Senthil, S. S., M. Vojta, PRL **90**, 216403 (2003);
R. K. Kaul, A. Kolezhuk, M. Levin, S. S., T. Senthil, PRB **75**, 235122 (2007);
R. K. Kaul, Y. B. Kim, S. S., T. Senthil, Nature Physics **4**, 28 (2008)

Doping an insulating antiferromagnet with holes of density p

Holon metal

Oshikawa anomaly is satisfied by sum of spin liquid (1) and Fermi surface anomalies (p)

Spin liquid with density p of spinless, charge $+e$ 'holons'. No coherent inter-layer transport, so no Yamaji effect.



Area $p/4$

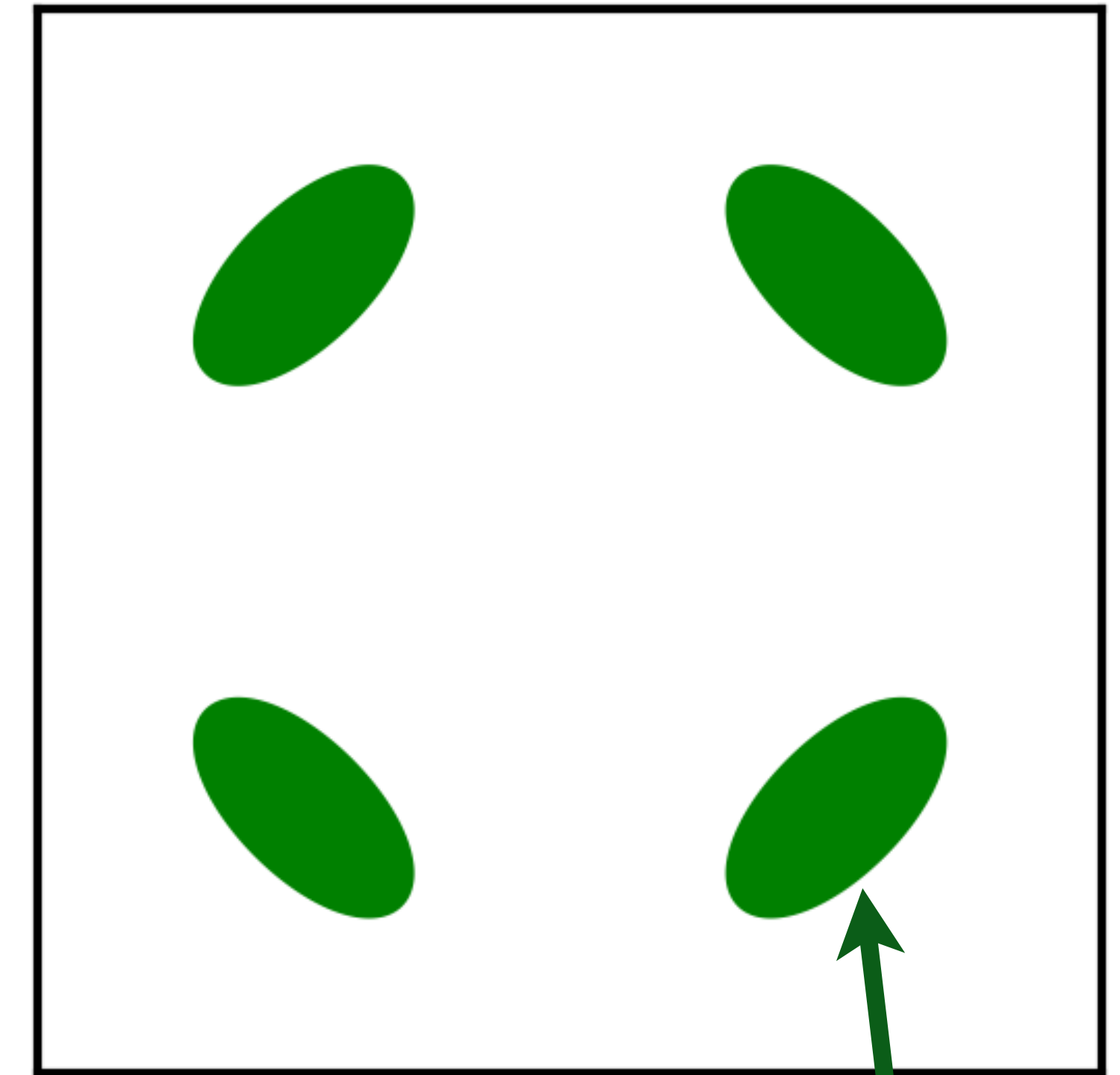
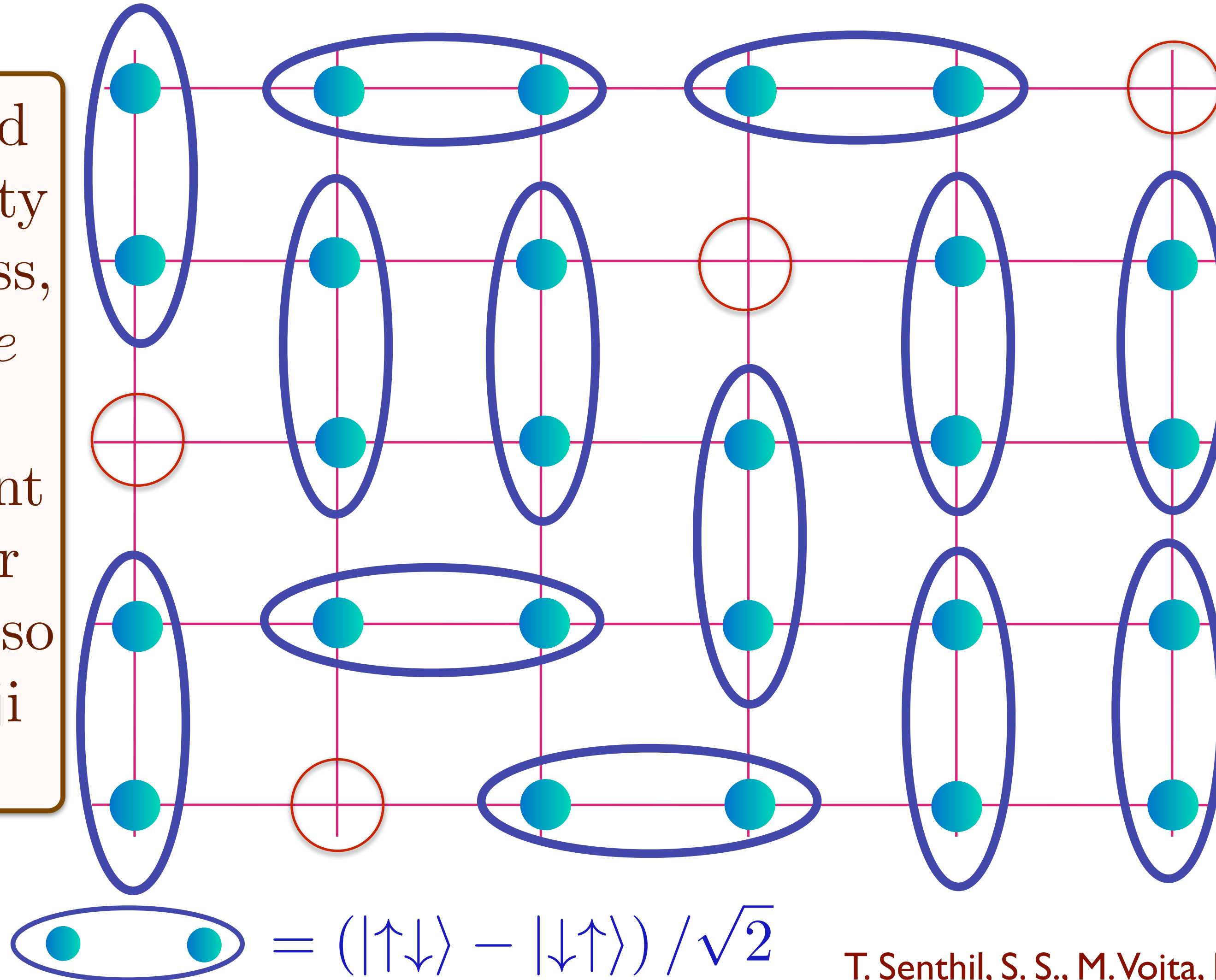
T. Senthil, S. S., M. Vojta, PRL **90**, 216403 (2003);
R. K. Kaul, A. Kolezhuk, M. Levin, S. S., T. Senthil, PRB **75**, 235122 (2007);
R. K. Kaul, Y. B. Kim, S. S., T. Senthil, Nature Physics **4**, 28 (2008)

Doping an insulating antiferromagnet with holes of density p

Holon metal

Oshikawa anomaly is satisfied by sum of spin liquid (1) and Fermi surface anomalies (p)

Spin liquid with density p of spinless, charge $+e$ 'holons'. No coherent inter-layer transport, so no Yamaji effect.



Area $p/4$

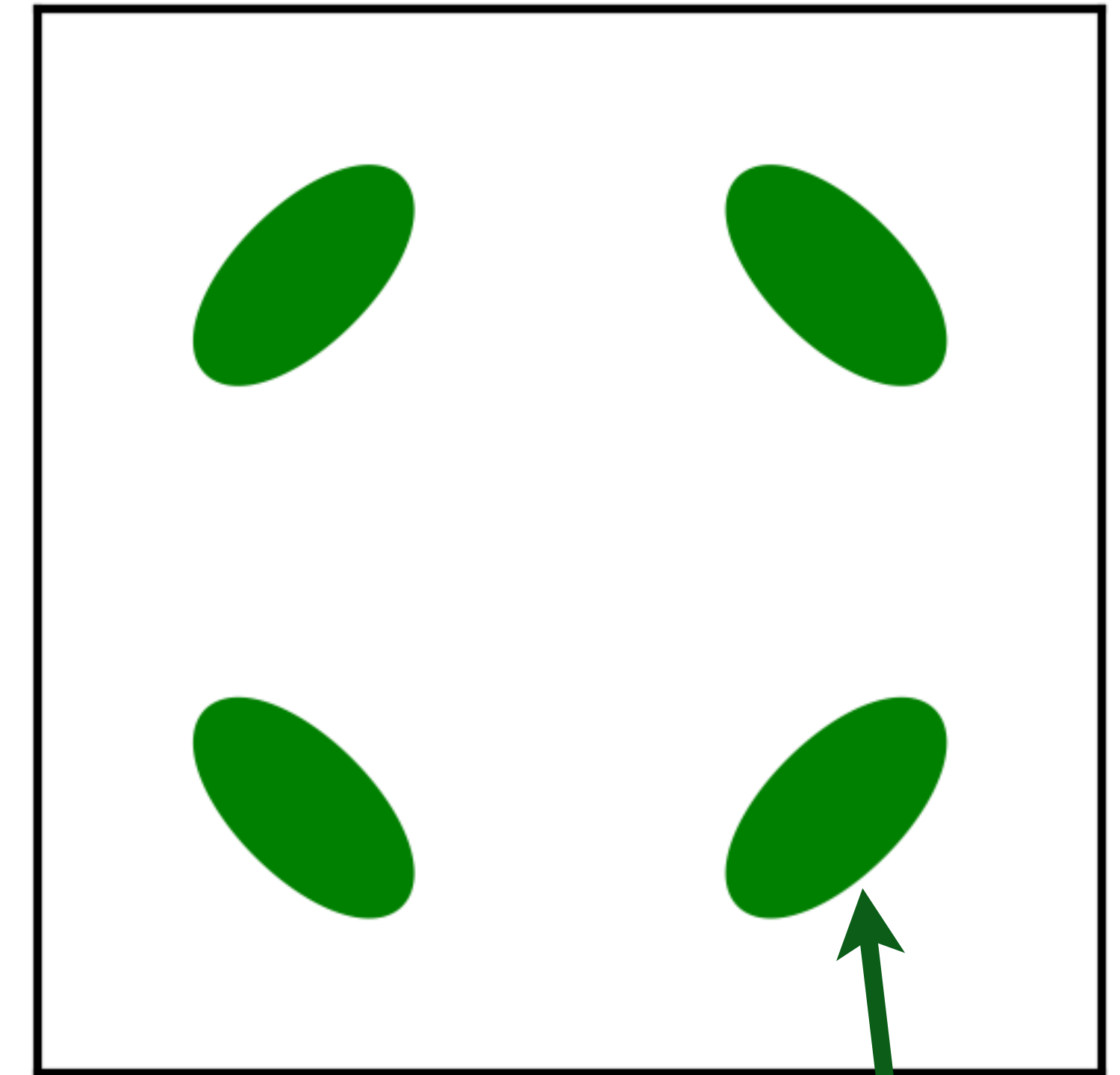
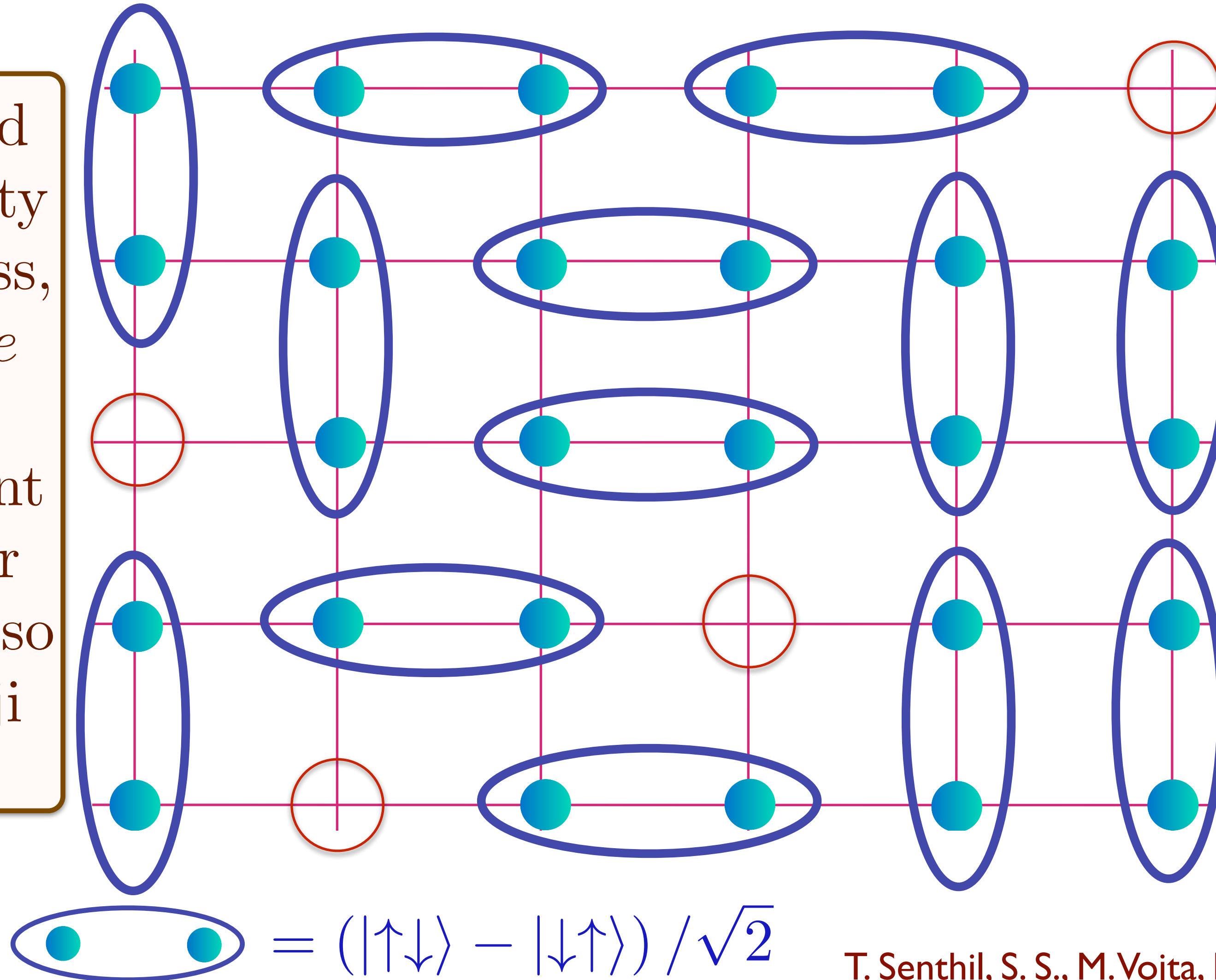
T. Senthil, S. S., M. Vojta, PRL **90**, 216403 (2003);
R. K. Kaul, A. Kolezhuk, M. Levin, S. S., T. Senthil, PRB **75**, 235122 (2007);
R. K. Kaul, Y. B. Kim, S. S., T. Senthil, Nature Physics **4**, 28 (2008)

Doping an insulating antiferromagnet with holes of density p

Holon metal

Oshikawa anomaly is satisfied by sum of spin liquid (1) and Fermi surface anomalies (p)

Spin liquid with density p of spinless, charge $+e$ 'holons'. No coherent inter-layer transport, so no Yamaji effect.



Area $p/4$

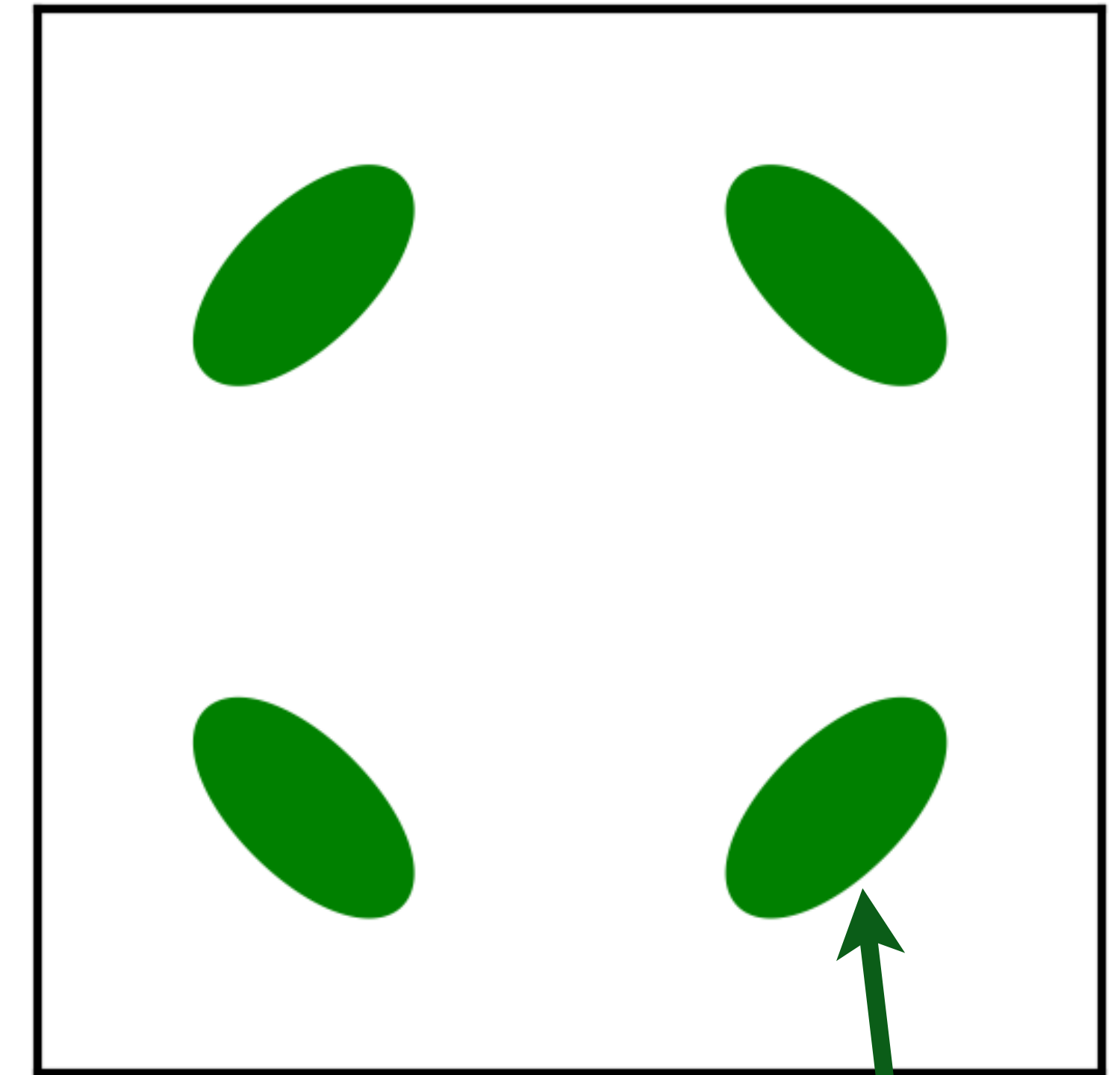
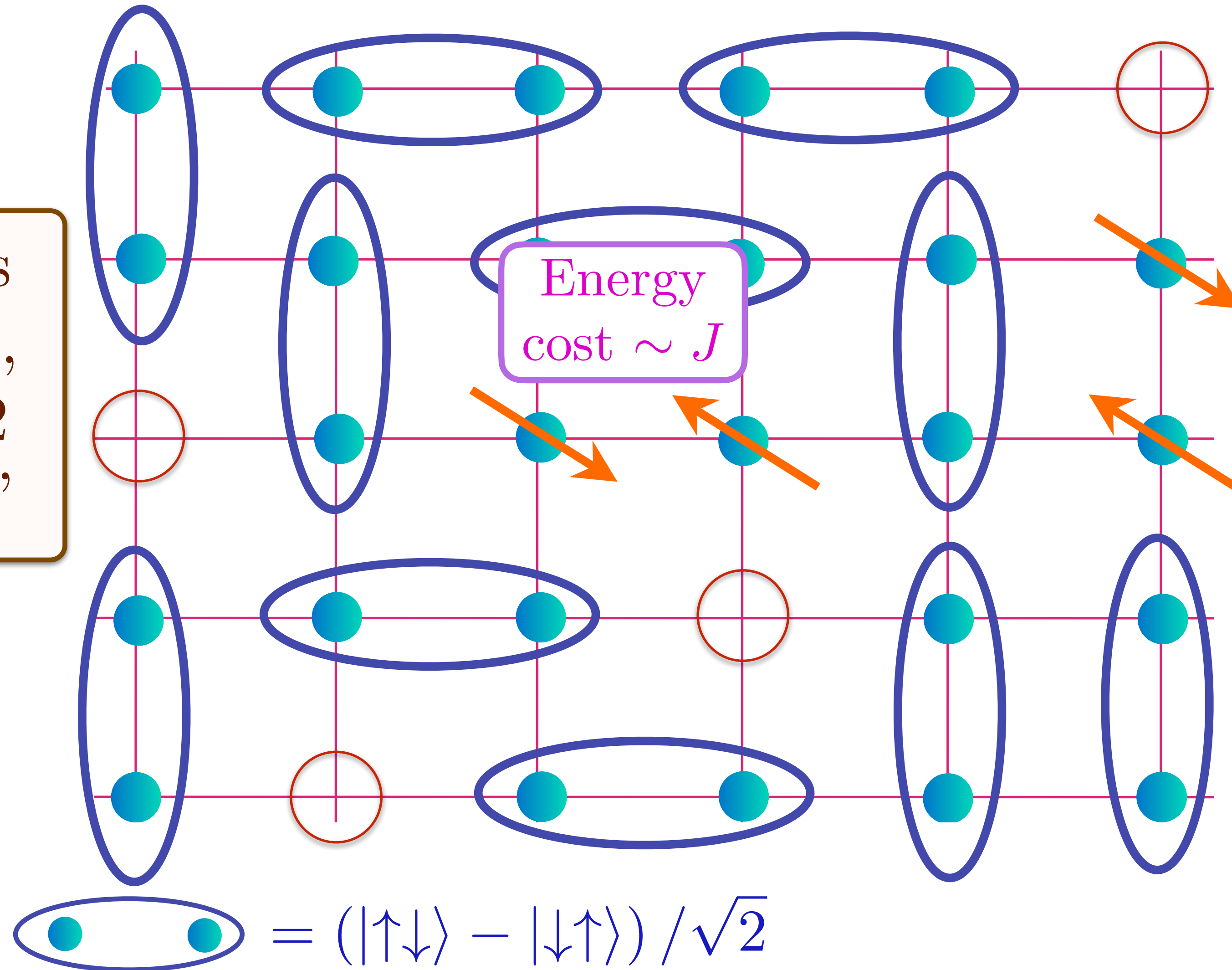
T. Senthil, S. S., M. Vojta, PRL **90**, 216403 (2003);
R. K. Kaul, A. Kolezhuk, M. Levin, S. S., T. Senthil, PRB **75**, 235122 (2007);
R. K. Kaul, Y. B. Kim, S. S., T. Senthil, Nature Physics **4**, 28 (2008)

Doping an insulating antiferromagnet with holes of density p

Holon metal

Oshikawa anomaly is satisfied by sum of spin liquid (1) and Fermi surface anomalies (p)

Also has charge 0, spin-1/2 'spinons'



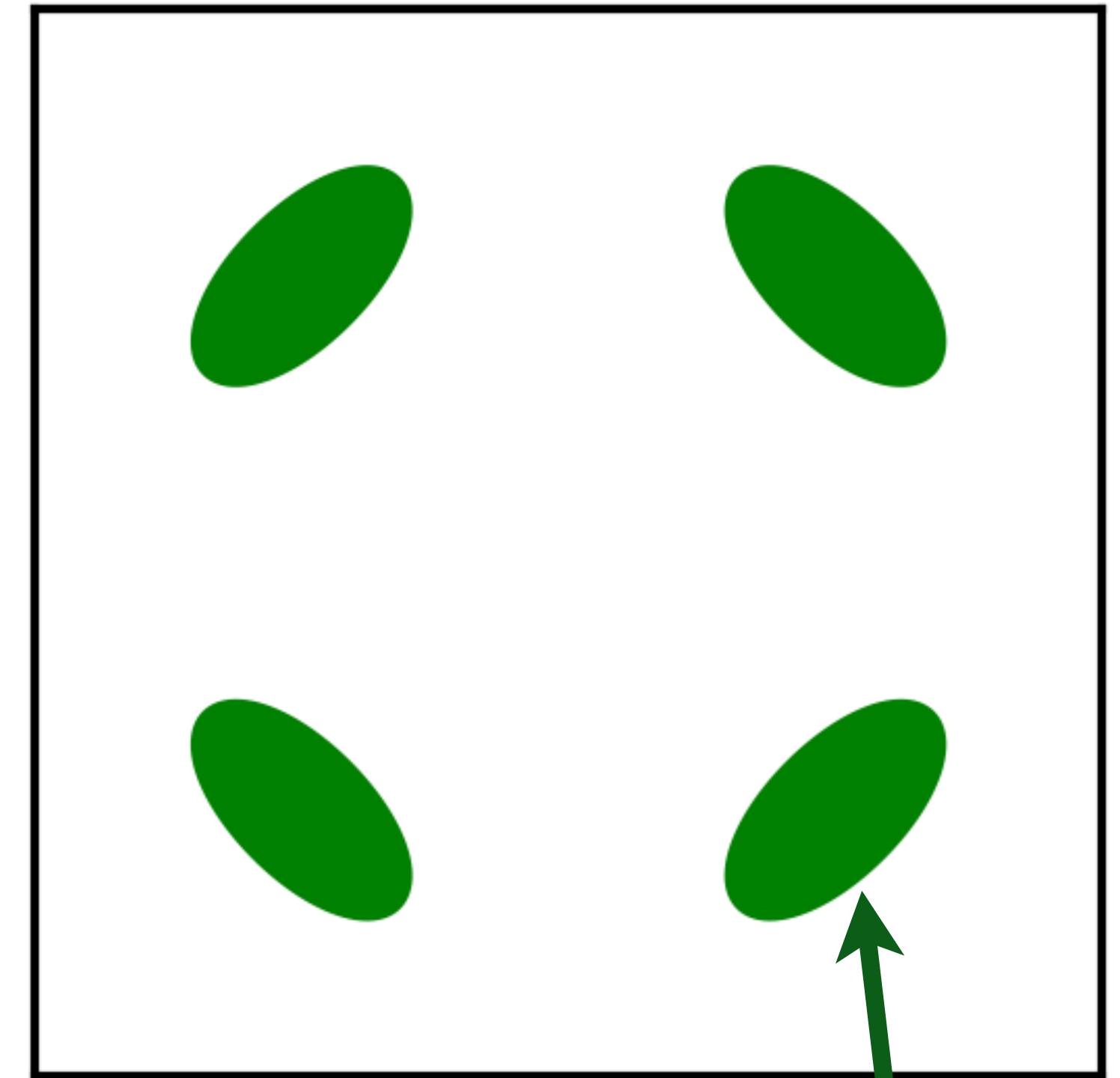
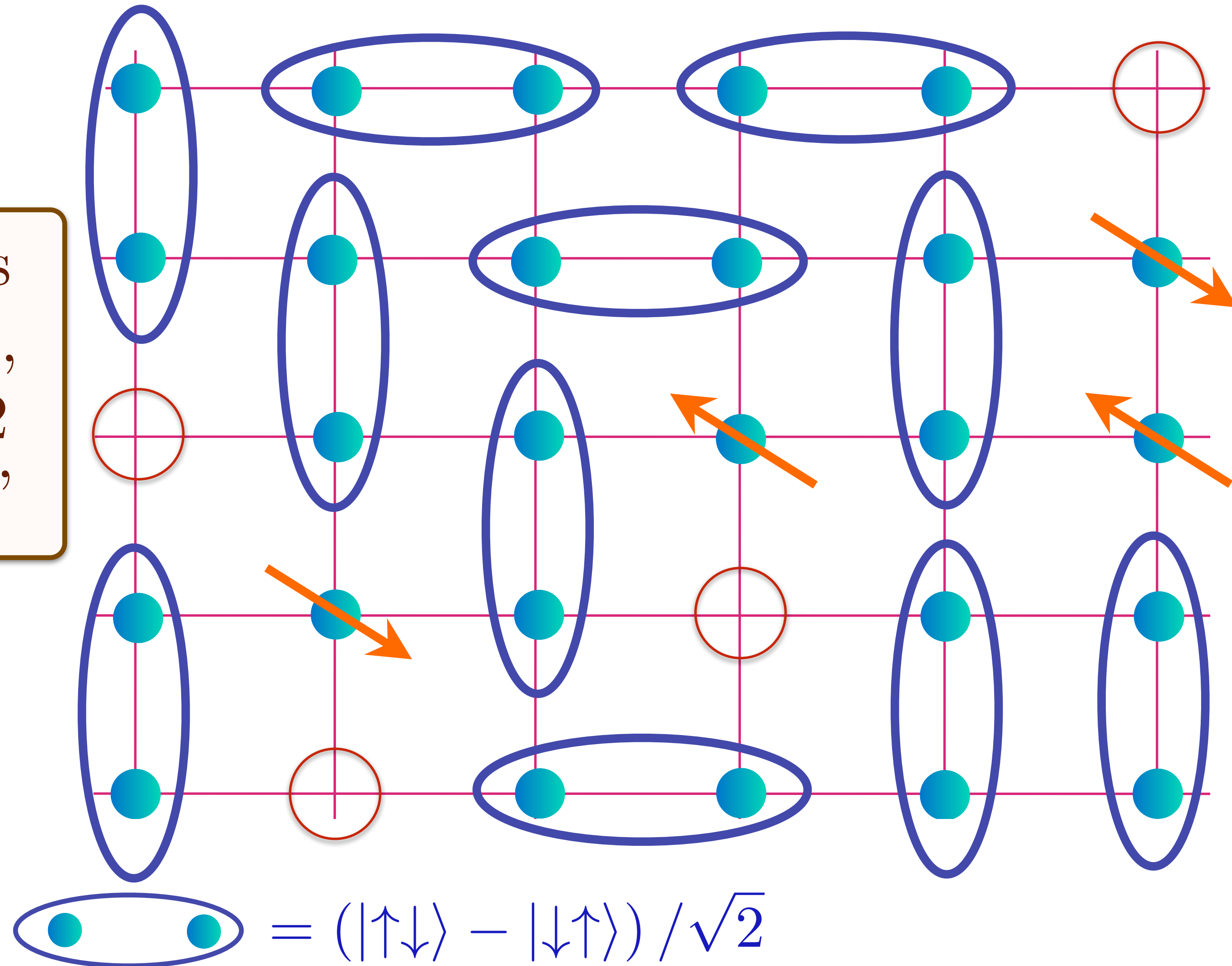
Area $p/4$

Doping an insulating antiferromagnet with holes of density p

Holon metal

Oshikawa anomaly is satisfied by sum of spin liquid (1) and Fermi surface anomalies (p)

Also has charge 0, spin-1/2 'spinons'



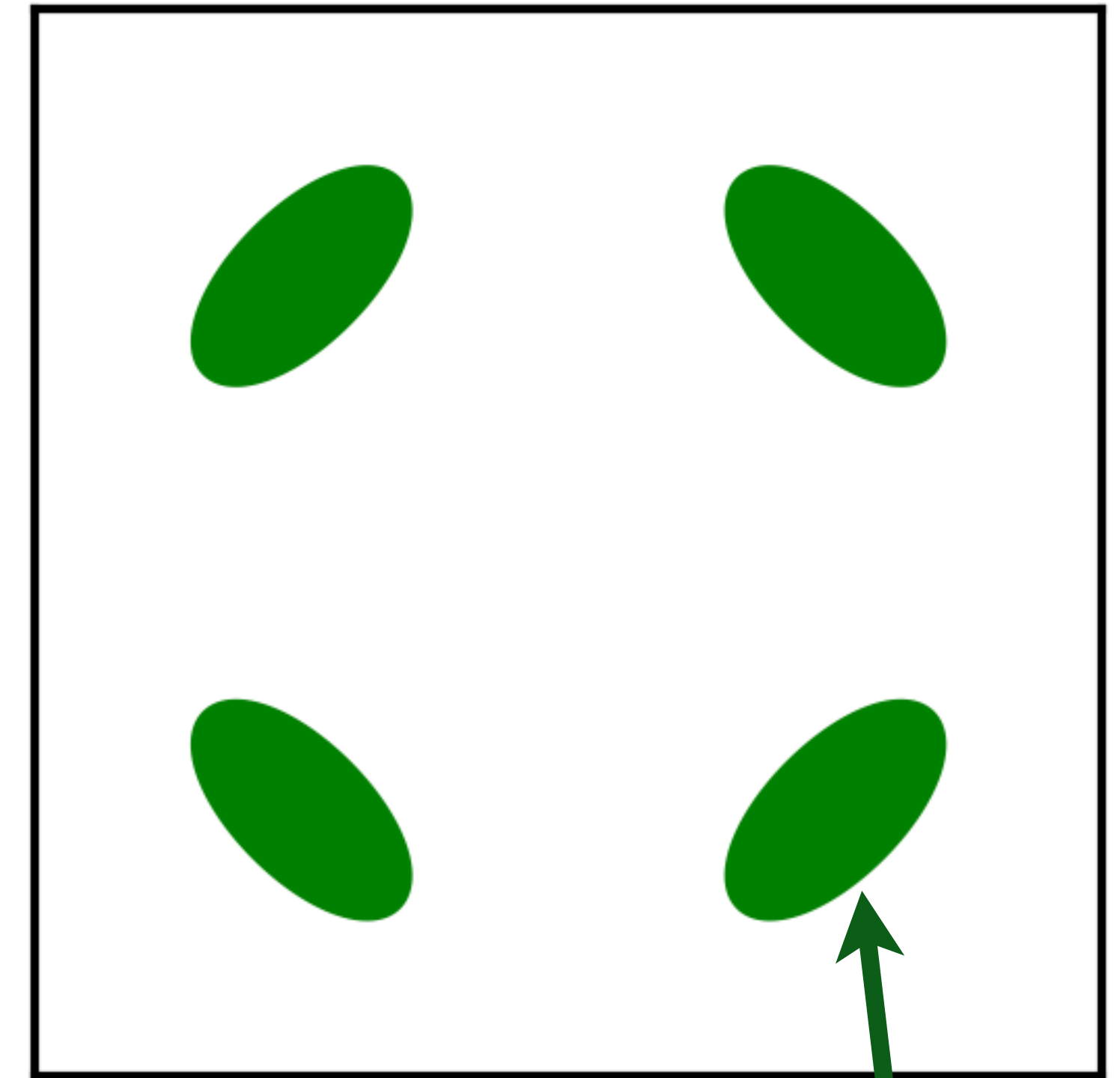
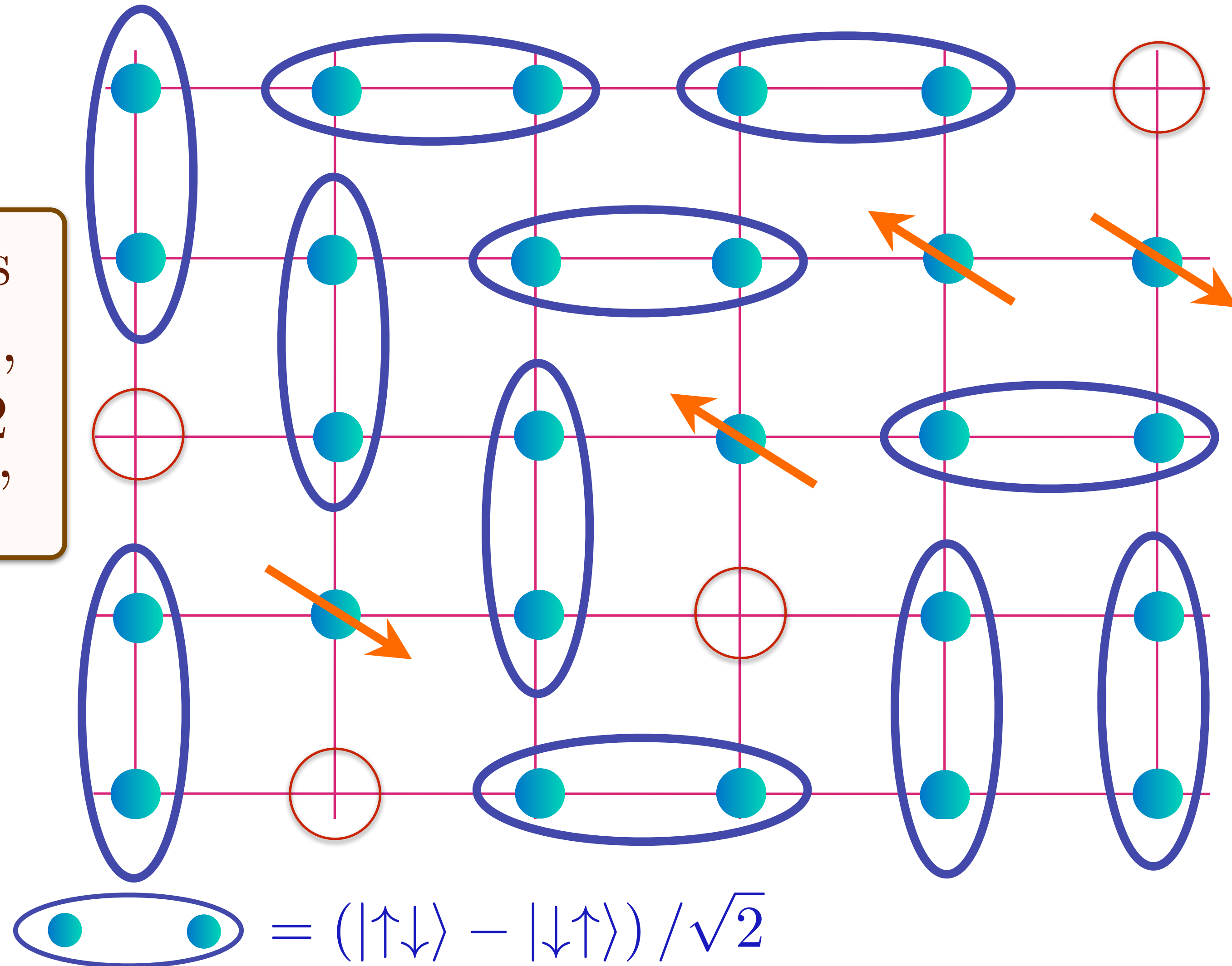
Area $p/4$

Doping an insulating antiferromagnet with holes of density p

Holon metal

Oshikawa anomaly is satisfied by sum of spin liquid (1) and Fermi surface anomalies (p)

Also has charge 0, spin-1/2 'spinons'



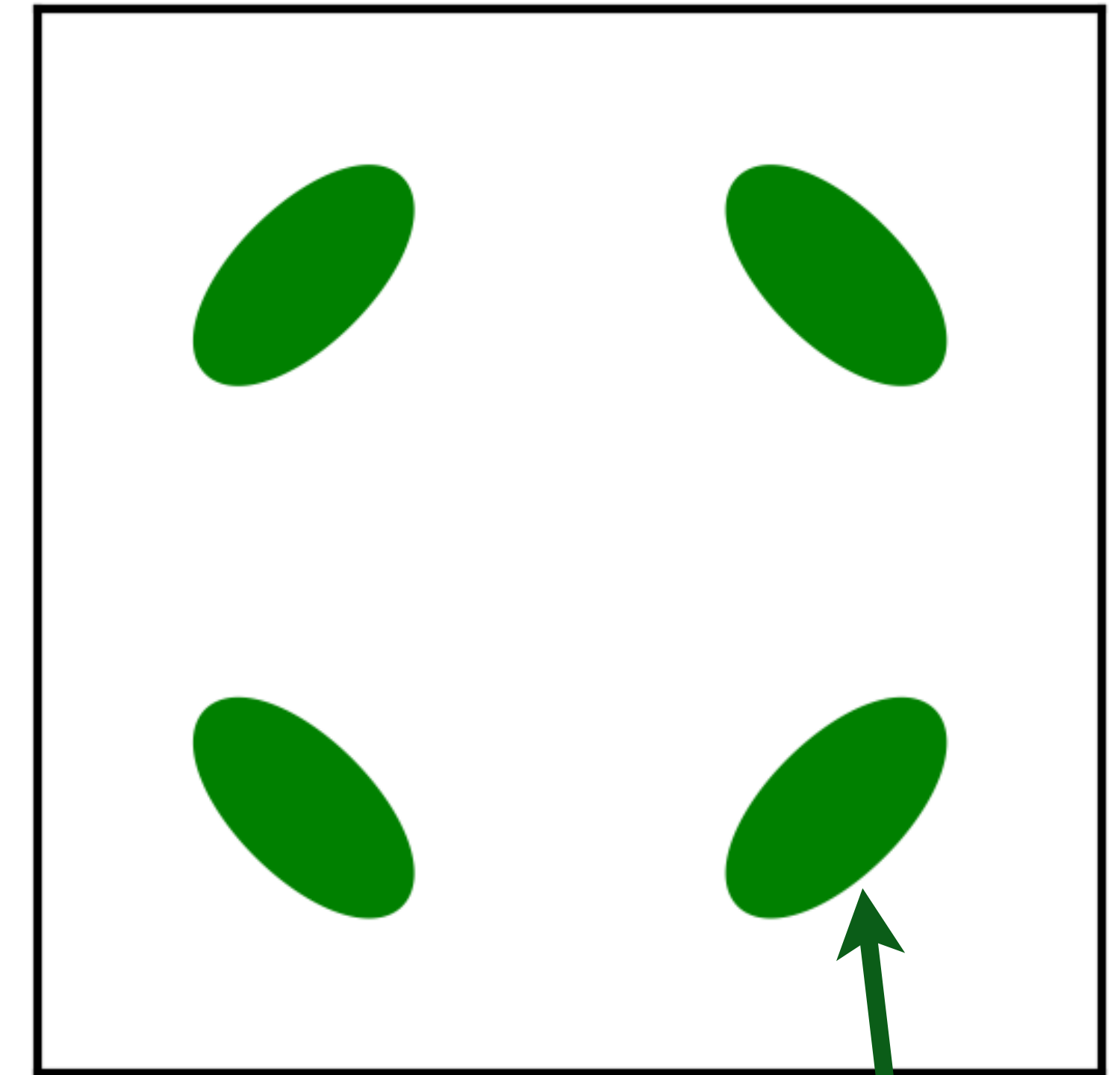
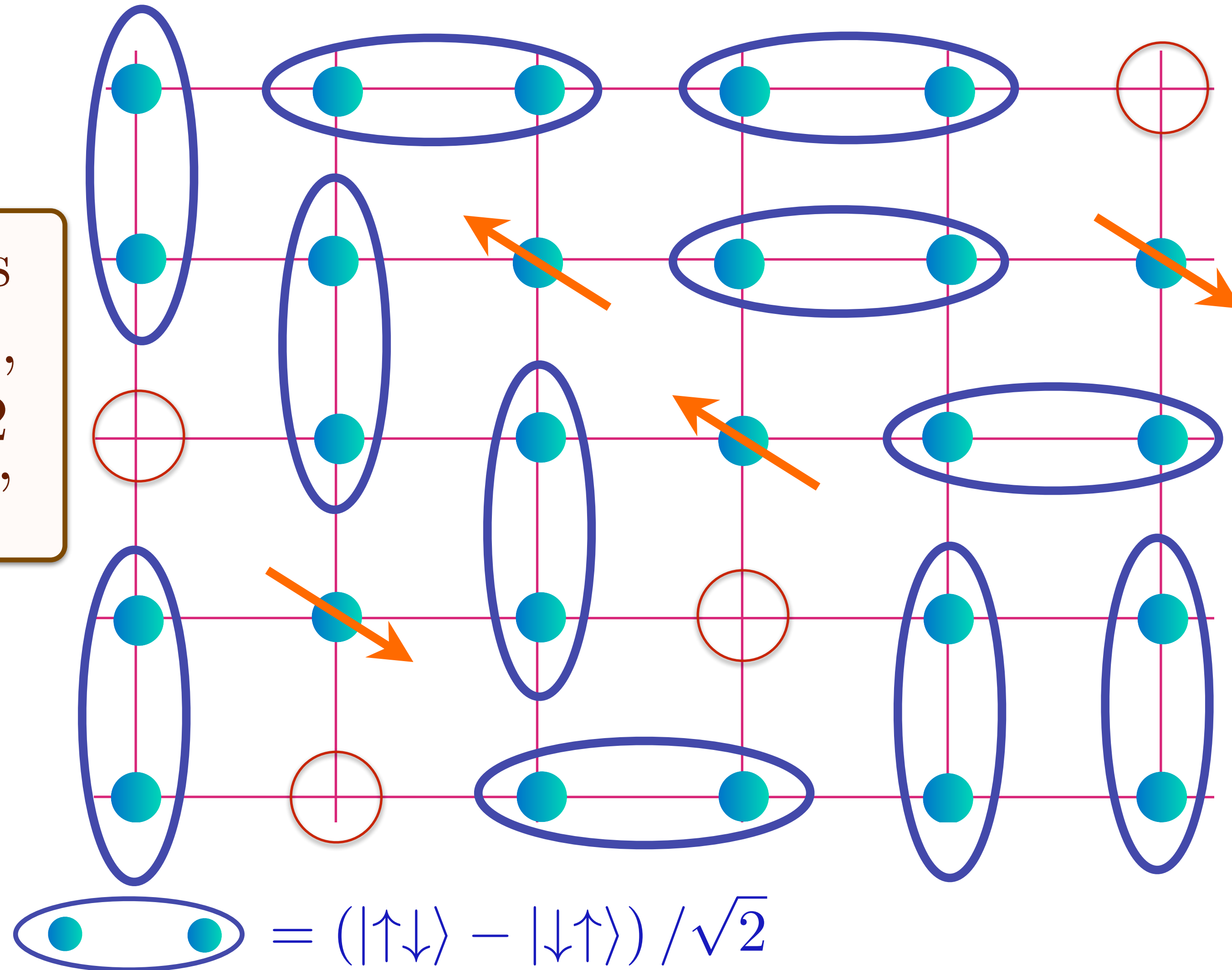
Area $p/4$

Doping an insulating antiferromagnet with holes of density p

Holon metal

Oshikawa anomaly is satisfied by sum of spin liquid (1) and Fermi surface anomalies (p)

Also has charge 0, spin-1/2 'spinons'



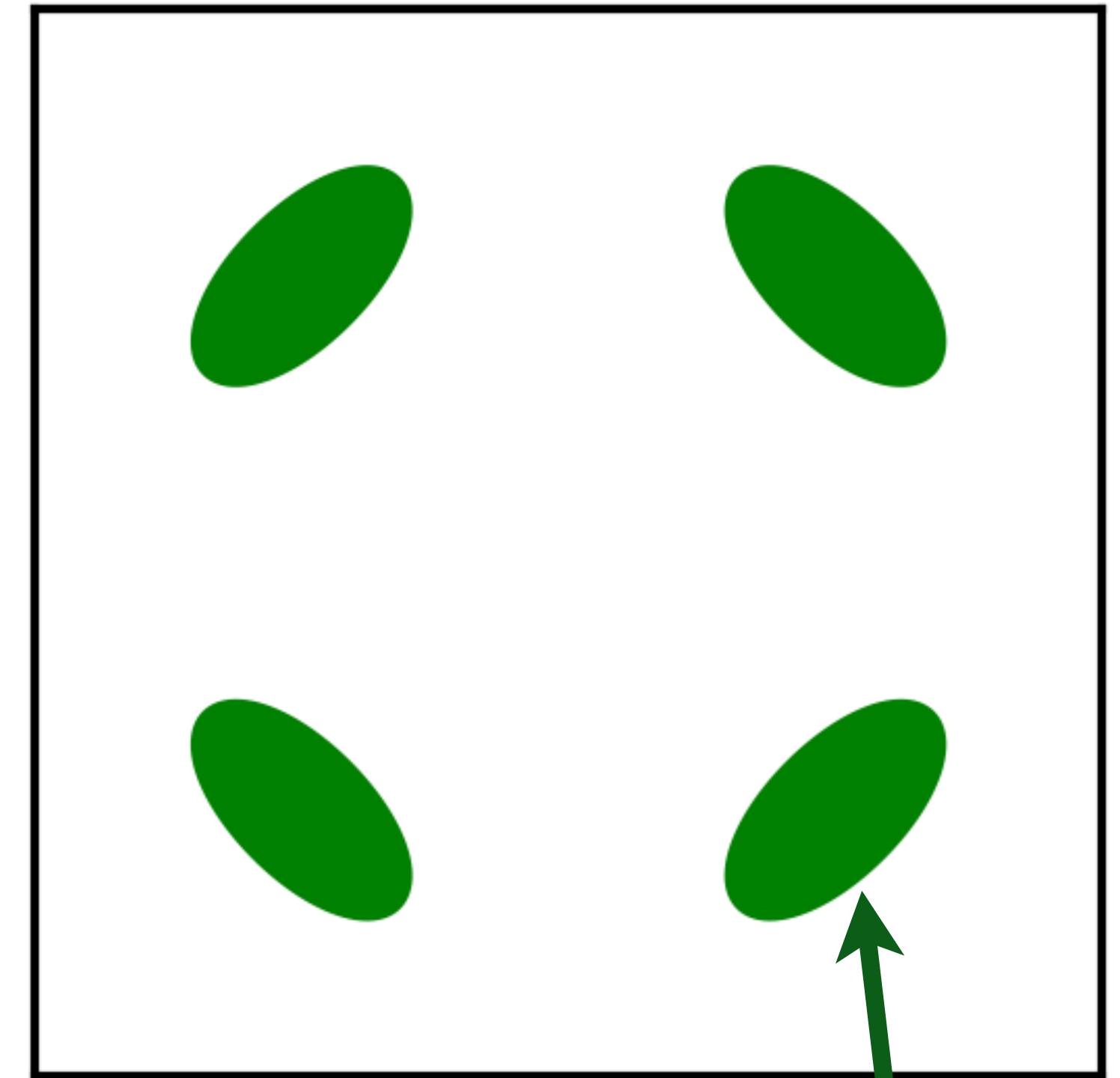
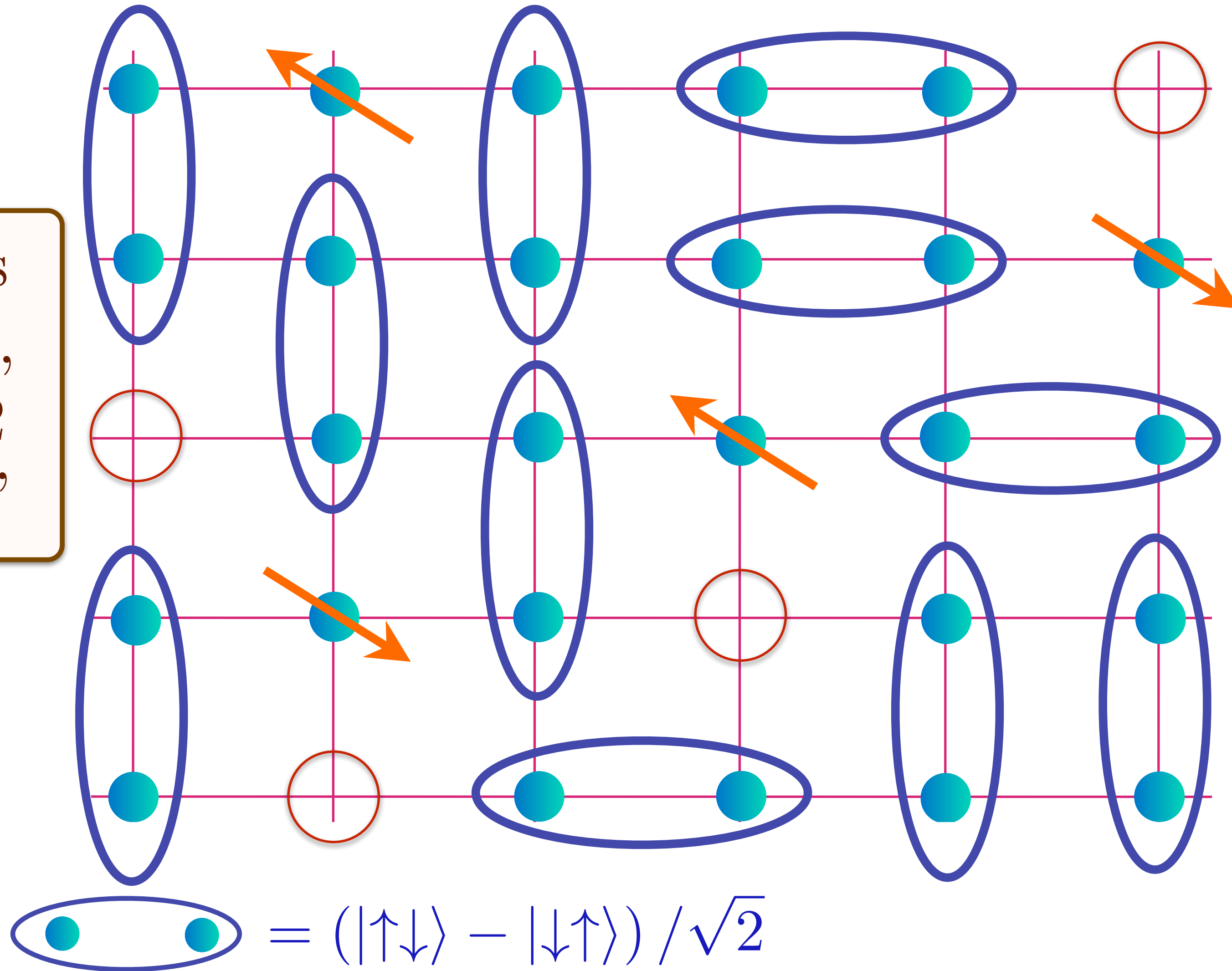
Area $p/4$

Doping an insulating antiferromagnet with holes of density p

Holon metal

Oshikawa anomaly is satisfied by sum of spin liquid (1) and Fermi surface anomalies (p)

Also has charge 0, spin-1/2 'spinons'



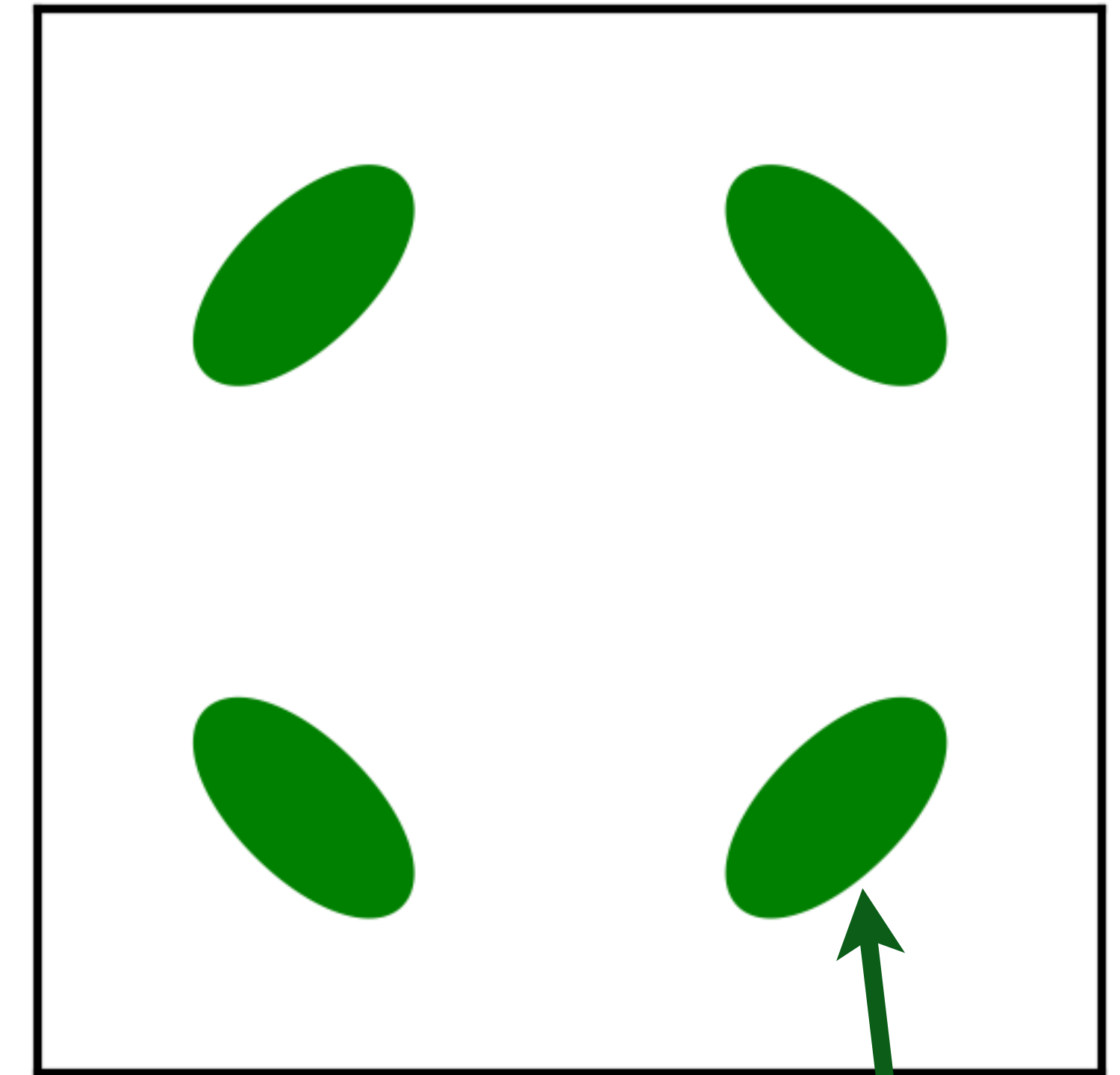
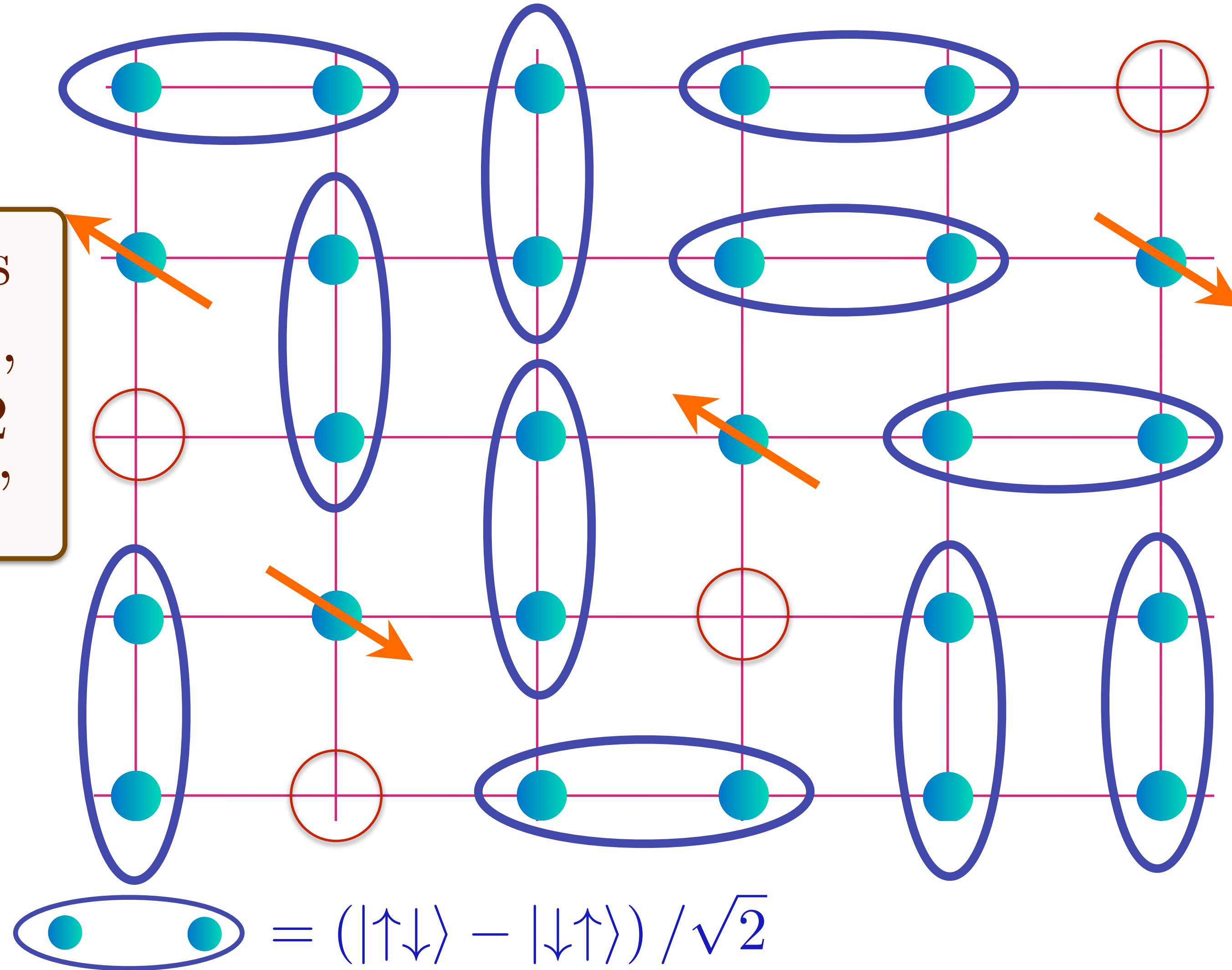
Area $p/4$

Doping an insulating antiferromagnet with holes of density p

Holon metal

Oshikawa anomaly is satisfied
by sum of spin liquid (1) and
Fermi surface anomalies (p)

Also has
charge 0,
spin-1/2
'spinons'



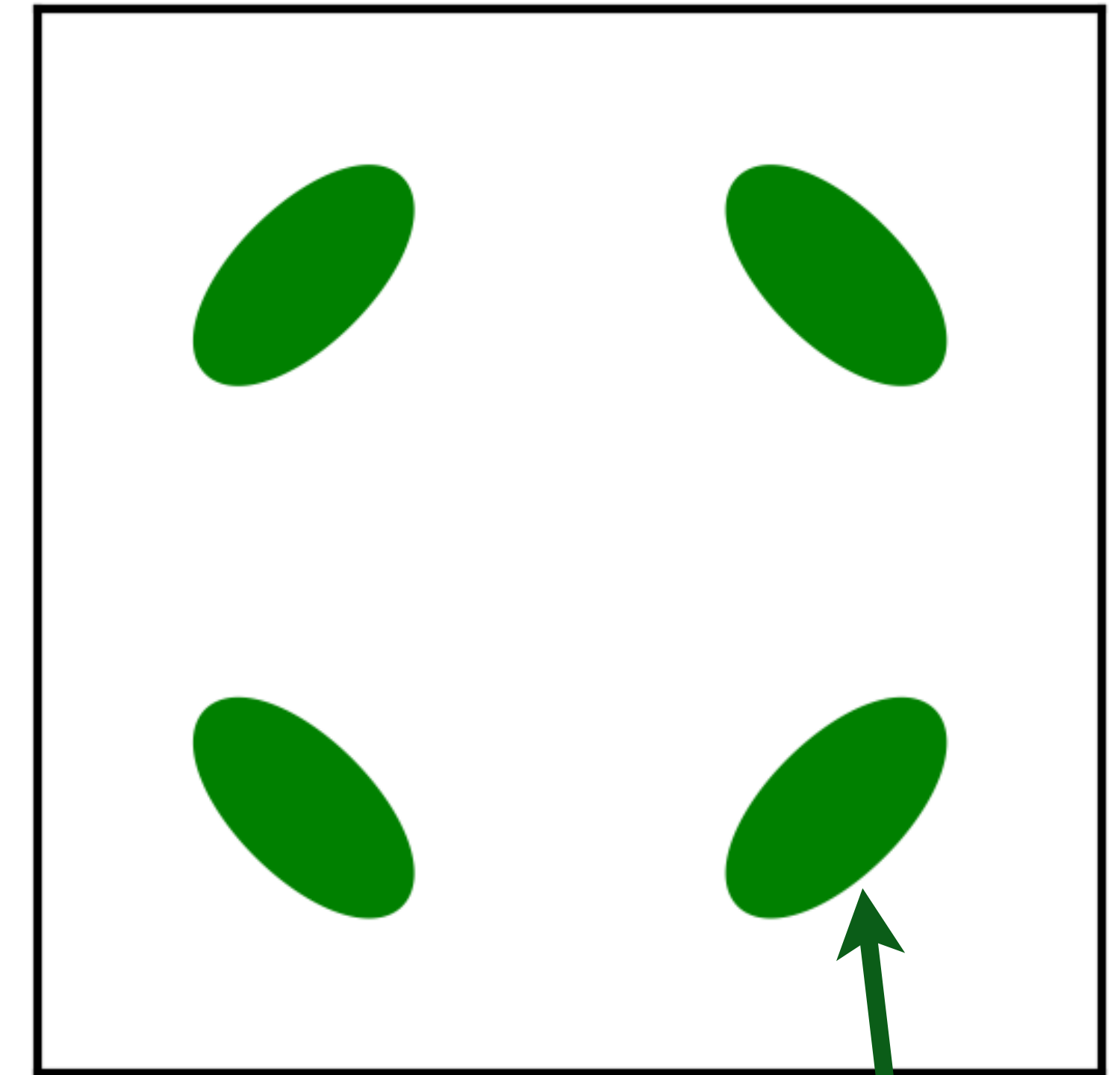
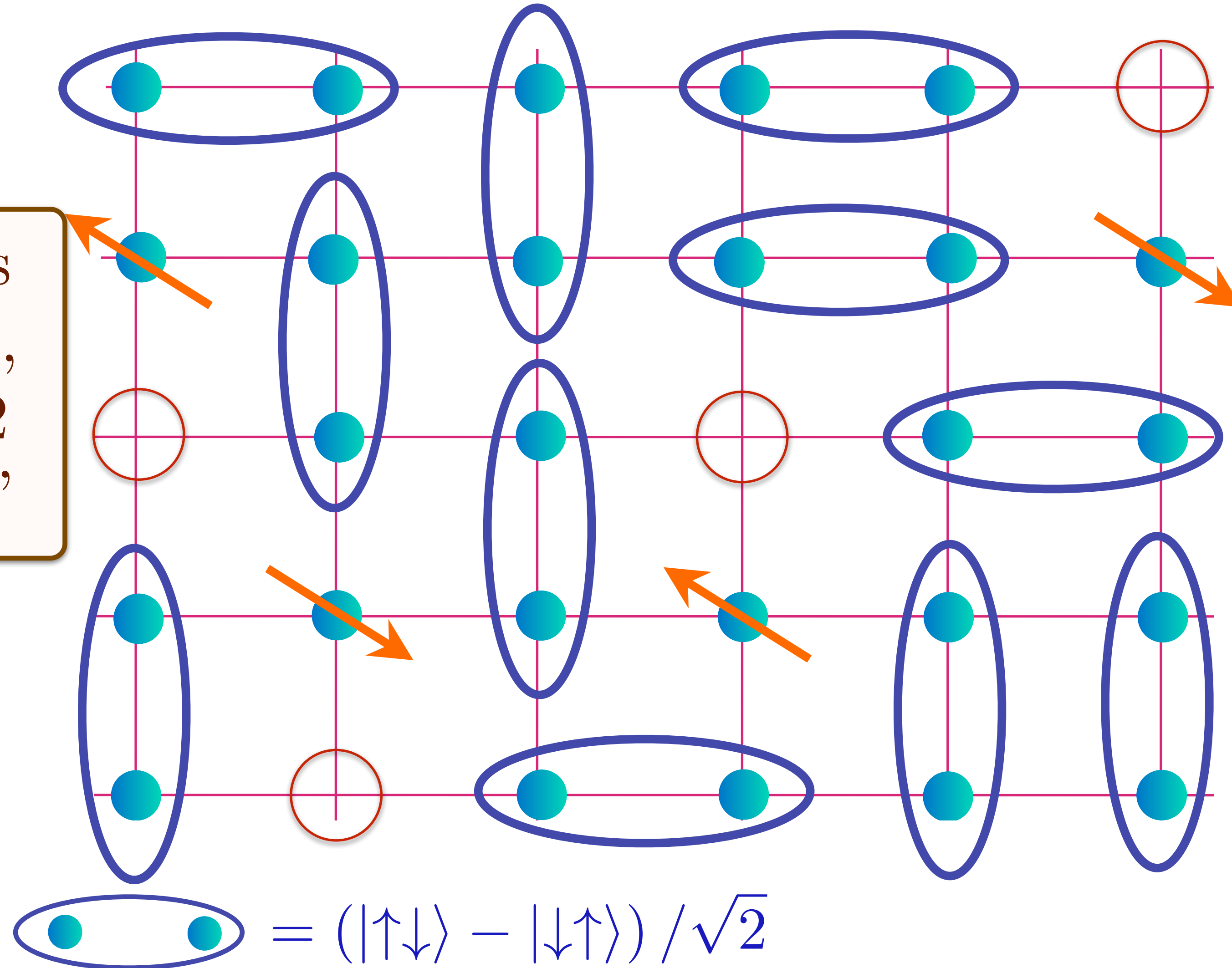
Area $p/4$

Doping an insulating antiferromagnet with holes of density p

Holon metal

Oshikawa anomaly is satisfied
by sum of spin liquid (1) and
Fermi surface anomalies (p)

Also has
charge 0,
spin-1/2
'spinons'



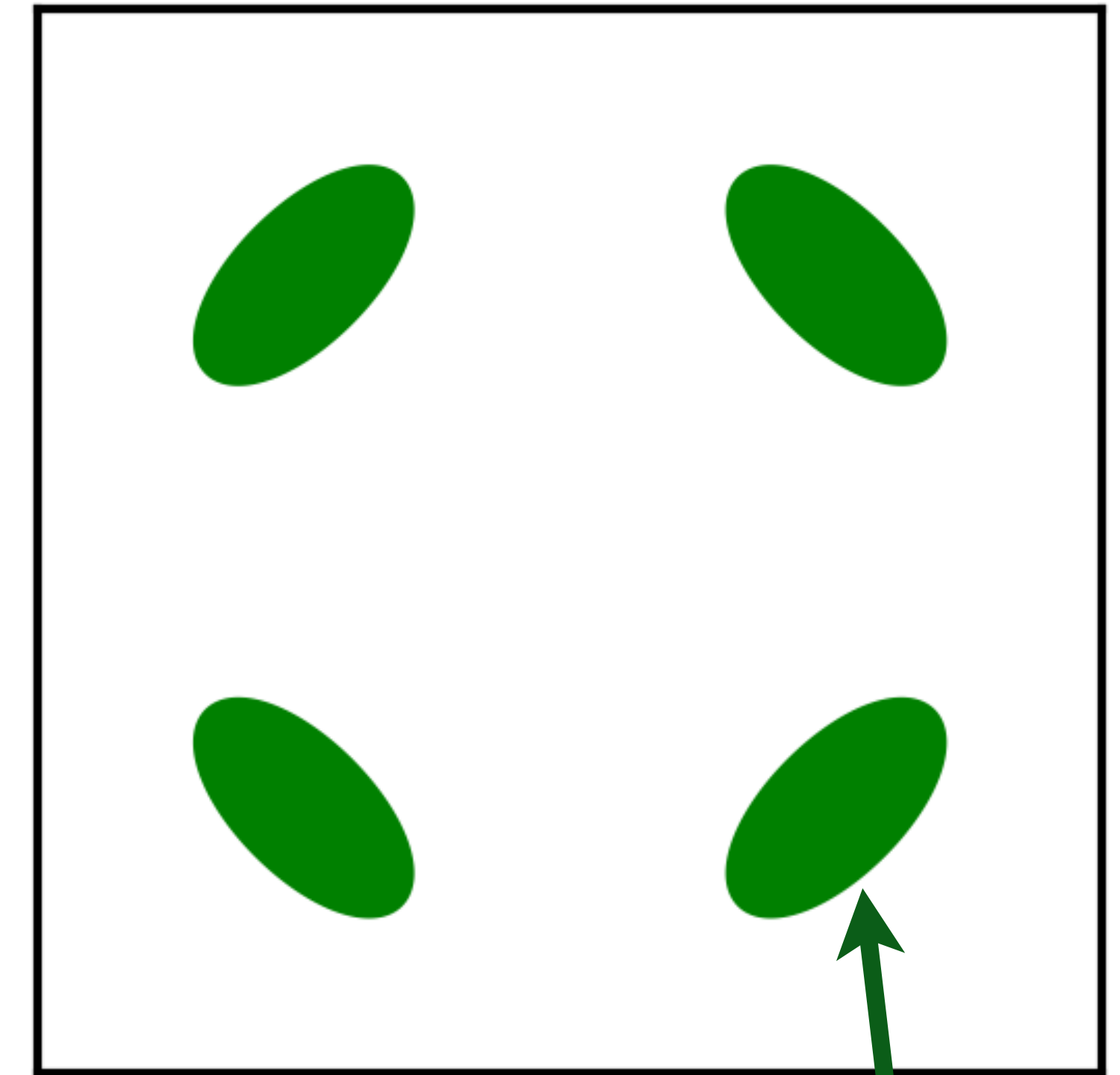
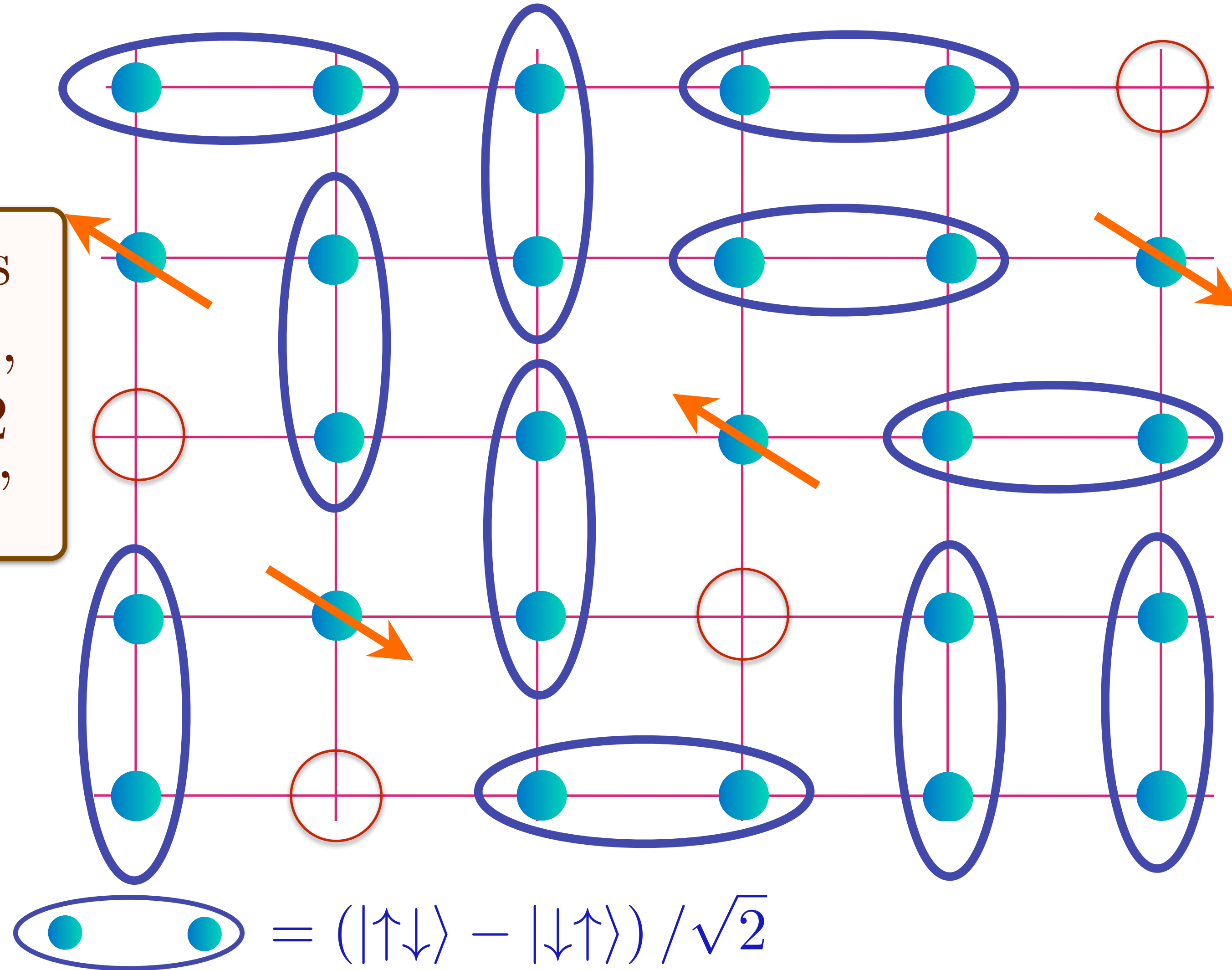
Area $p/4$

Doping an insulating antiferromagnet with holes of density p

Holon metal

Oshikawa anomaly is satisfied
by sum of spin liquid (1) and
Fermi surface anomalies (p)

Also has
charge 0,
spin-1/2
'spinons'



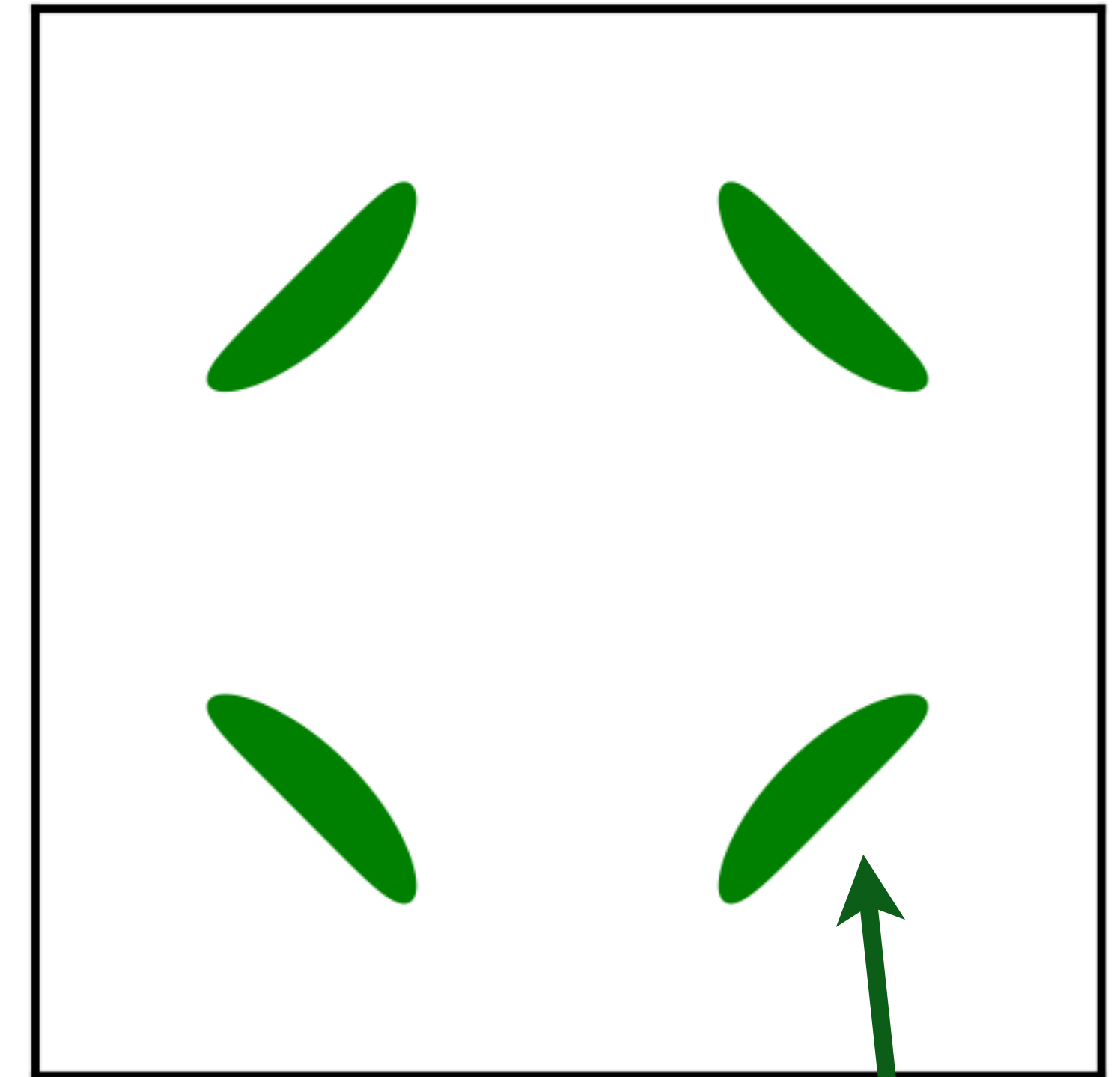
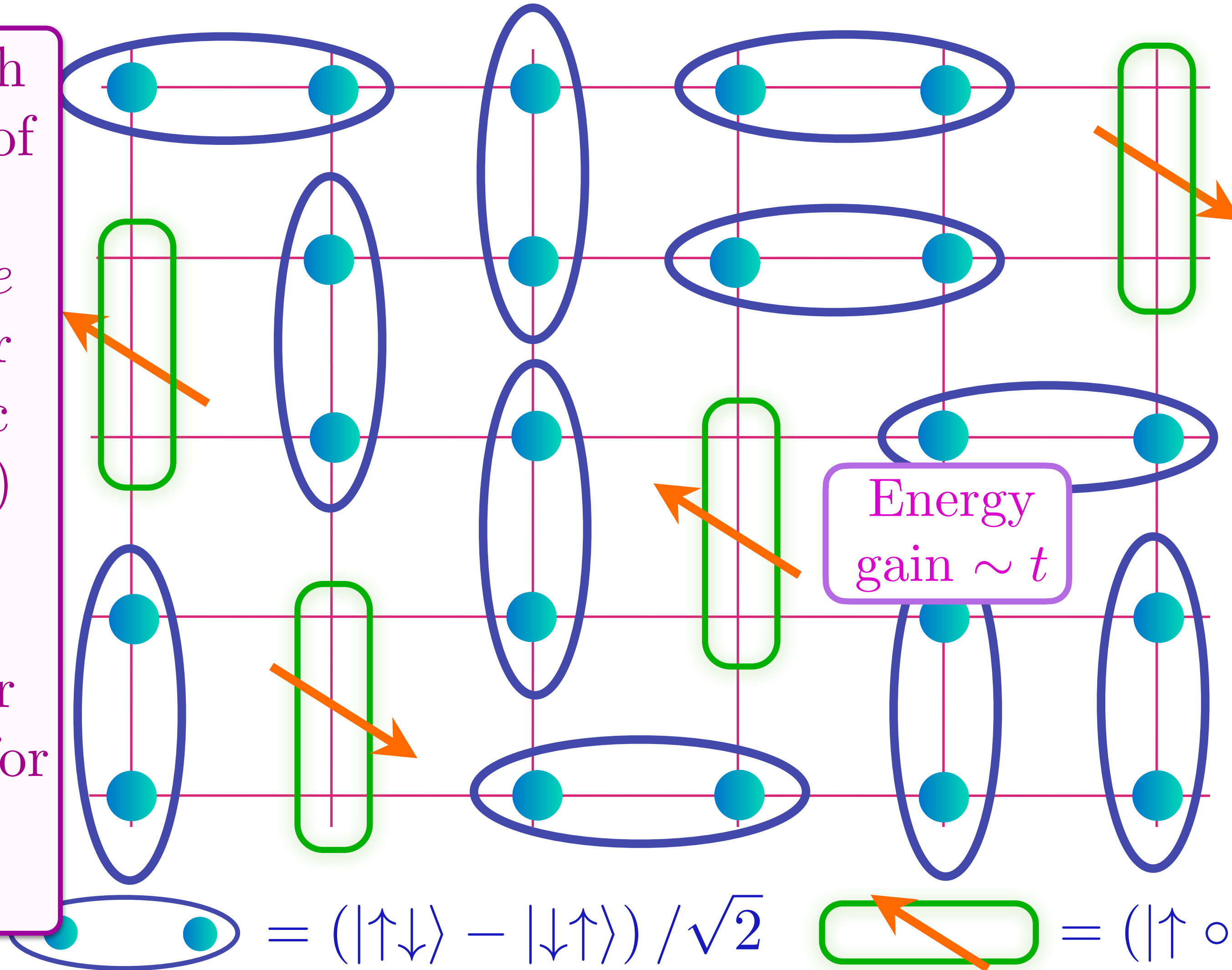
Area $p/4$

Doping an insulating antiferromagnet with holes of density p

FL*

Oshikawa anomaly is satisfied by sum of spin liquid (1) and Fermi surface anomalies (p)

Metal with density p of spin-1/2, charge $+e$ 'holes' (or 'magnetic polarons') with coherent inter-layer transport for Yamaji effect.



Area $p/8$

$$= (|\uparrow\downarrow\rangle - |\downarrow\uparrow\rangle) / \sqrt{2} \quad \text{green oval with arrow} = (|\uparrow\circ\rangle + |\circ\uparrow\rangle) / \sqrt{2}$$

T. Senthil, S. S., M. Vojta, PRL **90**, 216403 (2003); R. K. Kaul, A. Kolezhuk, M. Levin, S.S., T. Senthil, PRB **75**, 235122 (2007)

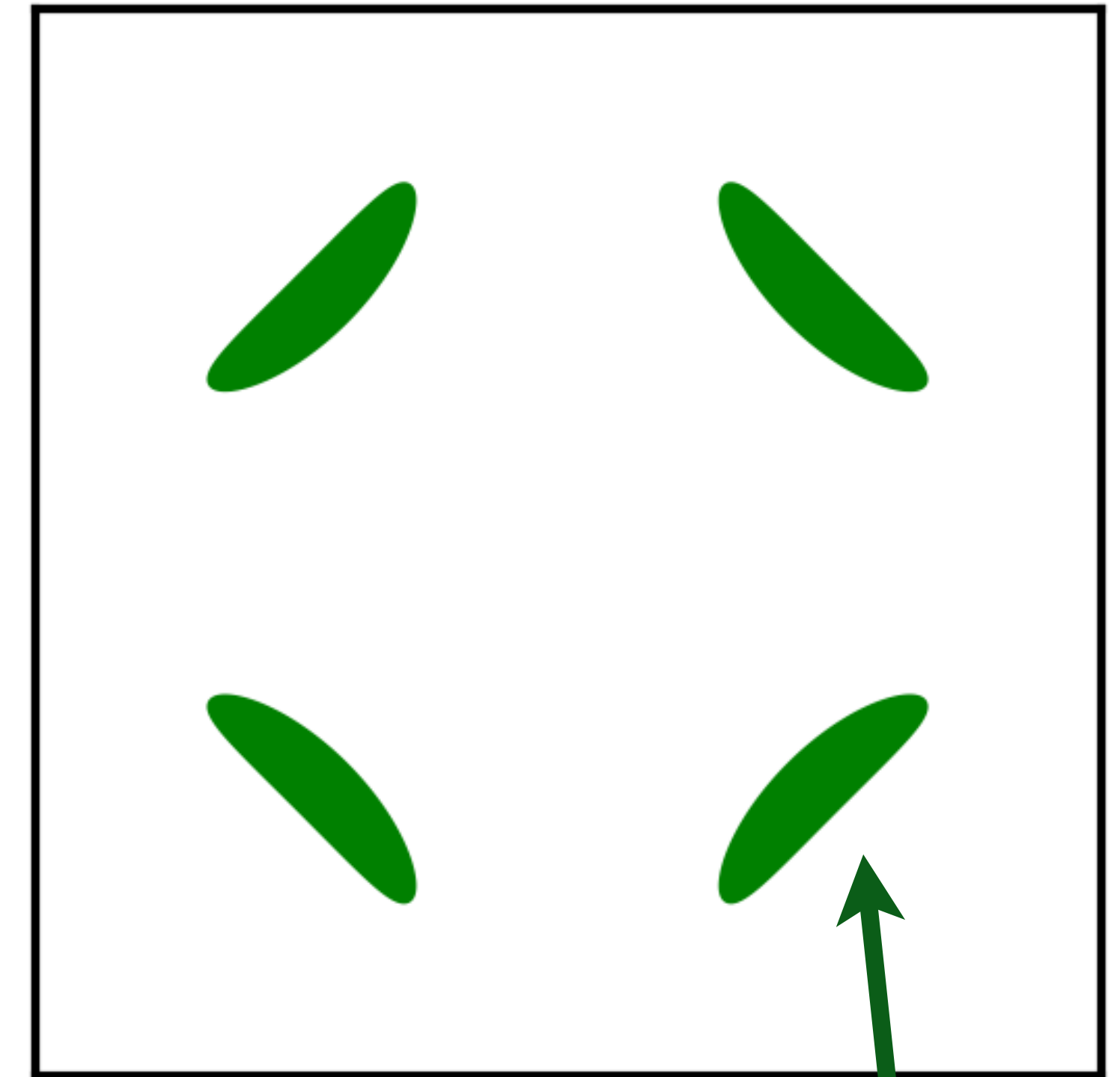
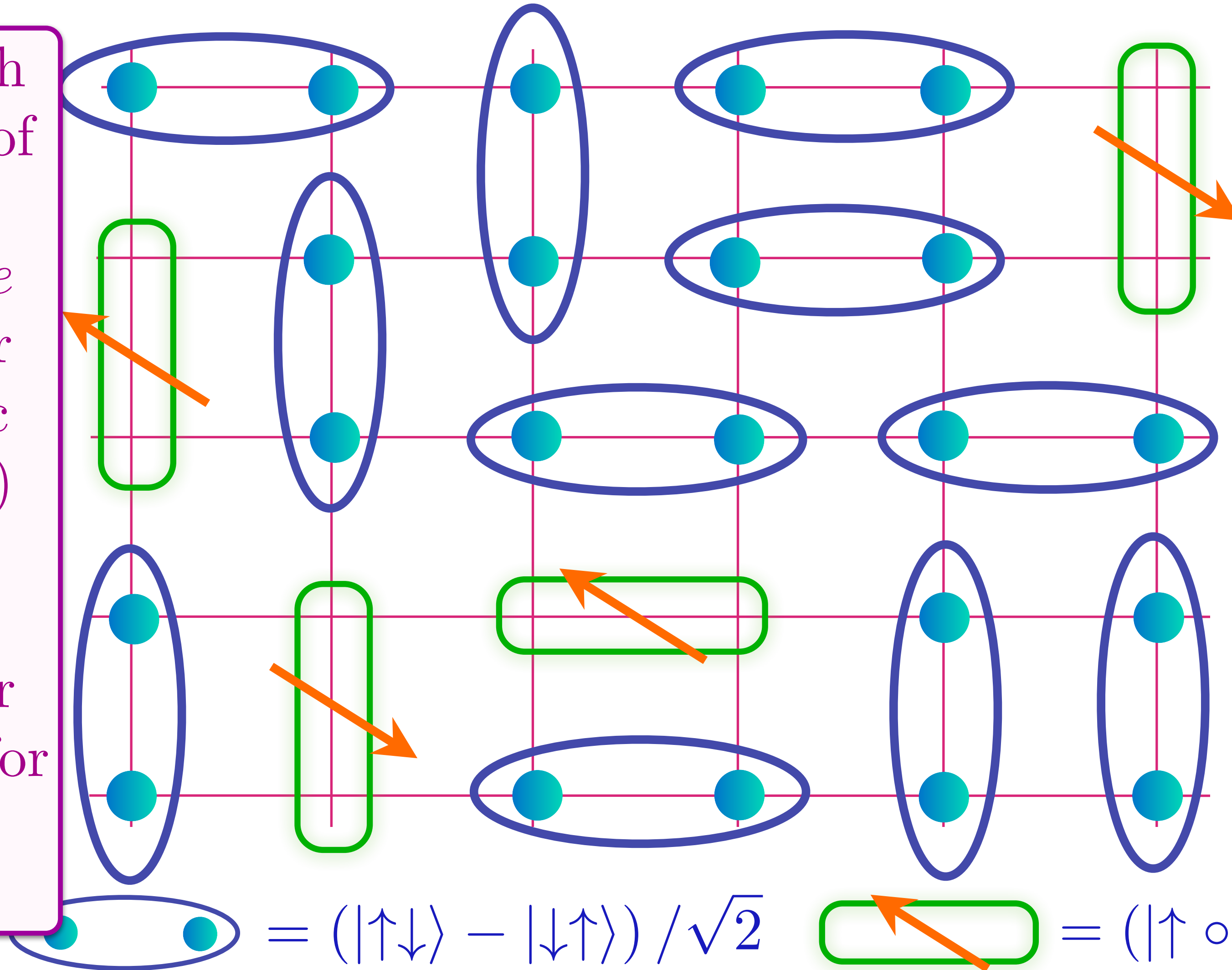
M. Punk, A. Allais, and S. Sachdev, PNAS **112**, 9552 (2015)

Doping an insulating antiferromagnet with holes of density p

FL*

Oshikawa anomaly is satisfied by sum of spin liquid (1) and Fermi surface anomalies (p)

Metal with density p of spin-1/2, charge $+e$ 'holes' (or 'magnetic polarons') with coherent inter-layer transport for Yamaji effect.



Area $p/8$

$$= (|\uparrow\downarrow\rangle - |\downarrow\uparrow\rangle) / \sqrt{2} \quad \text{green rectangle with orange arrow} = (|\uparrow\circ\rangle + |\circ\uparrow\rangle) / \sqrt{2}$$

T. Senthil, S. S., M. Vojta, PRL **90**, 216403 (2003); R. K. Kaul, A. Kolezhuk, M. Levin, S.S., T. Senthil, PRB **75**, 235122 (2007)

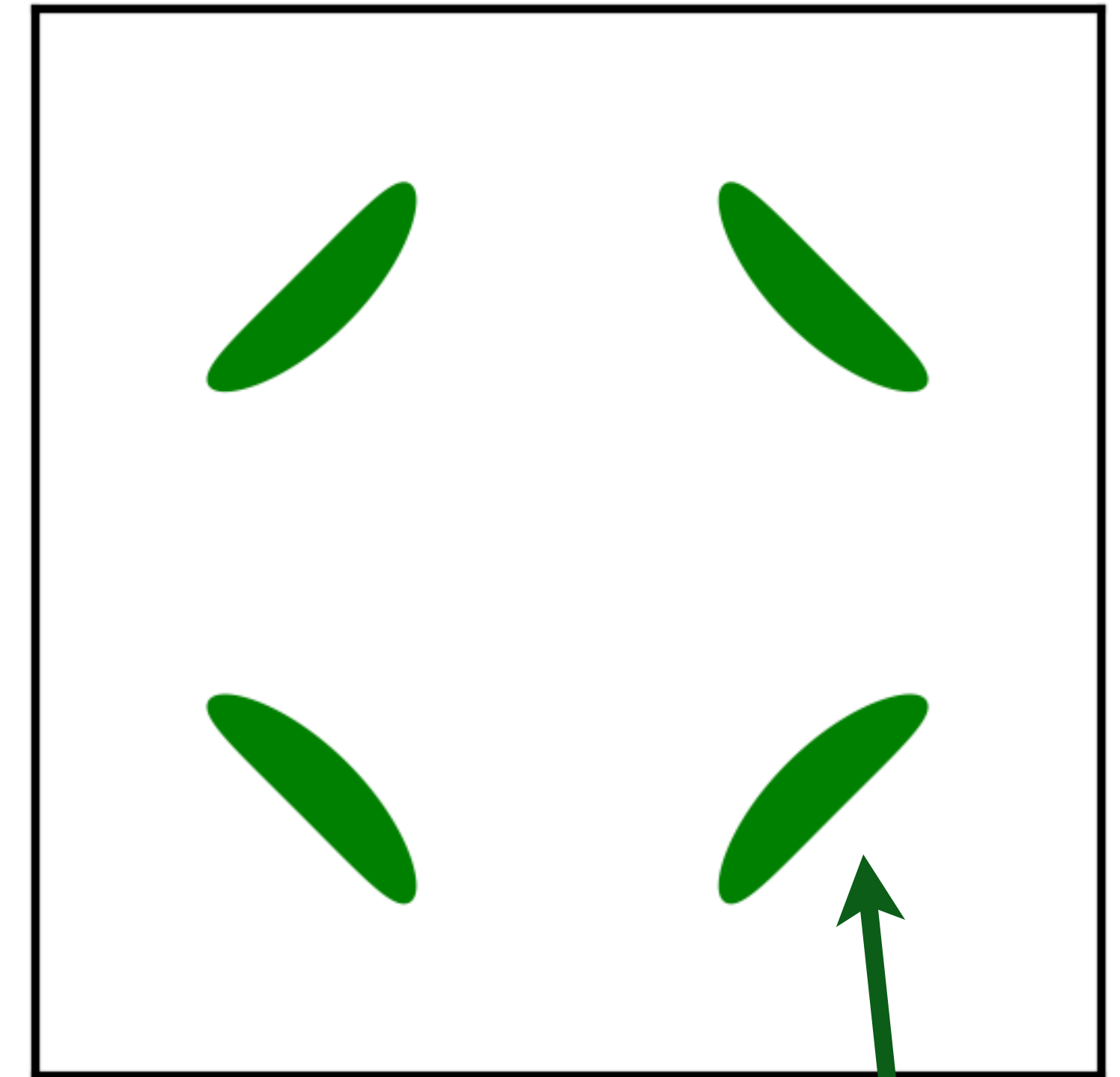
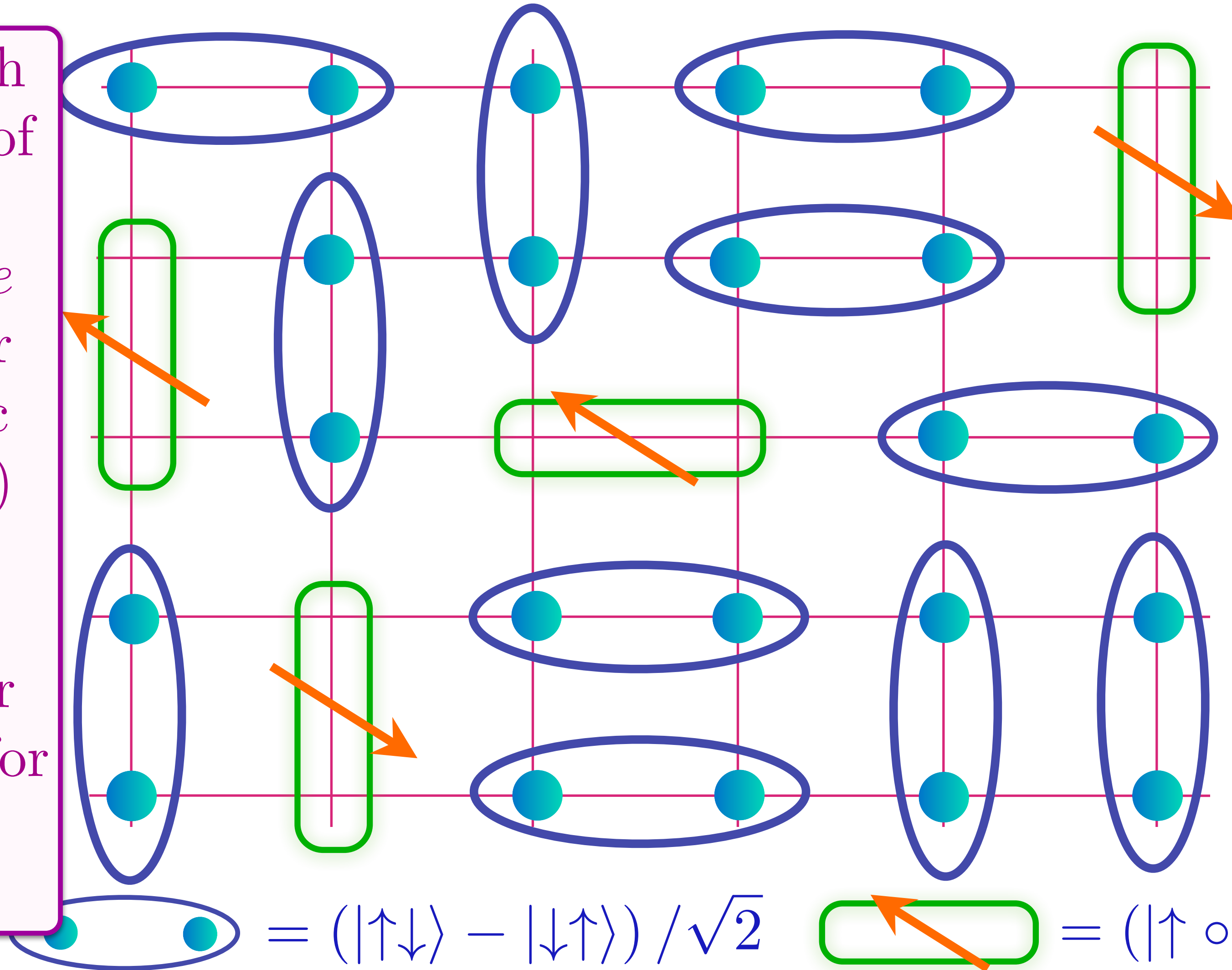
M. Punk, A. Allais, and S. Sachdev, PNAS **112**, 9552 (2015)

Doping an insulating antiferromagnet with holes of density p

FL*

Oshikawa anomaly is satisfied by sum of spin liquid (1) and Fermi surface anomalies (p)

Metal with density p of spin-1/2, charge $+e$ 'holes' (or 'magnetic polarons') with coherent inter-layer transport for Yamaji effect.



Area $p/8$

$$= (|\uparrow\downarrow\rangle - |\downarrow\uparrow\rangle) / \sqrt{2} \quad \text{green rectangle with arrow} = (|\uparrow\circ\rangle + |\circ\uparrow\rangle) / \sqrt{2}$$

T. Senthil, S. S., M. Vojta, PRL **90**, 216403 (2003); R. K. Kaul, A. Kolezhuk, M. Levin, S.S., T. Senthil, PRB **75**, 235122 (2007)

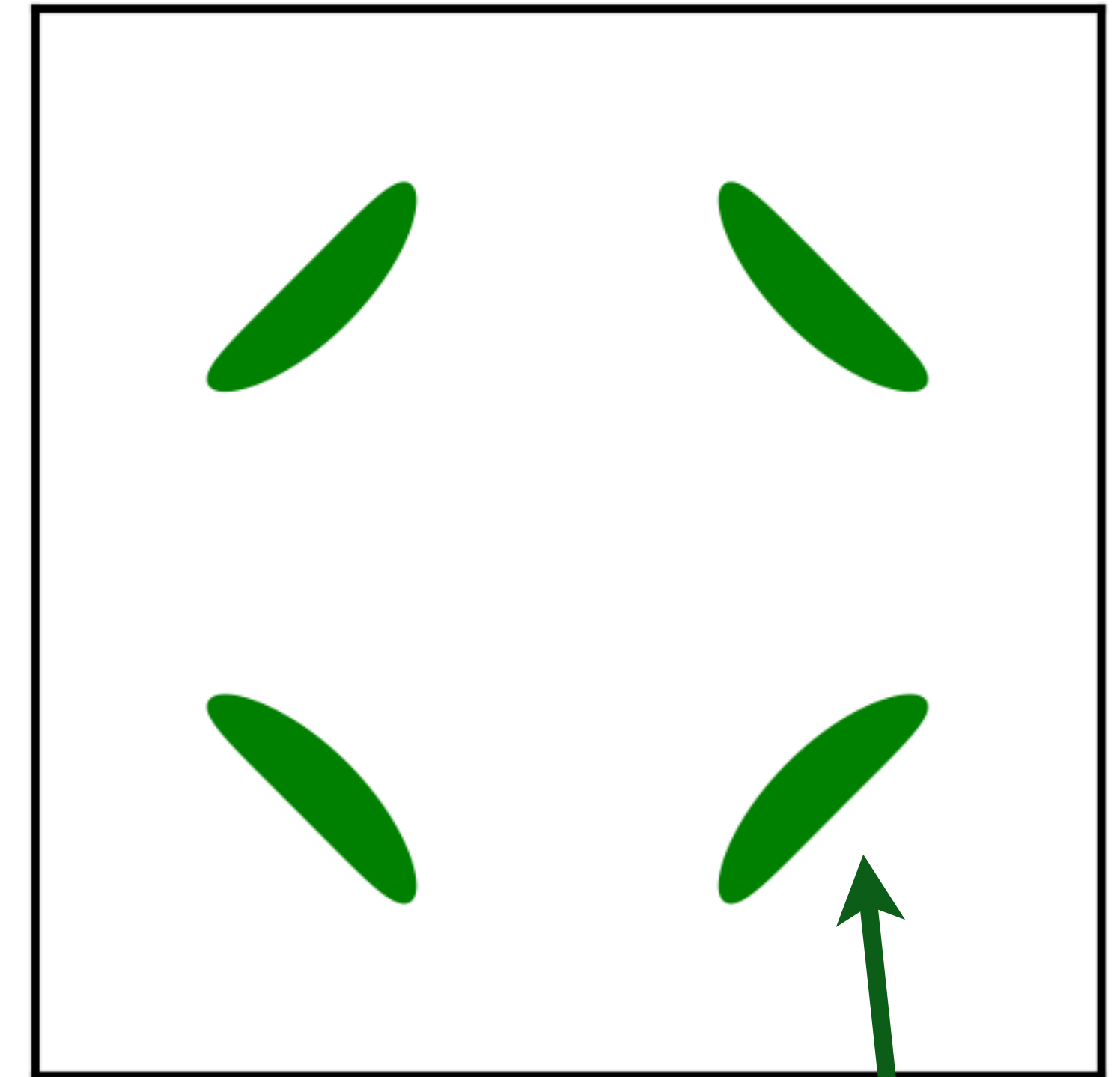
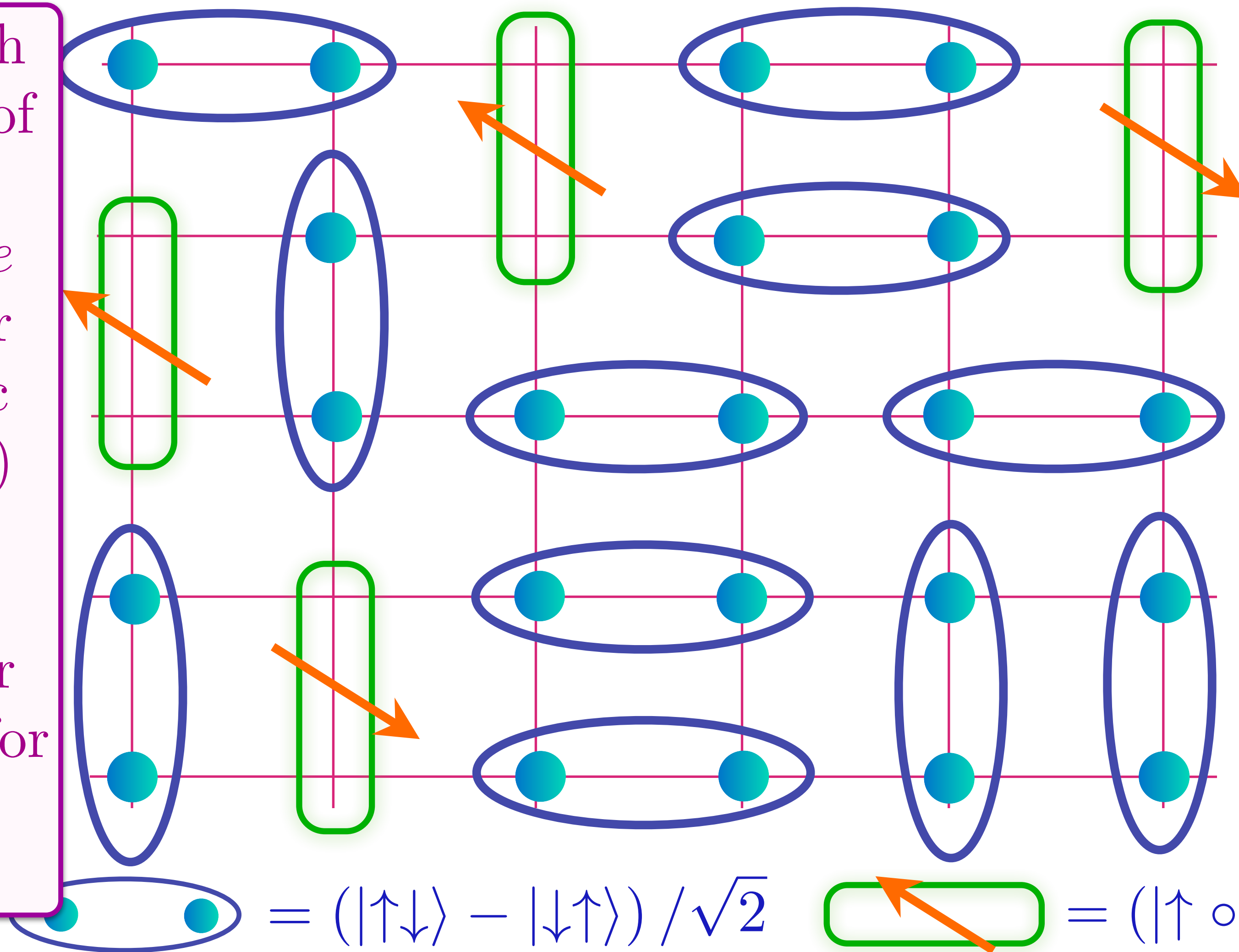
M. Punk, A. Allais, and S. Sachdev, PNAS **112**, 9552 (2015)

Doping an insulating antiferromagnet with holes of density p

FL*

Oshikawa anomaly is satisfied by sum of spin liquid (1) and Fermi surface anomalies (p)

Metal with density p of spin-1/2, charge $+e$ 'holes' (or 'magnetic polarons') with coherent inter-layer transport for Yamaji effect.



Area $p/8$

$$= (|\uparrow\downarrow\rangle - |\downarrow\uparrow\rangle) / \sqrt{2} \quad \text{green bar with arrow} = (|\uparrow\circ\rangle + |\circ\uparrow\rangle) / \sqrt{2}$$

T. Senthil, S. S., M. Vojta, PRL **90**, 216403 (2003); R. K. Kaul, A. Kolezhuk, M. Levin, S.S., T. Senthil, PRB **75**, 235122 (2007)

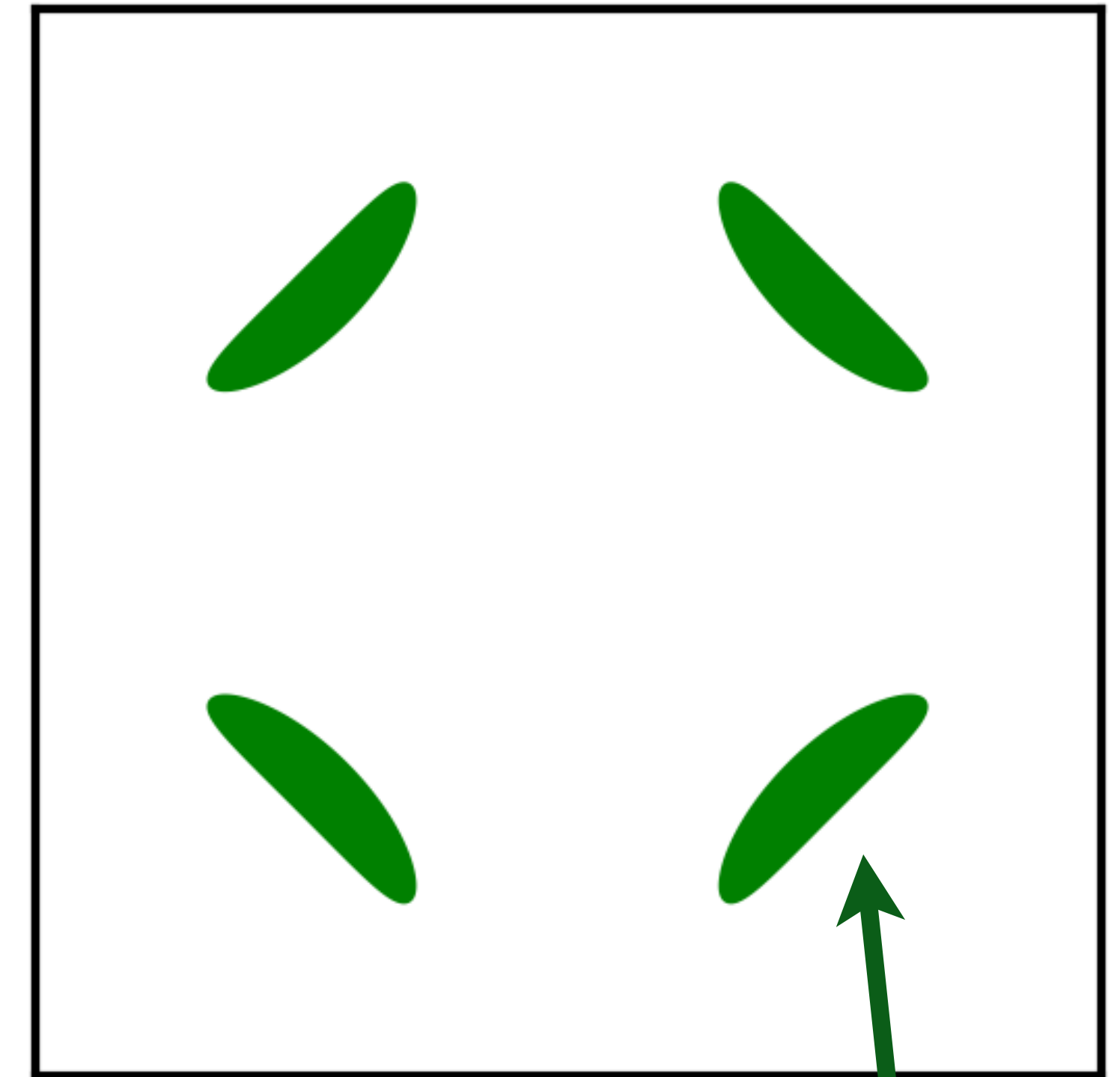
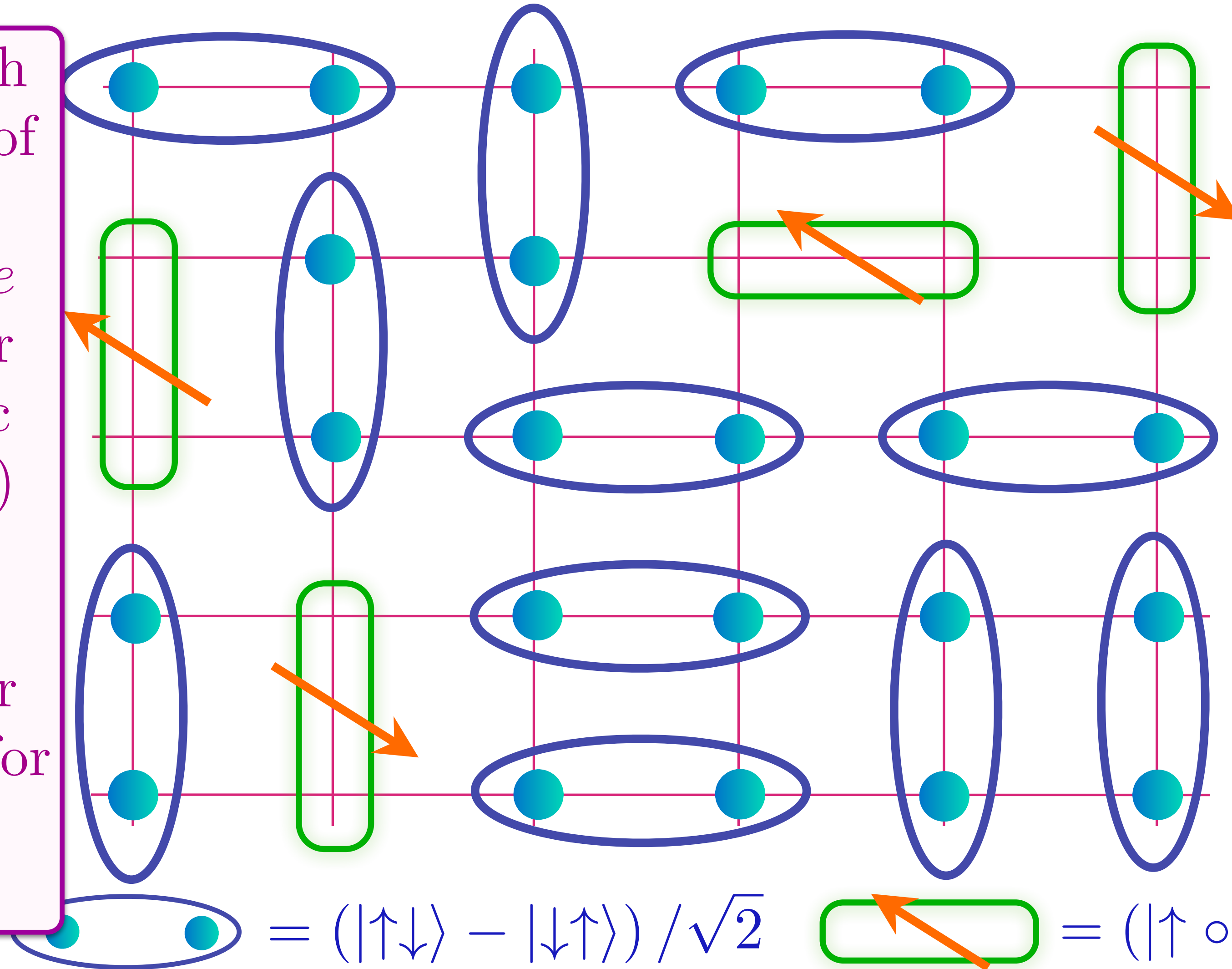
M. Punk, A. Allais, and S. Sachdev, PNAS **112**, 9552 (2015)

Doping an insulating antiferromagnet with holes of density p

FL*

Oshikawa anomaly is satisfied by sum of spin liquid (1) and Fermi surface anomalies (p)

Metal with density p of spin-1/2, charge $+e$ 'holes' (or 'magnetic polarons') with coherent inter-layer transport for Yamaji effect.



Area $p/8$

$$= (|\uparrow\downarrow\rangle - |\downarrow\uparrow\rangle) / \sqrt{2} \quad \text{green rectangle with arrow} = (|\uparrow\circ\rangle + |\circ\uparrow\rangle) / \sqrt{2}$$

T. Senthil, S. S., M. Vojta, PRL **90**, 216403 (2003); R. K. Kaul, A. Kolezhuk, M. Levin, S.S., T. Senthil, PRB **75**, 235122 (2007)

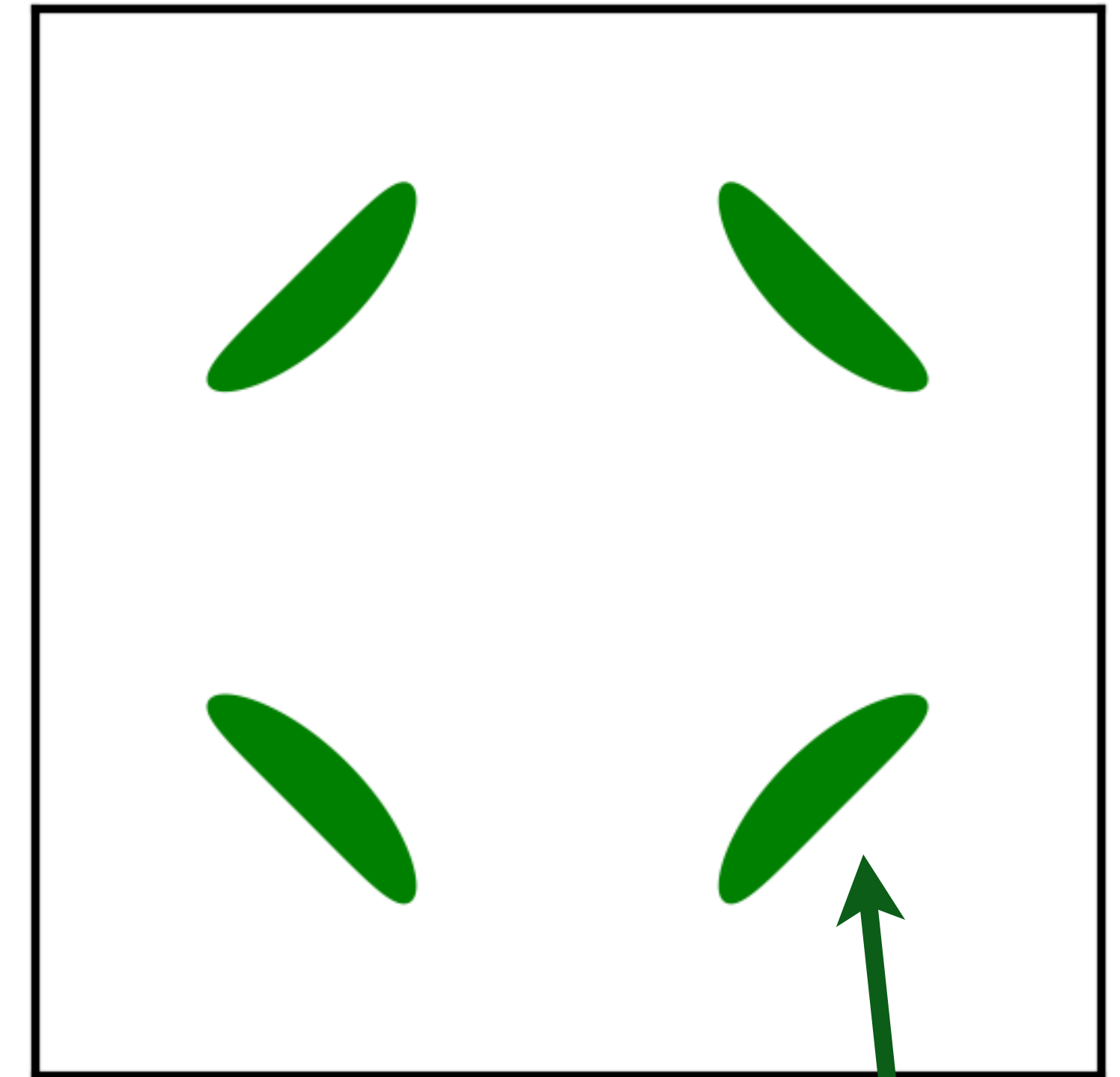
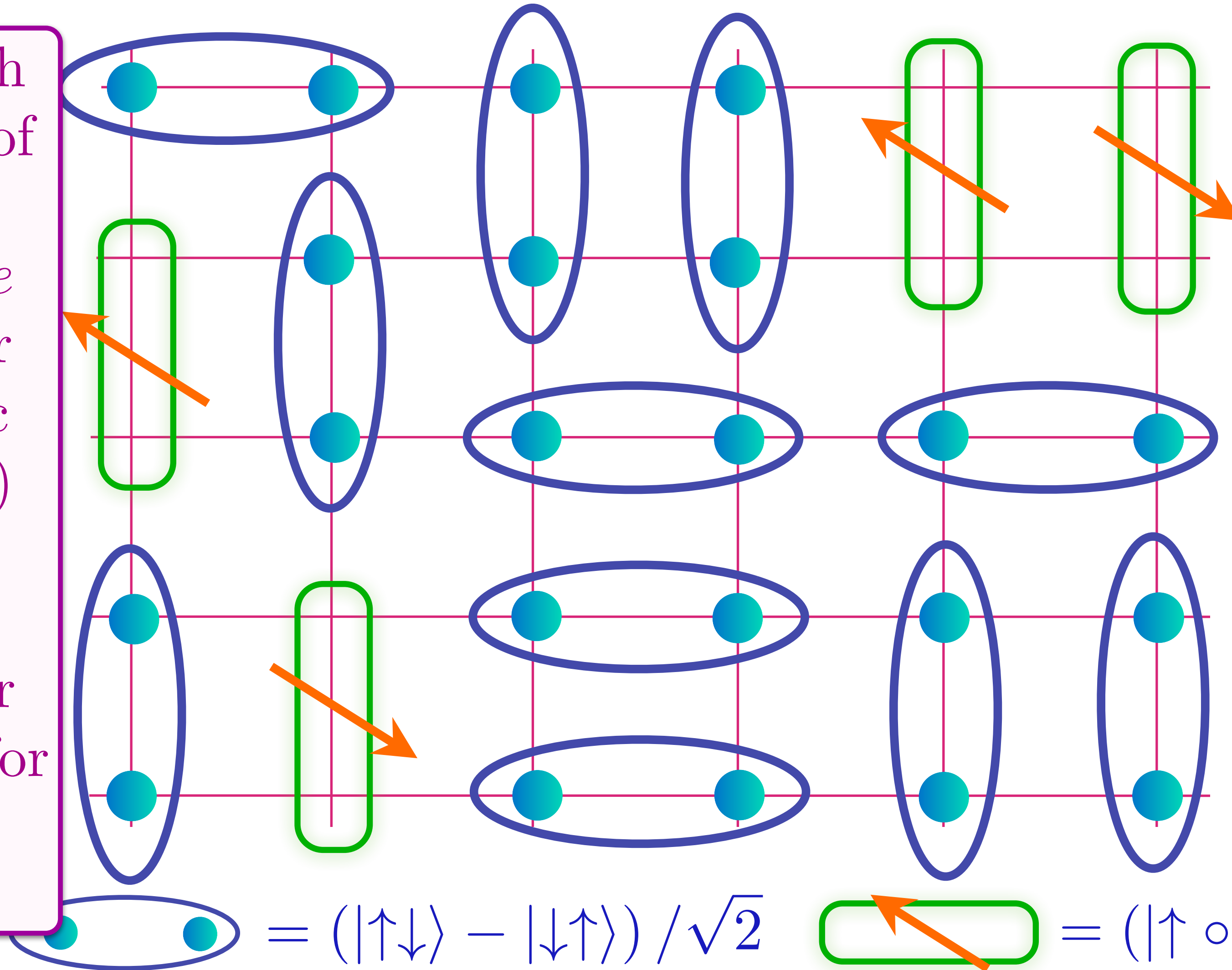
M. Punk, A. Allais, and S. Sachdev, PNAS **112**, 9552 (2015)

Doping an insulating antiferromagnet with holes of density p

FL*

Oshikawa anomaly is satisfied by sum of spin liquid (1) and Fermi surface anomalies (p)

Metal with density p of spin-1/2, charge $+e$ 'holes' (or 'magnetic polarons') with coherent inter-layer transport for Yamaji effect.



Area $p/8$

$$= (|\uparrow\downarrow\rangle - |\downarrow\uparrow\rangle) / \sqrt{2} \quad \text{green rectangle with arrow} = (|\uparrow\circ\rangle + |\circ\uparrow\rangle) / \sqrt{2}$$

T. Senthil, S. S., M. Vojta, PRL **90**, 216403 (2003); R. K. Kaul, A. Kolezhuk, M. Levin, S.S., T. Senthil, PRB **75**, 235122 (2007)

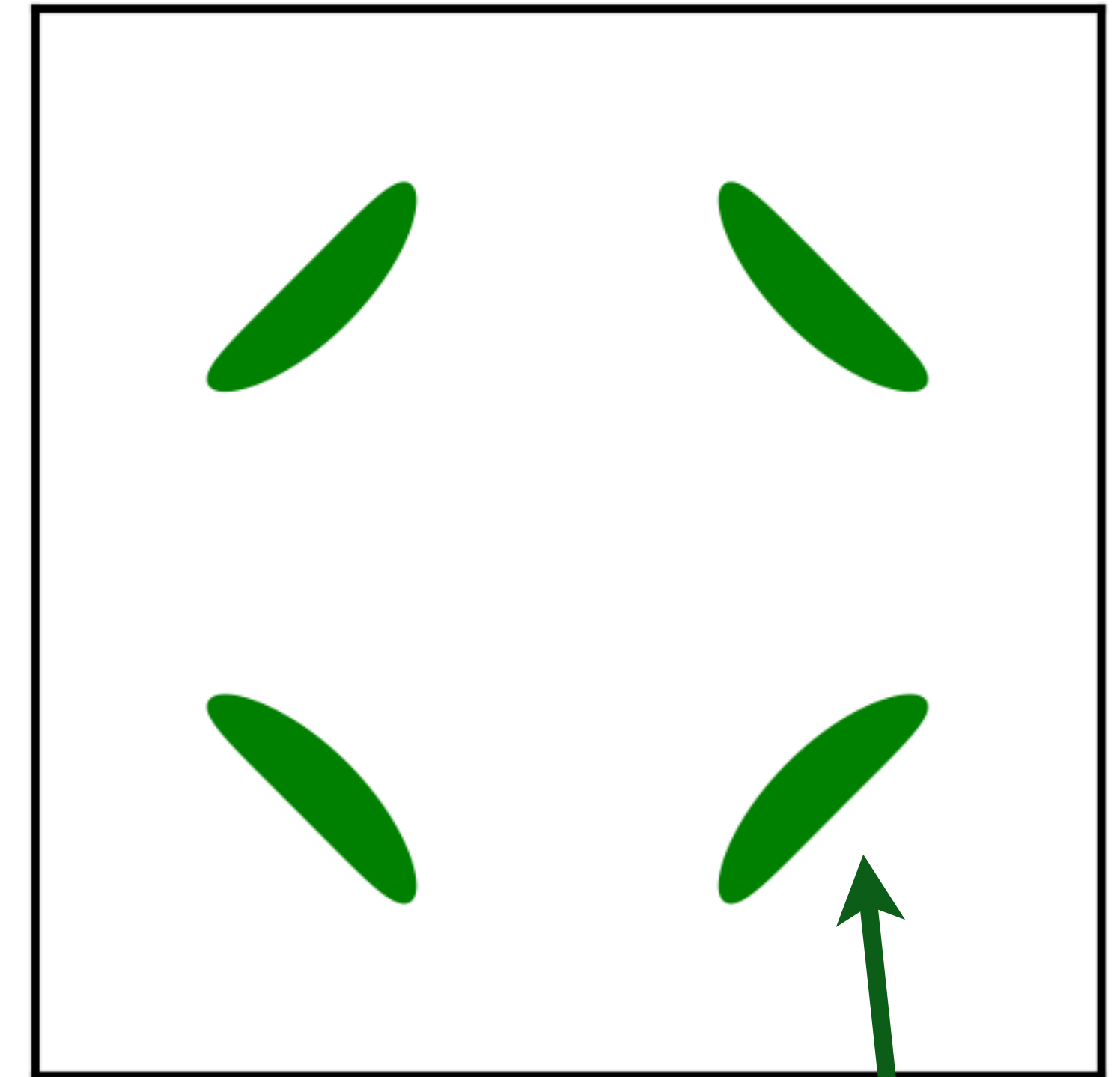
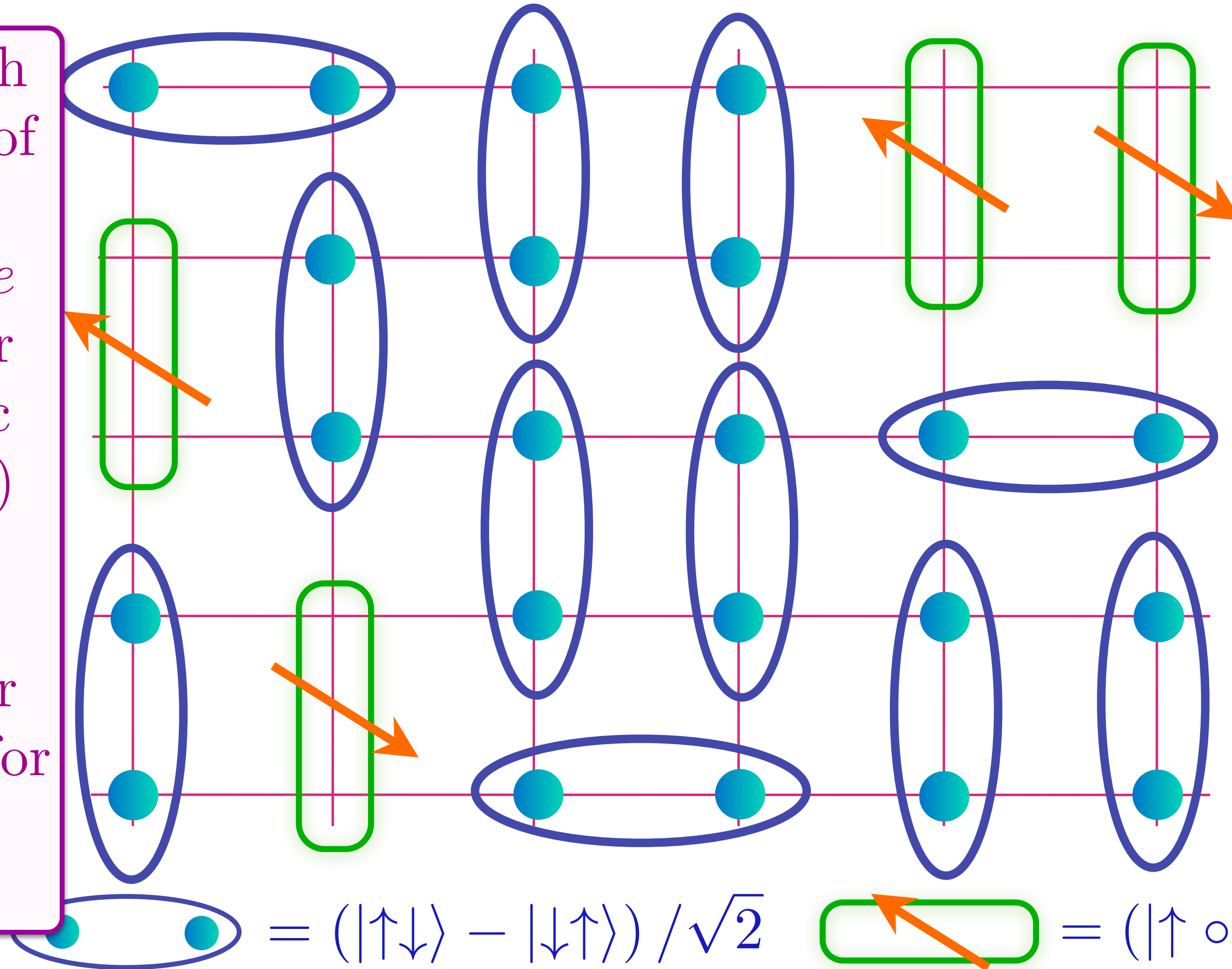
M. Punk, A. Allais, and S. Sachdev, PNAS **112**, 9552 (2015)

Doping an insulating antiferromagnet with holes of density p

FL*

Oshikawa anomaly is satisfied by sum of spin liquid (1) and Fermi surface anomalies (p)

Metal with density p of spin-1/2, charge $+e$ 'holes' (or 'magnetic polarons') with coherent inter-layer transport for Yamaji effect.



Area $p/8$

$$= (|\uparrow\downarrow\rangle - |\downarrow\uparrow\rangle) / \sqrt{2} \quad \text{green rectangle with arrow} = (|\uparrow\circ\rangle + |\circ\uparrow\rangle) / \sqrt{2}$$

T. Senthil, S. S., M. Vojta, PRL **90**, 216403 (2003); R. K. Kaul, A. Kolezhuk, M. Levin, S.S., T. Senthil, PRB **75**, 235122 (2007)

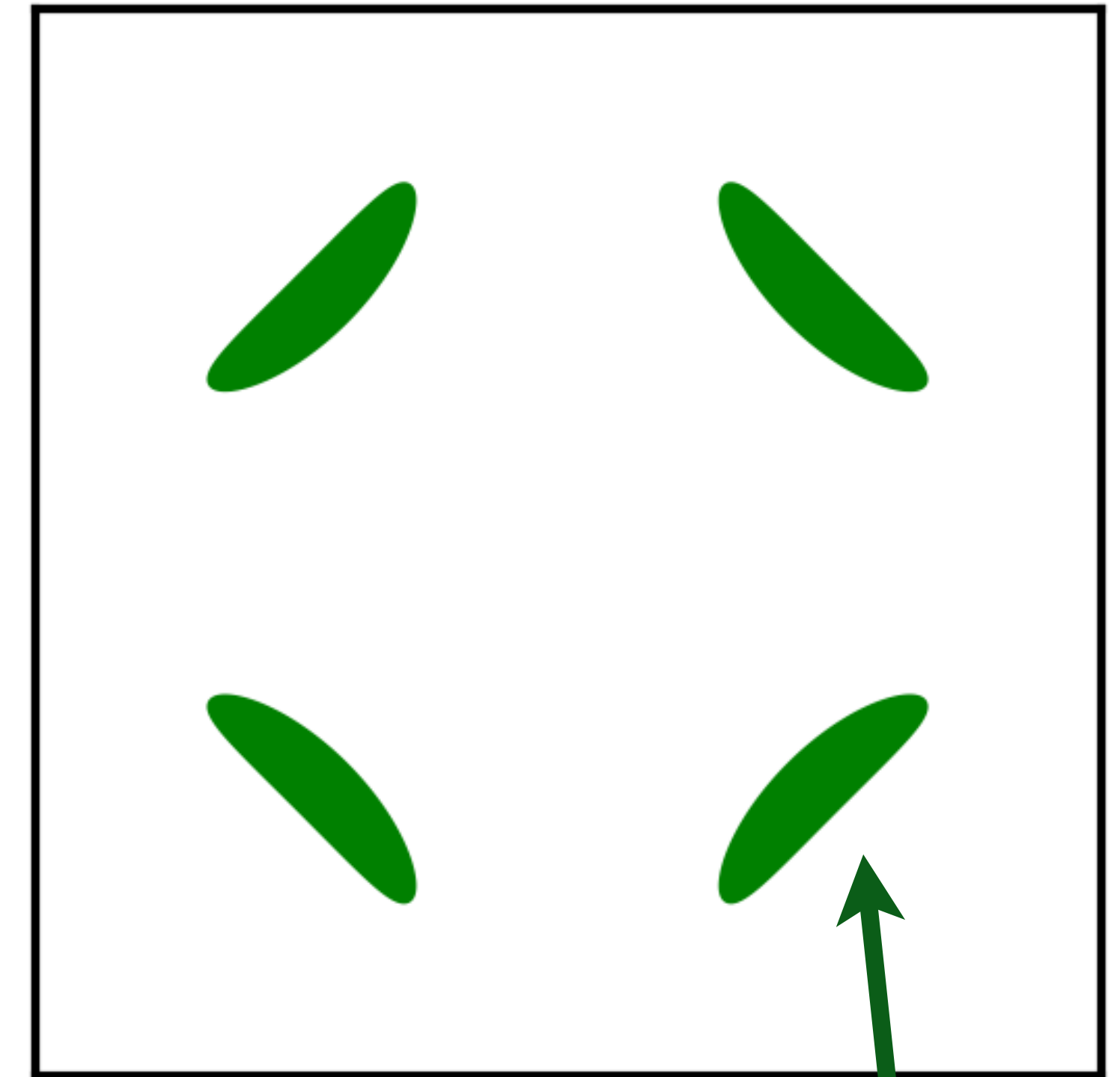
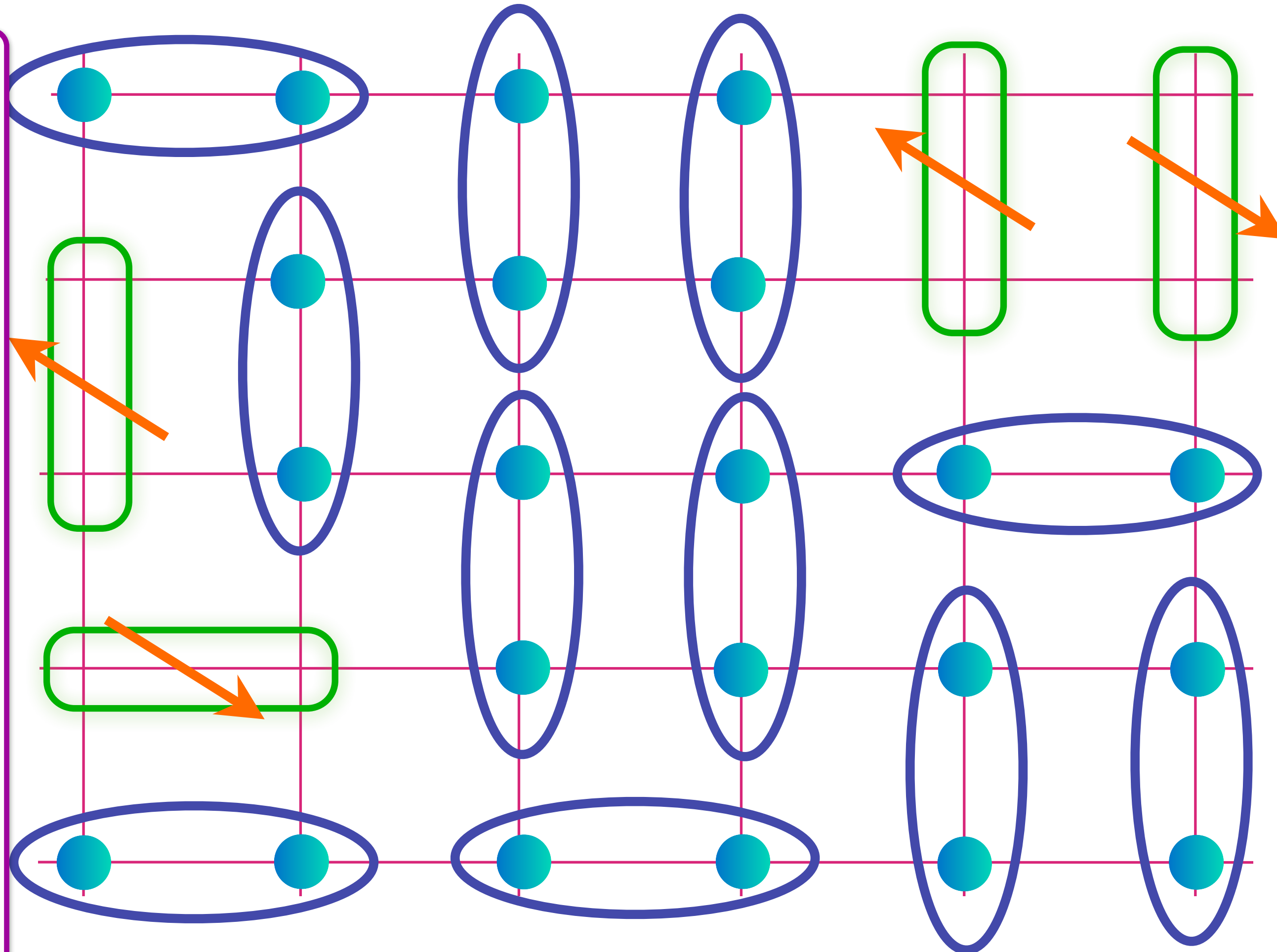
M. Punk, A. Allais, and S. Sachdev, PNAS **112**, 9552 (2015)

Doping an insulating antiferromagnet with holes of density p

FL*

Oshikawa anomaly is satisfied by sum of spin liquid (1) and Fermi surface anomalies (p)

Metal with density p of spin-1/2, charge $+e$ 'holes' (or 'magnetic polarons') with coherent inter-layer transport for Yamaji effect.



Area $p/8$

$$\text{Blue circle} = (|\uparrow\downarrow\rangle - |\downarrow\uparrow\rangle) / \sqrt{2} \quad \text{Green rectangle} = (|\uparrow\circ\rangle + |\circ\uparrow\rangle) / \sqrt{2}$$

T. Senthil, S. S., M. Vojta, PRL **90**, 216403 (2003); R. K. Kaul, A. Kolezhuk, M. Levin, S.S., T. Senthil, PRB **75**, 235122 (2007)

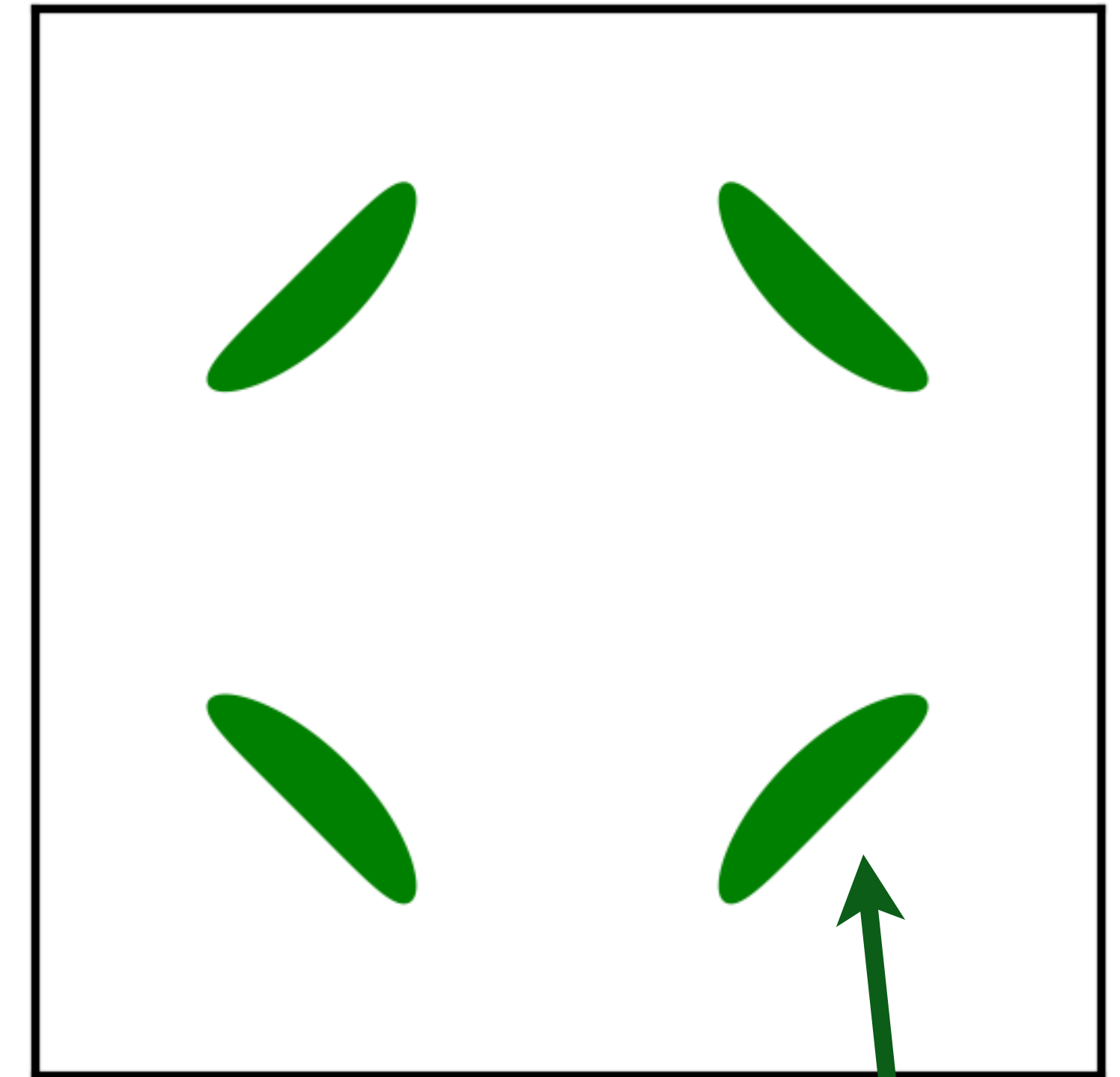
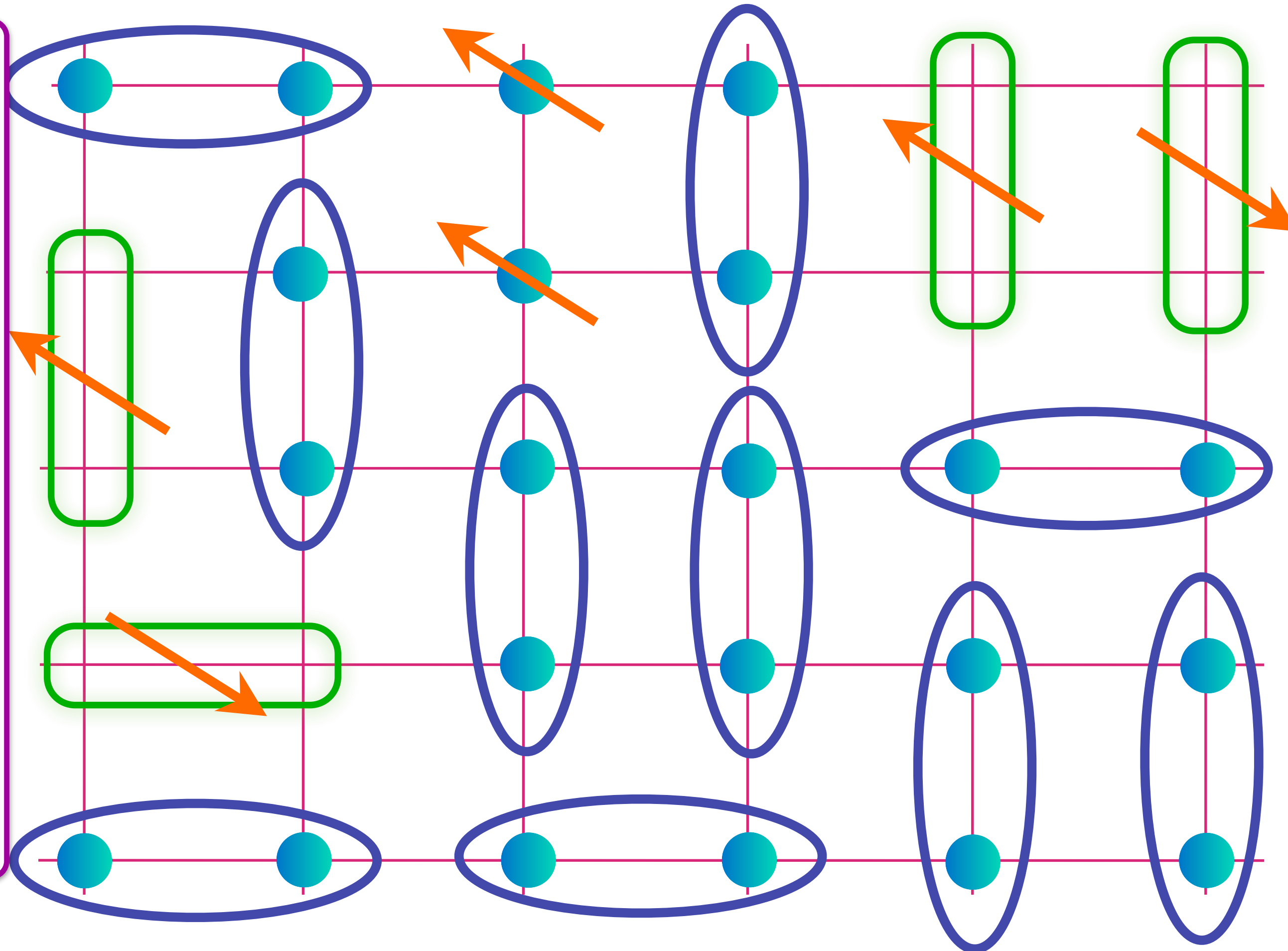
M. Punk, A. Allais, and S. Sachdev, PNAS **112**, 9552 (2015)

Doping an insulating antiferromagnet with holes of density p

FL*

Oshikawa anomaly is satisfied by sum of spin liquid (1) and Fermi surface anomalies (p)

Metal with density p of spin-1/2, charge $+e$ 'holes' (or 'magnetic polarons') and charge 0, spin-1/2 'spinons'



$$\text{Blue oval with two dots} = (|\uparrow\downarrow\rangle - |\downarrow\uparrow\rangle) / \sqrt{2} \quad \text{Green rectangle with arrow} = (|\uparrow\circ\rangle + |\circ\uparrow\rangle) / \sqrt{2}$$

Area $p/8$

T. Senthil, S. S., M. Vojta, PRL **90**, 216403 (2003); R. K. Kaul, A. Kolezhuk, M. Levin, S.S., T. Senthil, PRB **75**, 235122 (2007)

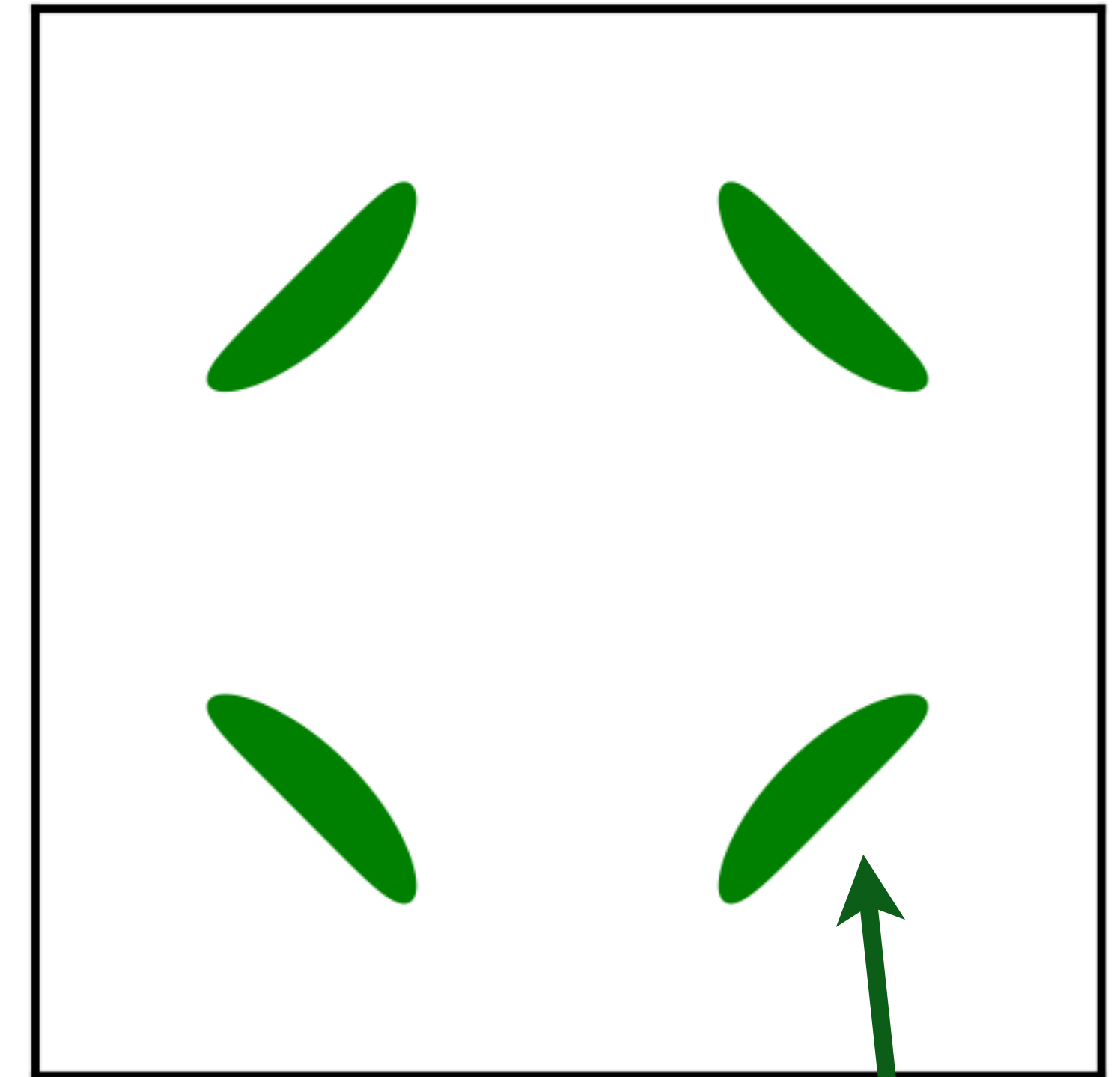
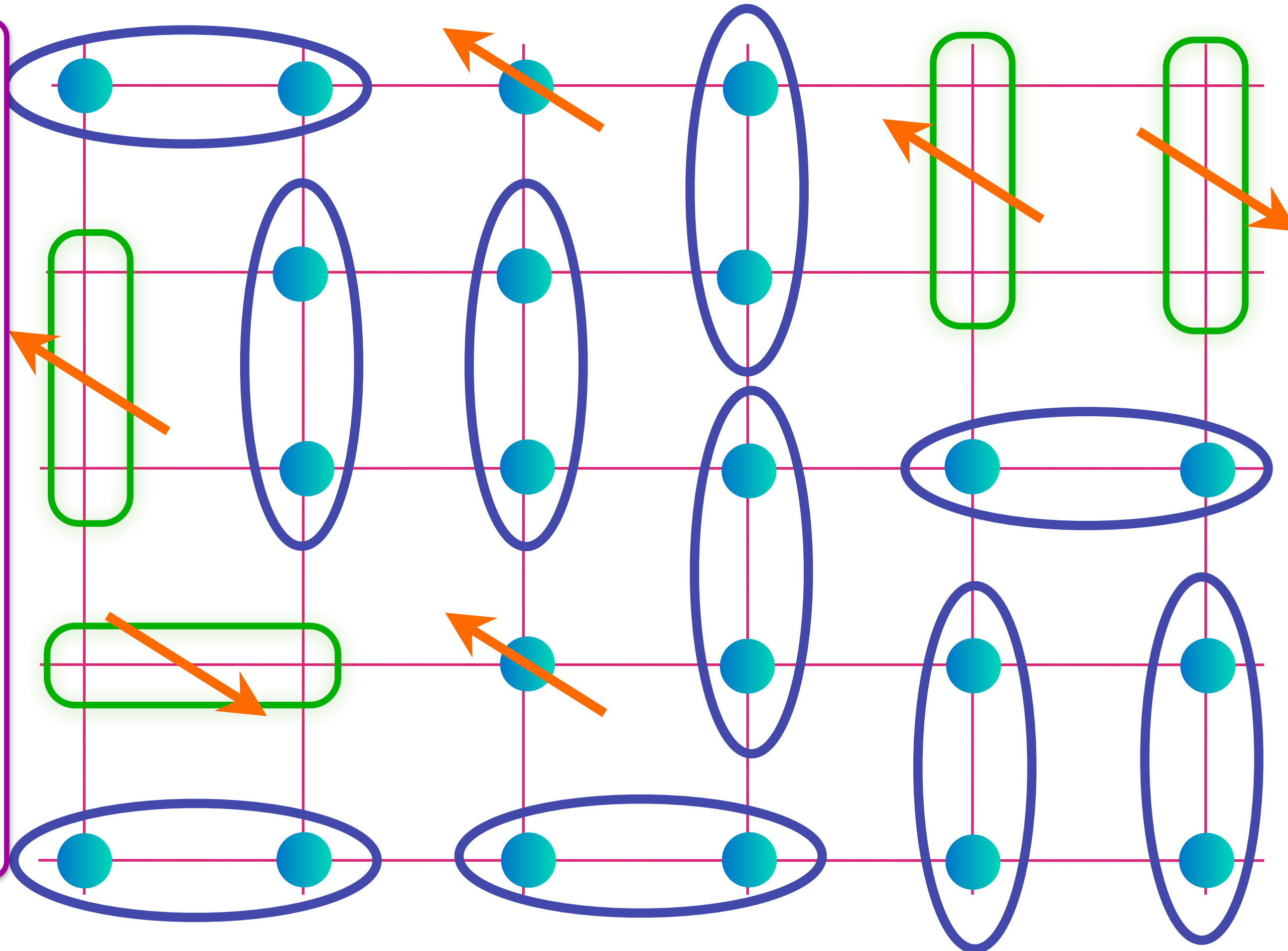
M. Punk, A. Allais, and S. Sachdev, PNAS **112**, 9552 (2015)

Doping an insulating antiferromagnet with holes of density p

FL*

Oshikawa anomaly is satisfied by sum of spin liquid (1) and Fermi surface anomalies (p)

Metal with density p of spin-1/2, charge $+e$ 'holes' (or 'magnetic polarons') and charge 0, spin-1/2 'spinons'



$$\text{Blue oval with two dots} = (|\uparrow\downarrow\rangle - |\downarrow\uparrow\rangle) / \sqrt{2} \quad \text{Green rectangle with two dots and an arrow} = (|\uparrow\circ\rangle + |\circ\uparrow\rangle) / \sqrt{2}$$

Area $p/8$

T. Senthil, S. S., M. Vojta, PRL **90**, 216403 (2003); R. K. Kaul, A. Kolezhuk, M. Levin, S.S., T. Senthil, PRB **75**, 235122 (2007)

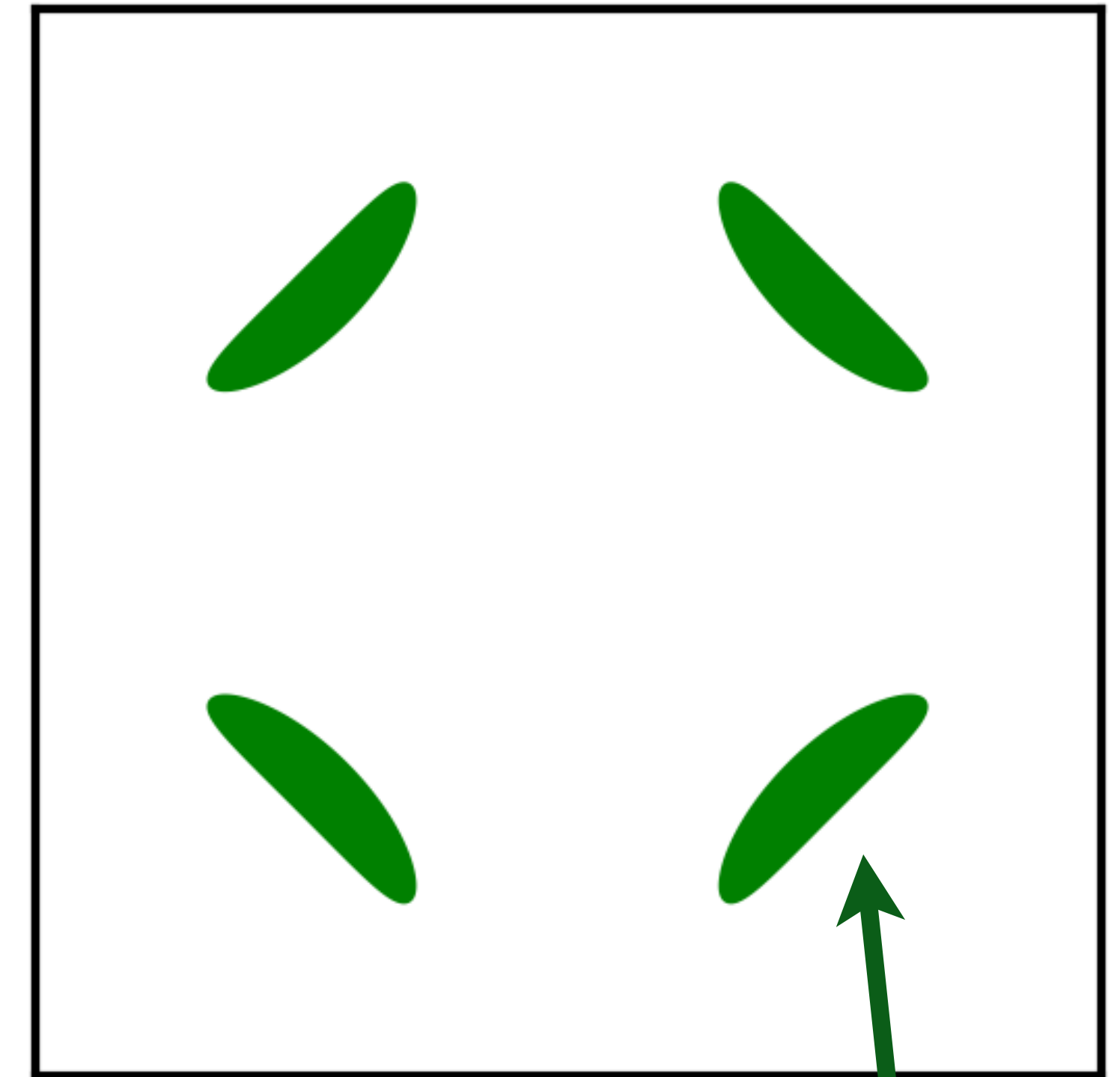
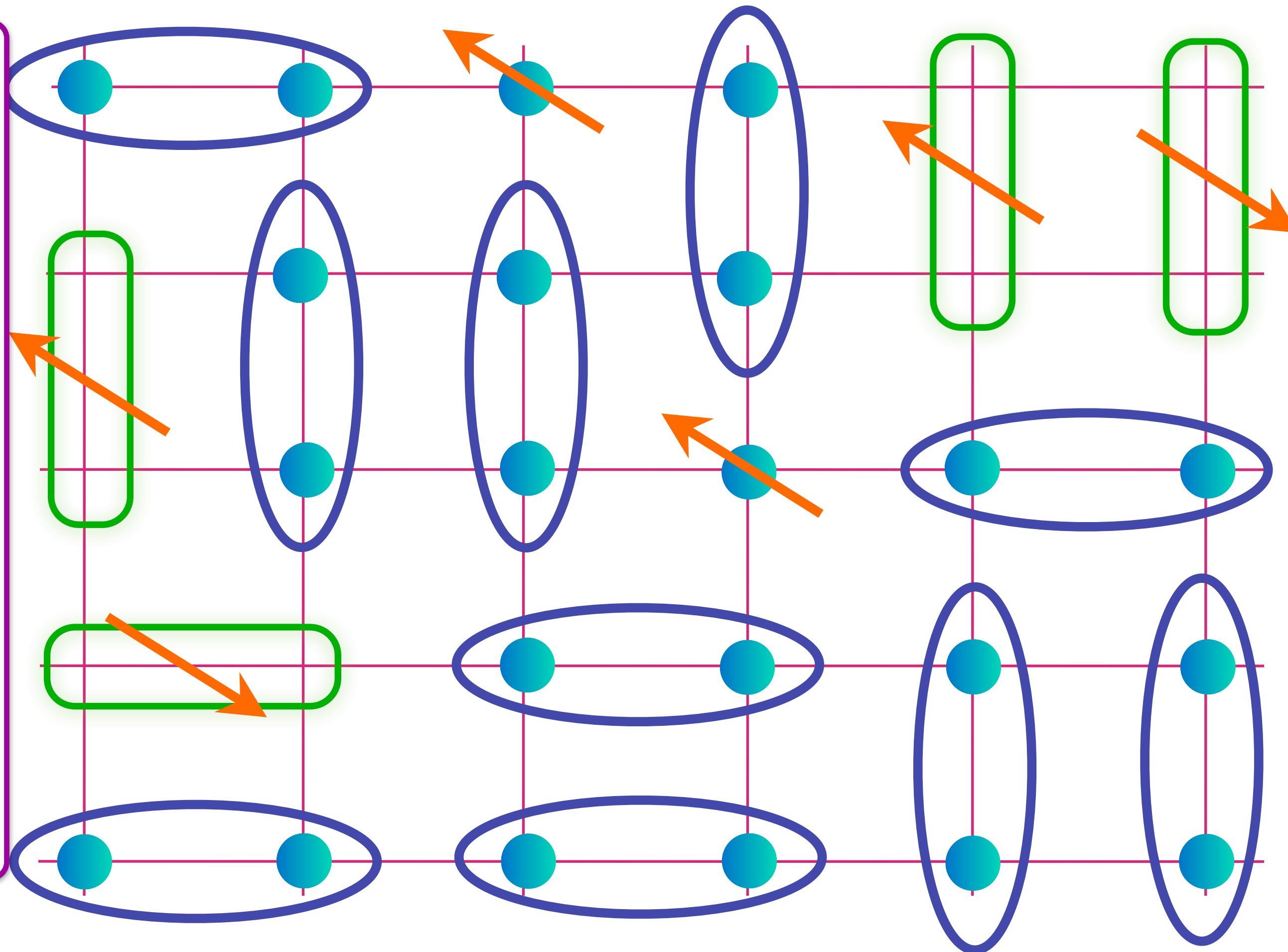
M. Punk, A. Allais, and S. Sachdev, PNAS **112**, 9552 (2015)

Doping an insulating antiferromagnet with holes of density p

FL*

Oshikawa anomaly is satisfied by sum of spin liquid (1) and Fermi surface anomalies (p)

Metal with density p of spin-1/2, charge $+e$ 'holes' (or 'magnetic polarons') and charge 0, spin-1/2 'spinons'



$$\text{Blue oval with two dots} = (|\uparrow\downarrow\rangle - |\downarrow\uparrow\rangle) / \sqrt{2} \quad \text{Green rectangle with arrow} = (|\uparrow\circ\rangle + |\circ\uparrow\rangle) / \sqrt{2}$$

Area $p/8$

T. Senthil, S. S., M. Vojta, PRL **90**, 216403 (2003); R. K. Kaul, A. Kolezhuk, M. Levin, S.S., T. Senthil, PRB **75**, 235122 (2007)

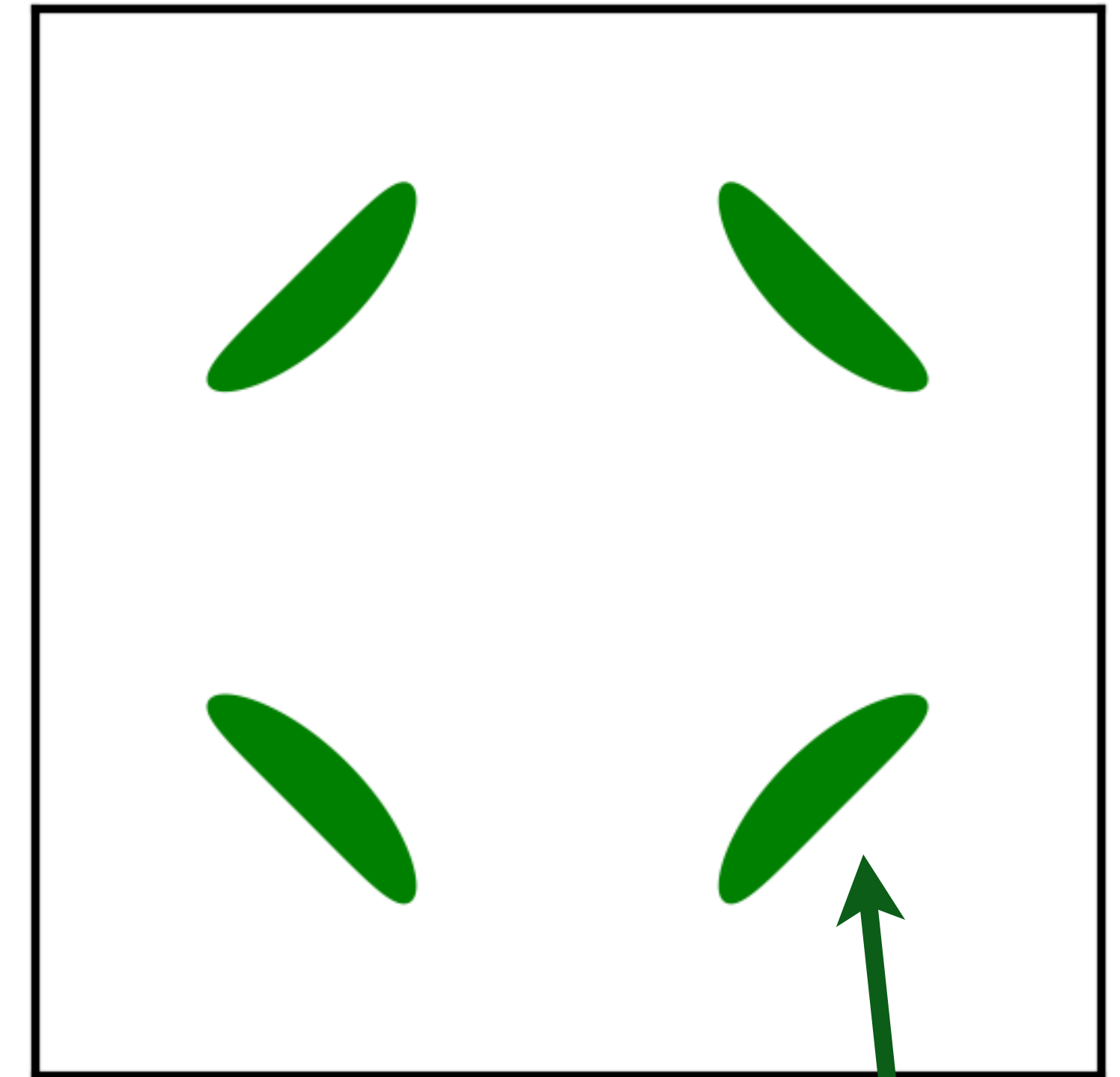
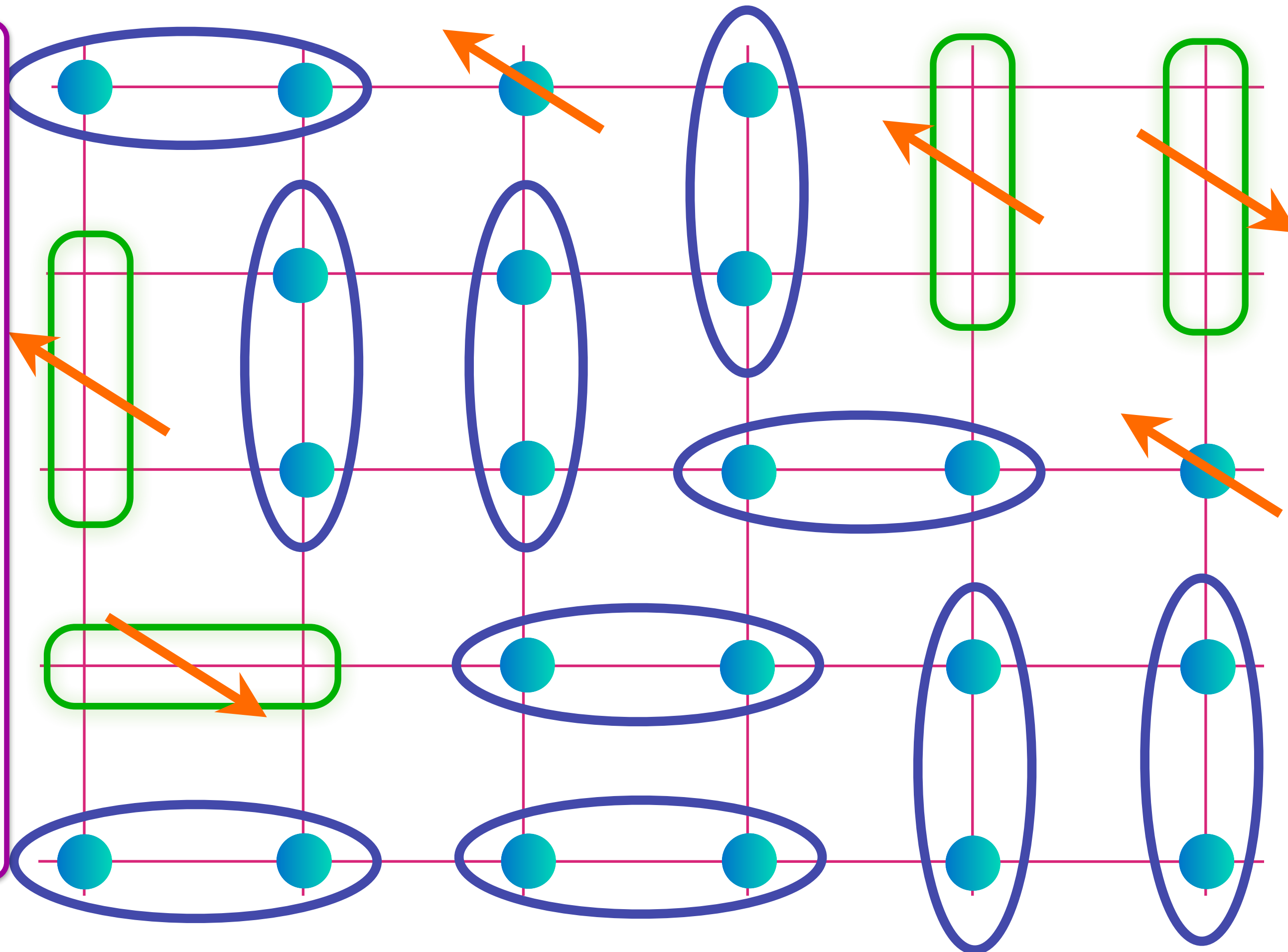
M. Punk, A. Allais, and S. Sachdev, PNAS **112**, 9552 (2015)

Doping an insulating antiferromagnet with holes of density p

FL*

Oshikawa anomaly is satisfied by sum of spin liquid (1) and Fermi surface anomalies (p)

Metal with density p of spin-1/2, charge $+e$ 'holes' (or 'magnetic polarons') and charge 0, spin-1/2 'spinons'



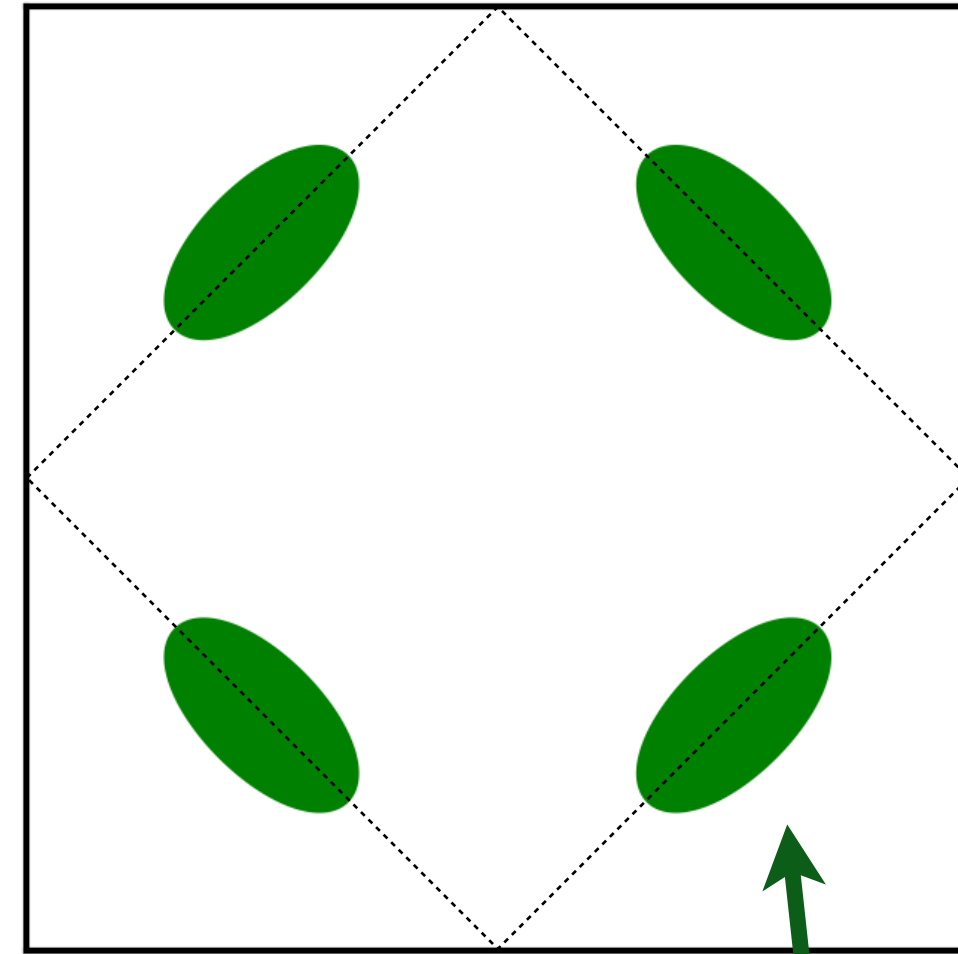
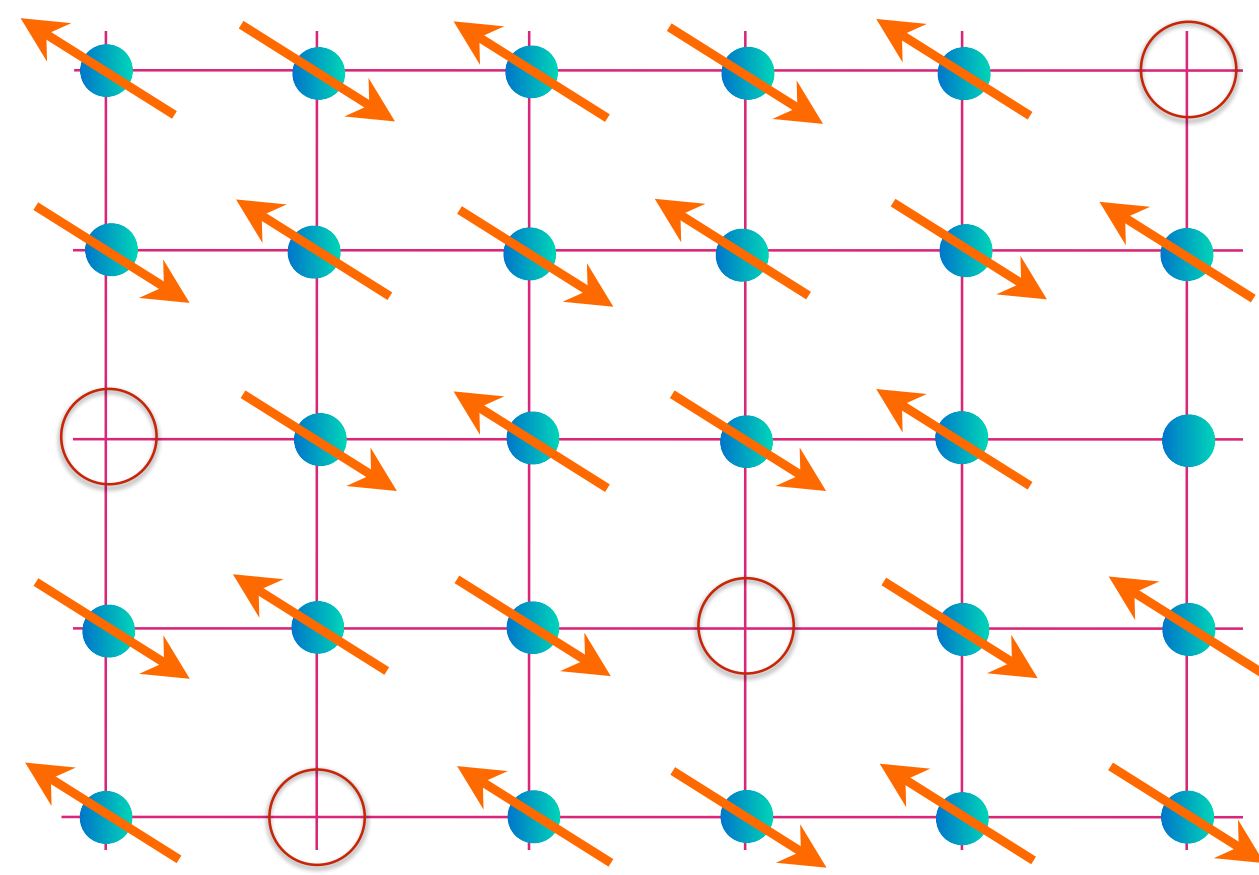
$$\text{Blue oval with two dots} = (|\uparrow\downarrow\rangle - |\downarrow\uparrow\rangle) / \sqrt{2} \quad \text{Green rectangle with two dots and an arrow} = (|\uparrow\circ\rangle + |\circ\uparrow\rangle) / \sqrt{2}$$

Area $p/8$

T. Senthil, S. S., M. Vojta, PRL **90**, 216403 (2003); R. K. Kaul, A. Kolezhuk, M. Levin, S.S., T. Senthil, PRB **75**, 235122 (2007)

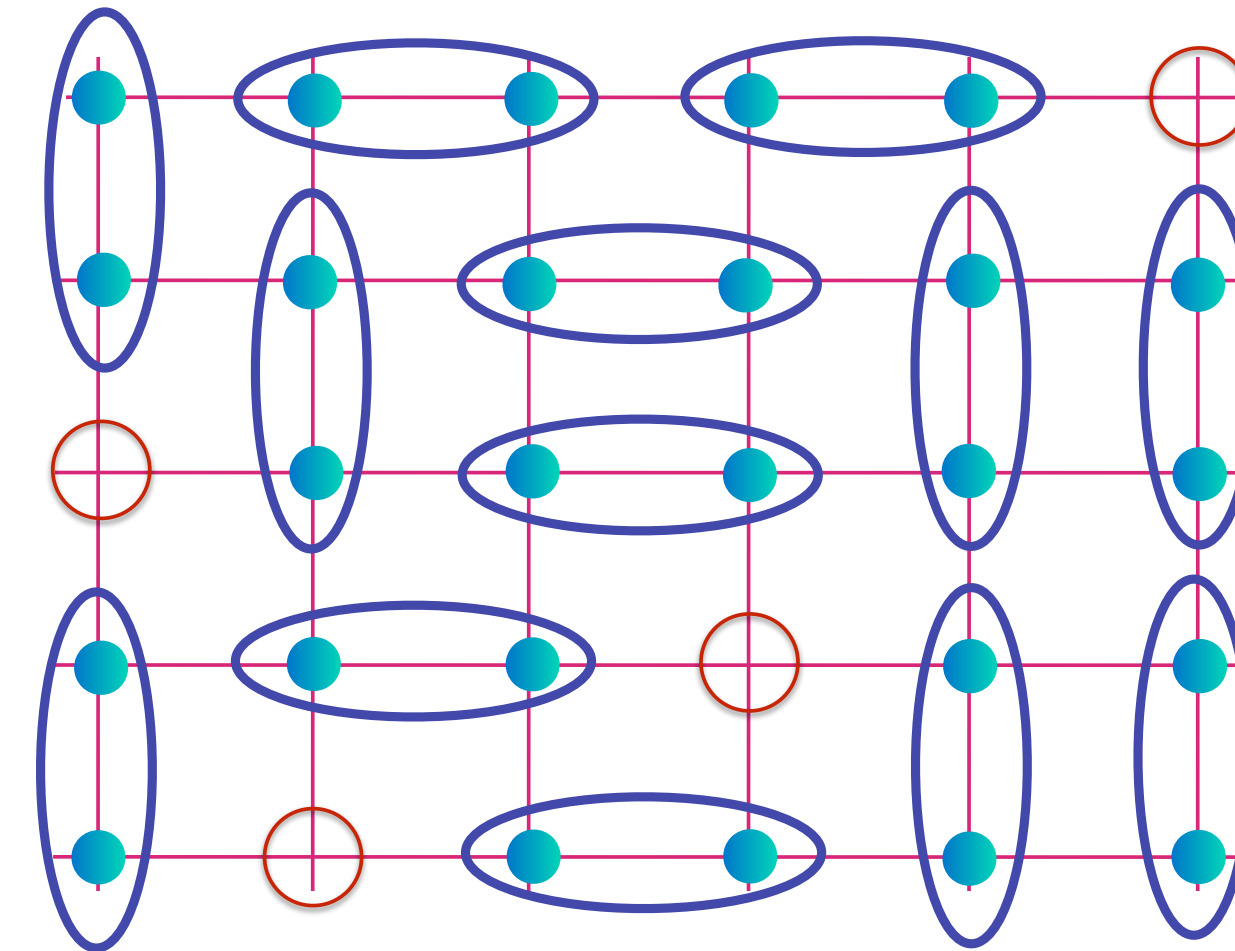
M. Punk, A. Allais, and S. Sachdev, PNAS **112**, 9552 (2015)

Doping an insulating antiferromagnet with holes of density p



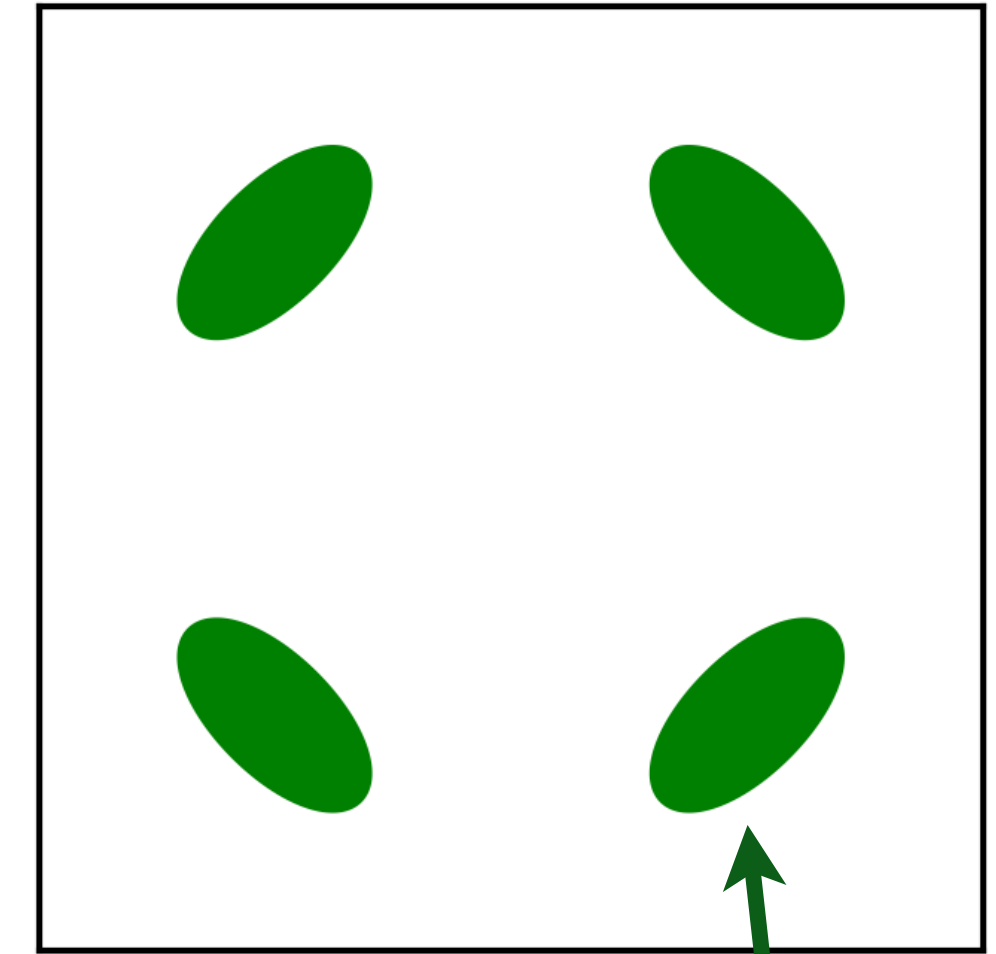
Area $p/4$

AF metal and SDW fluctuation

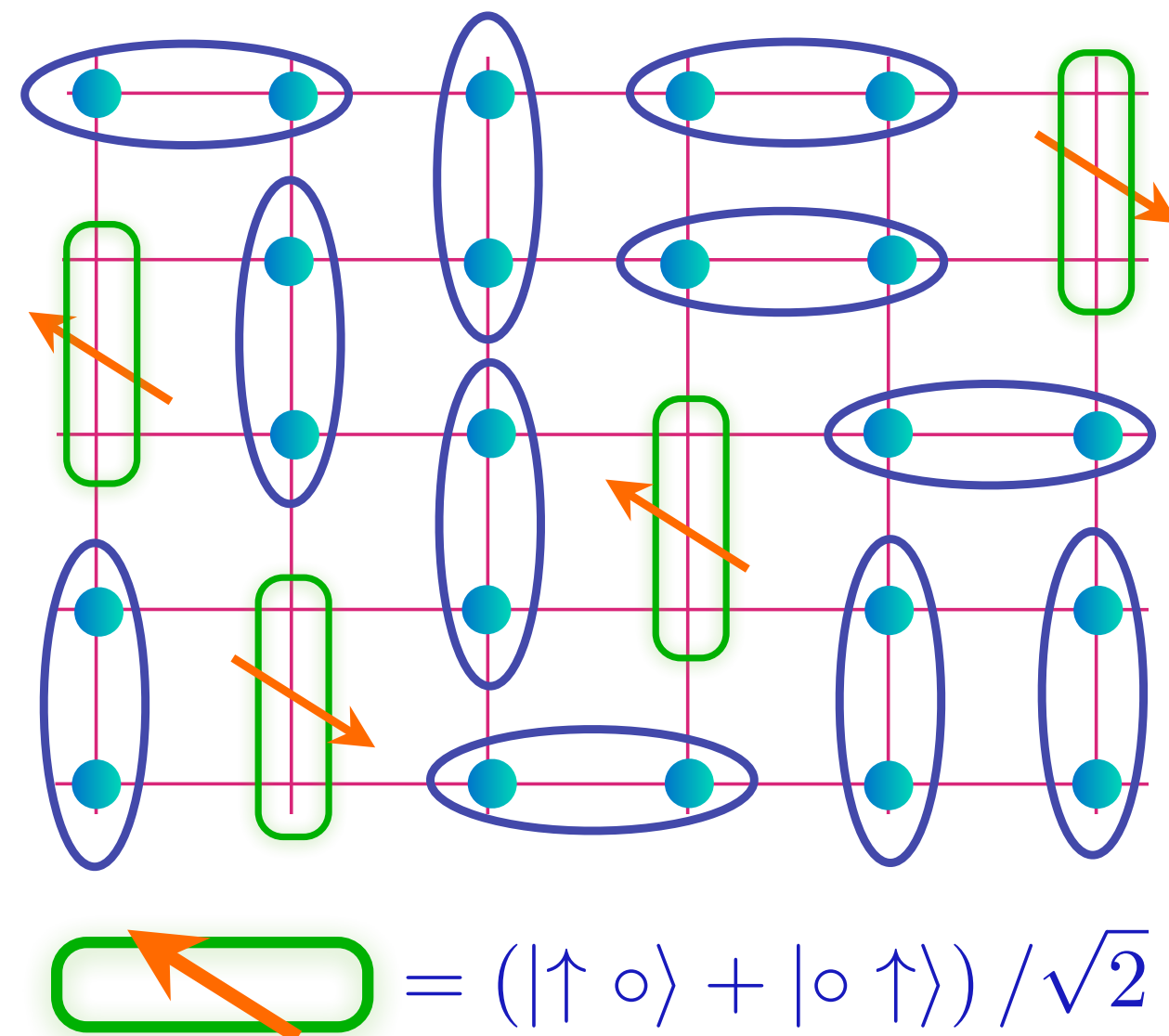


$$\text{blue ellipse} = (|\uparrow\downarrow\rangle - |\downarrow\uparrow\rangle) / \sqrt{2}$$

Holon metal

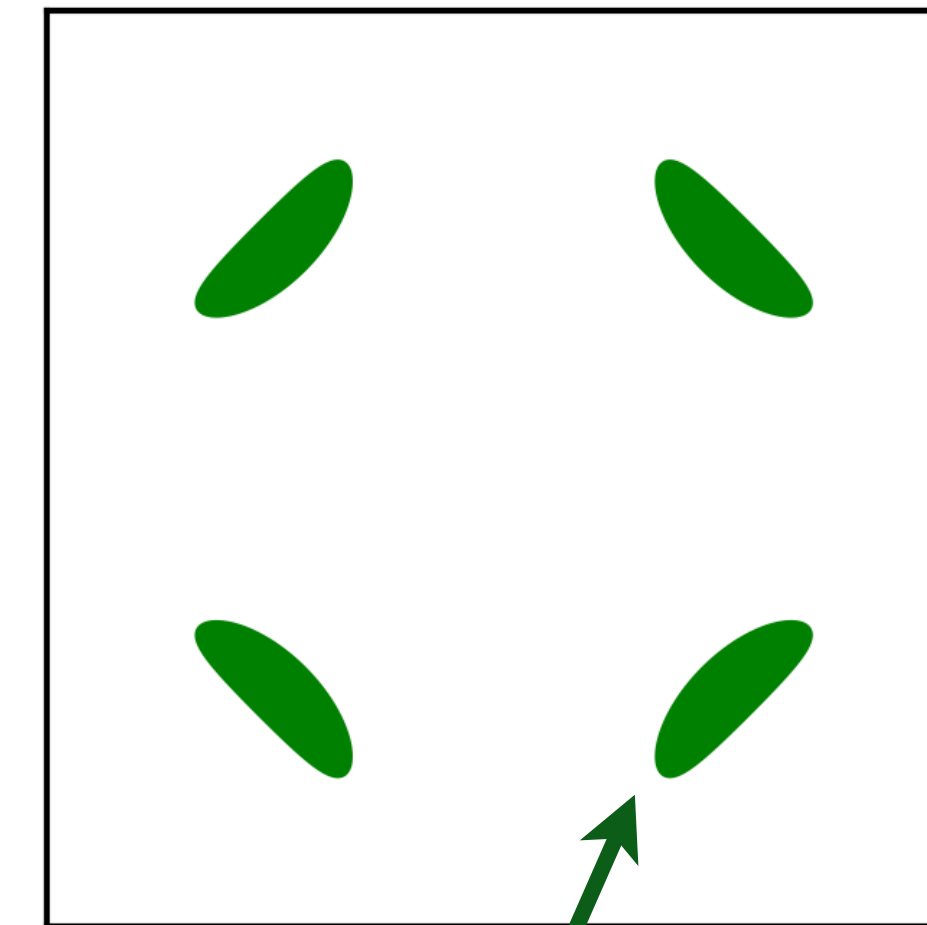


Area $p/4$



FL*

$$\text{green rectangle} = (|\uparrow\circ\rangle + |\circ\uparrow\rangle) / \sqrt{2}$$



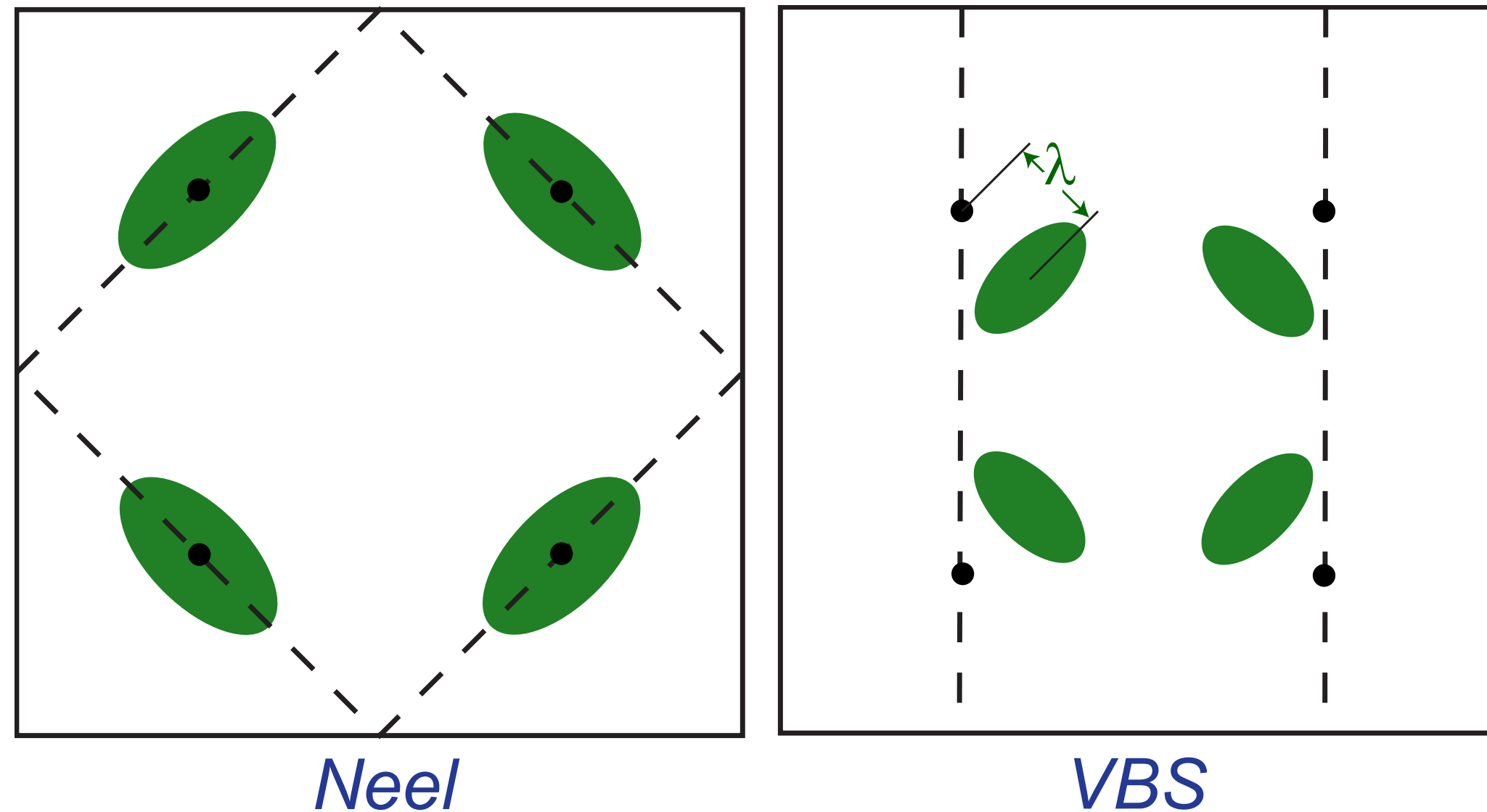
Area $p/8$

Quantization of spin liquid anomaly implies Fermi surface areas are also quantized and robust to all corrections.

T. Senthil, S. S., M. Vojta, PRL **90**, 216403 (2003);
 R. K. Kaul, A. Kolezhuk, M. Levin, S.S., T. Senthil, PRB **75**, 235122 (2007)
 M. Punk, A. Allais, and S. S., PNAS **112**, 9552 (2015)
 E. Mascot, A. Nikolaenko, M. Tikhanovskaya, Ya-Hui Zhang, D. K. Morr, S. S., PRB **105**, 075146 (2022)

Hole dynamics in an antiferromagnet across a deconfined quantum critical point

Ribhu K. Kaul,¹ Alexei Kolezhuk,^{1,2} Michael Levin,¹ Subir Sachdev,¹ and T. Senthil^{3,4}



The dashed line in the Néel phase indicates the boundary of the magnetic Brillouin zone. Only the Fermi surfaces within this zone contribute to the Luttinger counting, and so the area of each ellipse is $\mathcal{A}_F = (2\pi)^2 \delta/4$. In the VBS phase, all four pockets are inequivalent, and so the area of each ellipse is $\mathcal{A}_F = (2\pi)^2 \delta/8$.

Factor of 2 between
SDW fluctuation
and FL*

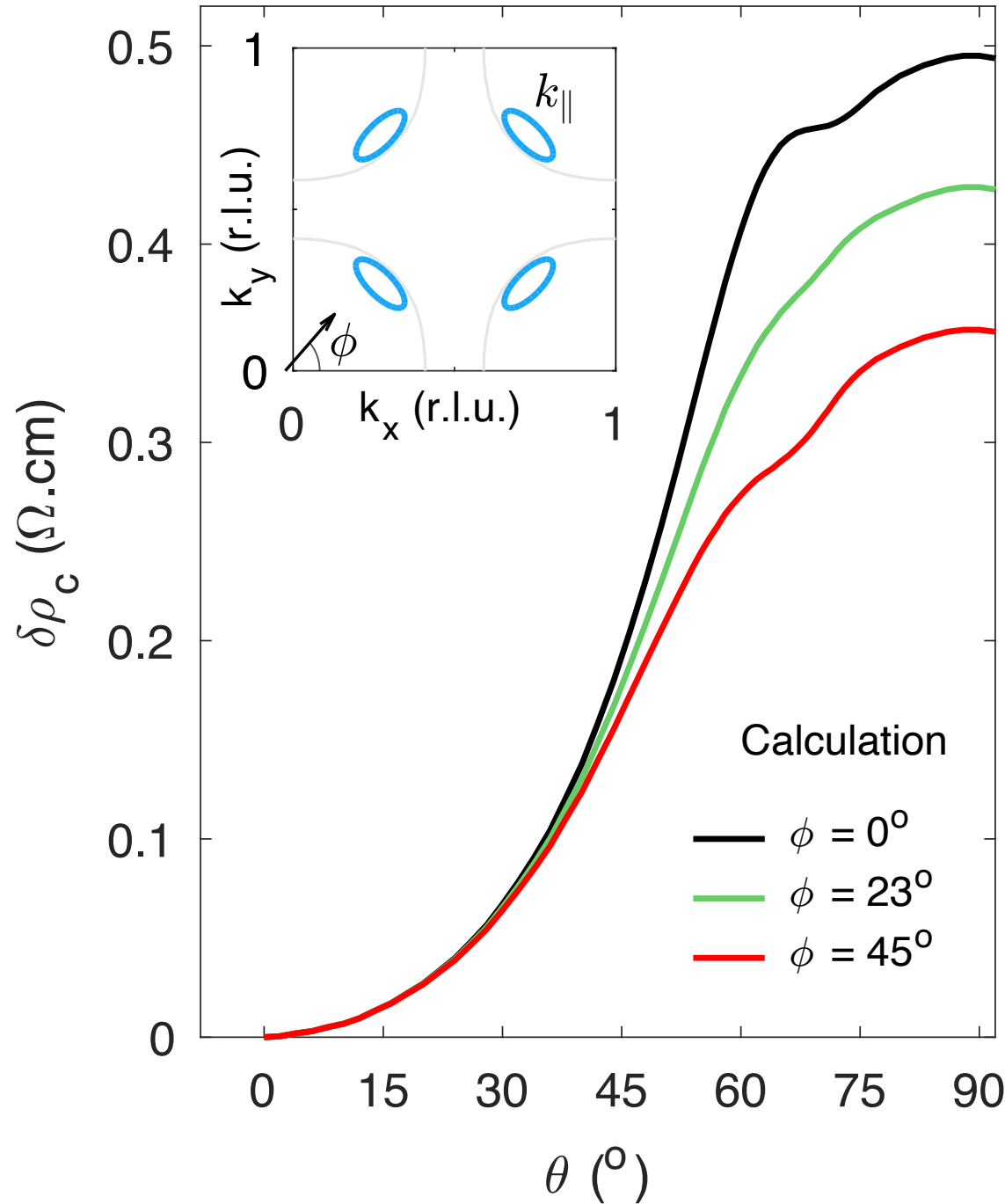
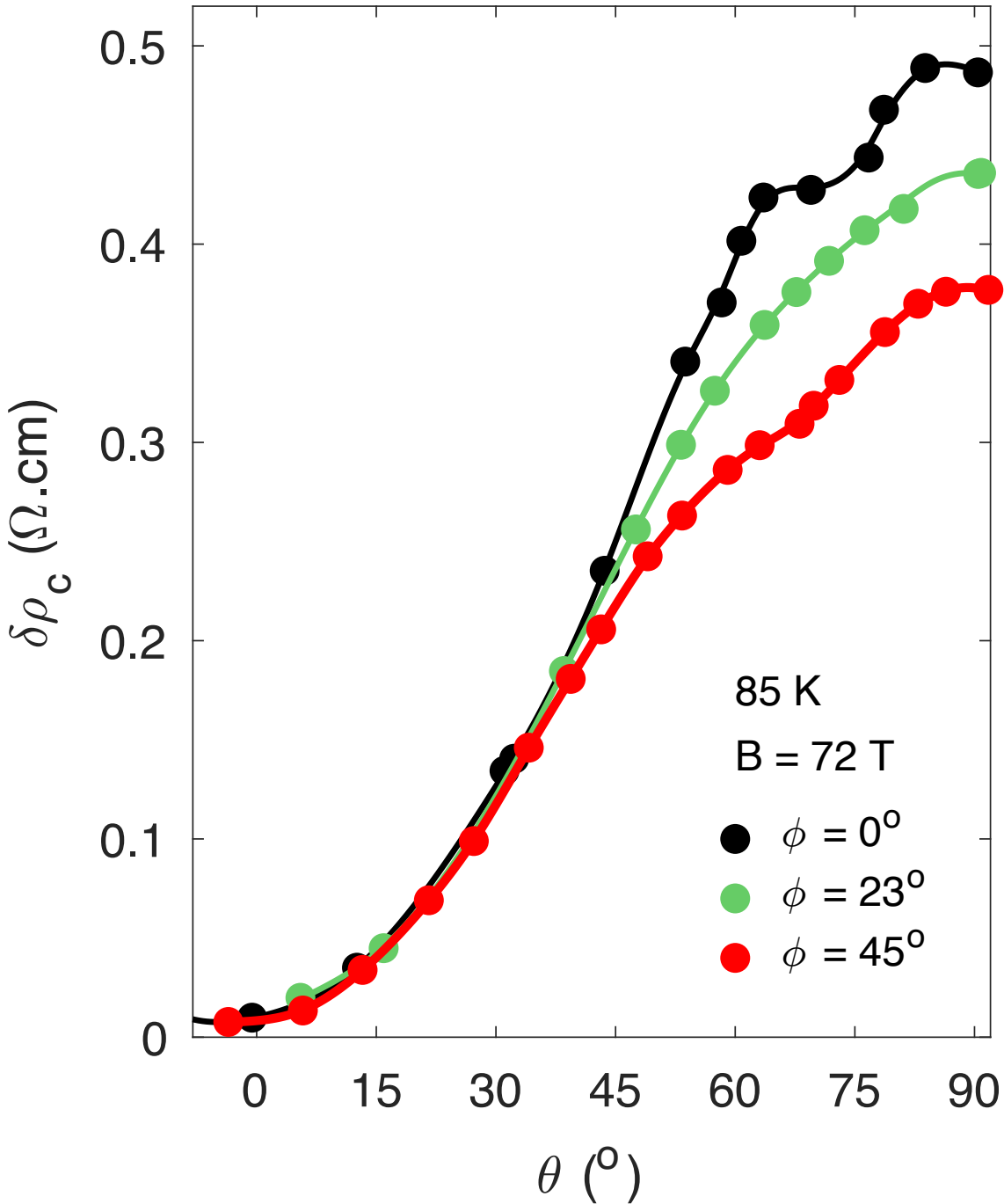
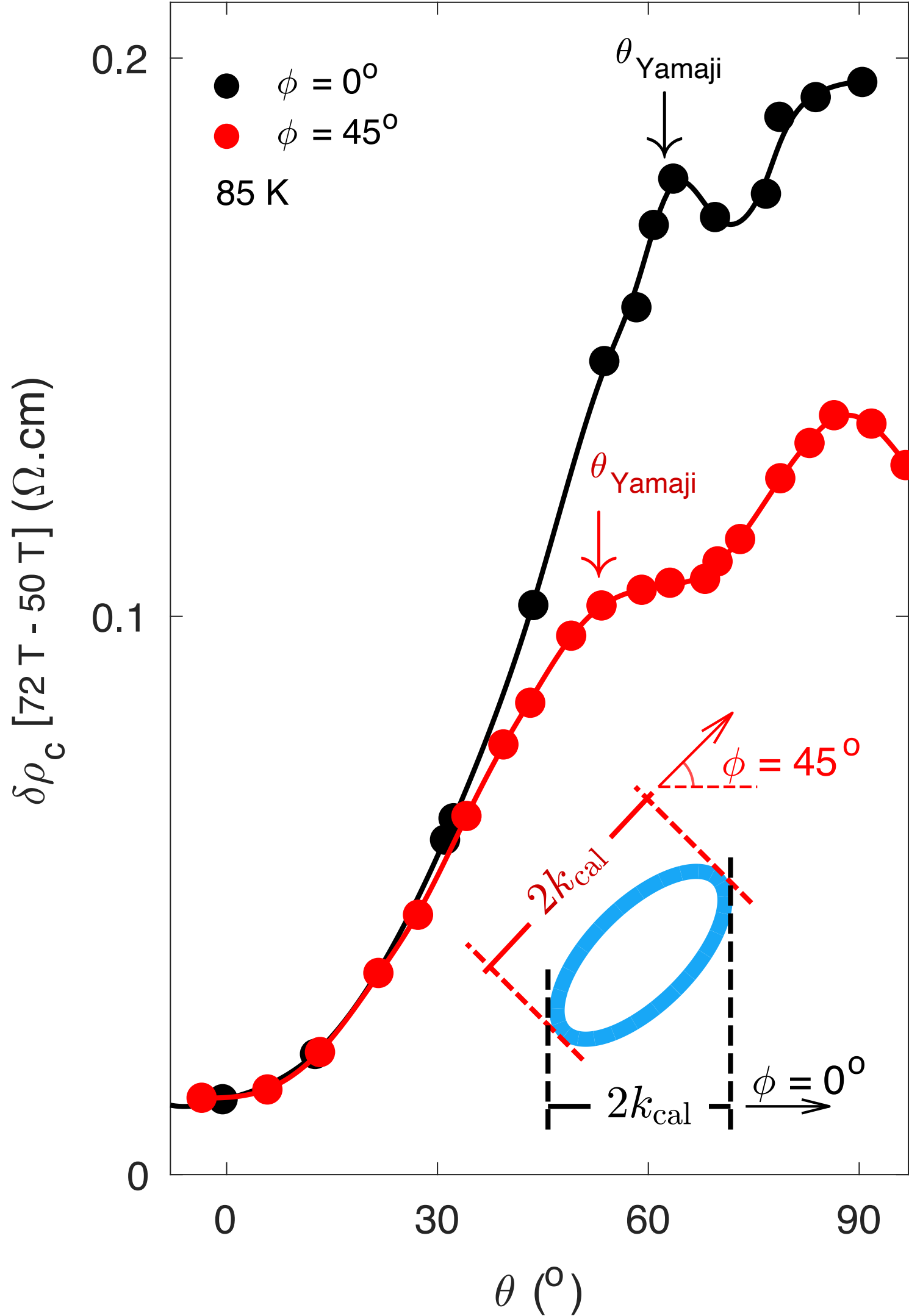
Observation of the Yamaji effect in a cuprate superconductor

nature physics

arXiv:2411.10631

Mun K. Chan¹, Katherine A. Schreiber¹, Oscar E. Ayala-Valenzuela¹,
Eric D. Bauer², Arkady Shekhter¹ & Neil Harrison¹

Published online: 16 September 2025



Doping
 $p = 0.1$

“The small size of the pockets determined from the Yamaji effect is ... approximately 1.3% of the Brillouin zone area”

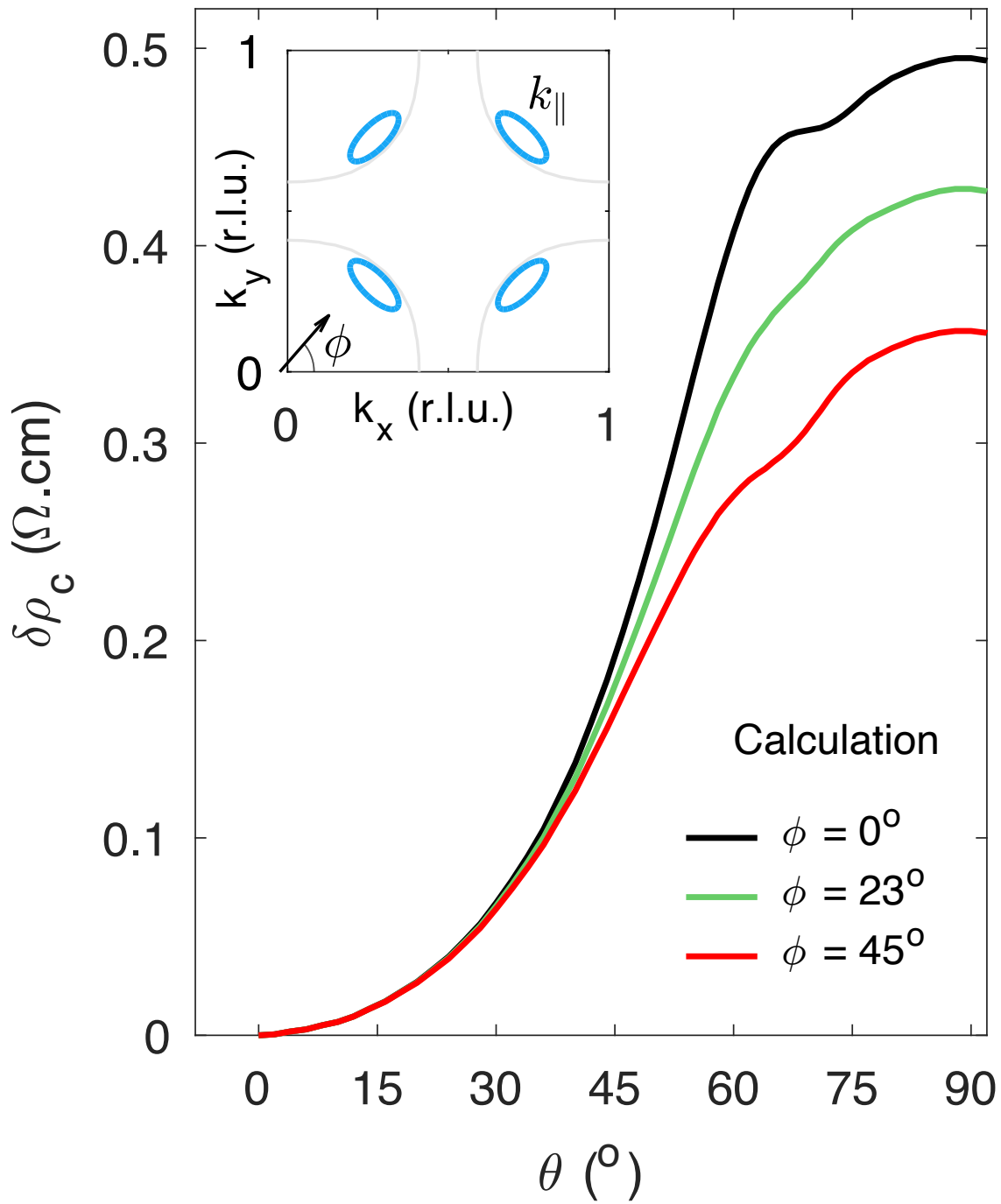
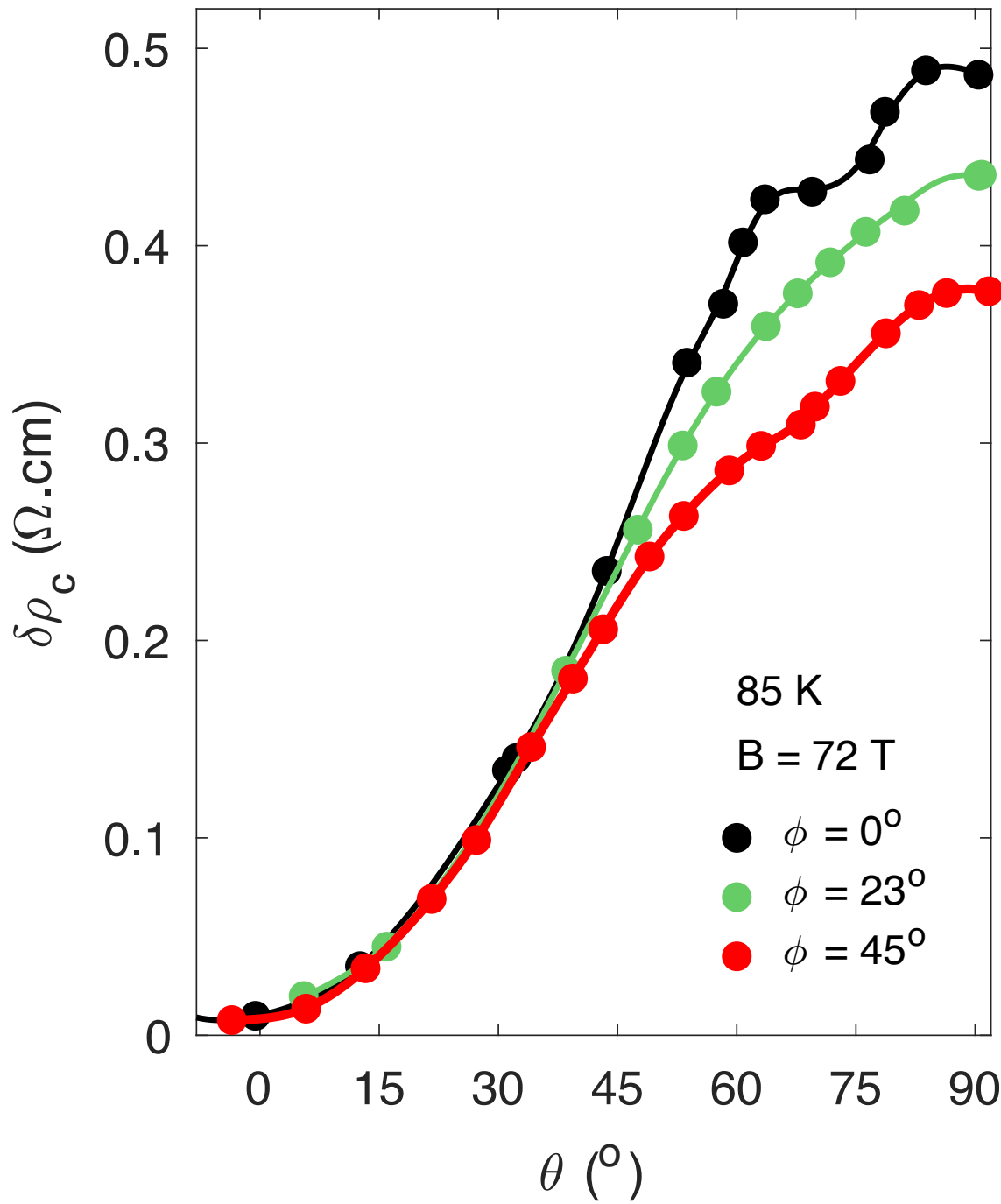
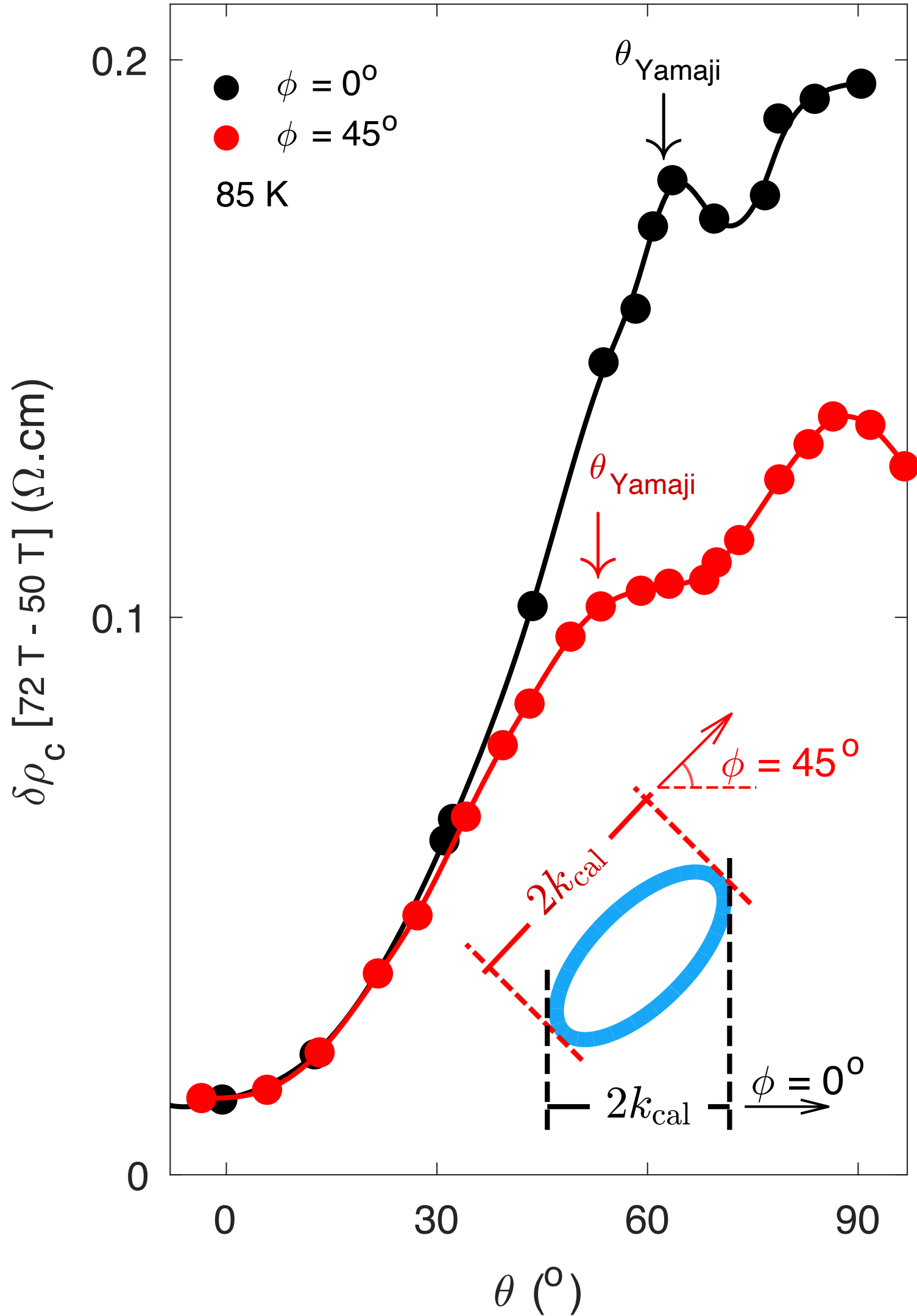
Observation of the Yamaji effect in a cuprate superconductor

nature physics

arXiv:2411.10631

Mun K. Chan¹, Katherine A. Schreiber¹, Oscar E. Ayala-Valenzuela¹,
Eric D. Bauer², Arkady Shekhter¹ & Neil Harrison¹

Published online: 16 September 2025



Doping
 $p = 0.1$

“The small size of the pockets determined from the Yamaji effect is ... approximately 1.3% of the Brillouin zone area”

FL* pocket fraction = $p/8 = 1.25\%$!

Fluctuating AF metal fraction = $p/4 = 2.5\%$. Yamaji effect requires correlated SDW order in the z direction, which is absent in $\text{HgBa}_2\text{CuO}_{4+\delta}$

Jing-Yu Zhao, S. Chatterjee, S. S., Ya-Hui Zhang, arXiv:2510.13943

($p/8$ also in YRZ ansatz, Peter Johnson photoemission, and Jenny Hoffman and Seamus Davis STMs; Stanescu-Kotliar)

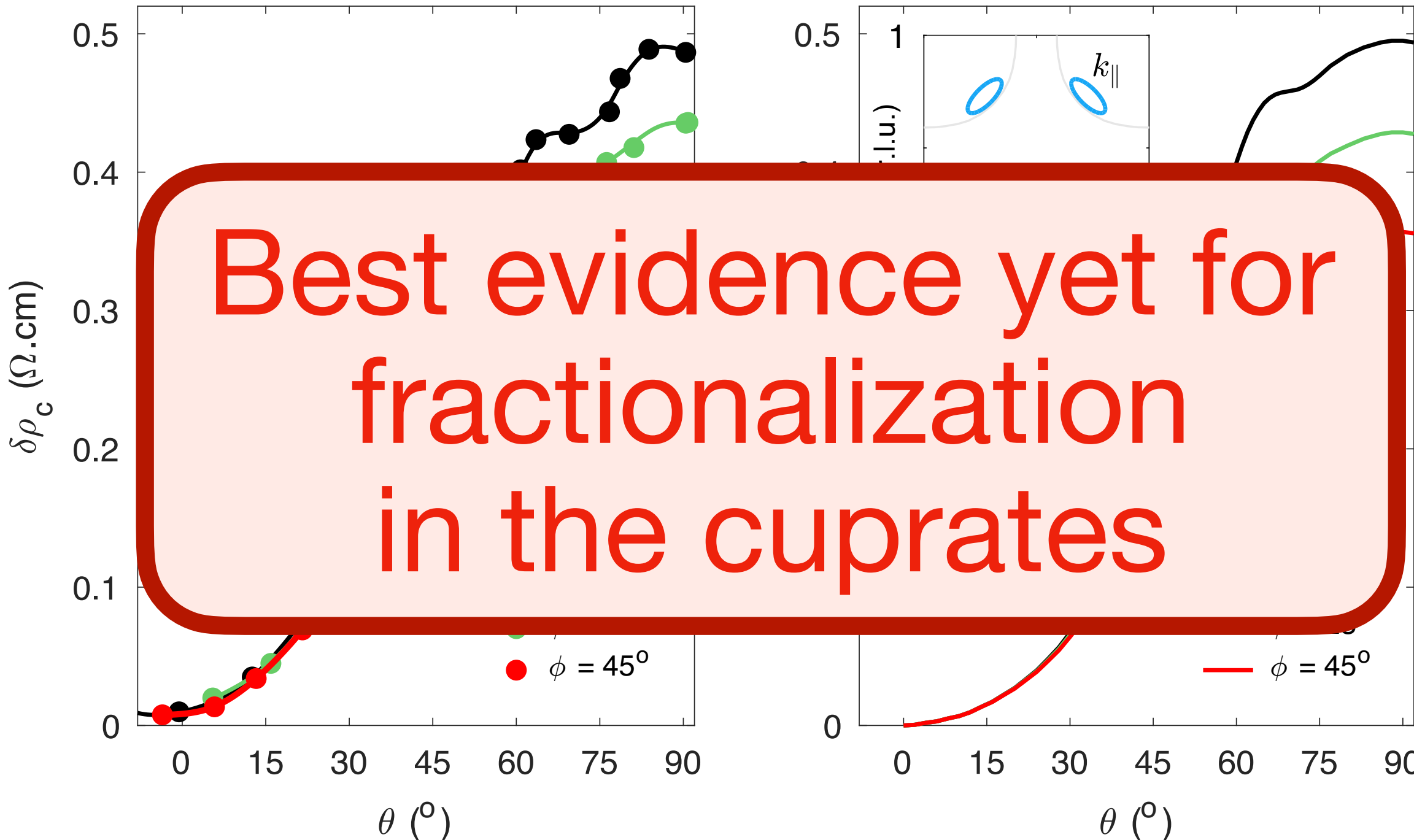
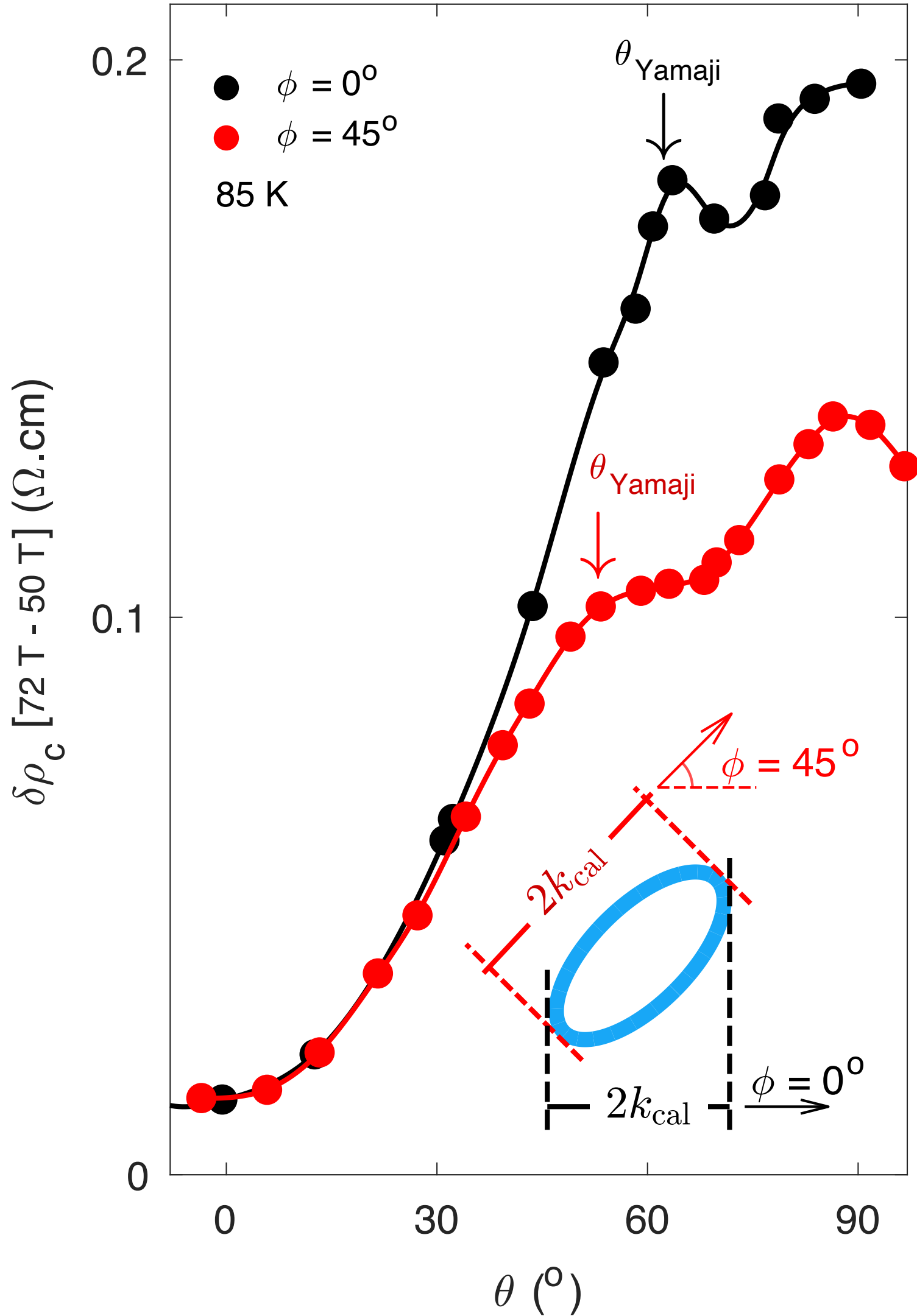
Observation of the Yamaji effect in a cuprate superconductor

nature physics

arXiv:2411.10631

Mun K. Chan¹, Katherine A. Schreiber¹, Oscar E. Ayala-Valenzuela¹,
Eric D. Bauer², Arkady Shekhter¹ & Neil Harrison¹

Published online: 16 September 2025



Best evidence yet for fractionalization in the cuprates

Doping $p = 0.1$

“The small size of the pockets determined from the Yamaji effect is ... approximately 1.3% of the Brillouin zone area”

FL* pocket fraction = $p/8 = 1.25\%$!

Fluctuating AF metal fraction = $p/4 = 2.5\%$. Yamaji effect requires correlated SDW order in the z direction, which is absent in $\text{HgBa}_2\text{CuO}_{4+\delta}$

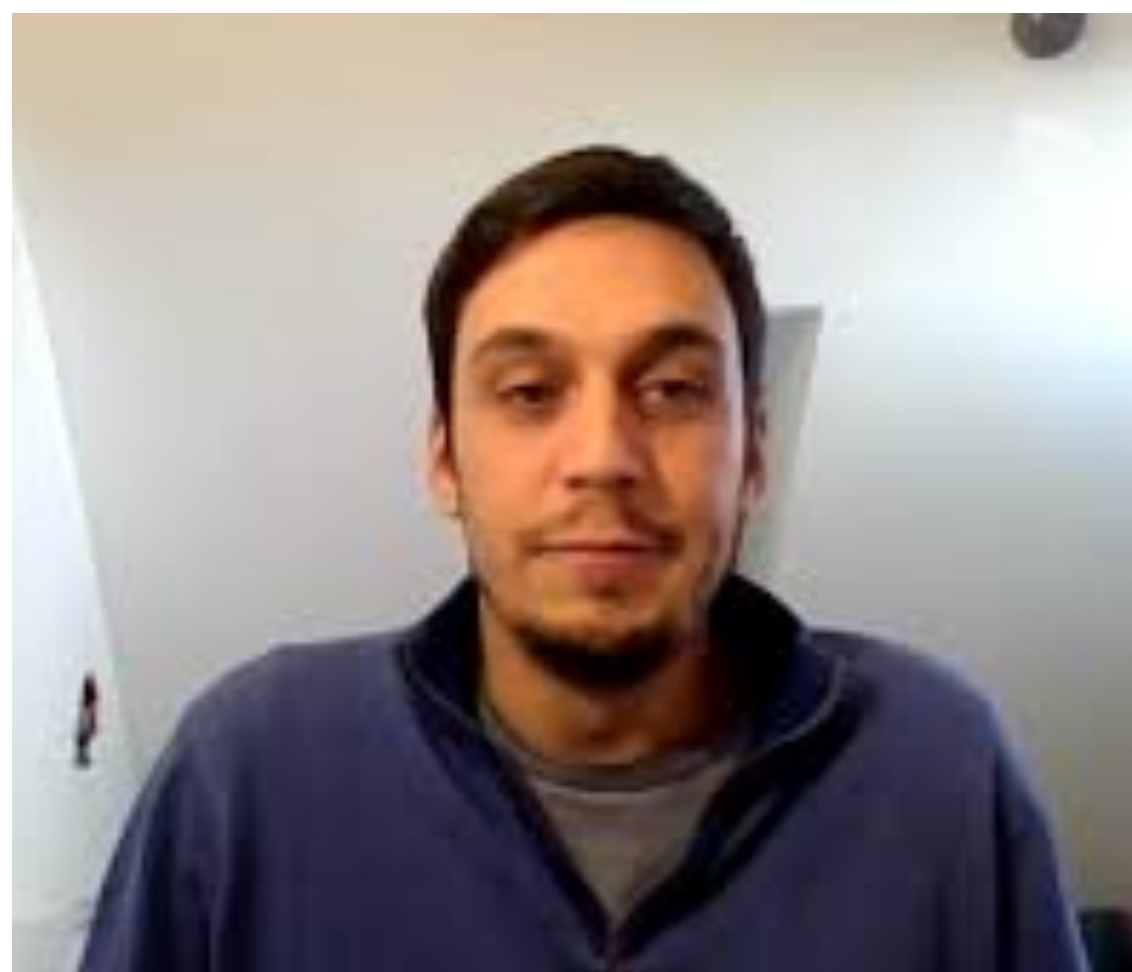
Jing-Yu Zhao, S. Chatterjee, S. S., Ya-Hui Zhang, arXiv:2510.13943

($p/8$ also in YRZ ansatz, Peter Johnson photoemission, and Jenny Hoffman and Seamus Davis STMs; Stanescu-Kotliar)

The cuprate phase diagram



Maine Christos
Caltech



Pietro Bonetti



Alexander
Nikolaenko



Aavishkar Patel
ICTS, Bengaluru

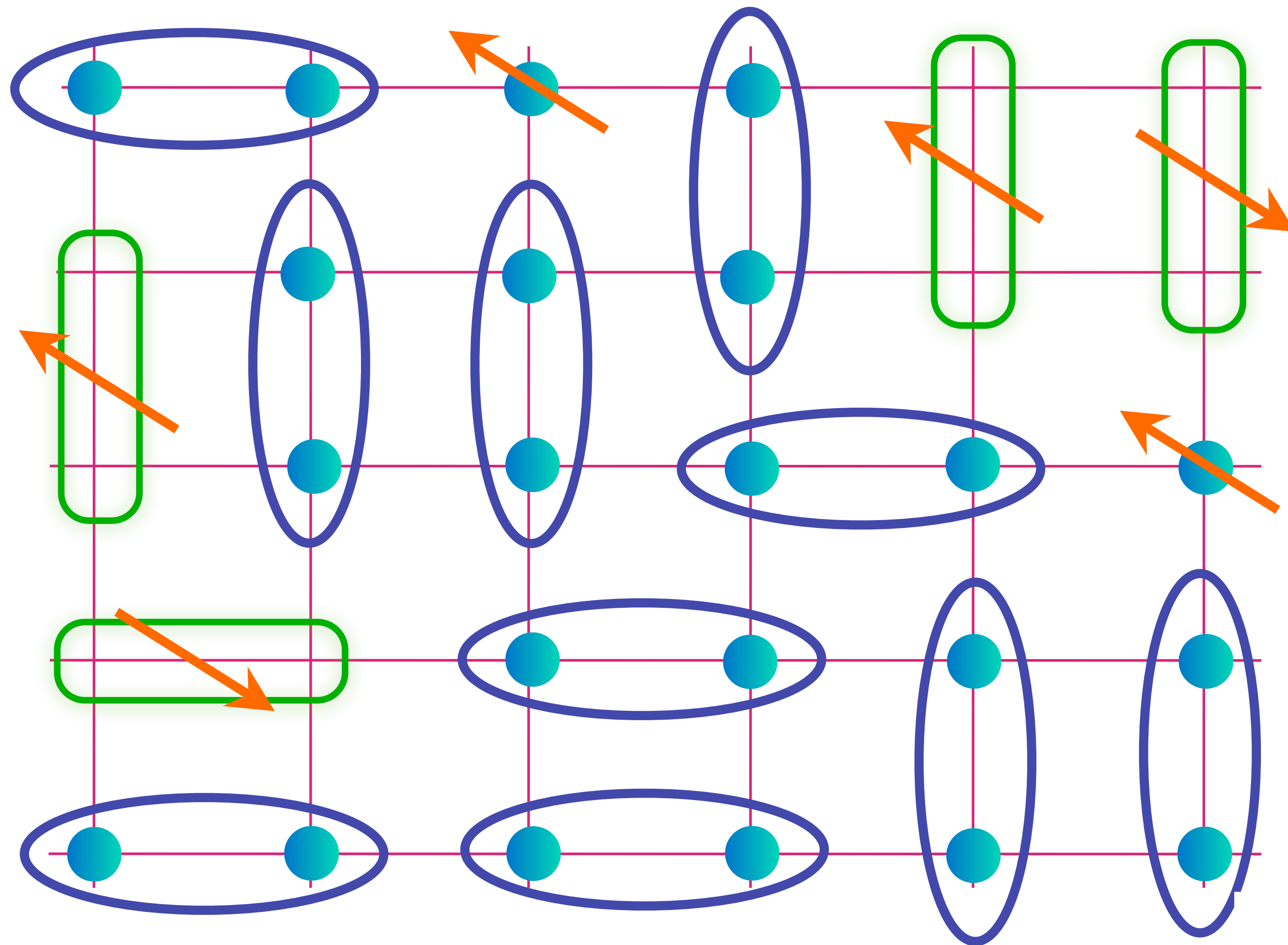
arXiv > cond-mat > arXiv:2508.20164

Condensed Matter > Strongly Correlated Electrons

[Submitted on 27 Aug 2025]

Critical quantum liquids and the cuprate high temperature superconductors

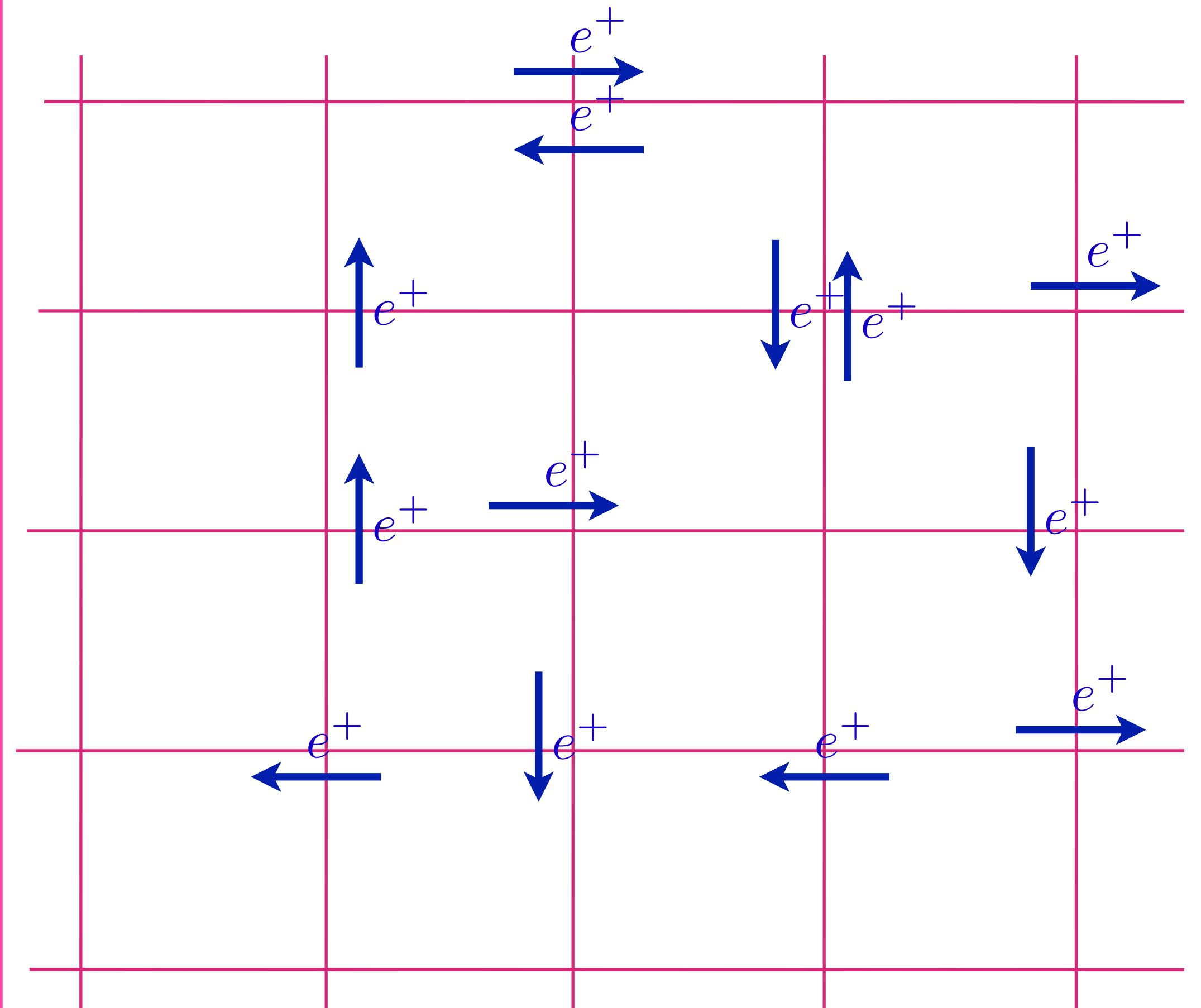
FL*



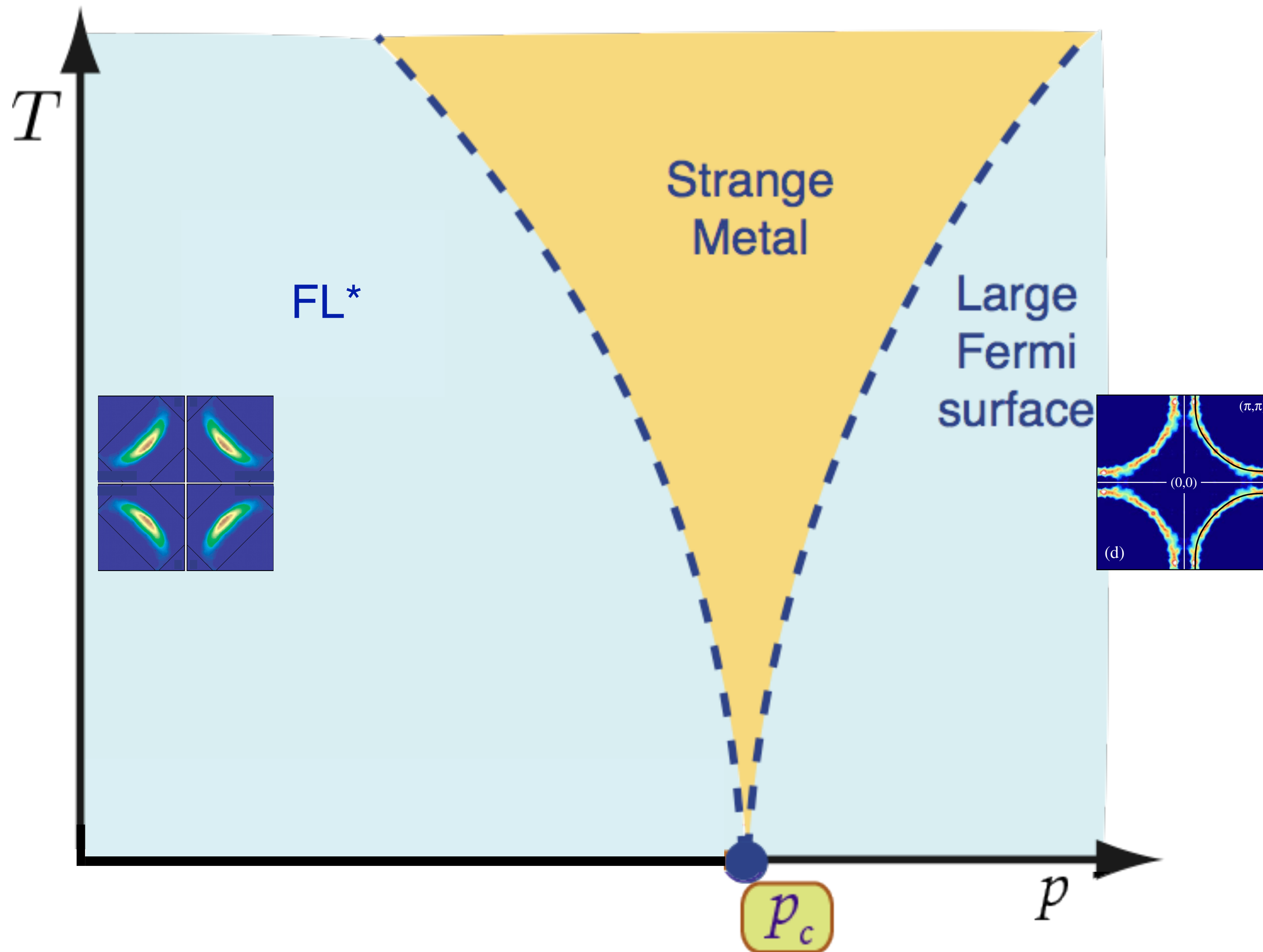
$$\begin{array}{|c|c|} \hline \bullet & \bullet \\ \hline \end{array} = (|\uparrow\downarrow\rangle - |\downarrow\uparrow\rangle) / \sqrt{2}$$

$$\begin{array}{|c|} \hline \bullet \\ \hline \end{array} \begin{array}{|c|} \hline \bullet \\ \hline \end{array} = (|\uparrow\circ\rangle + |\circ\uparrow\rangle) / \sqrt{2}$$

Ordinary metal



At large p , we obtain a gas of nearly free fermionic holes of density $1+p$ (relative to the filled band with 2 electrons per site)



Quantum-criticality
of a quantum phase transition
between two metals
(FL^* and FL) at $p = p_c$,
with no symmetry breaking.

1. Pick a spin liquid—a critical ‘Planckian’ spin liquid without quasiparticles: fermionic spinons f in π flux coupled to an emergent SU(2) gauge field U

M. Christos, Zhu-Xi Luo, L. Shackleton, Ya-Hui Zhang,
M. S. Scheurer, and S. S., PNAS **120**, e2302701120 (2023)

$S=1/2$ square lattice

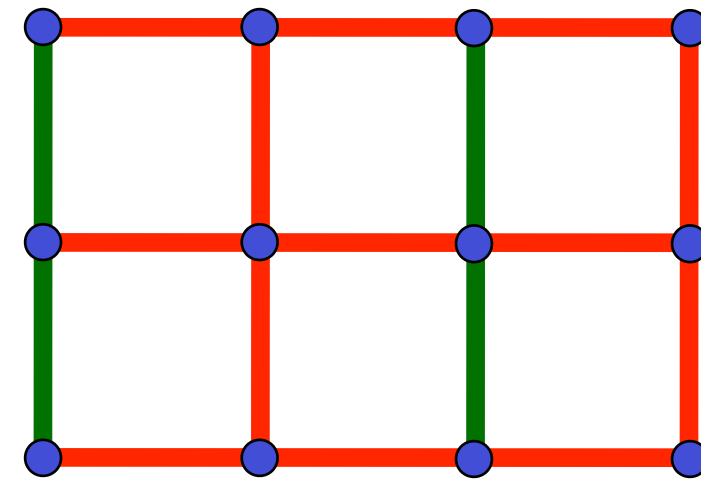
Represent spins in terms of
 $S = 1/2$ fermionic spinons $\mathbf{S} \sim f_{\alpha}^{\dagger} \boldsymbol{\sigma}_{\alpha\beta} f_{\beta}$

I. Affleck and J.B. Marston, PRB **37**, 3774 (1988)



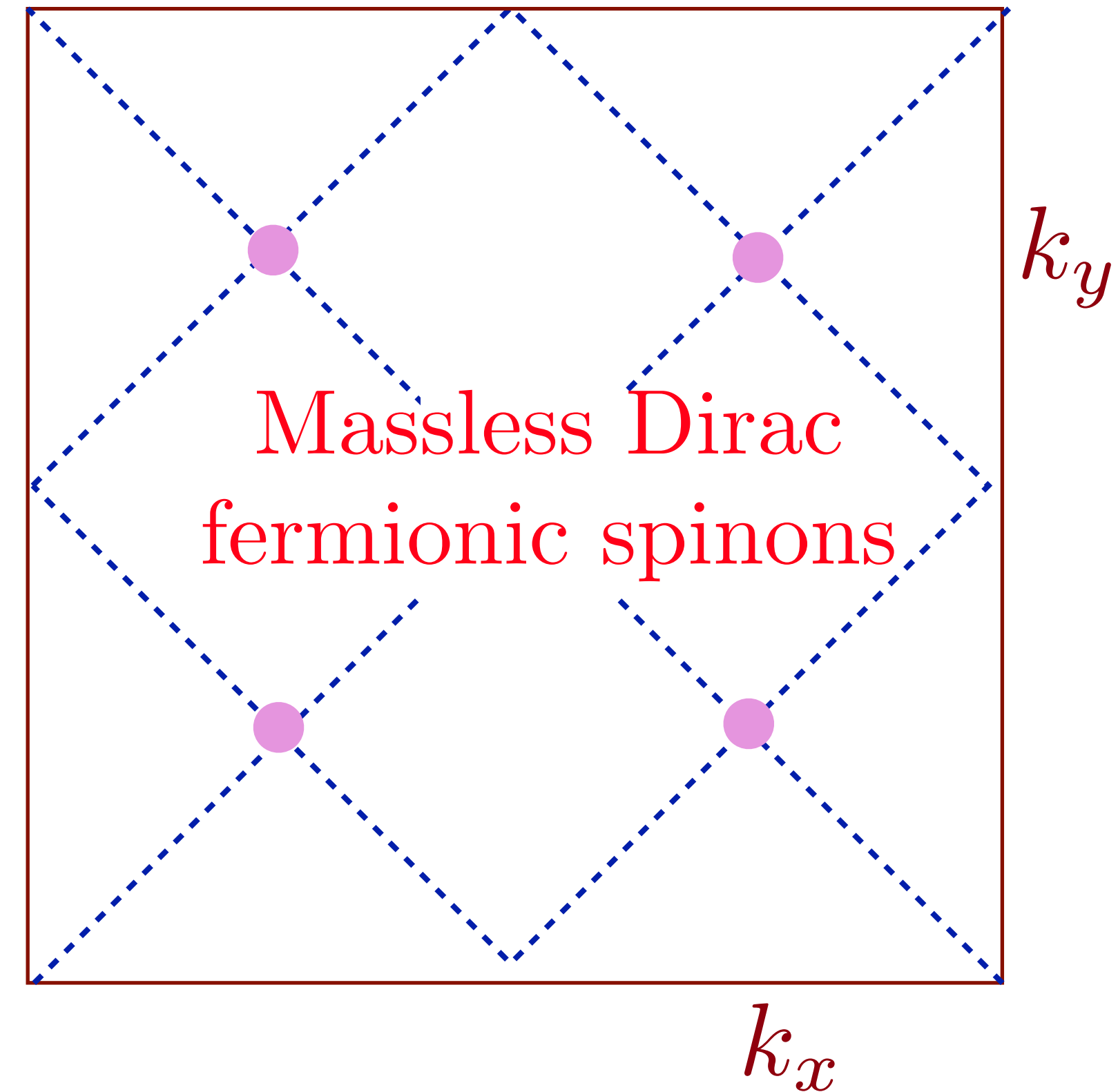
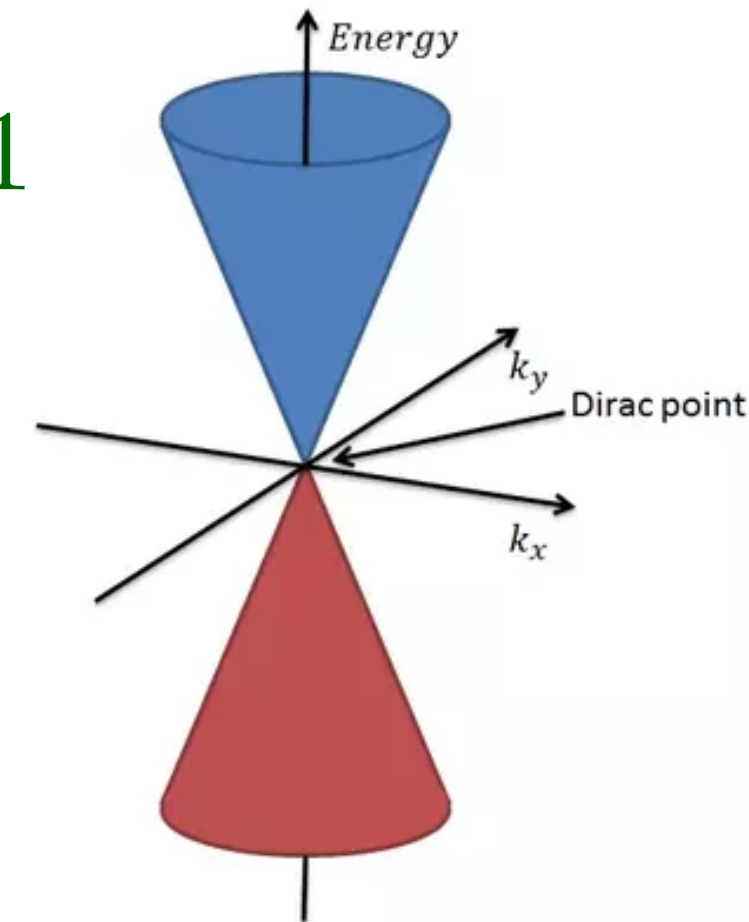
$$H_{\text{AFM}} = J \sum_{\langle ij \rangle} \mathbf{S}_i \cdot \mathbf{S}_j$$

$$H_{\text{Hartree-Fock}} = iJ \sum_{\langle ij \rangle} e_{ij} \left(\Psi_i^{\dagger} \Psi_j - \Psi_j^{\dagger} \Psi_i \right); \quad \Psi_i = \begin{pmatrix} f_{i\uparrow} \\ f_{i\downarrow} \end{pmatrix}$$



$$e_{ij} = 1$$

$$e_{ij} = -1$$

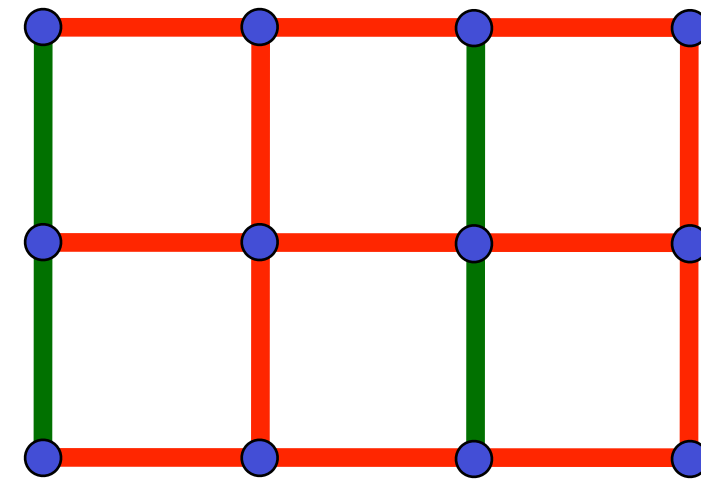


$S=1/2$ square lattice

Represent spins in terms of
 $S = 1/2$ fermionic spinons $\mathbf{S} \sim f_{\alpha}^{\dagger} \boldsymbol{\sigma}_{\alpha\beta} f_{\beta}$

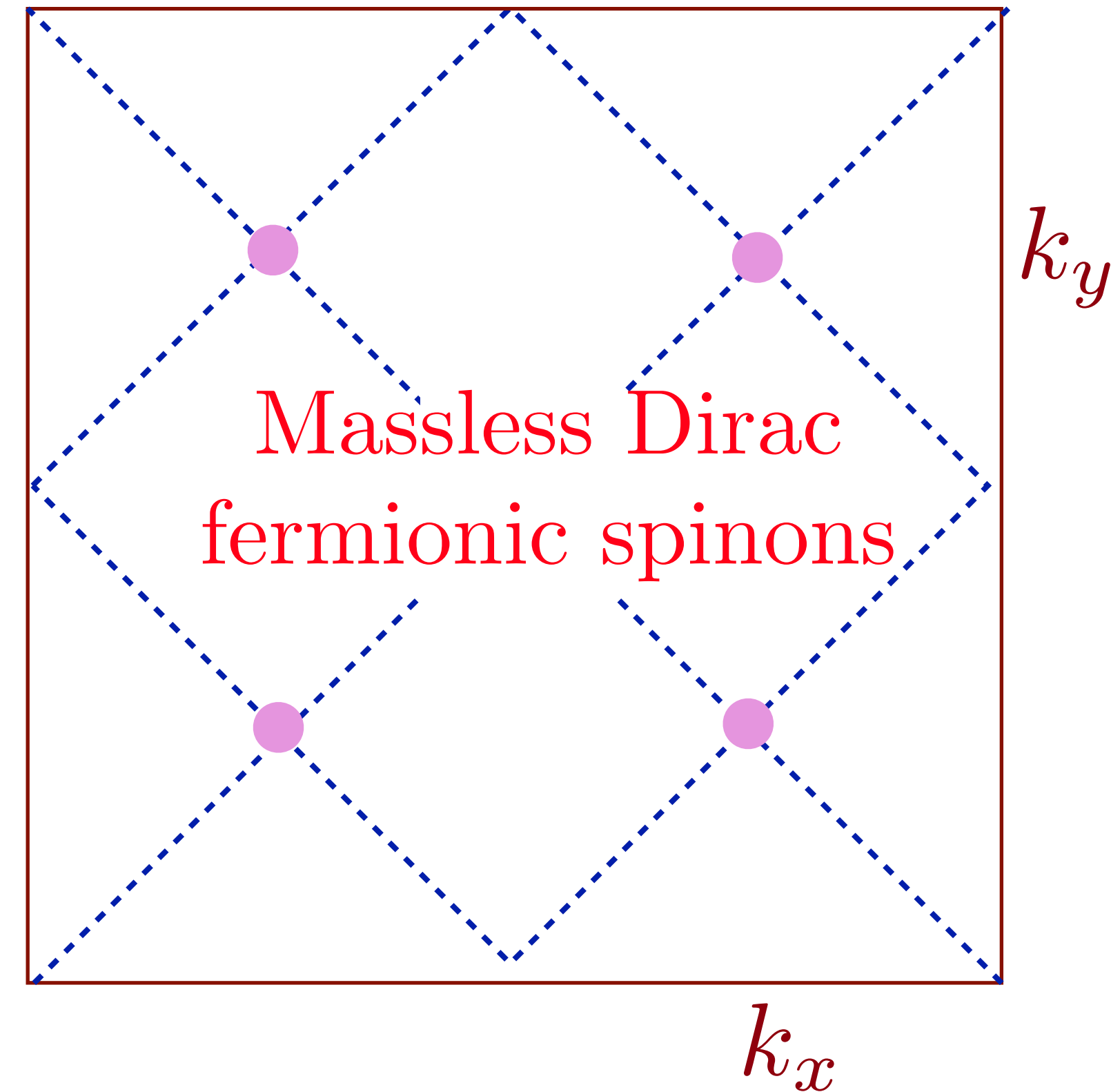
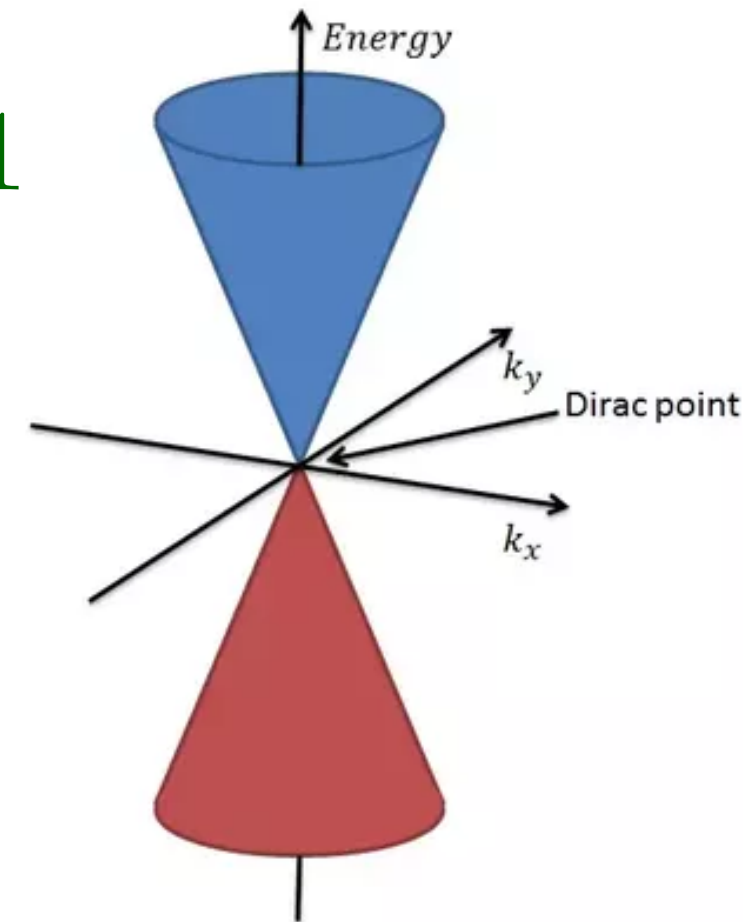
$$H_{\text{AFM}} = J \sum_{\langle ij \rangle} \mathbf{S}_i \cdot \mathbf{S}_j$$

$$H_{\text{spin liquid}} = iJ \sum_{\langle ij \rangle} e_{ij} \left(\Psi_i^{\dagger} U_{ij} \Psi_j - \Psi_j^{\dagger} U_{ji} \Psi_i \right); \quad \Psi_i = \begin{pmatrix} f_{i\uparrow} \\ f_{i\downarrow} \end{pmatrix}$$



$$e_{ij} = 1$$

$$e_{ij} = -1$$

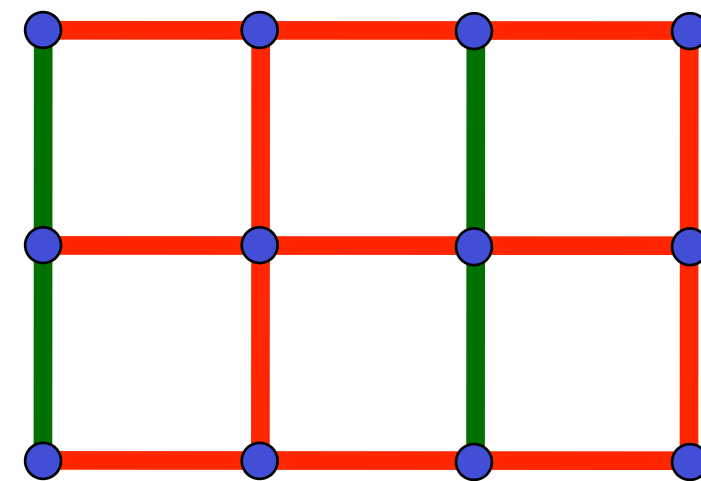


$S=1/2$ square lattice

Represent spins in terms of
 $S = 1/2$ fermionic spinons $\mathbf{S} \sim f_\alpha^\dagger \boldsymbol{\sigma}_{\alpha\beta} f_\beta$

$$H_{\text{AFM}} = J \sum_{\langle ij \rangle} \mathbf{S}_i \cdot \mathbf{S}_j$$

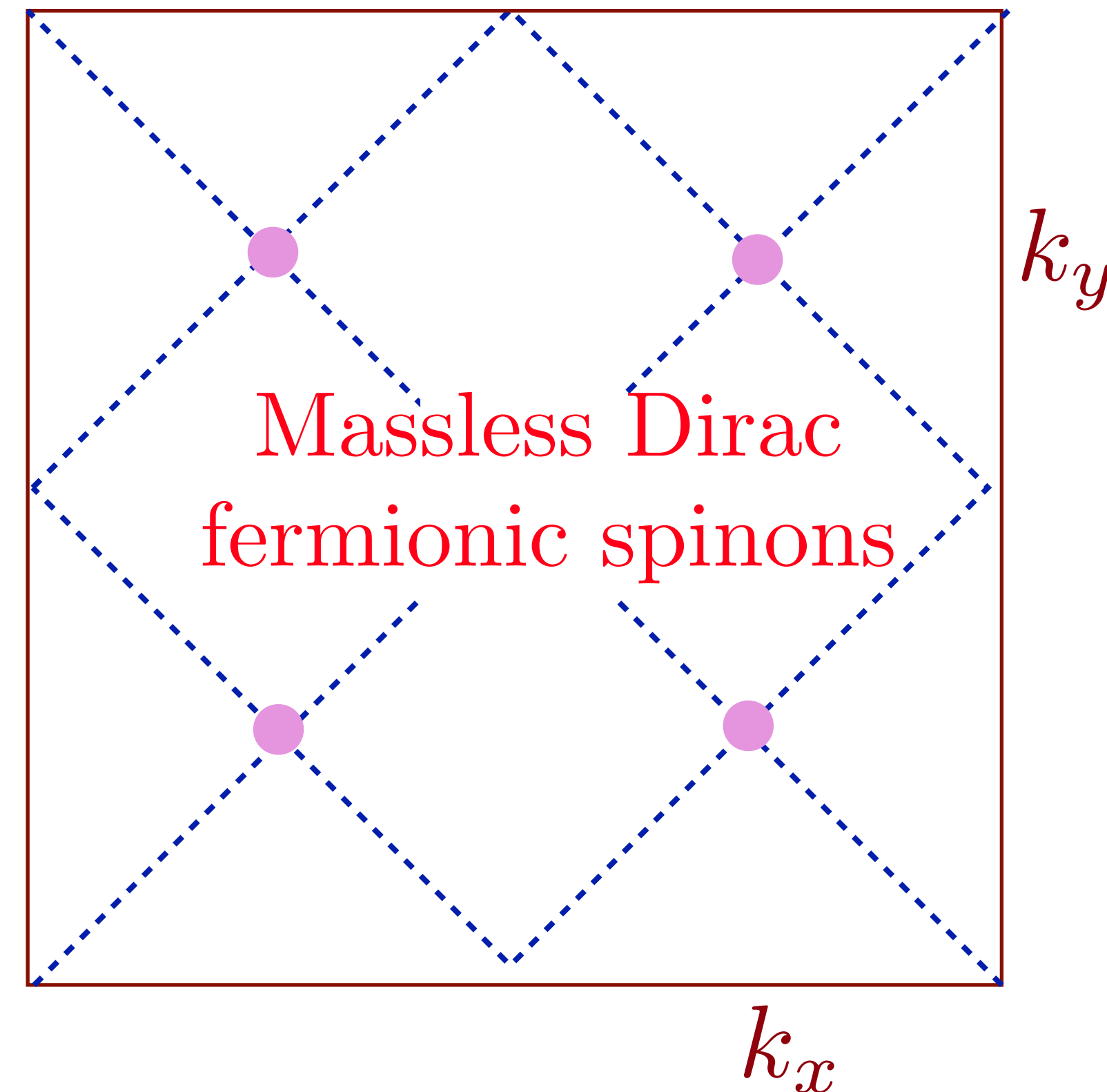
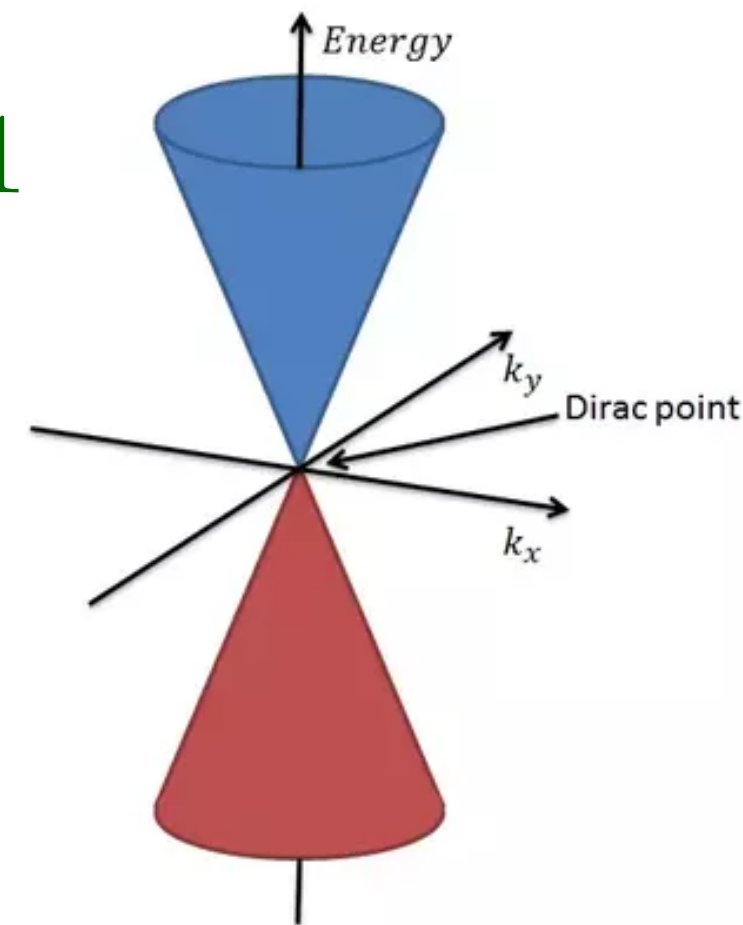
$$H_{\text{spin liquid}} = iJ \sum_{\langle ij \rangle} e_{ij} \left(\Psi_i^\dagger U_{ij} \Psi_j - \Psi_j^\dagger U_{ji} \Psi_i \right); \quad \Psi_i = \begin{pmatrix} f_{i\uparrow}^\dagger \\ f_{i\downarrow}^\dagger \end{pmatrix}$$



$$e_{ij} = 1$$

$$e_{ij} = -1$$

$$\mathcal{L} = i\bar{\psi}\gamma_\mu D_\mu \psi.$$

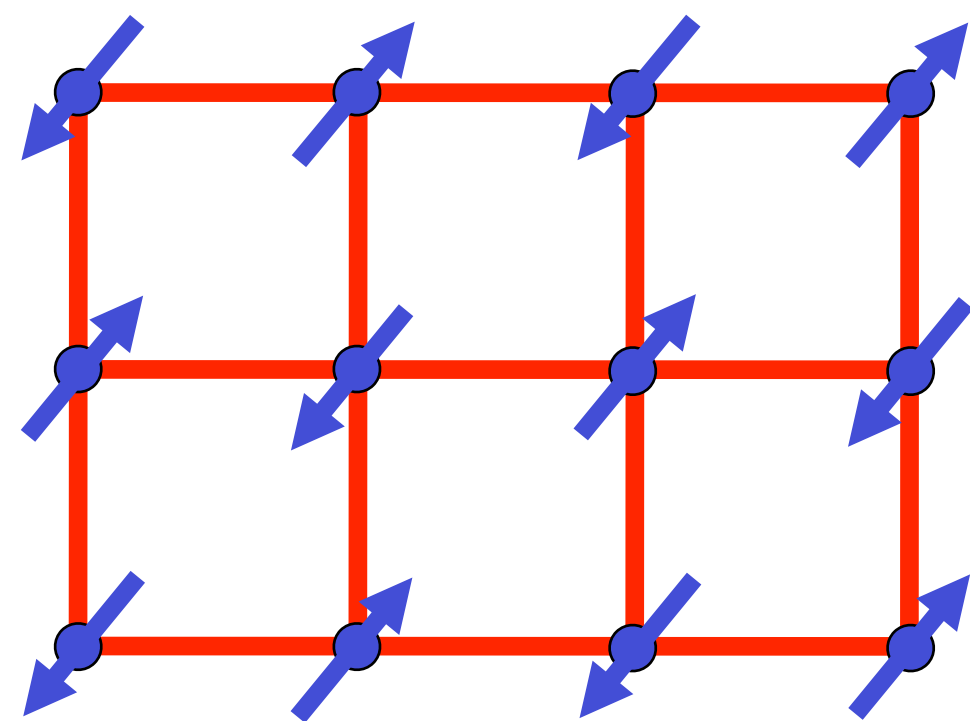


Low energy: $SU(2)$ gauge theory with $N_f = 2$
 massless Dirac spinons in 2+1 D.

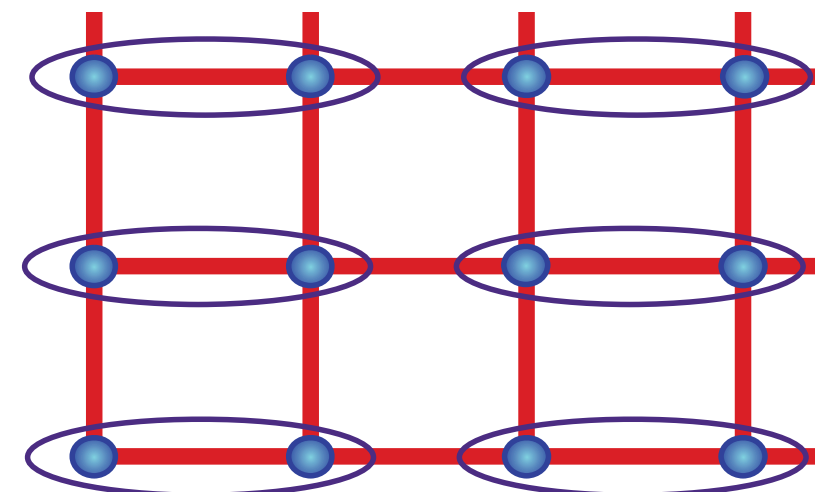
(QCD is a $SU(3)$ gauge theory with $N_f = 3$ massless Dirac quarks in 3+1 D.)

$S=1/2$ square lattice

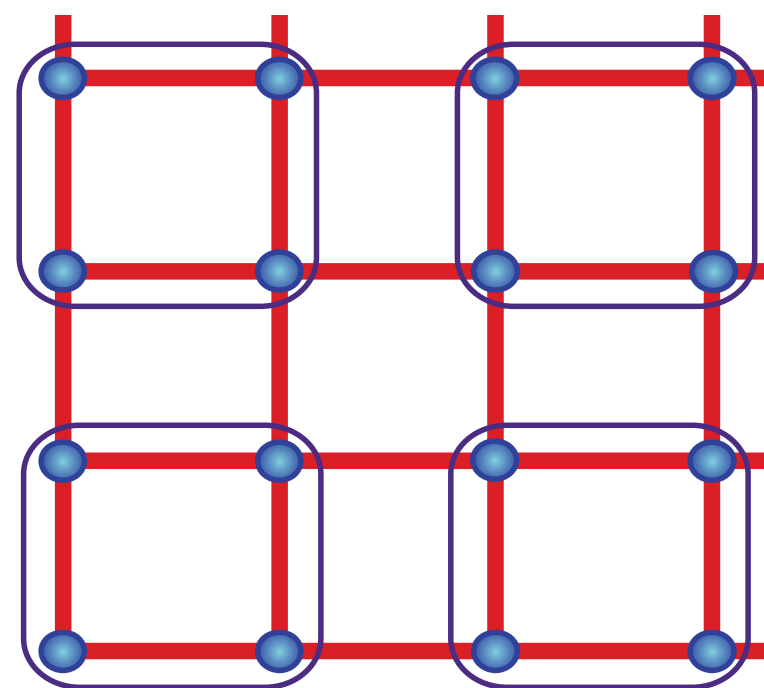
Represent spins in terms of
 $S = 1/2$ fermionic spinons $\mathbf{S} \sim f_\alpha^\dagger \boldsymbol{\sigma}_{\alpha\beta} f_\beta$



Néel order



or



Valence bond
solid (VBS)

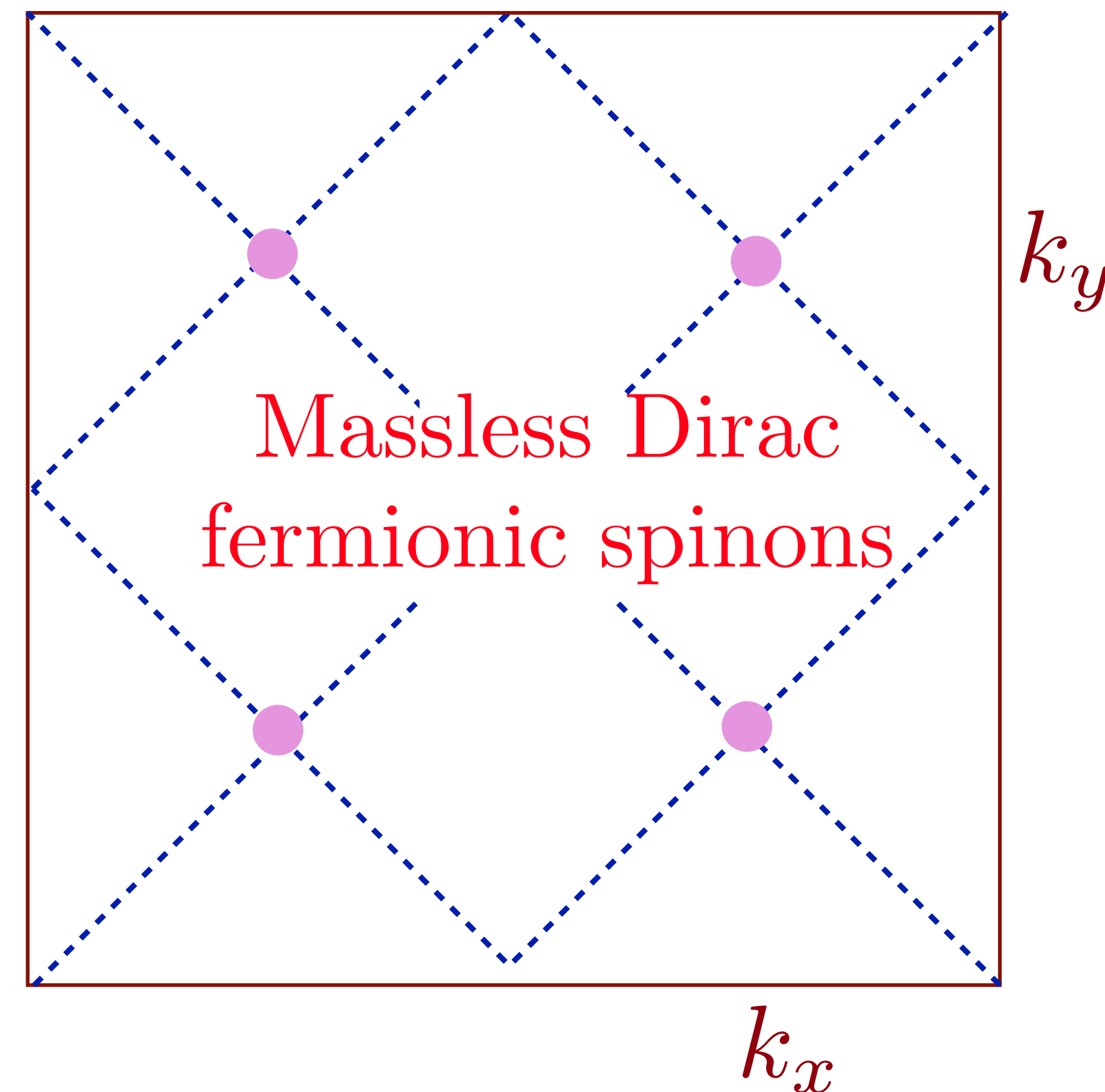
$$\mathcal{L} = i\bar{\psi}\gamma_\mu D_\mu\psi.$$

Critical spin liquid
without quasiparticles

Confining instability
to Néel and VBS,
as in \mathbb{CP}^1 theory of Read+SS

J_2/J_1

- I. Affleck and J.B. Marston, PRB **37**, 3774 (1988)
N. Read and S. Sachdev, PRL **62**, 1694 (1989)
C. Wang, A. Nahum, M. A. Metlitski, C. Xu,
T. Senthil, PRX **7**, 031051 (2017)
Zheng Zhou, Liangdong Hu, Wei Zhu,
Yin-Chen He, PRX **14**, 021044 (2024)

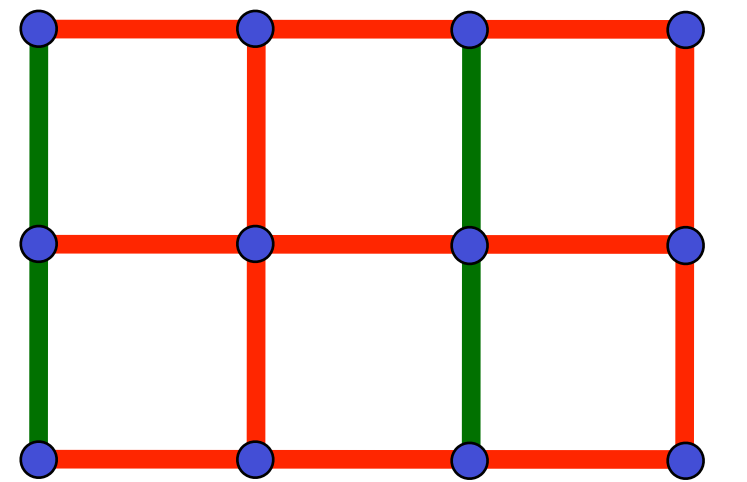


Massless Dirac
fermionic spinons

1. Pick a spin liquid—a critical ‘Planckian’ spin liquid without quasiparticles: fermionic spinons f in π flux coupled to an emergent SU(2) gauge field U

M. Christos, Zhu-Xi Luo, L. Shackleton, Ya-Hui Zhang,
M. S. Scheurer, and S. S., PNAS **120**, e2302701120 (2023)

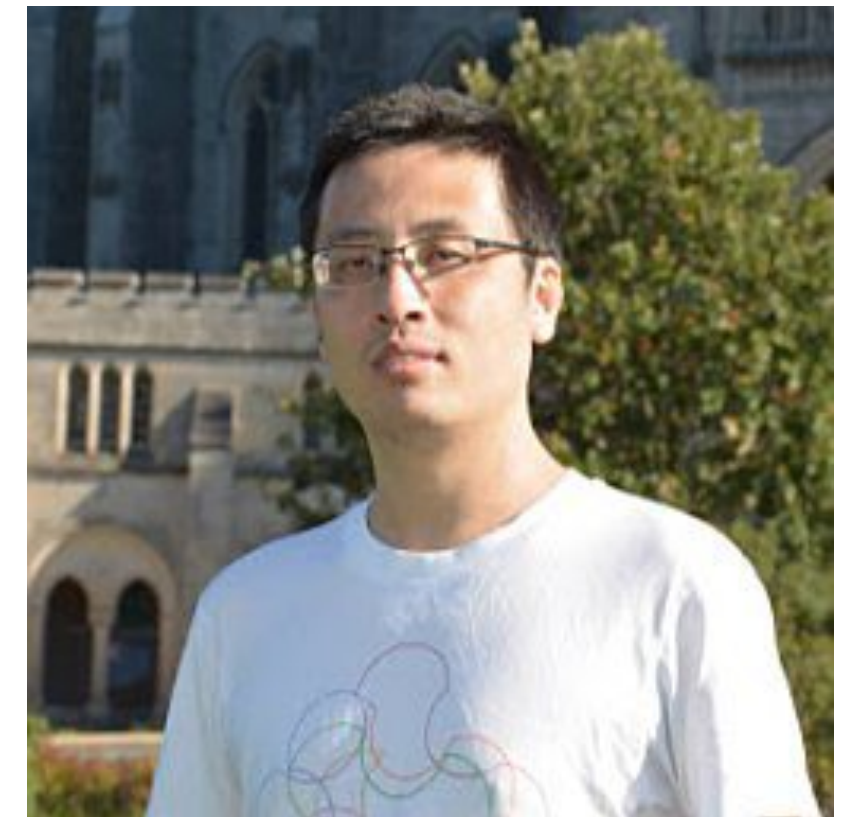
$$H_{\text{spin liquid}} = iJ \sum_{\langle ij \rangle} e_{ij} \left(\Psi_i^\dagger U_{ij} \Psi_j - \Psi_j^\dagger U_{ji} \Psi_i \right); \quad \Psi_i = \begin{pmatrix} f_{i\uparrow} \\ f_{i\downarrow}^\dagger \end{pmatrix}$$



$$e_{ij} = 1 \quad e_{ij} = -1$$

1. Pick a spin liquid—a critical ‘Planckian’ spin liquid without quasiparticles: fermionic spinons f in π flux coupled to an emergent SU(2) gauge field U
2. Dope spin liquid with *holes*, not holons.
The Ancilla Layer Model (ALM) puts the holes and spin liquid in different layers, and this enables a theory of both FL* and FL.

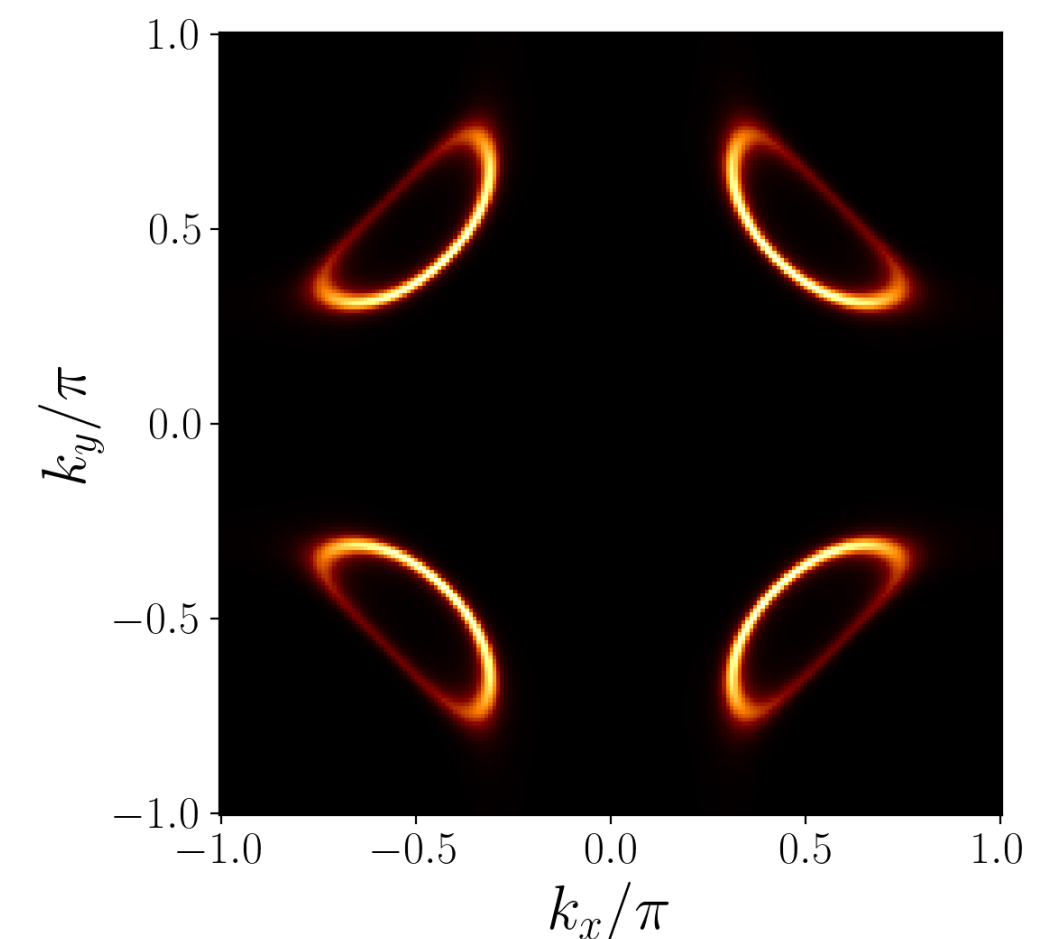
Ya-Hui Zhang and S. S., PRR **2**, 023172 (2020)



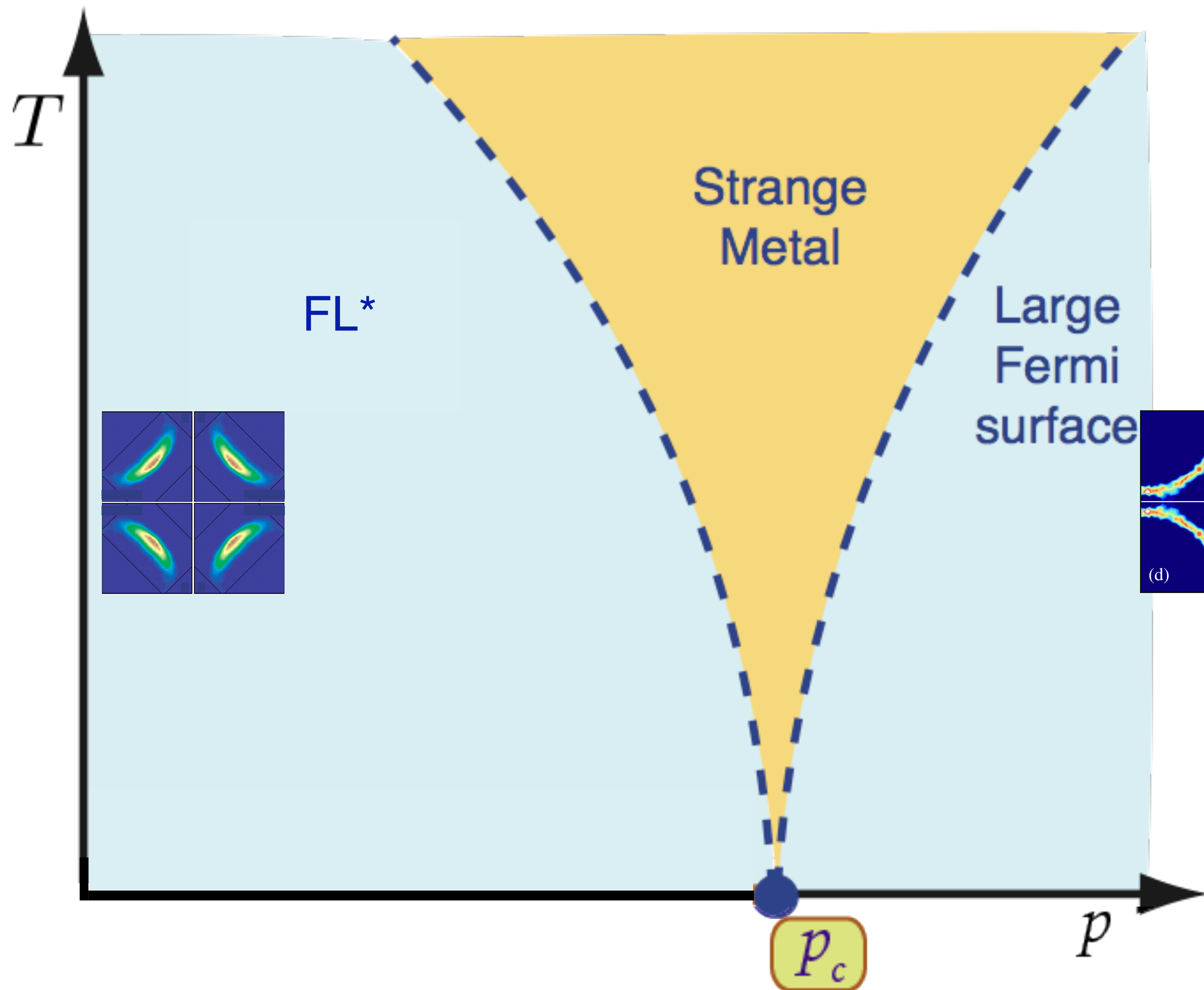
1. Pick a spin liquid—a critical ‘Planckian’ spin liquid without quasiparticles: fermionic spinons f in π flux coupled to an emergent SU(2) gauge field U
2. Dope spin liquid with *holes*, not holons.
The Ancilla Layer Model (ALM) puts the holes and spin liquid in different layers, and this enables a theory of both FL* and FL.
3. Hole pockets are obtained by hybridizing the large Fermi surface of $1 - p$ electrons c with the Fermi surface of 1 ancilla fermion f_1 . The hybridization Φ also determines the electronic gap near $(\pi, 0)$

Ya-Hui Zhang and S. S., PRR **2**, 023172 (2020)

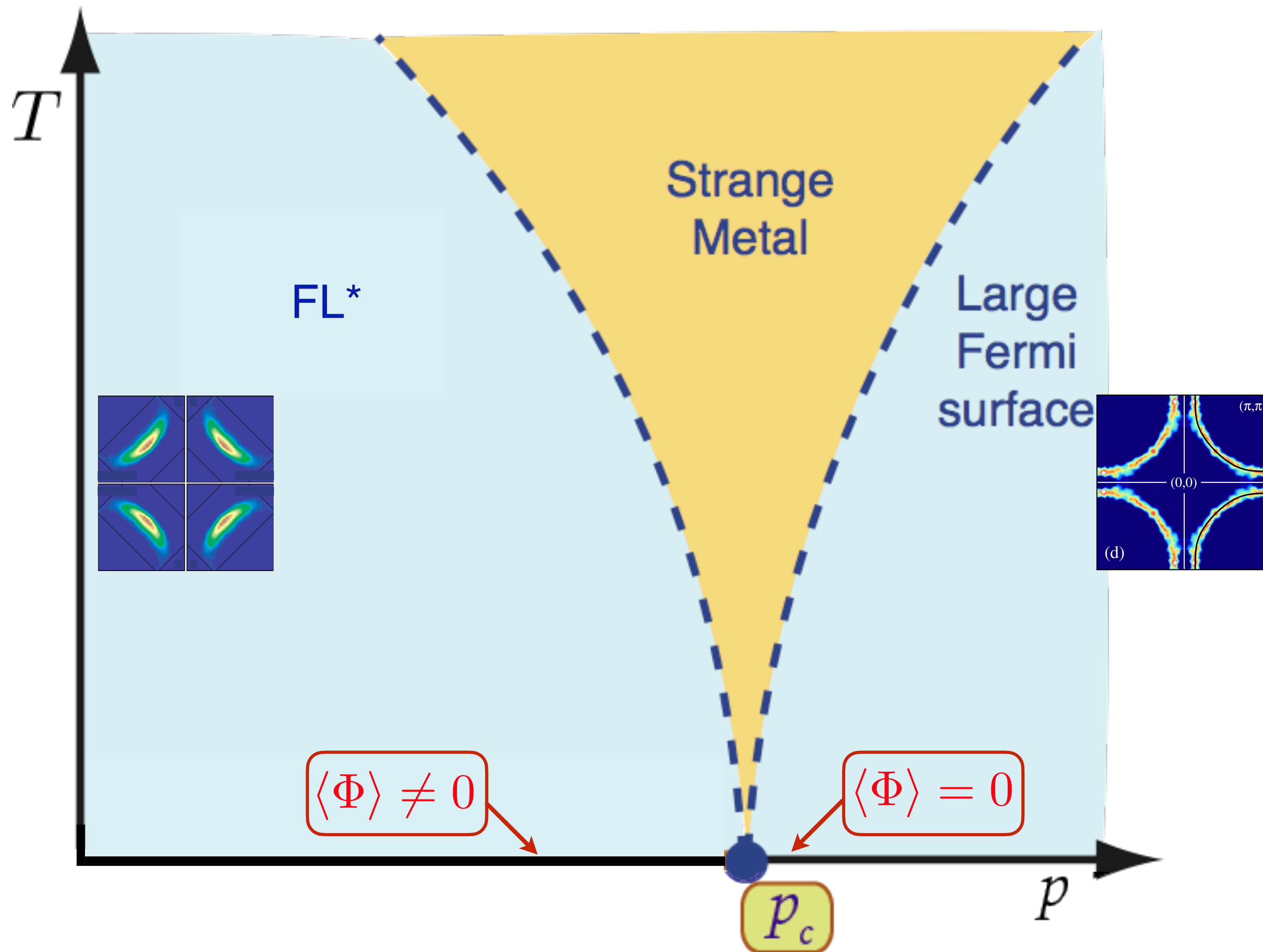
$$H_{\text{hole pockets}} = \sum_{i,j} \left[-t_{ij} c_{i\alpha}^\dagger c_{j\alpha} - t_{1,ij} f_{1i\alpha}^\dagger f_{1j\alpha} \right] - \sum_i \Phi (c_{i\alpha}^\dagger f_{1i\alpha} + f_{1i\alpha}^\dagger c_{i\alpha})$$



1. Pick a spin liquid—a critical ‘Planckian’ spin liquid without quasiparticles: fermionic spinons f in π flux coupled to an emergent SU(2) gauge field U (similar to neutrinos in Weinberg-Salam theory).
2. Dope spin liquid with *holes*, not holons.
The Ancilla Layer Model (ALM) puts the holes and spin liquid in different layers, and this enables a theory of both FL* and FL.
3. Hole pockets are obtained by hybridizing the large Fermi surface of $1 - p$ electrons c with the Fermi surface of 1 ancilla fermion f_1 . The hybridization Φ also determines the electronic gap near $(\pi, 0)$ (similar to electrons in Weinberg-Salam theory).
4. Couple hole pockets coupled to critical spin liquid by a charge e , SU(2) fundamental Higgs field B (similar to Yukawa coupling of Higgs field in Weinberg-Salam theory).



Quantum-criticality
of a quantum phase transition
between two metals
(FL* and FL) at $p = p_c$,
with no symmetry breaking.

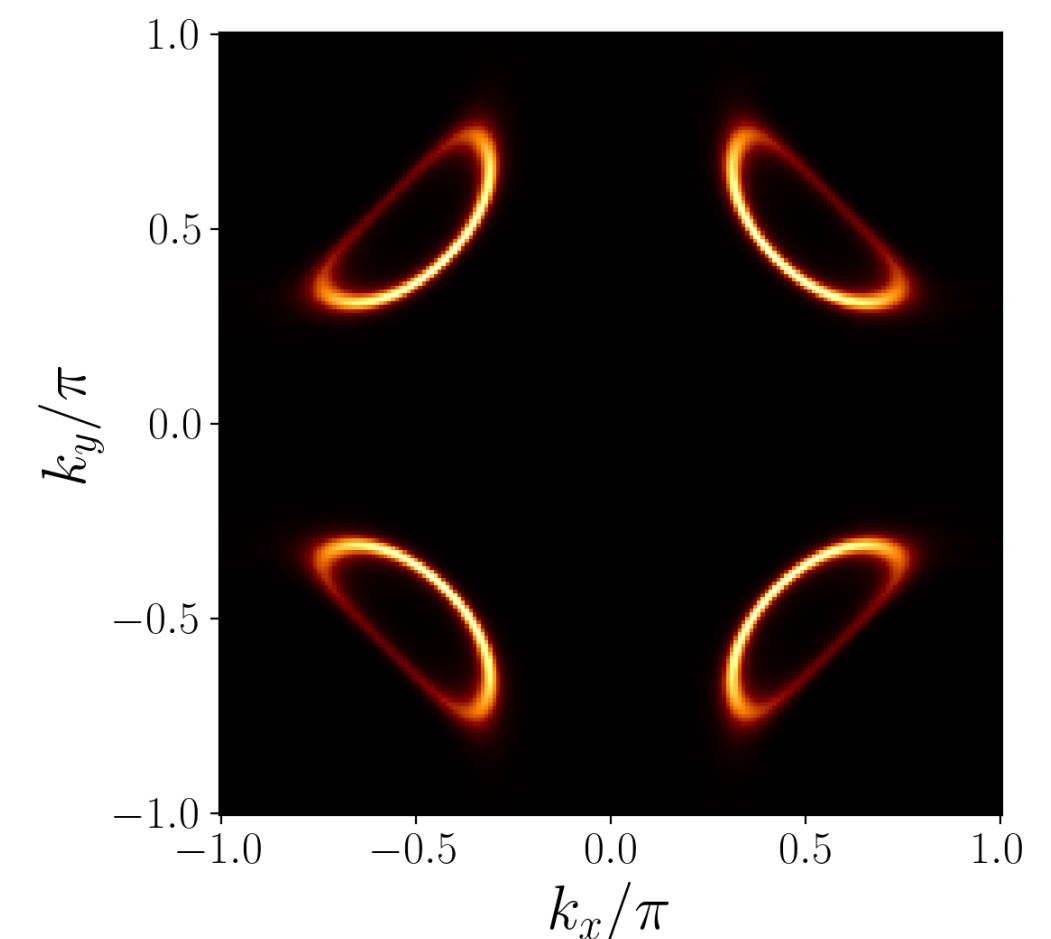


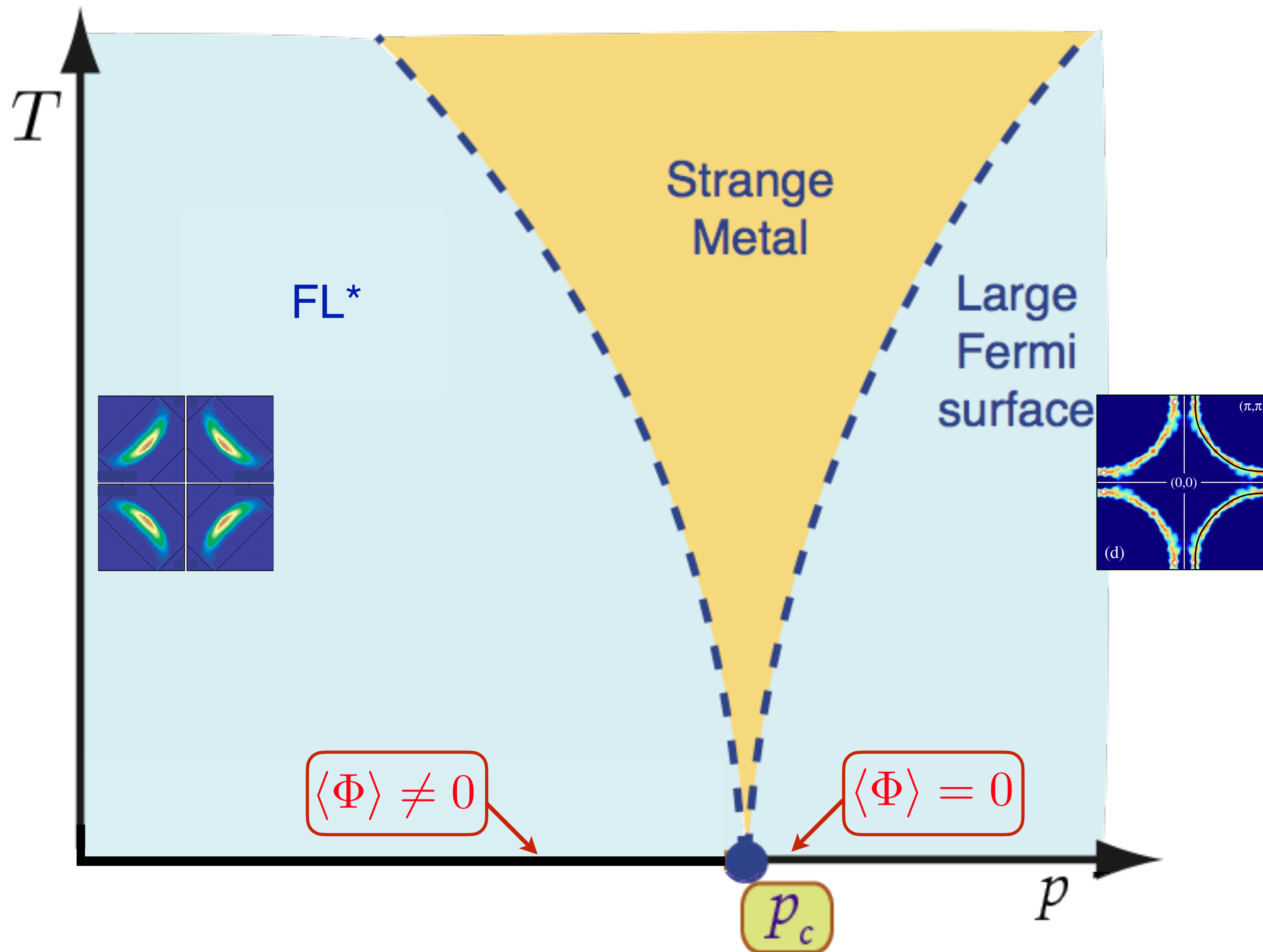
Quantum-criticality
of a quantum phase transition
between two metals
(FL^* and FL) at $p = p_c$,
with no symmetry breaking.
 Φ was the hybridization
between c and f_1 in theory of
hole pockets—it is
now a Higgs field.

1. Pick a spin liquid—a critical ‘Planckian’ spin liquid without quasiparticles: fermionic spinons f in π flux coupled to an emergent SU(2) gauge field U
2. Dope spin liquid with *holes*, not holons.
The Ancilla Layer Model (ALM) enables a theory of FL* with hole pockets and a general spin liquid.
3. Hole pockets are obtained by hybridizing the large Fermi surface of $1 - p$ electrons c with the Fermi surface of 1 ancilla fermion f_1 . The hybridization Φ also determines the electronic gap near $(\pi, 0)$

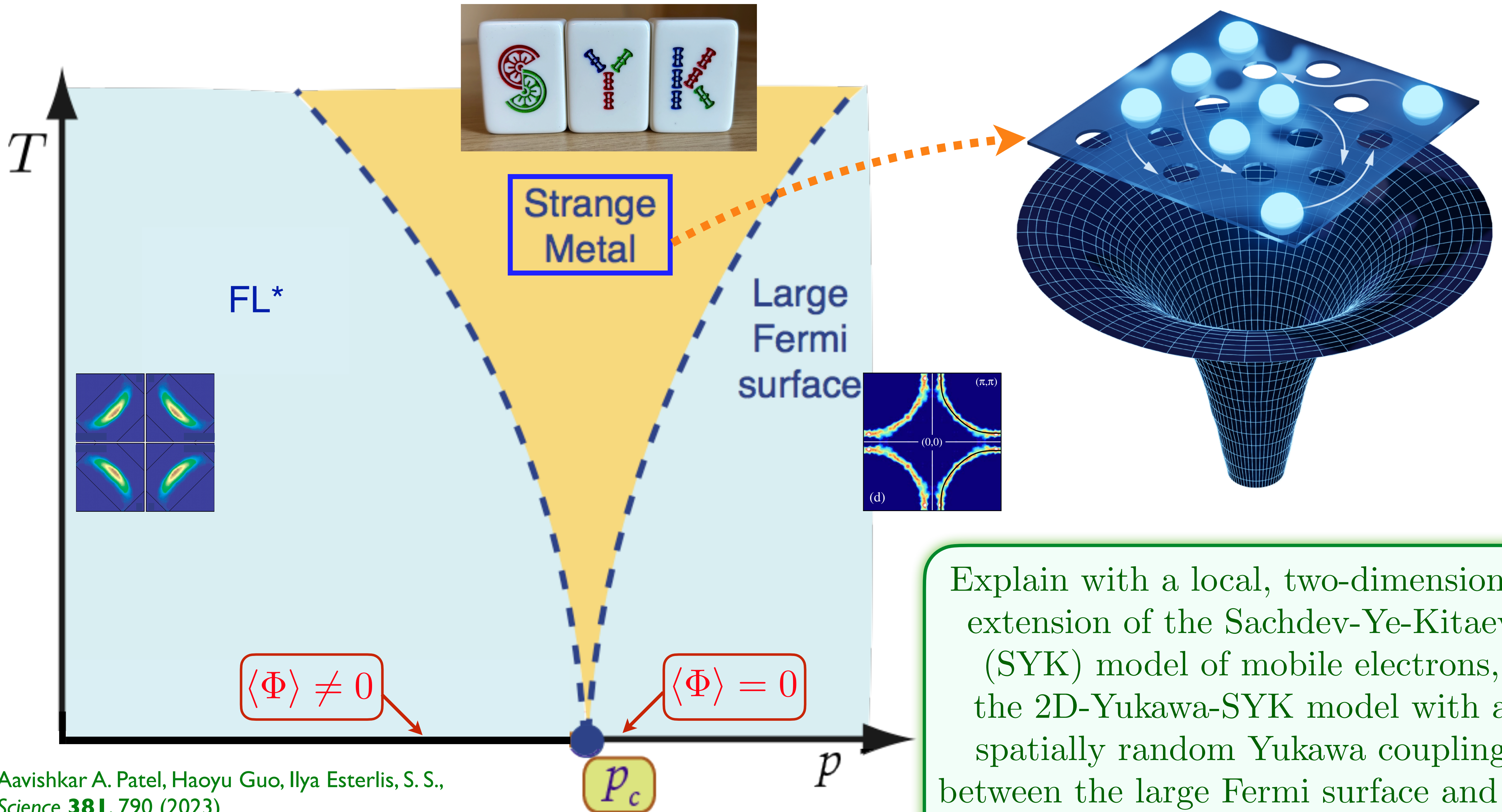
Ya-Hui Zhang and S. S., PRR **2**, 023172 (2020)

$$H_{\text{hole pockets}} = \sum_{i,j} \left[-t_{ij} c_{i\alpha}^\dagger c_{j\alpha} - t_{1,ij} f_{1i\alpha}^\dagger f_{1j\alpha} \right] - \sum_i \Phi (c_{i\alpha}^\dagger f_{1i\alpha} + f_{1i\alpha}^\dagger c_{i\alpha})$$



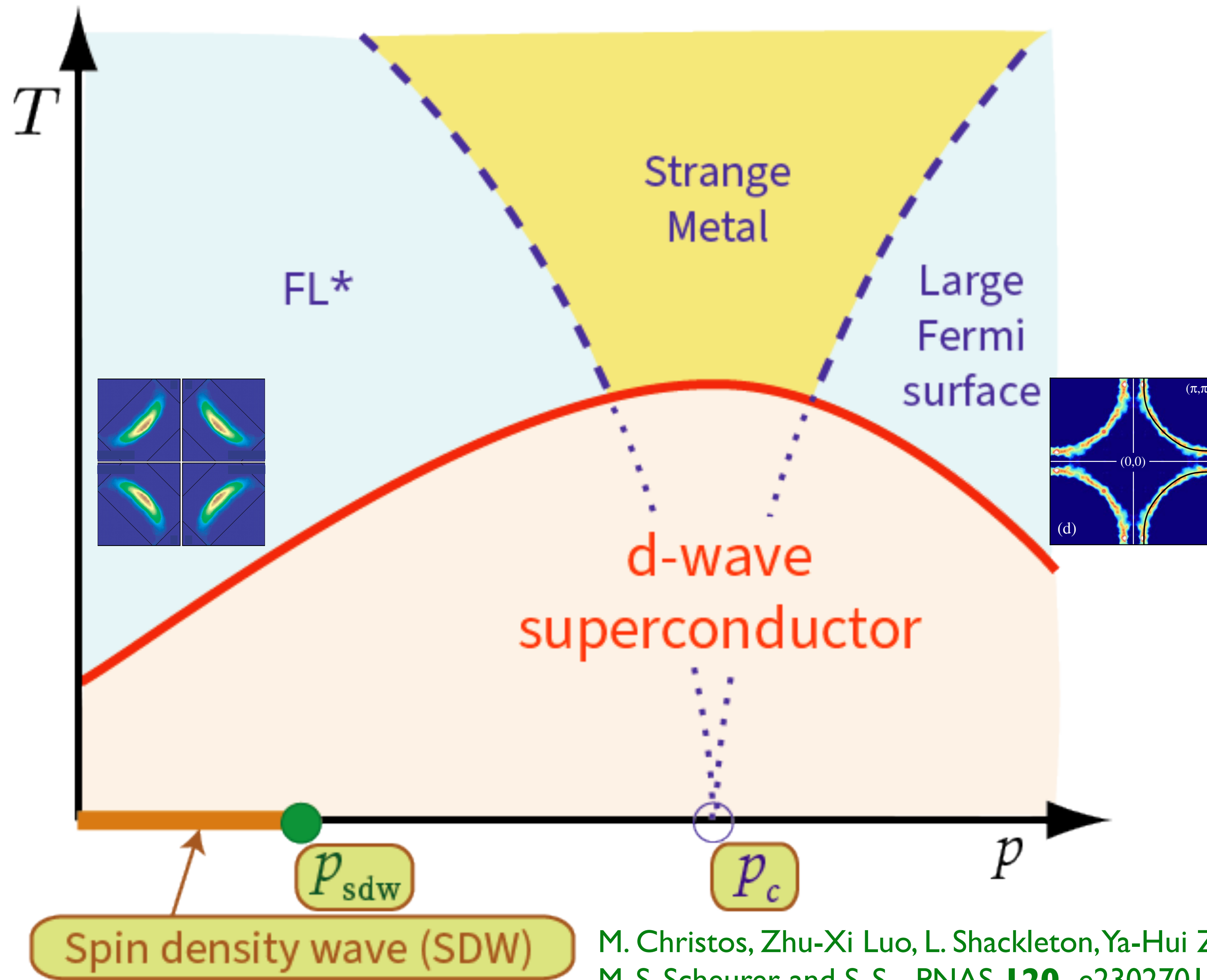


Quantum-criticality
of a quantum phase transition
between two metals
(FL^* and FL) at $p = p_c$,
with no symmetry breaking.
 Φ was the hybridization
between c and f_1 in theory of
hole pockets—it is
now a Higgs field.



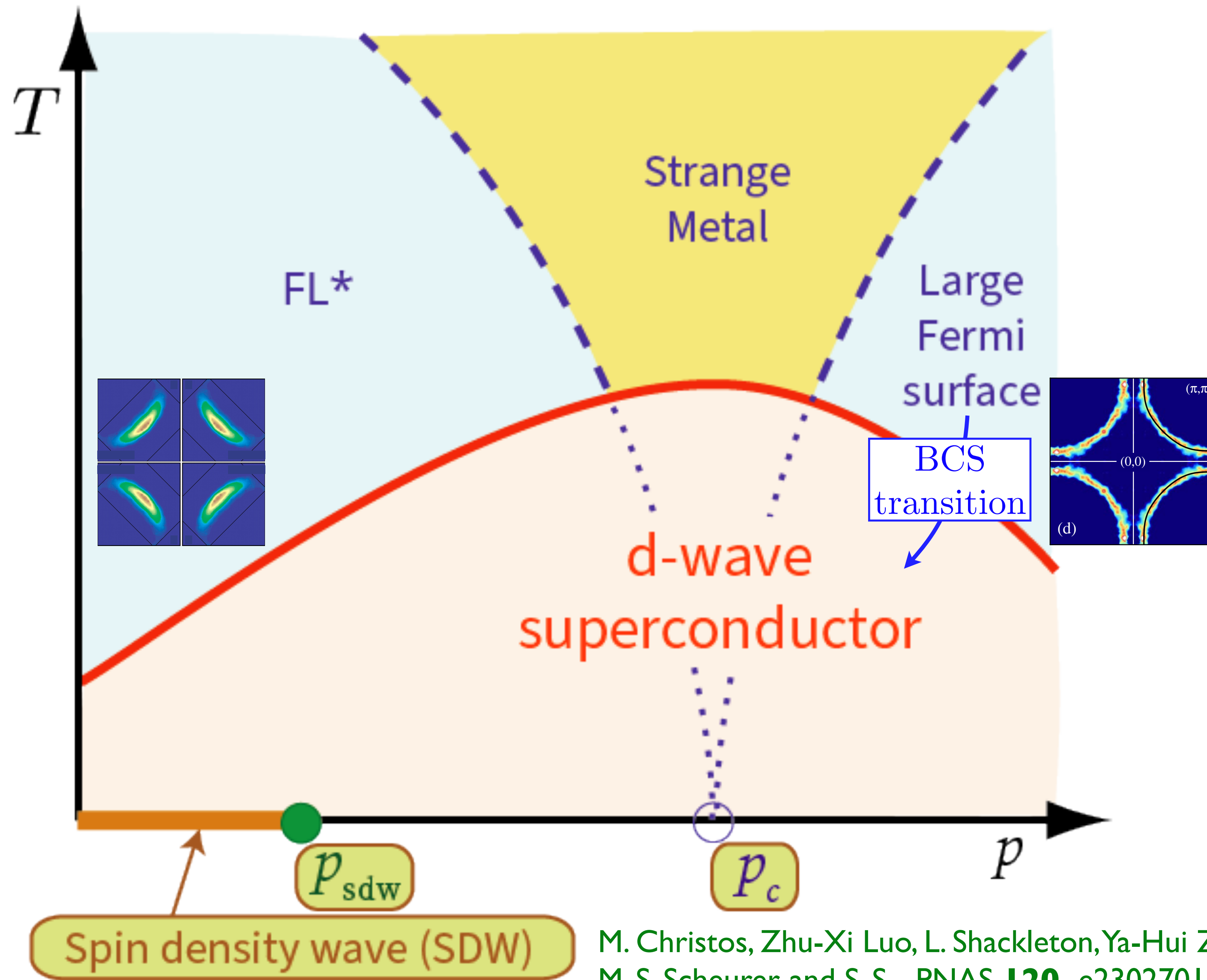
Explain with a local, two-dimensional extension of the Sachdev-Ye-Kitaev (SYK) model of mobile electrons, the 2D-Yukawa-SYK model with a spatially random Yukawa coupling between the large Fermi surface and Φ : a critical charge liquid

Aavishkar A. Patel, Haoyu Guo, Ilya Esterlis, S. S., *Science* **381**, 790 (2023)
 Chenyuan Li, Aavishkar A. Patel, Haoyu Guo, Davide Valentini, Jorg Schmalian, S.S., Ilya Esterlis, *PRL* **133**, 186502 (2024)



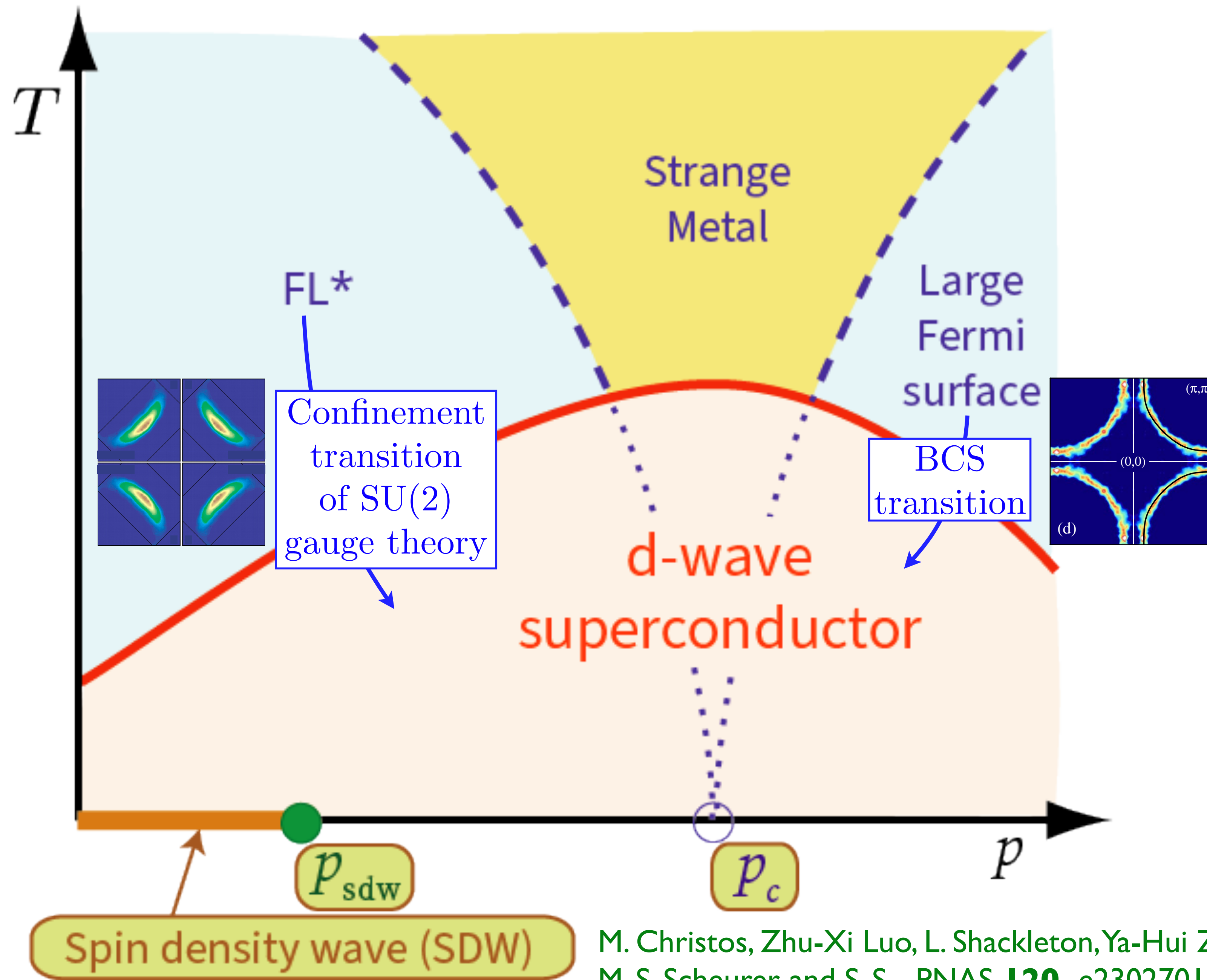
Quantum-criticality
of a quantum phase transition
between two metals
(FL* and FL) at $p = p_c$,
with no symmetry breaking.
 Φ was the hybridization
between c and f_1 in theory of
hole pockets—it is
now a Higgs field.

Both metals lead to the same
 d -wave superconductor at lower
temperatures, and so there is
transition at $p = p_c$ within the
superconducting state.



Quantum-criticality
of a quantum phase transition
between two metals
(FL* and FL) at $p = p_c$,
with no symmetry breaking.
 Φ was the hybridization
between c and f_1 in theory of
hole pockets—it is
now a Higgs field.

Both metals lead to the same
 d -wave superconductor at lower
temperatures, and so there is
transition at $p = p_c$ within the
superconducting state.



Quantum-criticality
of a quantum phase transition
between two metals
(FL* and FL) at $p = p_c$,
with no symmetry breaking.
 Φ was the hybridization
between c and f_1 in theory of
hole pockets—it is
now a Higgs field.

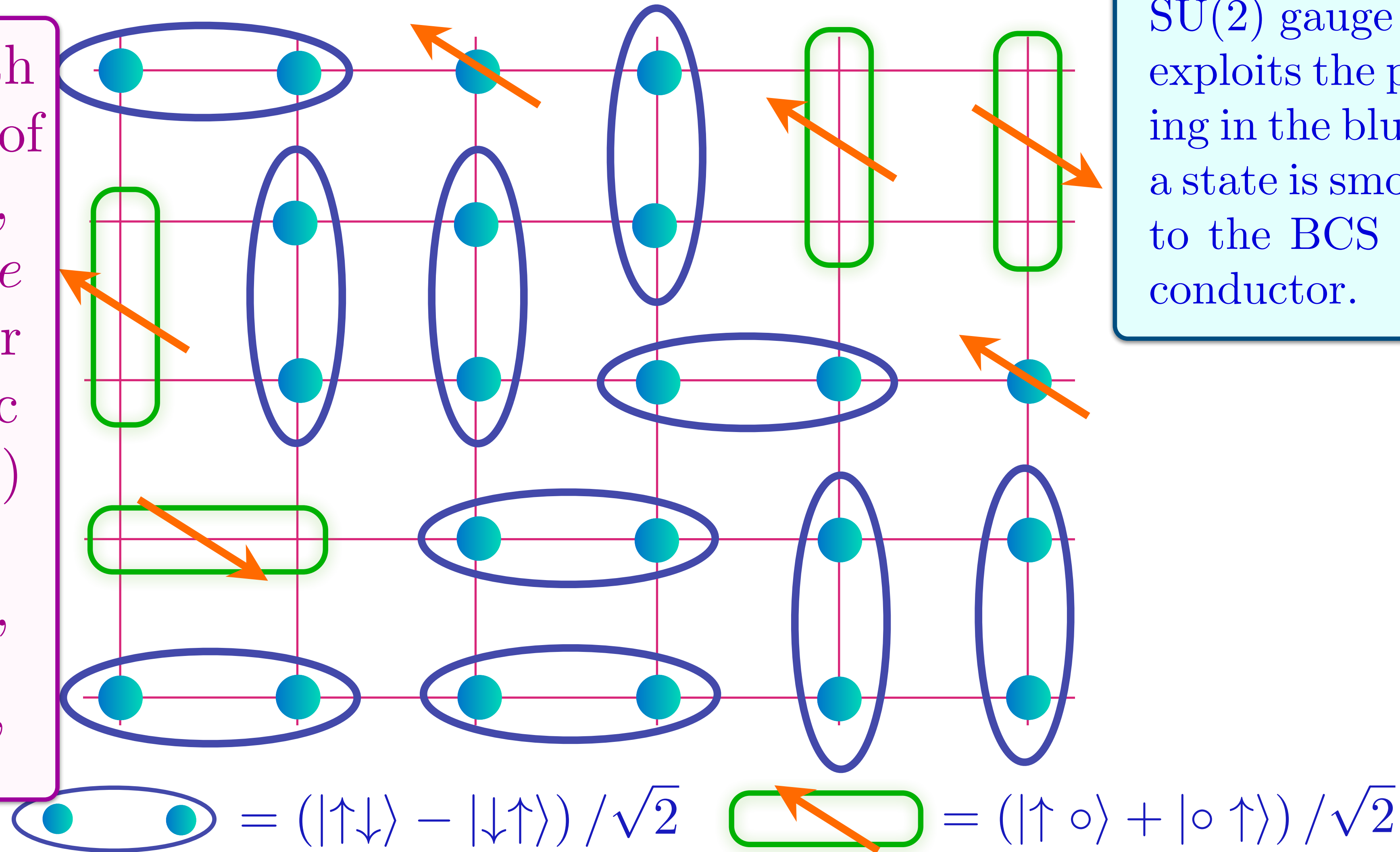
Both metals lead to the same
 d -wave superconductor at lower
temperatures, and so there is
transition at $p = p_c$ within the
superconducting state.

Doping an insulating antiferromagnet with holes of density p

FL*

Metal with density p of spin-1/2, charge $+e$ 'holes' (or 'magnetic polarons') and charge 0, spin-1/2 'spinons'

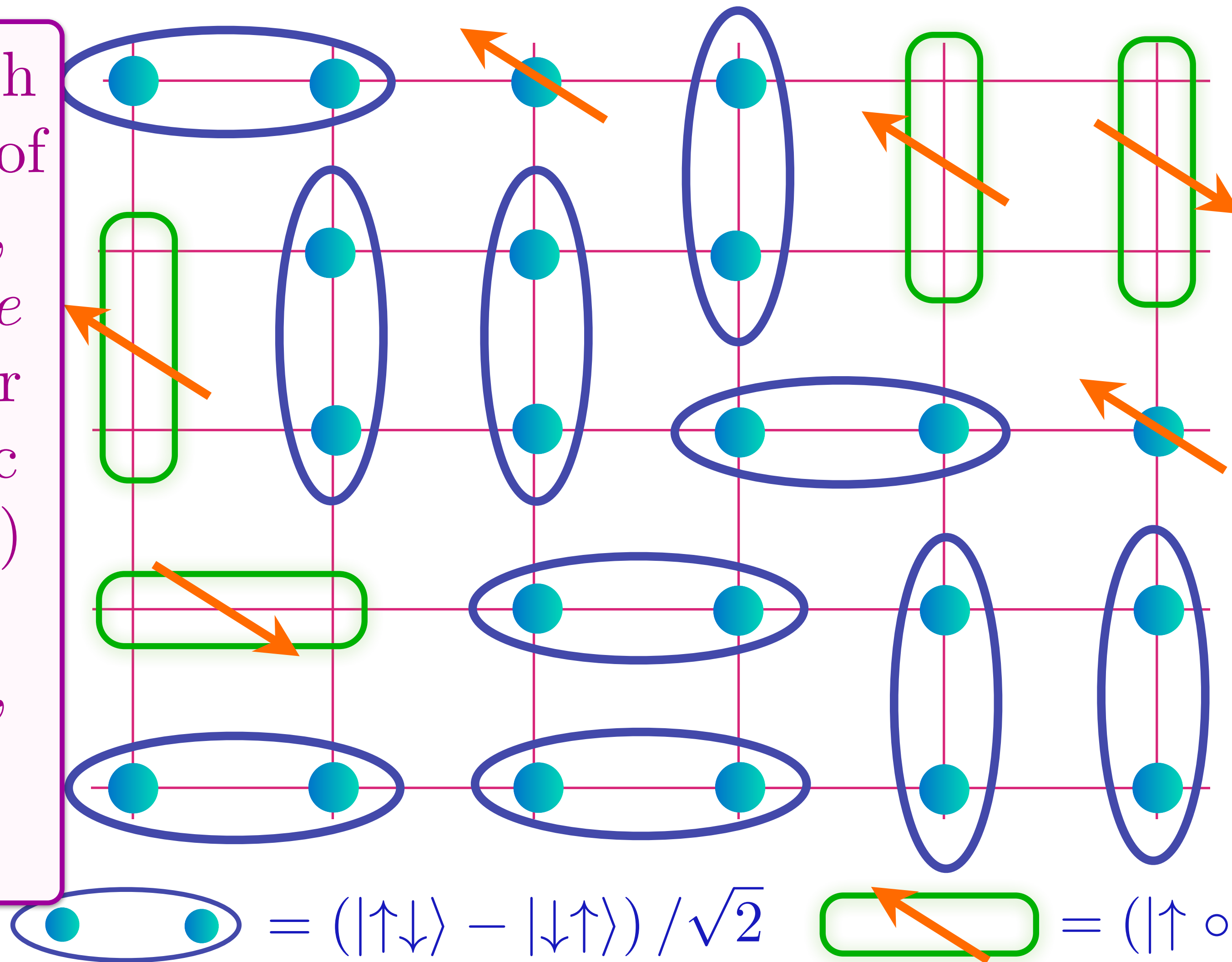
The d -wave superconductor is obtained by confining the SU(2) gauge field, and this exploits the pre-existing pairing in the blue dimers. Such a state is smoothly connected to the BCS d -wave superconductor.



Doping an insulating antiferromagnet with holes of density p

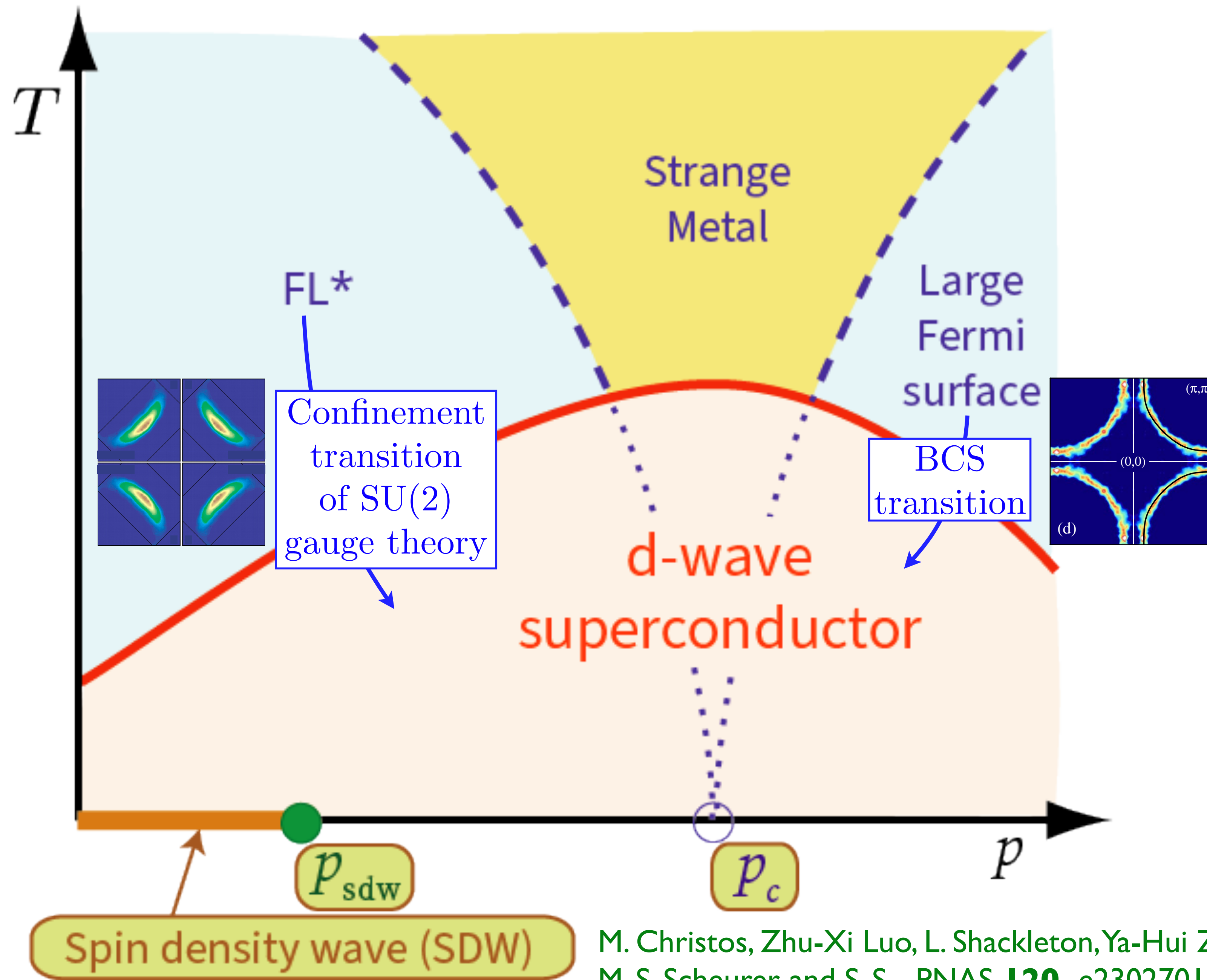
FL*

Metal with density p of spin-1/2, charge $+e$ 'holes' (or 'magnetic polarons') and charge 0, spin-1/2 'spinons'



The d -wave superconductor is obtained by confining the SU(2) gauge field, and this exploits the pre-existing pairing in the blue dimers. Such a state is smoothly connected to the BCS d -wave superconductor.

Applying BCS pairing to the hole pockets (green dimers) yields a distinct SC* state, which is *not* smoothly connected to the BCS d -wave state.



Quantum-criticality
of a quantum phase transition
between two metals
(FL* and FL) at $p = p_c$,
with no symmetry breaking.
 Φ was the hybridization
between c and f_1 in theory of
hole pockets—it is
now a Higgs field.

Both metals lead to the same
 d -wave superconductor at lower
temperatures, and so there is
transition at $p = p_c$ within the
superconducting state.